INTERNATIONAL JOURNAL OF HEAT AND MASS TRANSFER

VOLUME 3 1961

Vol. 3 1961

BOARD OF EDITORS

A. J. EDE
East Kilbride, Scotland

CARL GAZLEY, Jr.
Santa Monica, Calif.

U. GRIGULL
München, Germany

J. P. HARTNETT
Newark, Delaware

A. V. LUIKOV
Minsk, B.S.S.R.

TAKASHI SATŌ
Kyoto, Japan

D. B. SPALDING
London

Assisted by an Honorary Editorial Advisory Board

Co-chairmen

E. R. G. ECKERT
Minneapolis, Minn.

O. A. SAUNDERS
London

PERGAMON PRESS LTD.

OXFORD · LONDON · NEW YORK · PARIS

INTERNATIONAL JOURNAL OF HEAT AND MASS TRANSFER

BOARD OF EDITORS

A. J. EDE, National Engineering Laboratory, East Kilbride, Lanarkshire, Scotland
CARL GAZLEY, JR., The RAND Corporation, Santa Monica, California
U. GRIGULL, Technische Hochschule, München, Germany
J. P. HARTNETT, University of Delaware, Newark, Delaware, U.S.A.
A. V. LUIKOV, Institute of Energetics, Academy of Science, Podlesnaya 25, Minsk, B.S.S.R., U.S.S.R.
TAKASHI SATŌ, Kyoto University, Kyoto, Japan
D. B. SPALDING, Imperial College of Science & Technology, City & Guilds College, London S.W.7, England

HONORARY EDITORIAL ADVISORY BOARD

Co-chairmen:
E. R. G. ECKERT, *University of Minnesota, Minneapolis, Minnesota*
O. A. SAUNDERS, *Imperial College, London, England*

A. D. BAXTER, *Edgeware*
J. E. BIALOKOZ *Oxford*
L. M. K. BOELTER, *Los Angeles*
THOMAS W. F. BROWN, *Wallsend*
EDMUND A. BRUN, *Paris*
F. BOŠNJAKOVIĆ, *Stuttgart*
A. F. CHUDNOVSKY, *Leningrad*
Z. F. CHUKHANOV, *Moscow*
J. W. CIBOROWSKI, *Warsaw*
MILTON U. CLAUSER, *Los Angeles*
A. CRAYA, *Grenoble*
R. M. DRAKE, JR., *Princeton*
T. B. DREW, *New York*
HOWARD EMMONS, *Cambridge, Massachusetts*
P. GRASSMANN, *Zürich*
S. R. DE GROOT, *Leyden*
G. A. HAWKINS, *Lafayette, Indiana*
W. R. HAWTHORNE, *Cambridge, England*
T. HOBLER, *Gliwice*
J. N. HOOL, *Sydney*
H. C. HOTTEL, *Cambridge, Massachusetts*
BUSUKE HUDIMOTO, *Kyoto*
T. F. IRVINE, JR., *New York*
ARTHUR KANTROWITZ, *Cambridge, Massachusetts*
JOSEPH KESTIN, *Providence*
S. P. KEZIOS, *Chicago*
D. T. KOKOREV, *Moscow*
P. K. KONAKOV, *Moscow*
S. I. KOSTERIN, *Moscow*
V. D. LEBEDEV, *Moscow*
E. J. LE FEVRE, *London*
P. A. LIBBY, *New York*
D. J. MASSON, *Santa Monica*
T. MIZUSHINA, *Kyoto*
R. H. NORRIS, *Schenectady*
SIMON OSTRACH, *Cleveland*
R. L. PIGFORD, *Newark, Delaware*
A. A. POMERANTSEV, *Moscow*
A RAMACHANDRAN, *Bangalore*
H. L. RITZ, *Karlsruhe*
W. RIZK, *Whetstone*
W M. ROHSENOW, *Cambridge, Massachusetts*
E. SCHMIDT, *München*
H. SCHUH, *Linköping*
A. W. SCOTT, *Glasgow*
R. A. SEBAN, *Berkeley*
F. TACHIBANA, *Chiba City*
FUMIO TAMAKI, *Chiba City*
M. W. THRING, *Sheffield*
Y. S. TOULOUKIAN, *Lafayette, Indiana*
MYRON TRIBUS, *Los Angeles*
E. R. VAN DRIEST, *Downey, California*
K. YAMAGATA, *Fukuoka City*

Publishing Offices
Pergamon Press Limited, Headington Hill Hall, Oxford, England
Pergamon Press Inc., 122 East 55th Street, New York 22, N.Y.

Annual Subscription Rates

A. For libraries, government establishments, research laboratories, etc . . . £14 ($40.00).
B. For individuals who place their orders directly with the publisher and certify that the journal is for their personal use . . . £5 5s. ($15.00).

Copyright Pergamon Press Ltd. © 1961

PERGAMON PRESS LTD

Headington Hill Hall, Oxford — 122 East 55th Street, New York 22, N.Y.

Vol 3 196

VOLUME 3

NUMBER 1

PAGE

G. POOTS: Laminar natural convection in magneto-hydrodynamics 1

H. L. EVANS: Mass transfer through laminar boundary layers—3a. Similar solutions of the b-equation when $B = 0$ and $\sigma \geqslant 0{\cdot}5$ 26

E. R. G. ECKERT and E. M. SPARROW: Radiative heat exchange between surfaces with specular reflection 42

D. B. SPALDING and R. G. CRUDDACE: Theory of the steady laminar buoyant flow above a line heat source in a fluid of large Prandtl number and temperature-dependent viscosity 55

K. SREENIVASAN and A. RAMACHANDRAN: Effect of vibration on heat transfer from a horizontal cylinder to a normal air stream 60

E. R. G. ECKERT, E. M. SPARROW and W. E. IBELE: Heat transfer bibliography 68

Book Review 76

Vol.
3
1961

NUMBER 2

N. Z. AZER and B. T. CHAO: Turbulent heat transfer in liquid metals—Fully developed pipe flow with constant wall temperature 77

G. N. ABRAMOVICH, B. G. KHUDENKO and I. S. MAKAROV: Turbulence intensity, temperature and concentration of admixtures in a turbulent wake immediately behind a plate placed across a flow 84

KENNETH F. GORDON, T. SINGH and E. Y. WEISSMAN: Boiling heat transfer between immiscible liquids 90

M. PERLMUTTER and R. SIEGEL: Two-dimensional unsteady incompressible laminar duct flow with a step change in wall temperature 94

R. A. ALPHER: Heat Transfer in Magnetohydrodynamic flow between parallel plates 108

M. J. BALCERZAK and S. RAYNOR: Steady state temperature distribution and heat flow in prismatic bars with isothermal boundary conditions 113

A. G. SMITH and V. L. SHAH: Approximate calculation method for transfer in laminar boundary layers with constant surface temperature 126

J. KESTIN, P. F. MAEDER and H. E. WANG: Influence of turbulence on the transfer of heat from plates with and without a pressure gradient 133

Shorter Communication

WILLIAM SQUIRE: Application of the defect law to the determination of the average velocity and temperature in turbulent pipe flow 155

Letter to the Editor

A. WILLIAMS: Comment on Rogers' paper "Heat transfer at the interface of dissimilar metals" 159

Announcements 160

Book Reviews 161

Pioneer Paper

OSBORNE REYNOLDS: On the extent and action of the heating surface of steam boilers 163

NUMBER 3

PAGE

A. V. LUIKOV: Application of methods of thermodynamics of irreversible processes to investigation of heat and mass transfer in a boundary layer 167

LOUIS KAISER: Échange de masse entre phases constituées par des mélanges 175

A. M. MKHITARYAN, V. Y. FRIDLAND, V. S. MAKSIMOV and S. D. LABINOV: Investigation methods into flow in a boundary layer with a longitudinal pressure gradient 183

A. S. PREDVODITELEV: On aerodynamics of rarefied gases and problems of heat transfer 188

J. F. GROSS, J. P. HARTNETT, D. J. MASSON and CARL GAZLEY, JR.: A review of binary laminar boundary layer characteristics 198

E. R. G. ECKERT, T. F. IRVINE, JR., E. M. SPARROW and W. E. IBELE: Heat transfer, a review of current literature 222

Shorter Communications

LIANG-TSENG FAN: Experimental study of effect of gas injection on rate of mass transfer from solid to liquid 249

S. L. BRAGG and I. E. SMITH: Dimensional analysis of burnout heat transfer 252

Papers accepted for publication in future issues 254

NUMBER 4

R. A. SEBAN and L. H. BACK: Velocity and temperature profiles in a wall jet 255

E. M. SPARROW and R. D. CESS: The effect of a magnetic field on free convection heat transfer 267

BERNARD LE FUR: Convection de la chaleur dans un gaz en régime laminaire dans le cas d'un gradient de pression et d'une température de paroi quelconques 275

T. L. PERELMAN: On conjugated problems of heat transfer 293

A. A. ZHUKAUSKAS and A. B. AMBRAZYAVICHYUS: Heat transfer of a plate in a liquid flow 305

E. J. NEKHENDZI: Method of a regular regime for the determination of variable thermal coefficients 311

H. L. EVANS: Mass transfer through laminar boundary layers—6. Methods of evaluating the wall gradient (b_0'/B) for similar solutions; some new values for zero main-stream pressure gradient 321

B. GEBHART: Surface temperature calculations in radiant surroundings of arbitrary complexity—For gray, diffuse radiation 341

Shorter Communication

WILLIAM SQUIRE: A discrepancy in the published results on heat transfer to cryogenic fluids 347

Announcements 349

E. R. G. ECKERT, E. M. SPARROW and W. E. IBELE: Heat transfer bibliography 351

TAKASHI SATŌ: Heat transfer bibliography 358

Pioneer Paper

WILHELM NUSSELT: Die Verbrennung und die Vergasung der Kohle auf dem Rost 359

Papers accepted for publication in future issues 370

Vol 3 196

Int. J. Heat Mass Transfer. Vol. 3, pp. 1–25. Pergamon Press 1961. Printed in Great Britain.

LAMINAR NATURAL CONVECTION FLOW IN MAGNETO-HYDRODYNAMICS

G. POOTS

Department of Theoretical Mechanics, Bristol University

(*Received* 7 *August* 1960, *and in revised form* 28 *December* 1960)

Abstract—This paper deals with the two-dimensional laminar natural convection flow of an electrically conducting viscous fluid, such as mercury or liquid sodium, in the presence of electric or magnetic fields. Two different flow régimes are discussed. The first example considered is the steady fully developed natural convection flow, with and without heat sources, between two long parallel plane surfaces with uniform magnetic field applied normal to the surfaces. The plane vertical surfaces are open at both ends to the ambient fluid and are maintained at constant temperatures different from that of the ambient fluid. Tables are given from which the fully developed temperature, velocity and induced magnetic fields may be found. Flow characteristics such as the net mass flow and wall Nusselt numbers are also evaluated.

The second example considered is the steady two-dimensional natural convection flow set up by Joule heating when a direct current flows in the axial direction through a horizontal circular tube filled with an electrically conducting viscous fluid. The outside surface of the tube is maintained at constant temperature by a coolant which is assumed to be a non-conductor and non-magnetic. The influence of the non-uniform convection flow on the temperature distribution and wall Nusselt number is calculated.

Résumé—Cet article traite de l'écoulement de convection naturelle laminaire à deux dimensions dans un fluide visqueux conducteur tel que le mercure ou le sodium liquide, en présence de champs magnétiques ou électriques. Deux régimes d'écoulement différents sont étudiés. Le premier exemple considéré est celui de la convection naturelle, en régime permanent, avec ou sans source de chaleur, entre deux longues surfaces planes parallèles normalement auxquelles est appliqué un champ magnétique uniforme. Les surfaces planes verticales sont ouvertes aux deux extrémités vars le fluide ambiant et sont maintenues à des températures constantes, différentes de celle du fluide ambiant. Des tables, à partir desquelles on peut trouver la température de régime, la vitesse et les champs magnétiques induits, sont données. Des caractéristiques de l'écoulement, telles que le débit massique et le nombre de Nusselt à la paroi sont également évaluées.

Le deuxième exemple considéré est celui de la convection naturelle à deux dimensions qui s'établit dans le cas d'un chauffage par effet Joule, quand on fait circuler un courant continu dans l'axe d'un tube horizontal, à section circulaire, rempli d'un liquide visqueux conducteur. La surface extérieure du tube est maintenue à température constante par un réfrigérant que l'on suppose non conducteur et non magnétique. L'influence d'un écoulement de convection naturelle non-uniforme sur la distribution des températures et le nombre de Nusselt à la paroi est calculée.

Zusammenfassung—Die Arbeit behandelt die zweidimensionale, laminare, freie Konvektionsströmung in einer elektrisch leitenden, viskosen Flüssigkeit, wie Quecksilber oder flüssigem Natrium in Gegenwart von elektrischen oder magnetischen Feldern. Zwei verschiedene Strömungsarten werden besprochen: Als erstes Beispiel die stationäre, voll ausgebildete, freie Konvektionsströmung mit und ohne Wärmequellen zwischen zwei langen parallelen ebenen Flächen mit gleichmässigem, senkrecht zu den Oberflächen wirkendem Magnetfeld. Der Spalt zwischen den ebenen, senkrecht stehenden Oberflächen ist für die umgebende Flüssigkeit an beiden Enden geöffnet. Die Oberflächen werden auf konstanten Temperaturen gehalten, die sich von der Temperatur der angrenzenden Flüssigkeit unterscheiden. Aus angegebenen Tabellen können Temperatur-, Geschwindigkeits- und induzierte Magnetfelder ersehen werden. Weiterhin sind charakteristische Strömungsgrössen wie Mengenstrom und Nusseltzahl in Wandnähe berechnet.

Als zweites Beispiel wird die stationäre zweidimensionale freie Konvektionsströmung betrachtet, die infolge Joulescher Erwärmung auftritt, wenn Gleichstrom in Achsialrichtung durch ein waagerechtes, mit elektrisch leitender viskoser Flüssigkeit gefülltes Rohr von Kreisquerschnitt fliesst. Die Rohraussenfläche wird durch ein nichtleitendes und unmagnetisches Kühlmittel auf konstanter Temperatur gehalten. Der Einfluss des ungleichförmigen Konvektionsstromes auf die Temperaturverteilung und die Nusseltzahl in Wandnähe ist angegeben.

Vol. 3 1961

A

Аннотация—В статье рассматривается двухмерный ламинарный конвективный поток в условиях естественного движения электрически проводящей вязкой жидкости. Например, ртутр или натрий в жидком состоянии. Предусматривается наличие электрических или магнитных полей. Рассматриваются два раэличных режима потока. В первом случае—стационарный полностыо установившейся поток в условиях естественной конвекции между двумя длинными плоско-параллельными поверхностями при наличии источников тепла или без них и с равномерным магнитным полем, перпендикулярным к поверхности пластины. Температура плоских вертикальных поверхностей отлична от температуры окружающей жидкости, с которой соприкасаются оба конца пластины. Из приведенных таблиц можно найти полностью установившиеся поля температуры, скорости, а также индуктировнные магнитные поля, Вычислены характеристики чистого потока массы и число Нуссельта стенки.

Во втором случае рассматривается стационарный двухмерный поток в условиях естественной конвекции, создаваемый нагреванием при прохождении постоянного тока в аксиальном направлении через горизонтальную круглую трубу, заполненную электрически проводящей вязкой жидкостью. Температура внешней поверхности трубы поддерживается постоянной при помощи охлаждающей среды, которую принимают непроводящей и немагнитной. Вычислено влияние неравномерного конвективного потока на распределние температуры и на число Нуссельта стенки.

NOMENCLATURE

e.m.u. and c.g.s. system used throughout.

A dimensionless magnetic vector potential;

a characteristic length;

c_p specific heat at constant pressure;

E electrical intensity;

g gravitational force per unit of mass;

G Grashof number, $\frac{\beta g \theta_w a^3}{\nu^2}$ (Example I) or $\frac{\beta g J_0^2 a^5}{k\sigma\nu^2}$ (Example II);

G_M magnetic Grashof number, $4\pi\sigma\mu_e\nu G$;

H magnetic intensity;

J current density;

K dimensionless parameter, PGK_A;

K_A dimensionless parameter $\frac{\beta g a}{c_p}$;

k thermometric conductivity;

M Hartmann number, $\mu_e H_0 a \sqrt{\frac{\sigma}{\rho\nu}}$;

Nu Nusselt number;

p pressure;

p_d pressure p minus the hydrostatic pressure p_s;

P Prandtl number $\frac{\rho c_p \nu}{k}$;

Q heat added by heat sources;

q fluid velocity;

T temperature;

x, y, z Cartesian co-ordinates;

r, ϕ, z cylindrical co-ordinates.

Greek symbols

α dimensionless heat source parameter;

β coefficient of volumetric expansion;

γ dimensionless quantity, $\frac{\mu_{1e}}{\mu_{2e}}$;

Θ dimensionless local temperature distribution;

θ temperature difference, $T - T_s$;

λ ratio of wall temperature differences, $\frac{\theta_{w1}}{\theta_{w0}}$;

μ dynamic viscosity;

μ_e magnetic permeability;

ν kinematic viscosity;

η magnetic viscosity;

ρ fluid density;

σ electrical conductivity;

χ dimensionless group, $1/4\pi\sigma\mu_{1e}\nu$;

ϵ dimensionless group, $1/PK_A\chi$;

Ψ dimensionless stream function;

Φ magnetic scalar potential.

Subscripts

s reference condition (usually taken as the hydrostatic condition);

w wall condition;

1 and 2 wall condition at $y = 0$ and a respectively for Example I, and conditions in the fluid and coolant respectively for Example II.

Vol 3 196

Vol. 3 1961

1. INTRODUCTION AND BASIC THEORY OF TWO-DIMENSIONAL NATURAL CONVECTION IN MAGNETO-HYDRODYNAMICS

THE PROCESS of natural convection flow will occur when density variations due to heating exist in a fluid, and is generated entirely by the action of body forces due to gravity. This process has many applications as a mechanism for heat transfer and, for example, plays a major role in the cooling of nuclear power plants where liquid sodium is used as a coolant. It is the purpose of this paper to investigate some aspects of two-dimensional laminar natural convection flow of an electrically conducting viscous fluid, such as mercury or liquid sodium, in the presence of additional forces due to imposed electric and magnetic fields. In general two types of problem require investigation. In the first type if a natural convection flow exists we wish to know how this is modified, i.e. changes in heat transfer and net mass flow, when electric and magnetic fields are applied. The second type of problem which may occur is one in which the natural convection flow is a direct consequence of the applied electric and magnetic fields and would not exist in the absence of these fields. In this case temperature gradients are caused by Joule heating if the region under consideration is enclosed or partially enclosed by solid boundaries.

The paper treats two relatively simple two-dimensional natural convection flow régimes, representative of the above types. In the first example results are obtained for the steady fully developed natural convection flow, with and without heat sources, between two long parallel plane surfaces with uniform magnetic fields applied normal to the surfaces. The plane vertical surfaces are open at both ends to the ambient fluid and are maintained at constant temperatures different from that of the ambient fluid. This configuration is a modification of the magnetic field-free case as discussed by Ostrach [1] and the analysis of this example follows Ostrach's treatment of the thermal convection problem and that of Cowling [2] in the discussion of the Hartmann–Lazarus flow of an electrically conducting viscous fluid between parallel flat plates. The special case when the arithmetic average of the plate temperatures is equal to the temperature of the ambient fluid has been discussed by Gershuni and Zhukhovitskii* [3]. In this reference the viscous and Joulean dissipation have been neglected in the equation of thermal energy transport.

In the second example results are obtained for the natural convection flow régime set up by Joule heating when a direct current is passed axially through a horizontal cylindrical tube filled with conducting fluid. The outside surface of the tube is maintained at constant temperature by a coolant which is assumed to be a non-conductor and non-magnetic. End effects near the electrodes are neglected, so that it is assumed that the tube is sufficiently long to allow steady two-dimensional natural convection flow near the centre to be established.

Consider now the magneto-hydrodynamic equations and the equation of thermal energy transport relating to steady natural convection flow. The usual assumptions are made with regard to the physical properties of the fluid, i.e. the viscosity, electrical conductivity and magnetic permeability etc. are independent of the temperature and the strength of the magnetic or electric fields involved. The density of the fluid is assumed constant except in the case of density variation with temperature in producing the buoyancy force. The basic equations in e.m.u. and c.g.s. units are, in the usual notation,

$$\operatorname{div} \mathbf{q} = 0, \tag{1.1}$$

$$(\mathbf{q}.\nabla)\mathbf{q} = -1/\rho\, \nabla p_d + \nu\nabla^2 q + \frac{\mu_e}{\rho}\mathbf{J}\wedge\mathbf{H} - \beta(T - T_s)\mathbf{g}, \tag{1.2}$$

$$\rho c_p\, \mathbf{q}.\nabla T = k\nabla^2 T + \frac{\mathbf{J}^2}{\sigma} + Q + \Phi_q, \tag{1.3}$$

together with the electro-magnetic equations

$$\operatorname{div} \mathbf{H} = 0, \tag{1.4}$$

$$\operatorname{curl} \mathbf{H} = 4\pi J, \tag{1.5}$$

$$\operatorname{curl} \mathbf{E} = 0, \tag{1.6}$$

and finally Ohm's law for the moving fluid

$$\mathbf{J} = \sigma(\mathbf{E} + \mu_e\, \mathbf{q}\wedge\mathbf{H}). \tag{1.7}$$

* The author is indebted to a referee for this reference.

Here p_d is the pressure of the fluid minus the hydrostatic pressure, β is the coefficient of volumetric expansion, Q is the quantity of heat added by heat sources per unit of volume, and Φ_q is the viscous dissipation function. Furthermore equation (1.3) is valid only when the temperature difference $(T-T_s)$ is small compared with the hydrostatic temperature T_s, and all physical constants appearing in equations (1.1) to (1.7) must be evaluated at the hydrostatic condition.

These equations can now be reduced to their simplest two-dimensional form when the following conditions are satisfied within the fluid:

(i) the pressure gradient in the z-direction is zero i.e. $(\partial p_d/\partial z) = 0$,

(ii) the velocity and magnetic field components are

$$\mathbf{q} = [u(x, y), \quad v(x, y), 0], \tag{1.8}$$

and

$$\mathbf{H} = [H_x(x, y), H_y(x, y), 0]. \tag{1.9}$$

On using this assumed form for $\mathbf{H}$ equation (1.5) implies that $J_x = J_y = 0$ and

$$4\pi J_z = \frac{\partial H_y}{\partial x} = \frac{\partial H_z}{\partial y};$$

equation (1.6) implies that

$$\frac{\partial E_y}{\partial x} - \frac{\partial E_x}{\partial y} = 0$$

and $E_z = E_0$, a constant; equation (1.7) now implies on using (1.8) and (1.9) that $E_x = E_y = 0$ and $J_z = \sigma[E_0 + \mu_e(uH_y - vH_x)]$. Thus subject to the above conditions the equations governing the steady two-dimensional natural convection flow, taking the x-axis in the vertical direction, are

$$\frac{\partial u}{\partial x} + \frac{\partial v}{\partial y} = 0, \tag{1.10}$$

$$u\frac{\partial u}{\partial x} + v\frac{\partial u}{\partial y} = -\frac{1}{\rho}\frac{\partial p_d}{\partial x} + \nu\nabla^2 u - \frac{\mu_e}{\rho}J_z H_y + \beta g(T - T_s), \tag{1.11}$$

$$u\frac{\partial v}{\partial x} + v\frac{\partial v}{\partial y} = -\frac{1}{\rho}\frac{\partial p_d}{\partial y} + \nu\nabla^2 v + \frac{\mu_e}{\rho}J_z H_x, \tag{1.12}$$

$$\frac{\partial H_x}{\partial x} + \frac{\partial H_y}{\partial y} = 0, \tag{1.13}$$

$$J_z = \frac{1}{4\pi}\left(\frac{\partial H_y}{\partial x} - \frac{\partial H_x}{\partial y}\right) = \sigma[E_0 + \mu_e(uH_y - vH_x)], \tag{1.14}$$

and

$$\rho c_p\left(u\frac{\partial T}{\partial x} + v\frac{\partial T}{\partial y}\right) = k\nabla^2 T + \frac{J_z^2}{\sigma} + Q + \Phi_q, \tag{1.15}$$

where Φ_q is the two-dimensional form of the dissipation function

$$\Phi_q = 2\mu\left[\left(\frac{\partial u}{\partial x}\right)^2 + \left(\frac{\partial v}{\partial y}\right)^2 + \tfrac{1}{2}\left(\frac{\partial u}{\partial y} + \frac{\partial v}{\partial x}\right)^2\right]. \tag{1.16}$$

The boundary conditions for equations (1.10) and (1.16) will be derived later.

2. EXAMPLE 1: FULLY DEVELOPED NATURAL CONVECTION FLOW BETWEEN PARALLEL FLAT PLATES IN A MAGNETIC FIELD

2(a) *Statement of problem and governing equations*

The simplified configuration to be investigated in this section is the fully developed laminar flow of an electrically conducting viscous fluid, with and without heat sources, between two parallel flat plates orientated in the vertical direction (taken to be the x-direction) and distance a apart (i.e. $y = 0$ and a). The plate surfaces, which are open at both ends to the ambient fluid, are maintained at constant temperature $T = T_0$ at $y = 0$ and $T = T_1$ at $y = a$ respectively, and in general $T_0 \neq T_1 \neq T_s$, the ambient temperature. A uniform magnetic field of intensity H_0 is applied normal to the plates, i.e. parallel to Oy and perpendicular to

Ox and Oz respectively. If the dimensions of the plates are large compared with the distance between them such that fully developed flow exists everywhere (except near the edges of the plates) then as in the Hartmann–Lazarus flow (see Cowling [2]) a solution of the basic equations (1.10) to (1.16) is possible provided $u = u(y)$, $v = 0$, $T = T(y)$, $H_x = H_x(y)$ and $H_y = H_0$, the applied field. The equations for steady motion now become

$$\mu \frac{\mathrm{d}^2 u}{\mathrm{d}y^2} + \beta\rho g(T - T_s) - \mu_e H_0 J_z = \frac{\partial p_d}{\partial x}, \tag{2.1}$$

$$\mu_e J_z H_x = \frac{\partial p_d}{\partial y}, \tag{2.2}$$

$$J_z = -\frac{1}{4\pi}\frac{\mathrm{d}H_x}{\mathrm{d}y} = \sigma(E_0 + \mu_e H_0 u), \tag{2.3}$$

and

$$k \frac{\mathrm{d}^2 T}{\mathrm{d}y^2} + \mu \left(\frac{\mathrm{d}u}{\mathrm{d}y}\right)^2 + Q + \sigma(E_0 + \mu_e H_0 u)^2 = 0. \tag{2.4}$$

Now we are interested only in the case for which there is zero axial pressure gradient i.e. $\partial p_d/\partial x = 0$ and thus on using equations (2.2) and (2.3) the momentum equation yields

$$\mu \frac{\mathrm{d}^2 u}{\mathrm{d}y^2} + \beta\rho g(T - T_s) - \sigma\mu_e H_0(E_0 + \mu_e H_0 u) = 0. \tag{2.5}$$

The boundary conditions associated with (2.4) and (2.5) are

$$\left.\begin{aligned} u(0) = u(a) = 0,\ T(0) = T_0 \\ \text{and} \qquad T(a) = T_1. \end{aligned}\right\} \tag{2.6}$$

A solution of equations (2.4) to (2.6) may now be obtained for any specified value of the constant electric field E_0 and this would, on using equation (2.3), imply a flow of current in the z-direction. Suppose now the channel is bounded by electrically insulated walls in the planes $z = \pm d$, where $d \gg a$. For this model a non-uniform induced electric field is set up since J_z must vanish at $z = \pm d$. Equations (2.4) and (2.5) no longer apply to this situation since the condition that E_0 must be constant is violated. To represent this model as closely as possible Cowling [2] suggests that the constant E_0 is adjusted to make the total current $\int_0^a J_z \mathrm{d}y$ flowing between $z = \pm d$ vanish. This gives

$$E_0 = -\frac{\mu_e H_0}{a}\int_0^a u \,\mathrm{d}y \tag{2.7}$$

which is consistent with the boundary condition $H_x(0) = H_x(a) = 0$. This follows from the condition that there must be no discontinuity in the tangential component of **H** at the solid interfaces $y = 0, a$. Thus for a long rectangular duct, having aspect ratio $2\mathrm{d}/a \gg 1$, orientated in the vertical direction and with a uniform magnetic field imposed perpendicular to the isothermal walls $y = 0, a$, the steady fully developed natural convection flow near the central axis of the tube ($z = 0$) and sufficiently far away from the open ends, is determined by the equations

$$\mu \frac{\mathrm{d}^2 u}{\mathrm{d}y^2} + \rho\beta g(T - T_s) - \sigma\mu_e^2 H_0^2\left(u - \frac{1}{a}\int_0^a u\mathrm{d}y\right) = 0, \tag{2.8}$$

$$k \frac{\mathrm{d}^2 T}{\mathrm{d}y^2} + \mu\left(\frac{\mathrm{d}u}{\mathrm{d}y}\right)^2 + Q + \sigma\mu_e^2 H_0^2\left(u - \frac{1}{a}\int_0^a u\mathrm{d}y\right)^2 = 0, \tag{2.9}$$

subject to the boundary conditions (2.6). The terms in (2.8) denote the viscous, buoyancy and Lorentz forces respectively; the terms in (2.9) denote the transport of thermal energy by conduction, viscous dissipation, heat generation by heat sources, and Joulean dissipation. We note also that the Lorentz force opposes the buoyancy force, which leads to an effective decrease in velocity or net mass flow as H_0 increases.

As the units of field strength, temperature and velocity we choose H_0, $\theta_0 = (T_0 - T_s)$ and ν/a respectively. Dimensional analysis then leads to the introduction of four dimensionless parameters: the temperature difference ratio

$$\lambda = \frac{(T_1 - T_s)}{(T_0 - T_s)} = \frac{\theta_1}{\theta_0};$$

Vol. 3 1961

the heat source parameter $\alpha = Qa^2/k\theta_0$; the Hartmann number $M = \mu_e H_0 a(\sigma/\rho\nu)^{1/2}$; and, due to Ostrach [1], the dimensionless group $K = PGK_A$ where $P = (\rho c_p \nu/k)$ is the Prandtl number, $G = (\beta g \theta_w a^3/\nu^2)$ the Grashof number ($\theta_w = \theta_0$ or θ_1), and the dimensionless group $K_A = (\beta g a/c_p)$. We now introduce the new dimensionless variables

$$Y = y/a, \quad \Theta = K\frac{(T_1 - T_s)}{(T_0 - T_s)}, \quad U = K_A P \frac{\nu}{a} u. \tag{2.10}$$

When these substitutions are made in the basic equations of motion (2.8) and (2.9) we obtain

$$U'' + \Theta - M^2(U - \int_0^1 U \mathrm{d}Y) = 0, \tag{2.11}$$

$$\Theta'' + (U')^2 + M^2(U - \int_0^1 U \mathrm{d}Y)^2 + \alpha K = 0, \tag{2.12}$$

subject to the boundary conditions

$$\left.\begin{aligned} U(0) = U(1) = 0,\ \Theta(0) = K \\ \text{and} \qquad \Theta(1) = \lambda K. \end{aligned}\right\} \tag{2.13}$$

In equations (2.11) and (2.12) the prime denotes differentiation with respect to Y.

It remains now to choose representative values of α, λ, M and K applicable, for example, to liquid metals. Without loss of generality we shall take $\alpha = 0$, 10 and 100, $\lambda = -1(1)2$ and $M = 0, 2, 4$ and 10. However, as seen from Table 1, we are interested only in a range of small or moderately small values of K. For example, considering the convection flow of mercury in a gravitational field at room temperature (20°C), and taking $\theta_0 = T_0 - T_s = 5$°C and the plates 5 cm apart (i.e. $a = 5$), then $K = 1{\cdot}5$; for liquid sodium, if $T_s = 200$°C, $\theta_0 = 100$°C and $a = 10$ then $K = 1{\cdot}04$. In the next section series expansions in powers of K are obtained for U and Θ, valid for small K and all values of the remaining parameters α, λ and M.

2(b) *Series expansion for small K*

A series solution for U and Θ may be obtained by taking

Table 1

	Mercury, 20°C	Liquid sodium, 200°C
Density, ρ (g/cm^3)	13·55	0·904
Coefficient of cubical expansion, β (/°C)	$1{\cdot}82 \times 10^{-4}$	$2{\cdot}2 \times 10^{-4}$
Dynamic viscosity, μ (g/cm sec)	$1{\cdot}53 \times 10^{-2}$	$4{\cdot}5 \times 10^{-3}$
Kinematic viscosity, ν (cm^2/sec)	$1{\cdot}13 \times 10^{-3}$	$4{\cdot}97 \times 10^{-3}$
Permeability, μ_e (e.m.u.)	1	1
Resistivity, R (ohms-cm)	$9{\cdot}58 \times 10^{-5}$	$1{\cdot}36 \times 10^{-5}$
Specific heat, c_p (cal/°C)	$3{\cdot}33 \times 10^{-2}$	0·32
Thermal conductivity, K (cal/cm sec°C)	$1{\cdot}90 \times 10^{-2}$	0·195
Prandtl number, $P = \frac{\rho c_p \nu}{K}$	$2{\cdot}68 \times 10^{-2}$	$7{\cdot}38 \times 10^{-3}$
$\eta/\nu = \frac{1}{4\pi\sigma\mu_e\nu}$	$6{\cdot}74 \times 10^{6}$	$2{\cdot}18 \times 10^{5}$

$$\left.\begin{aligned} U = K\sum_{n=0}^{\infty} K^n U_n(Y) \\ \text{and} \qquad \Theta = K\sum_{n=0}^{\infty} K_n \Theta_n(Y). \end{aligned}\right\} \tag{2.14}$$

On substituting the expansions (2.14) into equations (2.11) to (2.13) and equating coefficients of like powers of K, there results a set of differential equations of which the first few are:

$$\left.\begin{aligned} \Theta_0'' + \alpha = 0,\ \Theta_0(0) = 1, \quad \Theta_0(1) = \lambda; \\ U_0'' + \Theta_0 - M^2(U_0 - \textstyle\int_0^1 U_0 \mathrm{d}Y) = 0, \\ U_0(0) = U_0(1) = 0; \end{aligned}\right\} \tag{2.15}$$

$$\left.\begin{aligned} \Theta_1'' + (U_0')^2 + M^2(U_0 - \textstyle\int_0^1 U_0 \mathrm{d}Y)^2 = 0, \\ \Theta_1(0) = \Theta_1(1) = 0; \\ U_1'' + \Theta_1 - M^2(U_1 - \textstyle\int_0^1 U_1 \mathrm{d}Y) = 0, \\ U_1(0) = U_1(1) = 0. \end{aligned}\right\} \tag{2.16}$$

Equations (2.15) yield the fully developed velocity and thermal profiles neglecting the viscous and Joulean dissipation.* The inclusion of equations (2.16) refines this approximation to include the dissipation functions.

* Note that the case $\lambda = -1$ is that treated by Gershuni and Zhukhovitskii [3].

Vol 3 196

For the zeroth-order functions U_0 and Θ_0 we obtain

$$\Theta_0 = 1 + b_1 Y + b_2 Y^2, \tag{2.17}$$

$$M^3 U_0 = B_0 S_0(M, Y) + B_1 S_1(M, Y) + b_1 + b_2 Y^2, \tag{2.18}$$

where

$$S_0(M, Y) = \sinh M - \sinh MY + \sinh M(Y-1),$$

$$S_1(M, Y) = \sinh M + \sinh MY + \sinh M(Y-1),$$

$$b_1 = \tfrac{1}{2}(a + 2\lambda - 2), \quad b_2 = -a/2,$$

$$B_2 = \frac{M^2(6 + 6\lambda + a - 12a/M^2)}{24(\cosh M - 1)}$$

and

$$B_2 = \frac{-M(\lambda - 1)}{\sinh M}.$$

The first-order functions are obviously more tedious to evaluate. They can be expressed as

$$M^4\Theta_1 = -\sum_{n=1}^{\infty} C_n g_n(Y),$$

$$M^4 U_1 = \sum_{n=1}^{\infty} C_n f_n(Y) \tag{2.19}$$

where

$$C_1 = B_1^2,\ C_2 = B_2^2,\ C_3 = 2B_1B_2,\ C_4 = 2B_1,$$
$$C_5 = 2B_2 \text{ and } C_6 = 1.$$

The subsidiary functions $g_n(Y)$ and $f_n(Y)$ are:

$$4M^2 g_1 = \cosh 2M(Y-1) - 2\cosh 2M(Y - \tfrac{1}{2}) + \cosh 2MY - (\cosh 2M - 2\cosh M + 1), \tag{2.20}$$

$$12M^4 f_1 = 4M^2 g_1 + \left\{\sinh M + \frac{3M(\cosh 2M - 2\cosh M + 1)}{2(\cosh M - 1)}\right\} S_0(M, Y), \tag{2.21}$$

$$4M^2 g_2 = \cosh 2M(Y-1) + 2\cosh 2M(Y - \tfrac{1}{2}) + \cosh 2MY - (\cosh 2M + 2\cosh M + 1), \tag{2.22}$$

$$12M^4 f_2 = 4M^2 g_2 + \left\{\sinh M \frac{(\cosh M + 1)}{(\cosh M - 1)} + \frac{3M(\cosh 2M + 2\cosh M + 1)}{2(\cosh M - 1)}\right\} S_0(M, Y), \tag{2.23}$$

$$4M^2 g_3 = (1 - 2Y)(1 - \cosh 2M) + \cosh 2M(Y-1) - \cosh 2MY, \tag{2.24}$$

$$12M^4 f_3 = 4M^2 g_3 - 4(1 - \cosh 2M)\left\{\frac{(\cosh M + 1)}{\sinh M}\sinh MY - \cosh MY + 1 - 2Y\right\} \tag{2.25}$$

$$M^2 g_4 = M\left[\left(b_0 + \frac{2b_2}{M^2}\right)\sinh M + (b_1 + b_2)Y\sinh M + \left\{b_0 + \frac{2b_2}{M^2} + b_1 Y + b_2 Y^2\right\} S_2(M, Y)\right] + b_1(\cosh M - 1) - 2(b_1 - b_2)(\cosh M - 1)Y - (b_1 + 2b_2 Y)C_0(M, Y), \tag{2.26}$$

$$M^2 g_5 = M\left[\left(b_0 + \frac{2b_2}{M^2}\right)\sinh M + Y\left(b_1 + b_2 - \frac{8b_2}{M^2}\right)\sinh M + \left\{b_0 + \frac{2b_2}{M^2} + b_1 Y + b_2 Y^2\right\} S_3(M, Y)\right] + b_1(\cosh M + 1) + 2b_2(\cosh M + 1)Y - (b_1 + 2b_2 Y)C_1(M, Y). \tag{2.27}$$

Vol. 3 1961

$$
\begin{aligned}
12Mf_p = {} & \frac{12M}{\sinh M}\left[\frac{2-2\cosh M+M\sinh M}{2(1-\cosh M)M^2}\left(b_0+\frac{b_1}{2}\right)-\frac{b_0}{M^2}\right]S_0(M,\,Y)\\
& +\frac{12b_1}{M}\left[\frac{\sinh MY}{\sinh M}-Y\right]+\left[\frac{3\delta(b_3+b_4)}{2M}-\left(3b_5+\tfrac{3}{2}b_3+b_4+\frac{3b_4}{2M^2}\right)\left(\frac{1+\delta\cosh M}{\sinh M}\right)\right.\\
& +\left\{\delta\left(6b_5+2b_4+3b_3+\frac{1}{M^2}(9b_3+21b_4)\right)+\frac{9}{M^2}b_3\right\}\frac{\sinh M}{2(\cosh M-1)}\\
& +\left(6b_5+\frac{21b_4}{M^2}\right)\frac{\cosh M+\delta}{2M(\cosh M-1)}-\left(6b_5+9b_4+9b_3+\frac{21b_4}{M^2}\right)\frac{1+\delta\cosh M}{2M(\cosh M-1)}\Big]\\
& \times\frac{S_0(M,\,Y)}{\sinh M}+\left[\frac{3\delta}{M}(b_3+b_4)+\left(6b_5+3b_3+2b_4+\frac{3b_4}{M^2}\right)\frac{1+\delta\cosh M}{\sinh M}\right]\sinh MY\\
& +\left[\left(6b_5+\frac{3b_4}{M^2}\right)Y+3b_3Y^2+2b_4Y^3\right][\cosh M(Y-1)+\delta\cosh MY]-\\
& -\frac{3}{M}[b_3Y+b_4Y^2][\sinh M(Y-1)+\delta\sinh MY]+3\left\{\frac{b_7}{2M}\,\frac{1+\delta\cosh M}{\sinh M}\right.\\
& -\frac{\delta}{2}(2b_6+b_7)-[\delta(2b_6+3b_7)-2b_6]\frac{\sinh M}{2M(\cosh M-1)}\\
& -\left(1+\frac{2}{M^2}\right)b_7\frac{\cosh M+\delta}{2M^2(\cosh M-1)}+\left(2b_6+b_7+\frac{b_7}{M}+\frac{2b_7}{M^2}\right)\frac{1+\delta\cosh M}{2(\cosh M-1)}\Big\}S_0(M,\,Y)\\
& +3\left[b_7\frac{(1+\delta\cosh M)}{\sinh M}-\delta(2b_6+b_7)\right]\sinh MY+3[2b_6Y+b_7Y^2]\,[\sinh M(Y-1)\\
& +\delta\sinh MY]-\frac{3b_7}{M}\,Y[\cosh M(Y-1)+\delta\cosh MY],
\end{aligned}
\tag{2.28}
$$

$$
g_6=\sum_{r=0}^{4}d_rY^{r+2}-Y\sum_{r=0}^{4}d_r,
\tag{2.29}
$$

$$
\begin{aligned}
f_6 = {} & \left[-\frac{1}{M^2\sinh M}\left\{(3d_1+6d_2+10d_3+15d_4+)\,\frac{1}{M^2}\left(60d_3+180d_4\right)\right\}\right.\\
& +\frac{M}{2(\cosh M-1)}\left\{(-\tfrac{1}{6}d_0+\tfrac{1}{4}d_1+\tfrac{3}{10}d_2+\tfrac{1}{3}d_3+\tfrac{5}{14}d_4)\right.\\
& +\frac{1}{M^2}(2d_0+3d_1+4d_2+5d_3+6d_4)+\frac{1}{M^4}(24d_2+60d_3+120d_4)\\
& \left.\left.+\frac{720d_4}{M^6}\right\}\right]S_0(M,\,Y)+\frac{1}{M^2\sinh M}\left[(6d_1+12d_2+20d_3+30d_4)\right.\\
& \left.+\frac{1}{M^2}(120d_3+360d_4)\right]\sinh MY+Y\left(\sum_{r=0}^{4}d_r-\frac{6d_1}{M^2}-\frac{120d_3}{M^4}\right)\\
& -Y^2\left(d_0+\frac{12d_2}{M^2}+\frac{360d_4}{M^4}\right)-Y^3\left(d_1+\frac{20d_3}{M^2}\right)-d_3Y^4-d_4Y^5.
\end{aligned}
\tag{2.30}
$$

Here $S_2(M, Y) = \sinh M(Y-1) - \sinh MY$, $S_3(M, Y) = \sinh M(Y-1) + \sinh MY$, $C_0(M, Y) = \cosh M(Y-1) - \cosh MY$, $C_1(M, Y) = \cosh M(Y-1) + \cosh MY$; in equations (2.27) $\delta = -1$ when $p = 4$ and $\delta = +1$ when $p = 5$, and the constants b_r are

$$b_0 = 1 - \frac{a}{M^2}, \; b_3 = \frac{b_1}{M}, \; b_4 = \frac{b_2}{M^2},$$

$$b_5 = \frac{1}{M}\left(b_0 + \frac{2b_2}{M^2}\right), \; b_6 = -\frac{b_1}{M^2}$$

and $$b_7 = -\frac{2b_2}{M^2}.$$

Finally in equations (2.28) and (2.29) the constants d_r are

$$d_0 = \tfrac{1}{2}(b_1^2 + M^2 b_0), \; d_1 = \tfrac{1}{3} b_1(b_2 + M^2 b_0),$$

$$d_2 = \tfrac{1}{12}\{4b_2^2 + M^2(2b_0 b_2 + b_1^2)\},$$

$$d_3 = \tfrac{1}{10} M^2 b_1 b_2 \text{ and } d_4 = \tfrac{1}{30} M^2 b_2^2.$$

The zeroth and first-order functions have been calculated from equations (2.17) to (2.30) for the following cases: $M = 0$, 2, 4 and 10, $a = 0$, 10, and 100 and $\lambda = -1(1)2$. These are tabulated at an interval of $Y = 0{\cdot}2$ in Tables 2 and 3. Note that in these tables and in all succeeding tables the figure in parenthesis, say n, denotes a multiplying factor of 10^{-n}.

2(c) *Flow and heat transfer characteristics*

From section 2(b) quantitative information may now be deduced for flow and heat transfer characteristics such as the net mass flow, the induced magnetic flux density, and the heat transfer coefficients at the wall.

(i) *Net mass flow.* The net mass flow per sec per unit breadth of wall in the z-direction when the isothermal walls are a distance a cm apart is given by

$$\bar{q} = \mu \bar{U}/PK_A \qquad (2.31a)$$

where on using (2.14) we obtain

$$\bar{U} = K\int_0^1 U_0 \mathrm{d}Y + K^2 \int_0^1 U_1 \mathrm{d}Y + 0(K^3). \quad (2.31b)$$

These integrals have already been evaluated in the determination of U_0 and U_1 and are tabulated in Table 4 for $a = 0$, 10 and 100, $\lambda = -1(1)2$ and $M = 0$, 2, 4, 10, 20, 40, 100 and 200.

(ii) *Induced magnetic flux density.* From Ohm's law as stated in equation (2.3) together with expressions (2.7), (2.10) and (2.14) the induced magnetic flux density $B_x = \mu_e H_x$ is evaluated to be

$$B_x = B_0 G_M \left[\int_0^Y (\bar{U}_0 - U_0)\mathrm{d}Y + K\int_0^Y (\bar{U}_1 - U_1)\mathrm{d}Y + 0(K^2)\right]. \quad (2.32)$$

Here $G_M = 4\pi\sigma\mu_e \nu G$ is the magnetic Grashof number and is the natural convection flow equivalent of the magnetic Reynolds number. The magnitude of B_x can then be calculated using equation (2.31) and Tables 2–4.

(iii) *Heat transfer coefficients.* The heat transfer coefficients at the wall can be expressed in the usual fashion by dimensionless Nusselt numbers. For the case when the walls are not at the same temperature i.e. $\lambda = 1$ then at the wall $y = 0$

$$Nu_0 = \left(\frac{\mathrm{d}T}{\mathrm{d}y}\right)_{y=0} \frac{a}{(T_{w1} - T_{w0})} = \frac{1}{(\lambda - 1)K}\left(\frac{\partial \Theta}{\partial Y}\right)_{Y=0}, \quad (2.33)$$

and at the wall $y = a$

$$Nu_1 = \left(\frac{\mathrm{d}T}{\mathrm{d}y}\right)_{y=a} \frac{a}{(T_{w1} - T_{w0})} = \frac{1}{(\lambda - 1)K}\left(\frac{\partial \Theta}{\partial Y}\right)_{Y=1}. \quad (2.34)$$

When the series expansion for Θ given by equations (2.14), (2.17) and (2.19) is substituted

Table 2

	u_0, $\alpha = 0$, $\lambda = 2$				u_1, $\alpha = 0$, $\lambda = 2$			
y	$M = 0$	$M = 2$	$M = 4$	$M = 10$	$M = 0$	$M = 2$	$M = 4$	$M = 10$
0·0	0	0	0	0	0	0	0	0
0·2	1·12 (−1)	1·07 (−1)	9·51 (−2)	6·25 (−2)	8·47 (−4)	7·23 (−4)	4·89 (−4)	1·25 (−4)
0·4	1·76 (−1)	1·63 (−1)	1·36 (−1)	7·25 (−2)	1·32 (−3)	1·10 (−3)	7·01 (−4)	1·44 (−4)
0·6	1·84 (−1)	1·70 (−1)	1·41 (−1)	7·44 (−2)	1·32 (−3)	1·10 (−3)	7·03 (−4)	1·44 (−4)
0·8	1·28 (−1)	1·21 (−1)	1·07 (−1)	6·71 (−2)	8·57 (−4)	7·31 (−4)	4·95 (−4)	1·23 (−4)
1·0	0	0	0	0	0	0	0	0

	u_0, $\alpha = 0$, $\lambda = 1$				u_1, $\alpha = 0$, $\lambda = 1$			
y	$M = 0$	$M = 2$	$M = 4$	$M = 10$	$M = 0$	$M = 2$	$M = 4$	$M = 10$
0·0	0	0	0	0	0	0	0	0
0·2	8·00 (−2)	7·61 (−2)	6·73 (−2)	4·32 (−2)	3·75 (−4)	3·20 (−4)	2·17 (−4)	5·4 (−5)
0·4	1·20 (−1)	1·11 (−1)	9·24 (−2)	4·90 (−2)	5·82 (−4)	4·85 (−4)	3·09 (−4)	6·3 (−5)
0·6	1·20 (−1)	1·11 (−1)	9·24 (−2)	4·90 (−2)	5·82 (−4)	4·85 (−4)	3·09 (−4)	6·3 (−5)
0·8	8·00 (−2)	7·61 (−2)	6·73 (−2)	4·32 (−2)	3·75 (−4)	3·20 (−4)	2·17 (−4)	5·4 (−5)
1·0	0	0	0	0	0	0	0	0

	u_0, $\alpha = 0$, $\lambda = 0$				u_1, $\alpha = 0$, $\lambda = 0$			
y	$M = 0$	$M = 2$	$M = 4$	$M = 10$	$M = 0$	$M = 2$	$M = 4$	$M = 10$
0·0	0	0	0	0	0	0	0	0
0·2	4·80 (−2)	4·53 (−2)	3·94 (−2)	2·39 (−2)	1·03 (−4)	8·8 (−5)	6·0 (−5)	2·1 (−5)
0·4	6·40 (−2)	5·92 (−2)	4·89 (−2)	2·54 (−2)	1·58 (−4)	1·32 (−4)	8·5 (−5)	1·7 (−5)
0·6	5·60 (−2)	5·20 (−2)	4·35 (−2)	2·36 (−2)	1·57 (−4)	1·31 (−4)	8·4 (−5)	1·8 (−5)
0·8	3·20 (−2)	3·08 (−2)	2·79 (−2)	1·93 (−2)	1·00 (−4)	8·5 (−5)	5·8 (−5)	1·5 (−5)
1·0	0	0	0	0	0	0	0	0

	u_0, $\alpha = 0$, $\lambda = -1$				u_1, $\alpha = 0$, $\lambda = -1$			
y	$M = 0$	$M = 2$	$M = 4$	$M = 10$	$M = 0$	$M = 2$	$M = 4$	$M = 10$
0·0	0	0	0	0	0	0	0	0
0·2	1·60 (−2)	1·46 (−2)	1·15 (−2)	4·65 (−3)	3·1 (−5)	2·6 (−5)	1·9 (−5)	9·0 (−6)
0·4	8·0 (−3)	7·17 (−3)	5·42 (−3)	1·84 (−3)	4·9 (−5)	4·2 (−5)	2·8 (−5)	1·1 (−5)
0·6	−8·0 (−3)	−7·17 (−3)	−5·42 (−3)	−1·84 (−3)	4·9 (−5)	4·2 (−5)	2·8 (−5)	1·1 (−5)
0·8	−1·60 (−2)	−1·46 (−2)	−1·15 (−2)	−4·65 (−3)	3·1 (−5)	2·6 (−5)	1·9 (−5)	9·0 (−6)
1·0	0	0	0	0	0	0	0	0

Vol 3 196

Table 2 (contd.)

	u_0, $\alpha = 10$, $\lambda = 2$				u_1, $\alpha = 10$, $\lambda = 2$			
y	$M = 0$	$M = 2$	$M = 4$	$M = 10$	$M = 0$	$M = 2$	$M = 4$	$M = 10$
0·0	0	0	0	0	0	0	0	0
0·2	1·89 (−1)	1·80 (−1)	1·59 (−1)	1·02 (−1)	2·49 (−3)	2·12 (−3)	1·43 (−3)	3·51 (−4)
0·4	3·00 (−1)	2·78 (−1)	2·30 (−1)	1·20 (−1)	3·88 (−3)	3·23 (−3)	2·05 (−3)	4·18 (−4)
0·6	3·08 (−1)	2·85 (−1)	2·36 (−1)	1·22 (−1)	3·88 (−3)	3·23 (−3)	2·05 (−3)	4·11 (−4)
0·8	2·05 (−1)	1·95 (−1)	1·71 (−1)	1·07 (−1)	2·51 (−3)	2·13 (−3)	1·44 (−3)	3·50 (−4)
1·0	0	0	0	0	0	0	0	0

	u_0, $\alpha = 10$, $\lambda = 1$				u_1, $\alpha = 10$, $\lambda = 1$			
y	$M = 0$	$M = 2$	$M = 4$	$M = 10$	$M = 0$	$M = 2$	$M = 4$	$M = 10$
0·0	0	0	0	0	0	0	0	0
0·2	1·57 (−1)	1·49 (−1)	1·31 (−1)	8·29 (−2)	1·62 (−3)	1·38 (−3)	9·26 (−4)	2·21 (−4)
0·4	2·44 (−1)	2·26 (−1)	1·87 (−1)	9·69 (−2)	2·52 (−3)	2·09 (−3)	1·32 (−3)	2·64 (−4)
0·6	2·44 (−1)	2·26 (−1)	1·87 (−1)	9·69 (−2)	2·52 (−3)	2·09 (−3)	1·32 (−3)	2·64 (−4)
0·8	1·57 (−1)	1·49 (−1)	1·31 (−1)	8·29 (−2)	1·62 (−3)	1·38 (−3)	9·26 (−4)	2·22 (−4)
1·0	0	0	0	0	0	0	0	0

	u_0, $\alpha = 10$, $\lambda = 0$				u_1, $\alpha = 10$, $\lambda = 0$			
y	$M = 0$	$M = 2$	$M = 4$	$M = 10$	$M = 0$	$M = 2$	$M = 4$	$M = 10$
0·0	0	0	0	0	0	0	0	0
0·2	1·25 (−1)	1·19 (−1)	1·03 (−1)	6·36 (−2)	9·46 (−4)	8·05 (−4)	5·40 (−4)	1·30 (−4)
0·4	1·88 (−1)	1·74 (−1)	1·43 (−1)	7·33 (−2)	1·47 (−3)	1·22 (−3)	7·71 (−4)	1·56 (−4)
0·6	1·80 (−1)	1·67 (−1)	1·38 (−1)	7·15 (−2)	1·46 (−3)	1·22 (−3)	7·70 (−4)	1·53 (−4)
0·8	1·09 (−1)	1·04 (−1)	9·19 (−2)	5·90 (−2)	9·38 (−4)	7·98 (−4)	5·36 (−4)	1·29 (−4)
1·0	0	0	0	0	0	0	0	0

	u_0, $\alpha = 10$, $\lambda = -1$				u_1, $\alpha = 10$, $\lambda = -1$			
y	$M = 0$	$M = 2$	$M = 4$	$M = 10$	$M = 0$	$M = 2$	$M = 4$	$M = 10$
0	0	0	0	0	0	0	0	0
0·2	9·33 (−2)	8·78 (−2)	7·55 (−2)	4·43 (−2)	4·73 (−4)	4·03 (−4)	2·70 (−4)	6·4 (−5)
0·4	1·32 (−1)	1·22 (−1)	9·97 (−2)	4·97 (−2)	7·31 (−4)	6·09 (−4)	3·85 (−4)	7·6 (−5)
0·6	1·16 (−1)	1·07 (−1)	8·88 (−2)	4·61 (−2)	7·29 (−4)	6·06 (−4)	3·83 (−4)	7·5 (−5)
0·8	6·13 (−2)	5·86 (−2)	5·25 (−2)	3·50 (−2)	4·63 (−4)	3·95 (−4)	2·65 (−4)	6·3 (−5)
1·0	0	0	0	0	0	0	0	0

Vol. 3 1961

Table 2 (contd.)

	u_0, $\alpha = 100$, $\lambda = 2$				u_1, $\alpha = 100$, $\lambda = 2$			
y	$M = 0$	$M = 2$	$M = 4$	$M = 10$	$M = 0$	$M = 2$	$M = 4$	$M = 10$
0·0	0	0	0	0	0	0	0	0
0·2	8·85 (−1)	8·39 (−1)	7·35 (−1)	4·59 (−1)	5·67 (−2)	4·82 (−2)	3·22 (−2)	7·63 (−3)
0·4	1·42	1·31	1·08	5·52 (−1)	8·82 (−2)	7·32 (−2)	4·62 (−2)	9·02 (−3)
0·6	1·42	1·32	1·08	5·53 (−1)	8·82 (−2)	7·32 (−2)	4·62 (−2)	9·03 (−3)
0·8	9·01 (−1)	8·53 (−1)	7·47 (−1)	4·64 (−1)	5·67 (−2)	4·82 (−2)	3·23 (−2)	7·63 (−3)
1·0	0	0	0	0	0	0	0	0

	u_0, $\alpha = 100$, $\lambda = 1$				u_1, $\alpha = 100$, $\lambda = 1$			
y	$M = 0$	$M = 2$	$M = 4$	$M = 10$	$M = 0$	$M = 2$	$M = 4$	$M = 10$
0·0	0	0	0	0	0	0	0	0
0·2	8·53 (−1)	8·08 (−1)	7·07 (−1)	4·40 (−1)	5·22 (−2)	4·44 (−2)	2·97 (−2)	7·01 (−3)
0·4	1·36	1·26	1·03	5·28 (−1)	8·12 (−2)	6·74 (−2)	4·25 (−2)	8·29 (−3)
0·6	1·36	1·26	1·03	5·28 (−1)	8·12 (−2)	6·74 (−2)	4·25 (−2)	8·29 (−3)
0·8	8·53 (−1)	8·08 (−1)	7·07 (−1)	4·40 (−1)	5·22 (−2)	4·44 (−2)	2·97 (−2)	7·01 (−3)
1·0	0	0	0	0	0	0	0	0

	u_0, $\alpha = 100$, $\lambda = 0$				u_1, $\alpha = 100$, $\lambda = 0$			
y	$M = 0$	$M = 2$	$M = 4$	$M = 10$	$M = 0$	$M = 2$	$M = 4$	$M = 10$
0·0	0	0	0	0	0	0	0	0
0·2	8·21 (−1)	7·77 (−1)	6·79 (−1)	4·21 (−1)	4·79 (−2)	4·07 (−2)	2·72 (−2)	6·41 (−3)
0·4	1·30	1·20	9·91 (−1)	5·04 (−1)	7·45 (−2)	6·19 (−2)	3·90 (−2)	7·59 (−3)
0·6	1·30	1·20	9·86 (−1)	5·03 (−1)	7·45 (−2)	6·19 (−2)	3·90 (−2)	7·59 (−3)
0·8	8·05 (−1)	7·63 (−1)	6·68 (−1)	4·16 (−1)	4·78 (−2)	4·07 (−2)	2·72 (−2)	6·41 (−3)
1·0	0	0	0	0	0	0	0	0

	u_0, $\alpha = 100$, $\lambda = -1$				u_1, $\alpha = 100$, $\lambda = -1$			
y	$M = 0$	$M = 2$	$M = 4$	$M = 10$	$M = 0$	$M = 2$	$M = 4$	$M = 10$
0·0	0	0	0	0	0	0	0	0
0·2	7·89 (−1)	7·47 (−1)	6·52 (−1)	4·02 (−1)	4·38 (−2)	3·72 (−2)	2·49 (−2)	5·85 (−3)
0·4	1·25	1·15	9·48 (−1)	4·81 (−1)	6·81 (−2)	5·66 (−2)	3·57 (−2)	6·92 (−3)
0·6	1·23	1·14	9·37 (−1)	4·77 (−1)	6·81 (−2)	5·65 (−2)	3·56 (−2)	6·92 (−3)
0·8	7·57 (−1)	7·17 (−1)	6·29 (−1)	3·92 (−1)	4·37 (−2)	3·71 (−2)	2·48 (−2)	5·84 (−3)
1·0	0	0	0	0	0	0	0	0

Vol 3 196

Table 3

	Θ_0, $\alpha = 0$				Θ_0, $\alpha = 10$				Θ_0, $\alpha = 100$			
y	$\lambda = 2$	$\lambda = 1$	$\lambda = 0$	$\lambda = -1$	$\lambda = 2$	$\lambda = 1$	$\lambda = 0$	$\lambda = -1$	$\lambda = 2$	$\lambda = 1$	$\lambda = 0$	$\lambda = -1$
0·0	1·0	1·0	1·0	1·0	1·0	1·0	1·0	1·0	1·0	1·0	1·0	1·0
0·2	1·2	1·0	0·8	0·6	2·0	1·8	1·6	1·4	9·2	9·0	8·8	8·6
0·4	1·4	1·0	0·6	0·2	2·6	2·2	1·8	1·4	13·4	13·0	12·6	12·2
0·6	1·6	1·0	0·4	−0·2	2·8	2·2	1·6	1·0	13·6	13·0	12·4	11·8
0·8	1·8	1·0	0·2	−0·6	2·6	1·8	1·0	0·2	9·8	9·0	8·2	7·4
1·0	2·0	1·0	0	−1·0	2·0	1·0	0	−1·0	2·0	1·0	0	−1·0

	Θ_1, $\alpha = 0$, $\lambda = 2$				Θ_1, $\alpha = 0$, $\lambda = 1$			
y	$M = 0$	$M = 2$	$M = 4$	$M = 10$	$M = 0$	$M = 2$	$M = 4$	$M = 10$
0·0	0	0	0	0	0	0	0	0
0·2	1·01 (−2)	8·97 (−3)	6·78 (−3)	2·57 (−3)	4·53 (−3)	4·04 (−3)	3·05 (−3)	1·16 (−3)
0·4	1·19 (−2)	1·07 (−2)	8·29 (−3)	3·30 (−3)	5·20 (−3)	4·70 (−3)	3·66 (−3)	1·47 (−3)
0·6	1·18 (−2)	1·07 (−2)	8·36 (−3)	3·39 (−3)	5·20 (−3)	4·70 (−3)	3·66 (−3)	1·47 (−3)
0·8	1·05 (−2)	9·36 (−3)	7·07 (−3)	2·71 (−3)	4·53 (−3)	4·04 (−3)	3·05 (−3)	1·16 (−3)
1·0	0	0	0	0	0	0	0	0

	Θ_1, $\alpha = 0$, $\lambda = 0$				Θ_1, $\alpha = 0$, $\lambda = -1$			
y	$M = 0$	$M = 2$	$M = 4$	$M = 10$	$M = 0$	$M = 2$	$M = 4$	$M = 10$
0·0	0	0	0	0	0	0	0	0
0·2	1·28 (−3)	1·14 (−3)	8·71 (−4)	3·42 (−4)	2·97 (−4)	2·80 (−4)	2·38 (−4)	1·13 (−4)
0·4	1·41 (−3)	1·28 (−3)	1·02 (−3)	4·20 (−4)	4·87 (−4)	4·46 (−4)	3·55 (−4)	1·46 (−4)
0·6	1·43 (−3)	1·29 (−3)	9·92 (−4)	3·88 (−4)	4·87 (−4)	4·46 (−4)	3·55 (−4)	1·46 (−4)
0·8	1·13 (−3)	1·01 (−3)	7·74 (−4)	2·96 (−4)	2·97 (−4)	2·80 (−4)	2·38 (−4)	1·13 (−4)
1·0	0	0	0	0	0	0	0	0

	Θ_1, $\alpha = 10$, $\lambda = 2$				Θ_1, $\alpha = 10$, $\lambda = 1$			
y	$M = 0$	$M = 2$	$M = 4$	$M = 10$	$M = 0$	$M = 2$	$M = 4$	$M = 10$
0·0	0	0	0	0	0	0	0	0
0·2	2·96 (−2)	2·64 (−2)	1·98 (−2)	7·34 (−3)	1·94 (−2)	1·73 (−2)	1·29 (−2)	4·77 (−3)
0·4	3·49 (−2)	3·15 (−2)	2·44 (−2)	9·52 (−3)	2·26 (−2)	2·04 (−2)	1·58 (−2)	6·19 (−3)
0·6	3·48 (−2)	3·15 (−2)	2·45 (−2)	9·67 (−3)	2·26 (−2)	2·04 (−2)	1·58 (−2)	6·19 (−3)
0·8	3·03 (−2)	2·70 (−2)	2·03 (−2)	7·54 (−3)	1·94 (−2)	1·73 (−2)	1·29 (−2)	4·77 (−3)
1·0	0	0	0	0	0	0	0	0

Vol. 3 1961

Table 3 (*contd.*)

	Θ_1, $\alpha = 10$, $\lambda = 0$				Θ_1, $\alpha = 10$, $\lambda = 1$			
y	$M = 0$	$M = 2$	$M = 4$	$M = 10$	$M = 0$	$M = 2$	$M = 4$	$M = 10$
0·0	0	0	0	0	0	0	0	0
0·2	1·14 (−2)	1·02 (−2)	7·62 (−3)	2·80 (−3)	5·75 (−3)	5·11 (−3)	3·83 (−3)	1·41 (−3)
0·4	1·31 (−2)	1·19 (−2)	9·23 (−3)	3·62 (−3)	6·55 (−3)	5·94 (−3)	4·65 (−3)	1·84 (−3)
0·6	1·33 (−2)	1·19 (−2)	9·19 (−3)	3·54 (−3)	6·73 (−3)	6·04 (−3)	4·61 (−3)	1·73 (−3)
0·8	1·11 (−2)	9·83 (−3)	7·37 (−3)	2·69 (−3)	5·26 (−3)	4·69 (−3)	3·54 (−3)	1·29 (−3)
1·0	0	0	0	0	0	0	0	0

	Θ_1, $\alpha = 100$, $\lambda = 2$				Θ_1, $\alpha = 100$, $\lambda = 1$			
y	$M = 0$	$M = 2$	$M = 4$	$M = 10$	$M = 0$	$M = 2$	$M = 4$	$M = 10$
0·0	0	0	0	0	0	0	0	0
0·2	6·74 (−1)	5·99 (−1)	4·47 (−1)	1·61 (−1)	6·22 (−1)	5·52 (−1)	4·12 (−1)	1·48 (−1)
0·4	7·96 (−1)	7·18 (−1)	5·54 (−1)	2·13 (−1)	7·33 (−1)	6·61 (−1)	5·10 (−1)	1·96 (−1)
0·6	7·95 (−1)	7·17 (−1)	5·54 (−1)	2·14 (−1)	7·33 (−1)	6·61 (−1)	5·10 (−1)	1·96 (−1)
0·8	6·77 (−1)	6·01 (−1)	4·49 (−1)	1·62 (−1)	6·22 (−1)	5·52 (−1)	4·12 (−1)	1·48 (−1)
1·0	0	0	0	0	0	0	0	0

	Θ_1, $\alpha = 100$, $\lambda = 0$				Θ_1, $\alpha = 100$, $\lambda = -1$			
y	$M = 0$	$M = 2$	$M = 4$	$M = 10$	$M = 0$	$M = 2$	$M = 4$	$M = 10$
0·0	0	0	0	0	0	0	0	0
0·2	5·71 (−1)	5·07 (−1)	3·78 (−1)	1·36 (−1)	5·23 (−1)	4·64 (−1)	3·46 (−1)	1·24 (−1)
0·4	6·72 (−1)	6·06 (−1)	4·68 (−1)	1·80 (−1)	6·14 (−1)	5·54 (−1)	4·28 (−1)	1·65 (−1)
0·6	6·73 (−1)	6·07 (−1)	4·68 (−1)	1·79 (−1)	6·16 (−1)	5·55 (−1)	4·28 (−1)	1·64 (−1)
0·8	5·69 (−1)	5·05 (−1)	3·77 (−1)	1·35 (−1)	5·18 (−1)	4·60 (−1)	3·43 (−1)	1·14 (−1)
1·0	0	0	0	0	0	0	0	0

Vol. 3 1961

Table 4

	$\int_0^1 u_0\,dY$, $\alpha = 0$				$\int_0^1 u_1\,dY$, $\alpha = 0$			
M	$\lambda = 2$	$\lambda = 1$	$\lambda = 0$	$\lambda = -1$	$\lambda = 2$	$\lambda = 1$	$\lambda = 0$	$\lambda = -1$
0	1·25 (−1)	8·33 (−2)	4·17 (−2)	0	9·01 (−4)	3·97 (−4)	1·07 (−4)	3·31 (−5)
2	1·17 (−1)	7·83 (−2)	3·91 (−2)	0	7·60 (−4)	3·35 (−4)	9·1 (−5)	2·9 (−5)
4	1·01 (−1)	6·72 (−2)	3·36 (−2)	0	5·00 (−4)	2·20 (−4)	6·0 (−5)	2·0 (−5)
10	6·00 (−2)	4·00 (−2)	2·00 (−2)	0	1·15 (−4)	5·1 (−5)	1·4 (−5)	5·0 (−6)
20	3·37 (−2)	2·25 (−2)	1·12 (−2)	0	2·1 (−5)	9·0 (−6)	3·0 (−6)	1·0 (−6)
40	1·78 (−2)	1·19 (−2)	5·94 (−3)	0	3·0 (−6)	1·0 (−6)	0	0
100	7·35 (−3)	4·90 (−3)	2·45 (−3)	0	—	—	—	—
200	3·71 (−3)	2·47 (−3)	1·24 (−3)	0	—	—	—	—

	$\int_0^1 u_0\,dY$, $\alpha = 10$				$\int_0^1 u_1\,dY$, $\alpha = 10$			
M	$\lambda = 2$	$\lambda = 1$	$\lambda = 0$	$\lambda = -1$	$\lambda = 2$	$\lambda = 1$	$\lambda = 0$	$\lambda = -1$
0	2·08 (−1)	1·67 (−1)	1·25 (−1)	8·33 (−2)	2·65 (−3)	1·71 (−3)	9·98 (−4)	4·97 (−4)
2	1·95 (−1)	1·56 (−1)	1·17 (−1)	7·79 (−2)	2·23 (−3)	1·44 (−3)	8·40 (−4)	4·18 (−4)
4	1·67 (−1)	1·33 (−1)	9·97 (−2)	6·61 (−2)	1·46 (−3)	9·42 (−4)	5·47 (−4)	2·73 (−4)
10	9·77 (−2)	7·77 (−2)	5·77 (−2)	3·77 (−2)	3·27 (−4)	2·10 (−4)	1·21 (−4)	6·0 (−5)
20	5·40 (−2)	4·28 (−2)	3·15 (−2)	2·03 (−2)	5·7 (−5)	3·6 (−5)	2·1 (−5)	1·0 (−5)
40	2·82 (−2)	2·22 (−2)	1·63 (−2)	1·03 (−2)	8·0 (−6)	5·0 (−6)	3·0 (−6)	1·0 (−6)
100	1·15 (−2)	9·06 (−3)	6·61 (−3)	4·16 (−3)	—	—	—	—
200	5·79 (−3)	4·56 (−3)	3·32 (−3)	2·08 (−3)	—	—	—	—

	$\int_0^1 u_0\,dY$, $\alpha = 100$				$\int_0^1 u_1\,dY$, $\alpha = 100$			
M	$\lambda = 2$	$\lambda = 1$	$\lambda = 0$	$\lambda = -1$	$\lambda = 2$	$\lambda = 1$	$\lambda = 0$	$\lambda = -1$
0	9·58 (−1)	9·17 (−1)	8·75 (−1)	8·33 (−1)	6·01 (−2)	5·53 (−2)	5·07 (−2)	4·64 (−2)
2	8·96 (−1)	8·57 (−1)	8·18 (−1)	7·79 (−1)	5·05 (−2)	4·65 (−2)	4·27 (−2)	3·90 (−2)
4	7·62 (−1)	7·28 (−1)	6·94 (−1)	6·61 (−1)	3·28 (−2)	3·02 (−2)	2·77 (−2)	2·53 (−2)
10	4·37 (−1)	4·17 (−1)	3·97 (−1)	3·77 (−1)	7·18 (−3)	6·60 (−3)	6·04 (−3)	5·50 (−3)
20	2·36 (−1)	2·25 (−1)	2·14 (−1)	2·03 (−1)	1·15 (−3)	1·05 (−3)	9·57 (−4)	8·68 (−4)
40	1·21 (−1)	1·15 (−1)	1·09 (−1)	1·03 (−1)	1·71 (−4)	1·57 (−4)	1·42 (−4)	1·29 (−4)
100	4·90 (−2)	4·65 (−2)	4·41 (−2)	4·16 (−2)	—	—	—	—
200	2·45 (−2)	2·33 (−2)	2·21 (−2)	2·08 (−2)	—	—	—	—

into equations (2.33) and (2.34) the following expressions are obtained:

$$\left.\begin{aligned} Nu_0 = {} & \frac{(\alpha + 2\lambda - 2)}{2(\lambda - 1)} + \frac{K}{(\lambda - 1)}\left[D_0(\alpha, \lambda, M) + (\lambda - 1)\left(\lambda + 3 - \frac{8\alpha}{M^2}\right)\frac{\cosh M + 1}{4M^3 \cosh M}\right. \\ & - D_1(\alpha, \lambda, M) + \frac{1}{240M^2}(\alpha^2 + 8\alpha\lambda + 20\lambda^2 - 8\alpha - 80\lambda - 60) \\ & \left. + \frac{1}{24M^2}(\alpha^2 + 8\alpha\lambda - 12\lambda^2 + 16\alpha - 24\lambda + 36) - \frac{1}{2M^6}(\alpha^2 - 8\alpha\lambda + 8\alpha)\right], \end{aligned}\right\} \quad (2.35)$$

and

$$\left.\begin{aligned} Nu_1 = {} & \frac{(2\lambda - \alpha - 2)}{2(\lambda - 1)} + \frac{K}{\lambda - 1}\left[D_0(\alpha, \lambda, M) + (\lambda - 1)\left(3\lambda + 1 - \frac{8\alpha}{M^2}\right)\frac{\cosh M + 1}{4M^3 \cosh M}\right. \\ & - D_1(\alpha, \lambda, M) - \frac{1}{240M^2}(\alpha^2 - 8\alpha\lambda - 60\lambda^2 + 8\alpha - 80\lambda + 20) \\ & \left. - \frac{1}{24M^2}(\alpha^2 + 8\alpha\lambda - 12\lambda^2 + 16\alpha - 24\lambda + 36) - \frac{1}{2M^6}(\alpha^2 - 8\alpha\lambda + 8\alpha)\right], \end{aligned}\right\} \quad (2.36)$$

where

$$D_0(\alpha, \lambda, M) = \left(6 + 6\lambda + \alpha - \frac{12\alpha}{M^2}\right)^2 \frac{\sinh M}{576M(\cosh M - 1)},$$

and

$$D_1(\alpha, \lambda, M) = (\lambda - 1)\left(6 + 6\lambda + \alpha - \frac{12\alpha}{M^2}\right)\left\{\frac{(M^2 - 4)\sinh 2M + M(\cosh 2M - 1) + 8\sinh M}{48M^4 \sinh M(\cosh M - 1)}\right\}.$$

When the walls are at equal temperature i.e. $\lambda = 1$ the Nusselt number may be defined as

$$\left.\begin{aligned} Nu = Nu_0 = Nu_1 &= \frac{a}{(T_{w0} - T_s)}\left(\frac{\mathrm{d}T}{\mathrm{d}y}\right)_0 \\ &= \frac{1}{K}\left(\frac{\partial \Theta}{\partial Y}\right)_{Y=0} \end{aligned}\right\} \quad (2.37)$$

On using the results of section 2(b) we obtain when $\lambda = 1$,

$$\left.\begin{aligned} Nu = {} & \frac{\alpha}{2} + K\left[D_0(\alpha, 1, M)\right. \\ & + \frac{1}{240M^2}(\alpha^2 - 120) \\ & \left. + \frac{1}{24M^4}\alpha(\alpha + 24) - \frac{\alpha^2}{2M^6}\right]. \end{aligned}\right\} \quad (2.38)$$

The Nusselt number $Nu_{0.1}{}^{(0)}$ due to ordinary conduction and $Nu_{0.1}{}^{(1)}$ due to dissipation effects have been evaluated for $\alpha = 0$, 10 and 100, $\lambda = -1(1)2$ and $M = 0$, 2, 4, 10, 50(50)200 and are given in Table 5. The actual wall Nusselt number is then given by

$$Nu_{0.1} = Nu_{0.1}{}^{(0)} + K \quad Nu_{0.1}{}^{(1)} + 0(K^2). \quad (2.39)$$

2(d) *Discussion*

The velocity and thermal profiles for fully developed flow depend on the four parameters K, α, λ and M. Let us first consider M fixed and examine general trends due to variations in K, α and λ. These are the same as in the magnetic field-free case and have been summarized by Ostrach [1] as follows:

(i) An increase in either the wall temperature difference ratio λ or the heat source parameter α increases the velocity, net mass flow and temperature.

(ii) The viscous dissipation was found to alter appreciably the velocity and temperature profiles in some cases, showing that as K was increased (α and λ remaining fixed) then the velocity was

Vol. 3 1961

Table 5

	$Nu_0^{(0)}$			$Nu_1^{(0)}$		
λ	$\alpha = 0$	$\alpha = 10$	$\alpha = 100$	$\alpha = 0$	$\alpha = 10$	$\alpha = 100$
2	1	6	51	1	4	49
1	0	5	50	0	5	50
0	1	4	49	1	6	51
−1	1	1·5	24	1	3·5	26

	$Nu_0^{(1)}$, $\alpha = 0$				$Nu_1^{(1)}$, $\alpha = 0$			
M	$\lambda = 2$	$\lambda = 1$	$\lambda = 0$	$\lambda = -1$	$\lambda = 2$	$\lambda = 1$	$\lambda = 0$	$\lambda = -1$
0	8·61 (−2)	4·16 (−2)	−1·39 (−2)	−1·39 (−3)	−1·02 (−1)	4·16 (−2)	8·33 (−3)	1·39 (−3)
2	8·14 (−2)	3·91 (−2)	−1·28 (−2)	−1·27 (−3)	−9·59 (−2)	3·91 (−2)	7·99 (−3)	1·27 (−3)
4	7·08 (−2)	3·35 (−2)	−1·07 (−2)	−1·01 (−3)	−8·13 (−2)	3·35 (−2)	7·15 (−3)	1·01 (−3)
10	4·35 (−2)	2·00 (−2)	−5·80 (−3)	−4·35 (−4)	−4·70 (−2)	2·00 (−2)	4·63 (−3)	4·35 (−4)
50	1·07 (−2)	4·80 (−3)	−1·21 (−3)	−2·9 (−4)	−1·09 (−2)	4·80 (−3)	1·18 (−3)	2·9 (−4)
100	5·49 (−3)	2·45 (−3)	−6·24 (−4)	−8·0 (−5)	−5·54 (−3)	2·45 (−3)	6·08 (−4)	8·0 (−5)
200	2·78 (−3)	1·23 (−3)	−3·12 (−4)	−2·0 (−6)	−2·43 (−3)	1·23 (−3)	3·27 (−4)	2·0 (−6)

	$Nu_0^{(1)}$, $\alpha = 10$				$Nu_1^{(1)}$, $\alpha = 10$			
M	$\lambda = 2$	$\lambda = 1$	$\lambda = 0$	$\lambda = -1$	$\lambda = 2$	$\lambda = 1$	$\lambda = 0$	$\lambda = -1$
0	2·48 (−1)	1·67 (−1)	1·03 (−1)	2·74 (−2)	2·75 (−1)	1·67 (−1)	8·72 (−2)	1·75 (−2)
2	2·33 (−1)	1·56 (−1)	9·53 (−2)	2·52 (−2)	2·56 (−1)	1·56 (−1)	8·19 (−2)	1·66 (−2)
4	2·00 (−1)	1·32 (−1)	7·96 (−2)	2·04 (−2)	2·16 (−1)	1·32 (−1)	7·01 (−2)	1·44 (−2)
10	1·17 (−1)	7·56 (−2)	4·27 (−2)	2·53 (−3)	1·22 (−1)	7·56 (−2)	4·06 (−2)	8·54 (−3)
50	2·67 (−2)	1·67 (−3)	9·17 (−3)	1·87 (−3)	2·70 (−2)	1·67 (−3)	8·90 (−3)	2·13 (−3)
100	1·34 (−2)	8·39 (−3)	4·49 (−3)	9·03 (−4)	1·36 (−2)	8·39 (−3)	4·45 (−3)	8·86 (−4)
150	9·03 (−3)	5·60 (−3)	2·98 (−3)	5·95 (−4)	9·06 (−3)	5·60 (−3)	2·97 (−3)	5·88 (−4)
200	6·78 (−3)	4·19 (−3)	2·23 (−3)	4·43 (−4)	6·46 (−3)	4·19 (−3)	2·41 (−3)	5·80 (−4)

	$Nu_0^{(1)}$, $\alpha = 100$				$Nu_1^{(1)}$, $\alpha = 100$			
M	$\lambda = 2$	$\lambda = 1$	$\lambda = 0$	$\lambda = -1$	$\lambda = 2$	$\lambda = 1$	$\lambda = 0$	$\lambda = -1$
0	5·50	5·09	4·70	2·16	5·62	5·09	4·59	2·06
2	5·13	4·74	4·37	2·01	5·23	4·74	4·28	1·92
4	4·32	3·98	3·66	1·68	4·39	3·98	3·60	1·62
10	2·40	2·19	2·00	9·08 (−1)	2·42	2·19	1·98	8·91 (−1)
50	4·95 (−1)	4·48 (−1)	4·04 (−1)	1·81 (−1)	4·96 (−1)	4·48 (−1)	4·02 (−1)	1·80 (−1)
100	2·45 (−1)	2·21 (−1)	1·99 (−1)	8·88 (−2)	2·45 (−1)	2·21 (−1)	1·99 (−1)	8·86 (−2)
150	1·63 (−1)	1·47 (−1)	1·32 (−1)	5·88 (−2)	1·63 (−1)	1·47 (−1)	1·32 (−1)	5·87 (−2)
200	1·22 (−1)	1·10 (−1)	9·85 (−2)	4·39 (−2)	1·30 (−1)	1·10 (−1)	1·08 (−1)	4·91 (−2)

increased and the heat transfer at the wall was greatly changed by this effect.

However when K, α and λ remain fixed and M increases the main feature is a reduction in magnitude of the velocity and temperature. The reason for this is as follows. An increase in M, i.e. the applied magnetic field strength causes greater interaction between the fluid motion and the magnetic field and hence an increase in the Lorentz force. Since this force opposes the buoyancy force the velocity will be decreased leading to a reduction in the viscous and Joulean dissipation and so a reduction in the temperature. The influence of large magnetic field on the net mass flow and heat transfer coefficients is readily seen from Tables 3–4. Thus if $\alpha = 100$, $\lambda = 1$, $K = 10$ and $M = 200$ then $\bar{q}$ is reduced to 2 per cent and Nu to 50 per cent of the magnetic field free case. In particular as $M \to \infty$ then $\bar{q} \to 0$ and the temperature profile tends to the ordinary conduction profile. Note also that when $\lambda = 1$, i.e. equal wall temperatures the velocity profile, evaluated neglecting dissipation effects, is similar to that in the Hartmann–Lazarus flow. Moreover as in the Hartmann–Lazarus flow a fluid boundary layer develops near the wall as M increases, and the velocity is then virtually constant across the gap and varies rapidly to zero near the walls.

It remains now to apply the above results to liquid metals such as mercury and liquid sodium. As an example the following natural convection flow configuration is chosen with mercury as the fluid. The plates, maintained at constant temperature 25°C, are taken to be 1 cm apart and the hydrostatic temperature to be 20°C. Thus $\alpha = 0$, $\lambda = 1$, $a = 1$ and $\theta_w = 5$°C. From Table 1 we obtain $P = 2{\cdot}68\ 10^{-2}$, $K_A = 1{\cdot}28\ 10^{-7}$, $G = 6{\cdot}99\ 10^{5}$ and the applied magnetic flux density $B_0 = 38{\cdot}4\ M$ gauss. Since $K = PG\ K_A = 2{\cdot}4\ 10^{-3}$ dissipation effects will be negligible and so the temperature across the gap will be constant and equal to 25°C. From Table 4 we may obtain the actual average velocity in cm/sec for various B_0. Hence if $B_0 = 0$, $\bar{u} =$ 66 cm/sec; if $B_0 = 76{\cdot}8$ gauss, $\bar{u} = 62$ cm/sec; if $B_0 = 3{\cdot}84\ 10^{2}$ gauss, $\bar{u} = 32$ cm/sec; if $B_0 = 1{\cdot}54\ 10^{3}$ gauss, $\bar{u} = 9$ cm/sec and finally if $B_0 = 7{\cdot}68\ 10^{3}$ gauss, $\bar{u} = 2$ cm/sec. These results imply imply that for mercury a field of order 10^4 gauss is necessary to reduce the flow rate to one per cent of that in the magnetic field free case. When liquid sodium is used as the fluid the field necessary for the same reduction is not quite so large, as shown by the following example. We consider the flow configuration for which $T_s = 200$°C, $\theta_w = 50$°C, $\lambda = 1$ and $a = 1$. From Table 1 $P = 7{\cdot}38\ 10^{-3}$, $K_A = 1{\cdot}61\ 10^{-8}$, $G = 4{\cdot}37\ 10^{5}$, $K = 5{\cdot}295\ 10^{-5}$ and $B_0 = 7{\cdot}84\ M$ gauss. Again from Table 4 if $B_0 = 0$, $\bar{u} = 181$ cm/sec; if $B_0 = 15{\cdot}7$ gauss, $\bar{u} = 170$ cm/sec; if $B_0 = 78{\cdot}4$ gauss, $\bar{u} = 109$ cm/sec; if $B_0 = 3{\cdot}14\ 10^{2}$ gauss, $\bar{u} = 25{\cdot}8$ cm/sec. Furthermore as in the previous example for mercury heat is transferred across the gap by conduction alone, giving $T = 250$°C for $0 \leqslant Y \leqslant 1$.

The induced magnetic flux density B_x is not without interest. Consider the magnitude of B_x for the mercury flow configuration cited above. From Table 1 the magnetic viscosity $\chi = (1/4\pi\sigma\mu_e\nu) = 6{\cdot}74\ 10^{6}$ and so the magnetic Grashof number $G_M = 0{\cdot}104$. If we choose $M = 10$ then the applied magnetic flux density $B_0 = 384$ gauss; from Table 4 if $\alpha = 0$, $\lambda = 1$, $M = 10$ then $\bar{u}_0 = 4\ 10^{-2}$, also $\int_0^Y U_0 \mathrm{d}Y$ may be evaluated by numerical integration at $Y =$ 0(0·2) 1·0 using the values of U_0 given in Table 2. Since $K = 2{\cdot}4\ 10^{-3}$ then from equation (2·32) we obtain that $B_x = 0$, 0·12, 0·04, 0, − 0·04, − 0·12, 0 gauss at $Y = 0(0{\cdot}1)1$ cm. The magnitude of the induced field is thus small in comparison with the applied magnetic field for this particular flow configuration. Moreover in this example B_x is small in comparison with the earth's magnetic field for which $B_x^{(E)} = 0{\cdot}44$ gauss and $B_0^{(E)} = 0{\cdot}17$ gauss approximately in the British Isles.

3. EXAMPLE II: ON THE TWO-DIMENSIONAL NATURAL CONVECTION FLOW DUE TO AN ELECTRIC CURRENT IN A HORIZONTAL CIRCULAR TUBE FILLED WITH AN ELECTRICALLY CONDUCTING VISCOUS FLUID

3(a) *Statement of problem and governing equations*

The special example to be considered is as follows: A long thin walled circular tube (made of

Vol. 3 1961

non-conducting material) is filled with electrically conducting viscous fluid and placed with its axis in a horizontal position. A direct current of mean density J_0 per unit of area flows axially through the tube whose outer surface is maintained at constant temperature T_s, i.e. the temperature of the coolant. Moreover the coolant is assumed to be non-magnetic and a non-conductor. The equations describing the resulting steady two-dimensional natural convection flow for the central portion of the tube (i.e. at sufficient distance from either electrodes at the ends of the tube) are given by equations (1.10) to (1.16) when $Q = 0$.

It is convenient to use cylindrical polar co-ordinates r, ϕ and z. The z axis is taken to be the axis of the cylinder and the angular co-ordinate ϕ is measured from a vertical plane through this axis; the velocity components are denoted by u_r and u_ϕ and the magnetic field components by H_r and H_ϕ. The basic equations (1.10) to (1.16) transformed to cylindrical polar co-ordinates give for the fluid or region (1) the set of equations:

$$\frac{\partial}{\partial r}(ru_r) + \frac{\partial u_\phi}{\partial \phi} = 0, \tag{3.1}$$

$$\left.\begin{aligned} u_r\frac{\partial u_r}{\partial r} + \frac{u_\phi}{r}\frac{\partial u_r}{\partial \phi} - \frac{u_\phi^2}{r} &= -\frac{1}{\rho}\frac{\partial p_d}{\partial r} \\ &\quad + \nu\left(\nabla^2 u_r - \frac{u_r}{r^2} + \frac{2}{r^2}\frac{\partial u_\phi}{\partial \phi}\right). \\ &\quad + \beta g(T - T_s)\cos\phi - \frac{\mu_e}{\rho}J_z H_\phi, \end{aligned}\right\} \tag{3.2}$$

$$\left.\begin{aligned} u_r\frac{\partial u_\phi}{\partial r} + \frac{u_\phi}{r}\frac{\partial u_\phi}{\partial \phi} + \frac{u_r u_\phi}{r} &= -\frac{1}{\rho}\frac{1}{r}\frac{\partial p_d}{\partial \phi} \\ +\nu\left(\nabla^2 u_\phi - \frac{u_\phi}{r^2} + \frac{2}{r^2}\frac{\partial u_r}{\partial \phi}\right) & \\ - \beta g(T - T_s)\sin\phi + \frac{\mu_e}{\rho}J_z H_r, & \end{aligned}\right\} \tag{3.3}$$

$$\frac{\partial}{\partial r}(r\,H_r) + \frac{\partial H_\phi}{\partial \phi} = 0, \tag{3.4}$$

$$J_z = \frac{1}{4\pi}\left(\frac{1}{r}\frac{\partial}{\partial r}(r\,H_\phi) - \frac{1}{r}\frac{\partial H_r}{\partial \phi}\right) = \sigma\{E_0 + \mu_e(u_r H_\phi - u_\phi H_r)\}, \tag{3.5}$$

and the energy equation is

$$\rho c_p\left(u_r\frac{\partial T}{\partial r} + \frac{u_\phi}{r}\frac{\partial T}{\partial \phi}\right) = k\nabla^2 T + \frac{J_z^2}{\sigma} + \Phi', \tag{3.6}$$

where $$\nabla^2 = \frac{\partial^2}{\partial r^2} + \frac{1}{r}\frac{\partial}{\partial r} + \frac{1}{r^2}\frac{\partial^2}{\partial \phi^2}.$$

The viscous dissipation function Φ' takes the form

$$\Phi' = 2\left(\frac{\partial u_r}{\partial r}\right)^2 + 2\left(\frac{1}{r}\frac{\partial u_\phi}{\partial \phi} + \frac{u_r}{r}\right)^2 + \left(\frac{1}{r}\frac{\partial u_r}{\partial \phi} + \frac{\partial u_\phi}{\partial r} - \frac{u_\phi}{r}\right)^2. \tag{3.7}$$

For the coolant or region (2) the relevant equations are:

$$\left.\begin{aligned} &\frac{1}{r}\frac{\partial}{\partial r}(r\,H_\phi) - \frac{1}{r}\frac{\partial H_r}{\partial \phi} = 0 \\ \text{and}\quad &\frac{\partial}{\partial r}(r\,H_r) + \frac{\partial H_\phi}{\partial \phi} = 0 \end{aligned}\right\} \tag{3.8}$$

The boundary conditions are:

$$\left.\begin{aligned} &u_r = u_\phi = 0,\ T = T_s,\ \mu_{1e}H_{1r} = \mu_{2e}H_{2r}, \\ &H_{1\phi} = H_{2\phi} \text{ on } r = a,\ u_r,\ u_\phi,\ T,\ H_r \text{ and} \\ &H_\phi \text{ are finite at } r = 0, \\ &\text{also } H_{2r} \text{ and } H_{2\phi} \to 0 \text{ as } r \to \infty, \end{aligned}\right\} \tag{3.9}$$

where a is the radius of the tube and the suffices refer to the fluid and coolant respectively.

In formulating the boundary conditions (3.9) the thickness of the non-conducting tube wall is assumed to be small in comparison with the radius of the tube and thus there is little variation in H_r and H_ϕ in the wall material and so the usual condition on **H** at the interface can be taken as between fluid and coolant. Furthermore at the interface there can be no normal flow of current, i.e. $J_r = 0$, a condition which is satisfied by this type of two-dimensional solution; also at the interface the tangential component of $E = E_0$ must be continuous implying that in the coolant there is a constant electric field $E_z = E_0$. Note that these boundary conditions on **H** and **E** are identical with those for the Joule heating, by a direct current, of an infinitely long cylindrical wire placed in a non-conducting medium.

On choosing J_0, $4\pi aJ_0$, $(J_0^2a^2/k\sigma)$ and ν/a as units of current, field strength, temperature and velocity respectively then the steady two-dimensional flow may be shown to depend on the following parameters: $\chi = (1/4\pi\sigma\mu_e)$, the magnetic viscosity; $G = (\beta g a^5 J_0^2/k\sigma\nu^2)$, the Grashof number; $P = (\rho c_p \nu/k)$, the Prandtl number; and the dimensionless group $K_A = (\beta g a/c_p)$. Equations (3.1) to (3.9) are thus reduced to non-dimensional form using the following dimensionless independent and dependent variables:

$$\left.\begin{aligned} R = r/a,\ U_R = \frac{au_r}{\nu K},\ U_\phi = \frac{au_\phi}{\nu K},\\ h_R = \frac{H_r}{4\pi aJ_0},\ h_\phi = \frac{H_\phi}{4\pi aJ_0},\\ E_0' = \frac{\sigma E_0}{J_0} \text{ and } \Theta = (T - T_s)\frac{k\sigma}{J_0^2a^2}, \end{aligned}\right\} \quad (3.10)$$

whereas in section (2) $K = PGK_A$.

In region (1) the stream function Ψ and the magnetic vector potential $\mathbf{A} = (0, 0, A)$ are defined by

$$RU_R = \frac{\partial\Psi}{\partial\phi},\ U_\phi = -\frac{\partial\Psi}{\partial R},\ Rh_R = \frac{\partial A}{\partial\phi},$$
$$h_\phi = -\frac{\partial A}{\partial R} \quad (3.11)$$

respectively, then on eliminating the pressure p_d the governing equations become:

$$\nabla^4\Psi + K\frac{\partial(\Psi, \nabla^2\Psi)}{\partial(R, \phi)} = \chi\epsilon^2\frac{\partial(A, \nabla^2A)}{\partial(R, \phi)} - \chi\epsilon\frac{\partial(R\cos\phi, \Theta)}{\partial(R, \phi)}, \quad (3.12)$$

$$j_z = -\nabla^2A = E_0' + \frac{K}{\chi}\frac{\partial(\Psi, A)}{\partial(R, \phi)}, \quad (3.13)$$

$$\nabla^2\Theta + (\nabla^2A)^2 + \frac{K}{\epsilon^2\chi^2}\Phi' + PK\frac{\partial(\Psi, \Theta)}{\partial(R, \phi)} = 0, \quad (3.14)$$

where $\dfrac{\partial(E, F)}{\partial(R, \phi)} = \dfrac{\partial E}{\partial R}\dfrac{1}{R}\dfrac{\partial F}{\partial\phi} - \dfrac{\partial E}{R\partial\phi}\dfrac{\partial F}{\partial R}$,

and $\epsilon = 1/PK_A\chi$ is a convenient dimensionless group. For the coolant or region (2) the magnetic field is determined by

$$h_R = \frac{\partial\Phi}{\partial R} \text{ and } h_\phi = \frac{1}{R}\frac{\partial\Phi}{\partial\phi}. \quad (3.15)$$

where the scalar potential Φ satisfies Laplaces equation

$$\nabla^2\Phi = 0. \quad (3.16)$$

The boundary conditions become

$$\Phi, \Theta, A \text{ finite at } R = 0,$$
$$\Psi = \frac{\partial\Psi}{\partial R} = \Theta = 0 \text{ at } R = 1,$$
$$\gamma\frac{\partial A}{\partial\phi} = \frac{\partial\Phi}{\partial R},\ \frac{\partial A}{\partial R} = -\frac{\partial\Phi}{\partial\phi} \text{ at } R = 1, \quad (3.17)$$

and $$\frac{1}{R}\frac{\partial\Phi}{\partial\phi} \to 0,\ \frac{\partial\Phi}{\partial R} \to 0 \text{ as } R \to \infty,$$

where $\gamma = \mu_{1e}/\mu_{2e}$ is the ratio of the magnetic permeability of the fluid to that of the coolant.

The above equations (3.12) to (3.17) have a non-zero solution provided the dimensionless electric field E_0' is non-zero. Since the velocity and magnetic field components are independent of z then equation (3.5) implies that $\iint_s J_z dr d\phi$ is constant and equal to the net flow of current crossing any tube cross-section in the z-direction. If this is chosen such that $\iint_s J_z r dr d\phi = \pi a^2 J_0$, then on integrating equation (3.13) over the tube cross-section and using Gauss's theorem together with the boundary condition that $\Psi = 0$ at $R = 1$, we obtain $E_0' = 1$. Thus the dimensionless form of Ohm's law is

$$j_z = -\nabla^2A = 1 + \frac{K}{\chi}\frac{\partial(\Psi, A)}{\partial(R, \phi)}. \quad (3.18)$$

Consider now the order of magnitude of the parameter K, χ and ϵ relevant to liquid metals such as mercury and liquid sodium. If the radius of the tube is a cm and the applied current is i_0 amp/cm^2 then from Table 1 we obtain for mercury ($T_s = 20°$C): $P = 2{\cdot}68\ 10^{-2}$, $K_A = 1{\cdot}28\ 10^{-7}a$, $\chi = 6{\cdot}74\ 10^6$, $\epsilon = 43{\cdot}3/a$, $G = 1{\cdot}69\ 10^2a^5i_0^2$ and $K = 5{\cdot}8\ 10^{-7}a^6i_0^2$; and for liquid sodium ($T_s = 200°$C): $P = 7{\cdot}38\ 10^{-3}$, $K_A = 1{\cdot}61\ 10^{-8}a$, $\chi = 2{\cdot}18\ 10^5$, $\epsilon = 3{\cdot}8510^4/a$, and $K = 1{\cdot}74\ 10^{-11}a^6i_0^2$. Thus in general if $a = 0(1)$ and i_0 is small or moderately large then $K \ll 1$, $\chi > \epsilon > 1$, and χ and ϵ^2 may be of the same order of magnitude. In fact, as in Example I, the magnitude of K controls the viscous and Joulean

Vol. 3 1961

dissipation. The next section deals with series expansions in powers of K for Ψ, Θ, A and Φ.

3(b) *Series expansion for small K*

We assume expansions of the type

$$\left.\begin{aligned}\Psi &= \Psi_0 + K\Psi_1 + \ldots,\\ A &= A_0 + KA_1 + \ldots,\\ \Theta &= \Theta_0 + K\Theta_1 + K^2\Theta_2 + \ldots,\\ \text{and } \Phi &= \Phi_0 + K\Phi_1 + K^2\Phi_2 + \ldots\end{aligned}\right\} \quad (3.19)$$

On substituting the equations (3.19) into (3.12), (3.14), and (3.18) and equating coefficients of like powers of K there results:

Zero-Order functions

$$\nabla^2 A_0 + 1 = 0, \quad (3.20)$$

$$\nabla^2 \Phi_0 = 0, \quad (3.21)$$

$$\nabla^2 \Theta_0 + 1 = 0, \quad (3.22)$$

$$\nabla^4 \Psi_0 + \chi\epsilon \frac{\partial(R\cos\phi, \Theta_0)}{\partial(R, \phi)} = 0; \quad (3.23)$$

First-Order functions

$$\nabla^2 A_1 + \frac{1}{\chi}\frac{\partial(\Psi_0, A_0)}{\partial(R, \phi)} = 0, \quad (3.24)$$

$$\nabla^2 \Phi_1 = 0, \quad (3.25)$$

$$\nabla^2\Theta_1 + 2\nabla^2 A_0 \nabla^2 A_1 + \frac{1}{\epsilon^2\chi^2}\Phi_0' + P\frac{\partial(\Psi_0, \Theta_0)}{\partial(R, \phi)} = 0, \quad (3.26)$$

$$\nabla^4\Psi_1 + \frac{\partial(\Psi_0, \nabla^2\Psi_0)}{\partial(R, \phi)} + \chi\epsilon\frac{\partial(R\cos\phi, \Theta_1)}{\partial(R, \phi)} - \chi\epsilon^2\left\{\frac{\partial(A_1, \nabla^2 A_D)}{\partial(R, \phi)} + \frac{\partial(A_0, \nabla^2 A_1)}{\partial(R, \phi)}\right\}; \quad (3.27)$$

Second-Order functions

$$\nabla^2 A_2 + \frac{1}{\chi}\left\{\frac{\partial(\Psi_0, A_1)}{\partial(R, \phi)} + \frac{\partial(\Psi_1, A_0)}{\partial(R, \phi)}\right\} = 0. \quad (3.28)$$

$$\nabla^2\Phi_2 = 0, \quad (3.29)$$

$$\nabla^2\Theta_2 + (\nabla^2 A_1)^2 + 2\nabla^2 A_0\nabla^2 A_2 + \frac{1}{\chi^2\epsilon^2}\Phi_1' + P\left\{\frac{\partial(\Psi_0, \Theta_1)}{\partial(R, \phi)} + \frac{\partial(\Psi_1, \Theta_0)}{\partial(R, \phi)}\right\}. \quad (3.30)$$

In equations (3.26) and (3.30) Φ_0' and Φ_1' are the zeroth and first-order viscous dissipation functions, which can be obtained using (3.7), (3.10), (3.11) and (3.17). The boundary conditions for A_n, Ψ_n, Θ_n and Φ_n for $n = 0$, 1 and 2 are as follows:

$$\left.\begin{aligned}&A_n, \Theta_n, \Psi_n \text{ are finite at } R = 0,\\ &\Psi_n = \frac{\partial\Psi_n}{\partial R} = \Theta_n = 0, \frac{\partial A_n}{\partial\phi} = \frac{\partial\Phi_n}{\partial R},\\ &\qquad \frac{\partial A_n}{\partial R} = -\frac{\partial\Phi_n}{\partial\phi} \text{ at } R = 1,\\ &\text{and } \frac{1}{R}\frac{\partial\Phi_n}{\partial\phi} \to 0, \frac{\partial\Phi_n}{\partial R} \to 0 \text{ as } R \to \infty.\end{aligned}\right\} \quad (3.31)$$

Here we have assumed that the fluid and coolant are non-magnetic, i.e. $\gamma = \mu_{1e}/\mu_{2e} = 1$.

The equations (3.20) to (3.31) are readily solved and higher approximations to A, Ψ, Θ and Φ could be obtained. However the incidental arithmetic involved in obtaining even the second-order functions indicates the limited usefulness of the series expansion (3.19). In the following we shall make use of the fact that $\chi > \epsilon > 1$ and $\chi = 0(\epsilon^2)$ if $a = 0(1)$ and thus give only the important terms in the rather lengthy expressions to be derived for A_n, Ψ_n, Θ_n and Φ_n.

Consider first the zeroth-order functions defined by equations (3.20) to (3.23) and (3.31). These are:

$$\left.\begin{aligned}&A_0 = -\tfrac{1}{4}(R^2 + a_0), \ \Phi_0 = \tfrac{1}{2}\phi + b_0,\\ &\Theta_0 = \tfrac{1}{4}(1 - R^2),\\ &\Psi_0 = \frac{\chi\epsilon}{384}(R^5 - 2R^3 + R)\sin\phi,\end{aligned}\right\} \quad (3.32)$$

where a_0 and b_0 are constants of integration. Hence in the fluid

$$h_R^{(0)} = 0, \ h_\phi^{(0)} = R/2, \ j_z^{(0)} = 1, \quad (3.33)$$

$$U_R^{(0)} = \frac{\chi\epsilon}{384}(R^4 - 2R^2 + 1)\cos\phi,$$

$$U_\phi^{(0)} = -\frac{\chi\epsilon}{384}(5R^4 - 6R^2 + 1)\sin\phi. \quad (3.34)$$

and for the coolant

$$h_R^{(0)} = 0, \ h_\phi^{(0)} = \frac{1}{2R}. \quad (3.35)$$

The first-order functions refine the above approximation by taking into account (a) the interaction of the fluid motion described by expression (3.34) and the magnetic field given by expression (3.33), and (b) the effect of viscous and Joulean dissipation. The solution of equations (3.24) to (3.27) subject to the boundary conditions (3.38) is:

$$\left.\begin{aligned} A_1 &= \frac{-\epsilon}{96\times 384}(R^7-4R^5+6R^3-4R)\cos\phi + a_1,\ \Phi_1 = \frac{\epsilon}{96\times 384}\frac{\sin\phi}{R} + b_1,\\ \Theta_1 &= -\frac{1}{96\times 384}\{\epsilon(2+\chi P)(R^7-4R^5+6R^3-3R)\cos\phi + 0(1)\},\\ \Psi_1 &= \frac{-\chi\epsilon}{240(384)^2}\{\chi\epsilon(R^{10}-4R^8+5R^6-2R^4)\sin 2\phi - \tfrac{1}{2}(2+\chi P)\epsilon(R^{10}-8R^8\\ &\quad +30R^6-40R^4+17R^2)\cos 2\phi + 2\epsilon^2(3R^9-20R^7+60R^5-72R^3+29R)\sin\phi + 0(1)\}, \end{aligned}\right\} \quad (3.36)$$

where a_1 and b_1 are constants of integration. Thus in the fluid

$$\left.\begin{aligned} h_R{}^{(1)} &= \frac{\epsilon}{96\times 384}(R^6-4R^4+6R^2-4)\sin\phi,\ h_\phi{}^{(1)} = \frac{\epsilon}{96\times 384}(7R^6-20R^4\\ &\quad +18R^2-4)\cos\phi,\ j_z{}^{(1)} = \frac{\epsilon}{768}(R^5-2R^3+R)\cos\phi, \end{aligned}\right\} \quad (3.37)$$

$$\left.\begin{aligned} U_R{}^{(1)} &= \frac{-\chi\epsilon}{(384)^2 240}\{2\chi\epsilon(R^9-4R^7+5R^5-2R^3)\cos 2\phi - \epsilon(2+\chi P)(R^9-8R^7\\ &\quad +30R^5-40R^3+17R)\cos 2\phi + 2\epsilon^2(3R^8-20R^6+60R^4-72R^2+29)\cos\phi + 0(1)\},\\ U_\phi{}^{(1)} &= \frac{\chi\epsilon}{(384)^2 240}\{\chi\epsilon(10R^9-32R^7+30R^5-8R^3)\sin 2\phi - \epsilon(2+\chi P)(10R^9-64R^7\\ &\quad +180R^5-160R^3+34R)\sin 2\phi + 2\epsilon^2(27R^8-140R^6+300R^4-216R^2+29)\sin\phi + 0(1)\}, \end{aligned}\right\} \quad (3.38)$$

and for the coolant

$$h_R{}^{(1)} = \frac{-\epsilon}{96\times 384}\frac{\sin\phi}{R^2},\ h_\phi{}^{(1)} = \frac{\epsilon}{96\times 384}\frac{\cos\phi}{R^2}. \quad (3.39)$$

For the second order functions $j_z^{(2)}$, A_2 and Φ_2 we obtain:

$$\left.\begin{aligned} j_z{}^{(2)} &= \frac{-\epsilon}{(384)^2 480}\{2\chi\epsilon(R^{10}-4R^8+5R^6-2R^4)\cos 2\phi - \epsilon\chi P(R^{10}-8R^8+30R^6\\ &\quad -40R^4+17R^2)\cos 2\phi + 2\epsilon^2(3R^9-20R^7+60R^5-72R^3+29R)\cos\phi + 0(\epsilon)\},\\ A_2 &= \frac{\epsilon}{(384)^2 480}\left\{\frac{\chi\epsilon}{840}(12R^{12}-70R^{10}+140R^8-105R^6+28R^2)\cos 2\phi - \frac{\epsilon\chi P}{420}(3R^{12}\right.\\ &\quad -35R^{10}+210R^8-525R^6+595R^4-273R^2)\cos 2\phi + \frac{\epsilon^2}{20}(R^{11}-10R^9+50R^7\\ &\quad \left.-120R^5+145R^3-86R)\cos\phi + 0(\epsilon)\right\} + a_2, \end{aligned}\right\} \quad (3.40)$$

and

$$\Phi_2 = \frac{\epsilon}{240(384)^2}\left\{\frac{5\epsilon\chi P}{42}\frac{\sin 2\phi}{R^2} + \frac{\chi\epsilon}{84}\frac{\sin 2\phi}{R^2} - 2\epsilon^2\frac{\sin\phi}{R} + 0(\epsilon)\right\} + b_2$$

where a_2 and b_2 are constants of integration.

Vol. 3 1961

It remains now to evaluate the second-order temperature function Θ_2 as defined by equations (3.30) and (3.31). The function Θ_2 can be written as

$$\Theta = \Theta_{2,0} + \Theta_{2,1} + \Theta_{2,2} \tag{3.41}$$

where the functions satisfy, respectively, the equations

$$\nabla^2\Theta_{2,0} + (\nabla^2 A_1)^2 + 2\nabla^2 A_0 \,.\, \nabla^2 A_2 = 0,$$

$$\nabla^2\Theta_{2,1} + \Phi_1' = 0,$$

and

$$\nabla^2\Theta_{2,2} + P\left(\frac{\partial(\Psi_0, \Theta_1)}{\partial(R, \phi)} + \frac{\partial(\Psi_1, \Theta_0)}{\partial(R, \phi)}\right) = 0.$$

The functions $\Theta_{2,0}$, $\Theta_{2,1}$ and $\Theta_{2,2}$ are the temperature distributions due to Joulean dissipation, viscous dissipation and heat transferred by convection, respectively. The boundary conditions are that $\Theta_{2,p}$ is finite at $R = 0$ and $\Theta_{2,p}(1, \phi) = 0$ for $p = 0, 1$ and 2 respectively.

The appropriate solutions of these equations are:

$$\left.\begin{aligned}
\Theta_{2,0} &= \frac{-\epsilon^2}{240(384)^2}\left\{\frac{\chi\epsilon}{840}(12R^{12} - 70R^{10} + 140R^8 - 105R^6 + 23R^2)\cos 2\phi - \frac{\epsilon\chi P}{420}(3R^{12}\right.\\
&- 35R^{10} + 210R^8 - 525R^6 + 595R^4 - 248R^2)\cos 2\phi + \frac{\epsilon^2}{20}(R^{11} - 10R^9 + 50R^7\\
&\left.- 120R^5 + 145R^3 - 66R)\cos\phi + 0(\epsilon)\right\},\\
\Theta_{2,1} &= \frac{1}{15(384)^3}\left\{\frac{\chi\epsilon}{1680}(693\,R^{13} - 2640\,R^{11} + 3220\,R^9 - 1344\,R^7 + 71\,R^3)\cos 3\phi\right.\\
&- \frac{\epsilon\chi P}{3360}(693\,R^{13} - 4920R^{11} + 14840R^9 - 15120R^7 + 3750R^5 + 937R^3)\cos 3\phi + \frac{2\epsilon^2}{5}\\
&\times(6R^{12} - 35R^{10} + 80R^8 - 60R^6 + 9R^2)\cos 2\phi - \frac{\chi\epsilon}{280}(170R^{13} - 756R^{11} + 1225R^9\\
&- 910R^7 + 280R^5 - 9R)\cos\phi - \frac{\epsilon^2}{10}(30R^{12} - 192R^{10} + 525R^8 - 640R^6\\
&\left.+ 360R^4 - 83) + 0(\epsilon)\right\},\\
\Theta_{2,2} &= \frac{P\chi\epsilon}{240(384)^2}\left\{\frac{\chi\epsilon}{840}(12R^{12} - 70R^{10} + 140R^8 - 105R^6 + 23R^2)\cos 2\phi - \frac{\epsilon\chi P}{1680}(72R^{12}\right.\\
&- 490R^{10} + 1540R^8 - 2625R^6 + 2380R^4 - 877R^2)\cos 2\phi + \frac{\epsilon^2}{20}(R^{11} - 10R^9 + 50R^7\\
&- 120R^5 + 145R^3 - 66R)\cos\phi - \frac{\epsilon\chi P}{144}(30R^{12} - 216R^{10} + 675R^8 - 1140R^6 + 1080R^4\\
&\left.- 540R^2 + 111) + 0(1)\right\}
\end{aligned}\right\} \tag{3.42}$$

In the next section the physical implications of these results are discussed.

3(c) *Results and Discussion*

Consider now the flow configuration as predicted by section 3(b) for small K. The zeroth-order approximation given by expressions (3.36) to (3.39) implies that the temperature distribution and magnetic field components are identical in form with those occurring in the Joule heating of an infinitely long solid cylinder with the same external conditions. Temperature gradients now exist in the fluid producing the buoyancy force resulting in the formation of a non-uniform fluid motion having convective cells on either side of the vertical plane $\phi = 0, \pi$ (see expression (3.34)). The fluid rises along the vertical plane and flows downward along the cool wall on either side of the vertical plane; also the fluid is stationary at $[1/(\sqrt{5}), \pi/2]$ and $[1/(\sqrt{5}), (3\pi)/2]$. The vertical flow along $\phi = 0, \pi$ now distorts the magnetic lines of force, given by expression (3.37), in the vertical direction. Thus we might expect an increase in local current density along the plane $\phi = 0$. This is borne out by the first approximation to j_z (see expression (3.37)) where $j_z^{(1)}$ has a maximum at $[1/(\sqrt{5}), 0]$. Along $\phi = \pi$ the vertical flow distorts the magnetic lines of force away from the tube surface thus producing a maximum decrease in local current density at $[1/(\sqrt{5}), \pi]$.

At this stage in the analysis the current density is no longer uniform over the tube cross-section and thus several modifications to the flow and temperature are necessary. Thus expression (3.36) for Θ_1 implies a maximum increase at (0·45, 0) and a maximum decrease at (0·46, π) coinciding approximately with the maximum increase and decrease for $j_z^{(1)}$ at $[1/(\sqrt{5}), 0]$ and $[1/(\sqrt{5}), \pi]$ respectively. A Lorentz force now exists opposing the buoyancy force and thus reduces in magnitude the velocity components. This is evident from the first-order velocity components as given by expressions (3.38). These components also imply that the "regions" of stationary fluid are now to the right of $[1/(\sqrt{5}), \pi/2]$ and to the left of $[1/(\sqrt{5}), (3\pi)/2]$. Finally as a consequence of the non-uniformity of current density there is an increase in the ϕ-component of the magnetic field in the neighbourhood of the axis $\phi = 0$ and a decrease in the neighbourhood of $\phi = \pi$ for both fluid and coolant [see expressions (3.37) and (3.39)]; furthermore a radial magnetic field is set up which acts radially inward for the coolant and fluid if $0 < \phi < \pi$ and radially outwards for $\pi < \phi < 2\pi$.

The second-order approximation adds little information to the above general trends. However, provided K is small there will be an overall small increase in j along the vertical axis and a slight decrease in the neighbourhood of the stationary points. A slight decrease in the local temperature will also occur in this neighbourhood [see expression (3.42)].

The above discussion gives some insight into the type of flow which may occur for large values of K. Thus we might expect isothermal cores on either side of the vertical plane. The fluid will rise in a narrow jet up the vertical plane and return down the wall on either side in a thin boundary layer which acts as a shield between the isothermal core and the wall. Furthermore there should be an increase in the local current density and temperature in the neighbourhood of (0·5, 0) and a corresponding decrease at (0·5, π).

Let us consider some thermal characteristics of the flow configuration when K is small. An average wall Nusselt number may be defined as

$$\overline{Nu} = \frac{a\int_0^{2\pi} (\mathrm{d}T/\mathrm{d}r)_{r=a}\,\mathrm{d}\phi}{2\pi(T_c - T_s)} \tag{3.43}$$

where $T_c - T_s = (J_0^2\, a^2/4K\sigma)$ is the temperature difference between the axis of the tube and the coolant when the thermal energy is transferred by conduction alone. Using the various transformations given by equation (3.10) and the complete expressions for the Θ_n as derived in section 3(b) we obtain

$$\overline{Nu} = 2 + \frac{1}{(96)^2} K + \frac{2}{5(384)^3}(8\epsilon^3 - 16\epsilon^2 + 1)K^2 + 0(K^3). \tag{3.44}$$

The axial temperature T_0 due to Joule heating and as modified by the non-uniform convection flow was found to be

Vol. 3 1961

$$T_0 = T_s + \frac{J_0^2 a^2}{4K\sigma}\left[1 + \frac{14}{3(384)^2}K + \frac{2}{75(384)^3}\left\{372\epsilon^3 + (83 + 350\chi P + 175\chi^2 P^2)\epsilon^2 + \frac{737}{168}\right\}K^2 + 0(K^3)\right] \quad (3.45)$$

In Table 6 the actual temperature difference $(T_0 - T_s)$, as calculated from expression (3.45), is compared with the fictitious temperature difference $(T_c - T_s) = (J_0^2 a^2)/(K\sigma)$. The fluids taken were mercury and liquid sodium with coolant temperatures 20° and 200°C respectively; the diameter of the tube is 1 cm and the current density is i_0 amp/cm². We note that for a tube of 1 cm diameter expression (3.45) is probably accurate for mercury if $i_0 \leqslant 80$ amp/cm² and for liquid sodium if $i_0 \leqslant 510^3$ amp/cm². Moreover within these current density limitations the average wall Nusselt number is 2 for both fluids [see expression (3.44)]. In view of this, and the small temperature differences existing between the fluid and the coolant when extremely large currents are applied, it seems unlikely that these results could be verified experimentally.

Table 6

Mercury (T_s = 20°C, dia. 1 cm)			Liquid sodium (T_s = 200°C, dia. 1 cm)		
i_0	$T_c - T_s$	$T_0 - T_s$	i_0	$T_c - T_s$	$T_0 - T_s$
40	0·12	0·12	1000	1·05	1·05
50	0·19	0·18	2000	4·20	4·18
60	0·27	0·25	3000	9·45	9·17
70	0·37	0·31	4000	16·8	15·2
80	0·48	0·35	5000	26·3	20·2

REFERENCES

1. S. OSTRACH, *N.A.C.A. Rep.* TN 2683 (1952).
2. C. G. COWLING, *Magnetohydrodynamics*, Interscience, New York (1957).
3. G. Z. GERSHUNI and E. M. ZHUKHOVITSKII, *Soviet Physics J.E.T.P.* **34**, 670 (1958).

Int. J. Heat Mass Transfer. Vol. 3, pp. 26–41. Pergamon Press 1961. Printed in Great Britain.

MASS TRANSFER THROUGH LAMINAR BOUNDARY LAYERS—3a. SIMILAR SOLUTIONS OF THE *b*-EQUATION WHEN $B = 0$ AND $\sigma \geqslant 0{\cdot}5$

H. L. EVANS
Commonwealth Scientific and Industrial Research Organization,
Division of Food Preservation, Homebush, N.S.W., Australia*

(*Received October* 1960)

Abstract—Using a form of expansion first suggested by Merk, series are given for evaluating accurately the "wall gradient" (b_0'/B) for the case when no mass flows through the phase boundary. These cover wide ranges of main-stream pressure gradient and give good accuracy for any value greater than 0·5 of the Prandtl/Schmidt number σ. Values obtained compare well both with the few exact solutions given in the literature and with exact numerical integration. Curves are drawn of a number of other functions obtained from this "wall gradient".

Résumé—Des séries, obtenues en utilisant une forme de développement préconisée primitivement par Merk, sont données pour le calcul précis du "gradient à la paroi" b_0/B dans le cas où aucun transport de masse ne s'effectue à la limite de la phase. Elles couvrent un grand domaine de gradient de pression de l'écoulement principal et assurent une bonne précision pour toute valeur σ du rapport du nombre de Prandtl au nombre de Schmidt supérieure à 0,5. Les valeurs obtenues se comparent bien aux quelques solutions exactes données dans la littérature et à celles de l'intégration numérique exacte. Des sourbes d'un certain nombre d'autres fonctions obtenues à partir de ce "gradient à la paroi" sont tracées.

Zusammenfassung—Mit Hilfe einer zuerst von Merk vorgeschlagenen Reihenentwicklung kann der „Wandgradient" (b_0'/B) genau berechnet werden, wenn kein Mengenstrom durch die Phasentrennschicht tritt. Diese Reihen umfassen ein grosses Gebiet des Druckgradienten der Hauptströmung und sind für beliebige Werte der Prandtl/Schmidtzahl σ die grösser als 0,5 sind, sehr genau. Die errechneten Werte stimmen gut überein mit den wenigen genauen Lösungen der Literatur und der exakten numerischen Integration. Kurven für eine Reihe anderer, mit Hilfe dieses „Wandgradienten" erhaltener Funktionen sind angegeben.

Аннотация—Используя вид разложения, впервые предложенный Мерком, приводятся ряды для точной оценки «пристенного градиента» (b_0/B) для случая, когда отсутствует поток массы через границу фазы. Эти разложения охватывают широкие области градиента давления основного потока и дают высокую точность во всех случаях, когда отношение числа Прандтля к числу Шмидта σ больше 0,5. Полученные величины хорошо сопоставимы как с некоторыми имеющимися в литературе точными решениями, так и с результатами точного численного интегрирования. Приводятся кривые некоторых других функций, полученных на основе «пристенного градиента».

NOTATION

a_q Coefficients in equation (13); see also Table 2 (—);

A_n Coefficients occurring in equation (9) and defined in equation (11) (—);

b Dimensionless conserved fluid property (see Paper 3 for discussion of its form and meaning) (—);

b_0' Gradient of b adjacent to the interface (—);

B Driving force for mass transfer (discussed in Paper 3) (—);

C_m Coefficients occurring in equation (18) and defined by equation (20) (—);

E Integral in equation (9); evaluated numerically using Table 2 (—);

E_{sep} Integral of equation (18); evaluated numerically from equation (21) (—);

* The Division is now located at P.O. Box 43, Ryde, N.S.W., Australia.

Vol. 3 1961

f Dimensionless stream function (defined and discussed in Paper 1) (—);

$f_0, f'_0, f''_0, f'''_0, f_0^{(n)}$ The value of f and its derivatives at the interface (—);

$F_2 \left(= \frac{u_G}{\nu} \frac{d\delta_2^2}{dx}\right)$ parameter giving rate of growth of the momentum thickness δ_2; discussed in Paper 1 (—);

g Mass transfer conductance (see Paper 3) (lb/ft²h);

g^* Value of g for $B = 0$. (See equation 27) (lb/ft²h);

m Number occurring in equation (20) specifying terms in equation (18). Also used to specify terms in equation (9) like that of equation (12) (—);

n Number occurring in equation (11) specifying terms in equation (9) (—);

Nu Local Nusselt number in terms of the length x (—);

q Number specifying terms in equation (13) (—);

r Number occurring in equation (15) (—);

Re Local Reynolds number ($= u_G x/\nu$) (—);

u Velocity component parallel to interface (ft/h);

u_G Value of u in the main-stream immediately outside the boundary layer (ft/h);

v Velocity component normal to interface (ft/h);

W Curvature parameter in terms of Δ_2 (equation 30) (—);

x Distance parallel to interface measured from start of boundary layer (ft);

X Curvature parameter in terms of Δ_4 (equation 28) (—);

X_{sep} Curvature parameter in terms of Δ_4 applicable to separation point (equation 39) (—);

y Distance perpendicular to interface (ft);

Y Parameter which is a measure of the rate of growth of Δ_4 (equation 29) (—);

Y_{sep} Parameter corresponding to Y applicable near separation point (equation 38) (—);

Z Parameter which is a measure of the rate of growth of Δ_2 (equation 31) (—).

Greek symbols

β Parameter occurring in velocity equation (equation 2); discussed in Paper 1 (—);

γ Fluid property called the "exchange coefficient" (diffusion coefficient times density, or thermal conductivity divided by specific heat at constant pressure) (lb/ft h);

δ_2 Momentum boundary layer thickness $= \int_0^\infty (u/u_G)(1 - u/u_G)\, dy$ (ft);

δ_4 Shear boundary layer thickness $= u_G/(\partial u/\partial y)_0$ (ft);

Δ_2 Convection boundary layer thickness $= \int_0^\infty (u/u_G)(1 - b/B)\, dy$ (ft);

Δ_4 Conduction boundary layer thickness $= B/(\partial b/\partial y)_0$ (ft);

η Dimensionless distance variable for "similar" solutions (—);

μ Dynamic viscosity of fluid (lb/ft h);

ν Kinematic viscosity of fluid ($= \mu/\rho$) (ft²/h);

ρ Density of fluid (lb/ft³);

σ Prandtl or Schmidt number ($= \mu/\gamma$) (—);

φ Integration variable occurring in equations (9) and (18) (—).

Subscripts

G Denotes fluid state in main-stream just outside the boundary layer;

sep Denotes "separation" conditions of section 3.2;

0 Denotes fluid state adjacent to the interface;

q Denotes terms in equation (13);

m Denotes terms in equation (18);

n Denotes terms in equation (9).

A prime ′ denotes differentiation with respect to η.

1. INTRODUCTION

1.1 *General remarks*

THE first two papers in the present series, Spalding [1], Spalding and Evans [2], were concerned exclusively with the velocity equation of laminar boundary layer theory when mass flows through the boundary layer, and Paper 3, Spalding and Evans [3], dealt with the b-equation. In this latter paper tables were given from which new approximate solutions to the b-equation could be evaluated. These gave reasonable agreement with known exact solutions over wide ranges of the Prandtl/Schmidt number, main-stream pressure gradient and the mass transfer driving force B.

The present paper is concerned with the case

when B, the driving force for mass transfer, is zero. The work has developed out of the methods employed in obtaining the earlier results so frequent reference will be made to the first three papers in the series.

Since the main aim of the present series is the prediction of mass transfer rates, the case when mass transfer is in fact zero may be thought to be irrelevant. But this is not the case, for, as was pointed out in Paper 3, we are interested in families of solutions to the boundary layer equations for both positive and negative values of B; the solutions for $B = 0$ must therefore form important members of these families. It is also found that many practical problems involving mass transfer correspond to very small values of B; this is often the case, for example, when water vapour either evaporates into or condenses out of the atmosphere at ordinary temperatures and pressures. The case for $B = 0$ can then serve as a useful first approximation, the effects of mass transfer being regarded as a small correction. In fact, Paper 3 contained an approximate formula for estimating the mass transfer conductance g from the value of g^*, the conductance when $B = 0$. Using tables to be given later it is possible to calculate g^* to high accuracy.

The present results are expected to be most useful, however, in problems when mass transfer is entirely absent; the most obvious case is that of heat transfer to or from an impervious wall. Although, in the literature, a number of papers consider this type of problem, comparatively few exact solutions to the equations could be found; most of these have already been quoted in Paper 3.

The quantity being evaluated in the present paper is (b_0'/B). Reference to formulae in Paper 3 indicates that when $B = 0$, so is b_0' $(= -\sigma f_0)$. The ratio (b_0'/B) is not zero, however, for, in terms of the familiar problem of pure heat transfer it is the gradient at the wall of the dimensionless temperature with respect to the "similar" distance variable η. In the customary nomenclature of heat transfer, therefore, we have:

$$(b_0'/B) = Nu\,(2 - \beta)^{1/2}/Re^{1/2}. \qquad (1)$$

where:

Nu = local Nusselt number,

Re = local Reynolds number, and

β = parameter occurring in the velocity equation.

1.2 *Outline of present paper*

The main purpose of the present paper is to give series expansions from which, knowing the solutions to the "similar" velocity equation, values of the "wall gradient" (b_0'/B) may be obtained to high accuracy for a range of values of the parameter β, which determines the magnitude of the main-stream pressure gradient, and for any value greater than 0·5 of the fluid property group σ.

The series from which values of (b_0'/B) are obtained are in increasing inverse powers of σ; they are therefore very accurate for high values of σ. Some exact values for $\sigma = 0{\cdot}7$ were found in the literature. Sufficient terms were therefore taken in the series to give close agreement in the fourth significant figure with these exact solutions. The values of (b_0'/B) quoted are then accurate to better than 0·1 per cent even when σ is as low as 0·7.

Using the series, a table of (b_0'/B) as a function of the parameters β and σ has been drawn up in which the interval in both these parameters is small enough to allow of rapid interpolation for intermediate values. In many cases, however, it may be more satisfactory to use the original series for intermediate values of σ.

As has been pointed out in earlier papers, the main interest in obtaining "similar" solutions to the boundary layer equations is not so much in their application to strictly "similar" physical configurations (e.g. flow over wedges) as in the way they can be used to solve more general problems involving non-similar flows.

Some functions which are useful for such calculations are plotted in Figs. 1–4 but are only briefly discussed here as their significance and applications are to be considered more fully in other papers in the series.

2. STATEMENT OF THE MATHEMATICAL PROBLEM

2.1 *Introduction*

It was shown in Paper 3 that the b-equation governs the distribution in the boundary layer of any conserved fluid property. The present paper

Vol. 3 1961

is mainly concerned with the "similar" solutions to this equation. It should be made clear, however, that the word "solution" is used in a restricted sense in that the important entity to be evaluated is the gradient of b at the phase boundary, although many other functions in the boundary layer may be obtained from this gradient. Interest is concentrated on this "wall gradient" because the present series of papers is mainly concerned with rates of transfer through the phase boundary, these rates being determined immediately the wall gradient is known. The distribution of b in the boundary layer is not evaluated, although obtaining the wall gradient is an important first step in getting this distribution.

Solutions to the b-equation depend, of course, on the distribution of the stream function. It will therefore be necessary to refer frequently to the velocity equation for "similar" flows. This will be quoted but not discussed; reference to discussions and tables given in Papers 1 and 2 will suffice for the purposes of the present paper.

2.2 *The velocity equation*

In Paper 1, Spalding [1], it was shown that, for "similar" solutions to the boundary layer equations the velocity distribution is governed by the ordinary differential equation:

$$f''' + ff'' + \beta(1 - f'^2) = 0. \tag{2}$$

When no mass flows through the interface, the boundary conditions associated with this equation are:

$$\left.\begin{aligned} \eta = 0,\ f = 0,\ f' = 0 \\ \eta \to \infty,\ f' \to 1 \end{aligned}\right\}. \tag{3}$$

In equations (2) and (3) the primes denote differentiation with respect to the dimensionless space co-ordinate η, f is the dimensionless stream function and β a parameter whose value depends on the acceleration of the main-stream. These functions are more fully defined in the notation list.

2.3 *The b-equation*

In Paper 3, Spalding and Evans [3], it was shown that for a certain restricted group of "similar" solutions to the boundary layer equations, the distribution of a function b, which represents a conserved fluid property in suitable dimensionless form, is governed by the ordinary differential equation:

$$b'' + \sigma f b' = 0 \tag{4}$$

with the boundary conditions:

$$\left.\begin{aligned} \eta = 0,\ b = 0 \\ \eta \to \infty,\ b \to B \end{aligned}\right\}. \tag{5}$$

In equation (4) the primes again denote differentiation with respect to η, f is the stream function occurring in equation (2) and σ is the fluid property group called the Prandtl or Schmidt number depending on the transferred fluid property which is under investigation. The quantity B occurring in equation (5) is the value of b in the main-stream and is assumed to be constant.

From equation (4) the gradient of b at the interface, namely b'_0, can in principle be evaluated once solutions to the velocity equation are known. This is done using the relationship:

$$(B/b'_0) = \int_0^\infty \exp -\{\sigma \int_0^\eta f \, d\eta\} \, d\eta. \tag{6}$$

It is convenient, for the present, to work in terms of the reciprocal of (b'_0/B).

The aim of the present paper is to evaluate this integral for a range of values of the parameter β occurring in equation (2) and for any value of σ greater than 0·5.

The tables given in Paper 3 included the case $B = 0$ and approximate values of this integral could be obtained from them. The accuracy of those tables increased with increasing σ. The present results are accurate for all high values of σ.

3. EVALUATING THE INTEGRAL AS A POWER SERIES IN σ

When evaluating the integral in equation (6) for various values of the parameter β, with the single exception of the separation point when $\beta = -0{\cdot}1988$, all values of β considered here could be treated by one general method. This will be given first and the separation point will then be treated by a modified form of this method.

3.1 *The general case*

It is clear that the integral in equation (6) for any value of σ depends only on the distribution with η of the stream function f. Unfortunately, however, only a few accurate values of the integral could be found in the literature.

On the other hand Merk [4] has shown that the integral can be expressed as a series in inverse powers of σ, which would be very accurate for large values of σ. Although the present work arose out of that paper, the method of deriving the series expansion differs in many respects from that given by Merk, and so will be given in outline below. It has also been possible to modify the present method to include cases when mass transfer occurs; this work is to be considered elsewhere.

Denoting quantities when evaluated at the interface by the suffix 0, the stream function f can be expanded in terms of derivatives there in the form:

$$f = \frac{f''_0\eta^2}{2!} + \frac{f'''_0\eta^3}{3!} + \frac{f^{iv}_0\eta^4}{4!} + \frac{f^{v}_0\eta^5}{5!} + \ldots \quad (7)$$

Inserting this into the integral in equation (6) and changing the variable from η to φ, where:

$$\varphi = \frac{\sigma f''_0}{3!}\eta^3 \quad (8)$$

the integral to be evaluated becomes:

$$E = \int_0^\infty e^{-\varphi}\varphi^{-2/3} \exp -\{A_3\varphi^{4/3} + A_5\varphi^{6/3} + A_6\varphi^{7/3} + \ldots\}\,\mathrm{d}\varphi. \quad (9)$$

The quantity (b'_0/B) is obtained from E using the relationship:

$$(b'_0/B) = \frac{3}{E}\left(\frac{\sigma f''_0}{3!}\right)^{1/3} \quad (10)$$

since f''_0 is known. The problem therefore reduces to the evaluation of E in equation (9).

The tables given in Paper 3 were approximate in that only the first two terms in the expansion given in equation (7) were used (remembering that we are considering here the case of no mass transfer so that f_0 is zero). In the present paper many more terms are included.

The coefficients A_n occurring in the expression for E are given by the general formula:

$$A_n = \frac{1}{\sigma^{(n-2)/3}}\frac{f_0{}^{(n)}}{(n+1)!}\left(\frac{3!}{f''_0}\right)^{(n+1)/3}. \quad (11)$$

Since the present discussion is restricted to the case when no mass flows through the interface the coefficients A_0, A_1 and A_4 are zero, and because of the transformation used in obtaining E, the coefficient A_2 is reduced to unity.

In order to calculate the coefficients A_n the values of $f_0{}^{(n)}$, the derivatives of f at the wall, were needed. These were obtained from equation (2) by successive differentiation. In this way each $f_0{}^{(n)}$ higher than f''_0 could be expressed in terms of f''_0 and the parameter β.

Values of the function f''_0 for the values of β considered in the present paper are given in Table 1. For values of β up to 2·0 these were taken from Falkner [5, 6]; the method used for evaluating f''_0 for higher values of β was given in Paper 2.

In the expression for E given in equation (9) the second exponential term in the integrand can be expanded as a series in powers of φ. Each term under the integral sign is then of the form $e^{-\varphi}\varphi^{m/3}$, where m has a different value for each term; the integral may then be readily evaluated term by term using the relationship:

$$\int_0^\infty e^{-\varphi}\varphi^{m/3}\,\mathrm{d}\varphi = \Gamma\left(\frac{m+3}{3}\right) \quad (12)$$

Table 1. Values of the stream function "wall gradient" f''_0 for the values of β considered in the present paper

β	−0·1988	−0·1	0·0	0·1	0·2	0·3	0·4	0·5
f''_0	0	0·3191	0·4696	0·5870	0·6869	0·7748	0·8542	0·9277
β	0·6	0·8	1·0	1·4	2·0	3·0	4·0	5·0
f''_0	0·9960	1·1200	1·2326	1·431	1·687	2·043	2·346	2·614

Vol. 3 1961

where Γ denotes the gamma function. The final step in obtaining the required series for E is to rearrange these terms into a series in inverse powers of σ having the form:

$$E = \Gamma(\tfrac{1}{3}) + \sum_{q=1}^{\infty} \frac{a_q}{\sigma^{q/3}} \tag{13}$$

in which the coefficients a_q are functions of the quantities A_n and gamma functions; these coefficients become more complicated as q increases.

The numerical values of only three gamma functions were needed, namely:

$$\Gamma(\tfrac{1}{3}) = 2{\cdot}67894,\ \Gamma(\tfrac{2}{3}) = 1{\cdot}35412,\quad \Gamma(1) = 1. \tag{14}$$

All other gamma functions which occurred could be expressed in terms of these using the relationship:

$$\Gamma(r+1) = r\Gamma(r) \tag{15}$$

which holds for any value of r for which the gamma function exists.

Numerical values of the first nine coefficients a_q are given in Table 2. This covers the range $-0{\cdot}1 \leqslant \beta \leqslant 5{\cdot}0$. In both directions outside this range the accuracy of the present method diminished, particularly when σ was less than unity. The region approaching conditions leading to "separation" of the velocity boundary layer, namely for $-0{\cdot}1988 \leqslant \beta \leqslant -0{\cdot}1$, was particularly difficult to treat. On the other hand the separation point itself, when $\beta = -0{\cdot}1988$, yielded a series which gave high accuracy.

3.2 *The separation point*

When $\beta = -0{\cdot}1988$ the velocity boundary layer is said to "separate" from the interface; for the present discussion this merely means that f_0'' becomes zero. The above analysis does not then apply because the transformation defined by equation (7) cannot be used. A modification of the procedure can, however, lead to an asymptotic series from which (b_0'/B) can be evaluated to high accuracy. Merk [4] also considered this case but as there appears to be a numerical error in the expansion he obtained, the derivation of the relevant series will be given here.

Table 2. Values of the first nine coefficients in the series expansion of the integral E.

$$\left(\frac{b_0'}{B}\right) = \frac{3}{E}\left(\frac{\sigma f_0'''}{3!}\right)^{1/3}; \qquad E = 2{\cdot}67894 + \sum_{q=1}^{\infty} \frac{a_q}{\sigma^{q/3}}$$

β	a_1	a_2	a_3	a_4	a_5	a_6	a_7	a_8	a_9
−0·1	−0·18808	0·04341	0·05748	−0·00357	0·00037	−0·00702	−0·00185	−0·00098	0·000968
0·0	0·0	0·0	0·05953	0·0	0·0	−0·00661	0·0	0·0	0·000717
0·1	0·08344	0·00854	0·04884	0·00153	−0·00001	−0·00587	−0·00062	−0·00013	0·00089
0·2	0·13533	0·02247	0·04092	0·00144	−0·00045	−0·00516	−0·00081	−0·00021	0·00092
0·3	0·17289	0·03668	0·03465	0·00110	−0·00118	−0·00456	−0·00086	−0·00018	0·00091
0·4	0·20240	0·05027	0·02930	0·00080	−0·00206	−0·00403	−0·00085	−0·00002	0·00090
0·5	0·22663	0·06302	0·02442	0·00057	−0·00302	−0·00352	−0·00086	0·00019	0·00086
0·6	0·24738	0·07509	0·01985	0·00042	−0·00403	−0·00301	−0·00089	0·00045	0·00086
0·8	0·28207	0·09763	0·01136	0·00040	−0·00612	−0·00189	−0·00103	0·00109	0·00056
1·0	0·31031	0·11816	0·00316	0·00053	−0·00834	−0·00061	−0·00127	0·00190	0·00018
1·4	0·35604	0·15555	−0·01247	0·00140	−0·01296	0·00262	−0·00201	0·00390	−0·00111
2·0	0·40841	0·20468	−0·03568	0·00315	−0·02078	0·00913	−0·00390	0·00787	−0·00464
3·0	0·47470	0·27651	−0·07325	0·00774	−0·03527	0·02523	−0·00889	0·01731	−0·01553
4·0	0·52632	0·33992	−0·11085	0·01306	−0·05227	0·04740	−0·01673	0·03016	−0·03392
5·0	0·56951	0·39798	−0·14828	0·01907	−0·07133	0·07600	−0·02728	0·04692	−0·06080

When $\beta = -0{\cdot}1988$, $\left(\frac{b_0'}{B}\right) = \frac{4}{E_{sep}}\left(\frac{\sigma f_0'''}{4!}\right)^{1/4}$; $E_{sep} = 3{\cdot}62561 + \frac{0{\cdot}084049}{\sigma} - \frac{0{\cdot}005907}{\sigma^2} - \frac{0{\cdot}0001405}{\sigma^3} + O(\sigma^{-4})$

Since f''_0 is zero the expansion for f takes the form:

$$f = f'''_0 \frac{\eta^3}{3!} + f^{\mathrm{VII}}_0 \frac{\eta^7}{7!} + f^{\mathrm{XI}}_0 \frac{\eta^{11}}{11!} + f^{\mathrm{XV}}_0 \frac{\eta^{15}}{15!} + \ldots . \quad (16)$$

Using the transformation:

$$\varphi = \left(\frac{\sigma f'''_0}{4!}\right) \eta^4, \quad (17)$$

the integral to be evaluated, denoted by E_{sep} since it applies only to the separation point, is:

$$E_{\mathrm{sep}} = \int_0^\infty e^{-\varphi} \varphi^{-3/4} \exp -\{C_7\varphi^2 + C_{11}\varphi^3 + C_{15}\varphi^4 + \ldots\} \, \mathrm{d}\varphi \quad (18)$$

and (b'_0/B) is obtained from E_{sep} using the relationship:

$$(b'_0/B) = \frac{4}{E_{\mathrm{sep}}} \left(\frac{\sigma f''''_0}{4!}\right)^{1/4}. \quad (19)$$

The coefficients C_m occurring in equation (18) are given by the general formula:

$$C_m = \frac{1}{\sigma^{(m-3)/4}} \frac{f_0^{(m)}}{(m+1)!} \left(\frac{4!}{f'''_0}\right)^{(m+1)/4}. \quad (20)$$

Again expanding the exponential term in the integrand of equation (18) gives a series for E_{sep} in terms of gamma functions and the coefficients C_m. Using the values $f'''_0 = 0{\cdot}1988$ and $\Gamma(\frac{1}{4}) = 3{\cdot}62561$ gives finally for E_{sep} the asymptotic expansion:

$$E_{\mathrm{sep}} = 3{\cdot}62561 + \frac{0{\cdot}084049}{\sigma} - \frac{0{\cdot}005907}{\sigma^2} - \frac{0{\cdot}0001405}{\sigma^3} + 0(\sigma^{-4}). \quad (21)$$

As has been noted the coefficients in this series differ from the values given by Merk [4]. The series also contains one more term than was given by Merk.

3.3 *Asymptotic behaviour at high* σ

It is clear from equation (13) that for high values of σ the integral E is constant. From equation (10) therefore, (b'_0/B) is proportional to $\sigma^{1/3}$. This is a well-known relationship which was exploited when plotting some of the figures given in Paper 3. In order to bring closer together curves for different values of σ, the group $\sigma^{-1/3}(b'_0/B)$ was plotted against the driving force B.

This relationship does not, however, hold for the separation point. From equations (19) and (21) it may be seen that for this case when σ is large, (b'_0/B) is proportional to $\sigma^{1/4}$.

These asymptotic relationships will be used later to include on the same figures curves relating to a wide range of σ.

4. FUNCTIONS OBTAINED FROM THE ASYMPTOTIC SERIES

4.1 *Introduction*

The asymptotic formulae given in Table 2 for evaluating (b'_0/B) should only be used for $\sigma \geqslant 0{\cdot}5$ since the accuracy decreases rapidly as σ decreases below this value.

Using these formulae values of (b'_0/B) have been calculated for wide ranges of β and σ; the results are given in Table 3.

The range of main-stream pressure gradient included in Table 3 covers the values encountered in a wide range of practical problems. It includes the point of separation for two-dimensional flow ($\beta = -0{\cdot}1988$), the case of zero pressure gradient ($\beta = 0$), the stagnation point for axially symmetric, three-dimensional flow (corresponding to $\beta = 0{\cdot}5$; see Paper 1), the stagnation point for two-dimensional flow ($\beta = 1{\cdot}0$) as well as some more highly accelerated main-streams than the last.

For application to problems involving heat transfer calculations, when σ is the Prandtl number, the table covers the case of most gases, which have a Prandtl number near 0·7, as well as the majority of liquids. The Prandtl number for water, for example, ranges from about 7 at room temperature to about 2·0 at 200°F. Typical values for a more viscous fluid like engine oil would be $\sigma = 10\,000$ at room temperature to $\sigma = 1000$ at 150°F. Fluids such as liquid metals, which have a high thermal conductivity and therefore a low Prandtl number (e.g. for mercury $\sigma = 0{\cdot}02$), are not however included.

Fluids will rarely have values of σ exactly equal to those given in Table 3 but the intervals in the

Vol. 3 1961

Table 3. Values of the wall gradient (b_0'/B) as a function of the parameter β and the fluid property σ

σ \ β	−0·1988	−0·1	0·0	0·1	0·2	0·3	0·4	0·5	0·6	0·8	1·0	1·4	2·0	3·0	4·0	5·0
0·5	0·2692	0·3443	0·3667(+3)	0·3811	0·3919	0·4003	0·4071	0·4130	0·4180	0·4263	0·4332	0·4437	0·4563	0·4725	0·4901	0·5111
0·6	0·2833	0·3669	0·3917(0)	0·4077	0·4197	0·4291	0·4367	0·4434	0·4491	0·4585	0·4663	0·4781	0·4918	0·5081	0·5231	0·5388
0·7	0·2957(+2)	0·3869(−4)	0·4139(+2)	0·4315	0·4445	0·4548	0·4633	0·4706(+1)	0·4769	0·4872	0·4958(0)	0·5089	0·5238	0·5409	0·5552	0·5686
0·8	0·3067	0·4049	0·4341(−1)	0·4530	0·4671	0·4782	0·4873	0·4953	0·5021	0·5134	0·5227	0·5370	0·5531	0·5712	0·5855	0·5980
0·9	0·3167	0·4214	0·4525(0)	0·4727	0·4878	0·4997	0·5095	0·5180	0·5253	0·5374	0·5475	0·5629	0·5799	0·5994	0·6141	0·6263
1·0	0·3258	0·4367	0·4696(0)	0·4910	0·5070	0·5196	0·5300	0·5390	0·5468	0·5598	0·5705	0·5869	0·6053	0·6258	0·6410	0·6534
1·1	0·3343	0·4509	0·4856(−2)	0·5081	0·5249	0·5382	0·5492	0·5587	0·5670	0·5806	0·5920	0·6094	0·6288	0·6506	0·6665	0·6791
1·2	0·3421	0·4643	0·5005	0·5241	0·5417	0·5557	0·5672	0·5773	0·5859	0·6003	0·6122	0·6306	0·5611	0·6740	9·6906	0·7036
1·4	0·3564	0·4889	0·5281	0·5536	0·5728	0·5880	0·6005	0·6114	0·6209	0·6365	0·6496	0·6697	0·6921	0·7173	0·7354	0·7494
1·6	0·3692	0·5111	0·5531	0·5804	0·6010	0·6172	0·6307	0·6424	0·6526	0·6695	0·6835	0·7053	0·7295	0·7568	0·7764	0·7914
1·8	0·3808	0·5314	0·5760	0·6050	0·6268	0·6441	0·6585	0·6709	0·6818	0·6998	0·7147	0·7380	0·7639	0·7933	0·8143	0·8304
2·0	0·3914	0·5503	0·5972(+1)	0·6278	0·6508	0·6691	0·6842	0·6974	0·7088	0·7279	0·7437	0·7684	0·7959	0·8272	0·8496	0·8667
2·5	0·4148	0·5923	0·6446	0·6788	0·7044	0·7248	0·7418	0·7565	0·7693	0·7907	0·8086	0·8364	0·8676	0·9032	0·9288	0·9484
3·0	0·4348	0·6289	0·6860	0·7232	0·7512	0·7735	0·7920	0·8081	0·8222	0·8456	0·8652	0·8959	0·9303	0·9698	0·9983	1·0201
3·5	0·4523	0·6616	0·7228	0·7628	0·7929	0·8169	0·8369	0·8542	0·8694	0·8947	0·9159	0·9491	0·9864	1·0294	1·0605	1·0844
4·0	0·4680	0·6911	0·7563	0·7988	0·8308	0·8564	0·8776	0·8961	0·9123	0·9393	0·9619	0·9974	1·0373	1·0837	1·1171	1·1430
4·5	0·4823	0·7183	0·7871	0·8319	0·8657	0·8926	0·9151	0·9346	0·9517	0·9803	1·0042	1·0419	1·0842	1·1336	1·1693	1·1969
5·0	0·4954	0·7435	0·8156	0·8626	0·8980	0·9263	0·9498	0·9703	0·9882	1·0183	1·0434	1·0831	1·1278	1·1799	1·2177	1·2471
6	0·5189	0·7892	0·8673	0·9183	0·9566	0·9873	1·0129	1·0351	1·0546	1·0873	1·1147	1·1580	1·2068	1·2641	1·3057	1·3382
7	0·5396	0·8299	0·9135(0)	0·9680	1·0090	1·0418	1·0692	1·0930	1·1139	1·1490	1·1784	1·2249	1·2775	1·3394	1·3845	1·4197
8	0·5582	0·8670	0·9554	1·0131	1·0566	1·0914	1·1204	1·1457	1·1678	1·2050	1·2362	1·2857	1·3418	1·4078	1·4561	1·4939
9	0·5750	0·9010	0·9940	1·0546	1·1003	1·1369	1·1674	1·1940	1·2173	1·2566	1·2894	1·3415	1·4008	1·4707	1·5219	1·5621
10	0·5905	0·9325	1·0298(0)	1·0932	1·1409	1·1792	1·2111	1·2389	1·2633	1·3044	1·3388	1·3935	1·4557	1·5291	1·5831	1·6255
15	0·6540	1·0646	1·1796(0)	1·2546	1·3110	1·3562	1·3941	1·4270	1·4559	1·5047	1·5457	1·6111	1·6855	1·7741	1·8396	1·8913
20	0·7031	1·1696	1·2988	1·3829	1·4463	1·4971	1·5396	1·5766	1·6092	1·6641	1·7103	1·7841	1·8684	1·9691	2·0438	2·1030
25	0·7436	1·2582	1·3994	1·4913	1·5605	1·6160	1·6625	1·7029	1·7385	1·7987	1·8492	1·9302	2·0227	2·1337	2·2162	2·2817
30	0·7784	1·3355	1·4873	1·5860	1·6603	1·7199	1·7698	1·8133	1·8515	1·9162	1·9706	2·0578	2·1576	2·2775	2·3668	2·4379
40	0·8366	1·4676	1·6373	1·7475	1·8306	1·8971	1·9530	2·0016	2·0443	2·1168	2·1778	2·2756	2·3878	2·5229	2·6239	2·7045
50	0·8847	1·5790	1·7639	1·8839	1·9743	2·0468	2·1076	2·1605	2·2071	2·2861	2·3526	2·4594	2·5820	2·7301	2·8409	2·9295
100	1·0523	1·9828	2·2239	2·3784	2·4954	2·5893	2·6681	2·7367	2·7972	2·8998	2·9863	3·1257	3·2861	3·4808	3·6273	3·7450
200	1·2515	2·4912	2·8010	3·0011	3·1517	3·2725	3·3739	3·4623	3·5402	3·6726	3·7843	3·9645	4·1725	4·4260	4·6173	4·7716
500	1·6442	3·3713	3·8018	4·0792	4·2878	4·4552	4·5958	4·7184	4·8265	5·0103	5·1655	5·4164	5·7065	6·0613	6·3302	6·5477
1000	1·8716	4·2403	4·7901	5·1438	5·4097	5·6231	5·8024	5·9586	6·0965	6·3310	6·5291	6·8497	7·2208	7·6757	8·021	8·301
2000	2·2258	5·3350	6·0352	6·4851	6·8231	7·0945	7·3224	7·5211	7·6964	7·995	8·247	8·655	9·128	9·709	10·151	10·509
5000	2·7988	7·2304	8·1910	8·808	9·270	9·642	9·954	10·226	10·467	10·876	11·221	11·781	12·431	13·229	13·837	14·331
10000	3·3284	9·102	10·320	11·101	11·687	12·158	12·553	12·898	13·202	13·720	14·158	14·868	15·692	16·705	17·477	18·105
20000	3·9581	11·461	13·003	13·991	14·732	15·328	15·828	16·264	16·649	17·304	17·859	18·757	19·801	21·805	22·063	22·860

Figures in brackets give differences in the last digit between the values given in the table and some exact values found in the literature. The accuracy is lower in the region marked off by broken lines.

parameters β and σ are believed to be convenient for interpolation over most parts of the table. This is clearly not true for decelerated flow approaching the conditions when the velocity layer separates. Although such interpolation would give the sort of accuracy needed for many practical problems, higher accuracy may sometimes be needed for some value of σ not given. It is then a simple matter to calculate new values of (b_0'/B) from the series given in Table 2.

4.2 *Accuracy of Table* 3

The series from which the values of (b_0'/B) given in Table 3 were calculated are asymptotically accurate for high values of σ. For sufficiently large σ therefore the figures should be correct to one place in the last digit. For $\sigma \leqslant 1$ however the accuracy may not be so high.

Some idea of the accuracy of the values may be obtained by comparing with exact solutions quoted in the literature. This is done in Table 3 by giving in brackets the differences in the final digit between the present values and exact solutions given in the literature. The exact values were taken from Mickley *et al.* [7], Merk [4], Livingood and Donoughe [8] and Howe and Mersman [9]. It should be realised, however, that exact solutions quoted in the literature are found to disagree with each other by up to three units in the fourth significant digit.

Exact calculations made since Table 3 was drawn up, using an entirely different method, have largely confirmed the figures in the table. Many values can be in error by one unit in the last place due to rounding off. This is, in fact, the case. Apart from these, however, the only serious errors in the table are for $\sigma = 0{\cdot}5$ and $0{\cdot}6$ but even so only amount to 3 units in the last significant digit. The results of exact calculations are to be published elsewhere.

No exact calculations have, however, been made for the region marked off in the table as inaccurate. Values in this region are almost certainly inaccurate.

4.3 *Other functions evaluated from* (b_0'/B)

It was shown in Paper 3 that a number of other functions related to the *b*-boundary layer may be evaluated from (b_0'/B). For ease of reference, and because many of the formulae take on a special form when no mass flows through the interface, the relevant formulae are listed below:

$$\frac{\Delta_4^2}{\nu}\frac{\mathrm{d}u_G}{\mathrm{d}x} = \frac{\beta}{(b_0'/B)^2} \tag{22}$$

$$\frac{u_G}{\nu}\frac{\mathrm{d}\Delta_4^2}{\mathrm{d}x} = \frac{2(1-\beta)}{(b_0'/B)^2} \tag{23}$$

$$\frac{\Delta_2^2}{\nu}\frac{\mathrm{d}u_G}{\mathrm{d}x} = \frac{\beta}{\sigma^2}\left(\frac{b_0'}{B}\right)^2 \tag{24}$$

$$\frac{u_G}{\nu}\frac{\mathrm{d}\Delta_2^2}{\mathrm{d}x} = \frac{2(1-\beta)}{\sigma^2}\left(\frac{b_0'}{B}\right)^2 \tag{25}$$

$$\frac{\Delta_2}{\Delta_4} = \frac{1}{\sigma}\left(\frac{b_0'}{B}\right)^2 \tag{26}$$

$$g^* = \frac{\gamma}{\Delta_4} = \gamma\left(\frac{1}{\nu\beta}\frac{\mathrm{d}u_G}{\mathrm{d}x}\right)^{1/2}\left(\frac{b_0'}{B}\right) \tag{27}$$

$$X = \frac{\Delta_4\delta_4}{\nu}\frac{\mathrm{d}u_G}{\mathrm{d}x} = \frac{\beta}{f_0''}\frac{1}{(b_0'/B)} \tag{28}$$

$$Y = \frac{1}{\gamma}\left(\frac{\delta_4}{u_G}\right)^{1/2}\frac{\mathrm{d}}{\mathrm{d}x}\left\{\Delta_4^3\left(\frac{u_G}{\delta_4}\right)^{3/2}\right\} = \frac{3}{2}\frac{\sigma f_0''}{(b_0'/B)^3} \tag{29}$$

$$W = \frac{\Delta_2^{1/2}\delta_4^{3/2}}{\nu}\frac{\mathrm{d}u_G}{\mathrm{d}x} = \frac{\beta(b_0'/B)^{1/2}}{\sigma^{\frac{1}{2}}(f_0'')^{3/2}} \tag{30}$$

$$Z = \frac{1}{\gamma}\left(\frac{\delta_4}{u_G}\right)^{1/2}\frac{\mathrm{d}}{\mathrm{d}x}(u_G\Delta_2)^{3/2} = \frac{3}{2}\frac{(b_0'/B)^{3/2}}{(\sigma f_0'')^{1/2}}. \tag{31}$$

In the literature many functions are written in terms of the distance x of the point in question from the start of the boundary layer. In terms of the present formulation of similar solutions some of these functions are:

$$Nu/Re^{1/2} = \frac{1}{(2-\beta)^{1/2}}\left(\frac{b_0'}{B}\right) \tag{32}$$

$$\frac{\Delta_4 Re^{1/2}}{x} = \frac{(2-\beta)^{1/2}}{(b_0'/B)} \tag{33}$$

$$\frac{\Delta_2 Re^{1/2}}{x} = \frac{(2-\beta)^{1/2}}{\sigma}\left(\frac{b_0'}{B}\right) \tag{34}$$

Vol. 3 1961

where the Nusselt number Nu and the Reynolds number Re have local values.

5. CURVES OF FUNCTIONS OBTAINED FROM TABLE 3

5.1 *General*

Curves have been drawn showing the relationships between many of the functions occurring on the left-hand sides of equations (22) to (31). Some interesting features about the curves will be indicated but their application for calculating functions in non-similar boundary layers will not be discussed. This is to be done in other papers in the series.

In Papers 1 and 2 it was shown that, in order to use the "similar" solutions to the velocity equation to obtain information about non-similar boundary layers, tables or curves were needed showing the variation of a quantity denoted by F_2 with the parameter $(\delta_2^2/\nu)(\mathrm{d}u_G/\mathrm{d}x)$. The latter is clearly a pressure gradient parameter related to the momentum boundary layer thickness δ_2 and F_2, which is $(u_G/\nu)(\mathrm{d}\delta_2^2/\mathrm{d}x)$, is a measure of the rate of growth of the momentum thickness with distance x.

Figures 1(a, b) and 2(a, b) give analogous relationships for thicknesses associated with the b-boundary layer. The relevant functions have been multiplied by an appropriate power of σ in order to bring closer together curves for different values of σ. Early forms of these curves for one value of σ, namely $\sigma = 0{\cdot}7$, were given by Smith and Spalding [10].

5.2 *Figure* 1(a)

This figure, which applies to the conduction thickness Δ_4, shows the relationship for accelerated and slightly decelerated flows. Because the wall gradient (b_0'/B) is almost exactly proportional to $\sigma^{1/3}$ when σ is large, the multiplying factor in this figure is $\sigma^{2/3}$. As σ becomes very

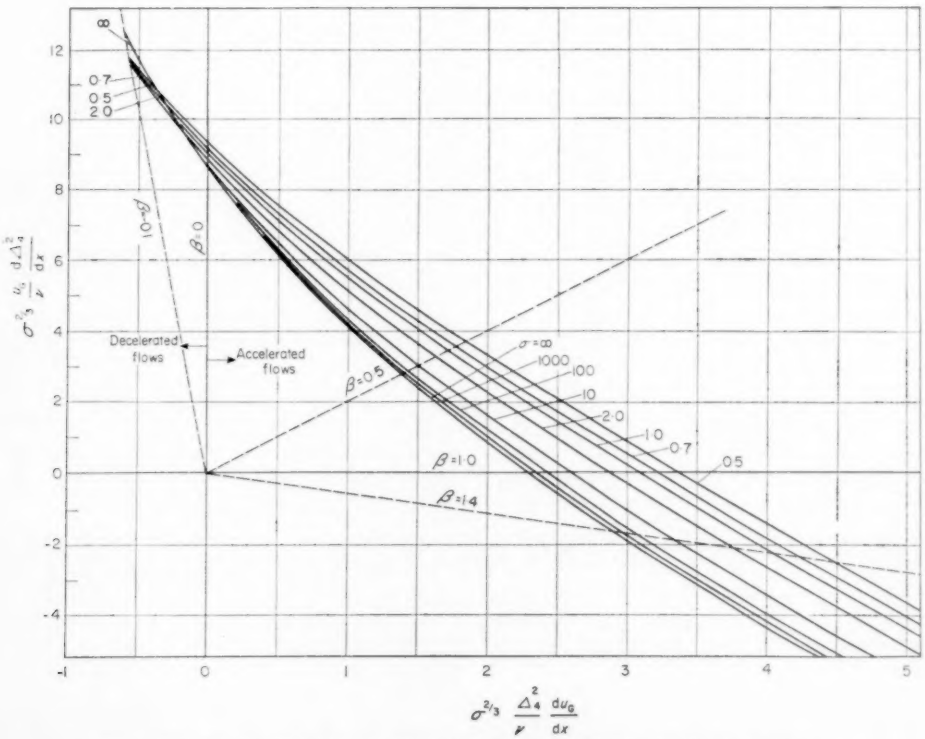

FIG. 1(a) Conduction thickness Δ_4, accelerated and slightly decelerated flows.

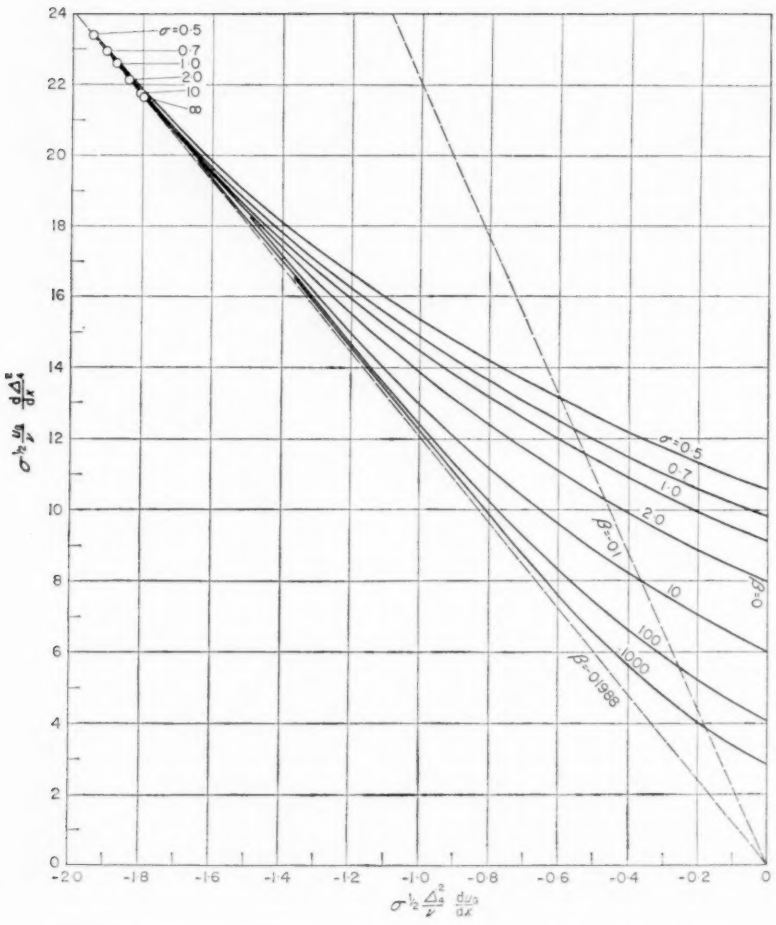

FIG. 1(b) Conduction thickness Δ_4, decelerated flows. ○ Separation points.

large the curves clearly tend to the asymptotic curve shown as $\sigma = \infty$.

It is clear from the curves for decelerated flows shown in this figure, which extend as far as $\beta = -0{\cdot}1$, that the wall gradient (b_0'/B) is not proportional to $\sigma^{1/3}$ in the lower part of the range covered. Hence the cross-over of the curves in this region. For more highly decelerated flows the curves diverge rapidly, particularly those for high σ.

Because of the scale of this figure it was convenient to omit parts corresponding to highly accelerated flows. Since the lines are only slightly curved in this region it is easy to see how they continue downwards and to the right.

5.3 *Figure* 1(b)

In section 3.3 it was noted that for the separation point (b_0'/B) is proportional to $\sigma^{1/4}$. The curves corresponding to Fig. 1(a), but for decelerated flows, have therefore been drawn using the multiplying factor $\sigma^{1/2}$. The separation points for a number of values of σ are shown on this figure.

There is some uncertainty about the shapes of these curves as only three values of β could be used from the present results. The curve for

Vol. 3 1961

$\sigma = 0{\cdot}7$ was drawn in using the results given by Livingood and Donoughe [8]. The other curves were then made to have the same general shape as this between $\beta = -0{\cdot}1$ and $\beta = -0{\cdot}1988$.

For $\sigma = \infty$ only the separation point is included because for both $\beta = 0$ and $\beta = -0{\cdot}1$ the relevant point is at the origin.

5.4 *Figure* 2(a)

This figure, which relates to the convection thickness Δ_2, corresponds to Fig. 1(a). The curves have not been extended into the region of decelerated flow, however, as the shapes of the curves could not be judged as was done for the earlier figure.

It was again convenient to omit the region of highly accelerated flows.

5.5 *Figure* 2(b)

This figure relates to the convection thickness Δ_2 for decelerated flows. The scale of the figure did not allow the curves for $\sigma > 1000$ to be included and parts of the curves for $\sigma \geqslant 10$ had to be omitted because their shapes could not be judged with any certainty from that for $\sigma = 0{\cdot}7$.

Again a few separation points are indicated.

5.6 *Figures* 3 *and* 4

In suggesting an approximate method for calculating rates of heat transfer between any laminar fluid stream and a solid surface, Spalding [11] set up differential equations which could be integrated numerically in a fairly straightforward manner. Referring to expressions defined in equations (28) to (31), the differential equation

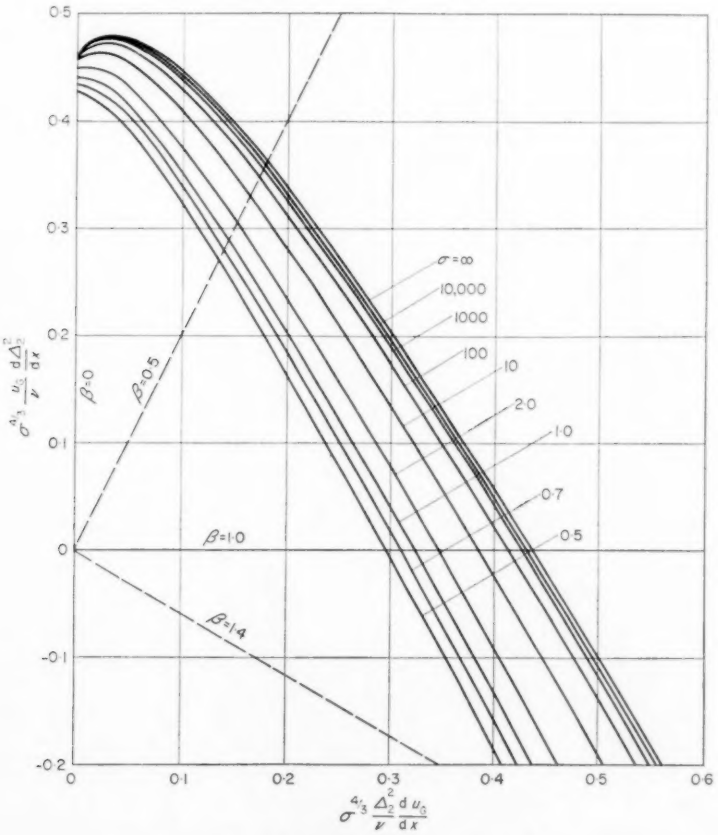

FIG. 2(a) Convection thickness Δ_2 accelerated flows.

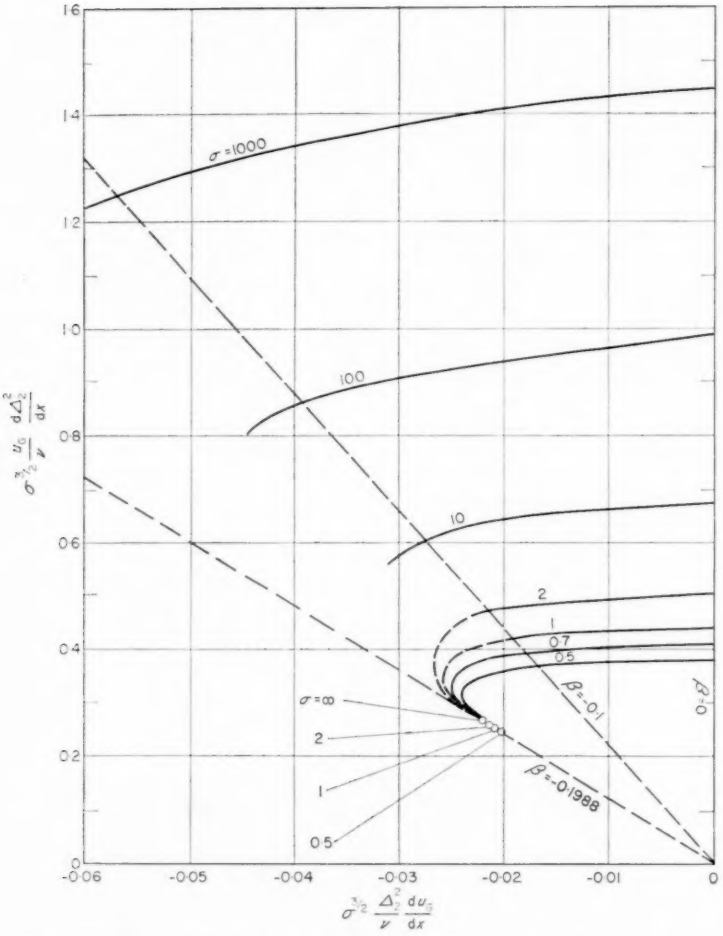

FIG. 2(b) Convection thickness Δ_2 decelerated flows. ○ Separation points.

for evaluating the conduction thickness Δ_4 was of the form:

$$Y = Y(X) \tag{35}$$

and for the convection thickness Δ_2 the equation was:

$$Z = Z(W). \tag{36}$$

In these equations the functions Y and Z are measures of the rate of growth of the relevant boundary layer thickness with distance x along the wall, and the functions X and W are curvature parameters which are a measure of the amount by which the b-boundary layer penetrates into regions where the velocity layer is appreciably curved. The forms of the functions Y and Z were obtained from the exact "similar" solutions to the boundary layer equations.

When plotting Y and Z as functions of X and W respectively, it was found that exact similar solutions for a wide range of Prandtl number were close to a single curve. Figs. 3 and 4 show these relationships obtained from the present results. Curves for only a few values of σ are drawn on these figures because such curves are very close together on this scale.

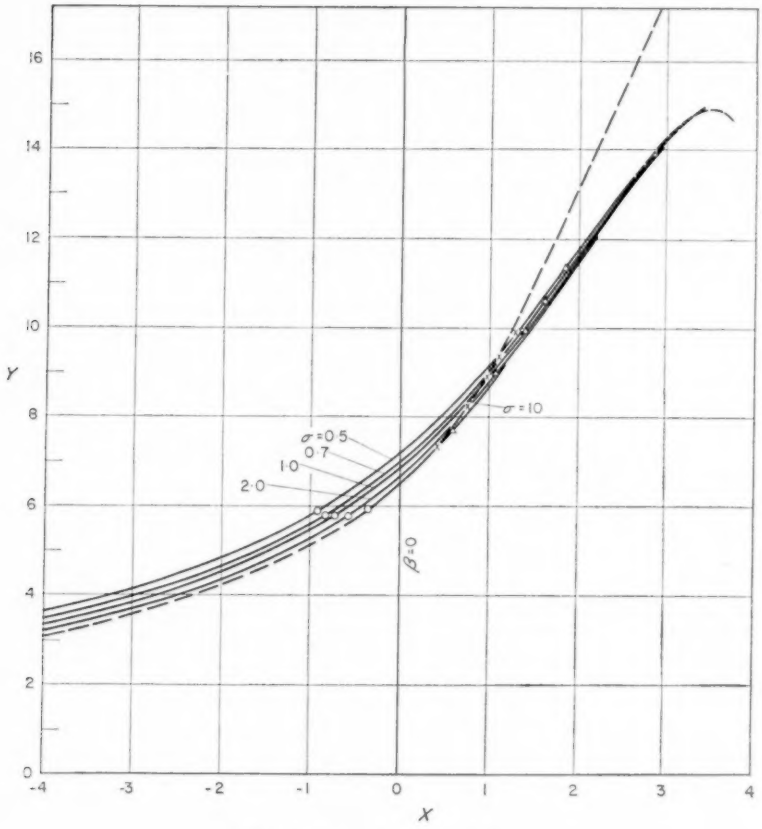

FIG. 3. Y as a function of X.

— — — σ large (from Paper 3).
——— present solutions.
- - - - - inaccurate region.

○ $\beta = -0{\cdot}1$
× $\beta = 0{\cdot}5$
△ $\beta = 1{\cdot}0$.

When $\sigma \geqslant 0{\cdot}5$, therefore, the assumption of a single curve for the relationships given in equations (35) and (36) would introduce only a small error in the estimation of boundary layer thicknesses for accelerated and slightly decelerated flows. For conditions approaching separation, however, the error would increase rapidly. These conditions occur for large negative values of the abscissae X and W, beyond the ranges of Figs. 3 and 4. The separation points themselves correspond to $X = -\infty$, $Y = 0$ and $W = -\infty$, $Z = \infty$ respectively.

In Figs. 3 and 4 the line for large σ was obtained from the approximate results given in Paper 3.

It should be noted that when $\sigma < 1{\cdot}0$ and $\beta > 2{\cdot}0$ the present results are inaccurate. This inaccurate region has already been indicated in Table 3. This shows up in Figs. 3 and 4 as a reversal in the slopes of the curves for large values of the abscissa.

In Fig. 3 all the results for $\sigma > 20$, except that for the separation point, are close to the point $X = 0$, $Y = 6{\cdot}41$, the well-known solution obtained by Lighthill [12].

The points on Figs. 3 and 4 give a few values of the parameter β. The curves from the present solutions have been extended beyond $\beta = -0{\cdot}1$ by giving them the same shape as those for $\sigma = 0{\cdot}7$ and σ-large whose shapes were known.

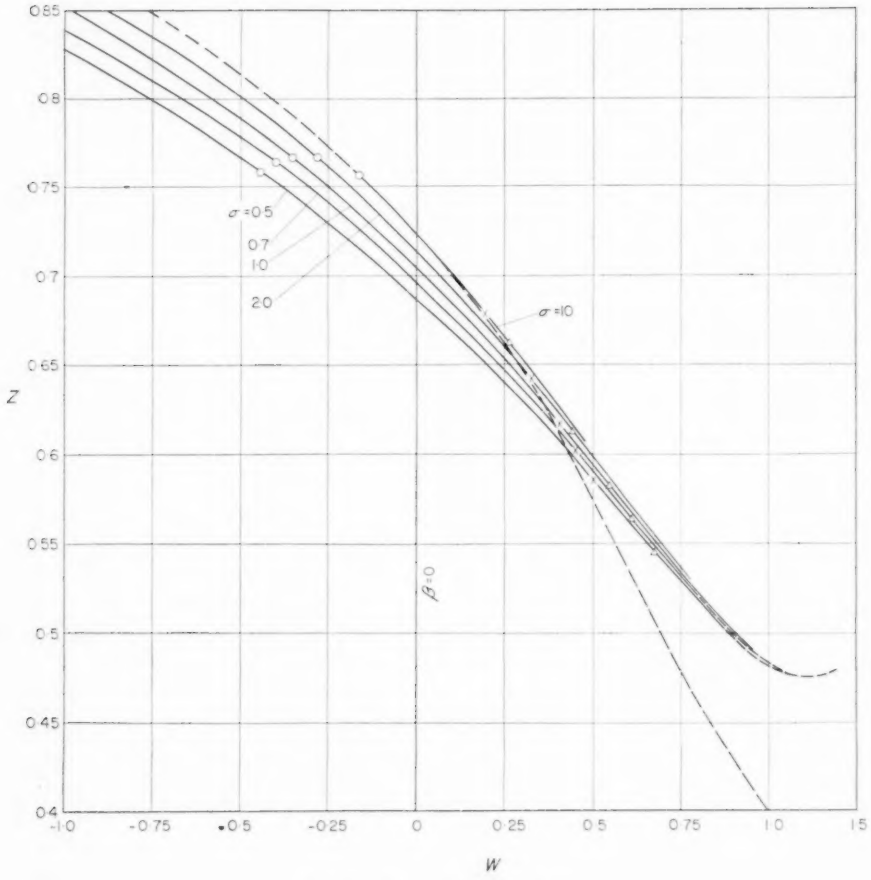

FIG. 4. Z as a function of W.

— — — σ large (from Paper 3).
——— present solutions.
- - - - - inaccurate region.

○ $\beta = -0{\cdot}1$
× $\beta = 0{\cdot}5$
△ $\beta = 1{\cdot}0$.

6. APPROXIMATE METHOD NEAR SEPARATION

It has been seen that, if it is greater than 0·5, the Prandtl/Schmidt number has only a small effect when boundary layer problems are formulated in terms of the functions X, Y, W and Z. It is, of course, for the same reason that the asymptotic series of Table 2 give good accuracy. The close connection between the present results and this approximate formulation may be seen by comparing, say, equations (10) and (29). The rate of growth parameter Y is related to the integral E of the present paper by:

$$Y = \frac{E^3}{3}. \tag{37}$$

This immediately suggests that near the point of separation the parameter Y should be replaced by Y_{sep} given by:

$$Y_{\text{sep}} = \frac{1}{\gamma}\left(\frac{\partial^2 u}{\partial y^2}\right)_0^{-1/3} \frac{\mathrm{d}}{\mathrm{d}x}\left\{\Delta_4^4\left(\frac{\partial^2 u}{\partial y^2}\right)_0^{4/3}\right\}$$

$$= \frac{4}{3}\frac{\sigma f'''_0}{(b'_0/B)^4} \tag{38}$$

where the second form is written in terms of

"similar" solutions. The corresponding curvature parameter is:

$$X_{\text{sep}} = \frac{(\partial^4 u/\partial y^4)_0 \Delta_4^2}{(\partial^2 u/\partial y^2)_0} = \frac{f_0^{\text{v}}}{(f_0''')(b_0'/B)^2} \qquad (39)$$

the second form again being in terms of "similar" solutions. For the case of no mass transfer, the gradients of f occurring in the last expression are given by $f_0''' = -\beta$ and $f_0^{\text{v}} = (2\beta - 1)(f_0'')^2$.

It should be noted that $(\partial^3 u/\partial y^3)_0$ cannot be used in the numerator of X_{sep} because it is identically zero for all β when no mass flows through the wall. For very large σ it may be shown that Y_{sep} tends to the value 21·599.

In the same way other functions can be derived to replace W and Z near the point of separation.

7. CONCLUSIONS

(a) Using the formulae and coefficients given in Table 2 and the values of f_0'' of Table 1, the wall gradient (b_0'/B) can be evaluated accurately for a wide range in the parameter β and for any value greater than 0·5 of the Prandtl/Schmidt number σ.

(b) From values of (b_0'/B) many other functions associated with the b-boundary layer can also be evaluated from the formulae of section 4.3.

(c) Using a different method of calculation more accurate results than those in Table 3 have now been obtained. They include results for values of β, in particular many negative values, not covered in the present paper as well as a range of low values of σ. These are to be published elsewhere.

ACKNOWLEDGMENTS

The work forms part of the research programme of the Division of Food Preservation, C.S.I.R.O., Homebush, N.S.W., Australia. The author is particularly indebted to Miss J. D. Hayhurst who was responsible for much of the computation associated with the present work.

REFERENCES

1. D. B. Spalding, Mass transfer through laminar boundary layers—1. The velocity boundary layer, *Int. J. Heat Mass Transfer* **2**, 15–32 (1961). Referred to as Paper 1.
2. D. B. Spalding and H. L. Evans, Mass transfer through laminar boundary layers—2. Auxiliary functions for the velocity boundary layer. *Int. J. Heat Mass Transfer* **2**, 199–221 (1961). Referred to as Paper 2.
3. D. B. Spalding and H. L. Evans, Mass transfer through laminar boundary layers—3. Similar solutions of the b-equation, *Int. J. Heat Mass Transfer* **2**, 314–341 (1961). Referred to as Paper 3.
4. H. J. Merk, Rapid calculations for boundary-layer transfer using wedge solutions and asymptotic expansions, *J. Fluid Mech.* **5**, 460 (1959).
5. V. M. Falkner, A further investigation of the boundary layer equation, *British Aero. Res. Council, R. and M.* 1884 (1937).
6. V. M. Falkner, A simplified calculation of the laminar boundary layer, *British Aero. Res. Council, R. and M.* 1895 (1941).
7. H. S. Mickley, R. C. Ross, A. L. Squyers and W. E. Stewart, Heat, mass and momentum transfer for flow over a flat plate with blowing and suction, *N.A.C.A.* T.N.3208 (1954).
8. J. N. B. Livingood and P. L. Donoughe, Summary of laminar boundary layer solutions for wedge-type flow over convection- and transpiration-cooled surfaces *N.A.C.A.* T.N.3588 (1955).
9. J. T. Howe and W. A. Mersman, Solutions of the laminar and compressible boundary-layer equations with transpiration which are applicable to the stagnation regions of axisymmetric blunt bodies, *N.A.S.A.* T.N. D-12 (1959).
10. A. G. Smith and D. B. Spalding, Heat transfer in a laminar boundary layer with constant fluid properties and constant wall temperature, *J. Roy. Aero. Soc.* **62**, 60 (1958).
11. D. B. Spalding, Heat transfer from surfaces of non-uniform temperature, *J. Fluid Mech.* **4**, 22 (1958).
12. M. J. Lighthill, Contributions to the theory of heat transfer through a laminar boundary layer, *Proc. Roy. Soc.* A **202**, 359 (1950).

Int. J. Heat Mass Transfer. Vol. 3, pp. 42–54. Pergamon Press 1961. Printed in Great Britain.

RADIATIVE HEAT EXCHANGE BETWEEN SURFACES WITH SPECULAR REFLECTION

E. R. G. ECKERT* and E. M. SPARROW*

Heat Transfer Laboratory, Department of Mechanical Engineering,
University of Minnesota, Minneapolis, Minnesota

(*Received* 14 *July* 1960; *and in revised form* 13 *January* 1961)

Abstract—A method has been developed for calculating the radiant interchange in an enclosure containing specularly reflecting surfaces. Consideration is given to systems composed of two specular surfaces and an unrestricted number of black surfaces. The method is illustrated by numerical examples and comparisons are made with the heat transfer results for diffusely reflecting surfaces.

Résumé—Une méthode de calcul des échanges thermiques par rayonnement, dans une enceinte ayant des surfaces à réflexion spéculaire, a été développée. Les systèmes composés de deux surfaces spéculaires et d'un nombre illimité de surfaces noires ont été considérés. La méthode est illustrée par des exemples numériques et les résultats sont comparés aux résultats de transmission de chaleur obtenus pour des surfaces à réflexion diffuse.

Zusammenfassung—Es wurde eine Methode entwickelt, den Strahlungsaustausch in einem von spiegelnd reflektierenden Oberflächen begrenzten Hohlraum zu berechnen. Besondere Berücksichtigung fanden Systeme aus zwei spiegelnden Oberflächen und einer unbeschränkten Zahl schwarzer Flächen. Die Methode wird durch numerische Beispiele erläutert und die übertragenen Wärmemengen werden mit denen diffus strahlender Oberflächen verglichen.

Аннотация—Разработан метод вычисления лучистого теплообмена между зеркально отражающими поверхностями. Рассмотрены системы, состоящие из двух зеркальных поверхностей и неограниченного количества чёрных поверхностей. Метод иллюстрируется численными примерами, даны сравнения с результатами по теплообмену для случая диффузно отражающих поверхностей.

Vol. 3 1961

NOMENCLATURE

- A surface area;
- e_b black-body emissive power;
- F angle factor;
- H incident radiant flux per unit time and area;
- h spacing between parallel plates;
- k summation index;
- L plate length
- Q overall rate of heat loss;
- q local heat loss rate per unit area;
- s distance between surface elements;
- T absolute temperature;
- X dimensionless distance, x/L;
- x co-ordinate measuring distance along plate;
- α absorptivity;
- γ spacing ratio, h/L;
- θ opening angle, see Fig. 7;
- ϵ emissivity;
- ϵ_i interchange emissivity;
- ρ reflectivity;
- σ Stefan–Boltzmann constant.

INTRODUCTION

ENERGY exchange by thermal radiation has in the literature been discussed almost exclusively for diffusely reflecting surfaces. Experiments [1, 2] on the spacial distribution of the reflected energy, on the other hand, indicate that the reflection on many surfaces of engineering importance actually is closer to the limit of specular than of perfectly diffuse reflection, even if this is not clearly evident by visual inspection of the surfaces. This will be amplified in the final section of the report.

* Professor of Mechanical Engineering.

The present paper develops a method of calculating the heat exchange between plane surfaces with specular reflection and presents numerical comparisons between specular and diffuse heat transfer results for a few typical geometries.

Before going into the analysis of the new calculation method, some consideration will be given to a geometry for which the analysis of radiative heat exchange with specular as well as diffuse reflection has been made in the past, namely, for two concentric cylinders or spheres. The relationships describing heat exchange by radiation between the two surfaces will be used to obtain information on the order of magnitude of the difference between specularly and diffusely reflecting surfaces.

Heat exchange between concentric spheres or cylinders with specularly and diffusely reflecting surfaces

We will consider two co-axial cylinders of infinite length or alternatively, two concentric spheres. The relations for these two geometries are identical and for the sake of simplicity we will in the future talk only about the spherical arrangement. Parameters for the inner sphere may be identified by a subscript 1 and those for the outer sphere by a subscript 2. A denotes the surface area, ϵ the surface emissivity, and e_b the black body emissive power (heat flux emitted per unit area and unit time). The heat loss of the inner surface 1 and the heat gain of the outer surface 2 is then described by the equation

$$Q = A_1 \, \epsilon_i \, (e_{b1} - e_{b2}). \tag{1}$$

The equations which specify the interchange emissivity ϵ_i are derived in the various textbooks on heat transfer for the situation where the surfaces emit according to Lambert's cosine law (for instance in Ref. 3). The relation for diffusely reflecting surfaces is

$$\frac{1}{\epsilon_i} = \frac{1}{\epsilon_1} + \frac{A_1}{A_2}\left(\frac{1}{\epsilon_2} - 1\right) \tag{2}$$

and for specularly reflecting surfaces

$$\frac{1}{\epsilon_i} = \frac{1}{\epsilon_1} + \frac{1}{\epsilon_2} - 1. \tag{3}$$

Introduction of monochromatic emissivities and emissive powers into those equations results in the heat exchange in a small band at a certain wave length. Usually, engineering calculations require knowledge of the total amount of energy transfer in the whole wave length range. For gray surfaces with emissivities independent of wave length, equation (1) specifies this energy exchange provided that total emissive powers are introduced into this equation. They are described by Stefan–Boltzmann's relation $e_b = \sigma T^4$. For surfaces with wave length-dependent emissivities, the radiative heat loss Q has to be calculated with equations (1) to (3) at first for monochromatic radiation, and the total heat loss is obtained by an integration of the monochromatic heat loss over the whole wave length range. This statement holds not only for the present section, but for all calculations in this paper.

The relations (1) to (3) may be used to establish the extent of the differences between specularly and diffusely reflecting surfaces which can be expected for the specific geometry. For the limiting situation that the inner sphere is very small compared to the outer one ($A_1/A_2 \to 0$), the relation for the interchange emissivity in diffuse reflection is $\epsilon_i = \epsilon_1$. Equation (3) remains unchanged. If one specifies in addition that both surfaces have the same emissivity ($\epsilon_2 = \epsilon_1$), equation (3) becomes $(1/\epsilon_i) = (2/\epsilon_1) - 1$. For small values of ϵ_1 the relation is approximated by $\epsilon_i = \epsilon_1/2$. This indicates that heat exchange for diffusely reflecting surfaces with equal emissivities is in the present geometry up to two times as large as for specularly reflecting surfaces.

The differences may become even larger when the emissivities of the two surfaces have different values. Let us assume surface 1 to be a black surface ($\epsilon_1 = 1$). This makes the interchange emissivity for diffuse reflection and $A_1/A_2 \to 0$ also equal to 1. The interchange emissivity ϵ_i for specularly reflecting surfaces, on the other hand, is equal to ϵ_2. It may, therefore, be by an order of magnitude smaller for specular reflection, when the emissivity ϵ_2 has a small value.

The differences which have just been established are, of course, extremes. It can, however, easily be checked that differences of the same order of magnitude may arise even

when the ratio of the two surface areas is not extremely small and when the emissivities have other values. It can also be expected that the geometries investigated in this section exhibit differences which will not be reached for other geometries. A slight eccentricity of the two surfaces, for instance, should bring the heat fluxes for diffuse and specular reflection more closely together.

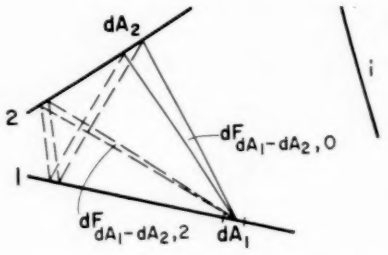

Fig. 1. Typical enclosure with two non-black surfaces.

HEAT EXCHANGE BETWEEN PLANE SURFACES WITH SPECULAR REFLECTION

Radiant interchange process

Consider a space which is enclosed by a number of plane surfaces. The temperature may be locally uniform on each of the surfaces, but may be different for the various surfaces. The space is filled by a medium which is perfectly transmittant and which does not participate in the radiative energy exchange. The surfaces emit energy by thermal radiation and the directional distribution of the emitted energy flux may follow Lambert's cosine law.* The analysis in this paper will be developed for an enclosure with two specular-reflecting surfaces, assuming that the rest of the surfaces are black. A calculation for a larger number of reflecting surfaces is straightforward, but soon becomes exceedingly involved. We will start by a consideration of the energy exchange between the two reflecting surfaces. Fig. 1 is a sketch of the two surfaces 1 and 2. Two area elements dA_1 and dA_2 may be located on the two surfaces. The heat flux emitted by the surface element dA_2 and traveling toward the element dA_1 can be expressed as

$$\epsilon_2 \, e_{b2} \, dA_2 \, dF_{dA_2-dA_1,0} \tag{4a}$$

where $dF_{dA_2-dA_1,0}$ denotes an "angle factor", i.e. that fraction of the energy emitted by dA_2 which impinges on dA_1. The first subscript $dA_2 - dA_1$ indicates radiative exchange between areas dA_2 and dA_1; while the second subscript 0 denotes direct interchange with zero reflections.

* Surfaces may approach Lambert's Law in emission while approaching specularity in reflection; see for example, copper oxide in Figs. 13-12 and 13-13 of Ref. 3.

Introducing the reciprocity relationship (Ref. 3, pp. 396–397)

$$dA_2 \, dF_{dA_2-dA_1} = dA_1 \, dF_{dA_1-dA_2}$$

expression (4a) can be rephrased as

$$\epsilon_2 \, e_{b2} \, dA_1 \, dF_{dA_1-dA_2,0}. \tag{4b}$$

The surface element dA_1 receives, in addition, radiative energy from dA_2 in an indirect way, for instance, on the path indicated by the dashed lines in Fig. 1. The energy arriving after two reflections is

$$\epsilon_2 \, e_{b2} \, \rho_1 \rho_2 \, dF_{dA_1-dA_2,2} \, dA_1 \tag{5}$$

$dF_{dA_1-dA_2,2}$ indicates the angle factor for the radiation traveling the dashed path in Fig. 1, with the second subscript 2 signifying that there have been two reflections. Energy also arrives at dA_1 after a larger number of reflections, for instance, after $2k$ reflections:

$$\epsilon_2 \, e_{b2} \, \rho_1^k \rho_2^k \, dF_{dA_1 \; dA_2,2k} \, dA_1. \tag{6}$$

The total energy emitted by dA_2 and arriving at dA_1 per unit area is obtained by a summation

$$\epsilon_2 \, e_{b2} \sum_0^\infty \rho_1^k \, \rho_2^k \, dF_{dA_1-dA_2,2k}. \tag{7}$$

The energy emitted by the whole surface area 2 and arriving at a unit area of dA_1 is

$$\epsilon_2 \, e_{b2} \sum_0^\infty \rho_1^k \, \rho_2^k \, F_{dA_1-A_2,2k} \tag{8}$$

where $F_{dA_1-A_2,2k}$ expresses the angle factor for radiation leaving surface 2 and arriving at dA_1 after $2k$ reflections on surfaces 1 or 2.

The surface element dA_1 receives also radiant

Vol. 3 1961

energy which originates at surface 1 and is reflected back to dA_1 by surface 2. The energy arriving is

after one reflection

$$\epsilon_1 e_{b1} F_{dA_1-A_1,1} \rho_2 \tag{9}$$

after three reflections

$$\epsilon_1 e_{b1} F_{dA_1-A_1,3} \rho_1 \rho_2^2 \tag{10}$$

after $2k + 1$ reflections

$$\epsilon_1 e_{b1} F_{dA_1-A_1,2k+1} \rho_1^k \rho_2^{k+1}. \tag{11}$$

The total amount of energy originating at surface 1 and arriving at dA_1 is again obtained by a summation

$$\epsilon_1 e_{b1} \sum_0^\infty \rho_1^k \rho_2^{k+1} F_{dA_1-A_1,2k+1}. \tag{12}$$

The surface element dA_1 will also receive radiation which is emitted by any of the black surfaces of the enclosure and arrives at the surface element after one or several reflections at surfaces 1 or 2. Let us consider the radiation originating from one of the black surfaces denoted by i. That part of the radiation for which the first reflection occurs at surface 2 can be treated formally in the same way as the expression (12), when the proper angle factor is introduced. The energy flux arriving at dA_1 after one or several reflections is

$$e_{bi} \sum_0^\infty \rho_1^k \rho_2^{k+1} F_{dA_1-A_i,2k+1}. \tag{13}$$

That part of the radiation for which the first reflection occurs at surface 1 will be described again by the same form as expression (8).

$$e_{bi} \sum_0^\infty \rho_1^k \rho_2^k F_{dA_1-A_i,2k}. \tag{14}$$

This expression also contains the radiation which arrives directly at dA_1.

The total flux H arriving at a unit area of surface 1 at the location of dA_1, either directly or after reflections from surfaces 1 and 2, can now be written as the sum of the expressions (8), (12), (13), and (14).

$$\left.\begin{aligned} H_1 = {} & \epsilon_1 e_{b1} \sum_0^\infty \rho_1^k \rho_2^{k+1} F_{dA_1-A_1,2k+1} \\ & + \epsilon_2 e_{b2} \sum_0^\infty \rho_1^k \rho_2^k F_{dA_1-A_2,2k} \\ & + \sum_{i=1}^n e_{bi} \left[\sum_0^\infty \rho_1^k \rho_2^{k+1} F_{dA_1-A_i,2k+1} \right. \\ & \left. + \sum_0^\infty \rho_1^k \rho_2^k F_{dA_1-A_i,2k}\right] \end{aligned}\right\} \tag{15}$$

The summation of radiation originating at black surfaces has to be extended over all n black surfaces. The net local heat loss per unit area at the element dA_1 finally can be expressed as the difference of the amount of radiation emitted by the surface and the amount absorbed by it.

$$q_1 = \epsilon_1 e_{b1} - \alpha_1 H_1. \tag{16}$$

The heat loss at any location of the reflecting surfaces can be calculated with equations (15) and (16) as soon as the various angle factors involved are known.

The overall net heat loss Q from surface 1 can be found from an equation similar to (16), with the modifications that the right side is multiplied by A_1 and the angle factors $F_{A_1-A_1}$, $F_{A_1-A_2}$, etc., are used in evaluating H. This same result can be obtained by integrating the local heat loss q over the area A_1.

Determination of angle factors

The angle factor for direct interchange $dF_{dA_1-dA_2,0}$ is given by the equation

$$dF_{d_1A-dA_2,0} = \frac{\cos\beta_1 \cos\beta_2}{\pi s^2} dA_2 \tag{17}$$

in which β denotes the angle between the line connecting the two area elements and the respective surface normal. s is the distance between the two surface elements. The angle factor $F_{dA_1-A_2,0}$ is obtained by an integration over the surface 2.

$$F_{dA_1-A_2,0} = \int_2 \frac{\cos\beta_1 \cos\beta_2}{\pi s^2} dA_2. \tag{18}$$

The angles β and the distance s have, of course, to be considered as functions of the location of dA_2.

The angle factor $F_{dA_1-A_2,\,2}$ is obtained by the following method, which is based on standard procedures in optics (see Fig. 2a). Consider the emitting area 2 as object and the planes 1 and 2 as mirrors. Mirror 1 creates an image 2_1 (Fig. 2a)

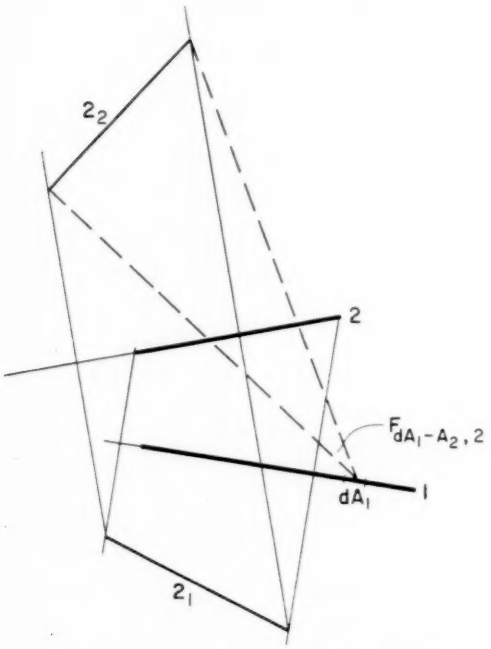

FIG. 2(a). Diagram illustrating angle factors $F_{dA_1-A_2,\,0}$ $F_{dA_1-A_2,\,2}$ etc.

of area 2. In turn, this first image 2_1 is reflected in mirror 2, creating image 2_2. The angle factor $F_{dA_1-A_2,\,2}$ is then identical with the angle factor between the area 2_2 and the element dA_1 for direct radiative interchange. It can be obtained from equation (18) when the area element dA_2 is located on the second image 2_2 and when the angle β_2 and the distance s are interpreted accordingly. Two more reflections on the mirrors 1 and 2 create a fourth image and the angle factor $F_{dA_1-A_2,\,4}$ is again identical with the angle factor for direct radiative interchange between the image 2_4 and the area element dA_1.

The angle factors $F_{dA_1-A_1,\,1}$, $F_{dA_1-A_1,\,3}$, and so on, are in the same way obtained by determination of the images 1_1, 1_3 and so on. Fig. 2(b) indicates the construction of these images.

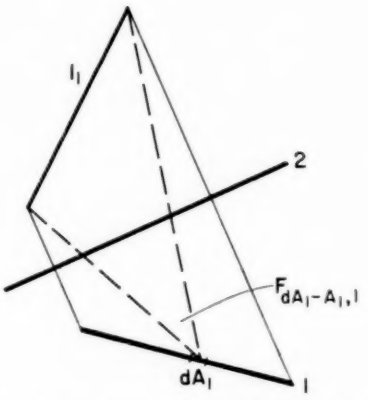

FIG. 2(b). Diagram illustrating angle factors $F_{dA_1-A_1,\,1}$ etc.

The angle factors $F_{dA_1-A,\,k}$ of any black surface are finally determined in the same way by constructing the images of the surface i in the mirrors 1 and 2.

In certain cases, the construction procedure as discussed above has to be modified to account for the fact that the participating areas may be too small to reflect the full images. Fig. 3

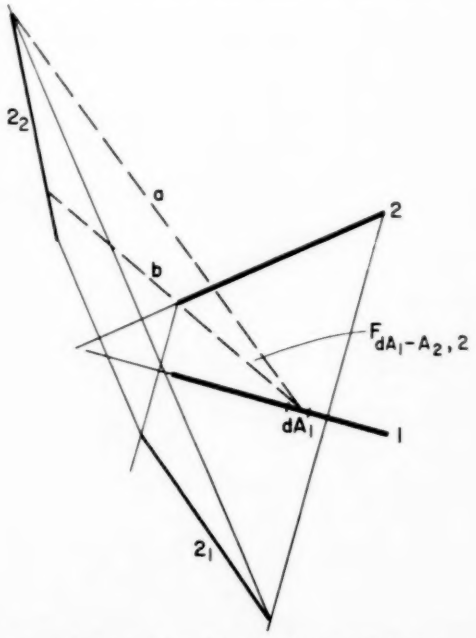

FIG. 3. Diagram illustrating partial use of images.

Vol. 3 1961

illustrates this point. Only that part of the image 2_2 between the rays a and b has to be used to determine the angle factor. Generally, that part of an image has to be considered from which the rays drawn towards the centre of dA_1 intersect area 2.

ILLUSTRATIVE RESULTS

It is useful to numerically illustrate the general method and, additionally, to make comparisons with results for diffusely reflecting surfaces. The particular situations treated below were selected on the basis of available exact solutions for gray, diffuse surfaces.

Two parallel plates of equal temperature

The sketch in Fig. 4 indicates two plates of width L arranged at a distance h. In the direction

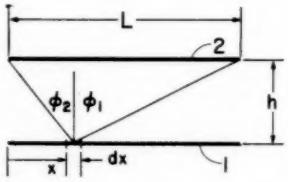

FIG. 4. Parallel plate system.

normal to the plane of drawing, the plates are taken to be infinite in extent. It will be assumed that the two plates are made of the same material so that they have equal radiation properties and that they are kept at the same temperature ($\epsilon_1 = \epsilon_2 = \epsilon$, $\rho_1 = \rho_2 = \rho$, $a_1 = a_2 = a$, $e_{b1} = e_{b2} = e_b = \sigma T^4$). The surroundings of the plates may be at a temperature of absolute zero so that no radiation enters the space between the two plates from the outside. The same condition for radiative exchange holds when the two plates are connected at their rim by two black surfaces at absolute zero temperature. Later on, the results will be generalized to account for a black surrounding at arbitrary temperature. The angle factor for an area element dA located at a distance x from the rim of plate 1 is, according to Ref. 3, p. 401,

$$F_0 = \tfrac{1}{2}(\sin\varphi_1 + \sin\varphi_2). \tag{19}$$

The angles φ_1 and φ_2 can be expressed by the length dimensions to obtain

$$F_0 = \tfrac{1}{2}\left[\frac{x}{\sqrt{(x^2+h^2)}} + \frac{L-x}{\sqrt{\{(L-x)^2+h^2\}}}\right] \tag{20}$$

It is not necessary to differentiate between radiation originating at surface 1 or 2 since both are at the same temperature. Accordingly, only one subscript is used for the angle factors to indicate the number of reflections. For k reflections, the image is located at a distance $(k+1)\,h$. The angle factor for this image is

$$F_k = \tfrac{1}{2}\left[\frac{x}{\sqrt{\{x^2+(k+1)^2\,h^2\}}} + \frac{L-x}{\sqrt{\{(L-x)^2+(k+1)^2\,h^2\}}}\right]. \tag{21}$$

The total flux H arriving at a unit surface area at the location of dA is obtained from equation (15) which simplifies to the following expression if use is made of the fact that the two emissivities and emissive powers are equal, that e_{bi} is equal to zero, and that no differentiation has to be made between the two types of angle factors in this equation.

$$H = \epsilon\, e_b \sum_0^\infty \rho^k\, F_k. \tag{22}$$

The relation (16) then determines the heat loss of the surface at location dA with the expression (22) for the incident flux H and the relation (21) for the angle factors. The following equation is obtained when, in addition, dimensionless parameters are introduced to characterize the length dimensions: $X = x/L$, $\gamma = h/L$

$$\frac{q}{\epsilon\sigma T^4} = 1 - \frac{a}{2}\left\{\sum_0^\infty \rho^k\left[\frac{X}{\sqrt{\{X^2+(k+1)^2\gamma^2\}}} + \frac{1-X}{\sqrt{\{(1-X)^2+(k+1)^2\gamma^2\}}}\right]\right\}. \tag{23}$$

The total heat loss of each one of the two plates is obtained in the same way by introducing the following relation for the average angle factor between two parallel plates

$$\bar{F}_k = \sqrt{\{1+(k+1)^2\gamma^2\}} - (k+1)\gamma = F_{A_1-A_2,\,k} \tag{24}$$

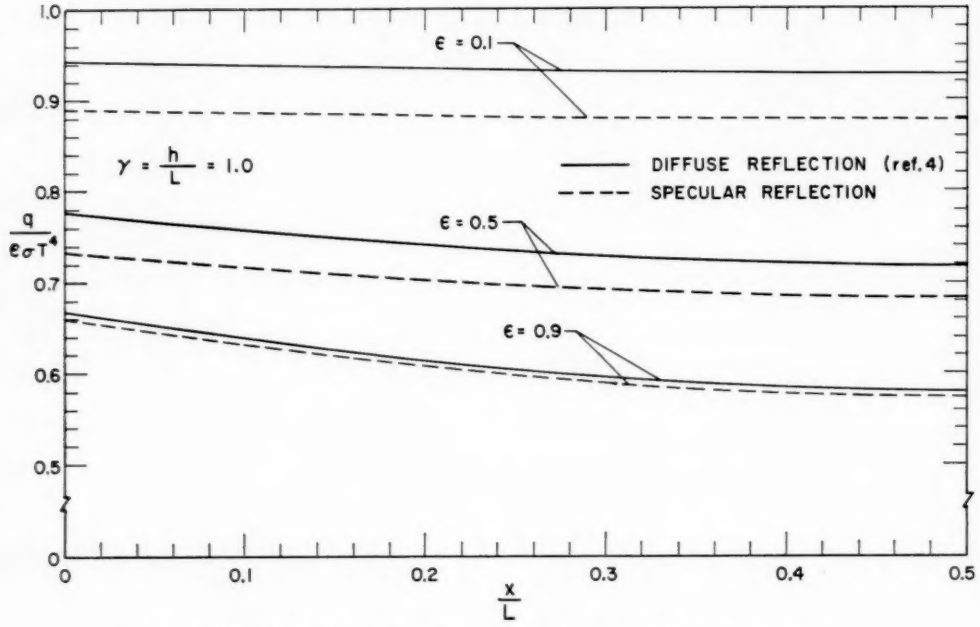

FIG. 5. Local heat flux results for parallel plate system with $\gamma = h/L = 1{\cdot}0$.

into equations (22) and (16). The following relation is obtained in this way

$$\frac{Q/L}{\epsilon\sigma T^4} = 1 - \alpha \sum_{0}^{\infty} \rho^k \left[\sqrt{\{1+(k+1)^2\gamma^2\}} - (k+1)\gamma\right]. \quad (25)$$

The infinite series in equations (23) and (25) have been evaluated on an electronic computer, type Remington–Rand 1103. The local heat loss on any of the parallel plates, made dimensionless by the energy emitted from the surface, is plotted in Figs. 5 and 6 over the dimensionless distance from the plate rim. The first of these is for a wide spacing, $h/L = 1$, while the second is for a close spacing, $h/L = 0{\cdot}05$. Curves are presented for emissivities 0·1, 0·5, and 0·9 as dashed lines, and the heat losses encountered by diffusely reflecting plates are also shown for comparison purposes as full lines. This last information was taken from the analysis published in Ref. 4.

The curves in Fig. 5 indicate that the heat loss of parallel plates is larger when the plates reflect diffusely. This can be explained by the fact that at each diffuse reflection the impinging ray is distributed in all directions and that by this process, in the average, the radiative flux has a better chance to escape through the opening between the plates. Additionally, the level of the curves increases with decreasing ϵ (increasing reflectivity), since radiative energy escapes not only as direct radiation, but also in the subsequent reflections. This increase in the heat loss in either reflection process is very slight for $\epsilon = 0{\cdot}9$, as can be recognized by a comparison of the pertinent curves of Fig. 5 with the heat loss results for black surfaces ($\epsilon = 1$). A simple calculation determines the heat loss parameter of black plates as 0·646 for $X = 0$ and as 0·552 for $X = \frac{1}{2}$.

Figure 6 presents, in the same way, the results for a close spacing of the plates ($h/L = 0{\cdot}05$). It can be seen that near the rim of the plates the relative position of the curves for specular and for diffuse reflection is the same as for the wider spacing of Fig. 5. In the inner part, however, the trend reverses and the heat loss of the plates with specular reflection is larger than the heat loss of the diffusely reflecting plates. This may be

Vol. 3 1961

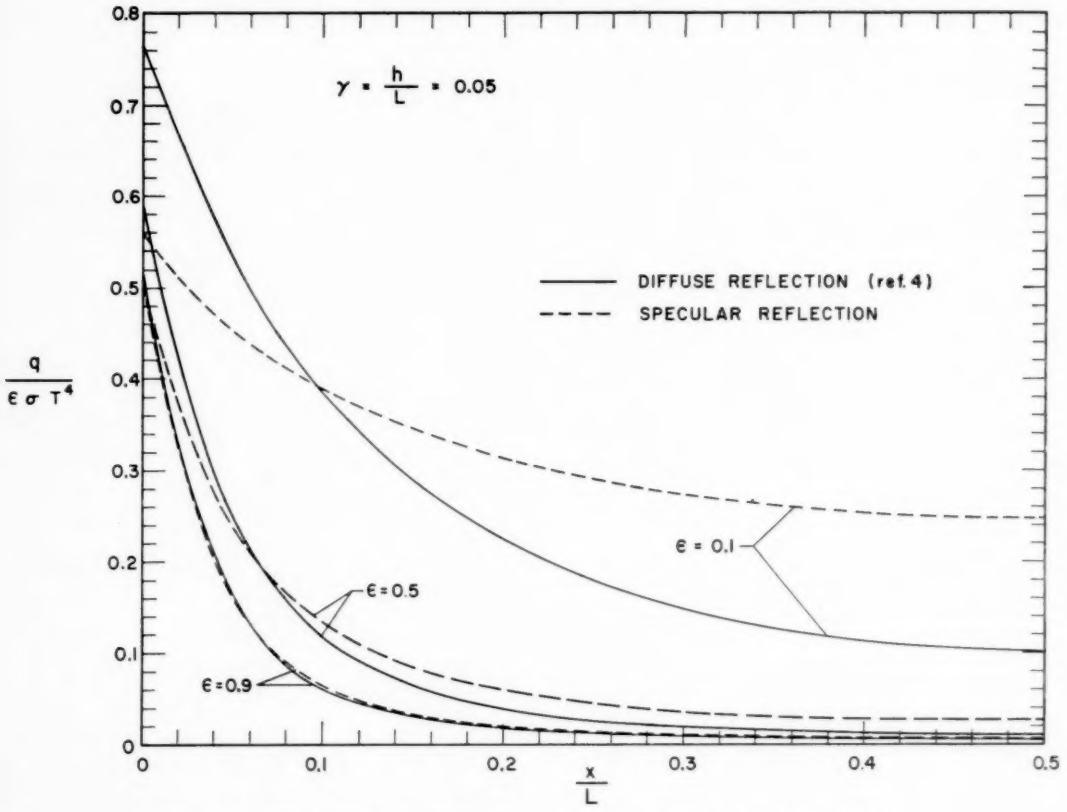

FIG. 6. Local heat flux results for parallel plate system with $\gamma = h/L = 0{\cdot}05$.

explained by the fact that radiation originating at the inner part of the plates escapes through the opening between the plates in general only after a larger number of reflections. The number of reflections, however, will, in an average, be smaller if the plates reflect specularly. It is again found that the curves for $\epsilon = 0{\cdot}9$ are located only slightly above the curve for $\epsilon = 1$, so that for this emissivity, reflections contribute only to a very small degree to the heat loss parameter.

The total heat loss from the surface of any plate has also been calculated from equation (25) and is presented in Table 1(a). The average heat flux Q/L per unit area and unit time has been divided by the energy flux leaving a unit area of a black surface at the plate temperature T. It is to be noted that the tabulated parameter has not been normalized by ϵ as were the ordinates of Figs. 5 and 6. Values for four plate spacings and for three emissivities have been entered for specular reflection as well as for diffuse reflection. Two sets of values for diffuse reflection were available from Ref. 4. One group of values presents the solutions of an integral equation describing the energy exchange process exactly. The second series of values results from a simplified analysis which neglects the local variation of the reflected radiative flux and replaces in this way the integral equation by an algebraic one. According to the specific definition of the heat loss parameter, the values of this parameter decrease with decreasing emissivity as contrasted to the behavior of the parameter presented in Figs. 5 and 6. The differences between specular and diffuse reflection are

Table 1. *Overall heat loss,* $(Q/L)/(\sigma T^4)$

(a) *Parallel plate system* (*Fig.* 4)

h/L	$\epsilon = 0{\cdot}1$			$\epsilon = 0{\cdot}5$			$\epsilon = 0{\cdot}9$		
	Specular	Diff. exact.	Diff. simpl.	Specular	Diff. exact.	Diff. simpl.	Specular	Diff. exact.	Diff. simpl.
1·0	0·08826	0·09338	0·09340	0·3503	0·3692	0·3694	0·5439	0·5500	0·5500
0·5	0·07948	0·08576	0·08607	0·2622	0·2747	0·2764	0·3632	0·3658	0·3664
0·1	0·04735	0·0442	0·05122	0·08575	0·07964	0·08677	0·09393	0·09269	0·09402
0·05	0·03220	0·0252	0·03388	0·04631	0·04128	0·04649	0·04848	0·04751	0·04848

(b) *Adjoint plate system* (*Fig.* 7)

θ	$\epsilon = 0{\cdot}1$			$\epsilon = 0{\cdot}5$			$\epsilon = 0{\cdot}9$		
	Specular	Diff. exact.	Diff. simpl.	Specular	Diff. exact.	Diff. simpl.	Specular	Diff. exact.	Diff. simpl.
135°	0·0992	0·0992	0·0992	0·481	0·480	0·480	0·838	0·838	0·838
90°	0·0971	0·0958	0·0960	0·427	0·412	0·414	0·663	0·655	0·656
60°	0·0938	0·0899	0·0909	0·358	0·327	0·333	0·484	0·472	0·474
45°	0·0906	0·0838	0·0861	0·304	0·268	0·277	0·376	0·365	0·367

Vol. 3 1961

largest for a close spacing and for a small emissivity. For $h/L = 0{\cdot}05$ and $\epsilon = 0{\cdot}1$, the heat loss of the specularly reflecting surface is larger by 28 per cent than the exactly calculated value for diffuse reflection. For this case, the error which is made by the use of the simplified analysis for diffuse reflection is even larger than the difference between specular and diffuse reflection.

The information in Figs. 5 and 6 and in Table 1 can immediately be used to determine the heat loss from parallel plates for the situation that they are in energy exchange by radiation with a black environment at a temperature T_e. The only change which has to be made in equations (23) and (25) as well as in the figures and table is that the term σT^4 in the denominator has to be replaced by $\sigma(T^4 - T_e^4)$. This is immediately evident from the fact that radiation entering from the environment consists of rays which experience exactly the same fate as rays starting from the plate surfaces and traveling to the environment. One can also consider the situation that the environment and the plates are at the same temperature. In this case the geometry corresponds to an isothermal, closed "hohlraum" and no net heat flux can exist in such an enclosure according to the second law of thermodynamics.

Two plates forming a groove

Figure 7 indicates two plates of width L arranged in such a way that they form a groove

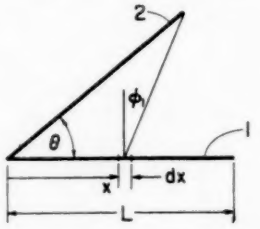

FIG. 7. Adjoint plate system.

with an opening angle θ. It will again be assumed that the plates have infinite length normal to the plane of drawing, and also, to provide comparisons with available diffuse results, that both

plates have equal and uniform temperatures. The angle factor under which an area element dA_1 sees the opposite plate is

$$F_{dA_1-A_2} = \tfrac{1}{2}(1 + \sin \varphi_1) \tag{26}$$

or expressed in the parameters $X = x/L$ and θ

$$F_{dA_1-A_2} = F_\theta = \tfrac{1}{2}\left\{1 + \frac{\cos\theta - X}{\sqrt{(1 - 2X\cos\theta + X^2)}}\right\}. \tag{27}$$

The situation in the present arrangement is different from the one in the previous section insofar that, after a finite number of reflections, an image is formed whose enveloping ray bundle as seen from dA_1 does not intersect the opposite surface. For an included angle of 90°, for instance, the image generated by the first reflection is already subject to this condition. Correspondingly, the heat flux q is described by the following equation which contains only the angle factor for direct radiative interchange

$$\frac{q}{\epsilon\sigma T^4} = 1 - \alpha F_{90°}. \tag{28}$$

For an included angle of 45°, the enveloping ray bundles drawn from dA_1 to the first and the second images 1_1 and 2_2 intersect the opposite plate. However, the enveloping ray bundles drawn from dA_1 to further images do not intersect A_2. Hence, the local heat loss q per unit area is described by an equation which contains three angle factors including the one for direct interchange as well as for the first image, which is a plate inclined under an angle $\theta = 90°$, and for the second image, which is a plate inclined under $\theta = 135°$

$$\frac{q}{\epsilon\sigma T^4} = 1 - \alpha(F_{45°} + \rho F_{90°} + \rho^2 F_{135°}). \tag{29}$$

The angle factors in equations (28) and (29) are obtained from equation (27) when the proper angle θ is inserted.

The results of the calculation are presented in Figs. 8 and 9, respectively, for 90° and 45° opening angles. The heat loss parameter has been calculated for emissivity values 0·1, 0·5, and 0·9. The dashed curves indicate the heat losses for specular reflection, and the corresponding

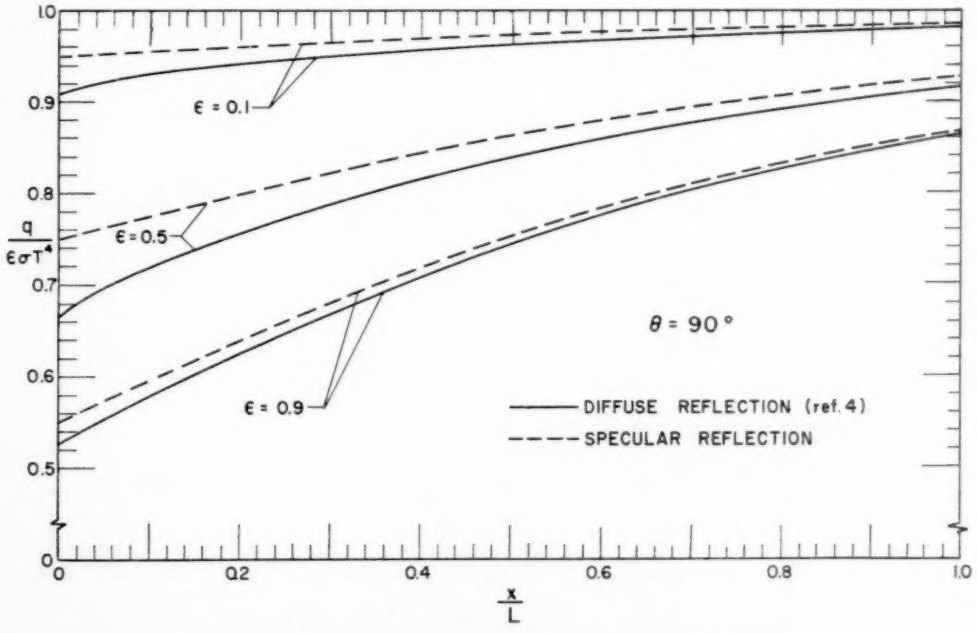

FIG. 8. Local heat flux results for adjoint plate system with $\theta = 90°$.

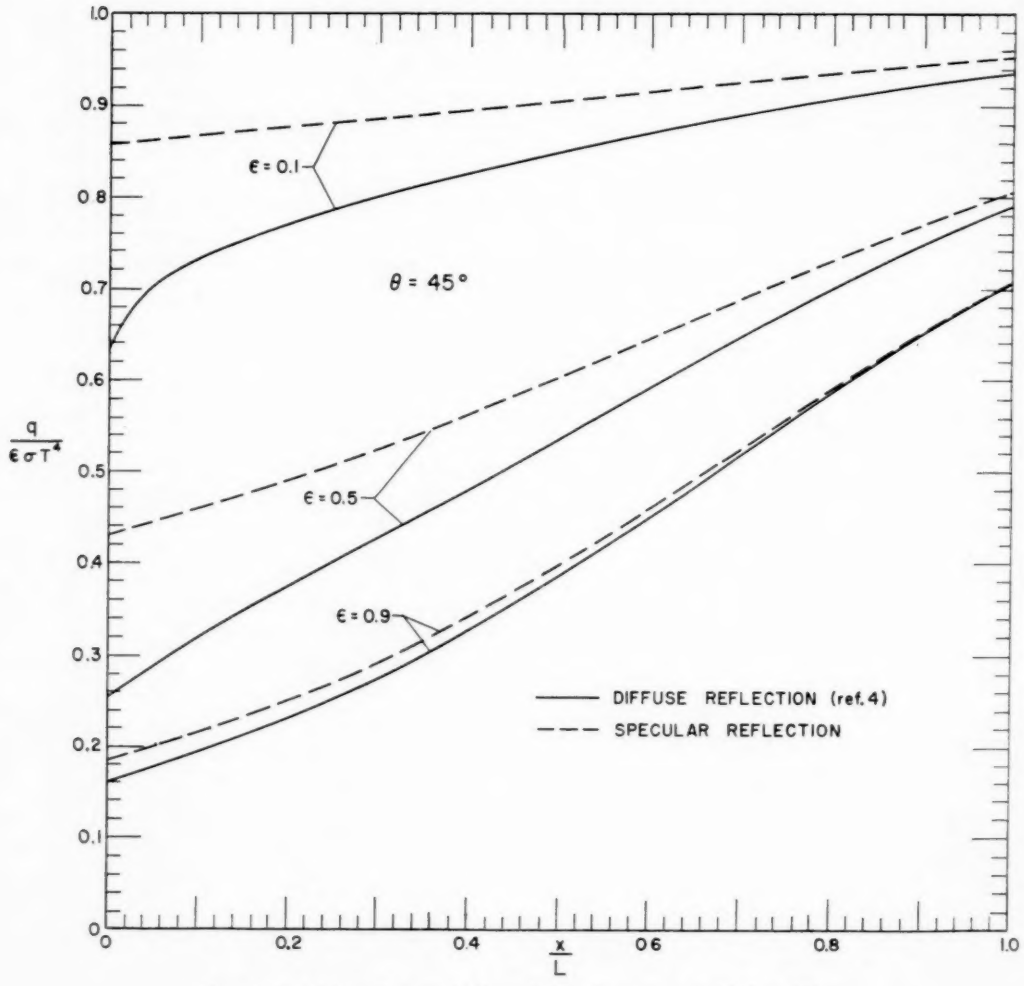

FIG. 9. Local heat flux results for adjoint plate system with $\theta = 45°$.

losses for diffuse reflection have again been entered as full lines for comparison purposes. These values have been taken from the analysis in Ref. 4. For both opening angles, the heat loss of plates with specular reflection is larger than the heat loss of diffusely reflecting surfaces. This is explained by the fact that the angular arrangement of the plates makes it easy for specularly reflected radiation to escape through the opening.

Table 1 (b) contains the average heat loss Q/L of the surfaces per unit area, divided by the energy emitted from a black surface at the specific temperature T. It should be noted that this parameter is not normalized by ϵ as were the ordinates of the figures. The results of calculations for four angles and for three emissivity values are presented. Results from Ref. 4 for diffuse reflection are also entered. The two columns for diffuse reflection present the results obtained by the solution of the integral equation and those from the simplified method. The heat loss parameter in this table compares the actual heat loss with the energy emitted by a

Vol. 3 1961

black surface, and it consequently decreases with decreasing emissivity values. The differences between specular and diffuse reflection are found to be largest for a small opening angle and for a low emissivity. The difference between the exact solution for diffuse reflection and the solution for specular reflection is 8 per cent for $\theta = 45°$ and $\epsilon = 0{\cdot}1$. Because the 45° angle is still a relatively open configuration, this difference is considerably smaller than the differences existing for concentric cylinders or spheres and also smaller than the differences between the closely spaced parallel plates.

ACTUAL DIRECTIONAL DISTRIBUTION OF REFLECTED RADIATION

Figures 10 and 11 present the angular distribution of reflected radiation for a few solid surfaces taken from Ref. 3. The curves have been

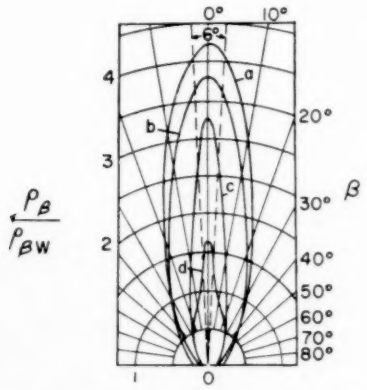

FIG. 10. Directional distribution of reflected radiation (black incident energy): *a*—aluminum paint; *b*—iron, scraped; *c*—black iron; *d*—copper oxide. ρ_β = measured reflectivity, $\rho_{\beta w}$ = reflectivity of a perfectly diffuse white surface. (From Ref. 3, Fig. 13-13).

obtained by directing a bundle of radiant energy with nearly normal incidence and with an opening angle of 6° towards the surface. The incident radiation came from a black body at the temperature 530°F and the reflecting surface was kept at atmospheric temperature. It can be recognized that the angular distribution of the reflected radiation for any of the surfaces is neither completely specular nor completely diffuse. The figures show that surfaces which appear specular to the eye approach more closely to specular reflection than to diffuse reflection for thermal radiation. But, even surfaces which appear diffuse to the eye (e.g. clay, scraped iron) may reflect a considerable

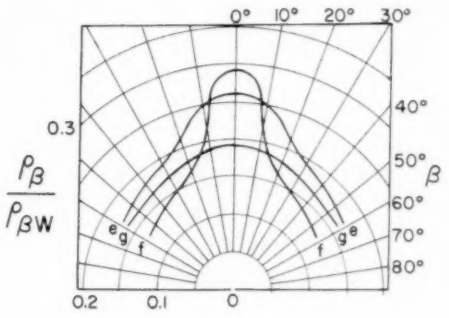

FIG. 11. Directional distribution of reflected radiation (black incident energy): *e*—cast iron; *f*—clay; *g*—wood. ρ_β = measured reflectivity. $\rho_{\beta w}$ = reflectivity of a perfectly diffuse white surface. (From Ref. 3, Fig. 13-14).

portion of thermal radiation in the proximity of the specularly reflected ray. The measurements reported in Ref. 2 indicate that the distribution of reflected radiation depends considerably on the angle of incidence.

A calculation which incorporates the actual distribution would be extremely involved and would be restricted to the specific surface. For this reason it is recommended that the data for specular and completely diffuse reflection be used to obtain limiting values for the heat loss. It is also possible to interpolate between these limiting values for a specific surface by assigning a certain fraction of the reflected energy to specular and the rest to diffuse reflection. Distribution curves like the ones presented in Figs. 10 and 11 may be used to make an estimate on these fractions.

ACKNOWLEDGEMENT

The support of the research by the National Science Foundation under grant G10177 is gratefully acknowledged.

REFERENCES

1. E. ECKERT, Messung der Reflexion von Wärmestrahlen an technischen Oberflächen. *Forsch. IngWes.* **7**, 265–270 (1936).
2. BENJAMIN MÜNCH, *Die Richtungsverteilung bei der Reflexion von Wärmestrahlung und ihr Einfluss auf die Wärmeübertragung*, Mitteilungen aus den Institut für Thermodynamik und Verbrennungsmotorenbau an der Eidgenössischen Technischen Hochschule in Zürich, nr. 16 (1955).
3. E. R. G. ECKERT and R. M. DRAKE, JR. *Heat and Mass Transfer*, McGraw-Hill, New York (1959).
4. E. M. SPARROW, J. L. GREGG, J. V. SZEL, and P. MANOS: Analysis, Results and Interpretation for Radiation Between Some Simply Arranged Gray Surfaces, A.S.M.E. paper 60-HT-4. Trans. Amer. Soc. Mech. Engrs., *J. Heat Transfer*, C **83**, May (1961).

Vol. 3 1961

Int. J. Heat Mass Transfer. Vol. 3, pp. 55–59. Pergamon Press 1961. Printed in Great Britain.

THEORY OF THE STEADY LAMINAR BUOYANT FLOW ABOVE A LINE HEAT SOURCE IN A FLUID OF LARGE PRANDTL NUMBER AND TEMPERATURE-DEPENDENT VISCOSITY

D. B. SPALDING* and R. G. CRUDDACE†

Mechanical Engineering Department, Imperial College of Science and Technology, London, S.W.7, England

(*Received* 13 *December* 1960)

Abstract—Schuh's [1] theory of steady laminar flow above a line heat source in a fluid with $Pr = 0{\cdot}7$ is extended to fluids such as heavy oils. The solution is valid for all fluids of high Prandtl number, regardless of whether the viscosity is temperature-dependent or not.

Résumé—Le théorie de Schuh de l'écoulement laminaire permanent, au-dessus d'une source de chaleur linéaire, dans un fluide dont $Pr = 0{,}7$, a été étendue aux fluides tels que les huiles lourdes. La solution est valable pour tous les fluides à grand nombre de Prandtl, que leur viscosité varie ou non avec la température.

Zusammenfassung—Die Theorie von Schuh der stationären Laminarströmung über einer linienförmigen Wärmequelle in einer Flüssigkeit mit $Pr = 0{,}7$ wird auf andere Flüssigkeiten wie Schweröle erweitert. Die Lösung gilt für alle Flüssigkeiten hoher Prandtlzahl, gleichgültig ob ihre Viskosität temperaturabhängig ist oder nicht.

Аннотация—Приложение теории Шаха 1 об установившемся ламинарном потоке над линейным источником тепла в жидкости с $Pr = 0{,}7$ распространяется на такие жидкости, как тяжелые масла. Это решение справедливо для всех жидкостей с большими числами Прандтля независимо от того, зависит ли вязкость от температуры.

NOTATION

c specific heat of the fluid at constant pressure;
f $\psi/\Lambda^{1/5}\nu_\infty x^{3/5}$;
g gravitational acceleration;
k thermal conductivity of fluid;
$\dot{m}'(x)$ vertical mass flux per unit length;
Pr_∞ $c_\infty\mu_\infty/k_\infty$, Prandtl number in the undisturbed fluid;
$\dot{q}'$ rate of heat transfer from unit length of source;
t fluid temperature;
u fluid velocity in vertical direction;
v fluid velocity in horizontal direction;
x vertical height above the heat source;
y horizontal distance from the plane of symmetry;
β volumetric thermal expansion coefficient;
ϵ a small number;
η $\Lambda^{1/5}/x^{2/5}\int_0^y \rho/\rho_\infty \cdot \mathrm{d}y$;
θ $(t - t_\infty)g\beta x^{3/5}/\nu_\infty^2\Lambda^{4/5}$;
Λ $\dot{q}'g\beta/c_\infty\rho_\infty\nu_\infty^3$;
μ dynamic viscosity of the fluid;
ν kinematic viscosity of the fluid;
ξ $-f''/f_0'^{3/2}$;
ρ fluid density;
τ $(t - t_\infty)$;
ψ stream function;
χ f'/f_0'.

* Professor of Heat Transfer.

† Present address—Rocket Propulsion Establishment, Westcott, Near Aylesbury, Bucks., England.

Subscripts

0 in the central plane;

∞ in the undisturbed fluid;

(0), (1), (2), . . . zeroth, first, second, . . . approximations.

1. INTRODUCTION

1.1 *The problem*

HEAVY oil stored in a tank is sometimes heated by horizontal steam pipes placed near the tank floor. When calculating the temperature distribution which will be found in the tank after heating has continued for a given time, it is important to know how much oil is convected upwards in the plume of heated fluid which forms itself above the pipe.

The present paper provides a theory for the steady laminar flow in a plume above a long horizontal heat source in a large tank of stagnant oil. Although this system is idealized, as compared with tanks of finite size containing several heating pipes and with slowly changing bulk temperature, it is thought that the analysis may form a first step towards predicting what happens in practice.

1.2 *Previous work on the subject*

Schuh [1] has developed a theory for the laminar buoyant flow above a two-dimensional heat source in a fluid of Prandtl number equal to 0·7. Since oils have Prandtl numbers which are very much greater than unity, we shall rework Schuh's problem for the case of infinite Prandtl number.

In Schuh's work the transport properties of the fluid were taken to be uniform. Since oils have viscosities which depend steeply upon temperature, we shall take account of this dependence. It will be shown that this involves trivial difficulty when the Prandtl number is large.

1.3 *Outline of main result*

The main result of the analysis is given in equation (19) below; this shows that the upward mass flow rate per unit length is proportional to the one-fifth power of the heat flux per unit length, the three-fifths power of the distance above the heat source, and the two-fifths power of the bulk viscosity of the oil.

2. MATHEMATICAL ANALYSIS

2.1 *Equations and boundary conditions*

The velocity and temperature distributions in the fluid are described by the following equations:

Mass continuity

$$(\rho u)_x + (\rho v)_y = 0 : \frac{u\rho}{\rho_\infty} = \psi_y : \frac{v\rho}{\rho_\infty} = \psi_x \quad (1)$$

Momentum

$$\rho u u_x + \rho v u_y = \rho\beta g\tau + (\mu u_y)_y \quad (2)$$

Energy

$$\rho u(c\tau)_x + \rho v(c\tau)_y = (k\tau_y)_y. \quad (3)$$

Dimensional analysis indicates that the variables are related by:

$$\frac{\psi}{\nu_\infty \Lambda^{1/5} x^{3/5}} \equiv f(\eta, Pr_\infty)$$

$$\frac{\tau g\beta x^{3/5}}{\nu_\infty \Lambda^{4/5}} \equiv \theta(\eta, Pr_\infty) \quad (4)$$

$$\eta \equiv \frac{\Lambda^{1/5}}{x^{2/5}} \cdot \int_o^y \frac{\rho}{\rho_\infty} \cdot dy.$$

Equations (1), (2) and (3) are transformed by equations (4) into the following ordinary differential equations, which are identical to Schuh's [1] equations for the case of constant properties:

$$\left[\frac{\rho\mu}{\rho_\infty \mu_\infty} \cdot f''\right]' + \tfrac{3}{5} f f'' + \theta - \tfrac{1}{5} f'^2 = 0 \quad (5)$$

$$\left[\frac{\rho k}{\rho_\infty k_\infty} \cdot \theta'\right]' + \tfrac{3}{5} Pr_\infty \left[\frac{c}{c_\infty} f\theta\right]' = 0, \quad (6)$$

where the prime denotes differentiation with respect to η, and other notation is given in section 5 below.

The boundary conditions may be expressed as:

$$\left.\begin{aligned} \eta = 0 : \; f'' = 0 : \theta' = 0 \\ \eta = \infty : f' = 0 : \theta = 0 \end{aligned}\right\} \quad (7)$$

and, in addition,

$$\int_0^\infty f'\theta d\eta = \tfrac{1}{2}. \quad (8)$$

The differential equations involve the usual boundary-layer assumptions. In addition it is

Vol. 3 1961

supposed that there is no influence of the force exerted on the fluid at the heat source. These assumptions are probably fulfilled in practice at a height which is sufficiently far above the steam pipe; they are responsible for the reduction of the partial differential equations to ordinary ones, i.e. for the existence of "similar" velocity and temperature profiles. Equation (8) equates the enthalpy flux through any horizontal plane to the rate of energy release from the heat source.

2.2 *Equations and boundary conditions for large Prandtl number*

The following argument shows that a solution to equations (5) and (6) may be obtained with little difficulty for the case of large Prandtl number.

Step (*i*). When the Prandtl number is high, the thermal boundary layer is much thinner than the velocity layer. (This fact, which is familiar from other boundary-layer studies, is proved *a posteriori* in section 2.3.)

Step (*ii*). Since the vertical velocity in the thin thermal layer is approximately uniform in a horizontal plane, we can write:

$$f' \approx f'_0 : \therefore f \approx \eta f'_0. \tag{9}$$

We assume that c, ρ, k are substantially invariant with temperature for oils, since it is the rapid variation in viscosity with temperature which is of major concern ($\mu \sim t^5$ approx.). Equation (6) now assumes the asymptotic form:

$$\theta'' + \tfrac{3}{5} Pr_\infty f'_0 [\eta\theta]' = 0. \tag{10}$$

Step (*iii*). A further consequence of Step (i) is that θ can be taken to be equal to zero in the region surrounding the thermal boundary layer, $\eta > \epsilon$, where ϵ is a small quantity. Equation (5) can therefore be re-written as:

$$0 \leqslant \eta \leqslant \epsilon : \left[\frac{\mu}{\mu_\infty} f''\right]' + \tfrac{3}{5} f'_0 \eta f'' + \theta - \tfrac{1}{5} f'^2_0 = 0 \tag{11}$$

$$\epsilon < \eta < \infty : f''' + \tfrac{3}{5} f f'' - \tfrac{1}{5} f'^2 = 0. \tag{12}$$

Step (*iv*). The boundary conditions for (11) and (12) become:

$$\left.\begin{aligned} \eta = 0 &: f'' = 0 \\ \eta = \epsilon &: f'' = f''_\epsilon \end{aligned}\right\} \tag{13}$$

$$\left.\begin{aligned} \eta = \epsilon &: f = 0 : f' = f'_0 : f'' = f''_\epsilon \\ \eta = \infty &: f' = 0 \end{aligned}\right\} \tag{14}$$

Conclusion. Our problem is thus reduced to the solutions of: equation (10) subject to the conditions (7) and (8), in the domain $0 \leqslant \eta \leqslant \epsilon$; equation (11) subject to the conditions (13) in the same domain; and equation (12) subject to the conditions (14) in the domain $\eta > \epsilon$. Only the last equation has to be solved numerically as will now be seen.

2.3 *Solution of the differential equations*

Equation (10) and its appropriate conditions are readily seen to be solved by:

$$\theta = \left(\frac{3Pr_\infty}{10\pi f'_0}\right)^{\frac{1}{3}} . \exp\left(-\frac{3Pr_\infty f'_0 \eta^2}{10}\right). \tag{15}$$

Were it not that f'_0 is an as yet undetermined number, equation (15) would completely describe the temperature distribution in the plume. It should be noted that the equation confirms that θ falls off rapidly with η when Pr_∞ is large. Correspondingly, the maximum value of θ, which occurs when $\eta = 0$, increases as the square root of Prandtl number.

Equation (11). By integrating with respect to η, we obtain:

$$\left[\frac{\mu}{\mu_\infty} f''\right]_0^\epsilon + \tfrac{3}{5} f'_0 [\eta f' - f]_0^\epsilon + \int_0^\epsilon \theta \, d\eta - \tfrac{1}{5} f'^2_0 \epsilon = 0. \tag{11a}$$

Introducing the boundary conditions (13) and the integral condition (8), and noting that ϵ is a small quantity, we see that equation (11a) reduces to:

$$f'_0 f''_\epsilon + \tfrac{1}{5} = 0. \tag{16}$$

This result is independent of the mode of variation of viscosity with temperature.

Equation (12). Equation (16) can be used to displace f''_ϵ from the conditions on equation (12), which can now be regarded as defining an eigenvalue problem, f'_0 being the quantity to be determined.

The procedure for solution of this problem is indicated in the Appendix; the equation has been solved by an iterative quadrature method after

the manner of Crocco [2]. For present purposes it suffices to note the result:

$$f'_0 = 0{\cdot}9335. \tag{17}$$

Also calculated was f_∞, which took the value:

$$f_\infty = \int_0^\infty f' \, \mathrm{d}\eta = 1{\cdot}346. \tag{18}$$

The variation of f' with η corresponding to the solution is shown in Fig. 1 as the curve marked: $Pr_\infty = \infty$.

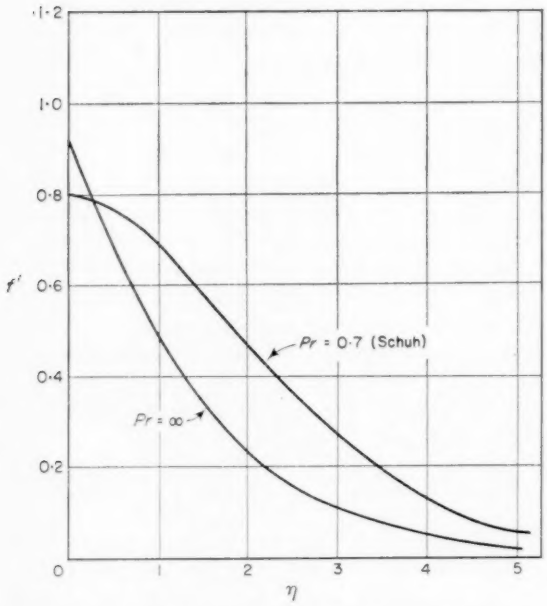

FIG. 1. Non-dimensional velocity distributions above heated line source in laminar steady flow.

3. DISCUSSION

3.1 *Interpretation of the result*

Equation (18), when translated into physical quantities, signifies:

$$\dot{m}'(x) = 2\int_0^\infty \rho u \, \mathrm{d}y = 2{\cdot}69[\dot{q}' g\beta\rho_\infty^2\mu_\infty^2 x^3/c_\infty]^{1/5}. \tag{19}$$

Thus the mass flow rate in the plume increases in accordance with the one-fifth power of the heating rate, the two-fifths power of the viscosity in the bulk of the fluid, and the three-fifths power of the distance above the heat source.

Neither the thermal conductivity nor the temperature-dependence of the viscosity have any influence on this result, the reason being that, when the Prandtl number is large, the region of non-uniform temperature is very thin and is moreover concentrated in a region of small shear stress.

Equation (17) correspondingly signifies that the upward velocity of fluid at the symmetry plane of the plume, u_0, is given by:

$$u_0 = 0{\cdot}934\ [\dot{q}' g\beta/c_\infty]^{2/5} \cdot [x/\rho_\infty\mu_\infty]^{1/5}. \tag{20}$$

This equation implies that the peak velocity in the plume increases with the one-fifth power of the height above the source, and with the two-fifths power of the strength of the heat source.

Equations (15) and (17), taken together, signify that the greatest temperature at any level in the plume is given by:

$$t - t_\infty = 0{\cdot}32\left[\frac{\dot{q}'}{c_\infty}\right]^{4/5} \cdot \frac{[c_\infty\mu_\infty/k_\infty]^{1/2}}{[g\beta\rho_\infty^2\mu_\infty^2]^{1/5}x^{3/5}}. \tag{21}$$

Hence we conclude that the maximum temperature in the plume falls off as the minus three-fifths power of the height; it is increased slightly (as the one-tenth power) by an increase in viscosity, but reduced by an increase in thermal conductivity.

It might be noted that the present theory is most easily checked experimentally by way of a measurement of the peak temperature in the plume.

3.2 *Comparison with Schuh's* [1] *result for* $Pr = 0{\cdot}7$

Figure 1 also contains, as a curve marked $Pr = 0{\cdot}7$, the result obtained by Schuh [1] for uniform transport properties. It is seen that the finite Prandtl number results in only modest changes in the $f'(\eta)$ curve, which now exhibits a rounded peak because the buoyancy forces now operate over a region of finite thickness.

It may be mentioned that Schuh found that the constant in the equation for $(t - t_\infty)$ was 0·37, instead of the 0·32 indicated above. This results, no doubt, from the fact that for $Pr = 0{\cdot}7$ the average velocity of the heated fluid is less than the maximum velocity in the plume, instead of

Vol. 3 1961

being nearly equal to it as when the Prandtl number is very large.

REFERENCES

1. H. SCHUH, Boundary Layers of Temperature, Section B.6 of W. TOLLMIEN's *Boundary Layers*, British Ministry of Supply, German Document Centre. Reference 3220T (1948).
2. L. CROCCO, Una carateristica transformazione delle equazione dello strato nei gas. *Atto di Guidonia*, No. 7 (1939).

APPENDIX

Procedure for solving equation (7) *by iterative quadrature*

The problem to be solved is the determination of f_0' and f_∞ from the solution to the equation:

$$f''' + \tfrac{3}{5} f f'' - \tfrac{1}{5} f'^2 = 0 \qquad \text{(A.1)}$$

with the boundary conditions:

$$\eta = 0 : \; f = 0 : f' = f_0' : f'' = -\frac{1}{2f_0'}$$
$$\eta = \infty : f' = 0. \qquad \text{(A.2)}$$

We introduce a transformation similar to that of Crocco [2]:

$$\xi \equiv -f'' f_0'^{-3/2} \qquad \text{(A.3)}$$

$$\chi \equiv f'/f_0'. \qquad \text{(A.4)}$$

Equation (A.1) then reduces to the first-order form:

$$\xi \frac{\mathrm{d}\xi}{\mathrm{d}\chi} + \tfrac{3}{5}\xi \int_1^\chi \frac{\chi}{\xi}\,\mathrm{d}\chi - \tfrac{1}{5}\chi^2 = 0 \qquad \text{(A.5)}$$

while the boundary conditions reduce to:

$$\chi = 1 : \xi = \tfrac{1}{2} f_0'^{-5/2} \qquad \text{(A.6)}$$

$$\chi = 0 : \xi = 0. \qquad \text{(A.7)}$$

Equation (A.5) can be integrated formally to yield, after substitution of equation (A.7):

$$\tfrac{1}{2}\xi^2 = \tfrac{3}{5}\int_0^\chi \xi \int_\chi^{'} \frac{\chi}{\xi}\,\mathrm{d}\chi\,\mathrm{d}\chi + \tfrac{1}{15}\chi^3. \qquad \text{(A.8)}$$

Now equation (A.8) can be used as an iteration formula for the determination of $\xi(\chi)$. The zero'th approximation $\xi_{(0)}$ is obtained by neglecting the quadrature expression entirely. Thus:

$$\xi_{(0)} = (\tfrac{2}{15}\chi^3)^{1/2}. \qquad \text{(A.9)}$$

The first approximation $\xi_{(1)}$ is obtained by substituting $\xi_{(0)}$ for ξ in the quadrature of (A.8). Thus:

$$\tfrac{1}{2}\xi_{(1)}^2 = \tfrac{3}{5}\int_0^\chi \chi^{3/2}\int \chi^{-1/2}\,\mathrm{d}\chi\,\mathrm{d}\chi + \frac{\chi^3}{15}$$
$$= \tfrac{12}{25}\chi^{5/2} - \tfrac{1}{3}\chi^3 \qquad \text{(A.10)}$$

which is a better approximation.

Further approximations involve numerical work. We here merely tabulate the resulting values for ξ^2 at $\chi = 1$, so that the rapidity of convergence can be seen. (See Table 1.)

The fifth approximation was regarded as sufficiently exact for our purposes.

Table 1

Approximation	Zero'th	First	Second	Third	Fourth	Fifth
ξ^2 at $\chi = 1$	0·133	0·293	0·334	0·346	0·3519	0·3526
f_0'	1·136	0·969	0·944	0·937	0·9339	0·93356

Int. J. Heat Mass Transfer. Vol. 3, pp. 60–67. Pergamon Press 1961. Printed in Great Britain.

EFFECT OF VIBRATION ON HEAT TRANSFER FROM A HORIZONTAL CYLINDER TO A NORMAL AIR STREAM

K. SREENIVASAN and A. RAMACHANDRAN

Mechanical Engineering Section, Indian Institute of Science, Bangalore, India

(*Received* 28 *November* 1960)

Abstract—The effect of vibration on heat transfer from a horizontal copper cylinder, 0·344 in. in diameter and 6 in. long, was investigated. The cylinder was placed normal to an air stream and was sinusoidally vibrated in a direction perpendicular to the direction of the air stream. The flow velocity varied from 19 ft/s to 92 ft/s; the double amplitude of vibration from 0·75 cm to 3·2 cm, and the frequency of vibration from 200 to 2800 cycles/min. A transient technique was used to determine the heat transfer coefficients. The experimental data in the absence of vibration is expressed by

$$N_{Nu} = 0{\cdot}226\ N_{Re}^{0{\cdot}6} \text{ in the range } 2500 < N_{Re} < 15\,000.$$

By imposing vibrational velocities as high as 20 per cent of the flow velocity, no appreciable change in the heat transfer coefficient was observed. An analysis using the resultant of the vibration and the flow velocity explains the observed phenomenon.

Résumé—L'effet des vibrations sur la transmission de chaleur a été étudié sur un tube de cuivre de 0,344 in. de diamètre et 6 in. de long. Le cylindre, placé normalement au courant d'air était animé d'une vibration sinusoïdale perpendiculaire à l'écoulement. La vitesse de l'écoulement variait de 19 ft/s à 92 ft/s, l'amplitude des vibrations de 0,75 cm à 3,2 cm et la fréquence de 200 à 2800 cycles/mn. Une technique de mesure transitoire a été utilisée pour déterminer les coefficients de transmission de chaleur. En l'absence de vibration, les données expérimentales s'expriment par

$$N_{Nu} = 0{,}226\ N_{Re}^{0{,}6} \text{ pour } 2500 < N_{Re} < 15\,000.$$

En imposant des vitesses de vibration atteingnant jusqu'à 20% de la vitesse de l'écoulement aucune modification des coefficients de transmission de chaleur n'a été observée. Une étude utilisant la résultante de la vibration et de la vitesse de l'écoulement explique le phénomène observé.

Zusammenfassung—Der Einfluss von Schwingungen auf den Wärmeübergang wurde an einem waagerechten Kupferzylinder von 0,875 cm Durchmesser und 15,2 cm Länge untersucht. Der Zylinder wurde quer zum Luftstrom angebracht und senkrecht zur Anströmrichtung in sinusförmige Schwingungen versetzt. Die Strömungsgeschwindigkeit reichte von 5,8 m/s bis 28 m/s; die Doppelamplitude der Schwingungen von 0,75 bis 3,2 cm und die Frequenz von 200 bis 2800 Schwingungen je min. Die Wärmeübergangszahlen wurden mit Hilfe eines Kurzzeitverfahrens bestimmt. Werden keine Schwingungen aufgebracht, lassen sich die Versuchsergebnisse im Bereich

$$2500 < Re < 15\,000 \text{ durch } Nu = 0{,}226\ Re^{0{,}6}$$

ausdrücken. Für Schwingungsgeschwindigkeiten bis 20% der Anströmgeschwindigkeit wurde keine merkliche Veränderung der Wärmeübergangszahlen festgestellt. Eine mit Hilfe der Resultierenden der Schwingungs- und Anströmgeschwindigkeit durchgeführte Analyse erklärt das beobachtete Phänomen.

Аннотация—Исследовано влияние вибрации на теплообмен горизонтального медного цилиндра диаметром 0,344 дюйма и длиною 6 дюймов. Цилиндр располагался перпендикулярно к потоку воздуха и вибрировал по синусоидальному закону в направлении, перпендикулярном потоку воздуха. Скорость потока изменялась от 19 до 92 футов в сек; двойная амплитуда вибрации изменялась в интервале от 0,75 до 3,2 см., частота вибрации—от 200 до 2800 колебаний в минуту. Для определения коэффициентов теплообмена использовался нестационарный метод. При отсутствии вибрации экспериментальные данные описываются зависимостью

Vol. 3 1961

$N_{Nu} = 0{,}226\ N_{Re}^{0{,}6}$ в интервале $2500 < N_{Re} < 15\,000$.

При скоростях вибрации даже равных 20 процентам скорости потока, никакого заметного изменения коэффициента теплообмена обнаружено не было. Наблюдаемое явление может быть объяснено, если учесть результирующую скоростей вибрации и потока.

NOMENCLATURE

The following nomenclature is used in this paper:

A	Area of the surface of the cylinder, ft²;
a	Constant;
b	Constant;
C_p	Specific heat at constant pressure, Btu/lb deg F;
D	Diameter of the cylinder, ft;
d	Amplitude of vibration, ft;
f	Frequency of vibration in cycle/min, 1/min;
h	Heat transfer coefficient, Btu/h ft² degF;
k	Thermal conductivity, Btu/h ft degF;
t	Temperature, °F;
t_a	Ambient temperature, °F;
t_0	Temperature at $\tau = 0$, °F;
t_s	Arithmetic mean of the temperature at cylinder axis at beginning and end of the cooling process, °F;
t_f	$(t_s + t_a)/2$, Film temperature, °F;
T	Temperature difference, $(t - t_a)$, degF;
U_v	Root-mean-square velocity in the direction of the air stream, ft/h;
V_F	Flow velocity, ft/h;
V_v	Root-mean-square velocity in the direction perpendicular to the air stream, ft/h;
V_R	Resultant velocity, ft/h;
W	Mass of the cylinder, lb;
X	Amplitude of vibration corresponding to a crank rotation of ψ, ft;
τ	Unit of time, h;
ρ	Density, lb/ft³;
μ	Viscosity, lb/h ft;
ψ	Crank angle with reference to bottom dead centre, radians;
N_{Nu}	Nusselt Number $= \dfrac{hD}{k_f}$, dimensionless;
N_{Re}	Reynolds Number $= \dfrac{DV_F\ \rho_f}{\mu_f}$, dimensionless;
$\dfrac{V_V}{V_F}$	Ratio of velocities, dimensionless.

INTRODUCTION

Heat convection is the transportation and exchange of heat due to the mixing motion of different parts of a fluid. Heat exchange by convection is promoted by the fluctuating motions in turbulent flow. Consequently heat transfer is higher in turbulent flow than in laminar flow. Vibration of the heat transfer surface may bring about the change from laminar to turbulent flow and hence result in higher heat transfer coefficients.

Studies in this field can be broadly classified into two types—one in which the heat transfer surface is vibrated and the other in which the flow medium is subjected to pulsation, vibrations or agitation.

Van der Hegge Zijnen [1] reported that the heat transfer from a tungsten wire, 0·0005 cm in diameter, to a normal air stream, decreased when the wire was subjected to vibrations in the direction of the air stream. A maximum decrease of 4·3 per cent in the heat transfer coefficient was observed when the ratio of the root-mean-square velocity of vibration to the flow velocity was as high as 45 per cent. Anantanarayanan and Ramachandran [2] observed an increase of 130 per cent in the heat transfer from a vibrating horizontal nichrome wire, 0·018 in. in diameter, to an air stream flowing parallel to the wire. The wire was vibrated in a vertical plane with varying values of vibrational velocity. The ratio of the vibrational velocity to the flow velocity used in their study varied from 0 to 30 per cent. Tessin and Jakob [3] while studying the effects of starting length on heat transfer from a cylinder to a parallel gas stream found that the heat transfer coefficients were not appreciably altered when the cylinder was subjected to a vibrational velocity of about 2 per cent of the flow velocity. While only the above three investigations have been reported on the effects of vibrations on heat transfer by forced convection, studies on the effect of vibration on heat transfer by free convection were reported by Martinelli and Boelter

[4], Lemlich [5], Tsui [6], Shine [7], Maxwell [8] and Richards [9].

In view of the meagre information available on the effect of vibration on heat transfer by forced convection, an investigation was undertaken to study the influence of vibration on heat transfer from a horizontal cylinder to a normal air stream. The basic vibrational parameters affecting the heat transfer are the amplitude and frequency of vibration. Previous investigations indicate that these three can be combined to give the following derived parameters: a vibrational velocity proportional to the product of amplitude and frequency of vibration, the ratio of the vibrational velocity to the flow velocity and the amplitude–diameter ratio. Besides the large accelerations and decelerations to which the heat transfer surface is subjected during the vibration, there appear to be other factors which decide whether the surface carries the boundary layer with it or vibrates in an enclosed fluid film. Indeed, the nature of the phenomenon associated with the vibration of the heat transfer surface is so complicated that a simple correlation or analysis of the mechanism is not possible at this time.

DESCRIPTION OF APPARATUS

The test apparatus consisted of a thermal "capacitor" with a high thermal capacity, an arrangement for vibrating the cylinder at various amplitudes and frequencies, provision for a controlled flow of air, and finally instrumentation to determine the temperature–time history of the capacitor during cooling. In Fig. 1 is shown the arrangement of the test apparatus. The honey-comb and the straightener in the 8 in. square duct straightened out the discharge from the blower. The duct discharged into atmosphere and the test cylinder was placed 1 ft from the duct. A pitot traverse indicated a uniform velocity profile at this section. The air velocity was measured with an impact tube made of standard dimensions. The velocity head was measured with a Meriam manometer, model A-750. The impact tube was swung into the plane of the test cylinder after each cooling run. This prevented the impact tube from disturbing the flow field around the cylinder during cooling. As the duct was discharging into the atmosphere, the impact tube directly gave the velocity head. In Fig. 2 is shown the solid copper rod, 6 in. long and 0·344 in. diameter, which was used as the thermal "capacitor" and which also provided the necessary heat transfer surface. The test cylinder constructed as shown in Fig. 2 satisfied the following conditions:

(a) The test cylinder made of copper was essentially isothermal at every instant of cooling.
(b) The end caps reduced the end leakage of heat to a negligible value.
(c) The radiation effects were reduced by the highly polished electroplated surface of the test cylinder.
(d) The test cylinder and its "transite" supports were heated simultaneously, thus reducing any parasitic heat transfer from the supports to the cylinder or vice versa, to a negligible value.

A 40 B and S gauge iron–constantan thermocouple was inserted inside the test cylinder. The reference junction of the thermocouple was placed upstream of the cylinder. The temperature at that station was measured using a mercury-in-glass thermometer reading accurately to 0·05°F. The copper cylinder with its transite supports was held in a yoke support fixed to the reciprocating member of the connecting rod and crank mechanism. A heater of a special design was used to heat the cylinder when fixed in position.

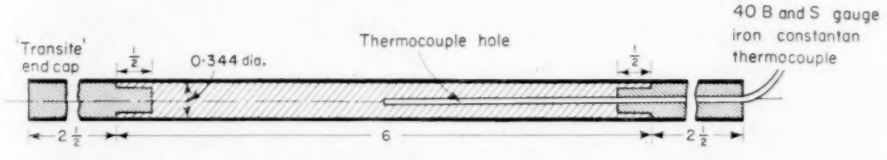

FIG. 2. Thermal capacitor.

Vol. 3 1961

ol.
3
961

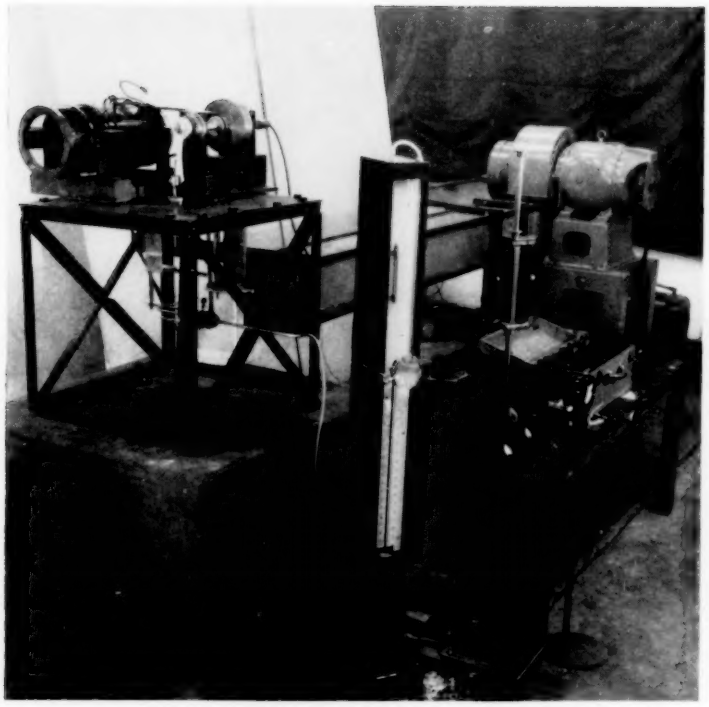

FIG. 1. General arrangement of the test apparatus.

Vol.
3
1961

In Fig. 3 is shown the connecting rod and crank mechanism which vibrated the cylinder in a vertical direction. The large length of the connecting rod gave a sensibly sinusoidal motion

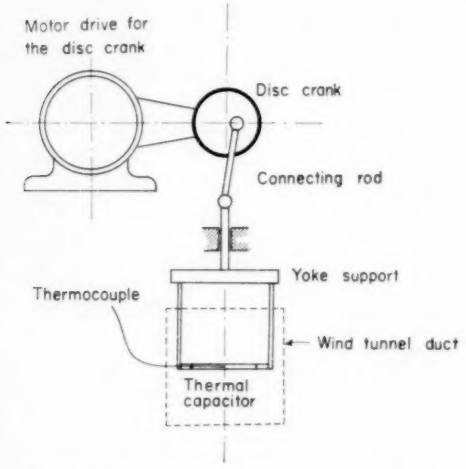

FIG. 3. Connecting rod and crank mechanism.

during vibration. A General Electric hand tachometer was used to measure the speed and the double amplitude of vibration was measured with a travelling telescope.

The size of the cylinder was so chosen that the cooling curve at the maximum velocity could be easily determined using a potentiometer and a stop watch. A Leeds and Northrup portable precision potentiometer was used along with an Anglo-Swiss stop watch for this purpose.

The transient technique adopted to determine the heat transfer coefficients was similar to the one suggested first by London *et al.* [10].

EXPERIMENTAL PROCEDURE

The initial runs were conducted to establish the heat transfer data in the absence of vibration. The test cylinder was heated by placing the heater near it. The blower was started. When the test cylinder had reached a temperature greater than a pre-set value, the heater was removed and the cylinder allowed to cool. One of the stop watches was started when the potentiometer balance was obtained at the pre-set value as indicated by the galvanometer. Immediately afterwards, the potentiometer reading was reduced by a known amount. When the poteniometer balance was reached at this value, the first stop watch was stopped and the second started. This procedure was repeated to obtain the complete cooling data. The temperature at the beginning of the cooling run was in the range 140° to 220°F. The temperature–time history was recorded till the surface reached a temperature of 90°F. The potentiometer current was obtained from a battery of six cells so as to minimize the de-standardization of the calibration during the cooling run. Further, the calibration was checked and rectified as and when the cooling rate permitted. At the conclusion of the test, all the non-transient data were recorded. This was repeated at various values of the flow velocity. The next set of runs was conducted with the cylinder vibrating. Keeping the amplitude of vibration and the flow velocity constant, the vibrational frequency was varied from 200 to 2800 cycle/min. This was repeated at the same amplitude for different values of flow velocity ranging from 19 ft/s to 92 ft/s. Further test data were obtained for different amplitudes of vibration. The range of parameters covered was

Flow velocity	19 ft/s to 92 ft/s
Double amplitude of vibration	0·75 cm to 3·2 cm
Frequency of vibration	200 cycle/min to 2800 cycle/min.

ANALYSIS OF DATA

The theory of the transient test technique [10] has been well established and will be briefly given here.

Writing the heat balance of the test cylinder at any instant of cooling,

$$W C_p \left(\frac{dt}{d\tau}\right) = - hA (t - t_a). \qquad (1)$$

Putting $T = t - t_a$

$$W C_p \left(\frac{dT}{d\tau}\right) = - hAT. \qquad (1a)$$

Equation (1) holds good only when the following assumptions are satisfied (a) the test cylinder loses all the heat through its

cylindrical surface only, i.e. no end conduction and radiation take place, (b) the test cylinder remains isothermal at every instant of cooling. Schneider [11] has pointed out that for the value of the modulus $K/h\ \delta_1 > 10$, where δ_1 is a surface radius, the temperature is nearly uniform through the cylinder. Under maximum heat flow conditions in this investigation, the value of the modulus is far in excess of 10, thus justifying the assumption that the cylinder is isothermal.

Equation (1a) can be integrated only when (i) h is independent of t and hence τ; (ii) C_p and t_a are assumed constants.

Equation (1a) can be written as

$$h = -\frac{W\ C_p}{A}\frac{1}{T}\frac{\mathrm{d}T}{\mathrm{d}\tau}. \tag{2}$$

Assuming that the chord has the same slope as the tangent at the mid-point of the chord, the value of $(1/T)\ (\mathrm{d}T/\mathrm{d}\tau)$ can be calculated from the temperature–time history.

Integration of equation (1) with the boundary conditions $\tau = 0$, $T = t_0 - t_a$; and $\tau = \tau$, $T = t - t_a$, yields

$$\frac{t - t_a}{t_0 - t_a} = \exp\left(-\frac{hA}{W\ C_p}\tau\right). \tag{3}$$

This relation should yield a straight line when plotted on a semi-log sheet. Fig. 4 is typical plot of a cooling run. Departure from linearity would reflect combinations of end leakage, variation of h and possibly instrument lag effects.

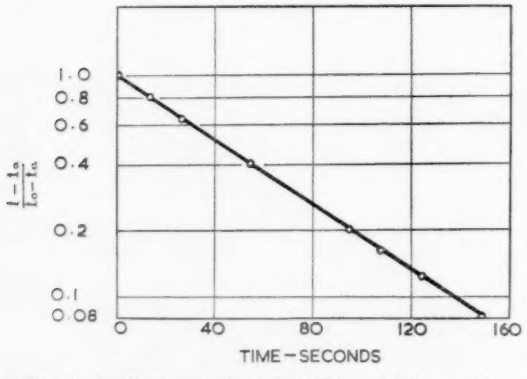

FIG. 4. Cooling curve in terms of $(t - t_a)/(t_0 - t_a)$ versus time.

After obtaining h, the Nusselt and Reynolds numbers were calculated using the values of the physical properties at the film temperature $t_f = (t_s + t_a)/2$.

As the length of the connecting rod was large the vibration was sensibly sinusoidal. The motion of the test cylinder under conditions of maximum amplitude is expressed by

$$\frac{X}{d} = \cos\psi + 0{\cdot}026\cos 2\psi. \tag{4}$$

The root-mean-square velocity of vibration was calculated from the equation

$$V_v = 60\ (\sqrt{2}\,\pi f d). \tag{5}$$

A similar equation was used by Martinelli and Boelter [4].

The ratio of the vibrational velocity to the flow velocity, V_v/V_F, was then calculated in each case.

ACCURACY OF INSTRUMENTATION

The following summarizes the accuracies of the various measurements:

Physical quantity	*Measured accurate to*
Temperature difference	± 0·2 degF
Time interval	± 0·1 s
Flow velocity	± 0·6 per cent
Frequency of vibration	± 10 cycle/min
Double amplitude of vibration	± 0·002 cm.

In some runs, a fluctuation of about 1·0 per cent in the flow velocity was observed. The cumulative error resulting from these inaccuracies was estimated to be 4 per cent. On this basis, the maximum error associated with the Nusselt and Reynolds numbers was 4 per cent under the most adverse conditions. A similar estimation indicated an error of 5 per cent in the vibrational velocity.

DISCUSSION OF RESULTS

The results in the absence of vibration are presented in Fig. 5. These can be expressed in the form

$$N_{Nu} = 0{\cdot}226\ N_{Re}^{\ 0{\cdot}6} \tag{6}$$

in the range $2500 < N_{Re} < 15\,000$.

Vol. 3 1961

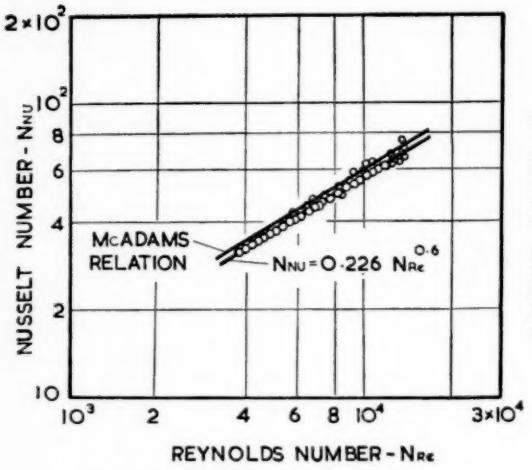

FIG. 5. Test results without vibration.

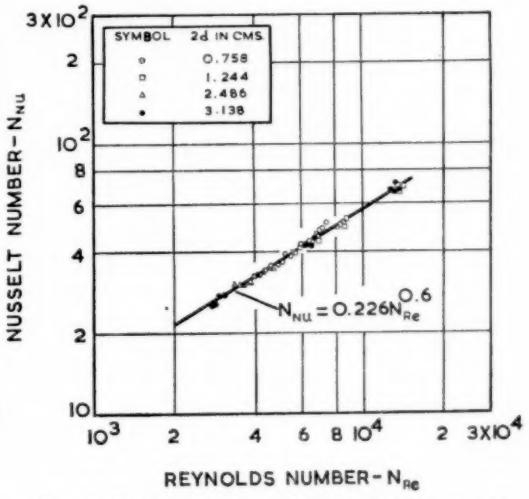

FIG. 7. Test results for a vibrational frequency of 990 cycle/min.

McAdams [12] recommends a relationship of the form

$$N_{Nu} = 0{\cdot}24\ N_{Re}^{0{\cdot}6} \qquad (7)$$

in the range $1000 < N_{Re} < 50{,}000$.

The heat transfer coefficients obtained in this investigation are 6 per cent lower than those given by equation 7.

In Figs. 6–8 are shown the results with vibration. In Fig. 6 is shown the test data for a constant amplitude with varying vibrational frequency and flow velocities. In Fig. 7 is presented test data at constant frequency with varying amplitude and flow velocities. In Fig. 8 is presented the data of all the sixty-four runs conducted with different combinations of flow velocity, amplitude and frequency of vibration. In each figure the forced convection correlation without vibration is also shown to facilitate comparison. They indicate that the heat transfer

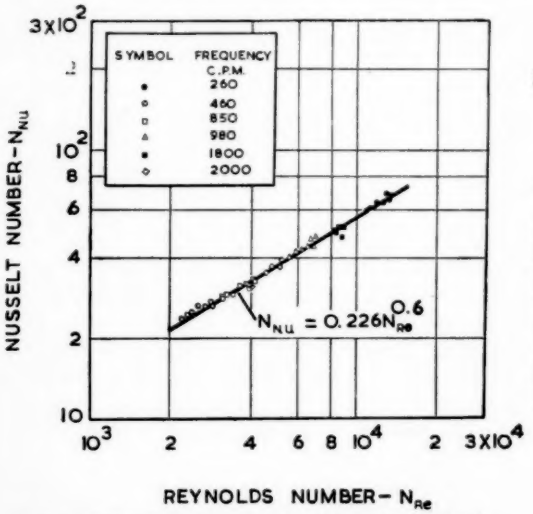

FIG. 6. Test results for a vibrational double amplitude of 1·244 cm.

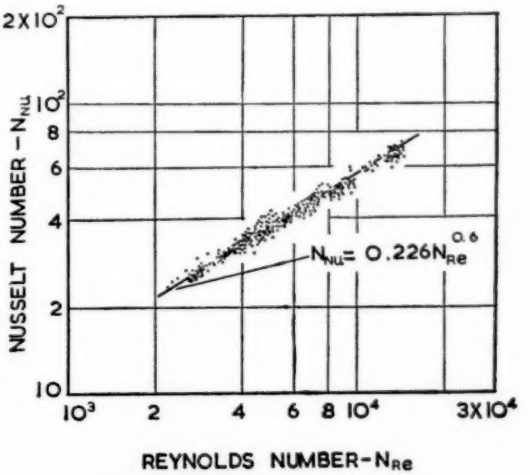

FIG. 8. Test results with vibration.

coefficients are not affected under the influence of vibrations in the range of parameters investigated. The root-mean-square velocity of vibration was varied from 0·5 ft/s to 4·2 ft/s. Further increase was prevented by mechanical limitations of the connecting rod and crank mechanism. The ratio V_v/V_F varied from 0·04 to 0·20. The trend of the results was the same in every run and no other characteristic behaviour was observed at the highest amplitude or at the highest flow velocity. A few runs were conducted wherein the frequency of vibration was varying throughout the cooling of the cylinder. Even these variations did not have any effect on the heat transfer coefficients.

Van der Hegge Zijnen [1] using the resultant of the flow velocity and the vibrational velocity found that the heat transfer from a wire subjected to velocity fluctuations perpendicular and parallel to the direction of flow could be expressed in the form

$$N_{Nu} = a + b\sqrt{(V_F)}\left[1 - \left(\frac{U_v}{V_F}\right)^2 + 0{\cdot}25\left(\frac{V_v}{V_F}\right)^2\right]. \quad (8)$$

This was obtained by substituting the resultant velocity for the flow velocity in the equation

$$N_{Nu} = a + b\sqrt{(V_F)}. \quad (9)$$

Higher power terms were neglected in the binomial expansion given in equation (8). His experimental results were in good agreement with equation (8).

A similar analysis is made below using equation (6) which gives the heat transfer data in the absence of vibration.

$$N_{Nu} = 0{\cdot}226\, N_{Re}{}^{0{\cdot}6} \quad (6)$$

$$N_{Nu} = K\, V_F^{0{\cdot}6} \quad (10)$$

where

$$K = 0{\cdot}226\left[\frac{D\rho}{\mu}\right]^{0{\cdot}6}.$$

On imposing a vibrational velocity V_v, the resultant velocity becomes

$$V_R = \sqrt{(V_F^2 + V_v^2)}. \quad (11)$$

On substituting this value, equation (10) transforms to

$$N_{Nu} = K\,(V_F^2 + V_v^2)^{0{\cdot}3} = K\, V_F^{0{\cdot}6}\left[1 + \left(\frac{V_v}{V_F}\right)^2\right]^{0{\cdot}3}. \quad (12)$$

Writing the binomial expansion of the terms in the parentheses, we get

$$N_{Nu} = K\, V_F^{0{\cdot}6}\left[1 + 0{\cdot}3\left(\frac{V_v}{V_F}\right)^2 - 0{\cdot}105\left(\frac{V_v}{V_F}\right)^4 + 0{\cdot}06\left(\frac{V_v}{V_F}\right)^6 - + \ldots\right] \quad (13)$$

As the highest value of V_v/V_F is 0·2, the third and the succeeding terms can be neglected. Then equation (13) reduces to

$$N_{Nu} = K\, V_F^{0{\cdot}6}\left[1 + 0{\cdot}3\left(\frac{V_v}{V_F}\right)^2\right]. \quad (14)$$

Substituting $(V_v/V_F) = 0{\cdot}2$ which is the maximum used in this investigation, we get

$$N_{Nu} = 1{\cdot}012\, K\, V_F^{0{\cdot}6} \quad (15)$$

thus indicating the improvement in heat transfer to be only 1·2 per cent. An increase of 1·2 per cent could not be observed with the instrumentation used in this investigation.

CONCLUSIONS

(1) The forced convection heat transfer from a horizontal cylinder to a normal air stream can be expressed in the form

$$N_{Nu} = 0{\cdot}226\, N_{Re}{}^{0{\cdot}6}$$

in the range $2500 < N_{Re} < 15\,000$.

(2) In the above range of Reynolds number, the heat transfer from the cylinder subjected to vibration in a direction perpendicular to the direction of the air stream remains unaffected when the ratio of the root-mean-square velocity of vibration to the flow velocity is varied from 4 to 20 per cent.

(3) An analysis using the resultant of the vibrational and the flow velocity indicated that there will be no appreciable change in the heat transfer coefficients.

Vol. 3 1961

ACKNOWLEDGEMENT

The authors thank the authorities of the Indian Institute of Science, Bangalore, for providing them with facilities for conducting the investigation.

REFERENCES

1. B. G. VAN DER HEGGE ZIJNEN, Heat transfer from horizontal cylinders to a turbulent air flow, *Appl. Sci. Res.* A **7**, 205–223 (1958).
2. R. ANANTANARAYANAN and A. RAMACHANDRAN, Effect of vibration on heat transfer from a wire to air in parallel flow, *Trans. Amer. Soc. Mech. Engrs*, **80**, 1426–32 (1958).
3. W. TESSIN and M. JAKOB, Influence of unheated starting section on heat transfer from a cylinder to gas streams parallel to the axis, *Trans. Amer. Soc. Mech. Engrs*, **75**, 473–481 (1953).
4. R. C. MARTINELLI and L. M. K. BOELTER, The effect of vibration on heat transfer by free convection from a horizontal cylinder, *Proc. of 5th Int. Congr. Appl. Mech.* 578–84 (1938).
5. R. LEMLICH, Effect of vibration on natural convective heat transfer, *Industr. Engng Chem.* **47**, 1175–80 (1955).
6. Y. T. TSUI, Ph.D. Dissertation, *The Effect of Vibration on Heat Transfer Coefficients*, The Ohio State University, Ohio (1953).
7. A. J. SHINE, *The Effect of Transverse Vibration on the Heat Transfer Rate from a Heated Vertical Plate in Free Convection*, Tech. Rept. 57–13, Wright Patterson Air Force Base, Ohio (1957).
8. R. S. MAXWELL, The escape of heat from a harmonically oscillating hot wire, *Phil. Mag.* **6**, 945–965 (1928).
9. R. C. RICHARDS, The resistance of a hot wire in an alternating air current, *Phil. Mag.* **45**, 926–934 (1923).
10. A. L. LONDON, H. B. NOTTAGE and L. M. K. BOELTER, Determination of unit conductances for heat and mass transfer by the transient method, *Industr. Engng Chem.* **33**, 467–473 (1941).
11. P. J. SCHNEIDER, *Conduction Heat Transfer*, p. 259. Addison-Wesley, Cambridge, Mass. (1955).
12. W. H. MCADAMS, *Heat Transmission*, p. 260. McGraw-Hill, New York (1954).

ol.
3
961

Int. J. Heat Mass Transfer. Vol. 3, pp. 68–75. Pergamon Press 1961. Printed in Great Britain.

HEAT TRANSFER BIBLIOGRAPHY

E. R. G. ECKERT, E. M. SPARROW and W. E. IBELE
Department of Mechanical Engineering, Heat Transfer Laboratory,
University of Minnesota, Minneapolis 14, Minnesota

APPLICATIONS

E. W. ADAMS, Radiation versus mass-transfer effects for ablating re-entry shields of a nonlifting satellite. *J. Aero. Space Sci.* **27**, No. 11, 868 (1960).

N. ANTONESCU, Calculation of optimal placement of the secondary heat exchange surfaces of steam boilers. *Acad. Rep. Pop. Romine, Inst. Energetica, Stud. Cerc. Energetica*, **9**, No. 1, 35 (1959). (In Roumanian).

T. BALASKA, A. L. MCKEAN and E. J. MERRELL, Long-time heat runs on underground cable. *Elect. Engng*, **79**, No. 11, 893 (1960).

K. BAMMERT, Optimale Auslegung von Kernheizkraftwerken mit Stickstoff als Arbeitsmittel. *Atomkernenergies*, **12**, 437 (1960).

F. J. BAYLEY, *Air-cooling Methods for Gas-turbine Combustion Systems*. Aero. Res. Coun. Lond. Rep. Mem. 3110 (1959).

B. H. BEAM, *Exploratory Study of Thermoelectric Power Generation for Space Flight Applications*. NASA TN D-336 (1960).

A. A. CHIRKOV and B. S. STEFANOVSKII, The dominating method of heat transfer in the cylinders of internal combustion motors. *Trudi Rostovsk. In-ta Inzh. Zh.-d. Transp.* No. 21, 96–111 (1958); *Ref. Zh. Mekh.* No. 6, Rev. 6441 (1959). (In Russian).

R. A. COLE, Dart-shaped satellite. *Aircraft & Missiles*, **3**, No. 9, 62 (1960).

H. HIDALGO, Ablation of glassy material around blunt bodies of revolution. *J. Amer. Rocket Soc.* **30**, No. 9, 806 (1960).

W. HUFSCHMIDT, Die Eigenschaften von Rippenrohr-luftkühlern im Arbeitsbereich der Klimaanlagen. *Forschnung. des Landes Nordrhein-Westfalen Herausgegeben durch das Kultusministerium*, No. 889, published by Westdutscher Verlag/Köln und Opladen (1960).

W. M. KAYS and T. R. LOESCHNER, *Heat Transfer and Flow Friction Characteristics of Elliptical Pin-fin Heat Exchanger Surface*. Stanford Univ., Dept. of Mech. Engng, TR 44 (1959).

O. A. KELLEY, JR., Parametric weight study of manned space entry vehicle. *Aero. Space Engng*, **19**, No. 10, 40 (1960).

V. F. KRAVETZ and V. F. STEPANCHUK, The calculation of regenerative heat exchange apparatus with revolving attachment. *Inzh.-Fiz. Zh.* **3**, No. 3, 133 (1960). (In Russian).

K. S. LEE and J. G. KNUDSEN, Local shell-side heat transfer coefficients and pressure drop in a tubular heat exchanger with orifice baffles. *J. Amer. Inst. Chem. Engrs*, **6**, 669 (1960).

J. L. LOCKARD and J. H. WEBER, Spined tubes in cross-flow exchangers. *Industr. Engng Chem.* **52**, No. 11, 925 (1960).

A. L. LONDON, J. W. MITCHELL and W. A. SUTHERLAND, *Heat Transfer and Flow Friction Characteristics of Crossed Rod Matrices*. Stanford Univ., Dept. of Mech. Engng, TR 41 (1959).

U. MENNICKE, Heat transfer in plate heat exchangers. *Kältetech.* **11**, No. 9, 278 (1959). (In German).

E. I. MOLCHANOV, The investigation of temperature fields arising in the cooled down rotor of a gas turbine. *Teploenergetika*, No. 4, 53 (1960). (In Russian).

E. I. MOLCHANOV, A method of approximating the calculation of temperature fields in cooled disc rotors of gas turbines. *Inzh.-Fiz. Zh.* **3**, No. 4, 99 (1960). (In Russian).

R. F. NEU, *Comparison of Localized Heat-transfer Rates in a Liquid-oxygen–heptane Rocket Engine Employing Several Injection Methods and Oxidant-fuel Ratios*. NASA TN D-286 (1960).

T. OGURI, On the coefficient of heat transfer between gases and cylinder walls of the spark-ignition engine. *Bull. Japan Soc. Mech. Engrs*, **3**, No. 11, 363 (1960).

T. OGURI, Theory of heat transfer in the working gases of internal combustion engines. *Bull. Japan Soc. Mech. Engrs*, **3**, No. 11, 370 (1960).

W. C. RAGSDALE and J. M. SMITH, Heat transfer in nozzles. *Chem. Engng Sci.* **11**, No. 4, 242 (1960).

W. H. ROBBINS, D. BACHKIN and A. A. MEDEIROS, *An Analysis of Nuclear-rocket Nozzle Cooling*. NASA TN D-482 (1960).

L. ROBERTS, *An Analysis of Ablation-shield Requirements for Manned Re-entry Vehicles*. NASA TR R-62 (1960).

D. J. I. RODERICK, M. V. MURRAY and A. G. WALL, Heat transfer and draught loss in the tube banks of shell boilers. *J. Inst. Fuel*, **32**, No. 225, 450 (1959).

S. M. SCALA and E. J. NOLAN, *Aerothermodynamic Feasibility of Graphite for Hypersonic Glide Vehicles*. Space Sciences Laboratory, General Electric Co., Missile and Space Vehicle Department, Technical Information Series, Report R60SD425 (1960).

C. G. SMITH, Heat-flux distribution over hemispherical-nosed bodies in hypersonic flight. *J. Aero. Space Sci.* **28**, No. 1, 69 (1961).

L. STEG, Materials for re-entry heat protection of satellites. *J. Amer. Rocket Soc.* **30**, No. 9, 815 (1960).

L. STEG and G. W. SUTTON, Prospects of MHD power generation. *Astronautics*, **5**, No. 8, 22 (1960).

R. T. SWANN, *Calculated Effective Thermal Conductivities of Honeycomb Sandwich Panels*. NASA TN D-171 (1959).

B. W. SWANSON and E. V. SOMERS, Refrigerator heat leak for sandwiched thermoelectric elements. *J. Heat Transfer*, C **83**, No. 1, 102 (1961).

B. W. SWANSON, E. V. SOMERS and R. R. HEIKES, Optimization of a sandwiched thermoelectric device. *J. Heat Transfer*, C **83**, No. 1, 77 (1961).

F. L. TEST, The influence of bypass channels on the laminar flow heat-transfer and fluid friction characteristics of shell and tube heat exchangers. *J. Heat Transfer*, C **83**, No. 1, 39 (1961).

Vol. 3 1961

W. T. THORNEYCROFT and M. W. THRING, A theoretical method for predicting heat transfer distribution in a petroleum heater. *Trans. Inst. Chem. Engrs*, **38**, No. 2, 63 (1960).

D. H. TRUSSELL and D. J. WEIDMAN, *A Radiant Heater to Stimulate Aerodynamic Heating in a Wind Tunnel.* NASA TN D-530 (1960).

V. W. UHL and H. P. VOZNICK, Anchor agitator. *Chem. Engng Progr.* **56**, No. 3, 72 (1960).

E. W. UNGAR, Particle impacts on melt layer of ablating body. *J. Amer. Rocket Soc.* **30**, No. 9, 799 (1960).

K. WANG and L. TING, Aerodynamic heating of re-entry vehicle. *J. Amer. Rocket Soc.* **30**, No. 12, 1180 (1960).

L. D. WING, Evaluation of thermal problems at relatively low orbital altitudes. *Aero. Space Engng*, **19**, No. 3, 58 (1960).

L. D. WING, Figuring heating of blunt shapes in hypersonic flight. *Space Aeronautics*, **34**, No. 4, 187 (1960).

T. J. WONG, G. GOODWIN and R. E. SLYE, *Motion and Heating During Atmosphere Re-entry of Space Vehicles.* NASA TN D-334 (1960).

BOOKS

F. BOŠNJAKOVIĆ, *Technische Thermodynamik, Part II*, 3rd Ed. Verlag von Theodor Steinkopff, Dresden (1960).

I. F. GOLUBEV, *Viscosity of Gases and Gaseous Mixtures:* A Reference Manual. Gosudarstvennoe Izdatel'stvo, Moscow, Fiziko-Matematichoskoi Literatury (1959).

V. J. JOHNSON (General Editor), *A Compendium of the Properties of Materials at Low Temperature (Phase 1), Parts I, II, and III.* Wright Air Development Division, WADD TR 60–56 (1960).

R. W. TRUITT, *Fundamentals of Aerodynamic Heating.* Ronald Press, New York (1960).

BOUNDARY LAYERS

M. C. ADAMS, W. E. POWERS and S. GEORGIEV, An experimental and theoretical study of quartz ablation at the stagnation point. *J. Aero. Space Sci.* **27**, No. 7, 535 (1960).

S. I. ANISIMOV and T. L. PERELMAN, On the investigation of heat transfer in the presence of chemical conversions. *Int. J. Heat Mass Transfer*, **1**, No. 4, 269 (1961).

A. SH. ASATURIAN and B. A. TONKOSHKUOV, Longitudinal flowing of highly viscous fluid around a heated cylinder. *Inzh.-Fiz. Zh.* **3**, No. 7, 106 (1960).

L. N. BATHISH and B. H. SAGE, Thermal transfer in turbulent gas streams: temperature distribution in boundary flows about spheres. *J. Amer. Inst. Chem. Engrs*, **6**, 693 (1960).

M. H. BERTRAM, *Boundary-layer Displacement Effects in Air at Mach Numbers of* 6·8 *and* 9·6. NASA TR R-22 (1959).

W. S. BRADFIELD, Conical turbulent boundary layer experiments and a correlation with flat plate data. *J. Heat Transfer*, C **82**, No. 2, 94 (1960).

L. T. CHAUVIN and J. J. BUGLIA, *Measurement of Aerodynamic Heat Transfer to a Deflected Trailing-edge Flap on a Delta Fin in Free Flight at Mach Numbers from* 1·5 *to* 2·6. NASA TN D-250 (1960).

S. I. CHENG and H. H. CHIU, Mixing and chemical reaction in an initially non-uniform temperature field. *Int. J. Heat Mass Transfer*, **1**, No. 4, 280 (1961).

J. W. CLEAVER and F. THOMSON, *Ablation Studies of Low Melting Point Bodies in a Pre-heated Supersonic Air Stream.* Coll. Aero., Cranfield, Report 127 (1960).

E. R. G. ECKERT, *Survey of Boundary Layer Heat Transfer at High Velocities and High Temperatures.* Wright Air Development Division, WADD TR 59-624 (1960).

R. EICHHORN, E. R. G. ECKERT and A. D. ANDERSON, An experimental study of the effects of nonuniform wall temperature on heat transfer in laminar and turbulent axisymmetric flow along a cylinder. *J. Heat Transfer*, C **82**, No. 4, 349 (1960).

R. D. ENGLISH and H. S. CARTER, *Variation in Heat Transfer During Transient Heating of a Hemisphere at a Mach Number of* 2. NASA TN D-399 (1960).

T. R. GOODMAN, *Nonsteady Incompressible Heat Transfer for Arbitrary Bodies and all Prandtl Numbers.* Allied Research Associates, Inc., Boston, Mass.; AFOSR TN 60-843 (1960).

P. G. HILL and A. H. STENNING, Laminar boundary layers in oscillatory flow. *J. Basic Engng*, D **82**, No. 3, 593 (1960).

G. R. INGER, An analogy between boundary-layer pressure gradient and chemical reaction-rate effects. *J. Aero. Space Sci.* **27**, No. 12, 956 (1960).

G. R. INGER, Specific heat inequality effect in the chemically frozen stagnation point boundary layer. *J. Amer. Rocket Soc.* **30**, No. 11, 1028 (1960).

S. I. KOSTERIN and YU. A. KOSHMAROV, Turbulent boundary layer on a flat plate in a stream of dissociating gas. *Int. J. Heat Mass Transfer*, **1**, No. 1, 46 (1960).

G. LUDWIG and M. HEIL, Boundary-layer theory with dissociation and ionization. *Advanc. Appl. Mech.* **6**, 39 (1960).

N. ROTT and M. L. ROSENZWEIG, On the response of the laminar boundary layer to small fluctuations of the free-stream velocity. *J. Aero. Space Sci.* **27**, No. 10, 741 (1960).

S. N. SAVULESCU, Betrachtungen über einige Lösungen des Falles der instationären inkompressiblen Grenzschicht. *Rev. Méchanique Appliquée*, **4**, No. 1, 7(1959).

D. A. SPENCE, A note on the recovery and Reynolds-analogy factors in laminar flat-plate flow. *J. Aero. Space Sci.* **27**, No. 11, 878 (1960).

H. THOMANN, *Measurement of the Recovery Temperature in the Wake of a Cylinder and of a Wedge at Mach Numbers Between* 0·5 *and* 3. The Aeronautical Research Institute of Sweden, Report 84, Stockholm (1959).

H. THOMANN, *Measurements of Heat Transfer and Recovery Temperature in Regions of Separated Flow at a Mach Number of* 1·8. The Aeronautical Research Institute of Sweden, Report 82, Stockholm (1959).

U. H. VON GLAHN, *Empirical Equation for Turbulent Forced-convection Heat Transfer for Prandtl Numbers* 0·001 *to* 1000. NASA TN D-483 (1960).

S. A. WAITER, *Reduction of the Boundary Layer Thickness in a Hypersonic Nozzle.* University of So. Calif. Engng Center, Report 56-213; AFOSR TN 60-514 (1960).

A. WALZ, Contribution to the approximation theory of compressible turbulent boundary layers. *Dtsch. Versuchsanstalt Luftfahrt, Ber.* 84 (1959). (In German).

P. P. WEGENER, Experiments on the departure from chemical equilibrium in a supersonic flow. *J. Amer. Rocket Soc.* **30**, No. 4, 322 (1960).

CHANGE OF PHASE

W. D. ALLINGHAM and J. A. MCENTIRE, Determination of boiling film coefficient for a heated horizontal tube

in water-saturated wick material. *J. Heat Transfer*, C **83**, No. 1, 71 (1961).
M. M. CHEN, An analytical study of laminar film condensation: Part 1, Flat plates. *J. Heat Transfer*, C **83**, No. 1, 48 (1961).
M. M. CHEN, An analytical study of laminar film condensation: Part 2, Single and multiple horizontal tubes. *J. Heat Transfer*, C **83**, No. 1, 55 (1961).
R. L. CLARK and L. A. BROMLEY, Multiple-effect rotating evaporation. *Chem. Engng Progr.* **57**, No. 1, 64 (1961).
R. COLE, A photographic study of pool boiling in the region of the critical heat flux. *J. Amer. Inst. Chem. Engrs*, **6**, 533 (1960).
S. ISHIGAI and K. SEKOGUCHI, On the flashing flow of saturated water through horizontal pipes. *Bull. Japan Soc. Mech. Engrs*, **2**, No. 8, 563 (1959).
R. T. JACOBS and J. A. MERRILL, The application of statistical methods of analysis for predicting the burnout heat flux. *Nucl. Sci. Engng*, **8**, No. 8, 480 (1960).
H. P. LÖW-FRÄULIN, Stoffaustausch zwischen Rieselfilm und gegenströmendem Dampf bei Zweistoffgemischen. *Chem.-Ing.-Tech.* **33**, No. 1, 39 (1961).
I. MABUCHI, Heat transfer by film condensation—An approximate theory of laminar film condensation. *Trans. Japan Soc. Mech. Engrs*, **26**, 1134 (1960).
P. W. MCFADDEN and R. J. GROSH, An analysis of laminar film boiling with variable properties. *Int. J. Heat Mass Transfer*, **1**, No. 4, 325 (1961).
I. S. PASTERNAK and W. H. GAUVIN, Turbulent heat and mass transfer from stationary particles. *Canad. J. Chem. Engng*, **38**, No. 2, 35 (1960).
F. E. ROMIE, S. W. BROVARNEY and W. H. GIEDT, Heat transfer to boiling mercury. *J. Heat Transfer*, C **82**, No. 4, 387 (1960).
R. J. SIERASKI and G. M. MACHWART, A nomograph for boiling temperature by the Meissner method. *Industr. Engng Chem.* **52**, No. 10, 869 (1960).
E. M. SPARROW and J. P. HARTNETT, Condensation on a rotating cone. *J. Heat Transfer*, C **83**, No. 1, 101 (1961).
B. STANISZEWSKI, Nucleate boiling bubble growth and departure. *Archiwum Budowy Maszyn*, **7**, No. 1, 3(1960).
M. UEDA, Rate of evaporation of water by forced convection. *J. Appl. Phys., Japan*, **29**, 443 (1960).
G. B. WALLIS, Gas-liquid analogue of nucleate boiling. *Nucl. Power*, **5**, No. 52, 99 (1960).

CHANNEL FLOW

H. ASAWO, An approximate solution of oil-cooling pipe. *Bull. Japan Soc. Mech. Engrs*, **2**, No. 7, 433 (1959).
H. ASAWO, Experiment on the heat-transfer of oil-cooling pipe. *Bull. Japan Soc. Mech. Engrs*, **2**, No. 7, 429 (1959).
H. BARROW, Convection heat transfer coefficients for turbulent flow between parallel plates with unequal heat fluxes. *Int. J. Heat Mass Transfer*, **1**, No. 4, 306 (1961).
D. E. BIRDSEYE, *Experimental Investigation of Heat-transfer Characteristics of Liquid Nitrogen Tetroxide*. Jet Propulsion Laboratory, Calif. Inst. Technology, JPL TR 32-37 (1960).
E. E. COVERT, *On an Approximate Solution of the Energy Equation and Its Application to the McClimans' Data*. Mass. Inst. Technology, Naval Supersonic Laboratory, TR 403 (1959).
H. FADU and T. J. HANRATTY, Effects of solids on turbulence in a fluid. *J. Amer. Inst. Chem. Engrs*, **6**, 624 (1960).
H. HARTMANN, Wärmeübergang bei laminarer Strömung durch Ringspalte. *Chem.-Ing.-Tech.* **33**, No. 1, 22 (1961).
T. W. JACKSON, K. R. PURDY, C. C. OLIVER and H. L. JOHNSON, *The Effects of Resonant Acoustic Vibrations on the Local and Overall Heat Transfer Coefficients for Air Flowing Through an Isothermal Horizontal Tube*. Aeronautical Research Laboratory, Air Force Research Division, ARL TR 60-322 (1960).
J. J. KEYES, JR., An experimental study of gas dynamics in high velocity vortex flow. *Proc. Heat Transfer and Fluid Mech. Inst.*, p. 31. Stanford Univ. Press, Stanford, Calif. (1960).
O. KRISCHER, Wärmeaustausch in Ringspalten bei laminarer und turbulenter Strömung. *Chem.-Ing.-Tech.* **33**, No. 1, 13 (1961).
K. S. KRISHNAN and R. SUNDARAM, Distribution of temperature along electrically heated tubes and coils, 1. Theoretical. *Proc. Roy. Soc.* A **257**, No. 1290, 302 (1960).
L. LEES and C. LIU, *Kinetic Theory Description of Plane, Compressible Couette Flow*. Guggenheim Aeronautical Laboratory, Calif. Inst. Technology, Hypersonic Research Project Memorandum No. 58 (1960).
A. M. MERCER, Growth of thermal boundary layer at inlet to circular tube. *Appl. Sci. Res.* A **9**, No. 6, 450 (1960).
W. B. NICOLL and W. M. KAYS, *Influence of Temperature Dependent Properties on Gas Flow Heat Transfer in Circular Tubes*. Stanford Univ., Dept. Mech. Engng, TR 43 (1959).
R. N. NOYES, A fully integrated solution of the problem of laminar or turbulent flow in a tube with arbitrary wall heat flux. *J. Heat Transfer*, C **83**, No. 1, 96 (1961).
T. OGURI, *Determination of Rate of Heat Transfer Between the Gases and the Cylinder Walls of a Spark-ignition Engine*. Yokohama National University, Faculty of Engineering Bulletin **9**, 1 (1960).
F. J. QUIRRENBACH, Wärmeübergang bei turbulenter Strömung in Ringspalten. *Allg. Wärmetech.* **9**, No. 13, 271 (1960).
G. F. C. Rogers and Y. R. MAYHEW, Evaluation of bulk velocity and temperature for turbulent flow in tubes. *Int. J. Heat Mass Transfer*, **1**, No. 1, 55 (1960).
E. M. ROSEN and E. J. SCOTT, The Leveque solution with a finite wall resistance. *J. Heat Transfer*, C **83**, No. 1, 98 (1961).
J. M. SAVINO and R. G. RAGSDALE, Some temperature and pressure measurements in confined vortex fields. *J. Heat Transfer*, C **83**, No. 1, 33 (1961).
W. R. SCHOWALTER and H. F. JOHNSTONE, Characteristics of the mean flow patterns and structure of turbulence in spiral gas streams. *J. Amer. Inst. Chem. Engrs*, **6**, 648 (1960).
D. E. SEVERSON, A. J. MADDEN and E. L. PIRET, Evaporation rates of liquids to flowing gas streams. *J. Amer. Inst. Chem. Engrs*, **5**, No. 4, 413 (1959).
M. SUZUKI, Theoretical and experimental studies on vortex-tube. *Inst. Phys. Chem. Res. (Tokyo), Sci. Papers*, **54**, No. 1, 42 (1960).
M. F. TAYLOR and T. A. KIRCHGESSNER, Measurements of heat transfer and friction coefficients for helium flowing in a tube at surface temperatures up to 5900 R. *J. Amer. Rocket Soc.* **30**, No. 9, 830 (1960).

CONDUCTION

E. L. ALBASINY, On numerical solution of cylindrical heat-conduction problem. *Quart. J. Mech. Appl. Math.* **13**, Pt. 3, 374 (1960).

Vol. 3 1961

H. R. BAILEY, Conduction-convection from a cylindrical source with increasing radius. *Quart. Appl. Math.* **18**, No. 4, 325 (1961).

A. N. BAXTER, Extension of the transient heating charts. *J. Amer. Rocket Soc.* **30**, No. 9, 905 (1960).

D. B. CONCER, Heat flow towards a moving cavity. *Quart. J. Mech. Appl. Math.* **12**, No. 2, 222 (1959).

E. DANTER, Periodic heat flow characteristics of simple walls and roofs. *Instn Heat. Vent. Engrs*, **28**, 136 (1960).

A. DEMETRIADES, Heat conduction in a circular cylinder rotating with its axis normal to the direction of flight. *J. Amer. Rocket Soc.* **29**, No. 9, 653 (1959).

G. M. DUSINBERRE, A note on the "Implicit" method for finite-different heat-transfer calculations. *J. Heat Transfer*, C **83**, No. 1, 94 (1961).

J. W. ENIG, *A Method for the Rapid Numerical Solution of the Heat Conduction Equation for Composite Slabs.* U.S. Naval Ordnance Laboratory, Report 6666 (1959).

K. GARDNER and T. C. CARNAROS, Thermal-contact resistance in finned tubing. *J. Heat Transfer*, C **82**, No. 4, 279 (1960).

T. R. GOODMAN, The heat-balance integral—Further considerations and refinements. *J. Heat Transfer*, C **83**, No. 1, 83 (1961).

R. J. GROSH, *Transient Temperature in a Semi-infinite, Porous Solid with Phase Change and Transpiration Effects.* U.S. Air Force, Wright Air Development Division, WADD TR 60-105 (1960).

G. R. GUINN, Aerodynamic heating charts for solid propellant rocket motors. *J. Amer. Rocket Soc.* **30**, No. 8, 776 (1960).

M. E. GURTIN, On the use of normal co-ordinates for the solution of lumped parameter transient heat-transfer problems. *J. Aero. Space Sci.* **27**, No. 5, 357 (1960).

W. H. HOLTER and J. H. GROVER, Insulation temperature for the transient heating of an insulated infinite metal slab. *J. Amer. Rocket Soc.* **30**, No. 9, 907 (1960).

G. HORVAY and R. H. EDSALL, The interface temperature of two media in poor thermal contact. *A.I.M.E. Metallurgical Soc. Trans.* **218**, No. 5, 927 (1960).

W. M. KAYS, Basic heat transfer and flow friction characteristics of six compact high-performance heat transfer surfaces. *J. Engng for Power*, A **82**, No. 1, 27 (1960).

J. A. LEWIS and T. D. RINEY, Temperature rise in infinite medium heated by planar source. *Soc. Industr. Appl. Math. J.* **8**, No. 2, 249 (1960).

C. H. LIEBERT, J. E. HATCH and R. W. GRANT, *Applications of Various Techniques for Determining Local Heat-transfer Coefficients in a Rocket Engine from Transient Experimental Data.* NASA TN D-277 (1960).

B. F. NOVITSKII, Calculations for the directed changes of temperature of an unbounded plate. *Trudi Leningrad Tekhnol. In-ta Pishch. Prom-sti.* **14**, 235 (1958); *Ref. Zh. Mekh.* No. 6, Rev. 6662 (1959). (In Russian).

J. R. PHILIP, General method of exact solution of the concentration-dependent diffusion equation. *Aust. J. Phys.* **13**, No. 1, 1 (1960).

J. S. PRZEMIENIECKI, Design charts for transient temperature and thermal stress distributions in thermally thick plates. *Aeronaut. Quart.* **11**, Pt. 3, 269 (1960).

R. W. SANDERS, Transient heat conduction in a melting finite slab: An exact solution. *J. Amer. Rocket Soc.* **30**, No. 11, 1030 (1960).

J. E. SCHMIDT and G. SONNEMANN, Transient temperatures and thermal stresses in hollow cylinders due to heat generation. *J. Heat Transfer*, C **82**, No. 4, 273 (1960).

M. S. SMIRNOV, Asymmetric heating of a plate when an internal source of heat is in operation. *Sb. Rabot. Vses. Zaochn. In-ta Pishch. Prom-sti.* No. 3, 49 (1958); *Ref. Zh. Mekh.* No. 6, Rev. 6663 (1959). (In Russian).

I. N. SOKOLOVA, Calculation of the heating of shells at high speeds. *J. Amer. Rocket Soc.* **30**, No. 4, 375 (1960).

W. UNTERBERG, Simple graphical method for temperature distribution in bodies with linear change in environment temperature. *J. Aero. Space Sci.* **28**, No. 1, 78 (1961).

V. VODICKA, Fourier's classical problem in case of stratiform bodies. *Archiwum Mechaniki Stosowanej*, **12**, No. 1, 3 (1960).

V. VODICKA, Steady temperature field in a composite doubly infinite strip. *J. Phys. Soc., Japan*, **15**, 1332 (1960).

K. T. YANG and A. SZEWCZYK, An approximate treatment of unsteady heat conduction in semi-infinite solids with variable thermal properties. *J. Heat Transfer*, C **81**, No. 3, 251 (1959).

FLOW WITH SEPARATED REGIONS

C. BOURQUE and B. G. NEWMAN, Reattachment of a two-dimensional, incompressible jet to an adjacent flat plate. *Aeronaut. Quart.* **11**, Pt. 3, 201 (1960).

M. COOPER, E. E. MAYO and J. D. JULIUS, *Influence of Low Wall Temperature on Boundary-Layer Transition and Local Heat Transfer on 2-in. Diameter Hemispheres at Mach Number of 4·95 and Reynolds Number per Foot of* $73{\cdot}2 \times 10^6$. NASA TN D-391 (1960).

K. R. CZARNECKI and J. R. SEVIER, JR., *Investigation o Effects of Roughness, Surface Cooling, and Shock Impingement on Boundary-layer Transition on Two-dimensional Wing.* NASA TN D-417 (1960).

D. KUNII and J. M. SMITH, Heat transfer characteristics of porous rocks. *J. Amer. Inst. Chem. Engrs*, **6**, No. 1, 71 (1960).

H. K. LARSON and J. K. STEPHEN, JR., *Transition Reynolds Numbers of Separated Flows at Supersonic Speeds.* NASA TN D-349 (1960).

G. B. SCHUBAUER and W. G. SPANGENBERG, Forced mixing in boundary layers. *J. Fluid Mech.* **8**, No. 1, 10 (1960).

W. SPRINGE, *Wärmeübergang an ein gekühltes Rohr im Lichtbogenplasma.* Friedr. Vieweg, Braunschweig (1960).

J. R. STERRETT and J. C. EMERY, *Extension of Boundary-layer-separation Criteria to a Mach Number of 6·5 by Utilizing Flat Plates with Forward-facing Steps.* NASA TN D-618 (1960).

A. A. TOWNSEND, The development of turbulent boundary layers with negligible wall stress. *J. Fluid Mech.* **8**, No. 1, 143 (1960).

J. WADSWORTH, *Experimental Examination of Local Processes in Packed Beds of Homogeneous Spheres. Part I. The Local Packing in Randomly Stacked Sphere Beds. Part II. The Local Heat Transfer over the Surface of Infinite Dimensions and Arranged in Rhombohedral Array.* National Research Council of Canada (1960).

S. YAGI and N. WAKAO, Heat and mass transfer from wall to fluid in packed beds. *J. Amer. Inst. Chem. Engrs*, **5**, No. 1, 69 (1959).

S. YAGI, D. KUNII and N. WAKAO, Studies on axial effective thermal conductivity in packed beds. *J. Amer. Inst. Chem. Engrs*, **6**, 543 (1960).

LOW-DENSITY HEAT TRANSFER

L. DUMITRESCU, On heat-transfer in free-molecule flows. *Rev. Méchanique Appliquée*, **4**, No. 2, 237 (1959).

T. FUJIMOTO and K. TAKAO, Heat transfer in the rarefied gases, Parts 1 and 2. *Bull. Japan Soc. Mech. Engrs*, **2**, No. 6, 197, 204 (1959).

M. Z. KRZYWOBLOCKI and R. E. BLOOMQUIST, On heat phenomena on rotating bodies in free molecule flow. *Acta Phys. Austr.* **12**, No. 3, 237 (1959).

S. E. NEICE, R. W. RUTOWSKI and K. K. CHAN, Stagnation-point heat-transfer measurements in hypersonic low-density flow. *J. Aero. Space Sci.* **27**, No. 5, 387 (1960).

A. TAKANO, Wall temperature and heat transfer of a flat plate in the slip flow. *Trans. Japan Soc. Aero. Space Sci.* **2**, No. 2, 11 (1959).

LIQUID METALS

J. S. MCDONALD and T. J. CONNOLLY, Investigation of natural convection heat transfer in liquid sodium. *Nucl. Sci. Engng*, **8**, No. 5, 369 (1960).

MAGNETOHYDRODYNAMICS

H. P. GREENSPAN, Flat plate drag in magnetohydrodynamic flow. *Phys. Fluids*, **3**, No. 4, 581 (1960).

R. X. MEYER, Heat-transfer near stagnation point of body of revolution in presence of magnetic field. *Z. Angew. Math. Phys.* **11**, No. 2, 127 (1960).

H. N. OLSEN, Thermal and electrical properties of an argon plasma. *Phys. Fluids*, **2**, No. 6, 614 (1959).

MEASUREMENT TECHNIQUES

T. AZUMA, T. CHIHARA and I. NIIKURA, The recording radiation thermometer. *Toshiba Rev.* **15**, 999 (1960).

W. H. CHRISTIANSEN, *Use of Fine Unheated Wires for Heat Transfer Measurements in the Shock Tube*. Guggenheim Aeronautical Laboratory, Calif. Inst. Technology, Hypersonic Research Project Memorandum 55 (1960).

J. C. COOK and H. S. LEVINE, Calorimeter and accessories for very high thermal radiation flux measurements. *Rev. Sci. Instrum.* **31**, No. 10, 1160 (1960).

S. CORRSIN, *Directional Sensitivity for a Finite Hot-wire Anemometer*. Johns Hopkins Univ., Mech. Engng Dept., AFOSR TN 60-171 (1960).

J. W. DAIBER, An optical boundary-layer probe. *J. Aero. Space Sci.* **27**, No. 11, 836 (1960).

W. T. EARHEART, JR. and D. S. BYNUM, *Hypervelocity Arc-tunnel Instrumentation*. Arnold Engng Development Center, Air Research and Development Command, USAF, AEDC-TN-60-227 (1960).

R. J. FRIAUE, Vacuum-tight sample holder for high-temperature conductivity measurements. *Rev. Sci. Instrum.* **31**, No. 10, 1161 (1960).

R. GARDON, A transducer for the measurement of heat-flow rate. *J. Heat Transfer*, C **82**, No. 4, 396 (1960).

R. GRANVILLE and G. BOXALL, Measurements of convective heat transfer by means of the Reynolds analogy. *Brit. J. Appl. Phys.* **11**, No. 10, 471 (1960).

P. GRASSMAN and W. STRAUMANN, An unsteady-state method for the measurement of thermal conductivities of gases and liquids. *Int. J. Heat Mass Transfer*, **1**, No. 1, 50 (1960). (In German).

M. L. GUPTA, Rapid *in situ* method for determining thermal conductivities. *J. Sci. Industr. Res.* B **19**, No. 7, 240 (1960).

R. A. HANEL, *The Dielectric Bolometer, A New Type of Thermal Radiation Detector*. NASA TN D-500 (1960).

M. HARA and T. OGURI, Measurement of piston temperature of spark-ignition engine. *Bull. Japan Soc. Mech. Engrs*, **2**, No. 7, 382 (1959).

A. HENDERSON, JR. and F. E. SWALLEY, *Effects of Air Contamination in Helium Tunnel*. NASA TN D-406 (1960).

M. K. JOVANOVIC and D. R. HAWORTH, *The Development of a Plasma Facility and a Survey of Spectroscopic Methods for Plasma Temperature Determination*. Oklahoma State Univ., Stillwater, Oklahoma (Dec. 1960).

M. A. KAGANOV and Y. L. ROZENSHTOK, The accuracy of measurement of heat flows with heat flow meters. *Inzh.-Fiz. Zh.* **3**, No. 3, 138 (1960). (In Russian).

E. R. KEBBON, Miscellaneous temperature-measuring methods. *Instrum. Control Systems*, Pt. 1, **33**, No. 11, 1921 (1960).

R. W. LARENZ, *Concerning a Method for the Measurement of Very High Temperatures in Nearly Transparent Arc Columns*. NASA TT F-54 (1960).

W. H. P. LESLIE, J. J. HUNTER and D. ROBB, Precision temperature measurement outside the laboratory. *Research, Lond.* **13**, No. 7, 250 (1960).

R. K. MCDONALD, Gas temperature by infrared. *Instrum. Control Systems*, **33**, Pt. 1, No. 11, 1926 (1960).

S. A. SHIPITSYN and V. V. PLASTININ, Determination of the temperature of the plasma of an electric arc. *Izv. Vysshikh Uchebnykh Zavadeniy. Fiz.* (*USSR*), No. 6, 169 (1959).

J. H. SIVITER and K. H. STRASS, *An Investigation of a Photographic Technique of Measuring High Surface Temperatures*. NASA TN D-617 (1960).

P. C. STAINBACK, *Visual Technique for Determining Qualitative Aerodynamic Heating Rates on Complex Configurations*. NASA TN D-385 (1960).

P. H. THOMAS and P. G. SMITH, Simple dosage meter for high-intensity thermal radiation. *J. Sci. Instrum.* **37**, No. 3, 73 (1960).

R. E. WALKER, N. DEHAAS and A. A. WESTERBERG, A new method of measuring gas thermal conductivity. *Phys. Fluids*, **3**, No. 3, 482 (1960).

O. C. WOLF, Hot-wire anemometer. *Instrum. Control Systems*, **33**, No. 6, 962 (1960).

NATURAL CONVECTION

A. ACRIVOS, A theoretical analysis of laminar natural non-Newtonian fluids. *J. Amer. Inst. Chem. Engrs*, **6**, 584 (1960).

J. BRINDLEY, Stability of flow in a rotating viscous incompressible fluid subjected to differential heating. *Phil. Trans.* A **253**, No. 1020 (1960).

T. FUJII, An analysis of turbulent free convection heat transfer from a vertical surface. *Bull. Japan Soc. Mech. Engrs*, **2**, No. 8, 559 (1959).

T. FUJII, Experimental studies of free convection heat transfer. *Bull. Japan Soc. Mech. Engrs*, **2**, No. 8, 555 (1959).

T. FUJII, On the development of a vortex street in a free convection boundary layer. *Bull. Japan Soc. Mech. Engrs*, **2**, No. 8, 551 (1959).

B. GEBHART, Transient natural convection from vertical elements. *J. Heat Transfer*, C **83**, No. 1, 61 (1961).

H. W. HAHNEMANN, Die Überlagerung von erzwungener und natürlicher Konvektion bei niedrigen Durchsätzen in einem lotrechten Rohr. *Z. Ver. Dtsch. Ing.* **102**, No. 36, 1789 (1960).

J. P. HOLMAN, The mechanism of sound field effects on heat transfer. *J. Heat Transfer*, C **82**, No. 4, 393 (1960).

Vol. 3 1961

D. A. KIRK, *The Effect of Gravity on Free Convection Heat Transfer; The Feasibility of Using an Electromagnetic Body Force*. Wright Air Development Division, WADD TR 60-303, Part 1 (1960).

F. W. LARSEN and J. P. HARTNETT, Effect of aspect ratio and tube orientation on free convection heat transfer to water and mercury in enclosed circular tubes. *J. Heat Transfer*, C **83**, No. 1, 87 (1961).

M. B. LARSON, *A Study of the Effects of Ultrasonic Vibrations on Convective Heat Transfer in Liquids*. Dept. of Mech. Engng, Stanford Univ., TR 48 (1960).

Y. MORI, On a laminar free-convection flow and heat transfer of electrically conducting fluid on a vertical flat plate in the presence of a transverse magnetic field. *Trans. Japan Soc. Aero. Space Sci.* **2**, No. 2, 22 (1959).

I. E. RANDALL and A. SESONSKE, Effect of a volume heat source on free-convection heat transfer, *J. Amer. Inst. Chem. Engrs*, **5**, No. 2, 150 (1959).

G. F. SCHEELE, E. M. ROSEN and T. J. HANRATTY, Effect of natural convection on transition to turbulence in vertical pipes. *Canad. J. Chem. Engng*, **38**, No. 3, 67 (1960).

E. SCHMIDT, Thermische Auftriebsströmungen und Wärmeübergang Vierte Ludwig-Prandtl-Gedächtnis-Vorlesung. *Z. Flugwissenschaften*, **8**, Nos. 10/11, 273 (1960).

E. E. SOEHNGEN and J. P. HOLMAN, *Experimental Studies on the Interaction of Strong Sound Fields with Free Convection Boundary Layers*. Aeronautical Research Laboratory, Air Force Research Division, ARL TR 60-323 (1960).

C. TELEKI, *The Influence of Vertical Vibrations on the Rate of Heat Transfer from a Horizontal Cylinder in Air*. Aeronatucal Research Laboratory, Air Force Research Division, WADC TN 59-357 (1960).

PROPERTIES

R. S. BROKAW, *Alignment Charts for Transport Properties Viscosity, Thermal Conductivity, and Diffusion Coefficients for Non-polar Gases and Gas Mixtures at Low Density*. NASA TR R-81 (1960).

H. W. DEEM, W. D. WOOD and C. F. LUCKS. *Thermal Properties of Materials at Elevated Temperatures*. WADC TN 59-215 (1959).

A. DEVRIES and M. F. LARANJEIRA, Thermal diffusion of ternary mixtures. *J. Chem. Phys.* **32**, No. 6, 1714 (1960).

E. DOBBS and L. FINEGOLD, Measurement of the velocity of sound in liquid argon and liquid nitrogen at high pressures. *J. Acoust. Soc. Amer.* **32**, No. 10, 1215 (1960).

W. C. EDMISTER, Applied hydrocarbon thermodynamics. *Petrol. Refin.* **39**, No. 7, 133; No. 8, 113; No. 9, 293; No. 10, 167 (1960).

J. W. FOX and A. C. H. SMITH, Viscosity of mixtures of hydrogen and water vapor at 295° K. *J. Chem. Phys.* **33**, No. 2, 623 (1960).

A. GOLDSMITH, T. E. WATERMAN and H. J. HIRSCHHORN, *Thermophysical Properties of Solid Materials: Vol. 1, Elements (Melting Temperature above 1000° F)*. Wright Air Development Division, WADC TR 58-476 (1960).

M. G. HARRIS, J. E. ROBERTS and J. G. TRULIO, Equilibrium properties of a partially ionized plasma. *Phys. Rev.* **119**, No. 6, 1832 (1960).

A. A. HASAPIS, M. B. PANISH and C. ROSEN, *The Vaporization and Physical Properties of Certain Refractories: Part 1. Techniques and Preliminary Studies*. Wright Air Development Division, WADD TR 60-463, Part 1 (1960).

E. HELFAND and S. RICE, Principle of corresponding states for transport properties. *J. Chem. Phys.* **32**, No. 6, 1642 (1960).

J. KESTIN and H. E. WANG, The viscosity of superheated steam up to 270°C. *Physica*, **26**, 575 (1960).

T. KIHARA, M. H. TAYLOR and J. O. HIRSCHFELDER, *Transport Properties for Gases Assuming Inverse Power Intermolecular Potentials*. Univ. of Wisconsin, Theor. Chem. Lab., WIS-OOR-27 (1960).

S. S. KVASHNINA, Dependence of internal energy of air on pressure and density at high temperatures. *J. Amer. Rocket Soc.* **30**, No. 9, 875 (1960).

E. S. NOWAK, R. J. GROSH and P. E. LILEY, Smooth pressure-volume-temperature data for water in the critical region derived from experimental measurements. *J. Heat Transfer*, C **83**, No. 1, 14 (1961).

E. S. NOWAK, R. J. GROSH and P. E. LILEY, A survey of P-V-T data for water in the critical region. *J. Heat Transfer*, C **83**, No. 1, 1 (1961).

H. J. PAIN and P. R. SMY, The electrical conductivity of shock-ionized argon. *J. Fluid Mech.* **9**, Pt. 3, 390 (1960).

R. W. POWELL and A. R. CHALLONER, Proposed values for thermal conductivities of some liquid refrigerants. *Mod. Refrig.* **63**, No. 742, 42 (1960).

S. M. SCALA, *A Note on the Thermal Diffusion Ratio in Dissociated Air*. Space Sciences Laboratory, General Electric Missile and Space Vehicle Dept., AFOSR Document No. 21, R60SD487 (1960).

S. N. SOKOLOV and L. N. ERASTOV, Lecture experiment on determination of the specific heat of a gas at constant pressure. *Soviet Phys.—Uspekhi*, **3**, No. 1, 171 (1960).

R. M. YARRINGTON and W. B. KAY, Thermodynamic properties of perfluoro-2-butyltetrahydrofuran. *J. Chem. Engng Data*, **5**, No. 1, 24 (1960).

RADIATION

H. E. BENNETT and J. O. PORTEUS, Relation between surface roughness and specular reflection at normal incidence. *J. Opt. Soc. Amer.* **51**, No. 2, 123 (1961).

R. W. BLISS, JR., The derivations of several "plate-efficiency factors" useful in the design of flat-plate solar heat collectors. *J. Solar Energy Sci. Engng*, **3**, No. 4, 55 (1959).

J. C. CAMM, B. KIVEL, R. L. TAYLOR and J. D. TEARE, *Absolute Intensity of Non-equilibrium Radiation in Air and Stagnation Heating at High Altitudes*. AVCO Everett Research Laboratory, Everett, Mass., AFBMD TR 60-184; Research Report 93 (1959).

H. G. ELROD, *Refinements of the Diffusion Theory for Radiative Transfer in Solids*. Air Force Ballistic Missile Division, Air Research and Development Command, USAF, Inglewood, Calif., TR RAD-TR-7-60-28 (1960).

R. M. GOODY, The influence of radiative transfer on the propagation of a temperature wave in a stratified diffusing atmosphere. *J. Fluid Mech.* **9**, Pt. 3, 445 (1960).

R. GOULARD, *The Coupling of Radiation and Convection in Detached Shock Layers*. Bendix Systems Division of the Bendix Corporation, Ann Arbor, Michigan, Research Note 23 (1960).

L. HARRIS and P. FOWLER, Absorptance of gold in the far infrared. *J. Opt. Soc. Amer.* **51**, No. 2, 164 (1961).

G. S. LEON and M. E. SHANK, Analysis of solar-furnace performance in mechanical testing at extremely high temperatures. *J. Engng for Power*, A **82**, No. 4, 325 (1960).

C. LIU, On minimum-weight rectangular radiating fins. *J. Aero. Space Sci.* **27**, No. 11, 871 (1960).
J. C. RICHMOND and W. HARRISON, Equipment and procedures for evaluation of total hemispherical emittance. *Bull. Amer. Ceram. Soc.* **39**, No. 11, 668 (1960).
R. G. STRUSS, Solar furnace determination of high-temperature absorption coefficients. *J. Solar Energy Sci. Engng*, **4**, No. 2, 21 (1960).
R. O. WHITAKER, Methodology for determination of performance characteristics of spectrally selective absorbers. *J. Solar Energy Sci. Engng*, **4**, No. 2, 40 (1960).
W. D. WOOD, H. W. DEEM and C. F. LUCKS, *Emissivity and Emittance—What Are They?* Battelle Memorial Inst., DMIC Memorandum 72 (1960).

ROTATING SURFACES

A. I. BORISENKO and A. D. MYSHKIS, Temperature and velocity distributions in a laminar flow of a fluid between rotating coaxial cylinders. *Appl. Math. Mech., Leningr.* **23**, No. 4, 1054 (1959).
D. FULTZ, R. R. LONG, G. V. OWENS, W. BOHAN, R. KAYLOR and J. WEIL, Studies of thermal convection in a rotating cylinder with some implications for large-scale atmospheric motions. *Met. Monogr.* **4**, No. 21 (1959).
J. P. HARTNETT and E. C. DELAND, The influence of Prandtl numbers on the heat transfer from rotating nonisothermal disks and cones. *J. Heat Transfer*, C **83**, No. 1, 95 (1961).

TRANSFER MECHANISMS

R. C. DIPRIMA, *The Stability of Non-rotationally Symmetric Disturbance for Viscous Flow Between Rotating Cylinders.* Rensselaer Polytechnic Inst., Research Division, Troy, N.Y., RPI MathRep 40 (1961).
R. A. DUTTON, *The Velocity Distribution in a Turbulent Boundary Layer on a Flat Plate.* Aero. Res. Coun., Lond., Curr. Pap. 453 (1959).
J. C. GIBBINGS, *On Boundary-layer Transition Wires.* Aero. Res. Coun., Lond., Curr. Pap. 462 (1959).
F. R. HAMA, *Boundary-layer Transition Induced by a Vibrating Ribbon on a Flat Plate.* Inst. Fluid Dynamics & Appl. Math., Univ. of Maryland, TN BN-195; AFOSR TN 60-290 (1960).
C. IDDINGS, *The Stability of Plasmas in the Presence of Conducting Walls.* Physical Research Laboratory, Space Technology Laboratories, Inc., Los Angeles, STL/TR-60-000-94316 (1960).
M. O. KRAMER, Boundary layer stabilization by distributed damping. *J. Amer. Soc. Nav. Engrs*, **72**, No. 1, 25 (1960).
A. L. LOEFFLER, JR. and R. G. DEISSLER, Decay of temperature fluctuations in homogeneous turbulence before the final period. *Int. J. Heat Mass Transfer*, **1**, No. 4, 312 (1961).
M. H. STEIGER and M. H. BLOOM, *Axially Symmetric Free Mixing with Swirl.* Dept. of Aerospace Engng & Appl. Mech., Polytechnic Inst. of Brooklyn, Brooklyn, N.Y., ARL TN 60-163; PIBAL Report 628 (1960).
N. TETERVIN (prepared by), *An Estimate of the Minimum Reynolds Number for Transition from Laminar to Turbulent Boundary-layer Flow by Means of Energy Considerations.* U.S. Naval Ordnance Laboratory, White Oak, Maryland, NAVORD Report 6854; Aeroballistics Research Report No. 98 (1960).
J. G. WOODLEY, *Measurements of the Effect of Surface Cooling on Boundary Layer Transition on a 15-degree Cone, Part 2: Tests at $M = 3$ and $M = 4$ in the 5-in. × 5-in. no. 5 Wind Tunnel at R.A.E. Farnborough.* Aero. Res. Coun., Lond., Curr. Pap. 479 (1960).

TRANSPIRATION AND MASS TRANSFER COOLING

G. E. ANDERSON, C. J. SCOTT and D. R. ELGIN, *Mass Transfer Cooling Experiments on a Hemisphere at $M = 5$.* Univ. of Minnesota, Inst. of Technology, Rosemount Aero. Lab. Research Report 166; AFOSR TN 59-1306 (1959).
R. J. BARRIAULT and J. YOS, Analysis of the ablation of plastic heat shields that form a charred surface layer. *J. Amer. Rocket Soc.* **30**, No. 9, 823 (1960).
P. M. CHUNG, *Effect of Localized Mass Transfer Near Stagnation Region of Blunt Bodies in Hypersonic Flight.* NASA TN D-141 (1960).
J. E. DANBERG, *Measurement of the Characteristics of the Compressible Turbulent Boundary Layer with Air Injection.* U.S. Naval Ordnance Laboratory, White Oak, Maryland, NAVORD Report 6683; Aeroballistics Research Report No. 67 (1960).
F. H. GAYNER and J. M. HOFFMAN, The transition from free to forced convection in mass transfer from solid spheres. *J. Amer. Inst. Chem. Engrs*, **6**, 579 (1960).
S. GEORGIEV, *Unsteady ablation.* AVCO Everett Research Laboratory, Everett, Mass., AFBMD TR-60-180; Research Report 94 (1959).
H. HIDALGO, Ablation of glassy material around blunt bodies of revolution. *J. Amer. Rocket Soc.* **30**, No. 9, 806 (1960).
P. D. LEBEDEV, Heat and mass transfer between moist solids and air. *Int. J. Heat Mass Transfer*, **1**, No. 4, 302 (1961).
P. D. LEBEDEV, Heat and mass transfer during the drying of moist materials. *Int. J. Heat Mass Transfer*, **1**, No. 4, 294 (1961).
L. LEES, Ablation in hypersonic flows, *Proc. Seventh Anglo-American Aeronautical Conference*, p. 344. Inst. of the Aeronautical Sciences, New York; Guggenheim Aeronautics Laboratory, Calif. Inst. of Technology, Pasadena, Publication 481 (1959).
W. R. LUCAS and J. E. KINGSBURY, ABMA reinforced plastics ablation program. *Mod. Plast.* **38**, No. 2, 135 (1960).
W. P. MANNING and W. H. GAUVIN, Heat and mass transfer to decelerating finely atomized sprays. *J. Amer. Inst. Chem. Engrs*, **6**, No. 2, 184 (1960).
Y. MIKHAILOV, Highly intensive heat and mass transfer in dispersed media. *Int. J. Heat Mass Transfer*, **1**, No. 1, 37 (1960).
H. MYERS, Aerodynamically heated surfaces—A chemical analysis. *Aero. Space Engng*, **19**, No. 2, 34 (1960).
A. H. NISSAN and D. HANSEN, Heat and mass transfer transients in cylinder drying: Part I. Unfelted cylinders. *J. Amer. Inst. Chem. Engrs*, **6**, 606 (1960).
A. V. RALKO, The experimental investigation of heat and mass transfer in the presence of chemical conversions. *Int. J. Heat Mass Transfer*, **1**, No. 4, 273 (1961).
D. L. SCHMIDT, Behavior of plastics in re-entry environments. *Mod. Plast.* **38**, No. 3, 131 (1960).

Vol. 3 1961

P. B. SCOTT, *Heat and Mass Transfer for Flow Past an Arbitrary Cylinder*. Mass. Inst. Technology, Naval Supersonic Laboratory TR 383; AFOSR TN 59-1268 (1959).

R. A. SEBAN, Effects of initial boundary-layer thickness on a tangential injection system. *J. Heat Transfer*, C **82**, No. 4, 392 (1960).

R. A. SEBAN, Heat transfer and effectiveness for a turbulent boundary layer with tangetial fluid injection. *J. Heat Transfer*, C **82**, No. 4, 303 (1960).

E. W. UNGAR, Particle impacts on the melt layer of an ablating body. *J. Amer. Rocket Soc.* **30**, No. 9, 799 (1960).

J. VAN DER BURGH, Thermal convection at a melting benzene surface. *Appl. Sci. Res.* A **9**, No. 4, 293 (1960).

C. H. E. WARREN, Experimental investigation of effect of ejecting coolant gas at nose of bluff body. *J. Fluid Mech.* **8**, Pt. 3, 400 (1960).

J. E. WELKER, *Comparison of Theoretical and Experimental Values for the Effective Heat of Ablation of Ammonium Chloride*. NASA TN D-553 (1960).

M. ZLOTNICK and B. NORDQUIST, *Calculation of Transient Ablation*. Air Force Ballistic Missile Division, Air Research and Development Command, USAF, Inglewood, Calif., Technical Memorandum RAD-9-TM-60-83 (1961).

Int. J. Heat Mass Transfer. Vol. 3, p. 76. Pergamon Press 1961. Printed in Great Britain.

BOOK REVIEW

Das Mollier *ix* Diagram für feuchte Luft und seine technischen Anwendungen. W. HÄUSSLER, Hochschule für Maschinenbau, Karl-Marx-Stadt. Verlag von Theodor Steinkopf, Dresden u. Leipzig, 1960. 167 pp.

THE diagrams introduced by Mollier for the representation of thermodynamic properties have been of great utility in engineering calculations; later workers have developed Mollier's methods and extended their field of application. This is particularly the case with the so-called *ix* diagram for moist air, which forms the subject of the present book. It is Professor Häussler's intention to show that, apart from some developments of his own, the "improvements" made by workers subsequent to Mollier have turned out not to be advantageous.

Chapter 3 contains a review of published diagrams for moist air. The authors of presentations differing from that of Mollier are dismissed rather patronizingly, a performance that is made easier by complete omission of reference to the valuable contributions of Busemann and Bošnjaković* in this field. Chapter 4 is devoted to the author's extension of the Mollier diagram to pressures other than atmospheric.

The remaining seven chapters contain discussions of: state changes, vaporization processes, humidity measurement, dehumidification, air-conditioning, drying, and the compression and expansion of moist air. There are twenty-six numerical examples, most of them solved with the aid of *ix* diagrams. More attention is devoted to the thermodynamic than the mass-transfer aspects of the problem.

The chapter on vaporization contains an account of experimental researches carried out by the author on the temperature distribution in the gas and liquid boundary layers adjacent to a vaporizing water surface. These lead the author to the conclusion that the difference between the interface temperature and the bulk-water temperature is about one eighth of the difference between the bulk-water temperature and the wet-bulb temperature; he recommends that this should be taken as valid for other circumstances than those of his experiments, in place of the "pure guesses" which have had to be used hitherto. Apparently he is not aware that very satisfactory methods have been long available for calculating the interface temperature as a function of the ratio of the conductances on the gas and liquid sides.

The author's method of calculating the gas-side mass-transfer conductance is equally primitive: he recommends use of a linear function of air velocity *alone*, and states that this has been satisfactorily confirmed experimentally in Germany and the Soviet Union. The standard equations involving the density and viscosity of the air, and the size and shape of the water surface, are entirely disregarded.

Chapter 6 also contains a remarkable discussion of the Lewis number (used in the older sense of the conductance ratio $a/\rho c_p$, rather than the more recent sense of a diffusivity ratio). Here some of the pioneering work of Merkel is described, very much in the tone used (it is hoped with more justice) in the present review. According to the author, Merkel's work showed that the Lewis number may vary between 1·45 and 4·12; Merkel nevertheless founded his theory on the brave declaration ("mit der mutigen Aussage") that the Lewis number was unity. Presumably Professor Häussler has misinterpreted Merkel's notation or the description of his data; for the val e of the Lewis number, and the factors influencing it, re now well established; and current understanding of the phenomena supports Merkel rather than Häussler. The author admits that Merkel's theory has shown itself to be useful for calculating vaporization processes, but states that further investigations are needed "to bring clarity into the relationships". The reviewer agrees, in a sense.

Nine large-scale diagrams are contained in a pocket at the end of the book. These will be useful.

D. B. SPALDING

* The *entropy*-composition diagram of Bošnjaković does get a reference; but even here doubt is cast on its accuracy.

Vol. 3 1961

Int. J. Heat Mass Transfer. Vol. 3, pp. 77–83. Pergamon Press 1961. Printed in Great Britain.

TURBULENT HEAT TRANSFER IN LIQUID METALS—FULLY DEVELOPED PIPE FLOW WITH CONSTANT WALL TEMPERATURE

N. Z. AZER* and B. T. CHAO†

*University of Alexandria, UAR (Egypt), and †University of Illinois, Urbana, Illinois

(*Received* 11 *July* 1960, *and in revised form* 27 *January* 1961)

Abstract—This paper is a continuation of the authors' earlier work on a mechanism of turbulent heat transfer in liquid metals [1]. Nusselt number and temperature profile for low Prandtl number fluids of constant properties flowing in a smooth pipe with constant wall temperature have been evaluated. Use is made of the theoretical expression for the ratio of eddy diffusivities for heat and momentum deduced in [1]. For practical calculation of film coefficient of heat transfer, an interpolation formula is proposed:

$$N_{Nu} = 5 + 0{\cdot}05\, N_{Pr}^{0{\cdot}25}\, N_{Pe}^{0{\cdot}77}$$

which fits the calculated data with a maximum deviation of less than 11 per cent for $N_{Pr} < 0{\cdot}1$ and $N_{Pe} < 15\,000$. Temperature profiles for several Prandtl and Reynolds numbers were compared with the case of constant wall flux.

Résumé—Cet article est la suite d'un travail précédent des auteurs sur le mécanisme de la transmission de chaleur turbulente dans les métaux liquides. Le nombre de Nusselt et le profil des températures sont déterminés pour des fluides, à propriétés constantes et faible nombre de Prandtl, s'écoulant dans une conduite lisse à température de paroi constante. On a utilisé l'expression théorique obtenue en [1] pour la détermination du rapport des diffusivités turbulentes de la chaleur et de la masse. Pour le calcul pratique du coefficient de transmission pariétale de chaleur, une formule d'interpolation est proposée

$$N_{Nu} = 5 + 0{,}05\, N_{Pr}^{0{,}25}\, N_{Pe}^{0{,}77}$$

dont les résultats diffèrent des données calculées de moins de 11% pour $N_{Pr} < 0{,}1$ et $N_{Pe} < 15\,000$. Les profils de température ont été comparés, pour plusieurs nombres de Prandtl et de Reynolds, avec le cas d'un flux de paroi constant.

Zusammenfassung—Eine frühere Arbeit der Autoren über den turbulenten Wärmeübergang in flüssigen Metallen wird fortgeführt. Für Flüssigkeiten konstanter Eigenschaften und kleiner Prandtlzahlen, die in glatten Rohren von gleichbleibender Wandtemperatur fliessen, wurden die Nusseltzahlen und die Temperaturprofile ermittelt. Von dem in [1] abgeleiteten theoretischen Ausdruck für das Verhältnis der Austauschgrössen von Wärme und Impuls wird Gebrauch gemacht. Die praktische Berechnung der auftretenden Wärmeübergangszahlen kann nach der Interpolationsformel

$$Nu = 5 + 0{,}05\, Pr^{0{,}25}\, Pe^{0{,}77}$$

erfolgen. Im Bereich $Pr < 0{,}1$ und $Pe < 15\,000$ ist die Maximalabweichung von den errechneten Werten geringer als 11%. Für verschiedene Prandtl- und Reynoldszahlen wurden die Temperaturprofile mit denen bei konstantem Wärmefluss an der Wand verglichen.

Аннотация—Настоящая статья является продолжением ранней работы автора по исследованию механиэма турбулентного переноса тепла в жидких металлах [1]. Вычислены критерий Нуссельта и профиль температуры для потоков с низким числом Прандтля и постоянными свойствами в гладкой трубе, температура стенок которой постоянна. Использовано теоретическое выражение, приведенное в [1] для отношения коэффициентов вихревой диффуэии тепла и количества движения. Предложена интерполяционная формула для практического вычисления коэффициента плёночного теплообмена:

$$N_{Nu} = 5 + 0{,}05\, N_{Pr}^{0{,}25}\, N_{Pe}^{0{,}77}$$

F

которая согласуется с вычисленными данными с максимальным отклонением в 11% для числа $N_{Pr} < 0{,}1$ и $N_{Pe} < 15\,000$. Дано сравнение профилей температуры для нескольких чисел Прандтля и Рейнольдса со случаем постоянного потока от стенки.

NOMENCLATURE

D, pipe inside diameter, $2r_w$ (ft);
h, surface conductance (Btu/ft² h degF)
k, thermal conductivity of fluid (Btu/ft h degF);
q_w, heat flux at pipe wall (Btu/ft² h);
r_w, inside radius of pipe (ft);
u, axial velocity (ft/h);
ϵ_H, eddy diffusivity for heat transfer (ft²/h);
ϵ_M, eddy diffusivity for momentum transfer (ft²/h);
κ, thermal diffusivity of fluid (ft²/h);
γ, kinematic viscosity of fluid (ft²/h).

Dimensionless quantities

N_{Nu}, Nusselt number, $\dfrac{hD}{k}$;

N_{Pe}, Peclet number, $N_{Re}\,N_{Pr} = \dfrac{u_b D}{\kappa}$;

N_{Pr}, Prandtl number, $\dfrac{\nu}{\kappa}$;

N_{Re}, Reynolds number, $\dfrac{u_b D}{\nu}$;

$U = \dfrac{u}{u_b}$;

$Z = \dfrac{r}{r_w}$;

$\alpha = \dfrac{\epsilon_H}{\epsilon_M}$, ratio of eddy diffusivity of heat to momentum.

Subscripts

b, bulk;
c, center of pipe;
w, wall.

1. INTRODUCTION

THE EFFECT of wall thermal conditions on surface conductance for fully developed turbulent flow in pipes was first reported by Reichardt [2]. For fluids whose Prandtl number is comparable to, or greater than, that of air, Reichardt found only small differences in heat transfer coefficient when results for constant wall flux were compared with those for constant wall temperature. Reichardt's findings have recently been confirmed by Siegel and Sparrow [3]. For fluids of low Prandtl number, such as liquid metals, Seban and Shimazaki [4] reported that the influence of wall-temperature variation was significant. In the latter analysis, the eddy diffusivity for heat ϵ_H was assumed to be identical to the eddy diffusivity for momentum, ϵ_M. However, experimental data indicate that this assumption is, in general, not valid [5, 6]. Based on a modification of Prandtl's mixing-length hypothesis, the authors [1] obtained an expression for the diffusivity ratio α [$= (\epsilon_H/\epsilon_M)$]. It depends on N_{Re}, N_{Pr} as well as radial location across the pipe. The theoretical expression gives fair agreement with available experimental data. In the following, Seban and Shimazaki's analysis is repeated but without the assumption of α being unity.

2. NUSSELT NUMBER AND TEMPERATURE PROFILE

For fully developed velocity and temperature distribution in constant property fluids flowing in pipes, with dissipation effects and axial conduction neglected, Seban and Shimazaki [4] showed that the Nusselt number and temperature profile are given respectively by:

$$N_{Nu} = \frac{N_{Pr}}{\psi(1)} \tag{1}$$

and

$$\frac{t_w - t}{t_w - t_c} = 1 - \frac{\psi(Z)}{\psi(1)} \tag{2}$$

where

$$\psi(Z) = N_{Pr}\int_0^Z \frac{\phi(Z)\,\mathrm{d}Z}{Z[1 + \alpha(\epsilon_M/\nu)\,N_{Pr}]} \tag{3}$$

and

$$\phi(Z) = \int_0^Z U\left(\frac{t_w - t}{t_w - t_c}\right) Z\,\mathrm{d}Z. \tag{4}$$

Vol. 3 1961

Since the evaluation of $\phi(Z)$ requires knowledge of the very temperature profile being sought, Seban and Shimazaki employed an iterative process in which the temperature profile obtained by Martinelli [7] for the case of constant wall flux was used as the first approximation. The ratio (ϵ_M/ν) was calculated from the universal velocity profile suggested by von Kármán [8]. They expressed their calculated values of Nusselt number by an interpolation formula of the form:

$$N_{Nu} = 5{\cdot}0 + 0{\cdot}025\, N_{Pe}{}^{0{\cdot}8}. \tag{5}$$

In the present analysis, values of α are calculated from:

$$\alpha = \frac{\epsilon_H}{\epsilon_M} = \frac{1 + 135\, N_{Re}{}^{-0{\cdot}45} \exp\left[-(y/r_w)^{0{\cdot}25}\right]}{1 + 380\, N_{Re}{}^{-0{\cdot}58} \exp\left[-(y/r_w)^{0{\cdot}25}\right]} \tag{6}$$

which is formulated from Prandtl's mixing-length hypothesis but modified for a continuous exchange of momentum and energy during the flight of the eddy. A detailed exposition is given in Ref. 1. Also, for reasons there expounded, the ratio (ϵ_M/ν) was evaluated directly from the velocity profile measurements of Nikuradse. In the first iteration, use was made of the temperature profile previously calculated for constant wall flux, also given in Ref. 1. Sufficient convergence was obtained after two iterations. Table 1 gives the results of computation. It is seen that the difference between the first and second iteration is small. Corresponding values for the constant wall flux case were also listed. Invariably, the Nusselt number is smaller under the constant wall temperature condition. Percentagewise, the difference is larger for smaller Prandtl numbers. For the highest Prandtl number considered, i.e. $N_{Pr} = 0{\cdot}100$, the difference becomes insignificant at large Reynolds numbers. These findings are in accord with those reported by Seban and Shimazaki. Fig. 1 compares the results obtained in this analysis with those reported in Ref. 4. The lower values of Nusselt number predicted are primarily due to the abandonment of the assumption that eddy diffusivities for heat and momentum are identical. While the use of such assumption definitely results in higher Nusselt number for both the constant flux and constant temperature wall condition, their ratio is not appreciably affected by variations in α, particularly for low N_{Pr} fluids. (See last two columns in Table 1.)

As is also seen from the Table, the Nusselt number tends to be insensitive to changes in N_{Re} for vanishingly small Prandtl numbers. It ranges only from 5·16 to 5·35 while N_{Re} varies

Table 1. Calculated values of Nusselt number

N_{Re}	N_{Pr}	N_{Pe}	$[N_{Nu,b}]_{q_w=\text{const.}}$	$[N_{Nu,b}]_{t_w=\text{const.}}$		$[N_{Nu,b}]_{t_w=\text{const.}}$	$[N_{Nu,b}]_{q_w=\text{const.}}$
				1st Iteration	2nd Iteration	Present analysis	Seban and Shimazaki* ($\alpha = 1$)
$4{\cdot}34 \times 10^4$	0·000	0	7	4·98	5·16	0·74	—
	0·001	43·4	7·04	5·01	5·18	0·74	0·73
	0·010	434	8·01	5·82	6·01	0·75	0·77
	0·100	4340	26·07	22·14	22·54	0·85	0·96
$3{\cdot}96 \times 10^5$	0·000	0	7	5·08	5·25	0·75	—
	0·001	396	7·46	5·48	5·66	0·76	0·76
	0·010	3960	16·90	14·12	14·37	0·85	0·83
	0·100	39600	107·99	102·48	102·41	0·95	0·89
$3{\cdot}24 \times 10^6$	0·000	0	7	5·16	5·34	0·76	—
	0·001	3240	12·51	10·01	10·30	0·82	—
	0·010	32400	65·17	60·49	63·55	0·98	—

* Taken from Fig. 2 in Ref. 4.

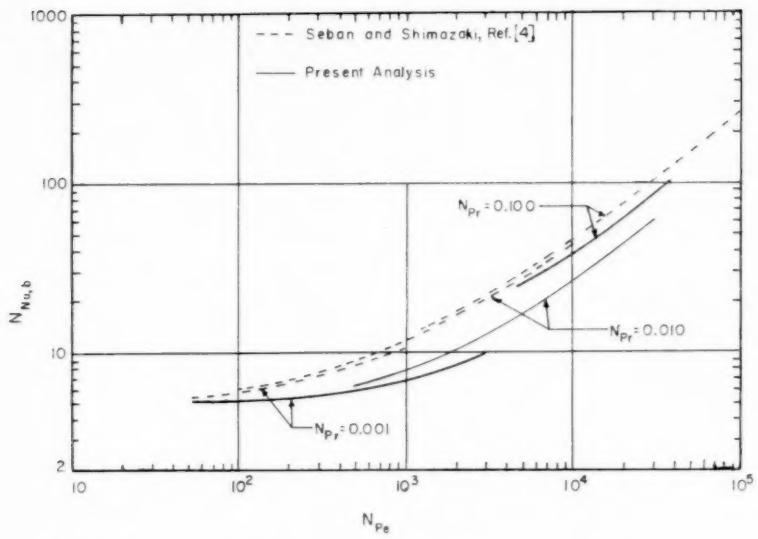

FIG. 1. Calculated values of Nusselt number at constant wall temperature.

Vol. 3 1961

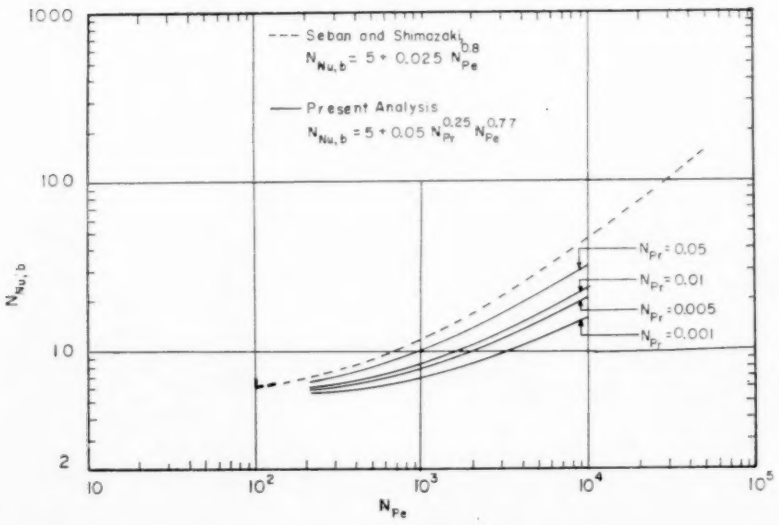

FIG. 2. Comparison of Seban and Shimazaki's equation with the present analysis.

nearly a hundredfold. It is interesting to note that the corresponding value of Nusselt number is 7 under constant wall flux condition. If, in addition, as $N_{Re} \to \infty$, the limiting Nusselt number has been found to be 5·88 which is the result obtained after three iterations. Under conditions of constant wall flux,

$$\lim N_{Nu,\,b} = 8$$

$$N_{Pr} \to 0$$

$$N_{Re} \to \infty.$$

Equation (5) asserts that the Nusselt number depends solely on Peclet number. The present analysis, however, reveals an independent Prandtl number effect. For $N_{Pr} < 0{\cdot}1$ and $N_{Pe} < 15\,000$ which cover the usual range of turbulent liquid metal heat transfer encountered in practice, the computed data shown in Table 1 could be represented by:

$$N_{Nu,\,b} = 5 + 0{\cdot}05\, N_{Pr}^{0{\cdot}25}\, N_{Pe}^{0{\cdot}77} \qquad (7)$$

which gives a maximum deviation of less than 11 per cent. Fig. 2 compares graphically Seban and Shimazaki's equation (5) with the proposed relation (7).

The difference in temperature profile for constant heat flux and constant wall temperature is illustrated in Fig. 3(a, b and c). For a given wall to center line temperature difference, the constant heat flux condition yields a steeper temperature gradient at wall and thus a higher rate of heat transfer. The deviation is most pronounced at the smallest N_{Pr}. For a given N_{Pr}, the deviation becomes less at higher N_{Re}.

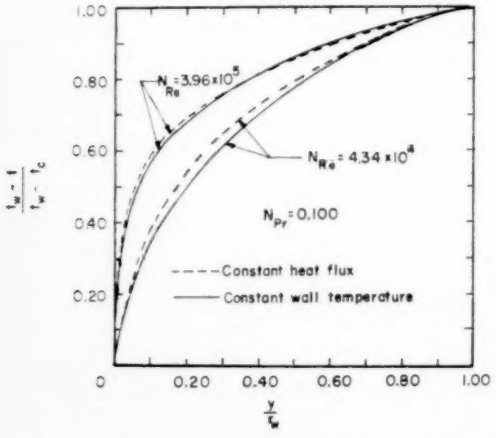

FIG. 3(a) Temperature profiles under conditions of constant wall flux and constant wall temperature. $N_{Pr} = 0{\cdot}1$.

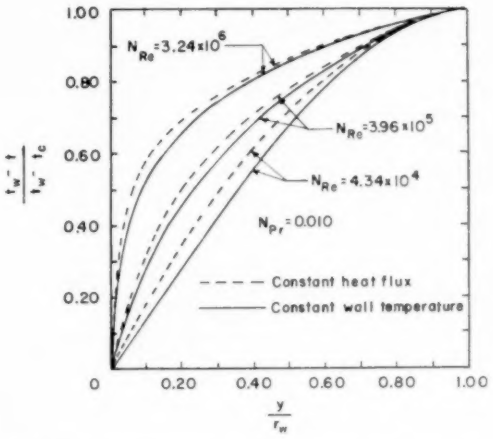

FIG. 3(b) Temperature profiles under conditions of constant wall flux and constant wall temperature. $N_{Pr} = 0{\cdot}01$.

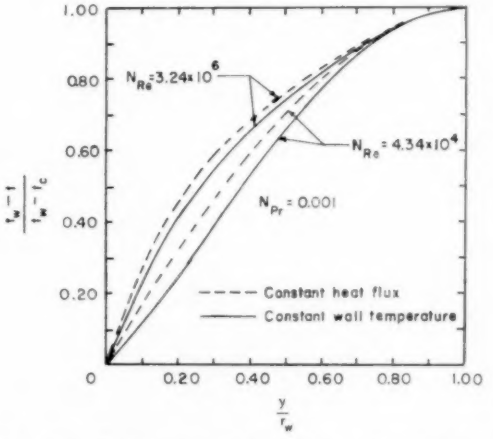

FIG. 3(c) Temperature profiles under conditions of constant wall flux and constant wall temperature. $N_{Pr} = 0{\cdot}001$.

Experimental data of heat transfer coefficient for fully developed turbulent flow of liquid metals in circular tubes under constant wall temperature conditions are practically non-existent. Gilliland *et al.* [9] reported some results

for mercury. Heating was done by dropwise condensation of steam on the outside of a vertical nickel tube, 0·319 in i.d. and 14·4 in long, thus approximating constant wall temperature condition. The Nusselt number reported was not for fully developed conditions but rather an overall average. For purpose of comparison, a small correction was introduced to take into account the finite length to diameter ratio of the test section [$(L/D) = 45$ in Gilliland's experiments] using the theoretical results of Deissler [10]. Fig. 4 compares their data so modified with the proposed correlation. Should

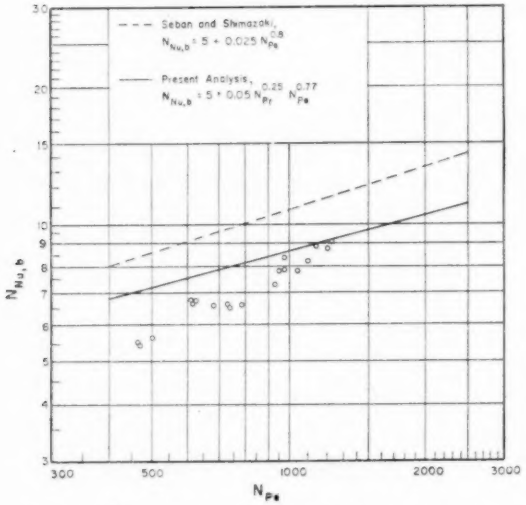

FIG. 4. Comparison of re-evaluated experimental data due to Gilliland *et al.* with the present analysis.

their raw data be used, the agreement would be even better. Shown also is a plot of equation (5) due to Seban and Shimazaki. At the present time, the authors do not construe that the proposed equation (7) gives a better correlation than equation (5). More experimental data are needed before a definite conclusion could be made.

Heating and cooling coefficients for mercury with and without sodium addition have been measured by Doody and Younger [11]. Their arrangement resulted in a wall condition somewhere between uniform wall temperature and uniform wall flux for some of the test runs. Others approximated more closely to uniform flux condition. Their heat balance indicated discrepancies as great as 140 per cent. Bailey *et al.* [12] reported cooling coefficients for mercury flowing in 0·437 in i.d. steel tube. At low Peclet numbers, their method of cooling resulted in approximately constant wall temperature condition. Unfortunately, the reliability of their data was open to question since no provision was made for mixing before exit temperatures were measured. Similar difficulty occurred in Doody and Younger's experiments. For these reasons, no attempt was made to compare these data with the theoretical predictions of equation (7).

3. FLUID BULK TEMPERATURE

It would be interesting to compare the fluid bulk temperatures under conditions of constant wall flux and constant wall temperature. A general expression for the temperature-difference ratio is:

$$\vartheta = \frac{t_w - t_b}{t_w - t_c} = \frac{\int_0^1 \left(\frac{t_w - t}{t_w - t_c}\right) UZ\, dZ}{\int_0^1 UZ\, dZ} \qquad (8)$$

which holds true irrespective of wall conditions. The numerator of equation (8) is seen to be $\phi(1)$. In Ref. 1, it has been demonstrated that the value of the integral $\int_0^Z UZ\, dZ$ is insensitive to changes in N_{Re} and could be closely approximated by $(Z^{1.75}/2)$ for N_{Re} ranging from 4×10^3 to over 3×10^6. Using this approximation, the denominator of equation (8) assumes a constant value of 1/2. The results of computation are briefly indicated below. Details may be found in [13].

The temperature-difference ratio, ϑ, defined by equation (8) has been found to be invariably smaller for the constant wall temperature condition when compared to the constant flux case. For instance, at $N_{Re} = 3{\cdot}96 \times 10^5$, $N_{Pr} = 0{\cdot}001$, ϑ is 0·470 and 0·504 respectively for the two wall conditions. However, as N_{Pr} increases, the ratio tends to be equal. As an illustration, we may cite that for $N_{Pr} = 0{\cdot}1$ the corresponding ratios are 0·740 and 0·742 at the said N_{Re}.

Under the condition of constant wall flux, Martinelli [7] computed and reported values of

Vol. 3 1961

ϑ for $a = 1$. Values of ϑ have also been evaluated by Lykoudis and Touloukian [14] using variable a. However, unlike the authors' expression for diffusivity ratio, Lykoudis and Touloukian's expression for a shows only Prandtl number dependency. The following compares the temperature-difference ratios evaluated for $N_{Re} = 3{\cdot}96 \times 10^5$.

$$\left[\vartheta = \frac{t_w - t_b}{t_w - t_c}\right]_{q_w = \text{const.}}$$

	Martinelli	Lykoudis and Touloukian	Present analysis
$N_{Pr} = 0{\cdot}1$	0·79	0·76	0·742
$N_{Pr} = 0{\cdot}001$	0·60	0·55	0·504

For very small N_{Pr}, ϑ tends to become insensitive to Reynolds number variation. In the limit, as $N_{Pr} \to 0$, $N_{Re} \to \infty$, $[\vartheta]_{q_w = \text{const.}} = 0{\cdot}5$ and $[\vartheta]_{t_w = \text{const.}} = 0{\cdot}446$. The former has also been reported in Ref. 14.

REFERENCES

1. N. Z. Azer and B. T. Chao, A mechanism of turbulent heat transfer in liquid metals. *Int. J. Heat Mass Transfer*, **1**, 121 (1960).
2. H. Reichardt, Heat transfer through turbulent friction layers, *N.A.C.A. TM* 1047 (1943).
3. R. Siegel and E. M. Sparrow, *J. Heat Transfer*, C **82**, 152 (1960).
4. R. A. Seban and T. T. Shimazaki, *Trans. Amer. Soc. Mech. Engrs*, **73**, 803 (1951).
5. S. E. Isakoff and T. B. Drew, *General Discussion on Heat Transfer*, p. 405, Institution of Mechanical Engineers, London (1951).
6. H. E. Brown, B. H. Amstead and B. E. Short, *Trans. Amer. Soc. Mech. Engrs*, **79**, 279 (1957).
7. R. C. Martinelli, *Trans. Amer. Soc. Mech. Engrs* **69**, 947 (1949).
8. T. von Kármán, *Trans. Amer. Soc. Mech. Engrs* **61**, 705 (1939).
9. E. R. Gilliland, R. J. Musser and W. R. Page, *General Discussion on Heat Transfer*, p. 402, Institution of Mechanical Engineers, London (1951).
10. R. G. Deissler, Analysis of turbulent heat transfer and flow in entrance regions of smooth passages, *N.A.C.A. TN* 3016 (1953).
11. T. C. Doody and A. H. Younger, *Heat Transfer Coefficients for Liquid Mercury and Dilute Solutions of Sodium in Mercury in Forced Convection* p. 77, Preprints of papers presented at the American Institute of Chemical Engineers Meeting, Atlantic City, New Jersey, (1951).
12. D. L. R. Bailey, W. F. Cope, and G. C. Watson, Heat transfer to mercury, *Heat Division Paper* No. 13, *Mech. Engng Res. Lab., E. Kilbride, Glasgow* (1952).
13. N. Z. Azer, Ph.D. Thesis, University of Illinois (1959).
14. P. S. Lykoudis and Y. S. Touloukian, *Trans. Amer. Soc. Mech. Engrs*, **80**, 653 (1958).

Int. J. Heat Mass Transfer. Vol. 3, pp. 84–89. Pergamon Press 1961. Printed in Great Britain.

TURBULENCE INTENSITY, TEMPERATURE AND CONCENTRATION OF ADMIXTURES IN A TURBULENT WAKE IMMEDIATELY BEHIND A PLATE PLACED ACROSS A FLOW

G. N. ABRAMOVICH, B. G. KHUDENKO and I. S. MAKAROV
Moscow Aviation Institute

(*Received January* 1961)

Abstract—Results of experimental investigations are presented for the wake region behind a plate (placed across the flow) in immediate proximity to this plate and at short distances from it.

Résumé—Cet article présente les résultats d'expériences faites dans le sillage d'une plaque normale à un écoulement, immédiatement derrière la plaque et à une certaine distance.

Zusammenfassung—Es werden Versuchsergebnisse für die von Luft quer angeströmte Platte mitgeteilt, und zwar für den Bereich unmittelbar dahinter und in einiger Entfernung stromabwärts.

Аннотация—В статье приводятся результаты экспериментальных исследований в области аэродинамического следа за пластинкой (установленной поперек потока) в непосредственной близости за ней и при небольшом удалении.

Vol. 3 1961

NOMENCLATURE

d, width of the plate;
h^*, dynamic pressure loss in mm of water column;
u, flow rate component (along axis x);
t, flow temperature in deg C;
x, y, z, co-ordinates;
$\bar{x} = x/d$, $\bar{y} = y/d$, relative longitudinal and transversal co-ordinates;
δ, width of the wake;
ϵ, dioxide gas volume concentration (per cent);
Π, temperature gauge reading;
θ, excess temperature in deg C.

Flow parameters

0, at the wind tunnel inlet;
m, axis of the wake;
max, in undisturbed potential flow downstream of the aerodynamic body.

1. EXPERIMENTAL

INVESTIGATIONS were carried out in a flat wind tunnel. A flow velocity of up to 40 m/s on a plate was obtained with this wind tunnel.

Measurements of the intensity of turbulence were carried out by apparatus of the ETAM type operating on the principle of an electrothermoanemometer.

Pickups previously evaluated by a known flow velocity were used for determination of pulsation values.

A steel plate 10 mm wide and 1·5 mm thick placed across the flow was heated by electric current up to a temperature ~500°C for investigation of heat transfer in the region of a wake. Constant heat supply was ensured at the expense of heat transfer between the plate and the flow in the region of an aerodynamic wake.

High air heating in the region of the wake could lead to essential change of air density. The search for the influence of gas compressibility on transfer processes in the region of the wake was not considered to be a purpose of the investigation, therefore heating of air in the wake did not exceed 20°C.

In a flat-parallel flow, gas parameters along a plate (along the ordinate z) must preserve a constant value. However, intensive heat removal from the heated plate into cold lateral fins through which the current was supplied, led to the fact that flow temperature in the wake

gradually decreased from the centre of the tube to the periphery and particularly sharply near the walls. In order to level the temperature field near the plate slots were cut in the bracing positions of the lateral fins which decreased essentially heat removal through lateral fins and temperature constancy was ensured in the centre of the tube on rather a greater distance along the co-ordinate z, i.e. the flow with all its parameters may be considered here to be flat-parallel.

Temperature measurement was made by two thermocouples (chromel–copel) the junction of which was 0·8 mm in diameter. Thermocouples were joined into a block for direct determination of the difference between the temperature t at a measurement point and that of a running flow t_0 which changed somewhat—by 0·1°C—while testing. Chromel terminals of both thermocouples were joined together and the copel terminals were attached to a measuring galvanometer. One of the thermocouples was placed in the running flow, the other at the measurement point. Thermocurrents with a different direction were reciprocally neutralized. In a small temperature range the relation between the electromotive force generated in the junction, and the temperature may be considered to be linear and the same for both thermocouples. Therefore, it was assumed that the resultant current supplied to the galvanometer, and indications Π were proportional to excessive temperature $\theta = t - t_0$.

In all cases with different errors of the indicator the calibration of the thermocouple block showed a linear dependence $\theta = k\Pi$.

Temperature fields were plotted graphically for each section (at a fixed distance from the plate $x = \text{const.}$) as follows: $\theta = \theta(y)$ where y is the distance of the measurement point from the axis of the wake.

Calculation of flow velocity was carried out according to measurements, both of total and static pressures and direction streamlines at each point where temperature measurements were made.

To measure carbon dioxide gas concentration the plate placed in the flow was made with an internal hollow. On the rear part of the plate holes 0·3 mm were drilled in chess-board order. The carbon dioxide gas was supplied through lateral tubes from both sides to the internal hollow of the plate, and through the holes entered the zone of reverse flow motion and was drawn away by air currents to the edges of the plate. The rear part of the plate (with openings) was pasted with a triple layer of tape that decreased the outflow velocity of the carbon dioxide gas and reduced its deep penetration into the zone of reverse currents.

The carbon dioxide gas was supplied to the plate from bulbs with a liquefied industrial gas through two reducing valves placed in succession. Precise regulation of gas consumption was carried out by the second reducing valve. The consumption was controlled by the pressure drop on a throttle plate and maintained constant while testing. Gas concentration remained constant in the centre of the wind tunnel over rather a wide zone along the co-ordinate z.

The removal of gas samples was carried out by T-shaped pickups whose receiving part was installed in each measuring point along the streamline. The air was pumped out by a vacuum-pump from an air main between the pickup and aspirator, after this the gas sample entered the aspirator. The determination of the carbon dioxide gas percentage in the sample was carried out on the VTI indicator to within 0·05 per cent.

Results of concentration measurements as a percentage (by volume) of the carbon dioxide gas in the air, κ, were plotted graphically for each section as follows: $\kappa = \kappa(y)$.

Comparison of the fields of total and static pressures at plate heating and at supply of the carbon dioxide gas to the zone of reverse currents with fields of these parameters under conventional conditions (i.e. without plate heating and gas supply through it) showed that in all cases the difference did not exceed the precision of measurements (1 mm water column), consequently, neither flow heating, nor the introduction of admixtures into it noticeably influenced the structure of the turbulent wake behind the plate.

2. RESULTS OF MEASUREMENTS OF THE TURBULENCE INTENSITY

According to the results of measurements the

turbulence intensity of the flow, ϵ, (ratio of a pulsing velocity component to its averaged value) changed considerably both over the width of the wake and its length.

Since the change of all the flow parameters behind the plate is closely connected with the gasodynamic structure of the turbulent wake, it is necessary to distinguish the following flow regions downstream of the plate:

(a) The region of a potential flow between the boundary of the turbulent wake and a boundary layer on the wall of the wind tunnel. Turbulent pulsations of the flow generated by the plate do not penetrate into this region; here total pressure remains just the same as in the upstream flow and, consequently, the measured losses of the total pressure, h^*, remain constant and equal to those of h_0^* at the inlet into the wind tunnel $|h^* = h_0^* = \text{const.}|$. In the region of the turbulent wake $h^* > h_0^*$ in contrast to that of the potential flow.

(b) The initial portion of the wake where boundary layers which left the edges of the plate have not yet managed to close up on the axis of the flow. Thus, in the initial portion of the wake it is necessary, in turn, to distinguish between two symmetrical regions of boundary layers and a core region of the reverse flow [2]. Moreover, because of values of the flow velocity in the initial portion, it is necessary to distinguish a region where the velocity component along the axis x (an expense component of the velocity u) has just the same direction as the approaching flow ($u > 0$) and a zone of reverse currents where ($u < 0$).

(c) The main portion of the wake behind the section where boundary layers close up along the axis of the flow as a result of which the change of velocity and total pressure in the wake region acquires a monotonous character both along the axis of the flow and in the direction of y.

Dealing with a more detailed consideration of the wake structure it is also necessary to single out a transient portion in it (between the initial and main ones). However, in the present paper we are confining ourselves to the description of only the qualitative picture of variation of flow properties, we shall not, therefore, distinguish the transient portion from the main one.

As measurements showed (Fig. 1), the intensity of turbulence ϵ was very low (<1 per cent) in the potential flow. Here, its precise value was not measured because for measurement of such low qualities of ϵ it is necessary to work at rather high amplification coefficients, at which the apparatus was unsteady.

In the wake region the intensity of turbulence increased sharply, achieving the value of 60–70 per cent at a short distance from the plate, i.e. pulsations of flow velocity, generated by a

Vol. 3 1961

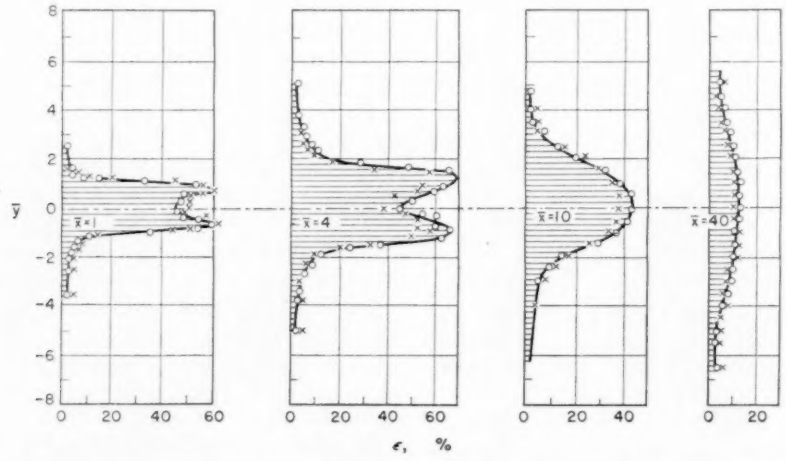

FIG. 1. Intensity of turbulence in different wake sections behind a plate $d = 40$ mm, ○—$u_0 = 38$ m/s, ×—$u_0 = 28$ m/s.

streamlined body, approached according to the order of magnitude the averaged value of the velocity.

In the initial portion of the wake region the intensity of turbulence increased while approaching the axis of the flow and achieved maximum, then it decreased noticeably immediately near the axis (in the core of the reverse flow), however, still preserving here rather high values (40–50 per cent). In all cases the maximum of ϵ coincided with a point where $u = 0$. In the main portion of the wake the variation of ϵ acquired a monotonous character with a very low maximum near the axis. While moving away from the plate, the turbulence generated by it attenuated gradually but rather slowly (ϵ decreased); and at a considerable distance from the plate it still differed noticeably from the turbulence in a potential flow.

In all cases the region of high turbulence coincided with the region where total pressure decreased in comparison with its value in the approaching flow (where $h^* > h_0^*$).

3. TEMPERATURE AND CONCENTRATION OF ADMIXTURES IN THE WAKE REGION

According to the results of measurements (Fig. 2), temperature in the whole region of potential flow was equal to that of the approaching flow ($\theta = 0$), i.e. heat spreading was limited by the region of the turbulent wake. From comparison of fields of temperature and total pressure it is seen (Fig. 3) that in all cases the region of temperature change coincided rather precisely with that of a total pressure change. At transition from the region of potential flow to that of the wake the flow temperature increased more sharply the closer the section was to the plate i.e. the thinner the boundary layer.

In the initial portion of the wake the temperature while approaching the axis of the wake, once it had achieved maximum, somewhat decreased. The temperature maximum corresponded here to the point where $u = 0$, i.e. temperature decrease occurred partially in the region of the boundary layer and partially in the region of the reverse flow core.

Such a character of the temperature change in the initial portion of the wake is closely connected with the existence of the zone of reverse currents downstream of the plate, as a result of which all the heat washed off by the flow from the front and back faces of the plate is carried away to its edges and thrown out into the flow by streams which leave the edges. In spite of a considerable temperature difference between heated streams and the approaching flow, practically all the heat carried away by the flow is distributed only in the boundary layer, since the intensity of turbulent exchange is considerably higher here than in the approaching undisturbed flow. Increase of wake width while

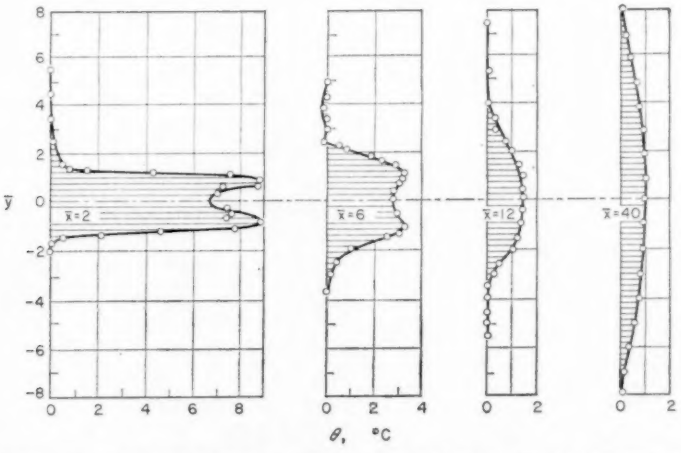

FIG. 2. Temperature change in different wake sections behind a plate $d = 10$ mm, $u_0 = 38$ m/s.

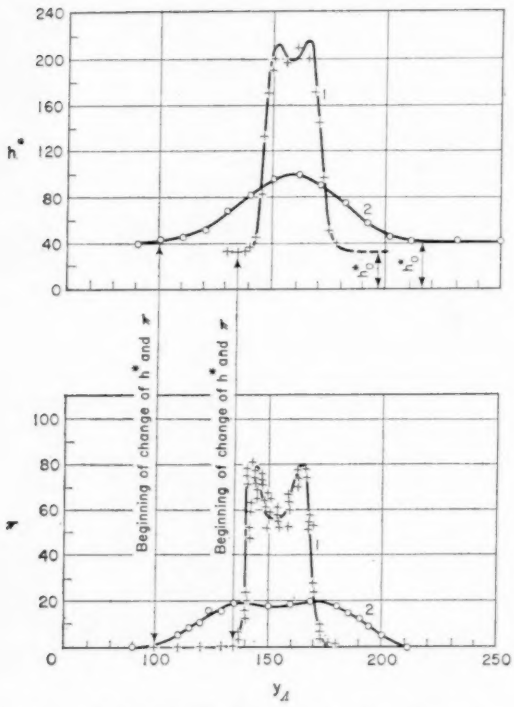

FIG. 3. Comparison of boundaries of a heat wake behind a plate $d = 10$ mm, $u_0 = 38$ m/s, y is distance of measuring point from the fixed one in the flow, in mm; h^*-mm water column, $1 - \bar{x} = 4$, $2 - \bar{x} = 20$.

moving from the plate leads to decrease of the flow temperature in the boundary layer since the total heat remains constant, and the region of its distribution increases.

In the zone of reverse currents where $u < 0$, the flow is formed in each section by streams having come not from the plate but from the portions of the boundary layer being farther from the body than the mentioned section. These streams brought to each section lower temperatures than the maximum temperature of the flow in this section. With such a mechanism of heat exchange the lower temperature corresponds to the axis of the wake, since here the flow is formed by streams having come from the sections which are removed further from the body.

While moving away from the body the difference between the maximum temperature in a section and that along the axis must decrease.

All these peculiarities of temperature distribution in the initial portion of the wake conditioned by flow structure are confirmed by experimental data.

In the main portion of the wake the temperature along the axis is gradually levelled. At rather great distances from the body ($\bar{x} = x/d > 25$, where d is the width of the plate) temperature profiles acquire a form with one maximum at the axis of the wake.

In well-known present works [3, 4, 5] on investigations of temperature fields in the region of a turbulent wake behind bluff bodies at great distances from them ($\bar{x} > 100$) it was determined that the ratio of the excess temperature θ in a measurement point to that of θ_m along the axis of the wake is a universal function of the dimensionless co-ordinate $\eta = y/\delta$ (δ is the width of the wake) for all sections, i.e. $\theta/\theta_m = f_T(\eta)$. It has also been determined that the analogous universal function $f(\eta)$ is valid for a velocity change in the region of the wake:

$$(u_{\max} - u)/(u_{\max} - u_m) = f(\eta).$$

Moreover, there is a ratio $f_T = \sqrt{f}$ between these functions for which a physical explanation has already been given in Taylor's works [6].

This fact facilitates a solution of the heat conductivity equation in the region of the wake and allows one to reduce rather simply a differential partial equation to an ordinary one, the solution of which is as follows:

$$\theta = \theta_m(x) \cdot f_T(\eta).$$

As the results of the present work show, velocity fields preserve their universality at short distances from the plate. The universal function $f(\eta)$ is valid both for the whole wake region in its main portion and for the boundary layer in the initial portion of it.

At the same time, near the body the temperature profiles change qualitatively along the wake, and the similarity of temperature fields does not take place here, as a result of which the solution of the heat conductivity equation must have the most general form $\theta = \theta(x, y)$ and only at $x \to \infty$ does it take the form

$$\theta = \theta_m(x) \cdot f_T(\eta).$$

Vol. 3 1961

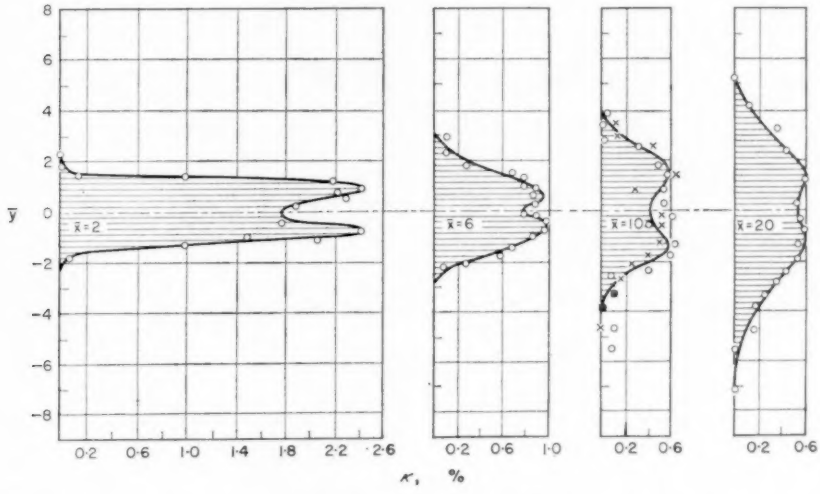

FIG. 4. Concentration change of carbon dioxide gas in different wake sections behind a plate $d = 10$ mm, $u_0 = 38$ m/s.

The results of measurements of concentrations of the carbon dioxide gas which was introduced into the zone of reverse currents behind the plate, are shown in Fig. 4.

All the mentioned peculiarities of temperature fields are also valid for concentration fields.

4. CONCLUSIONS

(1) The maximum speed pulsations immediately behind the plate reaches the values having the order of magnitude identical with that of averaged speed of flow.

(2) In the presence of slight turbulence in the approaching flow the heat and diffusion processes taking place behind the plate are restricted by the wake region.

(3) The similarity of temperature and concentration fields is absent immediately behind the aerodynamic body.

REFERENCES

1. P. V. CHEBYSHEV, Electrothermoanemometers. *Vestnik elektropromyshlennosti*, No. 1, 1–10 (1952).
2. I. V. BESPALOV and B. G. KHUDENKO, The turbulent flow pattern behind a poorly streamlined body. *Izv. VUZ Aviatsionn. Tekh.*, No. 2, 3–11 (1959).
3. G. SHLIKHTING, The boundary layer theory. *Teoriya pogranichnogo sloya*, IL, M. pp. 496–498 (1956).
4. H. REICHARDT, *Z. Angew. Math. Mech.* **21**, Heft 5, 270–271 (1941).
5. B. J. TRUBCHIKOV, The thermal method of measuring turbulence in wind tunnels. *Trud. ZAGI*, vyp. 372, 21–23 (1938).
6. G. I. TAYLOR, The transferring heat and vortices in turbulent movement of liquids. The problems of turbulence. *V kn. Problemy turbulentnosti*, 237–240, ONTI M-L (1936).

Int. J. Heat Mass Transfer. Vol. 3, pp. 90–93. Pergamon Press 1961. Printed in Great Britain.

BOILING HEAT TRANSFER BETWEEN IMMISCIBLE LIQUIDS

KENNETH F. GORDON, T. SINGH* and E. Y. WEISSMAN

Department of Chemical and Metallurgical Engineering,
University of Michigan, Ann Arbor, Michigan, U.S.A.

(*Received* 20 *September* 1960, *and in revised form* 3 *February* 1961)

Abstract—An investigation, apparently the first, was made of boiling heat transfer coefficients between immiscible liquids. Mercury with one of water, methanol or ethanol was used. The apparatus was a 2·5 in diameter glass tube with mercury heated by an external heating wire and the pool boiling liquid above. The data covered the range $\Delta T = 7°$–$103\,°F$, $q = 1500$–$110\,000$ Btu/ft² h with $h = 200$–1800 Btu/ft² h °F. Neither a peak flux nor a decline in h were reached.

Résumé—Une recherche, apparemment la première, a été effectuée sur le coefficient de transmission de chaleur par ébullition entre des liquides non miscibles. Le mercure avec de l'eau, de l'alcool éthylique ou de l'alcool méthylique a été utilisé. L'appareil est un tube de verre de 2,5 in. de diamètre contenant du mercure chauffé par une résistance extérieure; la nappe de liquide en ébullition se trouve à la surface du mercure. Les données couvrent le domaine $\Delta T = 7$–$103\,°F$, $q = 1500$–$110\,000$ Btu/ft² h avec $h = 200$–1800 Btu/ft² h °F. Aucune décroissance n'a été observée, ni pour le flux de chaleur, ni pour h.

Zusammenfassung—Offensichtlich zum ersten Male wurden Wärmeübergangszahlen beim Sieden zwischen nichtvermischbaren Flüssigkeiten ermittelt. In der Versuchsapparatur, einem Glasrohr von 6,35 cm Durchmesser wurde Quecksilber durch einem um das Rohr gewickelten Heizdraht erwärmt. Über das Quecksilber war die siedende Flüssigkeit Wasser, Methanol oder Äthanol geschichtet. Die untersuchten Werte erstreckten sich von $\Delta T = 4$–57 grd und $q = 4000$–$300\,000$ kcal/m² h mit $h = 980$–8800 kcal/m² hgrd, wobei kein Abfall des Wärmeflusses und der Wärmeübergangszahl zu beobachten war.

Аннотация—В статье, возможно впервые, даны результаты исследования по определению коэффициентов теплопереноса между несмешивающимися жидкостями при кипении. Для этой цели брали смеси ртути с водой, метиловым или этиловым спиртом. Установка состояла из стеклянной трубки диаметром 2,5 дюйма, заполненной ртутью, которая снаружи подогревалась электрическим нагревателем. Над трубкой находился резервуар с кипящей жидкостью. Экспериментальные данные соответствуют значениям: $\Delta T = 7$–$103°F$, $q = 1500$–110.000 Бте/кв. фут час и $h = 200$–1800 Бте/кв. фут час °F. Однако не было замечено уменьшение коэффициента теплообмена от потока тепла.

Vol. 3 1961

NOMENCLATURE

- h, boiling heat transfer coefficient, Btu/ft² h °F;
- k, thermal conductivity, Btu/ft h °F;
- q, heat flux, Btu/ft² h;
- ΔT, temperature difference, °F;
- Δx, distance, ft.

THE scarcity of published data on boiling from a liquid–liquid interface prompted a preliminary investigation using mercury with one of water, methanol and ethanol. This topic is of interest from both the fundamental and applied viewpoints. A liquid such as mercury would appear to have an unusual type of nucleation because a nucleation site at the interface might become displaced by the agitation from boiling, unlike that on a solid heat transfer interface. Nucleation with highly purified mercury, and another non-reactive liquid, might reasonably be expected to be closer to homogeneous rather than the usual heterogeneous nucleation. The required purity may be difficult to achieve and maintain. Because the mercury–boiling liquid surface might be greatly increased in area and constantly renewed by natural or mechanical agitation, by fluidization or by allowing the hot mercury to flow through the boiling liquid, there is the possibility of technological improvements in boiling equipment where increased capacity is desired, or where fouling presents a problem.

* Present address; Nylonge Corp., 1294 W. 70th St., Cleveland 2, Ohio, U.S.A.

Only one study of the topic has been found. As a portion of an investigation of two-phase boiling, Bonilla and Eisenberg [1] measured fluxes to butadiene boiling off water under pressure. The only temperature given is that of the metal surface heating the lower water phase which, with the boiling temperature of butadiene, gave a heat transfer coefficient. As most of the temperature drop occurred across the water the coefficients do not approximate the boiling heat transfer coefficients at the liquid–liquid interface.

There are several studies of related phenomena, the vaporization of liquid superheated drops in a second liquid [2] or at the interface of two other liquid phases [3, 4]. Fluxes are not measured for such discontinuous behavior. In these works it appears that homogeneous rather than heterogeneous nucleation is important.

EXPERIMENTAL

The apparatus (Fig. 1), consisted of a hard glass test-tube (2·5 in diameter and 21 in long) with the lower 6 in wrapped with nichrome heating wire plastered with asbestos cement. The top of the test tube was connected to two glass condensers in series to condense the boiled liquid and a separating funnel for filling the test-tube which was enclosed in a glass wool filled box. Reagent grade triple distilled mercury was used without purification between runs. Distilled water and reagent grade alcohols were employed.

After steady-state had been reached the boil-over was measured by timing the collection of condensate in a graduated cylinder. At high fluxes the batch hold-up of boiling liquid was relatively small compared with the rate so that the runs were from 1 to 30 min. The heat flow from condensation measurements ranged from 70 per cent of the electrical input at low fluxes to 100 per cent at high fluxes, fifty-fold greater, where the heat leak becomes of much less relative importance. The condensate rate yielded the heat flux while thermocouples in each phase gave the temperatures and differences. The mercury thermocouple was 0·5 in below the level interface, that in the boiling liquid was 2 in above the boiling interface as one 0·5 in above oscillated violently at high fluxes due to contact with the bouncing mercury.

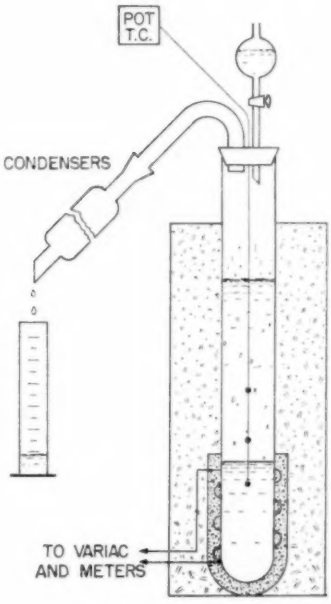

FIG. 1. Apparatus.

The temperature difference used employs the temperature of mercury 0·04 ft beneath the oscillating surface. The resistance of the mercury to heat transfer is unknown. If it were stagnant it would correspond to a $k/\Delta x$ of about 115 Btu/ft² h °F but as it is mixed due to convection currents and oscillation of the surface the effective value of $k/\Delta x$ may be more than an order of magnitude greater than this as indicated by heat transfer coefficients up to 1800 Btu/ft² h.

Despite great care a clean liquid–liquid interface could never be achieved during a run. Under a strong light a superficially clean surface would show many very small particles like white dust, most probably glass from the tube. Presumably these served as the nucleation sites. At low fluxes streams of bubbles rose from the center of the interface with no preference for bubbling at the wall. Droplets of the liquid being boiled would often form on the glass wall an inch or more below the interface remaining for tens of seconds before disappearing.

Runs were made on a roof with operators on the up-wind side with a mercury meter between

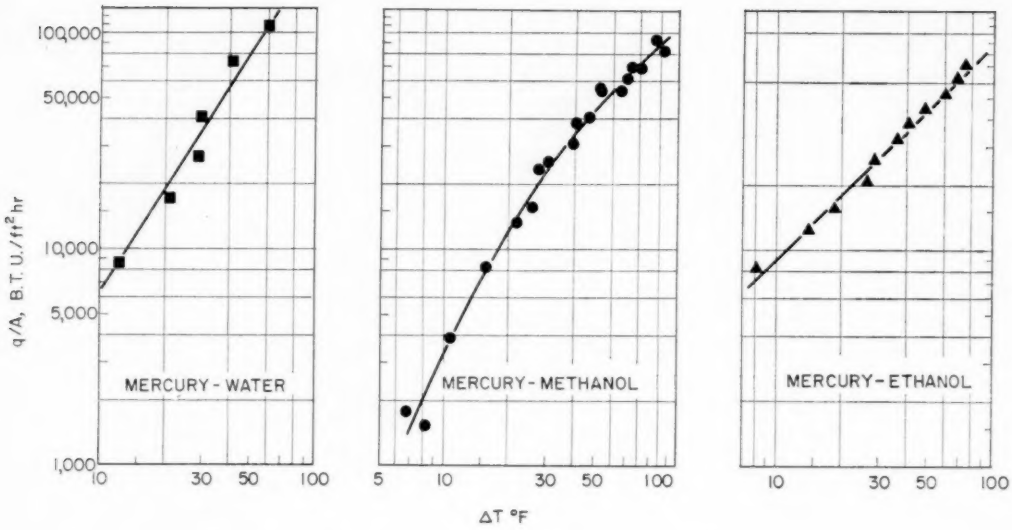

FIG. 2. Heat flux as a function of temperature difference.

Vol. 3 1961

themselves and the apparatus. There was an open metal box at the bottom of the wooden box to catch mercury in case of a break or leak. No trouble with mercury vapors was encountered.

Future investigations might employ guard heaters, continuous addition of the boiling phase, several thermocouples in the mercury, and a larger tube to reduce the possibility of appreciable entrainment at high boil-up rates. The effect of dirt should be examined.

RESULTS

In Figs. 2 and 3 the heat fluxes and transfer coefficients, based on the constant, level, superficial area, are shown as a function of the temperature difference between the two phases, ΔT.

Even up to a ΔT of 100°F neither the heat flux nor the transfer coefficient have started to decrease. This is possibly due to the violent oscillations of the interface increasing the actual interfacial area for heat transfer as ΔT is increased until at high fluxes there is violent churning with mercury droplets passing into the lighter liquid then falling back.

For submerged tubes in atmospheric pressure pool boiling, previous investigators [5] have

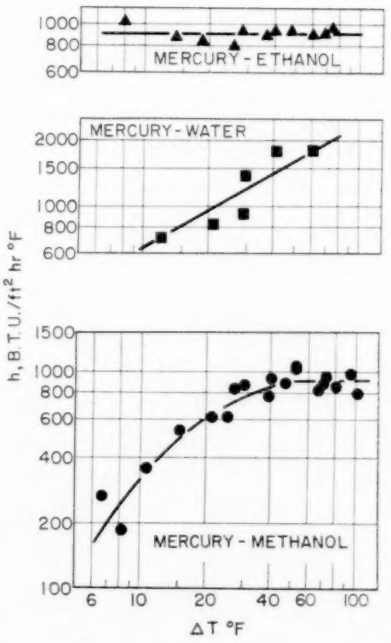

FIG. 3. Heat transfer coefficient as a function of temperature difference.

found peak fluxes of about 400 000 Btu/ft² h, at ΔT of about 50°F for water; about 126 000 Btu/ft² h at about 55–90°F for ethanol and about 124 000 Btu/ft² h at about 100°F for methanol. In the present work, no evidence of a heat flux peak or for a decrease in h may be seen up to a ΔT of 100°F leading to a belief that the use of a liquid pool rather than a solid surface for pool boiling might lead to record fluxes based on the horizontal area. Because boiling is such a strong function of surface condition, it is dangerous to generalize.

REFERENCES

1. C. F. Bonilla and A. A. Eisenberg, Heat transfer to boiling styrene and butadiene and their mixtures with water, *Industr. Engng Chem.* **40**, 1113 (1948).
2. G. R. Moore, Vaporization of superheated drops in liquids, *J. Amer. Inst. Chem. Engrs*, **5**, 458 (1959).
3. Dufour as quoted in E. Atkinson, *Elementary Treatise on Physics* translated and edited from A. Ganot, *Elements de Physique*, 10th Ed. William Wood, New York (1881).
4. L. Trefethen, Nucleation at a liquid–liquid interface, *J. Appl. Phys.* **28**, 923 (1957).
5. W. H. McAdams, *Heat Transmission*, 3rd Ed., pp. 370–387. McGraw-Hill, New York (1954).

ol.
3
961

Int. J. Heat Mass Transfer. Vol. 3, pp. 94–107. Pergamon Press 1961, Printed in Great Britain.

TWO-DIMENSIONAL UNSTEADY INCOMPRESSIBLE LAMINAR DUCT FLOW WITH A STEP CHANGE IN WALL TEMPERATURE

M. PERLMUTTER and R. SIEGEL

Lewis Research Center,
National Aeronautics and Space Administration, Cleveland, Ohio, U.S.A.

(*Received* 30 *September* 1960, *and in revised form* 6 *February* 1961)

Abstract—Analytical solutions are obtained of transient heat transfer for unsteady incompressible laminar flow between parallel plates. The transient is caused by simultaneously changing with time the driving pressure of the fluid and the wall temperature. The solution is first obtained for the case where the inside surfaces of the channel walls undergo a specified step in temperature, that is, the heat-transfer resistance of the wall is neglected. Then some results are given where the temperature is specified at the outside surfaces of the walls and the transient heat conduction through the walls is taken into account. A few numerical examples are carried out to illustrate the method.

Résumé—Des solutions analytiques sont obtenues pour la transmission de chaleur en régime transitoire, dans le cas d'un écoulement laminaire incompressible non permanent entre des plaques parallèles. Le régime transitoire est provoqué par des variations simultanées dans le temps de la pression motrice du fluide et de la température de paroi. La solution est tout d'abord obtenue dans le cas où les faces internes des parois du conduit subissent un saut donné de température, c'est-à-dire lorsque la résistance thermique de la paroi est négligée. Puis quelques résultats sont donnés dans le cas où la température des faces extérieures de la paroi est connue et où l'on tient compte de la conduction de chaleur transitoire à travers les parois. Quelques exemples numériques sont effectués pour illustrer la méthode.

Zusammenfassung—Für den veränderlichen Wärmeübergang einer nichtstationären inkompressiblen Laminarströmung zwischen parallelen Platten werden analytische Lösungen angegeben. Die Änderung wird dadurch hervorgerufen, dass man abhängig von der Zeit zugleich den Flüssigkeitsdruck und die Wandtemperatur variiert. Die Lösung ist zuerst für den Fall angegeben, dass die Innenfläche der Kanalwand eine bestimmte sprunghafte Temperaturänderung erleidet, der Wärmeleitwiderstand der Wand also vernachlässigt wird. Für einige weitere Ergebnisse ist die Temperatur auf die äussere Wandfläche bezogen und die veränderliche Wärmeleitung durch die Wand berücksichtigt. Einige numerische Beispiele veranschaulichen die Methode.

Аннотация—В статье дается аналитическое решение задачи неустановившегося теплопереноса для нестационарного ламинарного потока несжимаемой жидкости между параллельными пластинами. Неустановившееся состояние жидкости вызывается изменением давления жидкости и температуры стенки во времени. Задача решена для случаев, когда термическим сопротивлением стенки можно пренебречь, а также, когда его нужно учитывать. Выведенные расчётные формулы иллюстрируются численными примерами.

NOMENCLATURE

a, half-width of spacing between parallel plates;
$b_{n\,m}$, constants in series expansions of steady-state eigenfunctions, equation (6);
c_p, specific heat of fluid at constant pressure;
c_w, specific heat of channel walls;
d, thickness of channel walls;
E_i, eigenvalue, $(i + \frac{1}{2})\pi$; $E_m = (m + \frac{1}{2})\pi$;
F_n, function in problem where both pressure gradient and wall temperature change, equation (7);
f_n, constant defined in equation (15a);
G_n, function in problem where pressure gradient changes and wall temperature does not change, equation (18);
k, thermal conductivity of fluid;

Vol. 3 1961

k_w, thermal conductivity of wall;
Pr, Prandtl number of fluid, $c_p\mu/k = \nu/\alpha$;
p, static pressure;
q, local heat transferred per unit area from channel walls to fluid;
Re, Reynolds number, $\bar{u}4a/\nu$;
S, friction coefficient defined by equation (3);
s_w, shear stress at wall;
T, dimensionless temperature, $(t - t_0)/(t_w - t_0)$;
t, temperature;
t_0, temperature of fluid entering channel (a constant);
t_w, temperature at inside surface of wall in contact with fluid;
$t_{w,1}$, specified wall temperature before transient;
$t_{w,2}$, specified wall temperature during transient;
t_w^e, temperature at outside surface of wall;
u, fluid velocity;
$\bar{u}_1$, mean velocity before transient;
$\bar{u}_2$, final mean velocity after transient;
X, dimensionless co-ordinate, $8x/3a\ RePr$;
X_0, value of X at $\Theta = 0$ at beginning of a characteristic line;
x, axial distance from start of heated section of channel;
Y, dimensionless co-ordinate, y/a;
y, transverse co-ordinate measured from centerline of channel.

Greek symbols

α, thermal diffusivity of fluid, $k/\rho c_p$;
α_w, thermal diffusivity of wall, $k_w/\rho_w c_w$;
β_n^2, constant defined in equation (16);
Θ, dimensionless time, $\tau\nu/a^2Pr$;
Θ_0, value of Θ at $X = 0$ at beginning of a characteristic line;
θ, dimensionless time, $\tau\nu/a^2$;
λ_n^2, steady-state eigenvalue;
μ, absolute viscosity;
ν, kinematic viscosity;
ρ, fluid density;
ρ_w, density of wall;
σ_n, constant defined in equation (11a);
τ, time;
ψ_n, expansion for steady-state eigenfunction, equation (7a); average values,

$$\bar{\psi}_n = \int_0^1 \psi_n \, \mathrm{d}Y, \quad \overline{\frac{u}{\bar{u}_2}\psi_n} = \int_0^1 \frac{u}{\bar{u}_2}\psi_n \, \mathrm{d}Y.$$

INTRODUCTION

Unsteady internal flows with unsteady heat transfer are encountered in a wide variety of heat transfer devices. Some examples are the starting of a rocket engine, shutdown of a nuclear reactor, or during changes in propulsive power of a vehicle powerplant. There have been a number of papers dealing with unsteady heat transfer to flows in tubes and ducts, and [1] and [2] provide several references on this subject. These papers have been restricted to situations where the fluid velocity does not vary with time. For unsteady velocities, some information for flow in a circular tube with a constant wall temperature is given in [3].

In a previous paper [4] the authors considered heat transfer in the thermal entrance and fully developed regions for unsteady flow between parallel plates where the walls had either a constant temperature or had a uniform heat flux transferred from them. The transients were initiated by simultaneously changing with time the fluid pumping pressure and either the wall temperature or the wall heat flux. In [4] the problem was simplified by using a one-dimensional (slug flow) approximation for the velocity distribution in the channel. Within the limitation of this assumption, exact solutions for the fluid temperature distributions were obtained. One objective in the present work is to try to account for the variation in velocity across the channel cross section. A second objective is concerned with the heat conduction through the channel walls. In [4] the heat transfer resistance of the channel walls was neglected so that the thermal boundary conditions were assigned at the inside surfaces of the walls where they are in contact with the fluid. This restriction will be discussed in a later section of the paper, and some results for a finite wall resistance will be given.

The configuration selected for analysis is shown in Fig. 1. It consists of two parallel plates of thickness d with incompressible laminar flow between them. An unheated hydrodynamic entrance region is provided between the entrance of the channel and the start of the

heated section, so that within the heated section the velocity is no longer a function of axial position along the channel length. The first problem that is considered is the transient resulting from a step change in time of both the

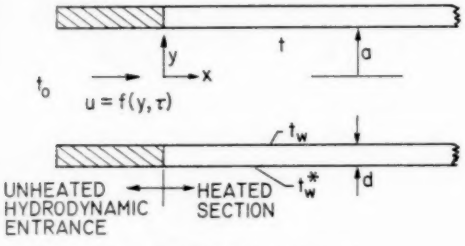

FIG. 1. Parallel-plate channel.

fluid pumping pressure and the temperature at the inside surface of the wall, t_w. The method used does not provide an exact solution of the governing partial differential equation, but involves an integral approximation at one step in the analysis. The validity of this approximation is tested by comparisons with exact results that are available for part of the solution. Then the results are extended to consider a change in temperature at the outside surface of the wall, t_w^*, and illustrative examples are given.

TRANSIENT VELOCITY DISTRIBUTION

Since the convective term in the energy equation contains the fluid velocity, the transient velocity must first be determined. The equation of motion for fully developed incompressible laminar flow between parallel plates is given by

$$\frac{\partial u}{\partial \tau} = -\frac{1}{\rho}\frac{\partial p}{\partial x} + \nu\frac{\partial^2 u}{\partial y^2} \tag{1}$$

where $\partial p/\partial x$ is a function of time. In the transient considered here, the fluid is moving initially with a steady mean velocity $\bar{u}_1$. Then the driving pressure difference is suddenly changed so that the velocity adjusts to a new mean value $\bar{u}_2$. The solution for the transient has been given in [4] as

$$\frac{u}{\bar{u}_2} = \frac{3}{2}(1 - Y^2) - 6\left(1 - \frac{\bar{u}_1}{\bar{u}_2}\right)\sum_{i=0}^{\infty}\frac{(-1)^i}{E_i^3}\exp(-E_i^2\theta)\cos E_i Y \tag{2}$$

where the dimensionless variables are defined in the nomenclature. In this solution the time required for the step pressure change to be transmitted throughout the fluid is neglected compared with the duration of velocity adjustment. The final pressure gradient imposed in the channel does not appear explicitly because it has been taken into account by the steady-state relation,

$$\bar{u}_2 = -\frac{a^2}{3\mu}\left(\frac{dp}{dx}\right)_2.$$

Equation (2) will apply for all transients except those where the final velocity $\bar{u}_2$ is zero, which occurs when the pressure gradient is dropped to zero. For this case we multiply equation (2) by $\bar{u}_2/\bar{u}_1$ and then let $\bar{u}_2 = 0$ to obtain the result,

$$\frac{u}{\bar{u}_1} = 6\sum_{i=0}^{\infty}\frac{(-1)^i}{E_i^3}\exp(-E_i^2\theta)\cos E_i Y. \tag{2a}$$

Equation (2a) has been plotted as a function of Y in Fig. 2 for various θ values. From these results all other transient velocity distributions can be found by using equation (2).

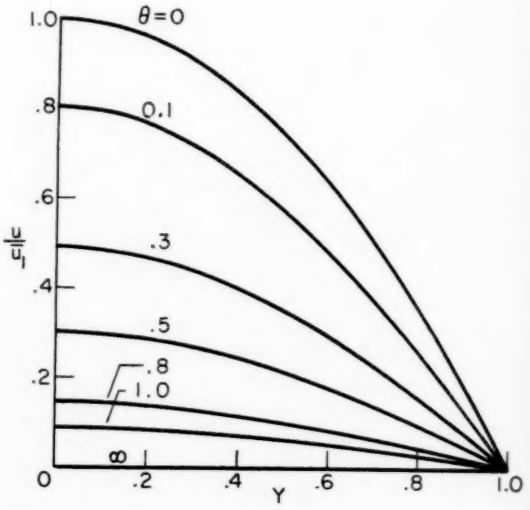

FIG. 2. Transient velocity profiles for case where pressure gradient is dropped to zero. These can be used to find all other profiles by using equation (2).

Vol. 3 1961

Wall friction

During the velocity transient, part of the pressure drop is used to change the momentum of the fluid and the remainder is used to overcome the fluid friction. As a matter of general interest we shall look at how the wall friction deviates from the steady value during the transient. A wall friction coefficient for laminar flow is defined as

$$S = \frac{s_w a}{\mu \bar{u}} \tag{3}$$

where s_w is the shear stress at the wall:

$$s_w = -\mu \left.\frac{\partial u}{\partial y}\right|_{y=a},$$

and $\bar{u}$ is the instantaneous mean velocity. By using the velocity as given in equation (2) we obtain the expression

$$S = \frac{1 - 2\left(1 - \dfrac{\bar{u}_1}{\bar{u}_2}\right)\displaystyle\sum_{i=0}^{\infty} \frac{1}{E_i^2} \exp\left(-E_i^2\theta\right)}{\dfrac{1}{3} - 2\left(1 - \dfrac{\bar{u}_1}{\bar{u}_2}\right)\displaystyle\sum_{i=0}^{\infty} \frac{1}{E_i^4} \exp\left(-E_i^2\theta\right)}. \tag{3a}$$

This is plotted as a function of θ in Fig. 3 for various pressure gradient ratios. For steady flow the value of S is 3. For a flow that is being accelerated $(\mathrm{d}p/\mathrm{d}x)_2 > (\mathrm{d}p/\mathrm{d}x)_1$, the friction coefficient rises above that for fully developed flow and then decreases to the steady value. This is caused by the fact that the fluid near the wall has a small momentum because of its low velocity and hence responds more quickly when the pressure force is changed. As a result, during the early part of the transient, the wall shear stress approaches the final value more rapidly than the mean fluid velocity, resulting in higher instantaneous values of the ratio S. During a deceleration the derivative at the wall decreases more rapidly than the mean velocity, and hence the friction coefficient goes through a minimum.

TRANSIENT HEAT TRANSFER FOR ZERO WALL RESISTANCE

The transient heat transfer results given in this paper are caused by a step change with time of the wall temperature in the heated section of the channel. In this section we consider a wall that is either very thin or has a very high thermal diffusivity so that the inside surface of the wall in contact with the fluid instantaneously reaches the value of the imposed wall temperature. The most general solution for this case is formed by superposing two more elementary results. These will be given first, and then the superposition will be described.

Step change in time of both pressure gradient and wall temperature from an unheated initial condition

Before the transient begins, the fluid is moving in a steady fashion with a mean velocity $\bar{u}_1$ that can also be zero as a special case. The walls of the channel are unheated, and the whole system is at the entering fluid temperature t_0. Then the pressure gradient in the channel is abruptly changed so that the fluid velocity undergoes a transient to a new mean velocity $\bar{u}_2$. At the same instant that the pressure gradient is changed, the temperature at the inside surface of the wall in the heated section of the channel is changed to a new value $t_{w,2}$. It is desired to compute how the heat transfer to the fluid varies with time and location along the channel.

In the analysis it is assumed that the fluid has constant properties. Axial heat conduction and viscous dissipation are neglected compared with heat conduction in the direction across the channel. With these restrictions, the energy equation for forced convection in the channel can be written as

$$\frac{\partial t}{\partial \tau} + u\frac{\partial t}{\partial x} = \alpha \frac{\partial^2 t}{\partial y^2}. \tag{4}$$

The unsteady velocity distribution equation (2) is then inserted, and the resulting equation is placed in the following dimensionless form:

$$\frac{\partial T}{\partial \Theta} + \left[1 - Y^2 - 4\left(1 - \frac{\bar{u}_1}{\bar{u}_2}\right) \times \sum_{i=0}^{\infty} \frac{(-1)^i}{E_i^3} \exp\left(-E_i^2 Pr\Theta\right) \cos E_i Y\right] \frac{\partial T}{\partial X} = \frac{\partial^2 T}{\partial Y^2}. \tag{4a}$$

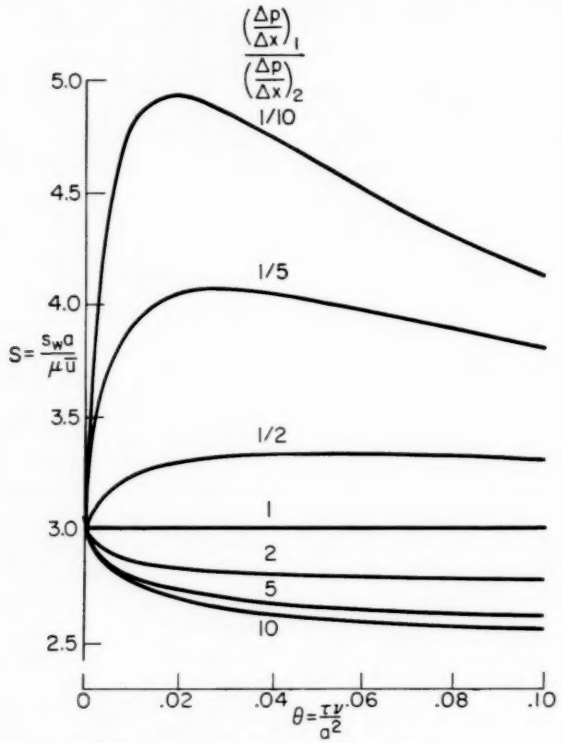

FIG. 3(a) Friction coefficients as a function of time for various pressure-gradient ratios.

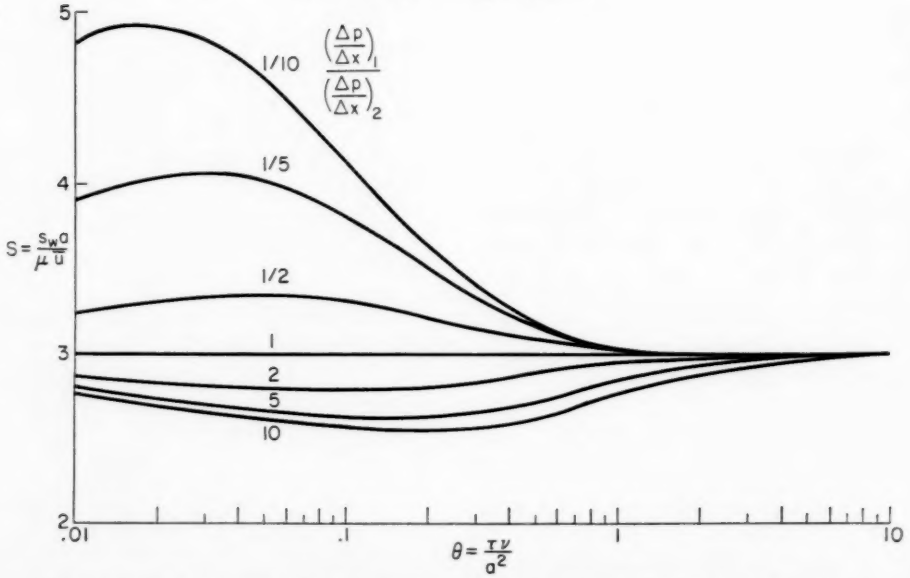

FIG. 3(b) Friction coefficients as a function of time for various pressure-gradient ratios.

Vol. 3 1961

This equation is to be solved subject to the boundary conditions:

$$T = 0 \text{ at } X = 0 \text{ for all } Y \text{ and } \Theta, \quad \text{entrance condition} \tag{5a}$$

$$T = 0 \text{ at } \Theta = 0 \text{ for all } Y \text{ and } X, \quad \text{initial condition} \tag{5b}$$

$$T = 1 \text{ at } Y = 1 \text{ for all } X \text{ and for } \Theta > 0, \quad \text{specified wall temperature} \tag{5c}$$

$$\frac{\partial T}{\partial Y} = 0 \text{ at } Y = 0 \text{ for all } X \text{ and } \Theta, \text{ symmetry} \tag{5d}$$

To obtain a solution to equation (4a), we first consider the steady-state solution in the thermal entrance region for flow between parallel plates with a constant surface temperature. One form of this solution has been given in [2] as

$$T_s = 1 - \sum_{n=0}^{4}\left(\sum_{m=0}^{4}\frac{b_{nm}}{b_{n0}}\cos E_m Y\right) b_{n0}\exp(-\lambda_n^2 X). \tag{6}$$

The summation in parenthesis is a series expansion for the eigenfunctions that arise from the product solution of the steady-state partial differential equation. The coefficients b_{nm}/b_{n0} and b_{n0}, and the eigenvalues λ_n^2 are given in Table 1 for a five-term expansion. This form of the steady solution is convenient for the present analysis as it enables the transient solutions to be carried out analytically rather than numerically.

Following the method given in [2], a transient solution is tried of the same general form as equation (6):

$$T = 1 - \sum_{n=0}^{4} b_{n0}\,\psi_n(Y)\,F_n(X,\Theta) \tag{7}$$

where for convenience we let

$$\psi_n(Y) = \sum_{m=0}^{4}\frac{b_{nm}}{b_{n0}}\cos E_m Y. \tag{7a}$$

Equation (7) already satisfies the boundary conditions (5c) and (5d). When Θ is very large, F_n should converge to the steady result, $\exp(-\lambda_n^2 X)$. To obtain the F_n, an approximation is made that the transient solution is only required to satisfy an integrated form of the energy equation. The validity of this approximation will be discussed a little later. The integrated form of equation (4a) is

$$\frac{\partial}{\partial\Theta}\int_0^1 T\,\mathrm{d}Y + \frac{2}{3}\frac{\partial}{\partial X}\int_0^1 \frac{u}{\bar{u}_2}T\,\mathrm{d}Y = \left.\frac{\partial T}{\partial Y}\right|_{Y=1}. \tag{8}$$

The trial solution equation (7) is substituted into equation (8), which yields a partial differential equation for F_n:

Table 1. *Coefficients in five-term approximation for flow between parallel plates*

n	b_{n0}	b_{n1}/b_{n0}	b_{n2}/b_{n0}	b_{n3}/b_{n0}	b_{n4}/b_{n0}
0	1·17776	0·0211834	−0·00113896	0·000207037	−0·0000586707
1	0·0579815	−5·37195	−0·838971	0·0230766	−0·00930795
2	0·0165696	−4·00649	9·45808	3·31526	0·101483
3	0·00706883	−3·59673	7·94700	−12·0113	−7·12402
4	0·0138607	−3·32432	6·61879	−11·0745	13·7624

n	λ_n^2	σ_n	β_n^2	f_n
0	2·82776	2·30858	2·82948	1·22564
1	32·1475	11·9441	32·3656	2·70975
2	93·4792	24·9156	95·2824	3·82421
3	187·388	37·4291	178·074	4·75764
4	414·761	92·5592	608·811	6·57754

$$\frac{\partial F_n}{\partial \Theta}\int_0^1 \psi_n \, dY + \frac{2}{3}\frac{\partial F_n}{\partial X}\int_0^1 \frac{u}{\bar{u}_2}\psi_n \, dY = F_n \frac{d\psi_n}{dY}\bigg|_{Y=1}. \tag{9}$$

This type of equation can be treated by using the method of characteristics (Ref. 5, p. 371). According to this method, the following set of auxiliary ordinary differential equations is formed from the coefficients in equation (9):

$$\frac{d\Theta}{\bar{\psi}_n} = \frac{dX}{\frac{2}{3}\frac{u}{\bar{u}_2}\psi_n} = \frac{dF_n}{F_n \frac{d\psi_n}{dY}\Big|_{Y=1}} \tag{10}$$

where a bar has been used to abbreviate the integral notation (e.g. $\bar{\psi}_n = \int_0^1 \psi_n \, dY$). If the first two terms of equation (10) are integrated, equations for characteristic curves on the X,Θ plane are obtained as shown schematically in Fig. 4. There is a different set of characteristic curves for each value of n. The characteristics beginning at the origin divide the plane into two regions: In region I the curves originate at the X axis, while in region II they originate from the Θ axis. By equating the last term in equation (10) with either of the other two terms, an equation for the F_n variation along the characteristic curves is obtained.

To determine F_n in region I, the first and last terms in equation (10) are equated and integrated:

$$\int_1^{F_n} \frac{dF_n}{F_n} = -\sigma_n \int_0^{\Theta} d\Theta \tag{11}$$

where

$$\sigma_n = -\frac{1}{\bar{\psi}_n}\frac{d\psi_n}{dY}\bigg|_{Y=1} = \frac{\sum_{m=0}^{4} E_m(-1)^m \frac{b_{nm}}{b_{n0}}}{\sum_{m=0}^{4} \frac{(-1)^m}{E_m}\frac{b_{nm}}{b_{n0}}}. \tag{11a}$$

Numerical values of σ_n are given in Table 1. The condition that $F_n = 1$ at $\Theta = 0$ is imposed to fulfill the initial condition (5b) which is satisfied because $1 - \sum_{n=0}^{4} b_{n0}\psi_n(Y) = 0$ as given by equation (6) at $X = 0$. The indicated integration in equation (11) is carried out to yield F_n in region I:

$$F_n = \exp(-\sigma_n \Theta). \tag{12}$$

To determine F_n in region II, the first and last terms in equation (10) are equated and then integrated along a region II characteristic curve:

$$\int_1^{F_n} \frac{dF_n}{F_n} = -\sigma_n \int_{\Theta_0}^{\Theta} d\Theta. \tag{13}$$

The boundary condition $F_n = 1$ at $\Theta = \Theta_0$, where $\Theta = \Theta_0$ corresponds to $X = 0$ on the characteristic curve, fulfills the entrance condition (5a). Integrating yields

$$F_n = \exp[-\sigma_n(\Theta - \Theta_0)]. \tag{14}$$

The arbitrary starting value Θ_0 must now be eliminated, and this is accomplished by utilizing

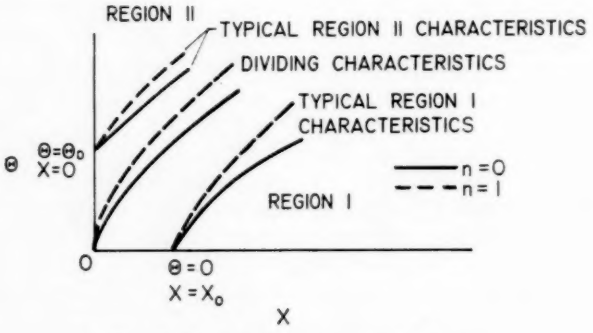

FIG. 4. Characteristic lines on X–Θ plane.

Vol. 3 1961

the equation of the characteristic curves originating at Θ_0. This is found by integrating the first two terms in equation (10):

$$\int_0^X \mathrm{d}X = \frac{2}{3}\int_{\Theta_0}^{\Theta} \frac{\overline{u}}{\bar{u}_2}\frac{\psi_n}{\bar{\psi}_n}\,\mathrm{d}\Theta. \tag{15}$$

After carrying out the integrations, this becomes

$$X = \frac{\Theta - \Theta_0}{f_n} + \frac{2\left(1 - \dfrac{\bar{u}_1}{\bar{u}_2}\right)}{Pr\,\bar{\psi}_n}\sum_{m=0}^{4}\frac{(-1)^m}{E_m^5}\frac{b_{nm}}{b_{n0}} \times [\exp(-E_m^2 Pr\Theta) - \exp(-E_m^2 Pr\Theta_0)] \tag{15a}$$

where

$$f_n = \frac{\bar{\psi}_n}{(1 - Y^2)\psi_n} = \frac{\displaystyle\sum_{m=0}^{4}\frac{(-1)^m}{E_m}\frac{b_{nm}}{b_{n0}}}{2\displaystyle\sum_{m=0}^{4}\frac{(-1)^m}{E_m^3}\frac{b_{nm}}{b_{n0}}}$$

and

$$\bar{\psi}_n = \sum_{m=0}^{4}\frac{(-1)^m}{E_m}\frac{b_{nm}}{b_{n0}}.$$

Numerical values of f_n are given in Table 1. Equation (14) is then solved for Θ_0, and this is substituted into equation (15a) to yield the following implicit expression for F_n as a function of X and Θ in region II:

$$X = -\frac{\log_e F_n}{\beta_n^2} + \frac{2\left(1 - \dfrac{\bar{u}_1}{\bar{u}_2}\right)}{Pr\,\bar{\psi}_n}\sum_{m=0}^{4}\frac{(-1)^m}{E_m^5}\frac{b_{nm}}{b_{n0}} \times \exp(-E_m^2 Pr\Theta)\left[1 - \exp\left(-E_m^2 Pr\frac{\log_e F_n}{\sigma_n}\right)\right] \tag{16}$$

where

$$\beta_n^2 = f_n\sigma_n = -\frac{1}{(1 - Y^2)\psi_n}\left.\frac{\mathrm{d}\psi_n}{\mathrm{d}Y}\right|_{Y=1}$$

The values of β_n^2 are given in Table 1. At steady state, since Θ is very large, the solution is found in region II, and equation (16) applies. When Θ is very large, the exponential term drops out and the equation reduces to

$$F_n = \exp(-\beta_n^2 X).$$

The steady-state solution equation (6) gave $F_n = \exp(-\lambda_n^2 X)$, and it is shown in Table 1 that the β_n^2 values are in good agreement with the λ_n^2 except for large n. If a larger number of terms were used for the series expansion in equation (6), then the agreement would improve, since the series approximation, ψ_n, for the eigenfunction would more closely approximate the exact function. As discussed in [2], if the exact eigenfunctions had been used, then β_n^2 would equal λ_n^2. Hence, within the limitation of the five-term approximation used here, the solution equation (16) approaches the exact solution at large time. The steady state results for the five-term approximation agree within a few per cent with the results in [6] and [7].

We can now summarize the solution. For each value of n, the X,Θ plane is divided into two regions by the characteristic curve passing through the origin. This dividing curve is given by equation (15a) with Θ_0 set equal to zero. For early times so that the solution is found in region I (Fig. 4) below the dividing characteristic, equation (12) is used for F_n. For later times so that the solution is found in region II above the dividing curve, equation (16) is used for F_n. For each F_n there is a different dividing characteristic curve. The F_n are then summed according to equation (7) to yield the transient temperature distribution.

The heat transferred from the wall to the fluid is obtained from Fourier's law:

$$q = k\left.\frac{\partial t}{\partial y}\right|_{y=a}.$$

By differentiating equation (7) and substituting into this relation, the heat flow becomes

$$\frac{qa}{k(t_{w,2} - t_0)} = -\sum_{n=0}^{4}\sum_{m=0}^{4} b_{n0}\frac{b_{nm}}{b_{n0}}E_m(-1)^m F_n. \tag{17}$$

To provide an illustrative example, this expression has been evaluated for a case when $\bar{u}_1 = 0$; that is, initially there is no flow and both the channel and fluid are isothermal at t_0. Then a pumping pressure is suddenly applied, and simultaneously the wall temperature in the

heated section is stepped to $t_{w,2}$. The resultant transient wall heat transfer for a fluid with $Pr = 0{\cdot}7$ is shown in Fig. 5. At each axial location the heat transfer goes through a minimum and then rises to the steady-state value. This type of behavior has been previously demonstrated in [4], where a slug-flow approximation was used for the velocity distribution. As pointed out in [2], for early times the heat transfer results for the example treated here can be predicted from the transient heat-conduction equation. This is due to the fact that after the initiation of the transient, the heat transfer at a given location proceeds as if the tube were of infinite length until fluid that was outside the entrance of the heated section at the start of the transient reaches that location. For this early part of the transient, there is no variation in temperature in the axial direction, and the convection term drops out of the energy equation. Hence, if the solution were exact, the curve moving downward at the left side of Fig. 5 would be in agreement with the transient heat conduction into a solid slab of thickness $2a$, which is initially isothermal at temperature t_0 and then receives a step in the surface temperature. This conduction solution is shown dashed in the figure, and the approximate solution is in good agreement with it. Thus, the transient solution obtained here yields good results for small times and also for large times as discussed earlier.

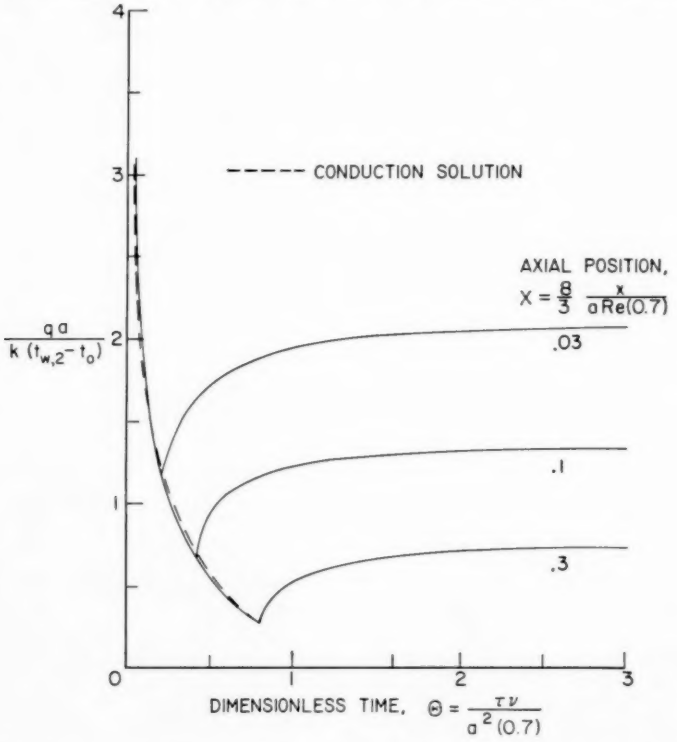

FIG. 5. Transient wall heat flux after a step change in pressure gradient and wall temperature. $Pr = 0{\cdot}7$; initially: $u = u_1 = 0$, $t_w = t_{w,1} = t_0$; finally: $u = u_2$, $t_w = t_{w,2}$.

Step change in pressure gradient with no change in wall temperature

Another type of transient will now be considered that can be superposed with the results in the previous section to solve a very general

Vol. 3 1961

case. The channel walls in the heated section are initially at a constant temperature different from that in the isothermal hydrodynamic entrance region, and there is a steady-state heat transfer. Then the pumping pressure is suddenly changed so that the flow velocity undergoes a transient change to a new steady value. Throughout the process the wall temperature is maintained at its original value.

A solution is tried that has the same form as equation (7):

$$T = 1 - \sum_{n=0}^{4} b_{n0}\psi_n(Y)\,G_n(X,\Theta). \tag{18}$$

The boundary conditions to be satisfied are the same as equations (5), except for the initial condition (5b). Since at time zero there is a steady heat transfer taking place, we have from the steady solution equation (6) that

$$G_n = \exp\,[-\lambda_n^2(\bar{u}_2/\bar{u}_1)X] \text{ at } \Theta = 0, \quad \text{initial condition.} \tag{19}$$

The ratio $\bar{u}_2/\bar{u}_1$ appears because X has been non-dimensionalized on the basis of $\bar{u}_2$, while at $\Theta = 0$ the fluid mean velocity is $\bar{u}_1$. The trial solution equation (18) is substituted into the integrated energy equation (8), and the resulting partial differential equation yields the same auxiliary ordinary equations as in equation (10), with F_n being replaced by G_n. Since the only boundary condition that has been changed is the initial condition, the expressions for the characteristic passing through the origin and for G_n in region II are the same as those for the F_n in the previous section. Hence, we only have to be concerned with region I.

For a characteristic curve in region I, the first two terms of equation (10) are integrated starting from a point $\Theta = 0$, $X = X_0$. This gives

$$X - X_0 = \frac{\Theta}{f_n} + \frac{2\left(1 - \dfrac{\bar{u}_1}{\bar{u}_2}\right)}{Pr\,\psi_n} \times \sum_{m=0}^{4} \frac{(-1)^m}{E_m^5}\,\frac{b_{nm}}{b_{n0}}\,[\exp\,(-E_m^2\,Pr\Theta) - 1]. \tag{20}$$

To obtain the variation in G_n along a characteristic in region I the first and third terms of equation (10) are integrated as follows:

$$\int_{\exp\,[-\lambda_n^2(\bar{u}_2/\bar{u}_1)X_0]}^{G_n} \frac{dG_n}{G_n} = -\sigma_n \int_0^{\Theta} d\Theta. \tag{21}$$

This gives

$$G_n = \exp\,[-\sigma_n\Theta - \lambda_n^2(\bar{u}_2/\bar{u}_1)X_0]. \tag{21a}$$

This is solved for X_0, and the result is substituted into equation (20) to eliminate the arbitrary starting point X_0. The final expression for G_n in region I then becomes

$$\frac{1}{\lambda_n^2}\frac{\bar{u}_1}{\bar{u}_2}\log_e G_n = -X - \frac{\sigma_n}{\lambda_n^2}\frac{\bar{u}_1}{\bar{u}_2}\Theta + \frac{\Theta}{f_n} + \frac{2\left(1 - \dfrac{\bar{u}_1}{\bar{u}_2}\right)}{Pr\,\psi_n} \sum_{m=0}^{4} \frac{(-1)^m}{E_m^5}\,\frac{b_{nm}}{b_{n0}} \times [\exp\,(-E_m^2 Pr\Theta) - 1]. \tag{22}$$

Now that the G_n are known, we can use equation (17) with G_n substituted for F_n to evaluate a numerical example. The example chosen is where the pressure gradient is given a step from an initially zero value. This means that, before the transient begins, there is no flow; and hence the heated section of the channel is filled with fluid at the wall temperature, which is different from the outside fluid temperature, and there is no heat transfer taking place. When the flow begins there is a transient period during which the fluid in the heated section of the channel is being swept out by fluid entering at t_0. During this early transient period no heat is being transferred. After this period, which occupies region I, heat flow begins, and the heat transfer rises toward the steady value. The results for a few axial locations and for $Pr = 0{\cdot}7$ are shown in Fig. 6. The slight discontinuities in derivative on the curve for $X = 0{\cdot}03$ occur where successive terms of the series in equation (17) are added together.

Step change in both pressure gradient and wall temperature with initial steady heating

The results given in the two previous sections can now be superposed to solve a more general situation. In this instance, there is initially a

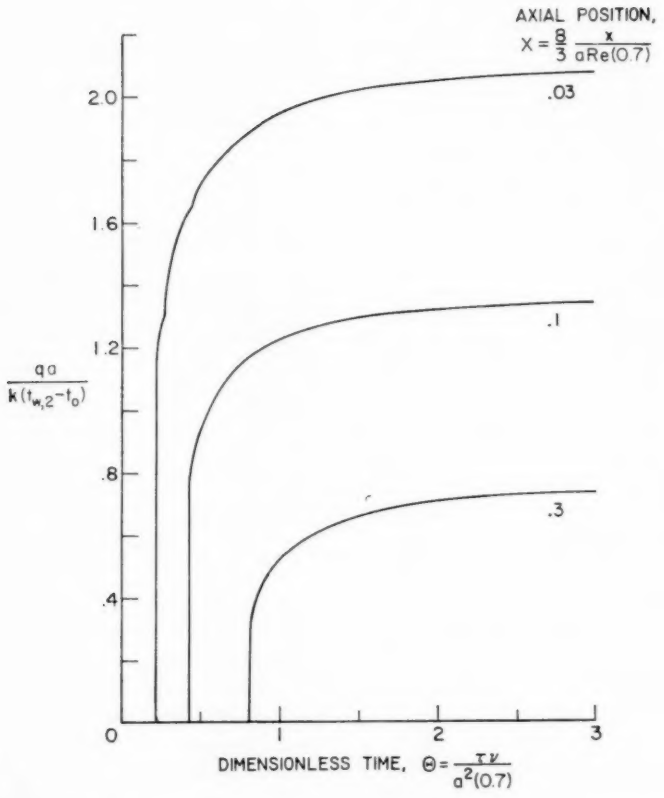

FIG. 6. Wall heat transfer after a step change in pressure gradient with the wall temperature kept constant ($t_{w,2} = t_{w,1}$). $Pr = 0{\cdot}7$; initially: $u = u_1 = 0$; finally: $u = u_2$.

steady heat transfer taking place. Then both the wall temperature in the heated section and the pressure gradient are suddenly changed to new values. The superposition used for this solution is illustrated in Fig. 7. The solution for the first part of the figure is given by the results of the first of the two preceding sections:

$$t = (t_{w,2} - t_{w,1})\,[1 - \sum_{n=0}^{4} b_{n0}\psi_n(Y)\,F_n(X,\Theta)].$$

The solution for the second part of the figure is given by the results in the preceding section:

$$t = (t_{w,1} - t_0)\,[1 - \sum_{n=0}^{4} b_{n0}\psi_n(Y)\,G_n(X,\Theta)] + t_0.$$

These results are then added to yield the general solution:

$$\frac{t - t_0}{t_{w,2} - t_0} = \left(\frac{t_{w,2} - t_{w,1}}{t_{w,2} - t_0}\right) \times [1 - \sum_{n=0}^{4} b_{n0}\psi_n(Y)\,F_n(X,\Theta)] + \left(\frac{t_{w,1} - t_0}{t_{w,2} - t_0}\right)[1 - \sum_{n=0}^{4} b_{n0}\psi_n(Y)\,G_n(X,\Theta)]. \quad (23)$$

TRANSIENT HEAT TRANSFER FOR FINITE WALL RESISTANCE

For the solutions in the previous section, the temperature t_w at the inside surface of the wall

Vol. 3 1961

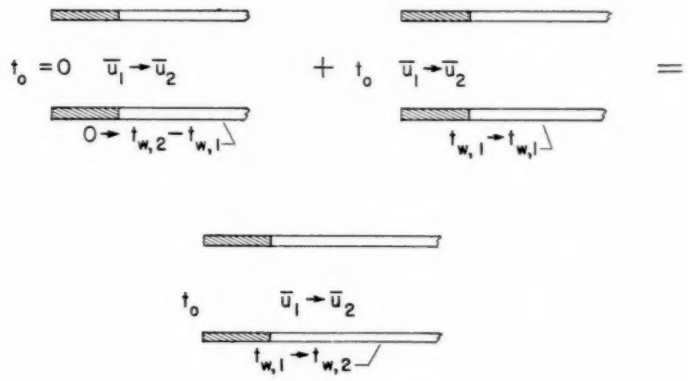

FIG. 7. Superposition of solutions for changing both pressure gradient and wall temperature.

was specified in the boundary conditions. We would now like to investigate the influence of a channel wall of finite thickness and finite thermal diffusivity where the temperature t_w^* at the outside surface is specified. In what follows we shall obtain part of the transient solution, and this will give an indication of how the additional factor of heat transport through the wall influences the transient response in the fluid.

The situation considered is as follows. The channel walls and fluid are initially isothermal at t_0 and there is no flow. Then both the outside surface temperature of the wall t_w^* in the heated section and the pressure gradient are simultaneously stepped to new values. As discussed previously, there follows an initial transient period of pure conduction in the fluid, and this continues at a given location until fluid that was originally outside of the heated section when the transient began reaches that location. Hence, for this initial period, if free convection is neglected the problem can be treated by considering the transient conduction through a two-layer slab. The first layer is the channel wall, and the second layer is the fluid contained between the wall and the center of the channel cross section. The boundary conditions are that the outside surface of the composite slab is suddenly given a step in temperature while the inside surface is kept perfectly insulated, which corresponds to the zero derivative in the fluid temperature distribution at the channel centerline. An analytical solution for this transient-conduction solution has been given in [8]. The heat transferred from the inside surface of the wall to the fluid is given by the relation

$$\frac{qa}{k(t_w^* - t_0)} = \frac{k_w a}{kd} \sum_{n=1}^{\infty} \frac{\rho_w c_w N_{1n} + \rho c_p N_{2n}}{\rho_w c_w D_{1n} + \rho c_p D_{2n}} \times (\Lambda_{1n} \cot \Lambda_{1n}) \exp(-\delta_n^2 \tau) \quad (24)$$

where the coefficients are found from

$$N_{1n} = \frac{d}{\Lambda_{1n}} [\sin \Lambda_{1n} + \cot \Lambda_{1n}(\cos \Lambda_{1n} - 1)]$$

$$N_{2n} = \frac{a}{\Lambda_{2n}} [\sin \Lambda_{2n} - \tan \Lambda_{2n}(\cos \Lambda_{2n} - 1)]$$

$$D_{1n} = \frac{d}{2\Lambda_{1n}} [(1 + \cot^2 \Lambda_{1n}) \Lambda_{1n} + (1 - \cot^2 \Lambda_{1n}) \sin \Lambda_{1n} \cos \Lambda_{1n} - 2 \cot \Lambda_{1n} \sin^2 \Lambda_{1n}]$$

$$D_{2n} = \frac{a}{2\Lambda_{2n}} [(1 + \tan^2 \Lambda_{2n}) \Lambda_{2n} + (1 - \tan^2 \Lambda_{2n}) \sin \Lambda_{2n} \cos \Lambda_{2n} + 2 \tan \Lambda_{2n} \sin^2 \Lambda_{2n}].$$

The Λ_{1n} are eigenvalues, which are determined from implicit equation

$$\tan \Lambda_{1n} = \left(\frac{k_w \rho_w c_w}{k \rho c_p}\right)^{1/2} \cot \left(\Lambda_{1n} \frac{a}{d} \sqrt{\frac{\alpha_w}{\alpha}}\right).$$

When the A_{1n} are known, the A_{2n} are then obtained from

$$A_{2n} = \frac{a}{d}\left(\frac{\alpha_w}{\alpha}\right)^{1/2} A_{1n}$$

and the δ_n are given by

$$\delta_n = \frac{\sqrt{\alpha_w}}{d} A_{1n}.$$

Two numerical examples were carried out to illustrate the transient process. The fluid in the channel was taken to be air at 170°F with the following properties: $c_p = 0{\cdot}241$ Btu/lb °F, $\rho = 0{\cdot}0623$ lb/ft^3, and $k = 0{\cdot}01735$ Btu/h ft °F. The channel walls were taken to be stainless steel (18 Cr–8 Ni) with the following properties: $c_w = 0{\cdot}11$ Btu/lb °F, $\rho_w = 488$ lb/ft^3, and $k_w = 10$ Btu/h ft °F. The channel half-width was fixed at $a = \frac{1}{8}$ in and two wall thicknesses were used: $d = \frac{1}{32}$ and $\frac{1}{16}$ in. The heat conducted from the wall to the fluid is given as a function of time by the solid lines in Fig. 8. The series in equation (24) was evaluated for the first four terms, which brought the conduction curves back to sufficiently early times for the examples given here; and the curves were then extended approximately to the origin. These conduction curves give the exact transient solutions for the forced-convection problem during the initial transient period. This period ends when fluid that was originally outside of the heated section starts to affect the heat transfer at a given point, and the time at which this occurs is given by the characteristic curve passing through the origin of the X–Θ plane for $n = 0$. These times correspond to the minimum points of the curves for $d = 0$ obtained earlier and shown again in Fig. 8. For each axial position, the pure conduction curve in the complete solution terminates at the time corresponding to this minimum point.

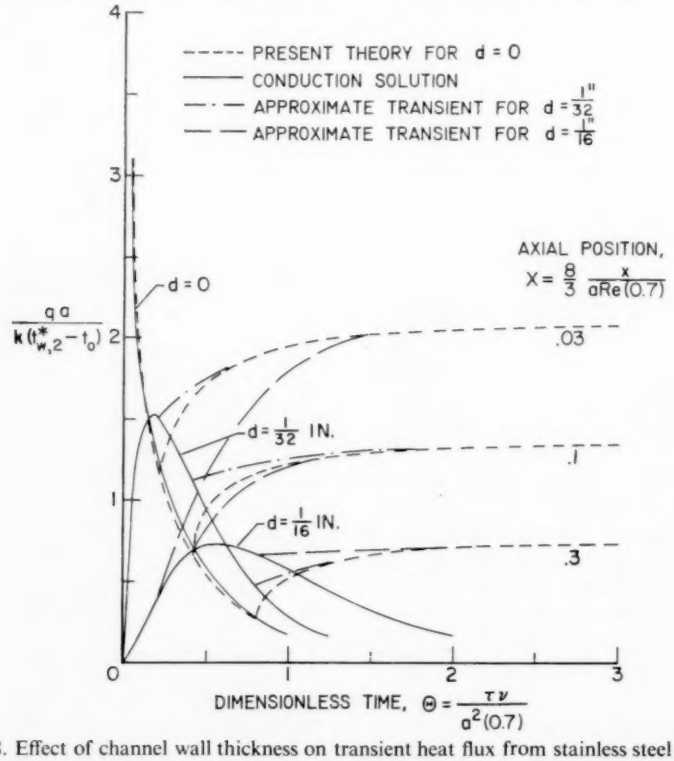

FIG. 8. Effect of channel wall thickness on transient heat flux from stainless steel walls to air for a step change in pressure gradient and outside wall temperature. $Pr = 0{\cdot}7$; initially: $u = u_1 = 0$, $t_w^* = t_{w,1}^* = t_0$; finally: $u = u_2$, $t_w^* = t_{w,2}^*$. Channel half width, $a = \frac{1}{8}$ in.

Vol. 3 1961

For large times, steady-state results must be achieved. For a finite wall resistance, the steady solution has been given in [6]. For the numerical examples given here, the wall resistance is sufficiently small that the final steady-state solution is uninfluenced by it, and the results for large times are the same as for the case with $d = 0$. For finite wall resistance we now have the solution for small and large times, and the time is known at which the initial period of pure conduction ends. For zero wall resistance we have the complete transient solution. Using this complete solution as a guide, the results for intermediate times are faired in for the finite wall resistance examples as shown in Fig. 8.

In some instances the presence of the wall has a considerable influence. Consider for example the curves for $X = 0{\cdot}1$. For $d = 0$ the heat flux starts from infinity, decreases with time to a minimum during the initial period of pure conduction, and then increases to the final steady value. When a wall of thickness $d = \frac{1}{32}$ in is introduced, the heat transfer to the fluid is initially zero. Then during the initial conduction process the heat flux rises rapidly to a maximum and then begins to decrease as the fluid temperature approaches the imposed outside wall temperature. For this example the fluid convection does not begin to have an influence until after the maximum in the pure conduction curve has been reached. Hence the heat transfer goes through a minimum and then the convection raises it to the final steady value. For $d = \frac{1}{16}$ in the heat comes through the wall so slowly that the heat flux by pure conduction is still increasing at the time that the convection begins to have an effect. Consequently, the heat flux rises from zero toward the steady value without passing through a minimum.

To have an indication of the actual time response in the channel, we note in Fig. 8 that, for the axial positions considered, the important transient effects occur during a dimensionless time Θ of about 1·0. Using $a = \frac{1}{8}$ in and $\nu = 22{\cdot}38 \times 10^{-5}$ ft^2/sec, this yields a value for τ of about $\frac{1}{3}$ sec. Hence for this example the transient period is quite short.

CONCLUDING REMARKS

Results have been presented for transient heat transfer arising from simultaneous changes with time of the channel wall temperature and fluid pumping pressure. In a previous paper [4] this type of transient solution was found for a one-dimensional velocity distribution in the channel, and the present work takes the two-dimensional velocity distribution into account. The present solutions exhibit the same general transient behavior as those in [4]. A method for investigating the effect of the heat-flow resistance of the channel walls has been demonstrated; and, as would be expected, this resistance can cause substantial changes in the heat transfer response. This is due to the fact that during the time delay required for the heat to flow through the wall the velocity is completing part of its transient.

This type of analysis is not restricted to abrupt pressure changes as considered here, but can also be carried out for other timewise pressure variations. Other types of boundary conditions can be treated for specified wall temperatures, such as one wall at uniform temperature and the other insulated. The analysis can be carried over in a straightforward fashion for the circular tube geometry.

ACKNOWLEDGEMENT

The authors would like to thank Miss Frances J. Schubert and Miss Eileen M. Norris who programed the machine computations for the examples presented here.

REFERENCES

1. V. S. Arpaci and J. A. Clark, Dynamic response of heat exchangers having internal heat sources—Part III, *J. Heat Transfer*, C **81**, 253 (1959).
2. R. Siegel, Heat transfer for laminar flow in ducts with arbitrary time variations in wall temperature, *J. Appl. Mech.* E **27**, 241 (1960).
3. K. Millsaps and K. Pohlhausen, Heat transfer to Hagen–Poiseuille flows, *Proc. Conf. on Differential Equations*, pp. 271–294, Univ. of Maryland (1955).
4. M. Perlmutter and R. Siegel, Unsteady laminar flow in a duct with unsteady heat addition. ASME paper no. 60 WA-174, to be published in *J. Heat Transfer*.
5. F. B. Hildebrand, *Advanced Calculus for Engineers*. Prentice-Hall, New York (1949).
6. J. A. W. Van Der Does De Bye and J. Schenk, Heat transfer in laminar flow between parallel plates, *Appl. Sci. Res.* A **3**, 308–316 (1953).
7. C. S. Yih and J. E. Cermak, Laminar heat convection in pipes and ducts, *Report No. 5, Civil Eng. Dept., Colorado Agricultural and Mechanical College*, Sept. (1951).
8. E. Mayer, Heat flow in composite slabs, *J. Amer. Rocket Soc.* **22**, 150 (1952).

Int. J. Heat Mass Transfer. Vol. 3, pp. 108–112. Pergamon Press 1961. Printed in Great Britain.

HEAT TRANSFER IN MAGNETOHYDRODYNAMIC FLOW BETWEEN PARALLEL PLATES*

R. A. ALPHER

General Electric Research Laboratory, Schenectady, New York

(*Received* 17 *October* 1960, *and in revised form* 27 *January* 1961)

Abstract—An analysis is presented of convective heat transfer in the fully developed laminar flow of an incompressible conducting fluid between parallel plates through a transverse magnetic field. In particular the earlier analysis of Siegel involving non-conducting plates is corrected and extended to plates of finite conductivity.

Résumé—Cet article présente une étude sur la transmission de chaleur par convection dans un écoulement laminaire pleinement établi d'un fluide conducteur incompressible, entre des plaques parallèles à travers un champ magnétique. En particulier, l'étude la plus récente de Siegel est corrigée et étendue à des plaques de conductivité finie.

Zusammenfassung—Es wird der konvektive Wärmeübergang in einer inkompressiblen elektrisch leitenden Flüssigkeit untersucht für voll ausgebildete Laminarströmung zwischen parallelen Platten und einem dazwischen angelegten Magnetfeld. Insbesondere wird die frühere Analyse von Siegel für nichtleitende Platten verbessert und auf elektrisch leitende Platten ausgedehnt.

Аннотация—В статье проводится анализ процесса конвективного переноса тепла при установившемся ламинарном движении несжимаемой электропроводящей жидкости между параллельными пластинами через поперечное магнитное поле. Уточняется метод Сигела для непроводящих пластин и осуществляется перенос его на случай движения между пластинами с конечной проводимостью.

Vol. 3 1961

NOMENCLATURE

α, thermal diffusivity;
A, mean temperature gradient;
B, magnetic induction;
c, velocity of light;
C_p, fluid specific heat at constant pressure;
E, electric field intensity;
H, magnetic field intensity;
h, thickness of channel wall;
j, current density;
k, thermal conductivity;
λ, magnetic viscosity;
L, half-height of channel;
μ, magnetic permeability;
M, Hartmann number;
ν, kinematic viscosity;
p, pressure;
P, pressure gradient;
Pr, Prandtl number;
q, heat flux;
ρ, density;
Re, hydrodynamic Reynolds number;
Re_m, magnetic Reynolds number;
σ, electrical conductivity;
u, fluid velocity;
$\bar{u}$, mean fluid velocity;
u_0, cosh M/(cosh M-1) times centerline velocity;
W, ratio of electrical resistances of channel walls and fluid;
x, co-ordinate in flow direction;
y, co-ordinate transverse to flow and magnetic field;
z, co-ordinate in magnetic field direction.

Subscripts

p, confining walls or plates;
f, fluid.

* This work was supported in part by the Ballistic Missile Division, U.S. Air Force, under Contract No. AF 04-(645)-24.

INTRODUCTION

RECENTLY an analysis was presented by Siegel [1] of the convective heat transfer for fully

developed laminar flow in a parallel plate channel with an imposed uniform wall heat flux, in the situation that the fluid is incompressible and electrically conducting, the plates are electrical insulators, and there is an impressed magnetic field transverse to the flow. The magnetic field flattens the parabolic velocity distribution usual to such a flow so that one then finds relatively higher fluid velocities near the wall as in turbulent flow [2]. As a consequence of this and of ohmic heating arising from induced currents in the fluid which provide an internal heat source, the temperature difference between wall and fluid is altered.

The problem becomes considerably more complex if one considers the plates to be electrically conducting. Now the fluid is not in a net-current-zero state, the magnitude and distribution of current in the fluid depends on the relative resistance of fluid and plates, and there is ohmic heating in the parallel plates as well as in the fluid. One can consider the plates to be electrically conducting without providing heat to the fluid by replacing them conceptually with plates of infinite conductivity connected in a coplanar sense (to preserve one-dimensionality) through an external load resistance [2, 3]. The situation is of some interest in that it provides a very crude model to a portion of the heat transfer problem in magnetohydrodynamic power-generating ducts of large aspect ratio, in the case when the walls normal to the applied field are nominally insulators but do in fact conduct under operating conditions.

It is the purpose of this note to extend Siegel's analysis to this case of plates of arbitrary electrical conductivity. For convenience and the sake of completeness some of the background is summarized. The results are presented only formally for the reason that they are complex and in practice one would doubtless resort to machine computation in such heat transfer problems in order to take into account more of the physical variables.

FLOW DESCRIPTION

Consider the steady laminar flow of a viscous incompressible fluid of constant conductivity σ_f through a parallel plate channel of height $2L$. (c.g.s. units are used throughout this paper.) A uniform magnetic field $B = B_z$ is applied. The walls parallel to the field are at $y = \pm\infty$. Continuity requires that the velocity $u = u_x(z)$ be uniform in x, with $u_y = u_z = 0$. Then one can show [3, 4] the fully developed velocity profile to be

$$u = u_0\left(1 - \frac{\cosh Mz/L}{\cosh M}\right) \tag{1}$$

where u_0, which is $\cosh M/(\cosh M - 1)$ times the fluid velocity on the channel center line, is given by

$$u_0 = \frac{Pc^2}{\sigma_f B_z^2}\,\frac{M(1+W)}{MW + \tanh M}, \tag{2}$$

the quantity $P = -\partial p/\partial x$ is the uniform pressure gradient in the channel, M is the Hartmann number, defined as $M = (B_z L/c)\,[\sigma_f/(\nu\rho)]^{1/2}$, with ν and ρ the kinematic viscosity and density, respectively, and W is the ratio of the electrical resistance of the fluid to that of the plates. Thus, with plates of equal thickness h and uniform conductivity σ_p, one may write

$$W = \frac{\sigma_p \,.\, 2h}{\sigma_f \,.\, 2L}. \tag{3}$$

If one is dealing not with parallel plates connected at $y = \pm\infty$ but with coplanar connection through an external load, the quantity $(2h\sigma_p)^{-1}$ should include the series resistance of the external load per unit channel length. The average fluid velocity in the channel is found from equations (1) and (2) to be

$$\bar{u} = u_0\left(1 - \frac{1}{M}\tanh M\right) = \frac{Pc^2}{\sigma_f B_z^2}\,\frac{(1+W)(M - \tanh M)}{MW + \tanh M}. \tag{4}$$

With the assumption that the induced magnetic field in the z-direction is small compared to the applied field, one obtains from the usual magnetohydrodynamic equations and boundary conditions [5] the following expression for the induced fields, current distributions and pressure gradient:

$$(E_x)_f = (E_x)_p = (E_z)_f = (E_z)_p = 0, \tag{5}$$

$$(E_y)_f = (E_y)_p = \frac{\bar{u}B_z}{c(1+W)}, \tag{6}$$

$$(\mu H_y)_f = (\mu H_y)_p = 0, \tag{7}$$

$$(\mu H_x)_f = \frac{Re_m B_z}{M}\left[\frac{\sinh M z/L}{\cosh M} - \frac{z}{L}\,\frac{MW + \tanh M}{1+W}\right], \tag{8}$$

$$(\mu H_x)_p = \frac{4\pi\mu_p\sigma_p}{c^2}\cdot\frac{\tilde{u}B_z}{1+W}\cdot z, \tag{9}$$

$$(j_y)_f = \frac{\sigma_f B_z}{c}\left(\frac{\tilde{u}}{1+W} - u\right), \tag{10}$$

$$(j_y)_p = \frac{\sigma_p \tilde{u} B_z}{c(1+W)}, \tag{11}$$

and

$$\frac{1}{\rho}\frac{\partial p}{\partial x} = -\frac{\sigma_f B_z^2}{\rho c^2}\left[u_0 - \frac{\tilde{u}}{1+W}\right], \tag{12}$$

in which μ is permeability, $Re_m = 2Lu_0/\lambda$ is the magnetic Reynolds number, and $\lambda = c^2/(4\pi\mu_f\sigma_f)$ is the fluid magnetic viscosity. Implicit in equations (5) through (9) is conservation of current within any element of channel length, viz.

$$\int_{-L}^{L}(j_y)_f dz + 2h(j_y)_p = 0.$$

Ohmic heating in the fluid and in the plates is computed as j^2/σ from equations (10) and (11).

HEAT TRANSFER ANALYSIS

Suppose that the externally imposed heat flux q through the confining walls is uniform with x, consistent with the fluid velocity being independent of x. If one neglects viscous dissipation compared to the transverse heat transport and, further, disregards any temperature effects due to ohmic losses in the plates, then the temperature gradient, A, in the channel can be written

$$A = \frac{\partial T_f}{\partial x} = \frac{\partial \bar{T}_f}{\partial x} = \frac{1}{L\tilde{u}\rho C_p}\left[g + \int_0^L \frac{(j_y)_f^2}{\sigma_f}\,dz\right], \tag{13}$$

where $\bar{T}_f$ is the mean fluid temperature and C_p is the fluid specific heat at constant pressure. It follows that one can take

$$T_f(x,z) = Ax + G(z). \tag{14}$$

The energy balance for the system can be written as

$$u\frac{\partial T}{\partial x} = \alpha\frac{\partial^2 T}{\partial z^2} + \frac{1}{\rho C_p}\frac{(j_y)_f^2}{\sigma_f}, \tag{15}$$

or, using equation (14), as

$$uA = \alpha\frac{d^2G}{dz^2} + \frac{1}{\rho C_p}\frac{(j_y)_f^2}{\sigma_f}, \tag{16}$$

with boundary conditions consistent with equation (14) being

$$G = 0,\ z = \pm L;\quad dG/dz = 0,\ z = 0. \tag{17}$$

The choice $G = 0$ rather than $G =$ constant is purely for convenience. The quantity α is the thermal diffusivity which for present purposes is defined by

$$\alpha = k/(\rho C_p), \tag{18}$$

where k is the thermal conductivity. (The validity of this definition for α must be examined in any real calculation, since replacing k by $\alpha\rho C_p$ in developing these results requires that ρC_p be constant in the fluid). Integration of equation (16) yields

$$G(z) = C_1\left(\frac{z^2}{L^2} - 1\right) + C_2\left(\frac{\cosh Mz/L}{\cosh M} - 1\right) + C_3\left(\frac{\cosh 2Mz/L}{\cosh 2M} - 1\right), \tag{19}$$

where

$$C_1 = \frac{u_0 AL^2}{2\alpha} - \frac{u_0^2 Pr M^2}{2C_p}\left[1 + \frac{\operatorname{sech}^2 M}{2} - \frac{2}{1+W}\frac{\tilde{u}}{u_0} + \left(\frac{1}{1+W}\frac{\tilde{u}}{u_0}\right)^2\right], \tag{20}$$

$$C_2 = -\frac{u_0 AL^2}{\alpha M^2} + \frac{2u_0^2 Pr}{C_p}\left[1 - \frac{\tilde{u}}{u_0(1+W)}\right], \tag{21}$$

and

$$C_3 = -\frac{u_0^2 Pr}{8C_p}\cosh 2M \operatorname{sech}^2 M, \tag{22}$$

in which $Pr = \nu/\alpha$ is the Prandtl number, and the quantity A, the mean temperature gradient defined in equation (13), can be written

$$A = (L\tilde{u}\rho C_p)^{-1}\left\{q + P^2L^3/(\rho\nu) \times\left[\frac{1}{M^2} - \frac{2(1+W)\tanh M}{M^2(MW + \tanh M)} + \frac{(1+W)^2}{2M}\,\frac{\sinh M\cosh M + M}{\cosh^2 M(MW + \tanh M)^2}\right]\right\}. \tag{23}$$

Vol. 3 1961

From equation (14), together with the obvious definition of mean fluid temperature, one may write the difference between wall and mean fluid temperature as

$$T_w - \bar{T}_f = Ax - \frac{1}{2L\bar{u}}\int_{-L}^{L} T_f(x,z)u(z)\mathrm{d}z$$

$$= -\frac{1}{2L\bar{u}}\int_{-L}^{L} G(z)u(z)\mathrm{d}z. \qquad (24)$$

Carrying out the indicated integrations yields

$$T_w - \bar{T}_f = \left(\frac{2}{3}\frac{u_0}{\bar{u}} - \frac{2}{M^2}\right) C_1$$

$$+ \left(\frac{3}{2} - \frac{u_0}{2\bar{u}}\tanh^2 M\right) C_2$$

$$+ \left(1 - \frac{u_0}{\bar{u}}\frac{\tanh 2M \operatorname{sech}^2 M}{6M}\right) C_3, \qquad (25)$$

where the coefficients C_1, C_2, and C_3 are as defined in equations (20–22). Inserting these coefficients and rearranging terms makes it possible to write equation (25) as

$$T_w - \bar{T}_f = \frac{qL}{k}\,\phi(M) + \frac{(RePr)^2\nu\alpha}{L^2C_p}\,\chi(M,W), \quad (26)$$

in which the Reynolds number is defined as $\bar{u}L/\nu$, and the function $\phi(M)$ can be written as

$$\phi(M) = \frac{1}{2M}\left(\frac{u_0}{\bar{u}}\right)^2\left[\frac{2M}{3} + \frac{1}{M}\left(\tanh^2 M - 5\frac{\bar{u}}{u_0}\right)\right]. \quad (27)$$

One can show $\phi(M)$ to be the same as that defined by Siegel. The function $\chi(M, W)$ is given by

$$\chi(M,W) = \frac{1}{2}\left(\frac{u_0}{\bar{u}}\right)^2\left\{\frac{u_0}{\bar{u}}\left(\frac{MW + \tanh M}{1+W}\right)^2\left[\frac{u_0}{\bar{u}}\left(\frac{2}{3} + \frac{\tanh^2 M}{M^2}\right) - \frac{5}{M^2}\right]\left[1 - \frac{2(1+W)\tanh M}{MW + \tanh M} + \right.\right.$$

$$\frac{(1+W)^2 M}{2}\,\frac{\sinh M\cosh M + M}{\cosh^2 M(MW + \tanh M)^2}\Bigg] - \left(\frac{2}{3}\frac{u_0}{\bar{u}} - \frac{2}{M^2}\right)M^2\left[1 + \frac{\operatorname{sech}^2 M}{2} - \frac{2}{1+W}\frac{\bar{u}}{u_0} + \right.$$

$$\left.\left(\frac{1}{1+W}\frac{\bar{u}}{u_0}\right)^2\right] + 2\left(3 - \frac{u_0}{\bar{u}}\tanh^2 M\right)\left[1 - \frac{\bar{u}}{u_0(1+W)}\right] - \frac{1}{4}\left(1 - \frac{\bar{u}}{u_0}\,\frac{\tanh 2M\tanh^2 M}{6M}\right)$$

$$\left.\times \cosh 2M \operatorname{sech}^2 M\right\}. \qquad (28)$$

Siegel's function $\chi(M)$, which should be the same as $\chi(M, 0)$ evaluated from equation (28), is not correct; the error in his paper apparently occurs in the steps between obtaining $G(z)$ and $T_w - \bar{T}_f$.

To illustrate the interplay of the quantities q, M, and W it is instructive to obtain an approximation for $T_w - \bar{T}_f$ with W arbitrary and M large (it appears that M may be of the order of 100 in typical magnetohydrodynamic power ducts). One finds for $\phi(M)$ the following

$$\phi(M) \cong \frac{1}{3} + \frac{2}{3M} - \frac{1}{M^2}, \qquad (30)$$

and for $\chi(M, W)$

$$\chi(M,W) \cong \frac{1}{2}\frac{M}{(1+W)^2}$$

$$\times\left[-\frac{1}{3}(1+W)^2 + \frac{1}{M}\left(-\frac{11}{6} + \frac{W}{3} + \frac{W^2}{6}\right)\right.$$

$$\left. + \frac{1}{M^2}\left(-\frac{27}{12} + \frac{3W}{2} + \frac{17W^2}{12}\right)\right]. \qquad (31)$$

For M sufficiently large, one finds that $\chi(M,W)$ becomes independent of W and equation (26) can be written

$$T_w - \bar{T}_f \cong \frac{1}{3}\frac{qL}{k} - \frac{(RePr)^2\nu\alpha}{6L^2C_p}M. \qquad (32)$$

To illustrate the magnitude of $T_w - \bar{T}_f$, one can rewrite equation (32) for mercury, viz.,

$$T_w - \bar{T}_f \cong 22qL - \tfrac{1}{6}\bar{u}^2M, \qquad (33)$$

with q in cal/cm² s, L in cm, and $\bar{u}$ in cm/s. It is interesting to note that equation (33) indicates a possibility of sign change in $T_w - \bar{T}_f$ for a given q as M is increased. This is physically

reasonable when one notes from equations (13) and (14) that for $M = 0$, with q as defined, the temperature difference corresponds to heat conduction into the fluid. If, on the other hand the magnetic field becomes high enough so that ohmic heating in the fluid exceeds the energy supplied to the fluid through q, the temperature difference should change sign.

Consider now the case when the term in χ is negligible compared to that in ϕ, as for example would be the case for a very low velocity flow through a strong magnetic field. Then one finds, as did Siegel, that $T_w - \bar{T}_f$ is reduced from its value with no field. In the case of M large, the decrease is from $(17/35)qL/k$ to $(1/3)qL/k$, or nearly 50 per cent.

One final comment with respect to equation (31) is that the value $W = 1$ corresponds to the optimum operating point of idealized magnetohydrodynamic ducts, i.e. $W = 1$ corresponds to equality of external load and internal generator resistances.

DISCUSSION

The foregoing is in some respects an exercise, insofar as its applicability to heat transfer calculations in real magnetohydrodynamic flows is concerned. Working fluids are generally compressible, conductivities are temperature and density dependent, uniform wall heat fluxes are only a convenient fiction, flows are in fact three-dimensional (side wall effects [4, 6] with or without power extraction) and also radiative heat transfer will play a role. Most important however, is the high probability that flows of real interest will be turbulent [7]. In power-generating devices the walls to which this parallel plate analysis refers will be nominally insulators when cool, but will conduct in operation as a result of property changes at high temperatures and possible reaction with seeding materials added to the working fluid to render it conducting. Moreover this conduction may be in addition to that provided by side wall electrodes. It would appear on the basis of preliminary studies made of magnetohydrodynamic power-generating devices that in practice one will be dealing with M large and $W \neq 0$.

ACKNOWLEDGEMENTS

The author wishes to acknowledge fruitful discussions with his colleagues P. Cannon and C. Muckenfuss.

REFERENCES

1. R. Siegel, Effect of magnetic field on forced convective heat transfer in a parallel plate channel, *J. Appl. Mech.* **25**, 415 (1958).
2. J. Hartmann, Hg-Dynamics—I. Theory of the laminar flow of an electrically conductive liquid in a homogeneous magnetic field, *Kgl. Danske Videnskab. Selskab Mat.-Fys. Medd.* **15**, No. 6 (1937); J. Hartmann and F. Lazarus, Hg-Dynamics—II. Experimental investigations on the flow of mercury in a homogeneous magnetic field, *Kgl. Danske Videnskab. Selskab Mat.-Fys. Medd.* **15**, No. 7 (1937).
3. R. A. Alpher, H. Hurwitz, Jr., R. H. Johnson and D. R. White, Some studies of free-surface mercury magnetohydrodynamics, *Rev. Mod. Phys.* **32**, 758 (1960).
4. C. C. Chang and T. S. Lundgren, The flow of an electrically conducting fluid through a duct with transverse magnetic field, *Proc.* 1959 *Heat Transfer and Fluid Mech. Inst.*, p. 41. Stanford Univ. Press, Stanford, Calif. (1959).
5. T. G. Cowling, *Magnetohydrodynamics*. Interscience, New York (1957).
6. S. C. R. Dennis, A. McD. Mercer and G. Poots, Forced heat convection in laminar flow through rectangular ducts, *Quart. Appl. Math.* **17**, 285 (1959).
7. L. P. Harris, *Hydromagnetic Channel Flows*. John Wiley, New York (1960).

Vol. 3 1961

Int. J. Heat Mass Transfer. Vol. 3, pp. 113–125. Pergamon Press 1961. Printed in Great Britain.

STEADY STATE TEMPERATURE DISTRIBUTION AND HEAT FLOW IN PRISMATIC BARS WITH ISOTHERMAL BOUNDARY CONDITIONS

M. J. BALCERZAK and S. RAYNOR

The Technological Institute, Northwestern University, Evanston, Illinois, U.S.A.

(*Received* 12 *September* 1960, *and in revised form* 4 *February* 1961)

Abstract—Steady state two-dimensional temperature distribution and heat flow in prismatic bars with isothermal boundary conditions and various external geometry were computed and tabulated. The method of conformal mapping was used.

Résumé—Le flux de chaleur et la distribution de température bidimensionnelle, en régime permanent, dans des barres prismatiques avec des conditions aux limites isothermes et des géométries extérieures variées ont été calculés et tabulés. La méthode de la représentation conforme a été utilisée.

Zusammenfassung—Mit Hilfe der konformen Abbildung wurde die stationäre zwei-dimensionale Temperaturverteilung und der Wärmefluss in prismatischen Körpern mit isothermer Begrenzung und verschiedenen äusseren Abmessungen berechnet und in Tabellen angegeben.

Аннотация—Дано аналитическое решение стационарного двухмерного температурного поля и определен тепловой поток в призматических брусках при изотермических граничных условиях и различной внешней геометрии брусков. Решение сопровождается расчётами, представленными в виде таблиц и рисунков.

NOMENCLATURE

General

- k, thermal conductivity;
- L, the axial dimension of a prismatic bar;
- Q, heat flow rate;
- S, shape factor;
- T, temperature at a point (x,y);
- T_i, temperature at the inner boundary;
- T_0, temperature at the outer boundary;
- w, complex number in the ϕ,Ψ plane;
- x,y, Cartesian co-ordinates of a point;
- z, complex number in the x,y plane;
- ∇^2, Laplacian operator;
- Δ, difference;
- ρ, θ, polar co-ordinates of a point;
- ϕ,Ψ, Cartesian co-ordinates of a point in the mapping plane;
- ϕ_0, Ψ_0, values of ϕ and Ψ at the outer boundary;
- ϕ_i, Ψ_i, values of ϕ and Ψ at the inner boundary.

n sided regular polygon

- A_n, coefficient of the n'th term in a polynomial;
- a, the shortest distance from the center to a side of a regular polygon;
- j, running index;
- n, number of sides of polygon;
- ρ, non-dimensional ratio of radii as defined by equation (4.1).

Rectangle

- a, one half of the shorter side of a rectangle;
- b, one half of the longer side of a rectangle;
- K, a constant term as defined for a rectangle by equation (5.5a).

Eccentric circle

- ϵ, eccentricity ratio as defined in Fig. 9.

Ellipse

- a, the major axis of the inner ellipse;

b, the minor axis of the inner ellipse;
c, the major axis of the outer ellipse;
d, the minor axis of the outer ellipse.

STATEMENT OF THE PROBLEM

THE steady state temperature distribution and heat flow in prismatic bars of various cross-sections are to be investigated. The bar material is assumed to be homogeneous, isotropic and with temperature-independent properties. The heat flow is due to central heat sources uniformly distributed along the bar axis maintaining uniform surface temperature.

The geometrical shapes considered are:

Class 1—"n-sided" regular polygon with small circular hole in the center. Special cases: triangle, square, pentagon, hexagon, heptagon, octagon, nonagon, decagon, circle.
A circular bar with an eccentric hole.

Class 2—Rectangle with small circular hole in the center, and with variable "aspect ratio".

Class 3—Elliptical cross-sections with a confocal elliptical hole, and with a confocal slit (a slit connecting the foci of the ellipse) as inner boundries.

THEORETICAL CONSIDERATIONS

Solutions of the problems will be obtained by the method of conformal mapping. A short review of the method follows [1].

The temperature distribution in the systems satisfied Laplace's equation,

$$\nabla^2 T = \frac{\partial^2 T}{\partial x^2} + \frac{\partial^2 T}{\partial y^2} = 0$$

in the domain of the x,y plane with the temperature $T = T_0$ and $T = T_i$ along the boundaries $\phi_0(x,y)$, the outer boundary, and $\phi_i(x,y)$, the inner boundary, respectively.

It can be shown if ϕ and Ψ form a new co-ordinate system given by

$$\phi = \phi(x,y)$$
$$\Psi = \Psi(x,y)$$

such that

$$w = \phi + i\Psi = f(x + iy) = f(\rho e^{i\theta}) = f(z)$$

with the conditions that $f(z)$ is analytic and $f'(z)$ is not equal to zero, then the temperature distribution in the new co-ordinate system also satisfies the Laplace's equation

$$\nabla^2 T = \frac{\partial^2 T}{\partial \phi^2} + \frac{\partial^2 T}{\partial \Psi^2} = 0$$

and the temperature at the boundary $\phi = \phi_0$ is T_0, and correspondingly, at $\phi = \phi_i$ is T_i [2–4].

The application of this method is done by choosing a known solution in the ϕ,Ψ plane, and by an appropriate choice of the mapping function, $f(x + iy)$.

The simplest solution in the ϕ,Ψ plane is for one dimensional heat flow, with the boundary conditions that along $\phi = \phi_0$, the temperature is T_0, and along $\phi = \phi_i$, it is T_i. Then

$$T - T_0 = (T_i - T_0)\frac{\phi - \phi_0}{\phi_i - \phi_0}. \tag{1}$$

The heat flow for the one dimensional case between the flow lines Ψ_1, and Ψ_2 is, according to Fourier's Law, equal to

$$Q = k(T_i - T_0)\frac{\Delta\Psi}{\phi_0 - \phi_i}L \tag{2}$$

where L is the width of the bar and $\Delta\Psi = \Psi_2 - \Psi_1$.

It can be shown that the resultant heat flow computed in the ϕ,Ψ plane is identical to the heat flow in the x,y plane. The heat flow per unit width is

$$\frac{Q}{L} = \frac{k\Delta\Psi}{\phi_0 - \phi_1}(T_i - T_0)$$

or

$$\frac{Q}{L} = kS(T_i - T_0)$$

where the shape factor, S, is defined as:

$$S = \frac{\Delta\Psi}{\phi_0 - \phi_i}. \tag{3}$$

STEADY TRANSVERSE HEAT FLOW IN PRISMATIC RODS WITH "n-SIDED" REGULAR POLYGON CROSS-SECTIONS

Consider a long regular prismatic rod with a concentric circular hole, Fig. 1. The temperatures at the inner circular boundary, and at the

Vol. 3 1961

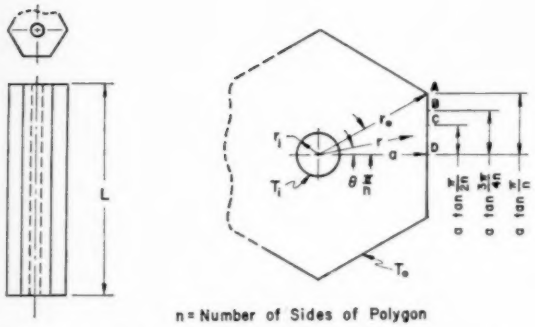

FIG. 1. Prismatic rod with "n-sided" regular polygonal cross-section.

outer prismatic boundary are T_i and T_0 respectively.

The mapping function which transforms the one dimensional heat flow in the ϕ,Ψ plane into the configuration of Fig. 1 is

$$w = \phi + i\Psi = 2 \ln z + \sum_{j=0}^{\infty} A_{jn} \rho^{jn} e^{ijn\theta} \qquad (4.1)$$

n = number of sides of polygon,

$$\rho = \frac{r}{r_e}.$$

The choice of this particular mapping function was due to:

(a) The influence of the power series diminishes toward the center. The lowest power of 3, for the case of a triangle, does not appreciably distort the temperature near the source.

(b) The "n" fold symmetry accounts for the geometry of the "n-sided" polygon. On the outer boundary the contribution from the source is small compared with that from the power series.

The real part (ϕ) is:

$$\phi = \ln \rho^2 + A_0 + A_n \rho^n \cos n\theta + A_{2n} \rho^{2n} \cos 2n\theta + A_{3n} \rho^{3n} \cos 3n\theta + \ldots \qquad (4.2)$$

and the imaginary part (Ψ) is:

$$\Psi = 2\theta + A_n \rho^n \sin n\theta + A_{2n} \rho^{2n} \sin 2n\theta + A_{3n} \rho^{3n} \sin 3n\theta + \ldots \qquad (4.3)$$

The coefficients A_0, A_n, A_{2n}, and A_{3n} can be computed to yield the value of T_0 or ($\phi_0 = 0$) at the points A, B, C, and D, considering only the first five terms of the series solution, (4.2). The values of these coefficients are given in Table 1 for various values of "n".

Table 1. *Coefficients* A_0, A_n, A_{2n}, *and* A_{3n} *for various values of* "n" *to be used with equations* (4.7) *and* (4.8)

n	A_0	A_n	A_{2n}	A_{3n}
3	1·13916	1·83402	1·09469	0·39984
4	0·54159	0·59131	0·05767	0·00796
5	0·32131	0·29838	−0·01111	0·01183
6	0·21339	0·18145	−0·01839	0·01355
7	0·15214	0·12233	−0·01704	0·01276
8	0·11397	0·08818	−0·01457	0·01123
9	0·08832	0·06642	−0·01218	0·00972
10	0·07076	0·05201	−0·01029	0·00841
.	.	.	.	.
.	.	.	.	.
.	.	.	.	.
∞	0	0	0	0

The method described above results in an approximation, and the outer boundary temperature is equal to T_0 at the few points selected. The maximum deviations from the constant value (T_0) were computed for the triangle and square, expecting the largest error in these cases. The deviation is less than $(T_i - T_0)/150$ in the case of the triangle, and $(T_i - T_0)/2000$ for the square. Therefore, for all practical cases, along the outer prismatic boundary, the value of ϕ is:

$$\phi_0 = 0. \qquad (4.4)$$

Along the inside circular boundary for small values of $\rho_i (\rho_i \ll 1)$

$$\phi_i = \ln \rho_i^2 + A_0 \qquad (4.5)$$

resulting in a constant temperature along the inner circular boundary.

Since θ varies from 0 to 2π in the x,y plane, then from (4.3)

$$\Delta\Psi = 4\pi. \qquad (4.6)$$

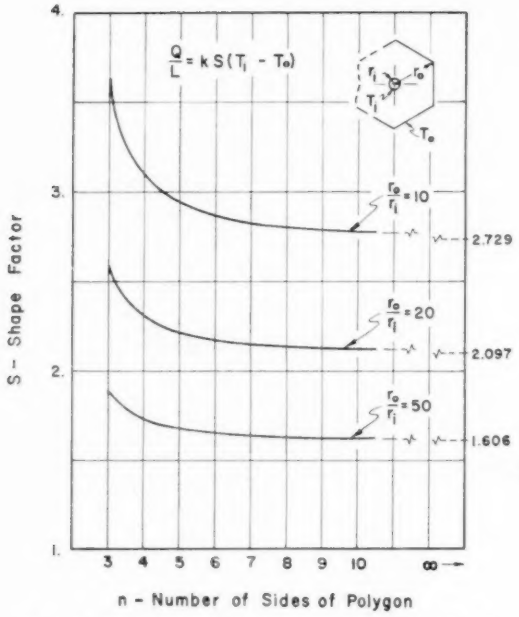

FIG. 2. Shape factor versus number of sides of regular polygon.

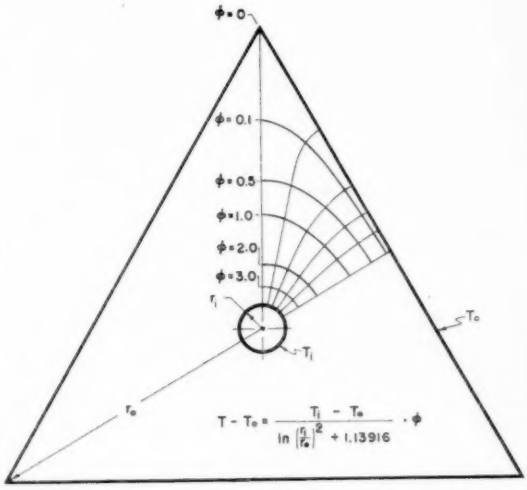

FIG. 3. Temperature distribution in a prismatic rod with triangular cross-section.

Vol. 3 1961

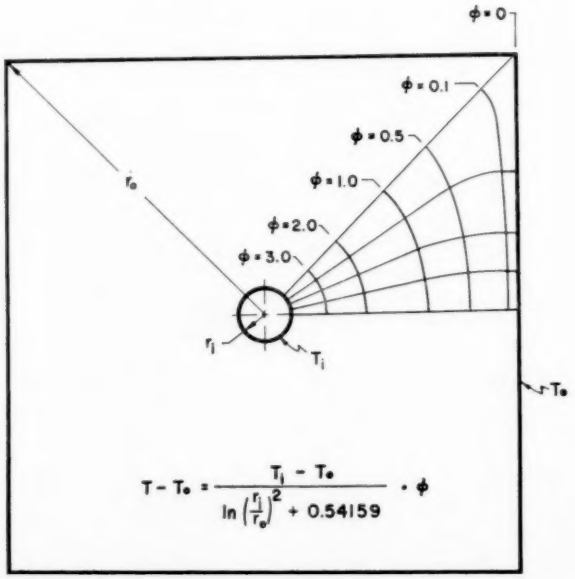

FIG. 4. Temperature distribution in a prismatic rod with square cross-section.

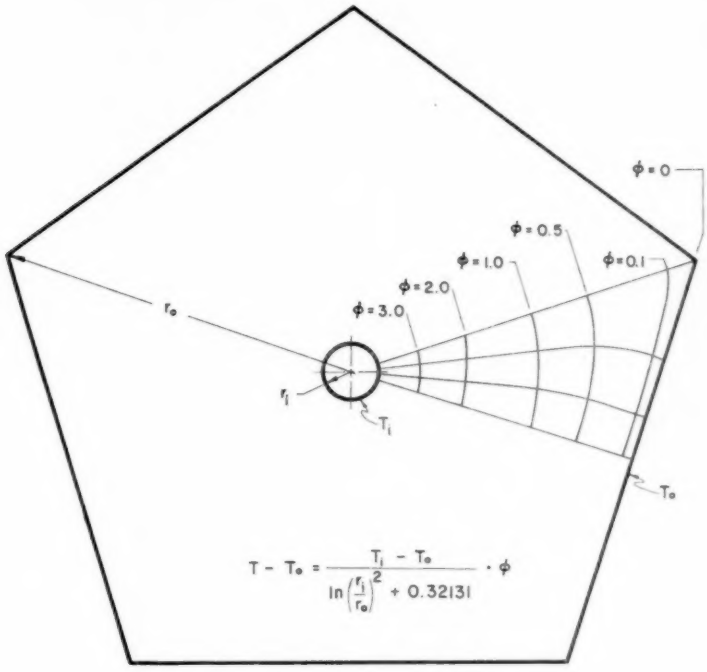

FIG. 5. Temperature distribution in a prismatic rod with pentagonal cross-section.

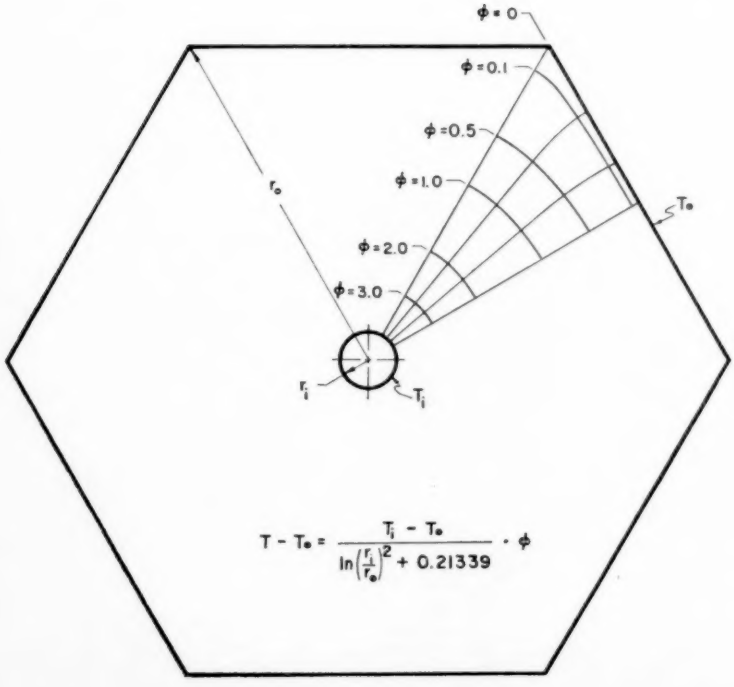

FIG. 6. Temperature distribution in a prismatic rod with hexagonal cross-section.

The temperature distribution is then obtained by substituting (4.2), (4.4), and (4.5) into (1).

$$T - T_0 = \frac{T_i - T_0}{\ln \rho_i^2 + A_0}(\ln \rho^2 + A_0 + A_n\rho^n \cos n\theta + A_{2n}\rho^{2n} \cos 2n\theta + A_{3n}\rho^{3n} \cos 3n\theta) \quad (4.7)$$

and substituting (4.4), (4.5), and (4.6) into (3) yields the shape factor

$$S = \frac{2\pi}{\ln \frac{r_0}{r_i} - \frac{A_0}{2}}. \quad (4.8)$$

It should be noted that A_0 is the only coefficient affecting the value of the shape factor for r_i/r_0 sufficiently small.

Values of the shape factor versus the number of sides of the polygon, "n", appear in Fig. 2. The temperature distribution for the triangle, square, pentagon, and hexagon are shown in Figs. 3, 4, 5 and 6.

Smith *et al.* [5] used an electrical analogue to determine the shape factor for a square with a central hole. From the graphical data, an empirical equation for the shape factor (written here with the notation used in this paper) was defined as

$$S = \frac{6{\cdot}42}{\ln \frac{r_0}{r_i} - 0{\cdot}264}. \quad (4.9)$$

It is interesting to notice the close similarity of this equation to the equation (4.8) as re-written in the form

$$S = \frac{6{\cdot}28318}{\ln \frac{r_0}{r_i} - 0{\cdot}27079}. \quad (4.10)$$

The agreement between the analysis and the experimental findings is excellent.

Moore [6] used field maps to study the problem of a square with a central hole. The result reported by Moore and Smith *et al.* show not only an excellent agreement for small values of r_i/a, but the agreement is close even for $r_i/a = 0{\cdot}7$.

STEADY TRANSVERSE HEAT FLOW IN PRISMATIC BARS WITH RECTANGULAR CROSS-SECTIONS

The configuration under study is represented in Fig. 7, and consists of a rectangle with sides $2a$ and $2b$, having a circular inner boundary. The temperatures at the inner and outer boundaries are T_i and T_0 respectively.

The mapping function which transforms the one-dimensional heat flow in the ϕ,Ψ plane with constant temperatures at ϕ_i and ϕ_0 to the configuration of Fig. 7 in the x,y plane is

$$w = \phi + i\Psi = 2\sum_{n=0}^{\infty}(-1)^n \ln\left[\coth\frac{\pi}{4a}(z \pm 2nb)\right]. \quad (5.1)$$

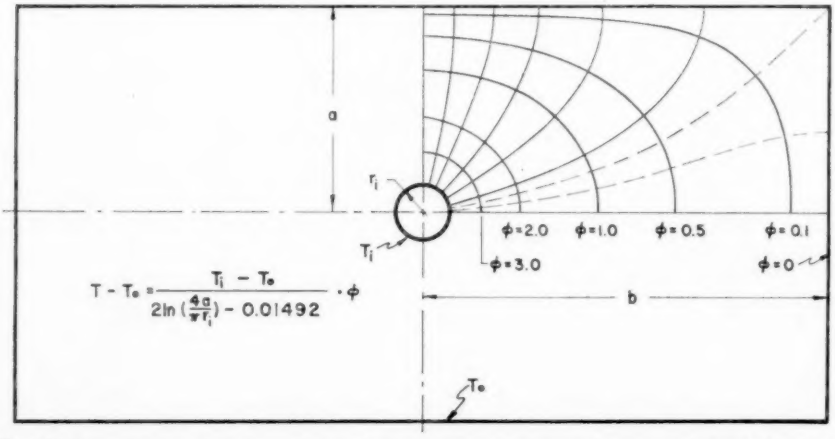

FIG. 7. Temperature distribution in a prismatic rod with rectangular cross-section ($b/a = 2$).

Vol. 3 1961

This form of the mapping function was obtained by filling the x,y plane with an infinite matrix of sources and sinks spaced by $2b$ in the x direction and by $2a$ in the y direction.

The real part (ϕ) is:

$$\phi = \sum_{n=0}^{\infty} (-1)^n \ln \left[\frac{1 + \dfrac{\cos \dfrac{\pi y}{2a}}{\cosh \dfrac{\pi}{2a}(x \pm 2nb)}}{1 - \dfrac{\cos \dfrac{\pi y}{2a}}{\cosh \dfrac{\pi}{2a}(x \pm 2nb)}} \right] \tag{5.2}$$

The imaginary part (Ψ) is:

$$\Psi = 2 \sum_{n=0}^{\infty} (-1)^{n+1} \tan^{-1} \left[\frac{\sin \dfrac{\pi y}{2a}}{\sinh \dfrac{\pi}{2a}(x \pm 2nb)} \right]. \tag{5.3}$$

The value of ϕ at the outer boundary of the rectangle is:

$$\phi_0 = 0 \tag{5.4}$$

at the inner circular boundary, when $r_i/2 \ll 1$, (or $x/a \ll 1$, $y/a \ll 1$), ϕ converges from (5.2) to

$$\phi_i = 2 \ln \frac{4a}{\pi r_i} - 4 \sum_{m=0}^{\infty} \sum_{n=1}^{\infty} \frac{(-1)^{n+1}}{(2m+1)} \operatorname{sech}^{(2m+1)} \frac{n\pi b}{a}. \tag{5.5}$$

The double-summed term can be shown to be convergent and it will henceforth be denoted by K, so that

$$\phi_i = 2 \ln \frac{4a}{\pi r_i} - 4K \tag{5.5a}$$

where:

$$K = \sum_{m=0}^{\infty} \sum_{n=1}^{\infty} \frac{(-1)^{n+1}}{(2m+1)} \operatorname{sech}^{(2m+1)} \frac{n\pi b}{a}.$$

The values of K are listed in Table 2 for various b/a ratios.

Table 2. Values of K for various b/a ratios to be used with equations (5.7) and (5.8)

$\frac{b}{a}$	K
1·00	0·08290
1·25	0·03963
1·50	0·01781
1·75	0·00816
2·00	0·00373
2·25	0·00170
2·50	0·00078
3·00	0·00016
4·00	$6{\cdot}9748 \times 10^{-6}$
5·00	$3{\cdot}0140 \times 10^{-7}$
10·00	$4{\cdot}5422 \times 10^{-14}$
. . . ∞	. . . 0

The variation of θ in the x,y plane from 0 to 2 corresponds to a variation in the ϕ,Ψ plane from $\Psi_1 = 0$ to $\Psi_2 = -4\pi$. Thus

$$\Delta\Psi = -4\pi. \tag{5.6}$$

The temperature distribution is then given by substituting (5.2), (5.4), and (5.5) into (1):

$$T - T_0 = \frac{T_i - T_0}{2 \ln \dfrac{4a}{\pi r_i} - 4K} \times \sum_{n=0}^{\infty} (-1)^n \ln \left[\frac{1 + \dfrac{\cos \dfrac{\pi y}{2a}}{\cosh \dfrac{\pi}{2a}(x \pm 2nb)}}{1 - \dfrac{\cos \dfrac{\pi y}{2a}}{\cosh \dfrac{\pi}{2a}(x \pm 2nb)}} \right]. \tag{5.7}$$

The shape factor is obtained by substituting (5.4), (5.5) and (5.6) into (3):

$$S = \frac{2\pi}{\ln \dfrac{4a}{\pi r_i} - 2K}. \tag{5.8}$$

The temperature distribution is illustrated for $b/a = 2$ in Fig. 7, and the values of the shape factor versus aspect ratio b/a are plotted in Fig. 8.

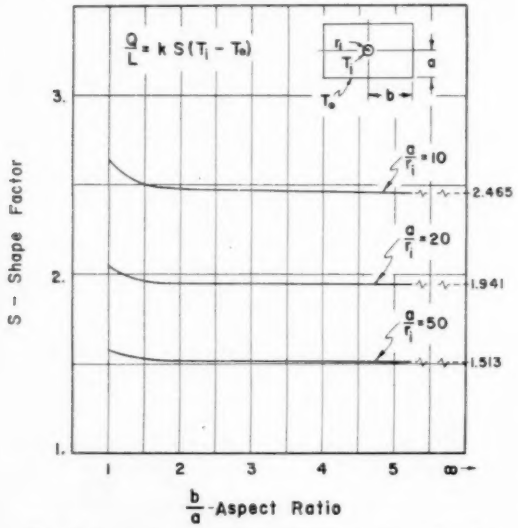

FIG. 8. Shape factor versus aspect ratio of rectangular.

When b/a tends to infinity, the temperature distribution of (5.7) and the shape factor, S, as given by (5.8), describe the case of an infinitely long strip with an inner circular boundary on the center line of the strip.

STEADY TRANSVERSE HEAT FLOW BETWEEN ECCENTRIC CIRCULAR CYLINDERS

Consider a bar with a circular outer boundary, and an eccentric circular inner boundary. The outer and inner boundary temperatures are T_0 and T_i respectively.

This problem is briefly discussed in Carslaw and Jaeger [2], and is quoted here briefly for the sake of completeness only.

The values of the shape factor versus eccentricity ratio, ϵ, are plotted in Fig. 9.

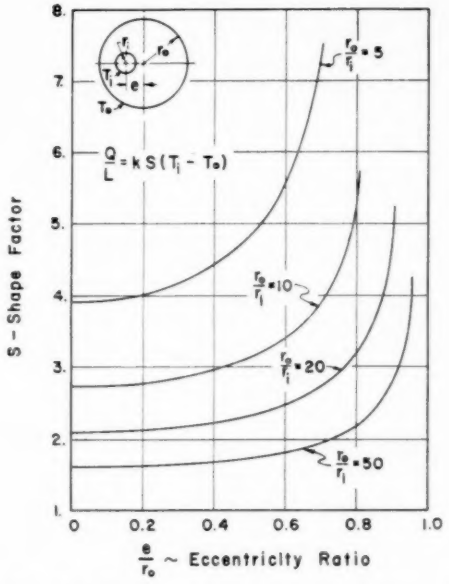

FIG. 9. Shape factor versus eccentricity ratio.

STEADY TRANSVERSE HEAT FLOW IN PRISMATIC BARS WITH ELLIPTICAL CROSS-SECTIONS

Consider a prismatic bar with confocal elliptical inner and outer boundaries. The temperatures of the outer and inner boundaries are T_0 and T_i, respectively.

The mapping function which transforms the one-dimensional heat flow in the ϕ,Ψ plane with constant temperatures at ϕ_i and ϕ_0 to the configuration of Fig. 10 in the x,y plane is [7]:

$$w = \phi + i\Psi = -i \sin^{-1} \frac{z}{f}. \tag{7.1}$$

The expressions for ϕ and Ψ are given in the implicit form

$$\frac{x^2}{f^2 \cosh^2 \phi} + \frac{y^2}{f^2 \sinh^2 \phi} = 1 \tag{7.2}$$

and

$$\frac{x^2}{f^2 \sin^2 \Psi} - \frac{y^2}{f^2 \cos^2 \Psi} = 1. \tag{7.3}$$

Along the outer boundary

$$\phi_0 = \tanh^{-1} \frac{d}{c} \tag{7.4}$$

Vol. 3 1961

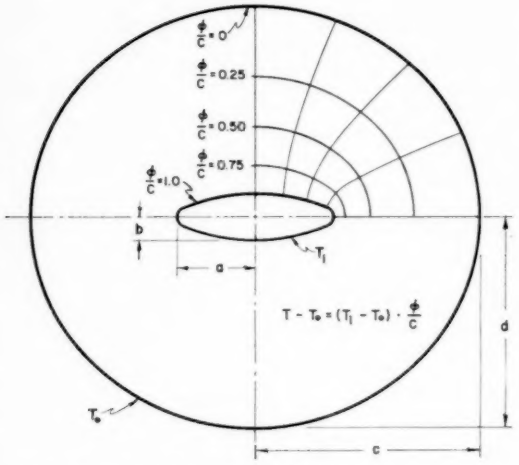

FIG. 10. Temperature distribution in a prismatic rod with confocal elliptical cross-section ($c/d = 1{\cdot}058$; $b/d = 0{\cdot}10$).

and along the inner boundary

$$\phi_i = \tanh^{-1}\frac{b}{a} \tag{7.5}$$

where

$$c^2 - d^2 = f^2$$

$$a^2 - b^2 = f^2.$$

The values of Ψ undergo a change of

$$\Delta\Psi = 2\pi. \tag{7.6}$$

The temperature distribution is given by substituting (7.4) and (7.5) into (1):

$$T - T_0 = (T_i - T_0)\frac{\phi - \ln\dfrac{c+d}{f}}{\ln\dfrac{a+b}{c+d}}. \tag{7.7}$$

The appropriate value of ϕ can be determined from (7.2) for particular values of x and y.

The shape is obtained by substituting (7.4), (7.5), and (7.6) into (3):

$$S = \frac{2\pi}{\ln\dfrac{c+d}{a+b}}. \tag{7.8}$$

The temperature distribution is shown in Fig. 10, and the shape factor is plotted versus the ratio of major to minor axis, c/d, in Fig. 11.

The case of the inner boundary degenerating into the focal slit, a slit connecting the foci of the outer elliptic boundary, is given by the curve $b/d = 0$.

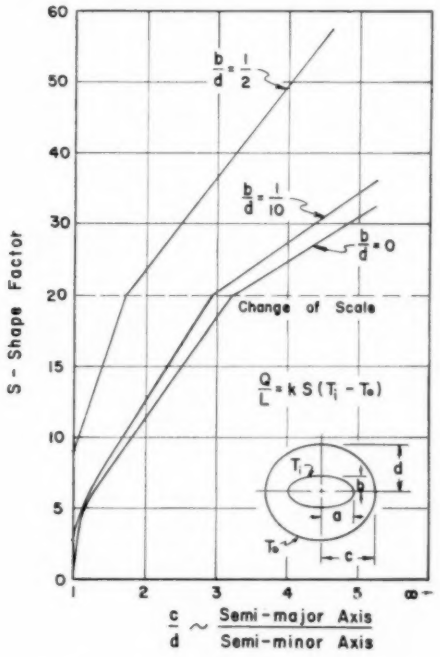

FIG. 11. Shape factor versus c/d ratio of confocal ellipses.

SUMMARY

The temperature distribution and the heat flow for long prismatic bars with constant temperatures at the outer and inner boundaries were computed and the results are summarized in Table 3.

ACKNOWLEDGEMENT

The authors would like to express their thanks to the Transportation Center at Northwestern University for supporting this study.

Table 3. *Summary of results*

Shape and notation	Temperature distribution	Shape factor, S $\frac{Q}{L} = kS(T_i - T_0)$
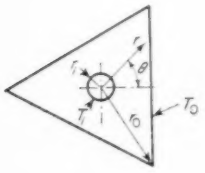 Triangle	$T - T_0 = \frac{T_i - T_0}{\ln\left(\frac{r_i}{r_0}\right)^2 + 1{\cdot}13916}\left[\ln\left(\frac{r}{r_0}\right)^2 + 1{\cdot}13916 + 1{\cdot}83402\left(\frac{r}{r_0}\right)^3\cos 3\theta + 1{\cdot}09469\left(\frac{r}{r_0}\right)^6\cos 6\theta + 0{\cdot}39984\left(\frac{r}{r_0}\right)^9\cos 9\theta\right]$	$\frac{2\pi}{\ln\frac{r_0}{r_i} - 0{\cdot}56958}$
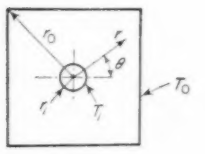 Square	$T - T_0 = \frac{T_i - T_0}{\ln\left(\frac{r_i}{r_0}\right)^2 + 0{\cdot}54159}\left[\ln\left(\frac{r}{r_0}\right)^2 + 0{\cdot}54159 + 0{\cdot}59131\left(\frac{r}{r_0}\right)^4\cos 4\theta + 0{\cdot}05767\left(\frac{r}{r_0}\right)^8\cos 8\theta + 0{\cdot}00796\left(\frac{r}{r_0}\right)^{12}\cos 12\theta\right]$	$\frac{2\pi}{\ln\frac{r_0}{r_i} - 0{\cdot}27079}$
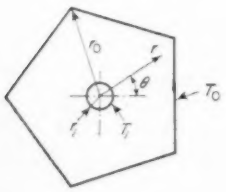 Pentagon	$T - T_0 = \frac{T_i - T_0}{\ln\left(\frac{r_i}{r_0}\right)^2 + 0{\cdot}32131}\left[\ln\left(\frac{r}{r_0}\right)^2 + 0{\cdot}32131 + 0{\cdot}29838\left(\frac{r}{r_0}\right)^5\cos 5\theta - 0{\cdot}0111\left(\frac{r}{r_0}\right)^{10}\cos 10\theta + 0{\cdot}01183\left(\frac{r}{r_0}\right)^{15}\cos 15\theta\right]$	$\frac{2\pi}{\ln\frac{r_0}{r_i} - 0{\cdot}16066}$
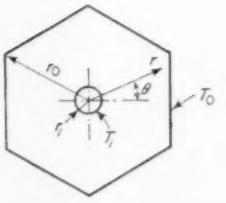 Hexagon	$T - T_0 = \frac{T_i - T_0}{\ln\left(\frac{r_i}{r_0}\right)^2 + 0{\cdot}21339}\left[\ln\left(\frac{r}{r_0}\right)^2 + 0{\cdot}21339 + 0{\cdot}18145\left(\frac{r}{r_0}\right)^6\cos 6\theta - 0{\cdot}01839\left(\frac{r}{r_0}\right)^{12}\cos 12\theta + 0{\cdot}01355\left(\frac{r}{r_0}\right)^{18}\cos 18\theta\right]$	$\frac{2\pi}{\ln\frac{r_0}{r_i} - 0{\cdot}10669}$

Vol. 3 1961

Table 3—continued

Shape and notation	Temperature distribution	Shape factor, S $\frac{Q}{L} = kS(T_i - T_0)$
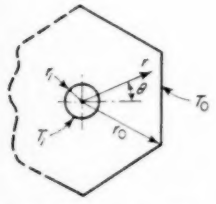 "n-Sided" regular polygon n = no. of sides	$T - T_0 = \frac{T_i - T_0}{\ln\left(\frac{r_i}{r_0}\right)^2 + A_0}\left[\ln\left(\frac{r}{r_0}\right)^2 + A_0 + A_n\left(\frac{r}{r_0}\right)^n \cos n\theta + A_{2n}\left(\frac{r}{r_0}\right)^{2n} \cos 2n\theta + A_{3n}\left(\frac{r}{r_0}\right)^{3n} \cos 3n\theta\right]$ (See Table 1 for A_0, A_n, A_{2n}, and A_{3n})	$\frac{2\pi}{\ln\frac{r_0}{r_i} - \frac{A_0}{2}}$
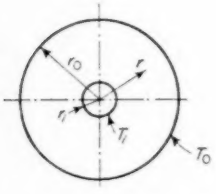 Concentric circles	$T - T_0 = (T_i - T_0)\frac{\ln\frac{r}{r_0}}{\ln\frac{r_i}{r_0}}$	$\frac{2\pi}{\ln\frac{r_0}{r_i}}$
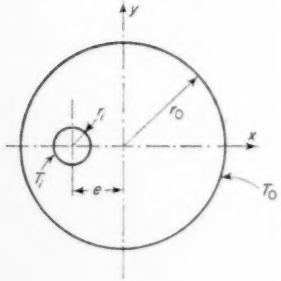 Eccentric circles	$T - T_0 = \frac{T_i - T_0}{2\cosh^{-1}\left(\frac{1+\rho_i^2-\epsilon^2}{2\rho_i}\right)}\left[\ln\frac{\left(\frac{x}{r_0}+\frac{h}{r_0}+\frac{a}{r_0}\right)^2+\left(\frac{y}{r_0}\right)^2}{\left(\frac{x}{r_0}+\frac{h}{r_0}-\frac{a}{r_0}\right)^2+\left(\frac{y}{r_0}\right)^2} - \cosh^{-1}\left(\frac{1-\rho_i^2+\epsilon^2}{2\epsilon}\right)\right]$ Where: $\rho_i = \frac{r_i}{r_0}; \quad \epsilon = \frac{e}{r_0}$ $\left(\frac{a}{r_0}\right)^2 = \frac{(1-\rho_i^2+\epsilon^2)^2}{4\epsilon^2} - 1$ $\frac{h}{r_0} = \frac{1-\rho_i^2+\epsilon^2}{2\epsilon}$	$\frac{2\pi}{\cosh^{-1}\left(\frac{1+\rho_i^2-\epsilon^2}{2\rho_i}\right)}$

Table 3—continued

Shape and notation	Temperature distribution	Shape factor, S $\frac{Q}{L} = kS(T_i - T_0)$
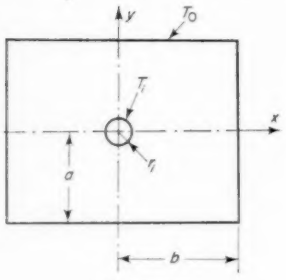 Rectangle	$T - T_0 = \frac{T_i - T_0}{2 \ln \frac{4a}{\pi r_i} - 4K} \sum_{n=0}^{\infty} (-1)^n \ln \left[\frac{1 + \frac{\cos \frac{\pi y}{2a}}{\cosh \frac{\pi}{2a}(x \pm 2nb)}}{1 - \frac{\cos \frac{\pi y}{2a}}{\cosh \frac{\pi}{2a}(x \pm 2nb)}} \right]$ (See Table 2 for K)	$\frac{2\pi}{\ln \frac{4a}{\pi r_i} - 2K}$
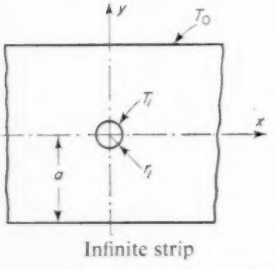 Infinite strip	$T - T_0 = \frac{T_i - T_0}{2 \ln \frac{4a}{\pi r_i}} \ln \left[\frac{1 + \frac{\cos \frac{\pi y}{2a}}{\cosh \frac{\pi x}{2a}}}{1 - \frac{\cos \frac{\pi y}{2a}}{\cosh \frac{\pi x}{2a}}} \right]$	$\frac{2\pi}{\ln \frac{4a}{\pi r_i}}$
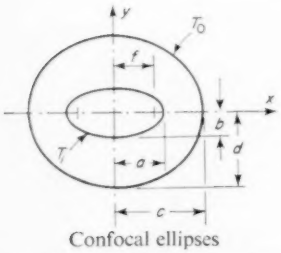 Confocal ellipses	$T - T_0 = \frac{T_i - T_0}{\ln \frac{a+b}{c+d}} \left(\phi - \ln \frac{c+d}{f} \right)$ Compute ϕ from: $\frac{x^2}{f^2 \cosh^2 \phi} + \frac{y^2}{f^2 \sinh^2 \phi} = 1$	$\frac{2\pi}{\ln \frac{c+d}{a+b}}$
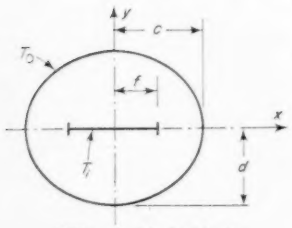 Ellipse with focal slit	$T - T_0 = \frac{T_i - T_0}{\ln \frac{f}{c+d}} \left(\phi - \ln \frac{c+d}{f} \right)$ Compute ϕ from: $\frac{x^2}{f^2 \cosh^2 \phi} + \frac{y^2}{f^2 \sinh^2 \phi} = 1$	$\frac{2\pi}{\ln \frac{c+d}{f}}$

Vol. 3 1961

REFERENCES

1. L. Bierberbach, *Conformal Mapping*. Chelsea Publishing, New York (1953).
2. H. S. Carslaw and J. C. Jaeger, *Conduction of Heat in Solids*, 2nd Ed., pp. 421–454. Oxford University Press, London (1959).
3. E. R. G. Eckert and R. M. Drake, Jr., *Heat and Mass Transfer*, pp. 64–69. McGraw-Hill, New York (1959).
4. M. Jakob, *Heat Transfer, Vol. I*, pp. 326–331. John Wiley, New York (1949).
5. J. C. Smith, T. E. Lind, Jr. and D. S. Lermond, Shape factors for conductive heat flow, *J. Amer. Inst. Chem. Engrs*, **4**, 330–331 (1958).
6. A. D. Moore, *Heat Transfer Notes for Electrical Engineering*, pp. 7–9. George Wahr, Ann Arbor, Michigan (1938).
7. R. V. Churchill, *Introduction to Complex Variables and Applications*. McGraw-Hill, New York (1948).

ol.
3
961

Int. J. Heat Mass Transfer. Vol. 3, pp. 126–132. Pergamon Press 1961. Printed in Great Britain.

APPROXIMATE CALCULATION METHOD FOR HEAT TRANSFER IN LAMINAR BOUNDARY LAYERS WITH CONSTANT SURFACE TEMPERATURE

A. G. SMITH* and V. L. SHAH†

Department of Aircraft Propulsion, College of Aeronautics, Cranfield

(*Received* 20 *January* 1961)

Abstract—A simple method for the calculation of heat transfer in a laminar, constant property and constant surface temperature flow, was described by Smith and Spalding [1]. In the present paper, the method is extended to the range of Prandtl numbers 0·7 to 10. Examples are given of heat transfer calculations for ellipses of 2:1 and 4:1 fineness ratio.

Résumé—Une méthode simple de calcul de la transmission de chaleur dans un écoulement laminaire à propriétés constantes et température de surface constante a été décrite par Smith et Spalding [1]. Dans cet article, la méthode est étendue au domaine des nombres de Prandtl compris entre 0,7 et 10. Des exemples de calcul de transmission de chaleur sont donnés pour les ellipses d'excentricité 2:1 et 4:1.

Zusammenfassung—Smith und Spalding [1] beschrieben eine einfache Methode zur Berechnung des Wärmeüberganges in einer Laminarströmung mit gleichbleibenden Stoffeigenschaften und konstanter Temperatur der Berandung. Diese Methode wird hier auf den Bereich der Prandtlzahlen von 0,7 bis 10 ausgedehnt. Als Beispiel wird der Wärmeübergang an Ellipsen vom Achsenverhältnis 2:1 und 4:1 berechnet.

Аннотация—Смит и Сполдинг [1] дали описание простого метода расчёта теплообмена в ламинарном потоке с постоянными физическими характеристиками и постоянной температурой поверхности. В публикуемой статье этот метод распространён на область чисел Прандтля от 0,7 до 10. Приводятся примеры расчёта теплообмена для эллипсов с соотношением осей равным 2:1 и 4:1.

NOTATION

A, number defined in equation (2);
a, thermal diffusivity, $k/\rho C_p$;
B, number defined in equation (2);
c, characteristic length of body, e.g. chord or major axis;
C_p, specific heat;
Δ_4, "heat flux thickness" defined by $h = k/\Delta_4$;
E_4, error term defined in equation (2);
h, heat transfer coefficient;
k, conductivity of the fluid;
Nu, Nusselt number, hc/k;
Nu_x, Nusselt number, hx/k;
μ, fluid viscosity;
ν, kinematic viscosity of the fluid;
Q, heat;
Re, Reynolds number, Uc/ν;
Re_x, Reynolds number, U_1x/ν;
r, radial dimension of axisymmetric body;
ρ, density;
σ, Prandtl number, ν/a;
θ, temperature;
U_1, mainstream velocity at a point on the surface;
U, approach or reference velocity;
u, fluid velocity within the boundary layer;
X, Y, Z, vectorial length;
x, distance along surface from stagnation point;
y, distance normal to surface.

* Professor of Thermodynamics, University of Nottingham, Nottingham.

† Department of Aircraft Propulsion, College of Aeronautics, Cranfield.

Vol. 3 1961

1. INTRODUCTION

EXACT solutions of the boundary layer equations are possible only for a limited range of mainstream velocity distributions. To solve a problem involving the flow of a fluid round a body of arbitrary shape, approximate methods are necessary. Numerous approximate methods are available to calculate heat transfer in a laminar boundary layer with constant fluid properties and constant wall temperature.

Frossling [2] carried out the calculations of the temperature distribution by assuming a power series for mainstream velocity distribution, velocity distribution in the boundary layer and the temperature distribution in the boundary layer, and solved the differential equation. The method is very cumbersome.

Eckert [3] solved the temperature equation by assuming that the rate of growth of the temperature layer is the same as for a wedge flow with the same temperature thickness and the same value of a certain pressure gradient parameter. However, by this method, the calculations for the thermal boundary layer are considerably more tedious than those for the velocity layers.

Squire [4] derived an approximate method by solving an approximate heat flux equation. The Blasius velocity profile was taken, but the displacement thickness was allowed to vary with x in a manner appropriate to the mainstream. The temperature profile was taken similar to the velocity profile but with scale in the y direction altered in a manner to be determined from the energy integral equation.

This method will give good results only for a streamline body because the profiles are assumed to be that of flat plate. Further the method involves more calculation than that of Smith and Spalding [1].

Ambrok [5] has solved an approximate heat flux equation by assuming that a relation of the type $Nu_x = A'(Re_x)^n$ which is true for flat plate, is also valid for a flow over a body of arbitrary shape. This method, though simple, gives lower values of heat transfer when compared to those of Eckert [3].

Allen and Look [6] have applied Reynolds analogy to calculate heat transfer from shear stress for fluids with Prandtl number unity. Frick and McCullough [7] extended this method for any Prandtl number by suggesting a simple multiplier for Prandtl number. This method gives very high values of heat transfer.

The simplest of all the methods appears to be that of Smith and Spalding [1] whose simple quadratures give results identical with those of Eckert [3]. The Smith and Spalding method is limited to fluid with Prandtl number $= 0{\cdot}7$ which is adequate for air and some other gases. However, to meet the case of liquids, the method has been extended in the present paper to cover a range of Prandtl numbers up to 10.

2. EXTENSION OF SMITH AND SPALDING METHOD TO A RANGE OF PRANDTL NUMBERS

From vectorial dimensional analysis, it can be shown that the rate of growth of a thermal boundary layer is dependent on the thickness of the layer and on the mainstream velocity gradient, i.e.

$$\frac{U_1}{\nu}\frac{\mathrm{d}(\Delta_4^2)}{\mathrm{d}x} = f\left(\frac{\Delta_4^2}{\nu}\frac{\mathrm{d}U_1}{\mathrm{d}x}, \sigma\right). \tag{1}$$

In deriving the above relation, the following assumptions are made in addition to the boundary layer assumptions:

(1) The rate of growth depends only on local conditions.
(2) Any dependence of the rate of growth on velocity layer shape or thickness can be ignored.

These assumptions lead to

$$\frac{\mathrm{d}\Delta_4}{\mathrm{d}x} = f\left(\Delta_4, U_1, \frac{\mathrm{d}U_1}{\mathrm{d}x}, \mu, k, C_p, \rho\right),$$

and when dimensionless groups are formed allowing a separate identity to the X, Y, Z, length dimensions, equation (1) follows. The dimensions $QT^{-1}\theta^{-1}X^{-1}YZ^{-1}$ and $MT^{-1}X^{-1}YZ^{-1}$ assigned to k and μ respectively, assert the usual boundary layer assumptions that k and μ "act" only through $\partial\theta/\partial y$ and $\partial u/\partial y$. This assertion leads to equation (1) instead of a more general and less useful relation obtained when the three length dimensions are undistinguished.

The unknown function in equation (1) can be obtained from the exact solutions of the thermal boundary layer equations. From exact solution

for the thermal boundary layers in "wedge" flows by Eckert [3] (Fig. 1), it can be seen that the relation between the two quantities is nearly linear.

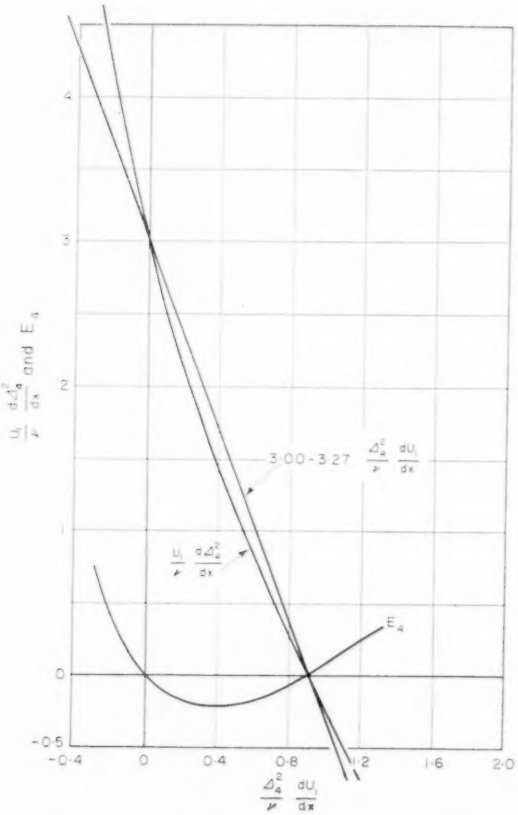

FIG. 1. Typical graph showing relation between $\frac{U_1}{\nu}\frac{\mathrm{d}\Delta_4^2}{\mathrm{d}x}$ and $\frac{\Delta_4^2}{\nu}\frac{\mathrm{d}U_1}{\mathrm{d}x}$ for $\sigma = 5$.

Writing the relation

$$\left[\frac{U_1}{\nu}\frac{\mathrm{d}\Delta_4^2}{\mathrm{d}x}\right] = A - B\left(\frac{\Delta_4^2}{\nu}\frac{\mathrm{d}U_1}{\mathrm{d}x}\right) + E_4 \qquad (2)$$

where E_4 is the error of the linear approximation, and is a small number dependent on

$$\left(\frac{\Delta_4^2}{\nu}\frac{\mathrm{d}U_1}{\mathrm{d}x}\right),$$

we may integrate, using the integrating factor U_1^{B-1} to

$$\left[\frac{U_1^B\,\Delta_4^2}{\nu}\right] = A\int_0^x U_1^{B-1}\,\mathrm{d}x + \int_0^x U_1^{B-1}E_4\,\mathrm{d}x. \qquad (3)$$

From this quadrature, knowing A and B, Δ_4 may be calculated everywhere, U_1 being a known function of x, and ν being known. The calculation is in principle iterative since E_4 cannot be found until a first approximation to Δ_4 has been obtained. This first approximation, called $\Delta_{4(1)}$ is calculated by omitting the last term from equation (3). From $\Delta_{4(1)}$, $E_{4(1)}$ is calculated, and hence $\Delta_{4(2)}$. Actually $E_{4(1)}$ is often so small that the first approximation $\Delta_{4(1)}$ suffices.

From Δ_4 the heat transfer coefficient may be found by the equation:

$$h = k/\Delta_4. \qquad (4)$$

It is preferable to work with the dimensionless forms of equations (3) and (4). They are:

$$\left(\frac{\Delta_4}{c}\right)^2\left(\frac{Uc}{\nu}\right) = \frac{A}{\left(\frac{U_1}{U}\right)^B}\int_0^{x/c}\left(\frac{U_1}{U}\right)^{B-1}\mathrm{d}\left(\frac{x}{c}\right) + \frac{1}{\left(\frac{U_1}{U}\right)^B}\int_0^{x/c}\left(\frac{U_1}{U}\right)^{B-1}E_4\,\mathrm{d}\left(\frac{x}{c}\right) \qquad (5)$$

and

$$\frac{hc}{k}\Big/\sqrt{\left(\frac{Uc}{\nu}\right)} = 1\Big/\left(\frac{\Delta_4}{c}\right)\sqrt{\left(\frac{Uc}{\nu}\right)} \qquad (6)$$

E_4 is now dependent on

$$\left(\frac{\Delta_4}{c}\right)^2\left(\frac{Uc}{\nu}\right)\frac{\mathrm{d}(U_1/U)}{\mathrm{d}(x/c)}.$$

At the front stagnation point, equation (5) becomes

$$\left(\frac{\Delta_4}{c}\right)^2\left(\frac{Uc}{\nu}\right) = \frac{A/B}{\frac{\mathrm{d}(U_1/U)}{\mathrm{d}(x/c)}}. \qquad (7)$$

Eckert [3] gives data sufficing for the calculation of A, B, and E_4 for $\sigma = 0{\cdot}7$, $0{\cdot}8$, $1{\cdot}0$, $5{\cdot}0$ and 10. Smith and Spalding [1] gave A, B, for $\sigma = 0{\cdot}7$ and the values for other σ are added below, in Table 1.

Vol. 3 1961

Table 1

σ	0·7	0·8	1·0	5	10
A	11·68	10·61	9·07	3·00	1·885
B	2·87	2·90	2·95	3·27	3·41
A/B	4·07	3·66	3·07	0·919	0·554

Figure 1 shows the relation between

$$\frac{U_1}{\nu}\frac{\mathrm{d}(\Delta_4^2)}{\mathrm{d}x} \text{ and } \frac{\Delta_4^2}{\nu}\frac{\mathrm{d}U_1}{\mathrm{d}x}$$

for $\sigma = 5$, as an example. Similar graphs were drawn for other σ values to obtain the A and B values of Table 1.

E_4 is given in Table 2.

Tables 1 and 2 give all the numerical data necessary for computing heat transfer in laminar layers over the range $\sigma = 0{\cdot}7$ to 10. For convenience in using the method at intermediate σ values, the dependence of A and B on σ has been plotted in Fig. 2.

Equations (5) and (6) have been computed by the authors, for flow over ellipses of major/minor axis ratio 4:1 and 2:1, and for Prandtl numbers 0·7, 0·8, 1·0, 5·0 and 10. Integration was performed by Simpson's rule using 0·01 intervals to $x/c = 0{\cdot}1$, then 0·05 intervals to $x/c = 0{\cdot}7$. An extract from the computation for $\sigma = 5$, for the 4:1 ellipse, is given in Table 3. The results of these calculations are shown in Figs. 3 and 4, and the velocity distributions which were used are shown in Fig. 5.

Comparison of these calculations with other theoretical results is not possible except at $\sigma = 0{\cdot}7$, where results from Eckert [3] and Schuh [8] are available. These results are in too close agreement with those of the present paper for differences to appear when plotting to the scale of Figs. 3 and 4.

3. AXISYMMETRIC FLOW

By the use of Mangler's transformations [9]:

(1) $$\bar{x} = \int_0^x \left(\frac{r}{c}\right)^2 \mathrm{d}x$$

(2) $$\bar{y} = \left(\frac{r}{c}\right) y$$

(3) $$\bar{\Delta} = \left(\frac{r}{c}\right) \Delta$$

Table 2

$\sigma = 0{\cdot}7$	$\frac{\Delta_1^2}{\nu}\frac{\mathrm{d}U_1}{\mathrm{d}x}$	6·05	4·07	2·26	1·01	0	−1·02
	E_4	1·042	0	−0·68	−0·67	0	2·06
$\sigma = 0{\cdot}8$	$\frac{\Delta_1^2}{\nu}\frac{\mathrm{d}U_1}{\mathrm{d}x}$	5·427	3·663	2·039	0·917	0	−0·937
	E_4	1·027	0·011	−0·618	−0·614	0	1·935
$\sigma = 1{\cdot}0$	$\frac{\Delta_1^2}{\nu}\frac{\mathrm{d}U_1}{\mathrm{d}x}$	4·541	3·074	1·721	0·779	0	−0·809
	E_4	0·919	−0·002	−0·551	−0·543	0	1·716
$\sigma = 5$	$\frac{\Delta_1^2}{\nu}\frac{\mathrm{d}U_1}{\mathrm{d}x}$	1·327	0·919	0·531	0·248	0	−0·287
	E_4	0·343	0	−0·202	−0·208	0	0·740
$\sigma = 10$	$\frac{\Delta_1^2}{\nu}\frac{\mathrm{d}U_1}{\mathrm{d}x}$	0·798	0·554	0·325	0·154	0	−0·185
	E_4	0·238	0	−0·126	−0·132	0	0·491

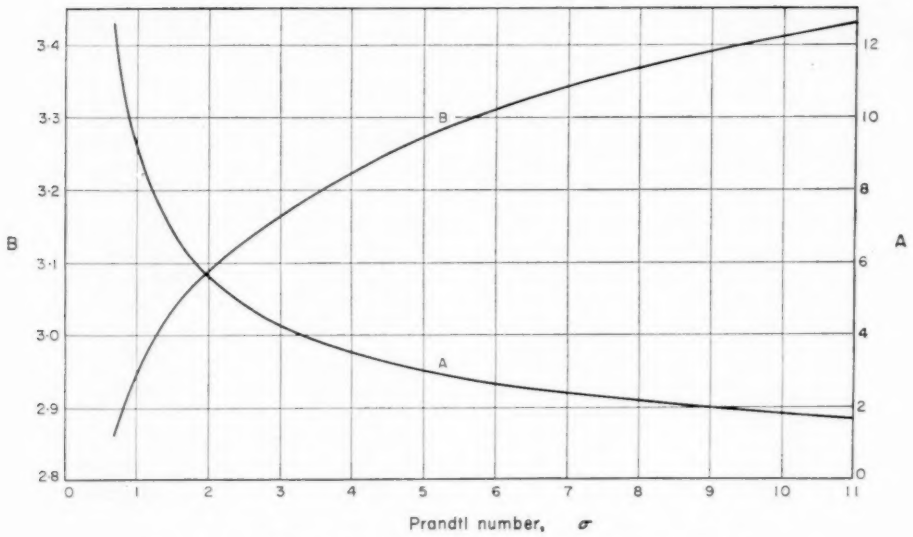

FIG. 2. Variation of A and B in equation (2) with Prandtl number.

Table 3

x/c	0	0·1	0·2	0·3	0·4	0·5	0·6	0·7	0·8
U_1/U	0	1·153	1·22	1·239	1·246	1·25	1·249	1·245	1·235
$I = \int_0^{x/c} (U_1/U)^{2\cdot27}\, \mathrm{d}\left(\frac{x}{c}\right)$	0	0·087	0·237	0·397	0·561	0·726	0·892	1·057	1·22
$\left(\frac{\Delta_4}{c}\right)^2\left(\frac{Uc}{\nu}\right) = \frac{3\cdot00\, I}{(U_1/U)^{3\cdot27}}$	0·023 *	0·164	0·371	0·591	0·821	1·295	1·295	1·55	1·839
$\frac{hc/k}{\sqrt{(Uc/\nu)}}$ 1st approx.	6·601	2·47	1·64	1·3	1·105	0·976	0·88	0·803	0·737
$\left(\frac{\Delta_4}{c}\right)^2\left(\frac{Uc}{\nu}\right)\frac{\mathrm{d}(U_1/U)}{\mathrm{d}(x/c)}$	0·919	0·232	0·113	0·07	0·041	0·011	−0·027	−0·098	−0·277
E_4	0	−0·204	−0·144	−0·105	−0·07	−0·02	−0·043	0·185	0·685
$\int_0^{x/c} (U_1/U)^{2\cdot27} E_4\, \mathrm{d}\left(\frac{x}{c}\right)$	0	−0·018	−0·044	−0·063	−0·078	−0·085	−0·084	−0·077	−0·004
$\frac{1}{(U_1/U)^{3\cdot27}}\int_0^{x/c}\left(\frac{U_1}{U}\right)^{2\cdot27} E_4\, \mathrm{d}\left(\frac{x}{c}\right)$	0	−0·011	−0·023	−0·031	−0·038	−0·041	−0·04	−0·038	−0·002
$\frac{hc}{k}\Big/\sqrt{\left(\frac{Uc}{\nu}\right)}$ 2nd approx.	6·601	2·559	1·694	1·336	1·13	0·995	0·893	0·813	0·738

No further cycles are needed.

* From the front stagnation point relation.

Vol. 3 1961

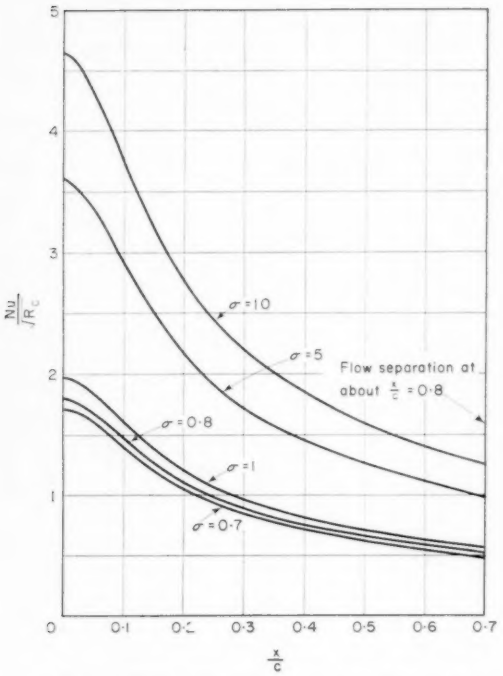

FIG. 3. Distribution of Nusselt number of the surface of a 2:1 ellipse for various Prandtl numbers.

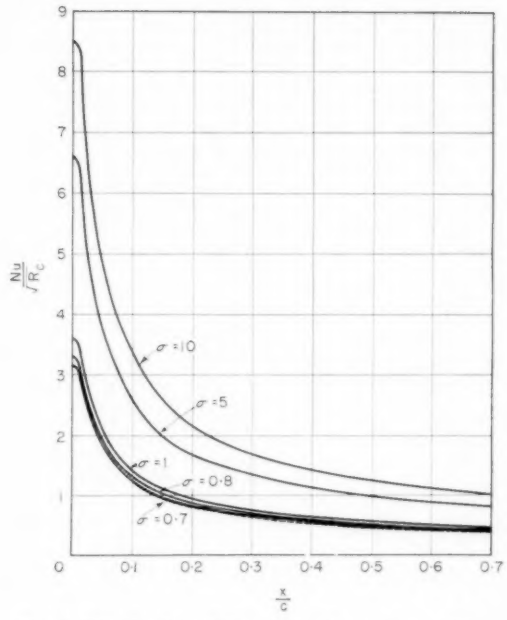

FIG. 4. Distribution of Nusselt number on the surface of a 4:1 ellipse for various Prandtl numbers.

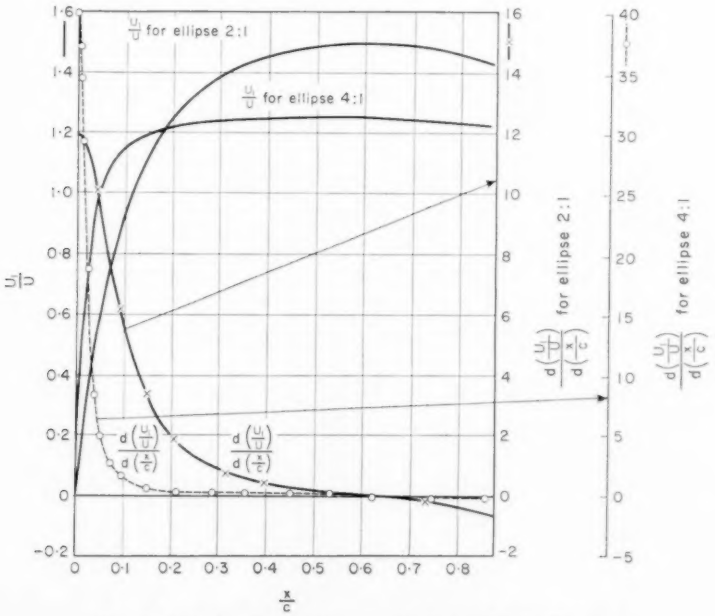

FIG. 5. Velocity distributions on the 2:1 and 4:1 ellipses.

$$\bar{h} = (c/r)\,h \tag{4}$$

$$\bar{U}_1 = U_1. \tag{5}$$

the method given above can be used for axisymmetric flows. Given $U_1(x)$ and $r(x)$, $\bar{U}_1(\bar{x})$ may be tabulated and $\bar{h}$ determined from equations (5) and (6) and hence h.

4. CONCLUSION

The method described and illustrated in detail above, gives a very rapid calculation of heat transfer in the two-dimensional or axisymmetric cases to which it can be applied. It is difficult to assess the accuracy of the calculations: for "wedge" flows the results should be exact, as should those of Eckert. The basis of the present method is in fact simply that on a surface with an arbitrary U_1 distribution, the rate of growth of thermal layer thickness is the same as it would be in a wedge flow with the same thermal thickness, U_1 and $\mathrm{d}U_1/\mathrm{d}x$. The present method is very unlikely to give highly misleading predictions of heat transfer: stagnation point solutions are exact within the usual boundary layer assumptions, and often large portions of subsequent velocity distributions are similar to "wedge" flow distributions. The method should be used with some regard for the velocity-layer phenomena—it would be fortuitous if the method gave accurate results in a region of flow separation, but the authors believe that it can be used with some confidence to near the calculated separation point.

REFERENCES

1. A. G. Smith and D. B. Spalding, Heat transfer in a laminar boundary layer with constant fluid properties and constant wall temperature. *J. Roy. Aero. Soc.* **62**, 60 (1958).
2. N. Frossling, Verdunstung, Wärmeübergang und Geschwindigkeitsverteilung bei zweidimensionaler und rotationssymmetrischer laminarer Grenzschichtströmung. *N.F. Avd.* **2**, 36 (1940).
3. E. R. G. Eckert, Die Berechnung des Wärmeübergangs in der laminaren Grenzschicht umströmter Körper. *Z. Ver. Dtsch. Ing. Forschungsheft* 416 (1942).
4. H. B. Squire, Heat transfer calculations for aerofoils. *Aero. Res. Coun. Lond. R. and M.* 1986 (1942).
5. G. S. Ambrok, Approximate solution of equations for the thermal boundary layer with variation of boundary layer structure. *Soviet Fiz. Tech. Fiz.* **2**, 1979 (1957).
6. H. J. Allen and B. C. Look, A method for calculating heat transfer in the laminar flow region of bodies. *N.A.C.A. Rep.* 764 (1943).
7. C. W. Frick, Jr. and G. B. McCullough, A method for determining the rate of heat transfer from a wing or streamline body. *N.A.C.A. Rep.* 830 (1945).
8. H. Schuh, A new method for calculating laminar heat transfer on cylinders of arbitrary cross-section and on bodies of revolution at constant and variable wall temperature. *K.T.H. Aero T.N.* 33, Stockholm (1953.)
9. W. Mangler, Zusammenhang zwischen ebenen und rotationssymmetrischen Grenzschichten in Kompressiblen Flussigkeiten. *Z. Angew. Math. Mech.* 28 (1948).

Vol. 3 1961

Int. J. Heat Mass Transfer. Vol. 3, pp. 133–154. Pergamon Press 1961. Printed in Great Britain.

INFLUENCE OF TURBULENCE ON THE TRANSFER OF HEAT FROM PLATES WITH AND WITHOUT A PRESSURE GRADIENT

J. KESTIN,* P. F. MAEDER* and H. E. WANG†
Brown University, Providence, R.I., U.S.A.

(*Received* 1 *February* 1961)

Abstract—The work described in this paper is a continuation of that done by Kestin and Maeder on the influence of free-stream turbulence on the coefficient of heat transfer from cylinders in cross-flow. The present work is concerned exclusively with the flat plate and deals at length with the case of zero incidence, i.e. of zero pressure gradient. The effect of adding a favorable pressure gradient was investigated in a preliminary way.

Kestin and Maeder have demonstrated the existence of two effects produced by an increase in the turbulence intensity of the free-stream in the case of cross-flow past a circular cylinder. (1) An increase in turbulence intensity causes earlier transition, and, generally, affects the flow pattern about the body. (2) An increase in turbulence intensity causes *local* changes in the coefficients of heat transfer and, presumably, in the flow pattern in the boundary layer. The existence of the local effect has also been observed by Kestin, Maeder and Sogin, Giedt, Sato and Sage, Sage *et al.*, Seban, and van der Hegge Zijnen.

The present investigation shows that the local effect is completely absent in the case of a flat plate at zero incidence, in good agreement with the work due to Edwards and Furber and Kline *et al.*, but in contradiction to the findings of Sugawara and Sato. This is a remarkable difference between the present case and that of a cylinder. A qualitative explanation of this difference was suggested by Kestin *et al.* The main conclusion reached by them was that large effects from changes in the free-stream turbulence can be produced only in the presence of pressure gradients. This conclusion was tested by imposing a favorable pressure gradient on the plate. It was found that small changes in the turbulence intensity of the free stream cause large changes in the coefficient of heat transfer in the laminar range. Experiments with a pressure gradient were carried out in a preliminary way, and no exhaustive measurements were undertaken at this stage. In particular, the effect on turbulent boundary layers as well as the effect of adverse pressure gradients were not investigated.

The experimental arrangement and the techniques used in measurement are described in detail; the accuracy is carefully examined and detailed check-measurements, in particular, measurements of velocity profiles were undertaken in order carefully to correlate the heat transfer measurements with the different flow regimes which are possible in the boundary layer.

Résumé—Le travail décrit dans cet article fait suite à celui de Kestin et Maeder sur l'influence de la turbulence de l'écoulement libre sur le coefficient de transmission de chaleur de cylindres placés normalement à l'écoulement. Le présent travail concerne exclusivement le cas de la plaque plane et traite en détail le cas de l'incidence nulle, c'est-à-dire du gradient de pression nul. L'effet de l'addition d'un gradient de pression favorable a été étudié de façon préliminaire.

Kestin et Maeder ont démontré, dans le cas de l'écoulement perpendiculaire à un cylindre, que l'augmentation de l'intensité de la turbulence dans l'écoulement libre avait pour effet:

1° d'avancer la transition et de modifier l'écoulement autour du corps;

2° d'affecter localement les coefficients de transmission de chaleur et probablement aussi l'écoulement dans la couche limite. L'existence d'un effet local a également été observé par Kestin, Maeder, Sogin, Giedt, Sato et Sage, Sage et ses collaborateurs, Seban et van der Hegge Zijnen.

La présente recherche montre que l'effet local est inexistant dans le cas d'une plaque plane à incidence nulle. Cette conclusion est en bon accord avec le travail de Edwards, Furber, Kline et ses collaborateurs, mais en contradiction avec les résultats de Sugawara et Sato. C'est une différence

* Professor of Engineering, Brown University, Providence, R.I.

† Formerly Research Assistant, Brown University, now with Systems Research Division, Aerospace Corp., Los Angeles, Calif.

remarquable entre le cas présent et celui du cylindre. Une explication qualitative de cette divergence a été suggérée par Kestin, Maeder et Wang. Leur conclusion principale est que la variation de la turbulence du courant libre n'a d'influence notable que s'il existe des gradients de pression. Cette conclusion a été contrôlée dans le cas de la plaque, en imposant un gradient de pression favorable. On a trouvé que des petites variations de l'intensité de la turbulence entraînaient de grandes variations du coefficient de transmission de chaleur dans la zone laminaire. Les expériences effectuées avec gradient de pression sont préliminaires, aucunes mesures complètes n'ont encore été entreprises à ce stade. En particulier, l'effet sur les couches limites turbulentes aussi bien que l'influence de gradients de pression défavorables n'ont encore été étudiés.

L'appareillage et les techniques utilisés pour les mesures sont décrits en détail; la précision est étudiée avec soin et les mesures de contrôle bien détaillées, en particulier, les mesures des profils de vitesse ont été effectuées pour les comparer aux mesures de transmission de chaleur pour les différents régimes d'écoulement dans la couche limite.

Zusammenfassung—Die Arbeit von Kestin und Maeder über den Einfluss der Freistromturbulenz auf den Wärmeübergangskoeffizienten bei Zylindern im Querstrom wird hier fortgesetzt für die ebene Platte im Fall der Null-Inzidenz d.h. für einen Druckgradienten von Null. In vorläufigen Versuchen wird der Einfluss günstiger Druckgradienten untersucht. Beim querangeströmten Kreiszylinder haben Kestin und Maeder zwei Effekte nachgewiesen, die von einer Erhöhung der Turbulenzintensität des Anblasstromes stammen. (1) Die Erhöhung der Turbulenzintensität verursacht einen vorzeitigeren Umschlag und beeinflusst ganz allgemein das Strömungsbild in der Umgebung des Körpers. (2) Die Erhöhung der Turbulenzintensität bedingt örtliche Veränderungen des Wärmeübergangskoeffizienten und wahrscheinlich auch des Strömungsbildes in der Grenzschicht. Diesen lokalen Effekt stellen auch Kestin, Maeder und Sogin, Giedt, Sato und Sage, Sage und andere, Seban und van der Hegge Zijnen fest.

Die vorliegende Untersuchung zeigt, dass ein lokaler Effekt bei der ebenen Platte vollkommen fehlt, was mit der Arbeit von Edwards und Furber und Kline und andere übereinstimmt, jedoch den Ermittlungen von Sugawara und Sato widerspricht. Dies bedeutet eine bemerkenswerte Abweichung des hier behandelten Falles vom Zylinder. Eine qualtitative Erklärung der Verschiedenheit geben Kestin, Maeder und Wang. Ihre Schlussfolgerung besagt, dass grosse Effekte durch Änderung der Freistromturbulenz nur in Gegenwart von Druckgradienten hervorgerufen werden können. Dies wurde mit Hilfe eines günstig gewählten Drucksgradienten an der Platte geprüft. Es ergab sich, dass kleine Änderungen der Turbulenzintensität des Freistromes grosse Änderungen des Wärmeübergangskoeffizienten im laminaren Bereich hervorrufen. Die Versuche mit dem Druckgradienten waren nur vorläufiger Art, es wurden noch keine eingehenden Messungen durchgeführt. Insbesondere ist noch nicht der Einfluss auf turbulente Grenzschichten und der Effekt weniger günstiger Druckgradienten untersucht.

Die Versuchseinrichtung und die Messmethode werden im Einzelnen beschrieben. Eingehende Kontrollmessungen sorgten für gute Genauigkeit. Besonders exakt wurden die Geschwindigkeitsprofile ermittelt, um die Wärmeübergangsmessungen mit den verschiedenen, in der Grenzschicht möglichen Strömungsarten in Beziehung setzen zu können.

Аннотация—Материалы, изложенные в настоящей статье, являются продолжением работы, проделанной Кестиным и Мидером по вопросу о влиянии турбулентности набегающего потока на коэффициент теплоотдачи цилиндров. В данной работе приведены результаты исследования теплоотдачи плоской пластины при условии, когда угол атаки равен нулю. В этом случае градиент давления равен нулю. Влияние величины градиента давления исследовалось отдельно.

Кестин и Мидер показали существование двух эффектов, которые возникают в результате повышения интенсивности турбулентности набегающего потока для случая, когда цилиндр расположен поперёк. (1) Повышение интенсивности турбулентности вызывает более ранний переход и, вообще, влияет на структуру потока над телом. (2) Повышение интенсивности турбулентности вызывает локальные изменения в коэффициентах теплообмена, повидимому, в структуре потока в пограничном слое. Это также наблюдали Кестин, Мидер и Зогин, Гидт, Сато и Саге, Саге и другие, Себан и Ван дер Хегге Цинен.

Настоящее исследование показывает хорошее совпадение с данными, приведенными в работах Эдвардса, Фурбера, Клайна и др., но противоречит данным, опубликованным в работах Сагавара и Сато, для случая плоской пластины с углом атаки равным нулю при полном отсутствии локального эффекта. В этом заключается существенное различие между настоящим случаем и случаем с цилиндром. Качественное объяснение этого различия было предложено Кестиным, Мидером и Уэнгом. Основной вывод, к которому

Vol. 3 1961

они пришли, заключается в следующем: большие эффекты, возникающие при изменении турбулентности набегающего потока, могут иметь место только при наличии градиентов давления. Этот вывод проверялся путём введения подходящего градиента давления. Было найдено, что небольшие изменения в интенсивности турбулентности набегающего потока вызывают большие изменения в коэффициенте теплообмена в ламинарной области. Опыты с градиентом давления проводились приближённым методом, а тщательные измерения не проводились на этом этапе. В частности, влияние на турбулентные пограничные слои, а также влияние неблагоприятных градиентов давления, не исследовалось.

В статье дано детальное описание экспериментальной установки. Точность её проверена, и, в частности, были проведены особо точные измерения профилей скорости для корреляции теплообмена с различными режимами, которые могут иметь место в пограничном слое.

LIST OF SYMBOLS

A, area of heater;
b, half-width of heater;
C, numerical factor in equation (31);
C_1, numerical factor in equation (10);
C_2, numerical factor in equation (12);
C_b, Stefan–Boltzmann radiation constant;
C_f, coefficient of skin friction;
f, correction factor, equation (27);
I, current flowing through heater;
k, thermal conductivity (average);
k_T, thermal conductivity (at temperature T);
L, length of plate;
Nu, Nusselt number (based on length co-ordinate for plate);
P_{atm}, atmospheric pressure;
P_r, radiation correction;
P_s, static pressure;
$P_{s\infty}$, static pressure in free stream;
P_t, total pressure;
q_∞, dynamic pressure in free stream;
Re, Reynolds numbers (based on length co-ordinate for plate);
r, pressure ratio, equation (3);
T, temperature;
T_a, air temperature;
$T_{a\infty}$, air temperature in free stream;
T_w, wall temperature;
ΔT, temperature difference ($=T_w - T_{a\infty}$);
Tu, intensity of turbulence (based on longitudinal oscillating component);
U_∞, free stream velocity;
u, longitudinal velocity component in boundary layer;
u', longitudinal fluctuating velocity component;
V, voltage across heater;
x, co-ordinate along plate in flow direction;
y, co-ordinate normal to plate.

Greek symbols

α, coefficient of heat transfer (mean value over heater);
α_1, coefficient of heat transfer (at centerline of heater);
Δ, dimensionless pressure gradient, equation (4);
δ, boundary layer thickness (calculated);
δ_m, boundary layer thickness (measured at $u/U_\infty = 0{\cdot}99$);
ϵ, emissivity;
ν, kinematic viscosity (average);
ν_T, kinematic viscosity (at temperature T);
ρ_∞, density in free stream.

1. INTRODUCTION AND RELATED WORK

IT HAS been known for some time that many experiments on forced convection show considerable, and inexplicable discrepancies in their results. It was suspected that some unknown factors must have been left out of account, in particular, the effect of the turbulence intensity of the free stream.

The present investigation is a continuation of that due to Kestin and Maeder [1] who gave an extensive discussion on the subject and reported experimental results on the overall coefficient of heat transfer from an "infinite" circular cylinder in cross-flow. The experiments showed unexpectedly large increases in the mean Nusselt number; for example, at a mean Reynolds number of 180 000, an increase in the mean Nusselt number of 14·3 per cent was observed for a change of turbulence intensity from 0·75 to 2·60 per cent only.

It is clear that the mean Nusselt number must be affected indirectly by the shifts of the points of transition and separation caused by different turbulence intensities in the free stream. However, by the use of tripping wires, these authors

demonstrated conclusively that, in addition, there exists a local effect. In other words, having fixed the flow pattern in the boundary layer about a cylinder by the use of tripping wires, and having made it insensitive to changes in turbulence intensity, these authors found that, nevertheless, small changes in turbulence intensity still caused large changes in the Nusselt number. For example, again at a mean Reynolds number of 180 000, the mean Nusselt number increased by 26 per cent when the intensity of turbulence was varied from 0·75 to 2·66 per cent.

This local effect was subsequently measured directly by Kestin *et al.* [2]. It was also noted in the earlier work by Giedt [3, 4], Sato and Sage [5] as well as in the subsequent work due to Sage *et al.* [6, 7], Seban [8] and van der Hegge Zijnen [9].

The case of a flat plate was studied by Edwards and Furber [10] who have undertaken experiments to determine the influence of the free-stream turbulence on the *mean* coefficient of heat transfer from a flat plate provided with a round nose of very small radius. Two screens were used to promote turbulence intensities of 1·5 and 2·5 per cent, but these values were estimated rather than measured directly. The investigation led to the conclusion that changes in the intensity of turbulence of the external stream had no influence on the rate of heat transfer across a laminar or a turbulent boundary layer except insofar that a higher intensity promoted transition at a lower Reynolds number. This showed the existence of an important difference between the flat plate at zero incidence and cylinders or spheres. The present investigation was conducted to confirm this result and to elucidate the reasons for such a fundamental divergence of behavior.

At an earlier time, Fage and Falkner [11] had performed experiments on a thin, electrically heated platinum foil and found no influence of the free-stream turbulence on the mean coefficient of heat transfer in the laminar regime to which their measurements were confined.

The local coefficient of heat transfer from a flat plate to a turbulent air stream was measured by Sugawara and Sato [12] who employed a non-steady method. Their measurements showed no effect in the laminar region for intensities up to 1 per cent, in agreement with Edwards and Furber. However, in the turbulent range they measured large increases in the Nusselt number. In contradiction to Edwards and Furber, they measured increases of up to 55 per cent in the Nusselt number for a variation in turbulence intensity from 1·0 to 8·0 per cent. We shall revert to these measurements in section 7.

Finally, Reynolds *et al.* [13] made measurements on a flat plate in the presence of a turbulent boundary layer. The measurements were made in a tunnel of relatively high intensity of turbulence (1·5 to 5·0 per cent) and it was found that irrespectively of the level of turbulence, the Nusselt numbers satisfied von Kármán's equation (see equation (36) later) with an accuracy of $\pm 4{\cdot}5$ per cent, i.e. with an accuracy of the order of their experimental error. These results can be interpreted as a confirmation of the findings due to Edwards and Furber. In addition to measuring rates of heat transfer, Reynolds *et al.* verified that the coefficient of skin friction was independent of the intensity of turbulence and agreed well with Schultz-Grunow's formula

$$\tfrac{1}{2}C_f = 1{\cdot}60\,(\ln Re)^{-2{\cdot}58}. \qquad (1)$$

The relation of the latter measurement to the former will be appreciated if it is remembered that in incompressible flow, the velocity field is independent of the temperature field, but the temperature field is solely determined by the velocity field and the boundary conditions. Consequently, any changes in the temperature profiles must be preceded by changes in the velocity profiles, although the two effects may be of different orders of magnitude.

2. STATEMENT OF PROBLEM

From what has been said in the preceding section, it is clear that the investigation of the following two problems would be both important and interesting. *First*, enough doubt existed about the effect of turbulence intensity on the rate of heat transfer from a flat plate at zero incidence to warrant new measurements. It was also clear that *local* measurements would be the most conclusive.

Secondly, as it turned out, no effect other than a change in the transition Reynolds number was

Vol. 3 1961

found, in full agreement with Edwards and Furber, and it became important to investigate the reasons for the fundamental difference in the behavior of flows past flat plates and those past cylinders or spheres. The difference in the flows passing over a cylinder and flat plate is the magnitude of the pressure gradient in the flow direction. At the forward portion of a cylinder or sphere there exists a strong favorable pressure gradient which is absent on a flat plate at zero incidence. Consequently, measurements were made on a flat plate with a positive pressure gradient imposed on it. Provisionally, and for the present, these measurements were confined to the laminar range only. This limitation was unavoidable, because a positive pressure gradient stabilizes the flow, and transition to a turbulent boundary layer could not be obtained with the present combination of tunnel speed and plate length.

A qualitative explanation of the part played by pressure gradients in the presence of free-stream oscillations was given by the present authors elsewhere [14]. It was shown that if free-stream oscillations are to produce an effective change in the boundary layer, the amplitude of the oscillation must be large, and must vary strongly in the main flow direction. As is known from numerous experiments, for example from the recent work by Crocker *et al.* [15], the amplitude of the oscillations in the free-stream is strongly affected by pressure gradients, particularly near a stagnation point.

In anticipation, it can be stated here that measurements on a flat plate with a pressure gradient imposed on it confirmed this hypothesis.

3. EXPERIMENTAL ARRANGEMENT

The measurements were carried out in the 22 in × 32 in Brown University low-speed tunnel described elsewhere [1]. The flat plate was placed vertically in the center-line of the tunnel. The local rate of heat transfer was measured electrically with the aid of two unit heaters at two positions along the plate. The combination of two heaters and variable wind velocity made it possible to cover a range of length Reynolds number from $Re = 35\,000$ to $Re = 600\,000$.

The unit heaters, exposing areas of 10 in × $\frac{1}{2}$ in to the air stream, were attached to the plate but insulated from it and heated electrically, the input into them being carefully metered. The flat plate was heated by steam which jacketed the unit heaters. The surface of the plate and the exposed surface of the heaters were maintained at a constant temperature thus eliminating all transfer of heat sideways. All temperatures were measured by copper–constantan thermocouples.

The turbulence intensity was increased by inserting a screen in the tunnel test-section upstream from the leading edge of the flat plate. The turbulence intensity was measured by a hot-wire anemometer and varied from 0·7 to 3·8 per cent. The scale of turbulence was not measured in the present experiment.

The pressure gradient along the flat plate and the velocity profiles of the boundary layers were measured with standard probes.

(a) *The flat plate*

A schematic diagram of the plate is shown in Fig. 1. The flat plate, 2 in thick, $20\frac{11}{16}$ in wide and $23\frac{25}{32}$ in high, consisted of a brass flat surface P, $\frac{1}{4}$ in thick and a brass cover B, $\frac{1}{16}$ in thick. The nose of the leading edge was round and had a radius of $\frac{1}{16}$ in. The brass cover joined the flat surface at $\frac{1}{2}$ in from the leading edge and right at the trailing edge through curved portions. Two end-pieces E, one on the top and one on the bottom, with taps of $1\frac{5}{32}$ in diameter were provided for circulating saturated steam to maintain a constant surface temperature on the plate. The jacket steam was obtained from a small laboratory boiler which was also described in Ref. 1. On the flat surface, two slots, each of 10·1 in × 0·6 in, were provided to accommodate the unit heaters a and b. The slots were about 6 in from the top and bottom walls of the tunnel test-section, thus eliminating any influence of the walls on the measurement of heat transfer. The first slot was $7\frac{3}{32}$ in from the leading edge and the second, $13\frac{19}{32}$ in from it. The design of the plate is shown in somewhat greater detail in Fig. 2.

The plate, owing to its 2 in thickness and the curved portions, aerodynamically formed an unsymmetrical wing section; the flow pattern over it was different from that over a "flat"

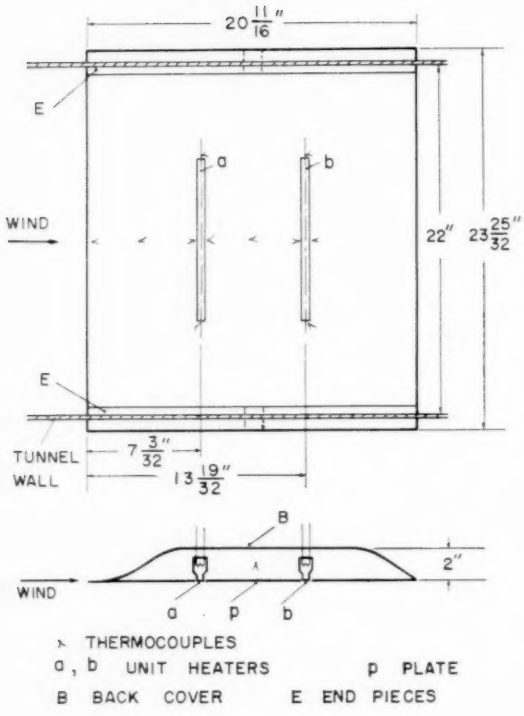

FIG. 1. Schematic drawing of flat plate.

plate at zero incidence and thickness. At the initial stage of the experiments, it was found that the flow separated at the leading edge and the pressure gradient along the plate was not negligible. In order to reproduce the flow pattern of a flat plate at zero incidence more precisely, two dividing plates P and B were provided, one upstream and one downstream, Fig. 3. The boundary layer formed on the front dividing plate was sucked away to the back of the plate through the suction slot. The pressure difference required for the suction was provided by four control louvers L mounted at the exit of the tunnel test-section. The control louvers were made of thin aluminium plates assembled in the form of a venetian blind and placed at approximately 40° to the direction of the flow as shown in Fig. 3. The front dividing plate was made of aluminum, $\frac{3}{8}$ in thick and 12 in wide and had a round nose and tapered trailing edge. The back dividing plate was made of wood, $\frac{3}{8}$ in $\times$ 9 in. With such an arrangement, a flat-plate flow pattern was successfully produced.

(b) *The unit heater*

The unit heater is first shown schematically in Fig. 4 and then in detail in Fig. 5. The heater was essentially a miniature boiler filled with saturated water and steam. It was made of copper and the heat-transferring surface e was 10 in $\times$ $\frac{1}{2}$ in. The heating element h was of the immersion type and had a rating of 30 W. During experiments the heating element was always kept immersed in water to prevent overheating. A baffle b was provided to cause circulation of the saturated water and steam inside the heater so that the surface temperature could be maintained uniform. The unit was charged with water from the bottom and the amount of water inside the heater could be examined by a gage m outside. Both the water inlet and the steam vent were provided with stop valves S which served to isolate the system during the experiments. The temperature of the steam inside the heater was measured by a thermocouple and the rate of heating was adjusted to provide a temperature equal to that of the jacket steam in the plate. Owing to the equal steam temperatures and to the provision of an insulating cover in the back of the heater, heat exchange between the heater and the jacket steam in the plate was reduced to

Vol. 3 1961

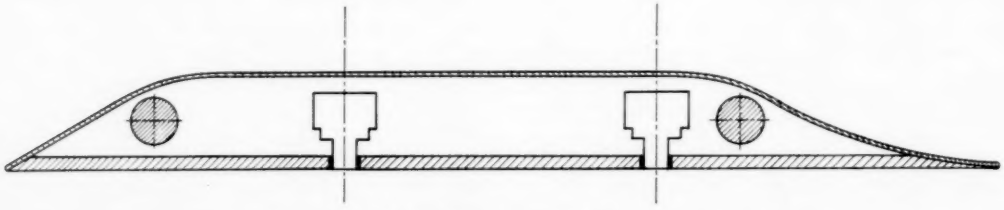

FIG. 2. Design drawing of flat plate.

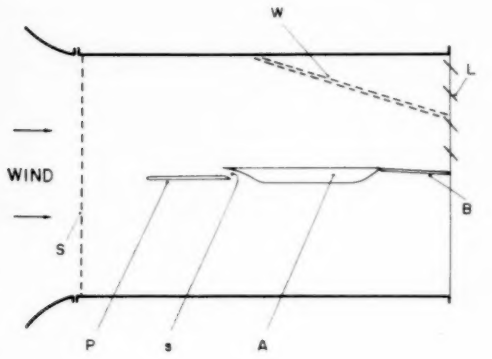

A FLAT PLATE
B BACK DIVIDING PLATE
P FRONT DIVIDING PLATE
W PLATE TO PROVIDE LARGE PRESSURE GRADIENT
S SCREEN
s SUCTION SLOT
L LOUVERS

FIG. 3. Arrangement of plate in tunnel.

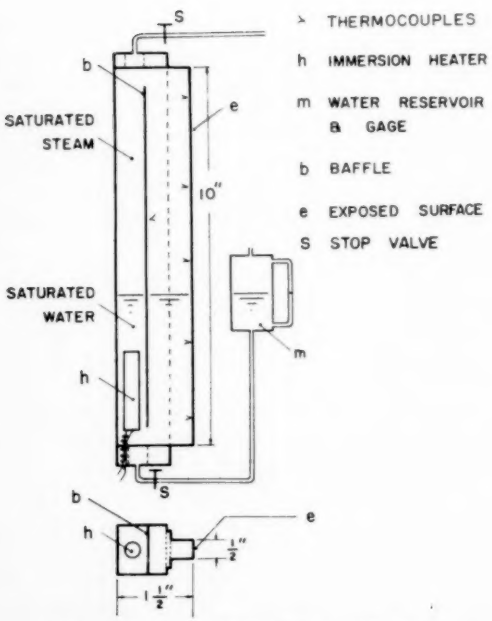

THERMOCOUPLES
h IMMERSION HEATER
m WATER RESERVOIR
B GAGE
b BAFFLE
e EXPOSED SURFACE
S STOP VALVE

FIG. 4. Schematic drawing of unit heater.

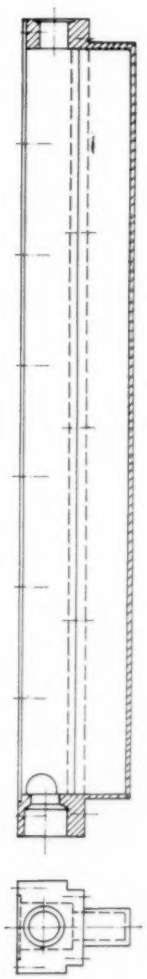

FIG. 5. Design drawing of unit heater.

a minimum. Therefore practically all of the electrical energy input into the heater was transferred through the exposed surface.

The unit heater was attached to the plate in such a way that its exposed surface was flush with that of the main plate at all temperatures. This was achieved by providing compensation for the different coefficients of linear thermal expansion of copper (heater) and brass (plate). The method of compensation can be best explained with reference to Fig. 6. It is seen from Fig. 6 that the unit heater e is attached to

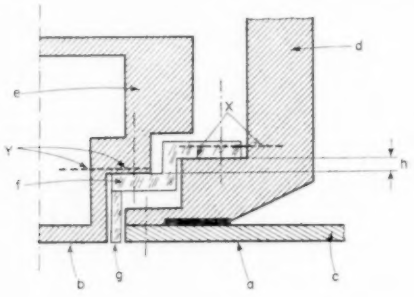

FIG. 6. Method of compensation for thermal expansion.

its cover d through a Teflon bridge f; and the cover is screwed to the plate c. When the arrangement was assembled at room temperature, the exposed surface b of the heater was made flush with the plate surface a and the contact surface X was higher than the contact surface Y by an amount h. At higher temperatures all parts would expand. Taking surfaces a and b as reference, surfaces X and Y would move backwards and reach a position shown by the dotted lines, say. If without the Teflon bridge, the heater would be a separate unit and surface X would recede more than surface Y would, because the main plate would expand more due to the fact that the coefficient of thermal expansion of brass (plate) is higher than that of copper (heater). The difference was compensated by the expansion of the Teflon bridge through the length h. The value of the length h was estimated and found to be fairly small.

The gap g between the heater and the plate was also filled with Teflon. Being an insulating material, the Teflon insert cut down the amount of heat conduction sideways, thus eliminating the complication of correcting for it when a mean area was taken for the evaluation of the Nusselt number.

It must be remarked here that the excellent experimental results obtained, as will be seen later, were due in great measure to the successful design of the heater.

(c) *Power-input measurement*

The electrical power-input to the heaters was supplied from a 230-V a.c.–d.c. converter set. The undesirably large voltage fluctuations were screened out by a voltage stabilizer which was described in detail in Ref. 1. The d.c. output from the stabilizer was constant to within 0·1 per cent.

The measuring circuit was also the same as in the Ref. 1, where it was shown that the rate of heat transfer could be measured with an accuracy of 0·3 per cent.

(d) *Temperature measurement*

All temperatures were measured by 0·005 in diameter copper and constantan thermocouples. Before setting-up, one piece of the thermocouple wire was calibrated with the aid of a high-precision potentiometer and with reference to two precision, etched-stem, mercury-in-glass thermometers provided with Bureau of Standards certificates. The accuracy of the calibration was to 0·005°C in the room-temperature range and to 0·01°C near the steam point.

The temperature of the plate surface was measured at eleven positions and that of each heater surface at five positions as shown in Figs. 1 and 4 respectively. The thermocouples used to measure the temperature of the plate surface were attached to the plate in the following way (see also Ref. 1). The bared ends of the copper and constantan wires were soldered into two very fine holes drilled in the plate. The two holes were very close to each other so that the two wires could be considered being soldered together. The thermocouples to measure the temperature of the heater surface were attached to the heater in the same way except that only

Vol. 3 1961

the constantan wires were soldered to it; the heater, being made of copper, served as the other wire.

Thermocouples to measure the jacket steam temperature and the temperature of the steam in each heater were also provided. The air temperature was deduced from the measurement of the stagnation temperature in the settling chamber of the wind tunnel.

All temperatures, except the air temperature, were measured relative to the jacket steam in the plate and the e.m.f. of the thermocouples was registered by a potentiometer recorder using a scale of 1 mV to 25 cm; in other words, differential measurements were made. Since all these temperatures were only slightly different from the jacket steam temperature a differential measurement was found very convenient and accurate.

The temperature of the jacket steam in the plate and the stagnation air temperature were measured independently by a portable potentiometer.

Owing to the successful design, the heaters had a surface temperature constant to within $\pm 0{\cdot}2°C$ in most runs. In one or two runs at high speeds it rose to $\pm 0{\cdot}5°C$. The plate surface temperature was maintained constant to within $\pm 0{\cdot}5°C$ at all positions except near the leading edge. Owing to the wedge-like shape of the leading edge where the heat transfer is extremely high, the supply of the jacket steam in the plate was insufficient to compensate for the cooling effect of the air-stream. Consequently the plate temperature near the leading edge varied from 92·6°C at the lowest speed to 67·3°C at the highest speed while the rest of the plate was always at nearly 100°C. The variation of the leading-edge temperature with the air speed is shown in Fig. 7. This was unavoidable and not very serious because the second thermocouple from the leading edge, $3\frac{1}{2}$ in away from it, already registered the normal plate temperature in all test runs. In view of the design of the leading edge, it was reasonable to assume a constant temperature, the value measured by the first thermocouple, $\frac{3}{4}$ in away from the leading edge, over a length of $1\frac{1}{2}$ in and then the normal plate temperature for the rest of the plate. The sudden jump, i.e. the discontinuity in temperature was assumed to occur at $x = 1{\cdot}5$ in. The rate of heat transfer was then corrected to the isothermal condition in the calculations of the Nusselt number according to the methods due to Eckert and Drake [16] and Rubesin [17]. The correction, as given in section 6, was only of the order of 5 per cent.

The heater surface temperature also differed somewhat from the plate surface temperature. In this case, however, the difference was only 1°C in most runs and rose to 3°C in a few runs at high speeds. Corrections were also applied by

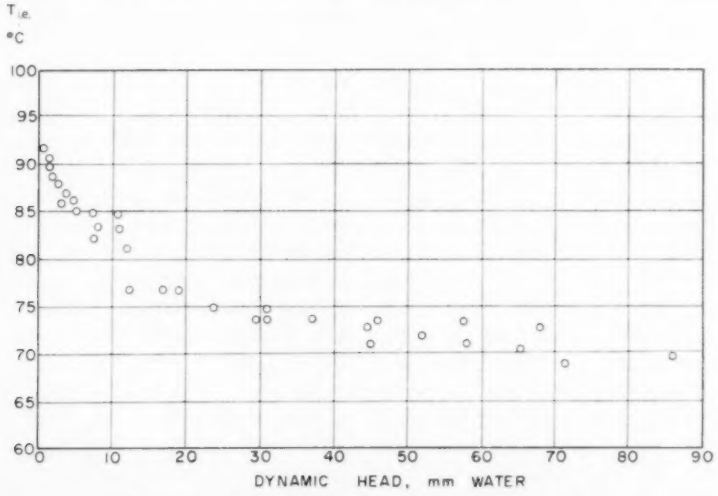

FIG. 7. Variation of temperature near leading edge.

the use of the same methods; the corrections turned out to be less than 1·5 per cent in all runs.

(e) *Measurement of turbulence intensity*

The turbulence intensity,

$$Tu = (\overline{u'^2})^{1/2}/U_\infty \qquad (2)$$

was measured by a hot-wire anemometer. All measurements were made at exactly the same flow conditions as in the heat transfer measurements but only after the latter had all been finished. It was done in such an order solely on the ground of convenience in practical operation.

In each measurement the probe (wire 0·00015 in in diameter) was placed opposite the heater at a distance of approximately 1·5 in from the surface of the plate, i.e. outside the boundary layer (the boundary layer thickness being of the order of 0·25 in). The turbulence intensity in the present wind tunnel remained approximately uniform for a given air speed throughout the entire test-section when it was clear. The uniformity was checked when the whole set-up was present in the test-section. Thus all the measurements were made in the presence of the flat plate and the dividing plates.

It was mentioned before that higher turbulence intensities were produced by placing a screen upstream of the plate. The screen S was of $\frac{3}{4}$ in mesh, 0·148 in diameter and placed 18·5 in upstream from the leading edge of the plate, as shown in Fig. 3. It is well known, e.g. as shown by Dryden *et al.* [18], that the turbulence intensity decreases in the downstream direction behind such a screen. They also found a perfect correlation between the local turbulence intensity and the screen-mesh length, Z/M, where Z is the distance downstream from the screen and M is the mesh size. Thus the value of the turbulence intensity at any position would be sufficient to determine the whole turbulence field. It is in the light of this fact that in the present experiments, when the turbulence screen was used, the turbulence intensity was also measured at one position only, i.e. opposite each heater and 1·5 in away from the flat plate. The measurements were also made when the flat plate and the dividing plates were present in the tunnel test-section.

As illustrated in Fig. 5 of Ref. 1, there were three fine screens in the settling chamber of the wind tunnel to equalize turbulence fluctuations. In the present experiments, one more fine screen was added at the entrance of the tunnel to reduce the amount of dust in the air before entering it. Moreover, all these screens were vacuum-cleaned at frequent intervals in order to gain a better control of the turbulence intensity and in order to prevent the hot-wire probes from becoming contaminated.

The accuracy of the turbulence measurements was believed to be well within 5 per cent.

4. AUXILIARY MEASUREMENTS

In addition to the measurements of the rate of heat transfer and temperature difference, it was necessary to perform measurements of the velocity profile in the boundary layer as well as to ascertain the deviation of the actual flow from the ideal flow as regards to the pressure gradient.

The static pressure in the free stream was investigated first. A standard static-pressure tube was employed. The static pressure in the transverse direction, i.e. normal to the flat plate, was found constant to within 0·5 per cent for all speeds with and without the turbulence screen. In the longitudinal direction, i.e. in the main stream direction, the static pressure varied slightly. The variation is shown in Fig. 8 in which the pressure ratio,

$$r = (P_s - P_{\text{atm}})/(P_t - P_{\text{atm}}) \qquad (3)$$

is drawn in terms of x, the distance from the leading edge. Here P_s P_t and P_{atm} denote the total, static and atmospheric pressures respectively. It is seen from Fig. 8 that the static pressure is highest near the leading edge. However, the maximum difference in the ratio r is only 0·025 over the entire length of the plate, which is considered negligible.

The static pressure on the surface of the plate was measured with the aid of three pressure taps, one near the leading edge, one between the two heaters and one near the trailing edge. The values of the ratio r for these measurements can also be seen in Fig. 8. They show a similar trend as that in the main stream, except near the

Vol. 3 1961

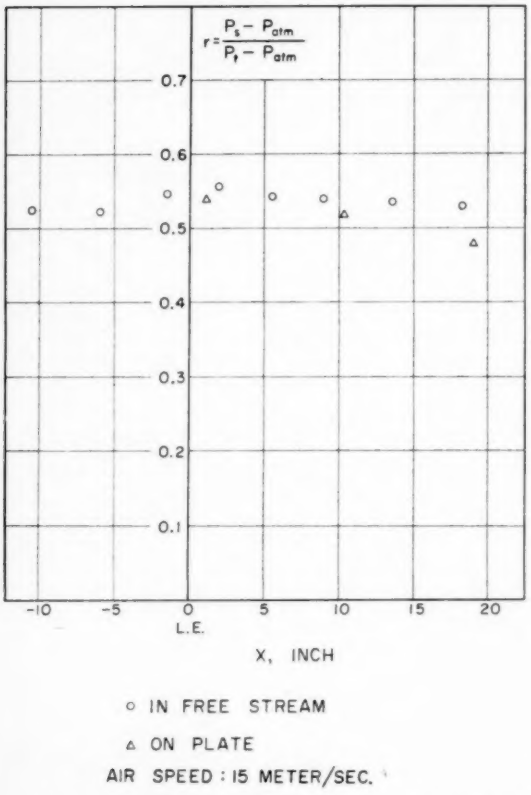

FIG. 8. Variation of static pressure; case of negligible pressure gradient.

trailing edge. The difference in the ratio r over the entire length of the plate is 0·06.

The pressure gradient can best be expressed by the following dimensionless quantity:

$$\Delta = \frac{L}{\frac{1}{2}\rho_\infty U_\infty} \cdot \frac{dP_s}{dx} \tag{4}$$

where L denotes the length of the plate, ρ_∞, the density of air in the free stream, and U_∞ is the free-stream velocity. In view of the fact that the pressure varies almost linearly with the distance from the leading edge, the pressure gradient can be assumed constant. Then the value of the quantity Δ is 0·056 in the free stream and 0·106 on the surface of the plate and it is independent of the air speed. It is noted from Fig. 8 that the static pressure also varies slightly across the

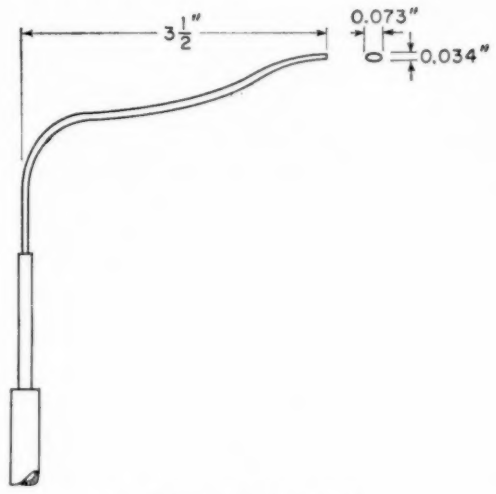

FIG. 9. Boundary layer probe.

boundary layer. The difference, however, is so small that it will be considered consistent with the boundary layer approximations to neglect it.

The velocity profile of the boundary layer was measured by a total-pressure probe with a rectangular face of 0·034 in × 0·073 in (Fig. 9). The probe was screwed to one end of a long stem which was fixed to a traversing mechanism. The traversing mechanism could be moved by a micrometer screw provided with a graduated head. In such a manner the distance of the probe from the flat plate could be determined to within 0·001 in.

The static pressure at each position in the boundary layer was not measured. In calculating the velocity profile, the static pressure measured at 1 in from the flat plate was used because the static pressure was approximately constant across the boundary layer.

The velocity profile and the heat transfer measurements were made immediately one after the other, in other words, the profiles were taken when the flat plate was hot. One profile was taken for each heat transfer determination. A typical laminar velocity profile is shown in Fig. 10(a), and a typical turbulent one, in Fig. 10(b). In Fig. 10(a), the profile is shown by a plot of u/U_∞ in terms of the Blasius parameter,

$$\eta = y(U_\infty/\nu x)^{1/2}, \tag{5}$$

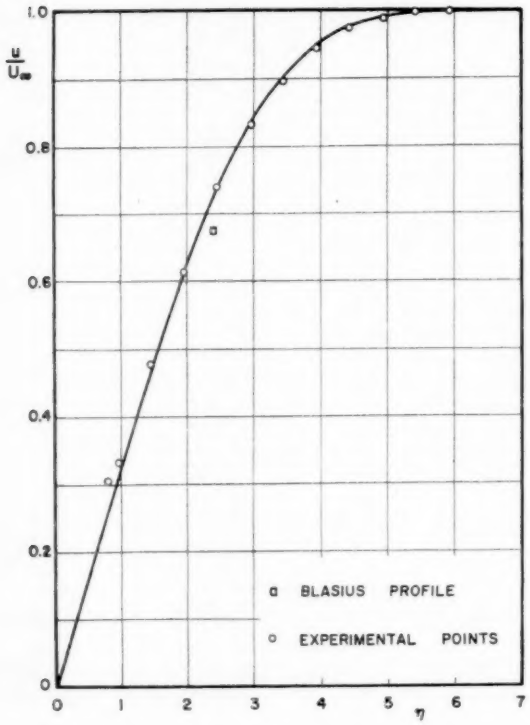

FIG. 10(a) Typical laminar velocity profile (hot)
$Re = 123\,000$ $Tu = 1{\cdot}0$ per cent.

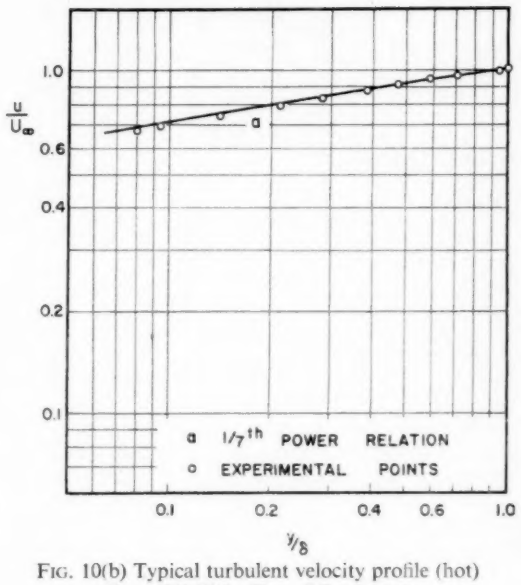

FIG. 10(b) Typical turbulent velocity profile (hot)
$Re = 289\,000$ $Tu = 3{\cdot}7$ per cent.

Vol. 3 1961

u being the velocity at distance y from the flat plate with ν denoting the mean value of the kinematic viscosity of air. It is seen that the velocity closely approximates a Blasius profile.

In Fig. 10(b), a turbulent velocity profile is shown by plotting u/U_∞ in terms of y/δ_m in logarithmic co-ordinates; here δ_m is the measured boundary layer thickness taken at the $u/U_\infty =$ 99 per cent position. The shape of the profile agrees very well with the 1/7th power relation. In most runs in the turbulent region, the calculated boundary layer thickness,

$$\delta = 0{\cdot}37\, x(U_\infty x/\nu)^{-0{\cdot}2}, \qquad (6)$$

agrees with the measured one.

In order to gain a better idea of the character of the boundary layers over the entire range of Reynolds numbers, six measurements of u/U_∞ are shown in terms of y/δ_m in Fig. 11 for six

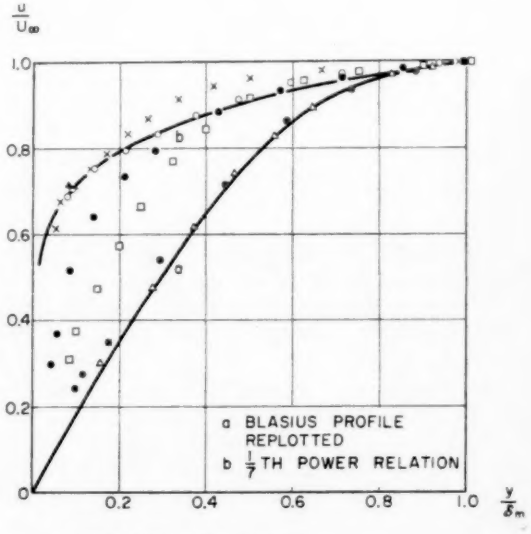

FIG. 11. Velocity profiles in boundary layer.

Reynolds numbers. In Fig. 11, curve a is the Blasius profile replotted, taking

$$\delta = 5{\cdot}0(\nu x/U_\infty)^{1/2} \tag{7}$$

as the boundary layer thickness and curve b is the 1/7th power relation. The character of the three regimes, laminar, transition and turbulent is clearly demonstrated. Edwards and Furber gave a similar illustration except that they used the cubic parabolic approximation for the Blasius profile. It may be remarked here that the cubic parabolic profile would lie slightly below the curve a in Fig. 11.

It is well known that transition from laminar to turbulent flow in the boundary layer can be clearly distinguished by a sudden and large increase in the boundary layer thickness. The dimensionless boundary layer thickness,

$$\delta(U_\infty/\nu x)^{1/2}, \tag{8}$$

is constant for laminar flow and the constant is approximately equal to 5, as can be seen from equation (7). Hansen [19] measured the boundary layer thickness along a flat plate in parallel flow at zero incidence, and found that the sudden change occurs at a Reynolds number,

$$U_\infty x/\nu = 320\,000. \tag{9}$$

His graph is reproduced in Fig. 12 which also contains the present results. It is seen that in the present experiment, the transition occurs at lower Reynolds numbers. This is evidently an influence of the free-stream turbulence.

In all the velocity profile explorations, the distance from the flat plate was always measured at the geometric center of the probe. It was shown experimentally by Young and Mass [20] that a displacement is associated with the geometric center of the face of the probe in measuring the total pressure in a region with transverse total-pressure gradient, such as in the boundary layer. A successful correction factor was reported for circular-faced probes but no reliable information was obtained for rectangular shapes. At any rate, applying such a displacement correction for the probe changes the shape of the profile only slightly, leaving its main character unaffected.

In addition to the displacement correction of the geometric center, MacMillan [21] also

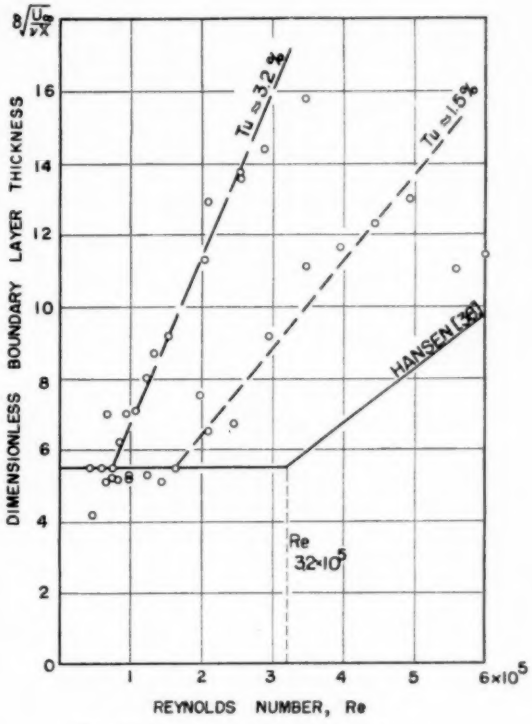

FIG. 12. Transition Reynolds numbers.

experimented on the wall effect when the total pressure at positions very close to a wall was to be taken. He also found a reliable correction for u/U_∞, but the correction was so small in the present case that it was entirely neglected.

It is thus believed that the uncorrected velocity profiles as presented in Figs. 10(a), (b) and 11 provide a fundamentally justifiable basis for the determination of the character of the boundary layers present in each case.

Velocity profiles were also measured for four Reynolds numbers when the flat plate was cold; no difference was found between them and those measured when the plate was hot if the kinematic viscosity of air was taken at the free-stream temperature.

5. EVALUATION OF RESULTS

The free-stream velocity U_∞, in m/s, was calculated by the following formula:

$$U_\infty = C_1(q_\infty/\rho_\infty)^{1/2} \tag{10}$$

where q_∞ denotes the dynamic head in mm H_2O, ρ_∞ denotes the density of air in kg/m³ and the constant C_1 is a conversion factor which has a value of

$$C_1 = 4{\cdot}3897 \text{ kg}^{1/2}/\text{m}^{1/2}\text{ s (mmH}_2\text{O)}^{1/2}. \quad (11)$$

The density ρ_∞, in kg/m³, was calculated from

$$\rho_\infty = C_2 \times (P_{s\infty}/T_{a\infty}), \quad (12)$$

where $P_{s\infty}$ denotes the static pressure in mm Hg, $T_{a\infty}$ denotes the air temperature in °K and the constant C_2 equals to

$$C_2 = 0{\cdot}46447 \text{ (kg °K)/m}^3\text{ (mmHg)}. \quad (13)$$

The Reynolds and Nusselt numbers were calculated in the following way. It is recalled that in order to justify the assumption of incompressibility, the difference between the surface temperature T_w and the free-stream air temperature $T_{a\infty}$ must be made small compared with the absolute temperature of the flow field, so that

$$(T_w - T_{a\infty})/T_{a\infty} \to 0. \quad (14)$$

When the surface temperature is different from the free-stream air temperature, there must be a variation in the fluid properties appearing in the Nusselt and Reynolds numbers. If the temperature difference is not too great, as in the present case, it is customary to correct for the influence of the variation in the thermodynamic properties with the temperature across the boundary layer by employing the integrated mean values of these properties. Thus Reynolds and Nusselt numbers were calculated from

$$Re = U_\infty x/\nu, \quad (15)$$

$$Nu = \alpha x/k, \quad (16)$$

where x denotes the distance from the leading edge, α denotes the local coefficient of heat transfer and ν and k represent the integrated mean values of the kinematic viscosity and the thermal conductivity of air respectively. The integrated mean values are defined by

$$\nu = \frac{1}{T_w - T_{a\infty}} \int_{T_{a\infty}}^{T_w} \nu_T(T)\mathrm{d}T, \quad (17)$$

$$k = \frac{1}{T_w - T_{a\infty}} \int_{T_{a\infty}}^{T} k_T(T)\mathrm{d}T \quad (18)$$

where $\nu_T(T)$ and $k_T(T)$ are the kinematic viscosity and the thermal conductivity of air at the temperature T, respectively. The numerical values of $\nu_T(T)$ and $k_T(T)$ have been interpolated from the NBS-NACA Tables of Thermodynamic Properties of Gases [22].

The local coefficient of heat transfer α was directly calculated from the electrical measurement of the power input to the heater and the temperature difference. It is true that the local values of α were measured over a length of 0·50 in, i.e. the heater width. However, only a negligible error was expected because the heaters were sufficiently far downstream from the leading edge. In order to justify this point, a simple estimation of errors is provided below.

For the laminar heat transfer, the local coefficient of heat transfer α_1, at the center line of the heater is given by

$$\alpha_1(x) \sim (x)^{-0{\cdot}5}. \quad (19)$$

If $2b$ denotes the width of the heater, the mean value of the coefficient over the heater width is given by

$$\alpha(x, b) \sim \frac{1}{2b} \int_{x-b}^{x+b} (x)^{-0{\cdot}5}\,\mathrm{d}x. \quad (20)$$

The ratio of the local value equation (19), to the mean value, equation (20), can be written as

$$\alpha_1/\alpha = \tfrac{1}{2}\{[1 + (b/x)]^{0{\cdot}5} + [1 - (b/x)^{0{\cdot}5}]\} \approx 1 - (1/8)\,(b/x)^2, \quad (21)$$

because $b/x \ll 1$. For the front heater, $b/x = 0{\cdot}0388$, and the ratio becomes

$$\alpha_1/\alpha \approx 0{\cdot}999 \quad (22)$$

and for the back heater the value of the ratio is even closer to unity because b/x is smaller.

For the turbulent heat transfer, the local coefficient of heat transfer α_1, at the center line of the heater is expressed by

$$\alpha_1(x) \sim (x)^{-0{\cdot}2} \quad (23)$$

while the ratio of the local value to the mean value becomes

$$\alpha_1/\alpha \approx 1 - (1/25)\,(b/x)^2. \quad (24)$$

The error is even smaller than that in the laminar case. The preceding calculations thus justify the

taking of the direct measurement of the heat transfer as the local value.

If V, I, and A denote the measured voltage, current and the mean area of the heater respectively, then the Nusselt number can be expressed as

$$Nu = \alpha x/k = 1{\cdot}01(VI)\, x/A\Delta Tk \qquad (25)$$

where $\Delta T = T_w - T_{a\infty}$. The mean area is the arithmetic mean value of the area of the slot on the plate surface and that of the exposed surface of the heater. Its value is $A = 35{\cdot}61$ cm² for both heaters. The factor 1·01 in equation (25) was deduced from the measuring circuit, as explained in Ref. 1. The accuracy of the determination of the Nusselt and Reynolds numbers was about 1·5 per cent.

The radiation correction was calculated from the following equation:

$$P_r = \epsilon C_b A \{(T_w/100)^4 - (T_{a\infty}/100)^4\} \qquad (26)$$

where $C_b = 5{\cdot}77$ W/m²C^4 and the emissivity ϵ was assumed to be 0·08.

6. CORRECTION DUE TO NON-ISOTHERMAL SURFACE

As already mentioned, the plate surface temperature was not uniform near the leading edge, and it also differed slightly from the heater surface temperature near the heaters. For the convenience of calculating the corrections, the plate surface temperature was assumed to have a discontinuity at 1·5 in from the leading edge and a second discontinuity at the front edge of each heater (Fig. 13).

The local coefficient of heat transfer from a flat plate with an unheated starting length was derived by Eckert [16] for a laminar boundary layer and by Rubesin [17] for a turbulent boundary layer. The coefficient $\alpha(L, x)$ is a function of the unheated length L and the distance from the leading edge x. Consequently $\alpha(0, x)$ denotes the coefficient of heat transfer without an unheated length, i.e. for the case when the momentum and thermal boundary layers both begin at the leading edge. The ratio between $\alpha(0, x)$ and $\alpha(L, x)$ denoted by

$$f(L, x) = \alpha(L, x)/\alpha(0, x) \qquad (27)$$

was calculated by Eckert and by Rubesin who found the following two expressions:

$$f(L, x) = \{1 - (L/x)^{0{\cdot}75}\}^{-1/3}\text{laminar}, \qquad (28)$$

$$f(L, x) = \{1 - (L/x)^{39/40}\}^{-7/39}\text{turbulent}. \qquad (29)$$

The present flat plate did not possess a portion which was entirely unheated; consequently the above two correction factors could not be applied directly to the present case.

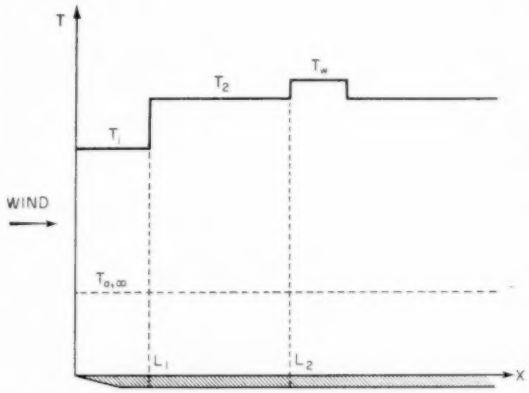

FIG. 13. Idealized temperature distribution on plate.

It was shown by Sogin [23] that the rate of heat transfer from a flat plate with a step-wise discontinuity in the surface temperature can be obtained as the sum of two simple solutions: (1) a simple solution for a heated plate at uniform temperature T_1, see Fig. 13; and (2) a simple solution for a heated step at temperature $T_2 - T_1$ with the step starting at L_1. The superposition of simple solutions can be extended to the case of n steps. In the present case, there are two steps for each heater. Therefore the coefficient of heat transfer $\alpha(L, x)$ can be expressed as

$$\alpha(L, x) = \frac{\alpha(0, x)}{T_w - T_{a\infty}} \{(T_1 - T_{a\infty}) + (T_2 - T_1) f(L_1, x) + (T_w - T_2) f(L_2, x)\}. \qquad (30)$$

Since the function f has a singularity at $x = L$, the integrated mean value of the left-hand side of equation (30) over the heater width must be taken in order to obtain the local coefficient of heat transfer. Thus

$$Nu(L, x) = Nu(0, x) \,.\, C. \qquad (31)$$

where

$$C = \frac{1}{T_w - T_{a\infty}} \left\{ (T_1 - T_{a\infty}) + \frac{T_2 - T_1}{2b\alpha(0, x)} \int_{x-b}^{x+b} \alpha(0, x) \, . \, f(L_1, x) \mathrm{d}x + \frac{T_w - T_2}{2b\alpha(0, x)} \int_{x-b}^{x+b} \alpha(0, x) \, . \, f(L_2, x) \mathrm{d}x \right\}. \quad (32)$$

The evaluation of the two integrals will be given in detail in the Appendix.

Together with the radiation correction, the corrected Nusselt number is given by

$$Nu = (1{\cdot}01\ VI - P_r)\ x/A(\Delta T)kC \quad (33)$$

All the Nusselt numbers were calculated from equation (33).

It is noted that the correction factor f was derived only for the laminar and turbulent boundary layers. In the transition region, half of the experimental points were corrected according to the laminar correction, and the other half, according to the turbulent correction.

7. EXPERIMENTAL RESULTS

The experimental results are given in Table 1 and Fig. 14. In Fig. 14 the results are shown as plots of the Nusselt number in terms of the Reynolds number in logarithmic co-ordinates. For the purpose of comparison, the well-known relations due to Pohlhausen [24, 25], Prandtl [25] and von Kármán [25, 26] are shown as lines a, b, and c respectively. Line a corresponds to Pohlhausen's equation

$$Nu = 0{\cdot}295\ Re^{1/2} \quad (34)$$

for laminar flow and $Pr = 0{\cdot}70$. Line b corresponds to Prandtl's semi-empirical relation for turbulent flow and $Pr = 0{\cdot}70$:

$$Nu = 0{\cdot}0236\ Re^{0{\cdot}8}. \quad (35)$$

Finally, line c corresponds to von Kármán's corresponding semi-empirical relation

$$Nu = 0{\cdot}0241\ Re^{0{\cdot}8}. \quad (36)$$

In the laminar region, the experimental points agree with Pohlhausen's solution to within $\pm 2{\cdot}0$ per cent, and the reader might recall that Pohlhausen's solution was derived for a free

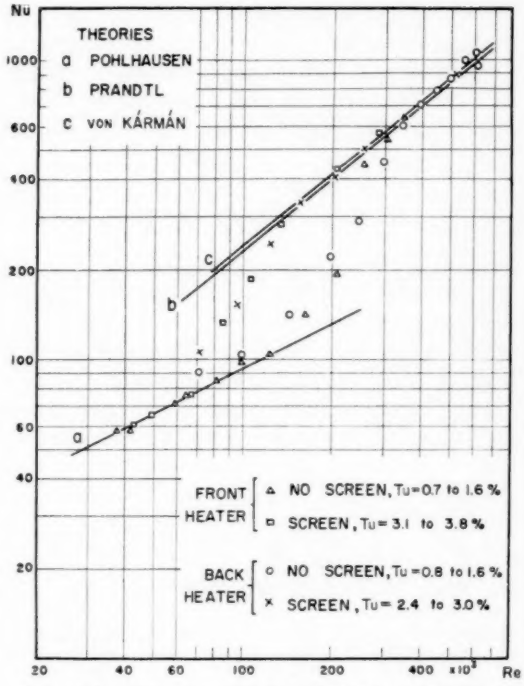

FIG. 14. Local heat transfer from flat plate; negligible pressure gradient.

stream of zero turbulence intensity. In the present experiment, the turbulence intensity varied from 0·75 to 3·82 per cent, as can be seen in Table 1. The agreement between the present experimental results and the theoretical prediction leads to the conclusion that the free-stream turbulence does not affect the local coefficient of heat transfer across a laminar boundary layer on a flat plate up to a turbulence intensity of 3·82 per cent. In other words, the random fluctuations in the free-stream velocity do not cause any measurable effect on the laminar boundary layer for a turbulence intensity in the present range. This constitutes a marked difference from the case of cylinders and spheres.

In the transition region, a great influence was detected as expected.

The effect of the free-stream turbulence on the position of the point of transition was first studied by Dryden [27]. Dryden examined the flow in the boundary layer on a flat plate and obtained initial results on the behavior of the

Vol. 3 1961

Table 1. *Experimental results*
(Negligible pressure gradient)

Air speed U_∞ (m/s)	Temp. difference ΔT (°C)	Measured power 1·01 (*VI*) (W)	Radiation correction P_r (W)	Correction for non-isothermal condition C	Corrected Nusselt number Nu	Reynolds number $Re \times 10^{-3}$	Turbulence intensity Tu (%)
First Heater							
4·00	78·20	2·8696	0·1965	1·025	58·5	37·8	1·60
4·42	79·00	2·8227	0·1974	1·019	57·2	41·9	1·60
4·57	76·46	2·9077	0·1942	1·028	60·4	42·9	3·82
5·25	75·30	3·1339	0·1915	1·022	66·8	49·2	0·90
6·25	78·48	3·4782	0·1970	1·029	71·3	59·1	0·75
6·75	79·21	3·7087	0·1976	1·023	76·1	64·0	0·75
7·06	74·50	3·6624	0·1887	1·063	76·6	66·3	3·17
8·77	73·39	3·9486	0·1884	1·048	85·2	81·9	0·81
10·72	73·19	4·5351	0·1879	1·056	98·0	99·9	1·09
13·18	73·55	5·1188	0·1887	1·060	110·2	123·0	1·00
9·03	77·16	6·3200	0·1932	1·043	133·4	85·3	3·26
11·09	76·86	8·5440	0·1923	1·013	187·8	105·0	3·58
17·48	73·60	6·5804	0·1886	1·077	140·6	163·0	1·46
22·19	73·66	9·0068	0·1877	1·073	194·5	208·0	1·38
26·98	70·69	18·9058	0·1820	1·030	446·5	251·0	1·04
32·54	70·28	22·7319	0·1800	1·030	540·8	302·0	1·07
14·17	77·12	12·9424	0·1928	1·018	284·5	134·0	3·37
22·12	74·67	19·6379	0·1881	1·021	445·3	208·0	3·72
31·00	71·42	24·7268	0·1828	1·029	580·7	289·0	3·68
37·89	63·29	23·8750	0·1656	1·039	644·4	347·0	1·15
Second Heater							
3·94	78·47	2·3262	0·1966	1·011	90·3	71·4	1·37
3·91	79·38	2·7088	0·1983	1·011	105·2	71·1	2·44
5·24	78·12	3·8386	0·1958	1·016	154·2	95·1	2·54
5·42	77·43	2·5637	0·1956	1·013	101·4	97·9	0·89
6·82	76·21	5·7401	0·1925	1·005	242·9	123·0	2·65
8·00	76·89	3·6085	0·1938	1·049	142·0	144·0	0·80
10·89	74·71	5·4310	0·1899	1·049	223·7	196·0	1·10
13·70	75·80	7·1263	0·1917	1·056	290·3	247·0	1·26
16·44	74·41	10·3499	0·1887	1·011	451·8	296·0	1·35
19·44	73·13	13·5958	0·1864	1·012	604·9	348·0	1·50
8·50	75·0	7·7685	0·1900	1·005	336·5	153·0	2·90
11·33	72·75	9·0182	0·1851	1·005	403·2	203·0	2·90
14·33	70·94	11·1454	0·1818	1·014	509·4	256·0	2·92
22·16	72·49	15·8986	0·1853	1·013	713·9	396·0	1·50
24·79	72·60	17·6986	0·1841	1·015	793·1	445·0	1·41
27·65	71·59	19·2864	0·1822	1·014	876·9	495·0	1·25
29·37	68·55	19·1867	0·1764	1·014	907·5	522·0	2·95
30·86	71·39	22·0417	0·1817	1·012	1008·1	522·0	1·07
33·69	68·86	22·2047	0·1767	1·014	1047·1	600·0	0·96
34·24	70·08	20·3622	0·1799	1·015	943·5	610·0	0·95

transition point. These results and others have been summarized by Gazley [28] who correlated the transition Reynolds number with the free-stream intensity. His correlation curves are reproduced in Fig. 15. When compared with Gazley's correlation, it is found that in the present experiment the transition Reynolds numbers were slightly lower for the respective turbulence intensities.

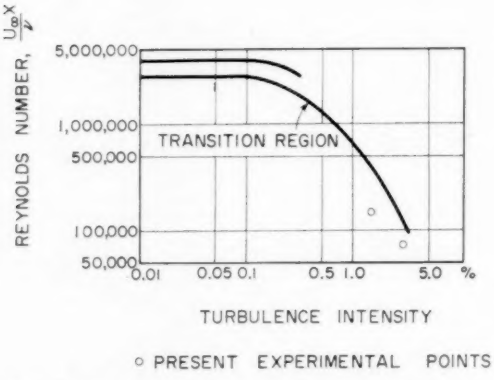

FIG. 15. Effect of free-stream turbulence on boundary layer transition from Gazley [28].

In the turbulent region, the experimental points are more scattered. It can be seen from Fig. 14 that most of the points lie on or in between lines b and c which are Prandtl's and von Kármán's equations respectively.

The largest deviation which appears at the highest Reynolds numbers is about +3·5 per cent from line c and −3·0 per cent from line b. In spite of these deviations, the general trend of the experimental points shows that the local coefficient of heat transfer was not affected by the change of the free-stream turbulence intensity in the range from 0·95 to 3·72 per cent. There is no evidence of any systematic effect of turbulence intensity.

The results of our experiments fully agree with the conclusions reached by Edwards and Furber [10] and Reynolds *et al.* [13]. The discordant results obtained by Sugawara and Sato [12] require further discussion.

As mentioned in section 1, Sugawara and Sato also measured the local coefficient of heat transfer from a flat plate to a turbulent air stream. Their results are replotted in Fig. 16 in which the Nusselt number *Nu*, instead of the ratio of the Nusselt number to the Reynolds

Vol. 3 1961

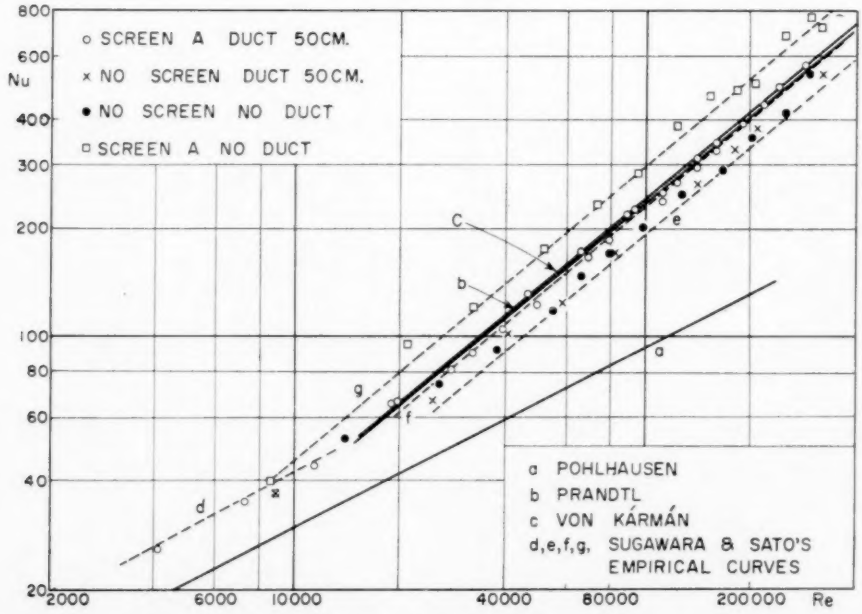

FIG. 16. Experimental results obtained by Sugawara and Sato [12].

number Nu/Re as in the original plot, is drawn in terms of the Reynolds number Re. The dotted lines in Fig. 16 are Sugawara and Sato's empirical expressions of their results for the laminar heat transfer (d) and the turbulent heat transfer (e, f, and g). The solutions due to Pohlhausen for the laminar heat transfer and that due to von Kármán for the turbulent heat transfer are also included. It is quite clear from Fig. 16 that Sugawara and Sato's experimental results in the laminar range deviate from Pohlhausen's solution by a large amount. In the turbulent range, some of their points lie much below von Kármán's equation and some lie considerably above it. However, the slope of line d is the same as that of line a and the slope of lines e, f, and g is the same as that of line c.

Clearly, the general features of their results do not agree with those of the others [10, 11, 13] and of the present investigation, Fig. 14. This divergence might be the result of the questionable accuracy of the non-steady method, or of some defects in their arrangement.

All these measurements, except those due to Sugawara and Sato, lead to the following conclusion: The free-stream turbulence does not exert a local effect on the coefficient of heat transfer through a laminar or a fully developed turbulent boundary layer *on a flat plate*. The only effect due to turbulence is to advance the position of the point of transition.

8. EFFECT OF PRESSURE GRADIENT

As already explained earlier in section 2, there are reasons to suppose that the imposition of a pressure gradient on the flat plate would restore the effect of turbulence intensity on the local rate of heat transfer.

The experimental arrangement employed for testing this supposition was identical with that used previously, except that a plate W was provided, as shown in broken lines in Fig. 3. This produced a large favorable pressure gradient along the test-plate A. The control louvers were removed, and the heat transfer determinations were made at the back heater only.

The static-pressure distribution in the free stream as well as along the plate is shown in Fig. 17 for one air speed. The average pressure

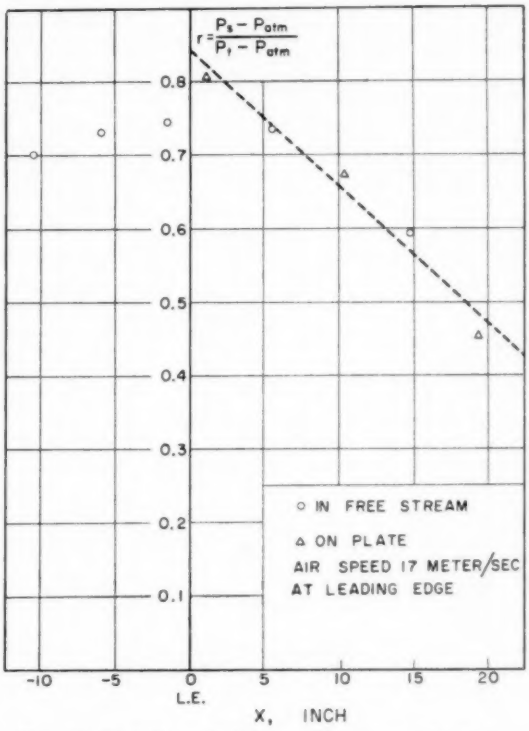

FIG. 17. Variation of static pressure; case of large pressure gradient.

gradient is indicated by the slope of the broken line. The dimensionless average gradient Δ, defined in equation (4) and based on the free-stream velocity at the leading edge has a value $\Delta = 1{\cdot}49$ which represents almost a fifteen-fold increase as compared with the case of a negligible pressure gradient.

The velocity profiles are shown in Fig. 18, in which the velocity profile u/U_∞ is plotted in terms of the dimensionless boundary layer thickness y/δ_m. Curve a is the convergent-channel solution given by Hartree [29] and replotted, taking $\eta = 3{\cdot}25$ as the boundary layer thickness. Curve b is the 1/7th power relation. Not all experimental points are included.

The heat transfer results are given in Table 1 and Fig. 19. It can be seen that in the laminar range, an increase in the turbulence intensity from 0·36 to 1·71 per cent in the range of Reynolds numbers $50\,000 < Re < 100\,000$ causes the Nusselt number to increase uniformly

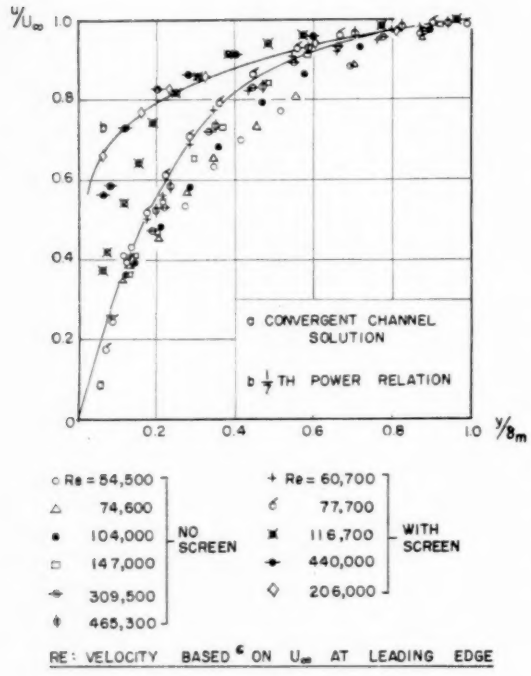

FIG. 18. Velocity profiles in boundary layer; large pressure gradient.

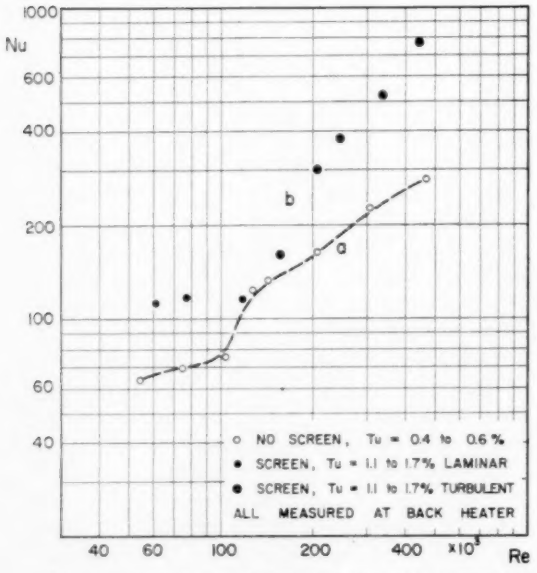

FIG. 19. Local rate of heat transfer with favorable pressure gradient.

by about 65 per cent which is very large and no longer surprising. The abrupt change in the Nusselt number near the Reynolds number $Re = 100\,000$ in Fig. 19 does not correspond to transition, because all the velocity profiles associated with the measurements along the lower line a in Fig. 19 turned out to be laminar in character. In contrast with that, along the upper line b, the velocity profiles below $Re \approx 100\,000$ were laminar, whereas those above $Re \approx 300\,000$ were turbulent, as can be seen from Fig. 18. Thus transition occurred at the higher turbulence intensity, but for the lower turbulence intensity, line a, the addition of the favorable pressure gradient seems to have stabilized the flow in the boundary layer and prevented transition in the range of Reynolds numbers covered by the experiments. Both the Nusselt and Reynolds numbers were based on the distance from the leading edge. The free-stream velocity at the leading edge was used to calculate the Reynolds number.

ACKNOWLEDGEMENTS

The authors wish gratefully to acknowledge the financial assistance received from the then NACA (now NASA) under a contract with Brown University. They also wish to record their thanks to Mr. C. C. Cometta, then Research Assistant at Brown University, for his help with the design of the flat plate and with the conduct of the experimental work. Mr. D. I. Paddison, former Research Assistant at Brown University, performed all the turbulence measurements.

REFERENCES

1. J. KESTIN and P. F. MAEDER, Influence of turbulence on the transfer of heat from cylinders. *N.A.C.A. Tech. Note* 4018 (1957).
2. J. KESTIN, P. F. MAEDER and H. H. SOGIN, The influence of turbulence on the transfer of heat from cylinders near the stagnation point. To be published in *Z. Angew Math. Phys.*
3. W. H. GIEDT, Effect of turbulence level of incident air stream on local heat transfer and skin friction on a cylinder. *J. Aero. Sci.* **18**, 725 (1951).
4. W. H. GIEDT, Investigation of variation of point unit heat transfer coefficient around a cylinder normal to an air stream. *Trans. Amer. Soc. Mech. Engrs*, **71**, 375 (1949).
5. K. SATO and B. H. SAGE, Thermal transfer in turbulent gas stream. Effect of turbulence on microscopic transport from spheres. *Trans. Amer. Soc. Mech. Engrs*, **80**, 1380 (1958).

Vol. 3 1961

6. N. T. Hsu and B. H. Sage, Thermal and material transfer in turbulent gas streams. Local transport from spheres. *J. Amer. Inst. Chem. Engrs*, **3**, 405 (1957).
7. W. W. Short, R. A. S. Brown and B. S. Sage, Thermal transfer in turbulent gas streams. Effect of turbulence on local transport from spheres. *Trans. ASME, J. Appl. Mech.* E **27**, 393 (1960).
8. R. Seban, The influence of free stream turbulence on the local heat transfer from cylinders. *Trans. ASME, J. Heat Transfer*, C **82**, 101 (1960).
9. B. G. Van der Hegge Zijnen, Heat transfer from horizontal cylinders to a turbulent air flow. *Appl. Sci. Res.* A **7**, 205 (1957).
10. A. Edwards and B. N. Furber, The influence of free-stream turbulence on heat transfer by convection from an isolated region of a plane surface in parallel air flow. *Proc. Inst. Mech.* E **170**, 941 (1956).
11. A. Fage and V. M. Falkner, On the relationship between heat transfer and surface friction for laminar flow. *Brit. Aero. Res. Council R and M* 1408 (1931).
12. S. Sugawara and T. Sato, Heat transfer on the surface of a flat plate in the forced convection. *Mem. Fac. Engng, Kyoto* **14**, 21 (1952).
13. W. C. Reynolds, W. M. Kays and S. J. Kline, Heat transfer in the turbulent incompressible boundary layer with constant wall temperature. *Stanford University Report*, NACA Contr. Naw-6494 (1957).
14. J. Kestin, P. F. Maeder and H. E. Wang, On boundary layers associated with oscillating streams. *Appl. Sci. Res.* **10**, 1–22 (1961).
15. G. H. Crocker, A. M. Kuethe and W. W. Willmarth, Velocity fluctuations and boundary layer stability near the nose of a blunt body. *AGARD Conference, London* (1960).
16. E. R. G. Eckert and R. M. Drake, Jr., *Heat and Mass Transfer*. McGraw-Hill, New York (1959).
17. M. W. Rubesin, The effect of an arbitrary surface-temperature variation along a flat plate on the convective heat transfer in an incompressible turbulent boundary layer. *N.A.C.A. Tech. Note* 2345 (1951).
18. H. L. Dryden, G. B. Schaubauer, W. C. Mock and H. K. Skramstad, Measurements of intensity and scale of wind-tunnel turbulence and their relation to the critical Reynolds number of spheres. *N.A.C.A. Rep.* 581 (1937).
19. M. Hansen, Die Geschwindigkeitsverteilung in der Grenzschicht an der längsangeströmten ebenen Platte. *Z. Angew. Math. Mech.* **8**, 185 (1928); also *N.A.C.A. TM* 585 (1930).
20. A. D. Young and J. N. Mass, The behavior of a Pitot tube in a transverse total-pressure gradient. *Brit. Aero. Res. Council R and M* 1770 (1936).
21. F. A. MacMillan, Experiments on Pitot tubes in shear flow. *Brit. Aero. Res. Council R and M* 3028 (1957).
22. J. Hilsenrath and others, Tables of thermal properties of gases. *Nat. Bur. Stand. Circular* 564, Washington (1955).
23. H. H. Sogin, Prediction of flat plate temperatures including low-density effects. *Republic Aviation Corp. Rep.* ETL-19 (1955).
24. E. Pohlhausen, Der Wärmeaustausch zwischen festen Körpern mit kleiner Reibung und kleiner Wärmeleitung. *Z. Angew. Math. Mech.* **1**, 115 (1921).
25. H. Schlichting, transl. and J. Kestin, *Boundary Layer Theory*, 4th Ed. McGraw-Hill, New York (1960).
26. Th. Von Kármán, The analogy between fluid friction and heat transfer. *Trans. Amer. Soc. Mech. Engrs*, **61**, 705 (1939).
27. H. L. Dryden, Air flow in the boundary layer near a plate. *N.A.C.A. Rep.* 562 (1936).
28. C. Gazley, Boundary layer stability and transition in subsonic and supersonic flow. *J. Aero. Sci.* **20**, 19 (1953).
29. D. R. Hartree, On an equation occurring in Falkner and Skan's approximate treatment of the equations of the boundary layer. *Proc. Camb. Phil. Soc.* **33**, Pt. 2, 223 (1937).

APPENDIX

Evaluation of the correction factor for non-isothermal conditions, equation (32)

For the first integral in equation (32), we can take the value calculated at the center line of each heater because the temperature jump occurs at L_1 which is far upstream from the heaters. Therefore the first integral becomes

$$I_1 \approx f(L_1, x).$$

The function $f(L_1, x)$ was given in equations (28) and (29). Thus we obtain the following values:

	Laminar	Turbulent
Front heater	$I_1 = 1{\cdot}14$	$I_1 = 1{\cdot}045$
Back heater	$I_1 = 1{\cdot}08$	$I_1 = 1{\cdot}022$

The second integral cannot be evaluated in the same way since the temperature jump occurs at L_2 which is the front edge of each heater. In the laminar region, the integral becomes

$$I_2 = \frac{1}{2b\alpha(0, x)} \int_{x_1}^{x_2} \gamma x^{-0{\cdot}25} (x^{0{\cdot}75} - x_1^{0{\cdot}75})^{-1/3} \, dx$$

where $x_1 = x - b = L_2$, $x_2 = x + b$ and γ is a constant. Note that the symbol x in the lower

and upper limits denotes the distance from the leading edge to the center line of each heater; thus it is a constant. Substituting $z = x^{3/4}$, the integral I_2 becomes

$$I_2 = (x_2^{0.75} - x_1^{0.75})^{2/3} (x_2^{0.5} - x_1^{0.5})^{-1}.$$

The numerical values of the integral I_2 are:

for the front heater: $I_2 = 4{\cdot}11$
for the back heater: $I_2 = 4{\cdot}96$.

In the turbulent region, the integral I_2 was evaluated numerically and the values are:

for the front heater: $I_2 = 1{\cdot}41$
for the back heater: $I_2 = 1{\cdot}54$.

Vol. 3 1961

Int. J. Heat Mass Transfer. Vol. 3, pp. 155–158. Pergamon Press 1961. Printed in Great Britain.

SHORTER COMMUNICATION

APPLICATION OF THE DEFECT LAW TO THE DETERMINATION OF THE AVERAGE VELOCITY AND TEMPERATURE IN TURBULENT PIPE FLOW*

WILLIAM SQUIRE

Southwest Research Institute, San Antonio, Texas, USA

(*Received* 22 *August* 1960, *and in revised form* 3 *April* 1961)

NOMENCLATURE

u, velocity;
r, radial co-ordinate;
r_0, radius of tube;
y, distance from wall;
$f(\ )$, function of;
T, temperature;
A, total Prandtl number;
D, a constant;
k, Nikuradze roughness parameter;
ν, kinematic viscosity;
κ, thermal diffusivity;
ϵ_M, eddy viscosity;
ϵ_H, eddy diffusivity;
λ, friction coefficient;
Δ, limit of velocity defect function as $r \to r_0$.

Dimensionless groups

Re, Reynolds number based on diameter and average velocity;
Pr, Prandtl number.

Subscripts

c, value at axis;
av, average value, for r_0 value at which local value equals average;
δ, value at edge of sublayer;
τ, friction.

INTRODUCTION

THE problem of determining the average velocity or temperature of a fluid flowing turbulently through a round pipe by a measurement at a single point is of some practical importance because of the inconvenience of making traverses or using mixing chambers.

Recently Rogers and Mayhew [1] analyzed two methods using the universal velocity and temperature distribution laws for turbulent flow in smooth pipes. The axial method uses the velocity or temperature on the axis and a correction factor which is a function of Reynolds number for the velocity and of Reynolds and Prandtl number for temperature. The ordinate method is based on measuring the velocity or temperature at a point where its value is equal to the average value.

This note considers the applications of defect profiles to these methods. While we are also limited to the restriction of essentially isothermal flow so that there is no marked variation of fluid properties across the profile, our results for the ordinate method are also applicable to rough pipes.

BACKGROUND ON TURBULENT FLOW

It is well known that the velocity profiles for both smooth and rough pipe are described quite well by the defect law

$$\frac{u_c - u}{u_\tau} = f(r/r_0). \tag{1}$$

The best known expression is the familiar logarithmic law

$$\frac{u_c - u}{u_\tau} = 5{\cdot}5 \log_{10} \frac{r_0}{r - r_0}. \tag{2}$$

We will refer to expressions such as this which become infinite as $r \to r_0$ as divergent. For parts of the present analysis it is preferable to have an expression for the velocity defect which approaches a finite value as $r \to r_0$. This type of expression will be referred to as convergent. The expression [2]

$$\left(\frac{r}{r_0}\right)^2 = 0{\cdot}189 \frac{u_c - u}{u_\tau} \exp\left(0{\cdot}0695 \frac{u_c - u}{u_\tau}\right) \tag{3}$$

is used for specific calculations, but the general method can be used with any expression.

A convergent expression is inconsistent with the usual assumption that the junction between the turbulent core and the laminar sublayer occurs at a fixed value of u_δ/u_τ as this would imply a constant friction coefficient. On the basis of Nikuradze's data, the relation

$$\frac{u_\delta}{u_\tau} = 5{\cdot}25 \log_{10}(Re \times 10^{-3}) \tag{4a}$$

was obtained [2]. For fully developed roughness it was found that

$$\frac{u_\delta}{u_\tau} = 5{\cdot}85 \log_{10}\left(\frac{r_0}{k} \times 10^{-1}\right). \tag{4b}$$

* This is a condensed version of a Southwest Research Institute report dated August 1960 on Internal Research Project 906-2.

The author [2, 3] has suggested that there is a relation between the temperature and velocity profiles of the form

$$\frac{T_c - T}{T_\tau} = A(Re, Pr)\frac{u_c - u}{u_\tau} \tag{5}$$

where the friction temperature T_τ is

$$\frac{\kappa}{u_\tau}\frac{\mathrm{d}T}{\mathrm{d}r}\bigg|_{r=r_0}.$$

The proportionality factor A can be interpreted as a total Prandtl number, i.e. the ratio of the sum of the eddy and molecular viscosities to the sum of the eddy and molecular diffusivities. An expression

$$A = \frac{1{\cdot}41\ Re\ Pr\ \sqrt{\lambda} + 40Pr}{1{\cdot}20\ Re\ Pr\ \sqrt{\lambda} + 40} \tag{6}$$

was proposed for A. While the direct experimental evidence is incomplete, particularly for $A \ll 1$, the derivation of a heat transfer relation in good agreement with experiment in the liquid metal range is an indirect verification.

There are two types of average temperature in the literature. The theorists prefer the average defined by

$$\frac{\int_0^{r_0} r\,T\,\mathrm{d}r}{\int_0^{r_0} r\,\mathrm{d}r}$$

while the experimentalists prefer the bulk average defined by

$$\frac{\int_0^{r_0} r\,u\,T\,\mathrm{d}r}{\int_0^{r_0} r\,u\,\mathrm{d}r},$$

since it is easier to measure. The difference is small and usually neglected.

THE ORDINATE METHOD

It is obvious that if the defect law is assumed the ordinate at which the local velocity is equal to the average velocity is independent of Reynolds number or roughness. This is related to the well-known Prandtl rule that

$$\frac{u_c - u_{\mathrm{av}}}{u_\tau} = D \cong 4{\cdot}07. \tag{7}$$

To obtain the value of the ordinate it is necessary to solve

$$D = f_1\left(\frac{r_{\mathrm{av}}}{r_0}\right). \tag{8}$$

Either a divergent or convergent velocity distribution may be used. Using expression (3) gives $r_{\mathrm{av}} = 0{\cdot}76\ r_0$ as the ordinate for the velocity determination. This agrees closely with Jakob [4] who claimed that a measurement at $0{\cdot}77\ r_0$ would determine the average velocity within 1 per cent. The variation obtained by Rogers and Mayhew is also relatively small going from $0{\cdot}808\ r_0$ at $Re = 10^4$ to $0{\cdot}777\ r_0$ at $Re = 10^7$.

Similarly if we assume the temperature defect law, equation (5), it can be seen that the ordinate at which the temperature is equal to the average temperature is the same as for the velocity determination, irrespective of the exact form of the expression for A. The evaluation of the ordinate for determining the bulk average temperature is more difficult and requires specific functional forms for the distributions. The ordinate will be a function of Reynolds and Prandtl number so that convenience is lost.

THE AXIAL METHOD

The simplification of the analytical results for the ordinate method obtained in the previous section does not change the fact that it uses a measurement at a point where the gradient is appreciable, while the axial method uses a measurement less subject to positioning error. While the calculation of the correction factor requires more specific assumptions, they are simpler than the corresponding assumptions utilizing the universal law.

To compute the ratio of average to maximum velocity, it is necessary to use a convergent (in the sense of this paper) velocity distribution. If we designate the limit of $(u_c - u)/u_\tau$ by Δ we have

$$\frac{u_{\mathrm{av}}}{u_c} = 1 - \frac{D}{(u_\delta/u_\tau) + \Delta}. \tag{9}$$

In conjunction with (4) this gives

$$\frac{u_{\mathrm{av}}}{u_c} = 1 - \frac{4{\cdot}07}{14{\cdot}4 + 5{\cdot}25\log_{10} Re \times 10^{-3}} \tag{10}$$

for smooth pipes. In Fig. 1 this correction factor is compared with these proposed by Rogers and Mayhew and by Jakob. Some of Nikuradze's experimental points, as tabulated by Bates [5] are shown for comparison. It should, however, be noted that there is some dispute [6] about the data reduction.

In conjunction with equation (5) the relation

$$\frac{u_{\mathrm{av}}}{u_c} = 1 - \frac{4{\cdot}07}{14{\cdot}4 + 5{\cdot}85\log_{10}(r_0/k) \times 10^{-1}} \tag{11}$$

is obtained for rough pipes. In Fig. 2 this is compared with some of Nikuradze's experimental data [7].

The derivation of the correction factor for the average temperature requires an explicit expression such as (6) for the total Prandtl number and an expression for T_δ/T_τ. In [3] the relation

$$\frac{T_\delta}{T_\tau} = Pr\frac{u_\delta}{u_\tau} \tag{12}$$

was proposed, but it is limited to smooth pipes and may not be valid for large Pr. However, the analysis employed by Rogers and Mayhew is in the same category in regard to behavior at large Pr. The analog of (10) is

$$\frac{T_{\mathrm{av}}}{T_c} = 1 - \frac{4{\cdot}07}{14{\cdot}4 + 5{\cdot}25\dfrac{1 + 0{\cdot}030\ Re\ Pr\ \sqrt{\lambda}}{1 + 0{\cdot}035\ Re\ \sqrt{\lambda}}\log_{10} Re \times 10^{-3}} \tag{13}$$

Vol. 3 1961

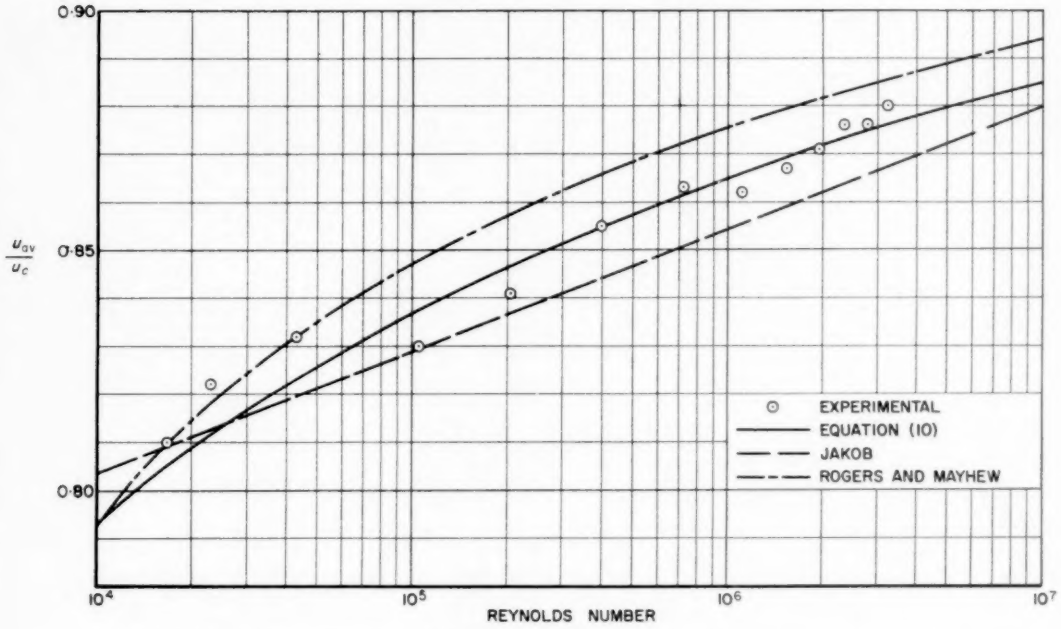

FIG. 1. Correction factor for axial method of average velocity determination in smooth pipe.

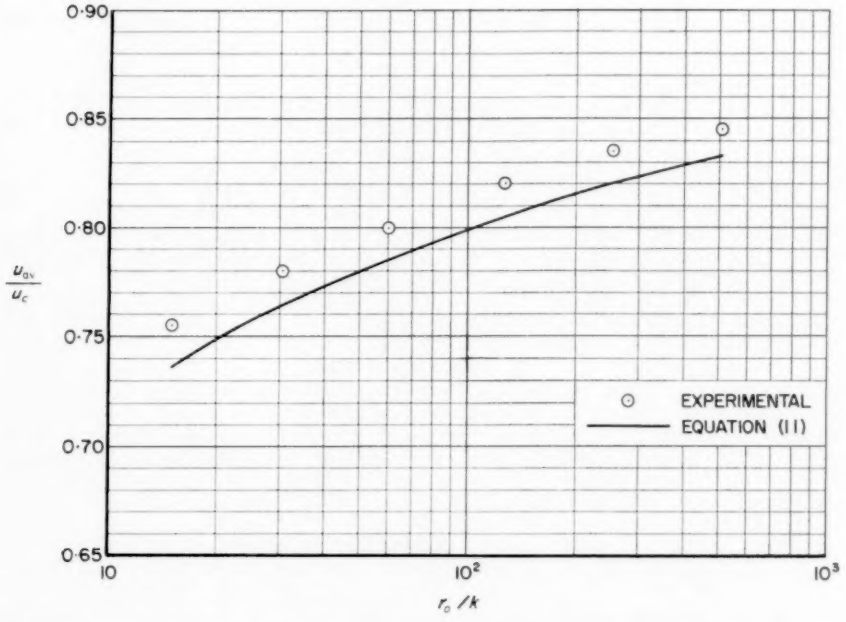

FIG. 2. Correction factor for axial method of average velocity determination in fully rough pipe.

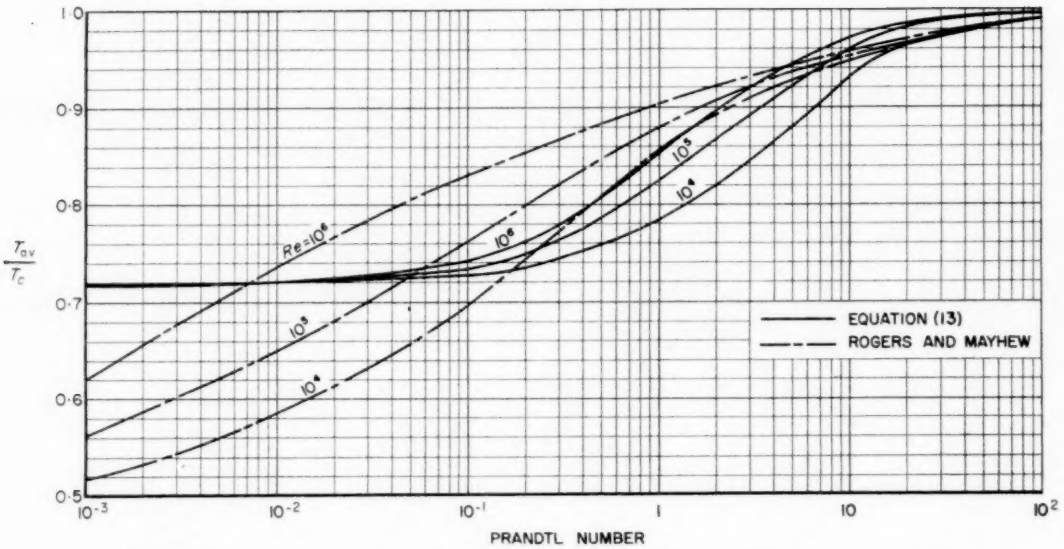

FIG. 3. Correction factor for axial method of average temperature determination in smooth pipe.

which is plotted in Fig. 3 with Mayhew and Rogers' factor for the bulk average. The calculation of the bulk average can be carried out by the present analysis but requires a specific expression for $f(r/r_0)$. It is believed that the difference between the average and bulk average is not large enough to account for the difference between the two analyses.

DISCUSSION

We have shown that the use of the defect laws results in an appreciable simplification of the analysis, but gives results somewhat different from those obtained using the universal laws. Actually, the defect law and the universal law are not exact mathematical relations but approximations of limited accuracy. For example, a critical examination of Nikuradze's data by Robertson [8] indicates a systematic difference in the value of D between smooth and rough pipes and a slight Reynolds number dependence. This may explain the small systematic discrepancy between the theoretical and experimental points in Fig. 2.

An advantage of our formulation of the ordinate method is that since the location is fixed the method should be applicable to cases where there is a slow time variation.

There is obviously a need for further experimental work, particularly on the temperature distribution, to resolve the discrepancies between the analysis based on the defect law and the analysis based on the universal profiles. In particular, closely spaced measurements in the neighborhood of the ordinate where the local value is equal to the average value are needed.

REFERENCES

1. G. F. C. ROGERS and Y. R. MAYHEW, *Int. J. Heat Mass Transfer*, **1**, No. 1, 55 (1960).
2. W. SQUIRE, *Appl. Sci. Res.* **A10**, 23 (1961).
3. W. SQUIRE, *Proceedings Sixth Midwestern Conference on Fluid Mechanics*, p. 16, Austin (1959).
4. M. JAKOB, *Trans. Amer. Inst. Chem. Engrs*, **36**, 657 (1940).
5. H. T. BATES, *Trans. Amer. Inst. Chem. Engrs*, **36**, 269 (1940).
6. B. MILLER, *Trans. Amer. Inst. Chem. Engrs*, **36**, 662 (1940).
7. J. NIKURADZE, *Forschung. Ver. Dtsch. Ing.* 361 July/August (1933).
8. J. M. ROBERTSON, *Proceedings Fifth Midwestern Conference on Fluid Mechanics*, p. 67, Ann Arbor (1957).

Vol. 3 1961

Int. J. Heat Mass Transfer. Vol. 3, p. 159. Pergamon Press 1961. Printed in Great Britain.

LETTER TO THE EDITOR

COMMENT ON ROGERS' PAPER "HEAT TRANSFER AT THE INTERFACE OF DISSIMILAR METALS"*

I READ with interest G. F. C. Rogers' paper in the March issue of the INTERNATIONAL JOURNAL OF HEAT AND MASS TRANSFER, entitled "Heat Transfer at the Interface of Dissimilar Metals". My own researches during the last year have been on the subject of thermal resistance of metal contacts and have dealt mainly with pairs of similar materials, although I have tested several combinations of copper/steel, aluminium/steel generally similar to those described in the above article.

For the tests carried out in a vacuum, the heat transfer across the faces is entirely by solid conduction, radiation being negligible at the temperatures quoted. The governing factors are thus:

(a) the number of microscopic metal to metal contacts (referred to as *a*-spots),
(b) the average size of these contacts,

and by no means least

(c) the condition of the surfaces within the contact spots.

For surfaces with the low surface roughness (2–19 μ in) tested by Rogers, the number of metal to metal contact spots can vary considerably from one pair of specimens to another pair of nominally identical geometry. This difference tends to diminish as the contact pressure increases, but at the low pressure of 122 lb/in^2 used for Rogers' tests, I have always found great difficulty in obtaining consistent experimental results. An important factor which accentuates this scatter is the initial flatness of the faces, and the quoted parallelism of 0·0003 in would seem to be the controlling factor, rather than the micro finish. It would be interesting to learn how the overall flatness was measured and just what shape the "flats" were.

Factor (c) may well be responsible for the effect measured by Rogers, a possible explanation being as follows.

The heat flux through the *a*-spots is the heat flux through the nominal contact area multiplied by the ratio of the nominal contact area to the true contact area. This ratio is usually calculated by dividing the applied pressure into the Meyer hardness of the softer metal. For typical conditions, e.g. 122 lb/in^2 with steel to aluminium specimens (Meyer hardness for pure aluminium is approximately 20 kg/mm^2), the area ratio is approximately 230. The heat flux through the *a*-spot is thus 230 times the nominal heat flux and when one considers that the thermal conductivities of any surface contaminant films may be about 1/50th of that of the parent metal, the overall effect of these films is to produce a temperature drop equivalent to that consequent upon an additional metal thickness of approximately 11,500 times the film thickness. With harder metals this effect is further exaggerated, although in many engineering contacts the interface fluid relieves the *a*-spots of some of their heat load. Rogers, in his paper, does not discuss these effects nor does he specify the previous history of his specimens.

I would suggest that the effect found by Rogers is a direct result of surface contamination, which could be presented before assembly or even deposited at the modest vacuum of 0·02 mm Hg quoted. In the case of heat flow from aluminium to steel the differential radial expansion of the aluminium surface across the hard steel surface could cause the film to be scoured off, thereby allowing better metallic contact compared with that of the reverse direction of heat flow, in which the relative movement is reduced. This effect may be exaggerated by the method of machining the contacting faces, i.e. diamond turning, as the differential radial movement will cause severe interference between the two sets of tool marks. There may be a further small contribution to the directional effect caused by the reduction in hardness of the aluminium as the temperature increases, but this is possibly negligible at the temperature quoted.

I would suggest that the simple mechanical engineer's explanation is adequate for a qualitative analysis of the effect but would be very interested to hear the opinions of the specialists in metal physics. I would be more convinced of the existence of a direction-conscious surface thermal potential barrier if the effects were found with tests having the following controls:

(a) a much higher contact pressure,
(b) a specified contact geometry,
(c) a controlled film thickness.

It would also be interesting to observe the results of repeated tests on the same pair of specimens to check whether the contact resistance remained at its low level once the film had been damaged.

You may be interested to hear that my own tests are being conducted at present with contact pressures rising above 3000 lb/in^2 the mating surfaces having previously been gold plated.

A. WILLIAMS

Engineering Department,
University of Manchester,
Manchester

* *Received* 25 *April* 1961.

Int. J. Heat Mass Transfer. Vol. 3, p. 160. Pergamon Press 1961. Printed in Great Britain.

ANNOUNCEMENTS

JOURNAL OF ENGINEERING PHYSICS

THE Journal publishes results of scientific investigations in physics which are of importance for modern technological development.

Papers on the following main subjects are printed; thermodynamics of irreversible processes and its application to the phenomena of energy and matter transfer in the presence of phase, chemical and nuclear transformations; heat and mass transfer in jet and rocket mechanism and in nuclear reactors; heat and mass transfer in the processes of combustion, gasification and drying; heat conduction theory; soil mechanics and physics, thermophysics of building constructions.

Summaries of all the fundamental articles published in the Journal, are given in English.

Parallel with original articles the Journal deals with reviews of current questions of modern science and technology and presents news of the most important events in scientific life.

The speciality of the Journal is a presentation of complex problems in the fields of physics and technology mentioned above; parallel with mathematical and experimental physical methods of research engineering, technical methods of solving these problems are discussed.

Material for publication in the Journal may be sent to: Journal of Engineering Physics, Podlesnaya 25, Minsk 13, B.S.S.R.

Subscription to the Journal of Engineering Physics for 1962 is taken through Mezhdunarodnaya kniga.

A. V. LUIKOV

THE COMBUSTION INSTITUTE

(British Section)

Chairman: DR. J. W. LINNETT, F.R.S.

A ONE-DAY symposium on carbon formation will be held on Wednesday, 27 September 1961 in The Department of Mechanical Engineering, City and Guilds College, South Kensington, London S.W.7.

The symposium is being organized by the British Committee of the Combustion Institute and will embrace discussions of the mechanism of carbon formation in flames and the application of fundamental data on carbon formation to practical combustion systems. There will be brief prepared contributions; the aim, however, will be to allow as much time as possible for discussion.

A business meeting for members of the British Section of the Combustion Institute will be arranged at a convenient time on the same day.

The symposium will be open to all members of the British Section and to others interested in the subject.

Further details of the Meeting may be obtained from N. S. W. Moore, Department of Mechanical Engineering, City and Guilds College, London S.W.7.

Vol. 3 1961

Int. J. Heat Mass Transfer. Vol. 3, pp. 161–162. Pergamon Press 1961. Printed in Great Britain.

BOOK REVIEWS

Elements of the Kinetic Theory of Gases. E. A. GUGGENHEIM. Pergamon Press, Oxford, 1960, 89 pp. 17*s* 6*d*.

IT IS a long time since the reviewer has obtained from a technical work the illumination and pleasure afforded by Professor Guggenheim's introduction to the kinetic theory of gases. In the hundred years which have elapsed since the work of Clausius and Maxwell, treatises on this subject have become so weighty and impenetrable that most scientists have had to content themselves with primitive theories of transport processes in gases. Yet here is a work of eighty-nine pages which brings the rigorous theory within the comprehension of the non-expert, an achievement which might well have been judged impossible.

The secret of the authors' success lies in his deep knowledge of the subject, which enables him always to choose the shortest path to his objective, and to eschew unprofitable digressions. He scorns to use the elaborate artifices of arrangement and illustration which lesser authors require to make their texts palatable, yet always provides sufficient insight into the mathematical derivations and enough discussion of their practical significance to carry the reader along with him.

The Maxwell distribution is derived by means of Maxwell's original method, the objections to which the author believes to have been misplaced. The formulae for the transport properties are derived by way of Maxwell's transport-equation along the lines first suggested by Chapman. The rigid-sphere model is given the most detailed attention; the formulae for other force laws are left in the form of quadratures, for the evaluation of which the reader can turn elsewhere. The relations between the force laws, gas imperfections and solid-state properties are given brief but penetrating treatment, with some original material relating to argon.

Despite the author's austere concentration on the bare bones of his subject, he finds space for a number of stimulating asides. For example page 80, if the reviewer interprets it correctly, suggests that the "Lennard–Jones 6–12" force law is perhaps incorrectly given this appellation. Professor Guggenheim's remark about the deduction of force laws by "fitting" their constants to measured values of viscosity deserves quotation: "This is a harmless exercise for those who have the patience. But if they believe that such an analysis, based on such a small temperature variation of the effective value of d (molecular diameter), leads to reliable information on the form of the interaction energy, they are deluding themselves."

The work under review is Volume 1 of Topic 6 of the new International Encyclopedia of Physical Chemistry and Chemical Physics, of which Professor Guggenheim is one of the three editors-in-chief. Let us hope that he can persuade the authors of subsequent volumes to emulate his style.

D. B. SPALDING

Physikalische Grundlagen der Chemie-Ingenieur-Technik. P. GRASSMANN. H. R. Sauerländer, Aarau and Frankfurt am Main, 1961, 939 pp. DM80.

FEW authors are nowadays courageous and hardworking enough to write a book which covers more than a restricted corner of science; yet, as the author reminds us in his preface, students are justifiably dismayed when they are required to master a field which is so large that a whole team of specialists is needed to display its complexities. Professor Grassmann has therefore done a great service to chemical engineers by showing that one man can indeed absorb and expound all the fundamental sciences which underlie their technology. His range is adequately exhibited by listing the chapter headings, which are (freely translated)—Quantity and energy balances; the concept and use of entropy; probability theory and kinetic theory of gases; mechanics of solids; particles, powders and porous materials; fundamentals of fluid flow; applications of fluid flow; dimensional analysis and the theory of models; the exchange of momentum, heat and mass; multi-phase flow phenomena; rheology; and general discussion.

Of course, even in a book of over nine hundred pages of small print, the treatment is bound to be somewhat superficial. This is perhaps particularly the case in the sections on heat and mass transfer; Fick's Law is presented in an exceedingly non-general form, and the author appears to have made an elementary error in modifying it (on p. 225) for the case of gases of non-uniform temperature.

Nevertheless, the author's energy of mind and individual viewpoint are evident throughout, and even readers who, at one point or another, would prefer a different treatment cannot fail to be stimulated; the book can be read with profit by students and teachers alike. Professor Grassmann's discussion of the motion of vapour bubbles in liquids is particularly to be commended.

D. B. SPALDING

Units, Dimensions and Dimensionless Numbers. D. C. IPSEN. McGraw-Hill, New York, 1960, 236 pp. 50*s* 6*d*.

THIS is an exasperating book. The cover blurb claims that it is "clearly written", but one wonders whether the writer of the blurb has read the book; the reviewer's pencilled marks against obscure passages are too numerous to let

the claim pass. The book is exasperating because, while there are some things in it that are worth saying, too many are said badly.

The subject demands precise treatment and clear definition of terms, but clear definitions we do not get; *vide:* "The physical variables that we use are of two *significantly* different sorts. The sort of variable that *probably first comes to mind* . . . we shall class as substantial variables." (Reviewer's italics.) The chapters on units are too often verbose and obscure. Those on similitude and dimensional analysis are more rewarding, though they are also unnecessarily laboured. This is not a book to be recommended to the busy reader who wishes to clarify his ideas with a minimum expenditure of effort.

R. W. HAYWOOD

Electrodynamics of Continuous Media. L. D. LANDAU and E. M. LIFSHITZ. Authorized translation from the Russian by J. B. SYKES and J. S. BELL. Pergamon Press, Oxford, 1960, 417 pp. 84*s*.

THIS work is the eighth in a series of publications by the authors on theoretical physics. The essential basic theory of electrodynamics of continuous media is presented rigorously and with great economy so that the reader is assumed to be familiar with the main mathematical techniques and theories of physics. Although the book deals primarily with the macroscopic theory the authors have successfully incorporated the atomic and molecular viewpoint.

The initial chapters deal with a very comprehensive study of the electrostatics of dielectric materials. Here temperature-dependent properties are fully discussed with the aid of classical thermodynamics. The conductivity tensor is introduced, and the theory relating to the flow of current in isotropic or anisotropic materials is developed and leads to a discussion of the Hall effect and thermoelectric phenomena. An exhaustive treatment, carefully supplemented by physical arguments, is then given on the structure of magnetic materials and the theory of superconductors. Some transient problems are discussed, namely the effect of a variable magnetic field on a conductor, i.e. eddy currents and the skin effect, together with a discussion on the excitation of currents by the motion of a conductor in an electromagnetic field.

The remainder of the book, apart from that section which deals with the electromagnetic field equations, is devoted to the discussion of some special topics. These are magnetohydrodynamics, magnetic-optical effects, ionization losses of fast particles in matter, black body radiation, dispersion theory of electromagnetic waves and finally the general theory of X-ray diffraction.

This book stands out as a piece of careful exposition and should have a strong appeal for both physicists and applied mathematicians. The translators are to be commended on the excellence of their work.

G. POOTS

Vol. 3 1961

Int. J. Heat Mass Transfer. Vol. 3, pp. 163–166. Pergamon Press 1961. Printed in Great Britain.

PIONEER PAPERS IN HEAT AND MASS TRANSFER

FOREWORD TO THE SERIES

MOST serious students of a scientific subject find that their understanding of its significance is deepened by an acquaintance with the works of the comparatively few writers who have made striking developments of a theoretical or experimental nature. Since many of the key papers are somewhat inaccessible however, and since the effort to keep up with current publications leaves few readers with sufficient energy for historical research, the editors of this journal propose to reprint selected works of pioneers in the field of heat and mass transfer. These will appear in alternate issues of the journal, as a rule. The papers will be mostly more than twenty-five years old and will be grouped according to subject. The papers will be reprinted in English, French or German, with editorial abridgement and comment where required.

The Editors

PIONEER PAPERS IN CONVECTIVE MASS TRANSFER

1. OSBORNE REYNOLDS: On the extent and action of the heating surface of steam boilers. (*Scientific Papers of Osborne Reynolds*, Vol. I, pp. 81–85. Cambridge University Press, London, 1901.) Reprinted by permission of The Manchester Literary and Philosophical Society.

Editor's Foreword

The first group of reprints will be devoted to contributions to the knowledge of convective mass transfer. It therefore seems proper to start by presenting Reynolds' often-cited but seldom-read paper relating heat transfer and friction to the "diffusion" processes in pipe flow. It is interesting to note that what has come to be known as the "Reynolds Analogy" is not spelled out in detail in this paper, which is more concerned with the influence of the flow velocity on the heat transfer coefficient: only proportionality is postulated between the constants in (1) and those in (2).

D.B.S.

ON THE EXTENT AND ACTION OF THE HEATING SURFACE OF STEAM BOILERS

OSBORNE REYNOLDS

[*From the Fourteenth Volume of the* "Proceedings of the Literary and Philosophical Society of Manchester." *Session* 1874–5.]

(*Read* October 6, 1874)

THE rapidity with which heat will pass from one fluid to another, through an intervening plate of metal, is a matter of such practical importance that I need not apologize for introducing it here. Besides its practical value, it also forms a subject of very great philosophical interest, being intimately connected with, if it does not form part of, molecular philosophy.

In addition to the great amount of empirical and practical knowledge which has been acquired

from steam boilers, the transmission of heat has been made the subject of direct inquiry by Newton, Dulong and Petit, Péclet, Joule, and Rankine, and considerable efforts have been made to reduce it to a system. But as yet the advance in this direction has not been very great; and the discrepancy in the results of the various experiments is such, that one cannot avoid the conclusion that the circumstances of the problem have not been all taken into account.

Newton appears to have assumed that the rate at which heat is transmitted from a surface to a gas, and vice versa, is, *ceteris paribus*, directly proportional to the difference in temperature between the surface and the gas, whereas Dulong and Petit, followed by Péclet, came to the conclusion from their experiments that it followed altogether a different law.[1]

These philosophers do not seem to have advanced any theoretical reasons for the law which they have taken, but have deduced it entirely from their experiments, "à chercher par tâtonnement la loi que suivent ces résultats[2]".

In reducing these results, however, so many things had to be taken into account, and so many assumptions have been made, that it can hardly be a matter of surprise if they have been misled. And there is one assumption which upon the face of it seems to be contrary to general experience, this is, that the quantity of heat imparted by a given extent of surface to the adjacent fluid is independent of the motion of that fluid or of the nature of the surface;[3] whereas the cooling effect of a wind compared with still air is so evident that it must cast doubt upon the truth of any hypothesis which does not take it into account.

In this paper I approach the problem in another manner from that in which it has been approached before. Starting with the laws, recently discovered, of the internal diffusion of fluids, I have endeavoured to deduce from theoretical considerations the laws for the transmission of heat, and then verify these laws by experiment. In the latter respect I can only offer a few preliminary results; which, however, seem to agree so well with general experience, as to warrant a further investigation of the subject, to promote which is my object in bringing it forward in the present incomplete form.

The heat carried off by air, or any fluid, from a surface, apart from the effect of radiation, is proportional to the internal diffusion of the fluid at and near the surface, i.e. is proportional to the rate at which particles or molecules pass backwards and forwards from the surface to any given depth within the fluid, thus, if AB be the surface and *ab* an ideal line in the fluid parallel to AB then the heat carried off from the surface in a given time will be proportional to the number of molecules which in that time pass from *ab* to AB—that is for a given difference of temperature between the fluid and the surface.

This assumption is fundamental to what I have to say, and is based on the molecular theory of fluids.

Now the rate of this diffusion has been shown from various considerations to depend on two things:

(1) The natural internal diffusion of the fluid when at rest.

(2) The eddies caused by visible motion which mixes the fluid up and continually brings fresh particles into contact with the surface.

The first of these causes is independent of the velocity of the fluid, and, if it be a gas, is independent of its density, so that it may be said to depend only on the nature of the fluid.[4]

The second cause, the effect of eddies, arises entirely from the motion of the fluid, and is proportional both to the density of the fluid, if gas, and the velocity with which it flows past the surface.

The combined effect of these two causes may be expressed in a formula as follows:

$$H = At + B\rho vt \qquad (1)$$

where t is the difference of temperature between the surface and the fluid, ρ is the density of the fluid, v its velocity, A and B constants depending on the nature of the fluid, and H the heat transmitted per unit area of the surface in a unit of time.

If, therefore, a fluid were forced along a fixed

[1] *Traité de la Chaleur*, Péclet, Vol. I, p. 365.
[2] *Ibid.*, p. 363.
[3] *Ibid.*, p. 383.
[4] Maxwell's *Theory of Heat*, Chap. XIX.

Vol. 3 1961

length of pipe, which was maintained at a uniform temperature greater or less than the initial temperature of the gas, we should expect the following results.

(1) Starting with a velocity zero, the gas would then acquire the same temperature as the tube.

(2) As the velocity increased the temperature at which the gas would emerge would gradually diminish, rapidly at first, but in a decreasing ratio until it would become sensibly constant and independent of the velocity. The velocity after which the temperature of the emerging gas would be sensibly constant can only be found for each particular gas by experiment; but it would seem reasonable to suppose that it would be the same as that at which the resistance offered by friction to the motion of the fluid would be sensibly proportional to the square of the velocity. It having been found both theoretically and by experiment that this resistance is connected with the diffusion of the gas by a formula:

$$R = A'v + B'\rho v^2 \qquad (2)$$

And various considerations lead to the supposition that A and B in (1) are proportional to A' and B' in (2).

The value of v which this gives is very small, and hence it follows that for considerable velocities the gas should emerge from the tube at a nearly constant temperature whatever may be its velocity.

This, as I am about to point out, is in accordance with what has been observed in tubular boilers, as well as in more definite experiments.

In the Locomotive the length of the boiler is limited by the length of tube necessary to cool the air from the fire down to a certain temperature, say 500°. Now there does not seem to be any general rule in practice for determining this length, the length varying from 16 ft to as little as 6, but whatever the proportions may be, each engine furnishes a means of comparing the efficiency of the tubes for high and low velocities of the air through them. It has been a matter of surprise how completely the steam-producing power of a boiler appears to rise with the strength of blast or the work required from it. And as the boilers are as economical when working with a high blast as with a low, the air going up the chimney cannot have a much higher temperature in the one case than in the other. That it should be somewhat higher is strictly in accordance with the theory as stated above.

It must, however, be noticed that the foregoing conclusion is based on the assumption that the surface of the tube is kept at the same constant temperature, a condition which it is easy to see can hardly be fulfilled in practice.

The method by which this is usually attempted is by surrounding the tube on the outside with some fluid the temperature of which is kept constant by some natural means, such as boiling or freezing, for instance the tube is surrounded with boiling water. Now although it may be possible to keep the water at a constant temperature, it does not at all follow that the tube will be kept at the same temperature; but on the other hand, since heat has to pass from the water to the tube, there must be a difference of temperature between them, and this difference will be proportional to the quantity of heat which has to pass. And again, the heat will have to pass through the material of the tube, and the rate at which it will do this will depend on the difference of the temperature at its two surfaces. Hence if air be forced through a tube surrounded with boiling water, the temperature of the inner surface of the tube will not be constant, but will diminish with the quantity of heat carried off by the air. It may be imagined that the difference will not be great: a variety of experiments lead me to suppose that it is much greater than is generally supposed. It is obvious that, if the previous conclusions be correct, this difference would be diminished by keeping the water in motion, and the more rapid the motion the less would be the difference. Taking these things into consideration the following experiments may, I think, be looked upon, if not as conclusive evidence of the truth of the above reasoning, yet as bearing directly upon it.

One end of a brass tube was connected with a reservoir of compressed air, the tube itself was immersed in boiling water, and the other end was connected with a small non-conducting chamber, formed of concentric cylinders of paper with intervals between them, in which was inserted the bulb of a thermometer. The air was then allowed to pass through the tube and paper chamber, the pressure in the reservoir being

maintained by bellows, and measured by a mercury gauge; the thermometer then indicated the temperature of the emerging air. One experiment gave the following results: With the smallest possible pressure the thermometer rose to 96°F, and as the pressure increased fell until with $\frac{1}{10}$ in. it was 87°, with $\frac{1}{4}$ in. it was 70°, with 1 in. it was 64°, with 2 in. 60°, beyond this point the bellows would not raise the pressure.

It appears, therefore, (1) that the temperature of the air never rose to 212°, the temperature of the tube, even when moving slowest; but the difference was clearly accounted for by the loss of heat in the chamber from radiation, the small quantity of air passing through it not being sufficient to maintain the full temperature, an effect which must obviously vanish as the velocity of the air increased; (2) as the velocity increased the temperature diminished, at first rapidly, and then in a more steady manner. The first diminution might be expected, from the fact that the velocity was not as yet equal to that at which the resistance of friction is sensibly equal to the square of the velocity, as previously explained. The steady diminution, which continued when the velocity was greater, was due to the cooling of the tube. This was proved to be the case, for at any stage of the operation the temperature of the emerging air could be slightly raised by increasing the heat under the water, so as to make it boil faster, and produce greater agitation in the water surrounding the tube. This experiment was repeated with several tubes of different lengths and characters, some of copper and some of brass, with practically the same results. I have not however as yet been able to complete the investigation, and I hope to be able before long to bring forward another communication before the Society.

I may state that should these conclusions be established, and the constant B for different fluids be determined, we should then be able to determine, as regards length and extent, the best proportion for the tubes and flues of boilers.

Vol. 3 1961

Int. J. Heat Mass Transfer. Vol. 3, pp. 167–174. Pergamon Press 1961. Printed in Great Britain.

APPLICATION OF METHODS OF THERMODYNAMICS OF IRREVERSIBLE PROCESSES TO INVESTIGATION OF HEAT AND MASS TRANSFER IN A BOUNDARY LAYER

A. V. LUIKOV
Institute of Energetics, Minsk, B.S.S.R.

(*Received* 18 *January* 1961)

Abstract—This paper considers the process of heat and mass transfer in a boundary layer at evaporation of a liquid. In this case heat and mass transfer mechanism differs from the process of heat transfer without mass transfer. Experimental results obtained showed that in the boundary layer over a plate there were submicroscopic particles of liquid whose evaporation was going on in the boundary layer itself. On the basis of the theory of thermodynamics of irreversible processes methods of calculation of mass transfer with regard for the action of all the thermodynamic forces including also a new effect of separation of gas mixture components during the process of molecular transfer of kinetic energy of a regulated motion have been developed.

Résumé—Cet article considère le processus du transport de chaleur et de masse dans la couche limite au cours de l'évaporation d'un liquide. Dans ce cas, le mécanisme de transport de chaleur et de masse diffère de celui de la transmission de chaleur sans transport de masse. Les résultats expérimentaux obtenus montrent que dans la couche limite sur une plaque il y a des particules submicroscopiques du liquide, dont l'évaporation est en cours, dans la couche limite elle-même. Des méthodes de calcul du transport de masse ont été développées, elles sont basées sur la théorie de la thermodynamique des phénomènes irréversibles et tiennent compte de l'action de toutes les forces thermodynamiques, y compris d'un nouvel effet de séparation des composants du mélange gazeux au cours du processus de transport moléculaire de l'énergie cinétique d'un mouvement contrôlé.

Zusammenfassung—Die Arbeit behandelt den Wärme- und Stoffübergang in der Grenzschicht beim Verdampfen einer Flüssigkeit. Der Mechanismus des Wärme- und Stofftransports unterscheidet sich in diesem Fall von dem des Wärmeüberganges ohne Stoffübertragung. Versuche zeigten, dass in der den Platten anhaftenden Grenzschicht submikroskopische Teilchen der Flüssigkeit vorhanden sind, die dort verdampfen. Auf Grund der Theorie der Thermodynamik irreversibler Prozesse wurden Berechnungsmethoden für den Stoffübergang entwickelt, die die Wirkung aller thermodynamischen Kräfte berücksichtigen, einschliesslich eines neuen Effektes der Trennung eines Gasgemisches während des Molekularüberganges der kinetischen Energie einer geordneten Bewegung.

Аннотация—В статье рассматривается процесс тепло-и массопереноса в пограничном слое при испарении жидкости. Механизм тепло-и массопереноса в этом случае отличается от процесса теплообмена, не осложнённого массообменом. Как показали результаты проведенных опытов, в пограничном слое над пластиной имеются субмикроскопические частицы жидкости, испарение которых происходит в самом пограничном слое. На основании теории термодинамики необратимых процессов разработаны методы расчётов массопереноса с учётом действия всех термодинамических сил, в том числе нового эффекта разделения компонентов газовой смеси в процессе молекулярного переноса кинетической энергии упорядоченного движения.

NOMENCLATURE

T, absolute temperature, °K($T = 273 + t$);

T_a and T_b, air temperature and temperature of the adiabatic air saturation (wet bulb temperature), respectively;

T_r, temperature of radiation surface;

u and u_c, moisture content and critical

M

moisture content of a porous body, respectively;

c_p, specific isobar heat capacity of humid air (of vapour–gas mixture);

ρ, density of humid air;

ν, coefficient of kinematic viscosity ($\nu = \eta/\rho$);

a, coefficient of thermal diffusivity ($a = \lambda/c_p\rho$);

λ, coefficient of heat conduction of humid air;

D_{12}, coefficient of reciprocal diffusion;

p_{10}, relative partial vapour pressure equal to the ratio of partial pressure of vapour p_1 to the total pressure of vapour–gas mixture p($p_{10} = p_1/p$);

w, air motion rate;

ρ_{i0}, relative concentration of the ith component in a mixture equal to the ratio of the volumetric concentration ρ_i to the density of the mixture ρ($\rho_{i0} = \rho_i/\rho$);

ρ_{10}, relative concentration of vapour in humid air;

ϕ, air humidity ($\phi = p_1/p_e$);

p_e, pressure of the saturated vapour;

μ_i, chemical potential of the ith component;

M_i, molecular weight of the ith component;

h_i, specific enthalpy of the ith component;

R, universal gas constant;

r, specific heat of evaporation of a liquid.

Indices

a, medium (humid air);

ω, surface (plate surface);

r, surface radiation;

1, water vapour;

2, dry air.

Numbers of similarity of heat and mass transfer

Nu and Nu', heat and diffusion Nusselt numbers, respectively;

Re, Reynolds number;

Pr, Prandtl number;

Pr', diffusional Prandtl number (Schmidt number $Pr' \equiv Sc$);

Gu, Gukhman number $\left(Gu = \dfrac{T_a - T_b}{T_a}\right)$;

Gu', modified Gukhman number $\left(Gu' = \dfrac{T_b}{T_a}\right)$.

HEAT transfer between a capillary porous body and flow of a mixture of gases is not only of theoretical interest but also is of great practical importance. If heat transfer is going on in the presence of evaporation of a liquid then mechanism of heat and mass transfer in a boundary layer near the surface of a body is complicated considerably and cannot be described by the classic regularities of heat and mass transfer of a matter.

For example, with the evaporation of a liquid from a free surface under conditions of forced convection the dependence between the numbers Nu, Re and Pr, as was shown by Nesterenko [1] and Polonskaya [2, 3], is not described by ordinary empirical relations which are applied to the theory of heat transfer. Nesterenko's formulae are of the following form

$$Nu = APr^{1/3}\, Re^{n}\, Gu^{0.175} \qquad (1)$$

$$Nu' = A'(Pr')^{1/3}\, Re^{n'}\, Gu^{0.135} \qquad (2)$$

where the constants A, A', n and n' are determined from Table 1.

On the basis of experimental investigations of heat transfer between moist porous plates and a

Table 1. *Value of constants in formulae by Nesterenko* [1]

Range of the Reynolds number variation	A	n	A'	n'
$Re > 3{\cdot}15 \times 10^3$	1·07	0·48	0·83	0·53
$3{\cdot}15 \times 10^3 < Re < 2{\cdot}2 \times 10^4$	0·51	0·61	0·49	0·61
$2{\cdot}2 \times 10^4 < Re < 3{\cdot}15 \times 10^5$	0·027	0·90	0·0248	0·90

Vol. 3 1961

flow of heated air the following empirical formula was obtained by Lebedev [4]

$$Nu = ARe^{0.5}(Gu')^{0.4}\left(\frac{T_r}{T_a}\right)^2\left(\frac{u}{u_c}\right)^n \qquad (3)$$

where the constants A and n are given for some bodies in Table 2.

Table 2. Value of constants in formula by Lebedev [4]

Material	A	n
Quartz sand	0·56	0·8
Clay	0·45	0·9
Wood	0·50	0·3

Other investigators [5–7] obtained formulae analogous to the formula (3).

Till recently no detailed substantiation of the introduction of new criteria of the form Gu, (T_r/T_a), (u/u_c) into relations (1–3) has been given for the case of heat and mass transfer between a porous body containing a liquid and a heated moving gas. This fact indicates that there is a necessity for special and detailed experimental investigations on heat and mass transfer mechanism in a boundary layer flowing over a porous body containing a liquid.

Lately such investigations have been carried out by A. V. Nesterenko, N. F. Dokuchaev [8] N. S. Mikheeva [9], and P. E. Mikhailov [10].

Temperature, partial pressure and velocity of humid air motion in a boundary layer were measured in these investigations.

Recently, applying improved methods, Mel'nikova [11] has carried out analogous investigations under the leadership of the author of this paper. In particular, the presence of a cooler inside the porous body made it possible to obtain any predetermined temperature head $\Delta t(\Delta t = t_a - t_w)$ and directly compare heat transfer of a dry porous plate with that of a moist one.

These investigations show that the heat transfer coefficient is higher in the process of evaporation of a liquid from a free surface or from a capillary-porous body in comparison with the case of net heat transfer, with other conditions equal. When increase in intensity of evaporation occurs, the heat transfer coefficient increases also.

While the calculations of heat transfer process between the surface of a porous wall and the flow of a gas, with blowing of an inert gas (hydrogen, helium), involve the theory of a boundary layer and produce the contrary phenomenon: i.e. with increase of intensity of gas supply into the boundary layer the coefficient of heat transfer decreases.

To reveal the mechanism of heat and mass transfer in the boundary layer special experiments were carried out. Temperature, partial pressure and velocity of air motion in a boundary layer flowing over a porous (gypsum) plate were measured by special devices. The plate was continuously moistened, i.e. the amount of evaporation of the liquid was calculated according to water flow rate and was controlled by weighing the whole plate.

A special cooler was mounted inside the plate so that the temperature of the plate surface t_w was maintained constant and at any predetermined value.

The heat flow was directed from the moving gas mixture to the plate (heat required for evaporation of the liquid) and supplied by forced convection from the air, moving with the velocity W_x.

The flow of mass (vapour) was directed from the surface of the plate into the surrounding air.

Distribution of temperature, partial pressure and motion velocity were thoroughly measured along the Y-axis and X-axis every 0·1 mm.

As a result it was determined that:

(1) At the evaporation of a liquid from the capillary porous body there are submicroscopical particles of liquid in the boundary layer whose evaporation is going on in the boundary layer itself (volumetric evaporation). The Gukhman number Gu or its modification Gu' as well as the parametric criterion T_r/T_a characterizes the volumetric evaporation of particles of the liquid in the boundary layer. The criterion u/u_c reflects the decrease in intensity of liquid particle emergence out of the porous body to the boundary layer as moisture content of the body decreases.

For well-known assumptions, differential equations of heat and mass transfer in a laminar boundary layer for the incompressible liquid flowing over a flat capillary porous plate will be as follows:

$$\rho w_x \frac{\partial \rho_{10}}{\partial x} + \rho w_y \frac{\partial \rho_{10}}{\partial y} = \frac{\partial}{\partial y}(j_{m1})_y + I_1, \quad (4)$$

$$c_p \rho w_x \frac{\partial t}{\partial x} + c_p \rho w_y \frac{\partial t}{\partial y} = \lambda \frac{\partial^2 t}{\partial y^2} + r I_1, \quad (5)$$

where I_1 is the specific capacity of a vapour source stipulated by evaporation of submicroscopic particles of the liquid in the boundary layer.

(2) In the range of variation of *Re* from 8000 to 100 000 for fine porous bodies, mass transfer constrained with the evaporation of a liquid has no influence upon the curves of air motion velocities distribution in a boundary layer (see Fig. 1). These results corroborate the detailed analysis of heat and mass transfer mechanism at evaporation of liquid from a free surface.

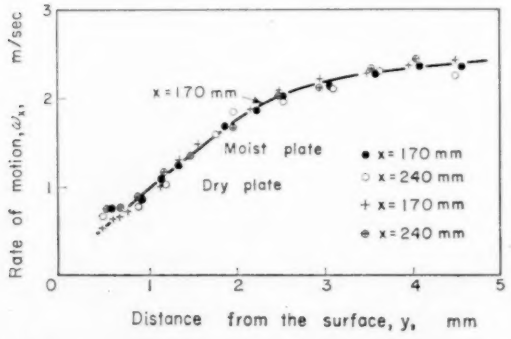

FIG. 1. Heated air flowing over a gypsum plate 350 mm in length ($l = 350$ mm) at $t_a = 35°C$ with the rate of $w_a = 2{\cdot}5$ m/s, temperature of the plate surface is $t_w = 22{\cdot}5°C$.

This analysis is given in a review-article by Polushkin [12].

(3) Water vapour partial pressure cannot be considered as a potential of mass transfer in a boundary layer. This may be confirmed by direct experiments. For example, from distribution curves $t^*(y)$ and $p_1^*(y)$ in Fig. 2 it follows that vapour transfer is going on from the lower partial pressure to the higher one.†

We shall dwell now on mass transfer potential without going into a detailed substantiation of introduction of the substance source I_1 into the differential equation of heat and mass transfer as is given in [11].

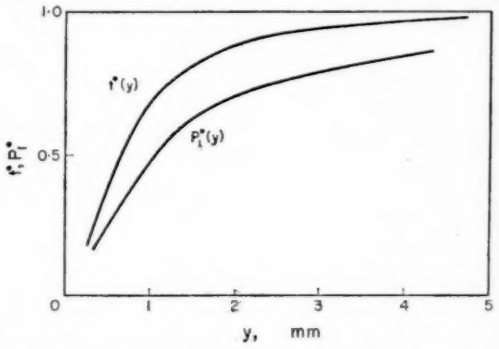

FIG. 2. Curves of distribution of temperature and partial pressure at the distance $x = 170$ mm from the plate edge ($t_a = 36{\cdot}5°C$, $t_w = 27°C$, $w_a = 5{\cdot}8$ m/s).

Usually the partial pressure p_1 or concentration ρ_1 is taken as the transfer potential of a condensing gas (vapour). Then the law of vapour transfer by diffusion in a binary mixture may be expressed in the following form:

$$j_{m1} = - D_{12} \rho \frac{M_1}{M} \nabla p_{10}. \quad (6)$$

Moreover, the value of thermal diffusion flow is assumed to be neglected.

However, the analysis by the methods of thermodynamics of irreversible processes shows that formula (6) is valid for non-condensing

† This somewhat unlooked-for result has been already displayed in earlier works. For example, it follows from Fig. 4, given in the paper "Investigation of drying mechanism of moist materials" [9] that at the distance equal to $y > 2$ mm from the surface of the gypsum plate humidity of air has practically no change, i.e. $\phi = \text{const}$. At the same time it is evident from Fig. 2 of the same paper that the humid air temperature continuously increases as it moves away from the surface up to the distance equal to $y = 10$ mm. Consequently, the vapour partial pressure $p_1 (p_1 = \phi p_s)$ will increase in the range of $2 < y < 10$.

Vol. 3 1961

gas mixtures and is not valid for condensing gases as well as for water vapour.

According to the Onsager theory the molecular transfer of heat and matter is interdependent and described by a system of linear equations. For a gas mixture we have:

$$j_{m1} = \sum_{j=1}^{n-1} L_{ij}(X_j - X_n) + L_{iT}X_T, \qquad (7)$$

$$j_q = L_{TT}X_T + \sum_{j=1}^{n-1} L_{Tj}(X_j - X_n), \qquad (8)$$

where the thermodynamic motive forces X_T and X_j are correspondingly equal to

$$X_T = -\frac{1}{T}\nabla T; \quad X_j = -\nabla T\left(\frac{\mu_j}{T}\right), \qquad (9)$$

j_q and j_{mi} are energy (heat) and mass flow of matter of the ith component conformably, L_{ij} are the Onsager kinetic coefficients.

The chemical potential μ_i of the ith component is the function of the temperature T, the pressure p and $(n-1)$ of the relative concentrations ρ_{i0}. In the absence of external forces and at the constant pressure ($p = \text{const}$) it is possible to write equation (7) as [13]:

$$j_{mi} = \sum_{j=1}^{n-1} L_{ij}\left\{\sum_{k=1}^{n-1}\left[\frac{\partial(\mu_j - \mu_n)}{\partial \rho_{k0}}\nabla\rho_{k0}\right]_T - (Q_j^* - h_j + h_n)\frac{\nabla T}{T}\right\} \qquad (10)$$

where Q_j^* is the heat of transfer equal to the amount of heat transferred per unit of mass of the component j at the constant temperature ($X_T = 0$). The value Q_j^* depends on coefficients L_{iT} and L_{ij} and enters the following relation:

$$L_{iT} = \sum_{j=1}^{n-1} L_{ij}Q_j^*. \qquad (11)$$

As an approximation we shall take humid air for a binary mixture consisting of water vapour ($M_1 = 18$) and dry air ($M_2 = 29$). In this case we may write equation (10) as:

$$j_{m1} = -j_{m2} = -L_{11}\left[\frac{1}{\rho_{20}}\left(\frac{\partial\mu_1}{\partial\rho_{10}}\right)_T\nabla\rho_{10} + (Q_1^* - h_1 + h_2)\frac{\nabla T}{T}\right]. \qquad (12)$$

Approximate evaluation of terms, which are in square brackets of formula (12), applying to the conditions of the experiment (see Fig. 2), shows that the first term is approximately equal to 34 cal/g cm and the second term is about equal to 80 cal/g cm, i.e. 2 or 3 times more. Moreover, the specific enthalpy of superheated vapour was taken equal to $h_1 = 595 + 0{\cdot}47t$ and the value $Q_1^* = L_{iT}/L_{11}$. Since the value $(Q_1^* - h_1 + h_2)$ is negative, then the molecular transfer of vapour is going on in the direction of the temperature gradient, i.e. from the surface of the plate into the surrounding medium.

Therefore, under certain conditions the molecular transfer of vapour is determined not by the drop of the vapour partial pressure but by the temperature drop, i.e. by the potential component μ_1/T the value of which depends on temperature change.

This type of transfer cannot be considered as thermal diffusion of a vapour, since the Soret thermo-diffusion effect in accordance with the system of the Onsager linear equations (7–8) is determined by the value $Q_1^*\nabla T/T$ which, in our case, is small in comparison with the value $(h_1 - h_2)\nabla T/T$.

Under certain conditions it is possible to take the difference between the chemical potentials in a state of saturation μ_{1e} and in a given state μ_1 at one and the same temperature [14] for the potential of vapour molecular transfer in order to obtain approximate calculations:

$$\tilde{\mu}_1 = \mu_{1e} - \mu_1. \qquad (13)$$

For the mixture of ideal gases we have:

$$\mu_1 = \mu_1^0(T) + \frac{RT}{M_1}\ln p_1. \qquad (14)$$

Then we shall get:

$$\frac{\tilde{\mu}_1}{T} = -\frac{R}{M_1}\ln\phi. \qquad (15)$$

Therefore, we may take air humidity for the potential of vapour molecular transfer. For the first time relation (15) based on some other assumptions was proposed in [9]. Here the curves of temperature distribution and of air humidity built in relative values are close to each other (Fig. 3).

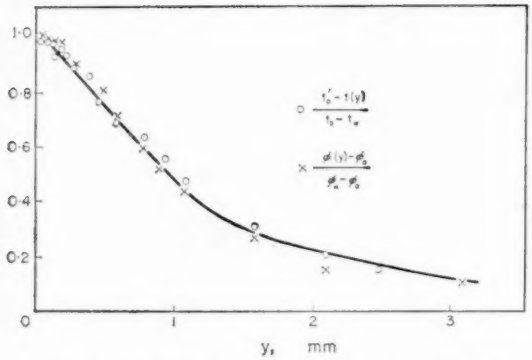

FIG. 3. Curves of distribution of temperature and air humidity in a boundary layer flowing over the moist gypsum plate (t_a = 36·5°C, t_w = 27°C, w_a = 5·8 m/s).

At the isothermal conditions (T = const) we can take the concentration ρ_{10} or the partial pressure p_{10} for the potential of vapour mass transfer. The calculations obtained with these assumptions for the uniform temperature process at small temperature drop in a boundary layer give a satisfactory result.

A new effect based on such a phenomenon as internal friction or viscosity influences vapour molecular transfer in a boundary layer.

Consider a general case of molecular transfer of heat, mass and impulse in the presence of chemical reactions, whose rate we shall designate through Γ_i. Now we write the system of the Onsager linear equations as follows

$$j_q = L_{TT}X_T + \sum_j L_{Tj}X_j, \tag{16}$$

$$j_{mi} = \sum_j L_{ij}X_j + L_{iT}X_T, \tag{17}$$

$$(\mathbf{P} - p\,\mathbf{1})_{ij} = \sum_{kl} L_{ij}^{kl}(X_w)_{kl}, \tag{18}$$

$$\Gamma_i = \sum_j L'_{ij}X_{ci} \tag{19}$$

where

$$X_w = -\nabla\,\mathbf{w}\,; \quad X_{ci} = A_i,$$

A_i is the chemical affinity, p is the statistic pressure which differs from the tensor of pressure $\mathbf{P}$, $\mathbf{1}$ is the single vector.

According to the principal relation of thermodynamics of irreversible processes the components of total flows are the combinations of generalized thermodynamic motive forces.

Motive forces are the tensors of various classes. It is possible to show by virtue of tensor transformations that some combinations cannot take place. If the system is an isotropic one then the combination may occur only between such tensors that have an even difference in classes.

The thermodynamic forces X_T and X_j are the vectors (tensors of the same class), therefore the combination may occur between them. This combination is observed as the Soret effect (thermal diffusion) and the Dufour effect (diffusional thermal conductivity).

The value X_w is the second class tensor and the chemical affinity X_{ci} is the zero class tensor. Consequently, there is no place in isotropic systems for the combination of effects from the action of these forces with diffusion and heat conduction. Therefore, the chemical reaction rate does not involve the emergence of concentration or temperature gradient. However, due to the fact that the difference in classes of X_{ci} and X_w is equal to 2 (an even number), generally speaking, the combination between these two processes is possible in essence. It should not take place in the case when the tensor difference $(\mathbf{P} - p\,\mathbf{1})$ is equal to zero.

For an incompressible liquid when dealing with one-dimensional problems (flat parallel laminar flow of a liquid over a body) internal friction phenomenon may be considered as molecular transfer of kinetic energy of translational movement of the liquid ($\epsilon = \frac{1}{2}\rho\omega_x^2$) along the normal, y, towards the body surface [15]. For one-component system one can write:

$$j_\epsilon = -\nu\nabla(\tfrac{1}{2}\rho w_x^2), \tag{20}$$

where

$$\nabla(\tfrac{1}{2}\rho w_x^2) \equiv \frac{\partial}{\partial y}(\tfrac{1}{2}\rho w_x^2).$$

Therefore, the molecular flow of energy of the regulated motion is directly proportional to the gradient of kinetic energy of translational motion of the liquid, i.e. the motive force of X_ϵ of such transfer is a vector (gradient from scalar).

It follows that in gas mixtures the motive

Vol. 3 1961

force X_ϵ may have a combination with forces X_T and X_j, since they all are the tensors of the same class.

Then equation (17) will be of the following form:

$$j_{mi} = \Sigma L_{ij}X_j + L_{iT}X_T + \sum_j L_{\epsilon ij}X_{\epsilon j}. \qquad (21)$$

From equation (21) it follows that in the process of molecular transfer by kinetic energy of motion at isothermal conditions ($X_T = 0$) the effect of moisture separation must take place; which is analogous to the Soret effect.

We have recognized the separation effect experimentally on a rotating separation column of the Clausius–Dickel type in the absence of temperature gradient (T = const) on molar solutions and binary gas mixtures (solution NaCl and binary mixture H_2 and N_2). This experiment was carried out on a column which was 1550 mm in height and had a clearance of 0·25 mm. We have obtained 70 per cent separation of NaCl at 20 rev/min for 1·5 h.

The separation process was going on at a constant temperature of 25·5°C. We are inclined to explain the separation coefficient increase on a rotating thermal diffusion separation column by this effect. This increase of separation coefficient was observed in [17] on separation of binary mixture n—$CH_3(CH_2)_{14}CH_3$—$C_{10}H_{18}$ (see Fig. 4). The kinetic curves of separation of binary mixture H_2–N_2 under the isothermal conditions on the rotating column at 20, 60 and 100 rev/min are given in Fig. 5.

The relative concentration of nitrogen at the bottom of the column is counted off along the ordinate axis and time in minutes is counted off along the abscissa axis. Fig. 5 shows that in 1 h at n = 100 rev/min 26 per cent of nitrogen separation was obtained.

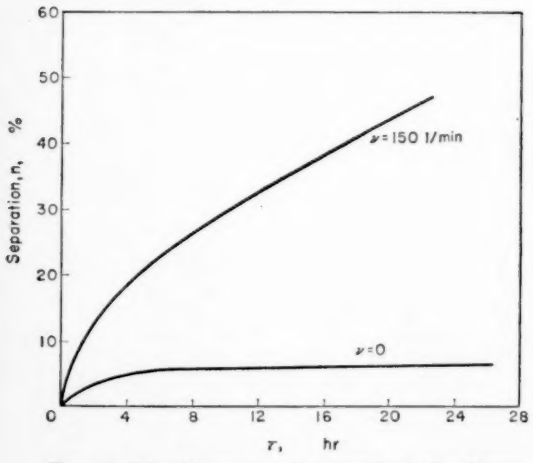

FIG. 4. Kinetic curves of separation of mixture n—$CH_3(CH_2)_{14}CH_3$—$C_{10}H_{18}$ on the rotating thermodiffusional column [17].

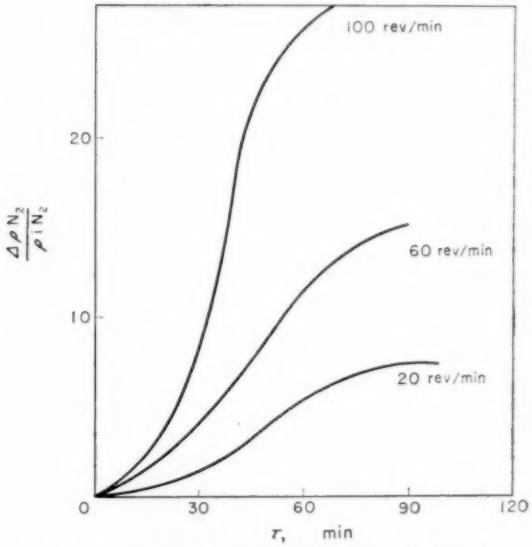

FIG. 5. Curves of kinetics of separation of the binary mixture (N_2–H_2).

From the analysis of experimental data as well as in accordance with equation (20) it follows that mass transfer under the action of the thermodynamic force X_ϵ is directly proportional to the gradient of the square velocity of the flow. The gradient of the square velocity in the separating column at 20 rev/min is approximately equal to 30 m/s² when the radius of the rotating cylinder is equal to 42·3 mm and the clearance is equal to 0·25 mm.

The value of ∇w_x^2 is much greater in a boundary layer. For example, from the curve $w_x(y)$ given in Fig. 1 we obtain ∇w_x^2 which is equal to 750 m/s², i.e. it is 25 times as much. If the rate of air motion is w_a = 5 m/s then the gradient of square velocity in a boundary layer according to the experimental data is equal to 1200 m/s²,

i.e. it is 400 times as much in comparison with the value of Δw^2 in the separating column. Consequently, the value of Δw_x^2 in the boundary layer is greater by 2–3 orders, therefore, the influence of the thermodynamic force $X_{\epsilon i}$ on molecular transfer of matter may be of importance. It is necessary to have the experimental data for the transfer coefficients $L_{\epsilon ij}$ to obtain a final conclusion, then we can calculate in detail the molecular transfer of matter in a boundary layer taking into account all the thermodynamic forces.

Therefore, in the boundary layer flowing over a moist porous plate the water vapour ($M = 18$) will strive (under the action of the force X_ϵ) to move in the direction y, while the air (the reduced molecular weight of which is $M = 29$) will strive to move in the opposite direction, i.e. to the surface of the plate, under certain conditions the motive force X_ϵ may be greater than the force X_y, therefore water vapour will move from the lower partial pressure to the higher, as happened in our experiments.

An analogous phenomenon will occur when air flows over a porous plate with hydrogen supply into the boundary layer. The moving force X_ϵ will intensify the transfer of molecules of hydrogen from the wall to the flow of gas. The contrary phenomenon may be observed with a heavy gas, for example, CO_2 supplied to the boundary layer, through the pores of the plate.

In this case the molecules of CO_2, under the action of the force X_ϵ, will move into the region of low velocities of the regulated air motion, i.e. to the wall surface. Consequently, the force X_ϵ will prevent mass transfer of the cooled gas.

In the general case we shall introduce the corresponding expression from relation (21) instead of the flow j_{m1} into the differential equation of mass transfer (4). In this case differential equation (4) will be interconnected with that of heat transfer.

Interconnection between the phenomena of molecular transfer directly follows from the physical nature of these phenomena. The analytical description of transfer phenomena in their interconnection is possible on the basis of thermodynamics of irreversible processes, the theory of which was founded by Dutch and Belgian physicists (Onsager, de Groot, Prigogine [13, 18]).

The application of thermodynamics of irreversible processes to the transfer phenomena makes it possible not only to define more exactly the existing methods of heat and mass transfer calculation but also to obtain quite new solutions for a number of problems which are of importance in modern engineering.

REFERENCES

1. A. V. Nesterenko, Teplo-i massoobmen pri isparenii zhidkosti so svobodnoi poverkhnosti, *Zh. Tekh. Fiz.* **24**, No. 4 (1954).
2. F. M. Polonskaya, Issledovanie temperaturnogo polya vlazhnykh materialov v protsesse sushki (period postoyanoi skorosti), *Zh. Tekh. Fiz.* **23** 796, 802 (1953).
3. F. M. Polonskaya, Teplo-i massoobmen v period postoyannoi skorosti sushki, *Zh. Tekh. Fiz.* **23**, 802 (1953).
4. P. D. Lebedev, Sushka infrakrasnymi luchami, *Gosenergoizdat* (1954).
5. B. I. Piatachkov, Kinetika sushki kuskovogo torfa, (Dissertatsiya), Moskovskii Energeticheskii Instituut (1954).
6. Sbornik, Teplo-i massoobmen v kapillyarno-poristykh telakh, *Gosenergoizdat* (1957).
7. Sbornik, Teplo-i massoobmen v protsessakh ispareniya, *Izd. Akad. Nauk SSSR* (1958).
8. N. F. Dokuchaev, Primenenie termo-gigrometricheskikh metodov k issledovaniyu protsessa ispareniya, (Dissertatsiya), MTIPP (1951).
9. Sbornik, Teplo-i massoobmen v pishchevykh produktakh, vyp. 6, *Pishchepromizdat* (1956).
10. P. E. Mikhailov, Issledovanie teplo-i massoobmena v protsessakh ispareniya, (Dissertatsiya), Energeticheskii nauchno-issledovatel'skii instituut (1957).
11. A. V. Luikov and I. S. Mel'nikova, Teplo-i massobmen v protsessakh ispareniya, *Izd. Akad. Stroitel'stva i Arkhitektury SSSR* (1959).
12. A. A. Polushkin, O kriteriakh podobia i massoobmena v protsessakh isparenia zhidkosti, *Inzh. Fiz. Zh.* **2**, 129 (1959).
13. S. R. de Groot, Thermodynamics of irreversible process, *Gostekhizdat* (1956).
14. A. M. Rozen, Teoriya razdeleniya izotopov v kolonnakh, *Atomizdat* (1960).
15. A. V. Luikov, Teplo-i massoobmen v protsessakh sushki, *Gosenergoizdat* (1956).
16. A. V. Luikov, K issledovaniju teplo—i massoperenosa v binarnykh gasovykh smesiyakh, *Inzh. Fiz. Zh.* **2**, 20 (1959).
17. L. Sullivan, T. Ruppel and C. Willingham, *Industr. Engng Chem.* **47**, 209 (1955).
18. I. Prigogine, Vvedenie v termodinamiku neobratimykh protsessov, *Inostrannaya Literatura* (1960).
19. P. D. Lebedev, Heat and mass transfer during the drying of moist materials, *Int. J. Heat Mass Transfer*, **1**, No. 4, 294 (1961); Heat and mass transfer between moist solids and air, *Int. J. Heat Mass Transfer*, **1**, No. 4, 302 (1961).

Vol. 3 1961

Int. J. Heat Mass Transfer. Vol. 3, pp. 175–182. Pergamon Press 1961. Printed in Great Britain.

ÉCHANGE DE MASSE ENTRE PHASES CONSTITUÉES PAR DES MÉLANGES

LOUIS KAISER†
Laboratoire de Chimie de l'Ecole Centrale, Paris

(*Received* 23 *January* 1961)

Résumé—L'étude de l'échange de masse entre phases constituées par des mélanges révèle l'existence de domaines de variation de la hauteur globale de l'unité de transfert distincts suivant la nature du régime d'écoulement. En écoulement non purement laminaire, la théorie des films interfaciaux exprime mal les faits.

Par un procédé optique sont mises en évidence des déformations interfaciales que n'envisageait pas la théorie des films.

Pour traduire les écarts à la théorie des films, on propose une fonction γ, susceptible d'une détermination expérimentale et unique pour tout domaine d'écoulement.

Le développement du modèle ondulatoire d'oscillateurs couplés, introduit ici, permet de retrouver par voie théorique la fonction expérimentale γ et d'en préciser l'expression formelle.

Abstract—The study of mass transfer between phases composed of solutions shows the existence of distinct ranges of variation of the height of an overall transfer unit depending on the nature of the flow regime. In flows which are not purely laminar the two film theory does not offer a good explanation of the results.

Interfacial deformations which are not accounted for in the film theory are demonstrated by an optical method.

To explain these deviations from film theory, a function γ is proposed; this function can be determined experimentally and is the same for the flow regime.

The development of a wave model of coupled oscillators, introduced here, makes it possible to find theoretically the experimental function γ and to give a formal expression for the function.

Zusammenfassung—Die Untersuchung des Stoffaustauches zwischen Mischphasen zeigt, dass der Änderungsbereich der gesamten Höhe der Übertragungseinheit je nach dem Strömungszustand verschieden ist. In nicht rein laminarer Strömung gibt die Theorie der Grenzflächenfilme die Tatsachen schlect wieder.

Durch ein optisches Verfahren werden Grenzflächendeformationen nachgewiesen, die die Filmtheorie nicht berücksichtigt hat.

Un die abweichungen auf die Filmtheorie zu übertragen, wird eine Funktion γ angenommen, die sich experimentell bestimmen lässt und die für jeden Strömungsbereich einheitlich ist.

Die Entwicklung eines Wellenmodells mit gekoppelten Schwingern, wie es hier eingeführt wird, erlaubt eine theorietische Deutung der experimentellen Funktion γ, wodurch der formale Ausdruck präzisiert wird.

Аннотация—Исследование явлений массопереноса между фазами смешения показывает, что интенсивность этого продесса зависит от состояния потока. Теория пограничного слоя, вводимая для описания процессов обмена в турбулентном потоке, плохо отражает сущность данного явления.

Оптическим способом доказана деформация пограничной плёнки, которая не была отражена плёночной теорией.

Для учёта этого фактора вводится определяемая экспериментально поправочная функция γ, единая для любого потока.

Для теоретической трактовки введенной функции γ создана волновая модель явления со связанными вибраторами, позволяющая объяснить физическую сущность этой величины и обосновывающая её формальное введение.

† Docteur ès Sciences.

NOTATIONS UTILISÉES

N_G, nombre global d'unités de transfert rapporté aux paramètres de la phase gazeuse;

x et y, composition de la phase liquide et de la phase gazeuse respectivement (fraction molaire du constituant le plus volatil);

y^*, composition de la phase gazeuse en équilibre thermodynamique avec le liquide de composition x;

y_1 et y_2, composition de la vapeur à la base et au sommet de la colonne, respectivement;

H_G, hauteur globale de l'unité de transfert liée aux paramètres de la phase vapeur;

Z, hauteur de la colonne;

G, débit molaire du gaz par unité de section droite de la colonne;

$\mathscr{R}_G$, nombre de Reynolds de la phase gazeuse;

a, aire active de la surface d'échange par unité de volume de la colonne;

$K_G a$, coefficient global de transport (défini dans le texte);

n_D^{25}, indice de réfraction par rapport à la raie D du sodium, à 25°C;

n_1 et n_2, indice de réfraction des mélanges prélevés à la base et au sommet de la colonne, respectivement;

$\gamma = \dfrac{N_G}{N_G^0} = \dfrac{H_G^0}{H_G}$ fonction d'écart proposée; où N_G^0 est le nombre global d'unités de transfert théorique, selon la théorie des films, et H_G^0 la hauteur globale de l'unité de transfert correspondante;

θ et φ, fonctions harmoniques associées au mouvement de la phase vapeur et à celui de l'interface, au moyen des fonctions ψ et τ, respectivement;

Ω et Ω_i, pulsations des fonctions θ et φ, respectivement;

ω, pulsation de couplage;

t, temps.;

$\lambda, k, A, a, \beta, \delta, \epsilon, \Gamma, a', \beta', \delta', \epsilon', \Gamma'$, constantes.

L'ÉTUDE du transport de masse est ici facilitée par l'application de la notion d'unité de transfert [1] à une rectification en tube vide.

La variable fondamentale est le nombre de Reynolds qui caractérise bien la nature de l'écoulement au travers duquel les constituants de chaque phase diffusent. Mais on peut envisager l'influence de cette variable sur le comportement de l'interface qui subit, à partir d'une certaine vitesse, des déformations qui, agitant les phases plus ou moins en profondeur, en facilitent l'échange des constituants.

EXPRESSIONS DISTINCTES ET EXPRESSIONS UNIFIÉES DE L'ÉCHANGE DE MASSE POUR DIVERS ÉCOULEMENTS

Expressions distinctes

Définition et détermination des unités de transfert. Le nombre global N_G d'unités de transfert pour la phase vapeur [1] est défini par l'intégrale suivante:

$$N_G = \int_{y_1}^{y_2} \frac{\mathrm{d}y}{y^* - y}$$

dans laquelle y^* est la composition de la vapeur qui serait en équilibre thermodynamique avec le liquide de composition x, en un point donné de la colonne où la composition réelle de la vapeur est y. Les limites d'intégration y_1 et y_2 représentent les compositions respectives de la vapeur à la base et au sommet de la colonne. Nous exprimerons les compositions en fraction molaire du constituant le plus volatil.

La hauteur globale H_G de l'unité de transfert liée aux paramètres de la phase vapeur:

$$H_G = \frac{Z}{N_G} = \frac{G}{K_G a}$$

s'exprime [2] en terme résistance au transport $1/K_G a$, en appelant:

Vol. 3 1961

Z, la hauteur de la colonne;

G, le débit molaire de la phase gazeuse par unité de section droite de la colonne;

$(K_G a)$, le coefficient global de transport qui est le nombre de molécules diffusées par unité de temps, unité de volume et unité de fraction molaire où apparaît l'aire a de la surface d'échange par unité de volume;

N_G, le nombre global d'unités de transfert.

La quantité N_G est obtenue à partir du diagramme expérimental d'équilibre liquide–vapeur qui relie y^* à x et à partir de la courbe opératoire qui lie x à y. (Sous reflux total nous aurons $x = y$.)

Dans la détermination pratique de l'enrichissement (y_1, y_2) on remplace les compositions des mélanges par les indices de réfraction correspondants, après avoir établi une courbe d'étalonnage.

Evolution expérimentale de la hauteur globale de l'unité de transfert avec le régime d'écoulement. A partir des données expérimentales de l'equilibre liquide–vapeur [3], nous avons dressé, pour un mélange de 1,2-dichloréthane et de toluène, le Tableau 1 de valeurs de l'intégrale indéfinie $\int dy/(y^* - y)$ en fonction de l'indice de réfraction pour la raie D à 25°C.

Tableau 1

n_D^{25}	$\int \frac{dy}{y^* - y}$
1,4912	0
1,4890	0,75
1,4868	1,20
1,4845	1,45
1,4822	1,76
1,4798	2,05
1,4774	2,31
1,4750	2,57
1,4727	2,82
1,4703	3,08
1,4678	3,34
1,4665	3,62
1,4625	3,92
1,4598	4,25
1,4570	4,62
1,4542	5,06
1,4513	5,61
1,4484	6,33
1,4456	7,62
1,4426	∞

Le pouvoir de résolution $\int_{y_1}^{y_2} dy/(y^* - y)$ se déduit de la différence des valeurs du tableau qui correspondent aux indices des mélanges prélevés au sommet (n_2) et à la base (n_1) de la colonne expérimentée, voisine de celle de Chahvekilian [4], où les débits sont mesurés avec un chronomètre au 1/10 de seconde et convertis en nombres de Reynolds $\mathscr{R}_G$ de la phase gazeuse.

D'où le Tableau 2 (a) des résultats relatifs à une composition moyenne de rectification de 0,65 et leur traduction graphique (Fig. 1).

Tableau 2 (*a*) *et* (*b*)

(a) et (b) $\mathscr{R}$	n_1	n_2	N_G	(a) (b) H_G	(b) γ
1070	1,4726	1,4543	2,21	31,7	0,88
1145	1,4726	1,4540	2,26	31,0	0,96
1150	1,4730	1,4536	2,40	29,2	1,02
1160	1,4730	1,4546	2,22	31,6	0,96
1200	1,4730	1,4525	2,60	27,0	1,15
1235	1,4736	1,4550	2,23	31,4	1,02
1360	1,4680	1,4526	2,04	31,4	1,01
1377	1,4626	1,4543	2,19	32,0	1,11
1480	1,4680	1,4533	1,90	36,8	1,04
1530	1,4680	1,4539	1,80	39,0	1,02
1740	1,4683	1,4555	1,62	43,2	1,05
1740	1,4683	1,4550	1,70	41,2	1,10
1819	1,4686	1,4560	1,60	43,8	1,12
2030	1,4683	1,4553	1,64	42,7	1,23
2058	1,4695	1,4566	1,52	46,1	1,16
2200	1,4690	1,4563	1,50	46,7	1,22
3179	1,4690	1,4576	1,31	53,5	1,54
3300	1,4693	1,4583	1,26	55,6	1,54
3500	1,4669	1,4569	1,18	59,4	1,53
3780	1,4673	1,4570	1,20	58,4	1,68
4448	1,4690	1,4583	1,16	60,5	1,91
4790	1,4673	1,4575	1,14	61,5	2,01
5208	1,4673	1,4576	1,12	62,5	2,16
6549	1,4673	1,4580	1,06	66,1	2,58
6875	1,4669	1,4576	1,08	65,0	2,74
7050	1,4693	1,4600	1,04	67,4	2,72
7375	1,4676	1,4583	1,04	67,4	2,85
7950	1,4673	1,4585	1,00	70,0	2,96
8100	1,4669	1,4579	1,04	67,4	3,10
8600	1,4669	1,4580	1,02	68,6	3,26
8800	1,4673	1,4576	1,02	68,6	3,34
9000	1,4693	1,4603	1,00	70,0	3,34
9310	1,4676	1,4586	1,00	70,0	3,46

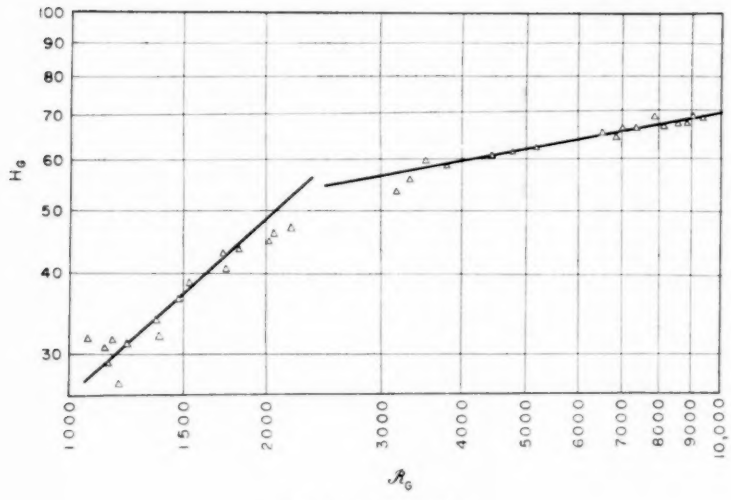

FIG. 1. $H_G = f(\mathscr{R}_G)$.

On déduit de ces résultats les expressions empiriques de la variation de la hauteur globale de l'unité de transfert H_G en fonction du nombre de Reynolds.

(1) *Pour l'écoulement laminaire:*

$$H_G = 0{,}0547 \,.\, \mathscr{R}_G^{0,89}. \qquad (1)$$

L'exposant de $\mathscr{R}_G$ est voisin de l'unité. Ceci concorde assez avec certains résultats expérimentaux et théoriques [5–8].

(2) *Pour l'écoulement turbulent:*

$$H_G = 13{,}8 \,.\, \mathscr{R}_G^{0,19}. \qquad (2)$$

Cette loi s'accorde avec d'autres relations [1, 5, 9–12].

De ces *deux types d'expressions distinctes* nous avons pu dégager [13] l'existence d'une structure commune cependant insuffisante pour représenter, *sous la même forme*, le domaine de transition qui apparaît entre $\mathscr{R}_G = 2000$ et $\mathscr{R}_G = 3600$, dans cette étude.

N'est-il pas possible de réunir ces *trois domaines* en une seule expression sous une notion continue?

Expressions unifiée ecarts à la théorie des films

La théorie des films [14] localise toute la résistance au transport de masse dans deux régions situées de part et d'autre de l'interface, régions appelées films interfaciaux.

Le procédé que nous proposons ici permet la détermination d'une loi empirique de la variation des écarts à la théorie des films, sans formuler d'abord d'hypothèse sur la nature de tels écarts. Plus loin, une interprétation quantitative sera abordée en proposant alors la notion d'oscillateurs couplés.

Représentation des écarts à la théorie des films interfaciaux. Introduisons le quotient γ du nombre d'unités de transfert expérimental N_G par le nombre d'unités de transfert N_G^0 que donne la rectification quand la théorie des films est vérifiée. Considérons les hauteurs H_G^0 et H_G de l'unité de transfert qui correspondent respectivement à N_G^0 et N_G. On a évidemment, pour une colonne donnée:

$$\gamma = \frac{H_G^0}{H_G}.$$

Suivant la théorie des films [2], H_G^0 est de la forme $k\mathscr{R}_G$ ($k = C^{te}$) relativement vérifiée par les données expérimentales pour le domaine laminaire d'écoulement.

Dans ce domaine nous avons, en effet, à partir de $\mathscr{R}_G = 1000$, l'expression réelle (1).

Admettons que nos résultats ne divergent de

Vol. 3 1961

façon sensible des valeurs théoriques qu'à partir de $\mathscr{R}_G = 1000$. Nous aurons encore, à ce régime, égalité entre notre expression empirique (1) et l'expression théorique $H_G^0 = k\mathscr{R}_G$. Ceci conduit à adopter, pour le mélange et le tube vide envisagés, l'expression conforme à la théorie des films:

$$H_G^0 = 26 \,.\, 10^{-3} \,.\, \mathscr{R}_G. \qquad (3)$$

Loi de variation de la fonction γ avec le régime d'écoulement. L'expressions (3) de H_G^0 et nos données expérimentales de H_G (Tableau 2a) relatives à diverses valeurs de $\mathscr{R}_G$ permettent le calcul de la fonction γ (Tableau 2b).

D'où la représentation graphique suivante (Fig. 2) de la variation des écarts à la théorie des films, qui présente l'allure d'une hyperbole dont nous établirons l'equation théorique, en proposant une interprétation ondulatoire de ces écarts.

Analyse de la courbe et conclusion. (a) L'existence d'expressions (1) et (2) de la hauteur de l'unité de transfert, distinctes suivant que l'écoulement est laminaire ou turbulent; *cette discontinuité* s'explique ici par *la variation continue des écarts à la théorie des films interfaciaux.* (b) On peut conserver la structure formelle de la théorie des films si l'on remplace H_G par le produit γH_G. Notre fonction γ joue ici le même rôle que le coefficient d'activité dans la thermodynamique des mélanges en phase fluide.

ASPECT ONDULATOIRE DES PHÉNOMÈNES

La théorie des films [14] n'envisage aucune *perturbation possible* à la surface de séparation des phases en présence.

Examinons ce que révèle une étude du comportement de l'interface.

Caractérisation du profil interfacial

Pour mettre en évidence le profil de l'interface liquide–vapeur, nous avons imaginé le procédé suivant:

La colonne en verre est entourée d'un écran opaque (0) sur lequel nous avons pratiqué une ouverture annulaire (A) (Fig. 3).

Le système optique permet d'éclairer la colonne par un faisceau de rayons quasi parallèles à l'axe de symétrie de la colonne. La lumière frappe l'interface sous une incidence quasi rasante. Les rayons qui émergent au travers de l'espace annulaire (A), sont recueillis sur un écran d'observation (E).

En régime laminaire lent on observe un anneau lumineux. *Si l'interface présente* des déformations, on doit observer des modifications de l'anneau lumineux.

Résultats de l'expérience. L'idéal eût été de filmer le phénomène. Nous avons dû procéder par photographie, en faisant de la pose. Une interprétation est possible, si l'on adopte, pour une même série d'expériences à divers régimes d'écoulement, un même temps de pose. On

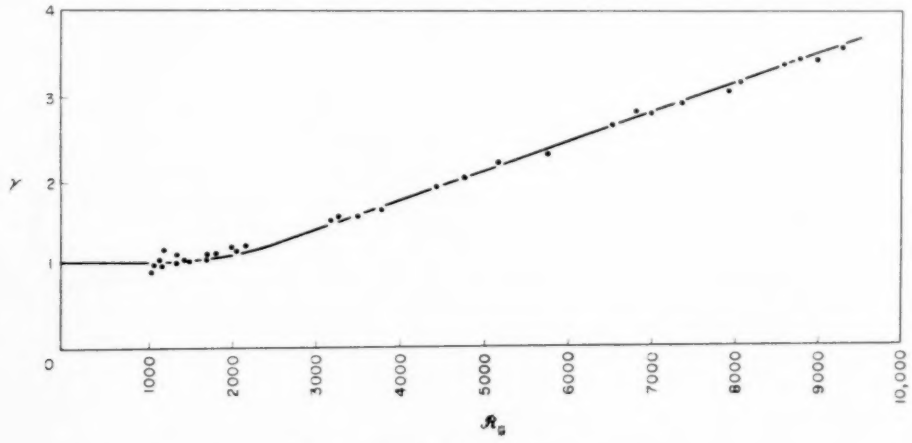

FIG. 2. Variations de la fonction d'écart γ.

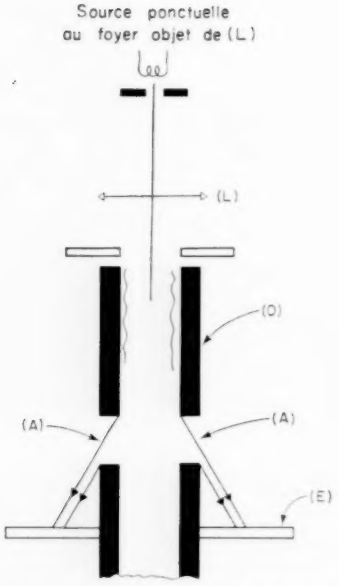

FIG. 3. Dispositif de mise en évidence des déformations interfaciales.

impressionne le papier sensible disposé sur l'écran d'observation.

En absence de tout écoulement, on obtient un anneau caractérisé par un certain éclairement. *Lorsque l'interface oscille*, deux halos entourent l'anneau initial.

(a) L'intensité de tels halos enregistre une valeur moyenne des positions successivement occupées par l'anneau oscillant pendant la pose.

(b) Ces halos donnent une image de l'amplitude des déformations: ils s'élargissent à mesure que le régime d'écoulement croît. On arrive finalement à un éclairement uniforme.

Nous présentons ci-dessous deux enregistrements du phénomène (Figs. 4 et 5).

Interprétation ondulatoire des écarts à la théorie des films

Envisageant les perturbations observées à l'interface, nous allons substituer, au schéma statique de la théorie des films, un modèle ondulatoire d'oscillateurs couplés.

L'état de l'interface est, en première approximation, uniquement conditionné par le régime d'écoulement des phases, donc par le nombre de Reynolds. Nous supposerons qu'en régime permanent, l'interface, soumis à des déformations, se comporte comme un système oscillant, sous l'action du régime d'écoulement assimilé à un oscillateur qui impose les vibrations interfaciales de couplage.

Pour vérifier une telle hypothèse, nous poserons le système suivant:

$$\Omega^2 = \mathscr{R}_G \,.\, \psi \tag{4}$$

$$\omega^2 = \gamma \,.\, \tau \tag{5}$$

$$\Omega_i^2 = \lambda \,.\, \tau \tag{6}$$

qui exprime que:

(a) *Au nombre de Reynolds $\mathscr{R}_G$ mesurable, nous associons une onde de pulsation Ω au moyen de la fonction ψ dont l'équation* (4) *est l'équation de définition.*

(b) *A l'effet de la perturbation interfaciale* (exprimé ici par le terme adimensionnel γ proposé plus haut) *est associée une onde de pulsation ω (de couplage)* au moyen de la fonction τ, définie par l'équation (5), analogue à la fonction ψ.

(c) La pulsation Ω_i de l'interface oscillant, *pris isolément* sera exprimée par l'équation (6); où λ *est une constante.*

Soient θ et φ les fonction harmoniques correspondant respectivement au mouvement de la phase gazeuse et à l'interface oscillant, liées aux pulsations des relations (4) et (6). Les équations différentielles générales du mouvement sont, pour les deux oscillateurs couplés:

$$\begin{cases} \alpha \dfrac{d^2\theta}{dt^2} + \beta \dfrac{d^2\varphi}{dt^2} + \delta \dfrac{d\theta}{dt} + \Gamma\theta = \epsilon \dfrac{d\theta}{dt}; \\ \alpha' \dfrac{d^2\varphi}{dt^2} + \beta' \dfrac{d^2\theta}{dt^2} + \delta' \dfrac{d\varphi}{dt} + \Gamma'\varphi = \epsilon' \dfrac{d\varphi}{dt}. \end{cases}$$

Nous supposerons qu'en régime de fonctionnement stationnaire (donc entretenu):

(a) L'amortissement est compensé par l'entretien du mouvement ($\delta = \epsilon$, $\delta' = \epsilon'$).

(b) L'action mutuelle est parfaite ($\beta = \beta'$) et le terme α' doit son existence au régime d'écoulement ($\beta = \beta' = \alpha'$). D'où le système:

$$\begin{cases} \dfrac{d^2\theta}{dt^2} + \dfrac{\beta}{\alpha} \dfrac{d^2\varphi}{dt^2} + \dfrac{\Gamma\theta}{\alpha} = 0; \\ \dfrac{d^2\varphi}{dt^2} + \dfrac{d^2\theta}{dt^2} + \dfrac{\Gamma'}{\alpha'} \varphi = 0. \end{cases}$$

Vol. 3 1961

ol.
3
961

f. p. 180

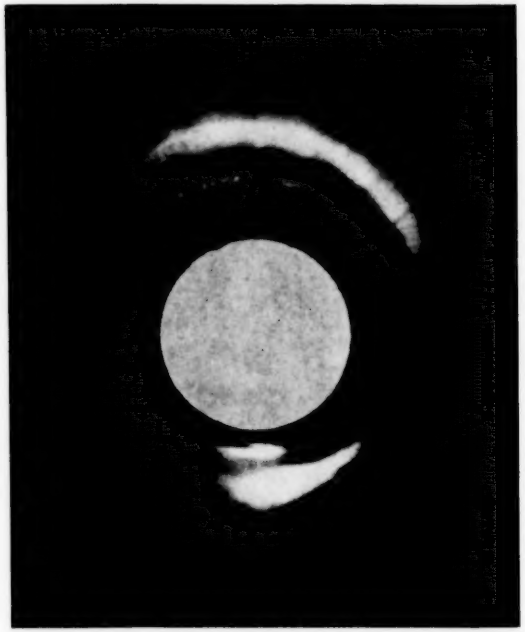

FIG. 4. Deformations interfaciales

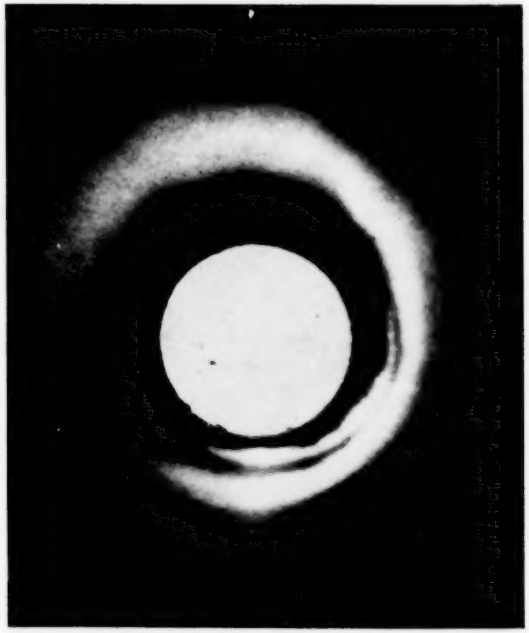

FIG. 5. Deformations interfaciales

Vol.
3
1961

Il est aisé de voir que Γ/a représente le carré de la pulsation Ω propre au régime d'écoulement. De la même façon symétrique, on a: $\Gamma'/a' = \Omega_i^2$.

D'où le nouveau système:

$$\begin{cases} -\theta\omega^2 - A\omega^2 q + \Omega^2\theta = 0 \\ -q\omega^2 - \omega^2\theta + \Omega_i^2 q = 0 \end{cases}$$

en posant $\beta/a = A$, analogue à un coefficient de couplage. Le terme ω est la pulsation commune prise par les deux systèmes envisages, déjà définie par l'équation (5). On en déduit:

$$(\Omega^2 - \omega^2)(\Omega_i^2 - \omega^2) = A\omega^4.$$

La réciprocité de l'action mutuelle entre les deux systèmes couplés exige, sinon l'égalité des fonctions ψ et τ, du moins la proportionnalité $\psi = k\tau$. D'où, en revenant aux équations de définition:

$$(k\mathscr{R}_G - \gamma)(\lambda - \gamma) = A\gamma^2.$$

On déterminera λ en écrivant que l'écart à la théorie des films, dû aux oscillations de l'interface, est négligeable lorsque $\mathscr{R}_G$ tend vers zéro: $\mathscr{R}_G = 0$; $\gamma = 1$. D'où la relation:

$$(\gamma - k\mathscr{R}_G)(\gamma + A - 1) = A\gamma^2.$$

Les valeurs du tableau suivant:

$\mathscr{R}_G$	1150	8800	Mélange 1,2-dichloréthane-toluène
γ	1,02	3,34	

permettent, pour le système envisagé, de préciser k et A. En rapportant ces valeurs à l'échelle graphique de la Fig. 2 on a:

$$A = 0{,}03; \quad k = 0{,}36.$$

L'étude mathématique de la courbe:

$$(\gamma - 0{,}36\mathscr{R}_G)(\gamma - 0{,}97) = 0{,}03\gamma^2$$

montre qu'il s'agit d'une hyperbole d'asymptotes:

$$\gamma = 0{,}97; \quad \gamma = 0{,}37\mathscr{R}_G + 0{,}03.$$

Le centre est défini par:

$$\gamma = 0{,}97; \quad \mathscr{R}_G = 2{,}55.$$

Verification expérimentale de la théorie proposée. Notre courbe théorique se superpose bien à la courbe expérimentale d'écarts (Fig. 2) et nous retrouvons par voie théorique la loi de variation des écarts à la théorie des films, comme le montre la représentation graphique (Fig. 6).

Compte tenu de l'échelle graphique, le centre de l'hyperbole correspond à la zone de transition localisée plus haut entre $R_G = 2000$ et $R_G = 3600$.

Les deux formes empiriques de la hauteur de l'unité de transfert (1) et (2) correspondent aux régions asymptotiques de la loi présentée. Il est un fait que les auteurs ont seulement vérifié ce type d'expression en régime turbulent extrême [1, 5, 9–12] et laminaire pur [5–8], le

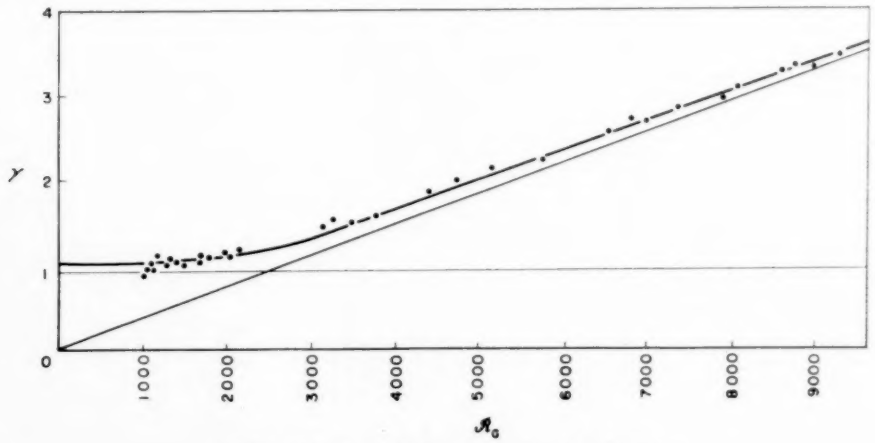

FIG. 6. Courbe theorique de la fonction d'écart γ.

domaine de transition échappant à ce genre de représentation.

Conclusion sur la théorie proposée

Sans sous-estimer la classification en régime d'écoulement laminaire et en régime d'écoulement turbulent, nous pensons qu'il est commode de parler d'un régime oscillant et d'un régime non oscillant de l'interface. Le régime non oscillant de l'interface correspond au *seul* régime laminaire d'écoulement où la théorie des films est satisfaite. Le régime oscillant de l'interface s'installe progressivement, à partir d'une certaine vitesse, dans l'écoulement laminaire: la théorie des films est satisfaite *de manière approchée*. La fréquence des oscillations augmente rapidement, à partir de la zone de transition, au-delà de laquelle les *écarts importants* à la théorie des films vont croissant.

Le modèle proposé permet la formulation d'un transport de masse, essentiellement variable avec le régime d'écoulement, en rapportant ce transport à une expression de référence $H_G^0 = k\mathscr{R}_G$ résultant de la théorie des films.

Plus généralement, si la théorie des films avait été mal vérifiée dans l'écoulement laminaire, nous aurions pu choisir, comme expression de référence, la loi expérimentale $H_G^0 = k\mathscr{R}_G^a$ du transport en écoulement laminaire où a eût alors pu être bien différent de l'unité.

BIBLIOGRAPHIE

1. T. H. Chilton et A. P. Colburn, Distillation and absorption in packed columns. *Industr. Engng Chem.* **27**, 255 (1935).
2. J. M. Coulson et J. F. Richardson, *Chem. Engng (Distillation)* t II, Pergamon Press, Paris (1955).
3. C. A. Jones, E. M. Schoenborn et A. P. Colburn, Equilibrium still for miscible liquids. *Industr. Engng Chem.* **35**, 666 (1943).
4. E. Chahvekilian, Contribution à l'étude de la distillation et à l'échange de matière entre phases. *Revue de l'Inst. Franç. du Pétrole*, XIII, **5**, 782 et **6**, 997 (1958).
5. A. Bogner, Diplôme d'études supérieures. Paris (1957).
6. L. B. Bragg, Laboratory columns for close fractionation. *Industr. Engng Chem. Anal.* **11**, 283 (1939).
7. A. Rose, Distillation efficiency in 3- and 6-mm fractionating columns. *Industr. Engng Chem.* **28**, 1210 (1936).
8. J. W. Westhaver, Theory of open-tube distillation columns. *Industr. Engng Chem.* **34**, 126 (1942).
9. K. S. Chari et J. A. Storrow, Film resistances in fractionation. *J. Appl. Chem.* **1**, 45 (1951).
10. T. H. Chilton et A. P. Colburn, Mass transfer coefficients. *Industr. Engng Chem.* **26**, 1183 (1934).
11. E. R. Gilliland et T. K. Sherwood, Diffusion of vapors into air streams. *Industr. Engng Chem.* **26**, 516 (1934).
12. H. F. Johnstone et R. L. Pigford, Distillation in a wetted-wall column. *Trans. Amer. Inst. Chem. Engrs*, **38**, 25 (1942).
13. L. Kaiser, Transfert de matière entre phase liquide et phase vapeur dans une colonne de rectification. *C.R. Acad. Sci., Paris*, **248**, 2873 (1959).
14. W. K. Lewis et W. G. Whitman, Principles of gas absorption. *Industr. Engng Chem.* **16**, 1215 (1924).

Vol. 3 1961

Int. J. Heat Mass Transfer. Vol. 3, pp. 183–187. Pergamon Press 1961. Printed in Great Britain.

INVESTIGATION METHODS INTO FLOW IN A BOUNDARY LAYER WITH A LONGITUDINAL PRESSURE GRADIENT

A. M. MKHITARYAN, V. Y. FRIDLAND, V. S. MAKSIMOV and S. D. LABINOV
Polytechnical Institute, Kiev, the Ukrainian SSR, U.S.S.R.

(*Received* 2 *February* 1961)

Abstract—The paper deals with a method and results of investigation of a boundary layer with a longitudinal pressure gradient. A two-dimensional problem of the external flow round a body is modelled in a channel of a "tray" type, one wall of which represents an investigated profile.

Résumé—Cet article traite d'une méthode d'étude d'une couche limite avec gradient de pression et des résultats obtenus. Le problème bidimensionnel de l'écoulement autour d'un corps est étudié dans une soufflerie du type "tray" dont une des parois est constituée par le profil à étudier.

Zusammenfassung—Es wird die Methode und das Ergebnis der Untersuchung einer Grenzschicht mit einem Druckgradienten in Längsrichtung besprochen. Ein zweidimensionales Problem der äusserem Umströmung eines Körpers wird in einem Kanal vom "Schalen"-Typ modellmässig so nachgebildet, dass eine Kanalwand das untersuchte Profil darstellt.

Аннотация—В статье излагаются методика и результаты исследования пограничного слоя с продольным градиентом давления. Двухмерная задача внешнего обтекания тела имитируется в канале типа "лоток", одна стенка которого представляет собой изучаемый профиль.

ol.
3
961

In the presence of a longitudinal pressure gradient the boundary layer flow follows curvilinear surfaces, for example, aerodynamic profiles used in aviation and for submerged wings of ships.

The whole picture of the flow profile depends on the character of the boundary layer. The non-separated flow profile is the most important condition for obtaining qualitative aerodynamic properties of the profile. Usually, the non-separated flow is disturbed at large attack angles, this is characteristic for aviation, e.g. for flight-landing regimes. The problem of the increase both in the attack angle and, consequently, in the lifting power is of great importance in water transport on ships with submerged wings. The annihilation of separated flow is achieved with the help of different ways of boundary-layer regulation.

For investigation of the ways of boundary-layer regulation in the presence of a longitudinal pressure gradient we developed and mastered special working sections of two types on an aerodynamic stand.

When investigating aerodynamic parameters of a boundary layer the gradient flow was created above a flat surface (Fig. 1a).

The air stream flowing from a rectangular nozzle passes through a tray formed by the blowed flat element, two flat lateral surfaces and by an upper curvilinear plate whose corresponding form creates the pressure distribution character required.

Such a type of working section allows one to carry out a precise experiment and when measuring makes it possible to single out the most important phenomena from a complicated series. Moreover, the use of a micrometer screw is simplified since the blowed flat element may serve over its whole area as a base for counting out a vertical co-ordinate.

Pressure curves along the flat surface compared well with a modelled surface of a wing profile. (Fig. 1b).

The experiment, if thoroughly carried out, allows one to obtain almost a complete coincidence of pressure curves.

In the working section there is a strongly

N

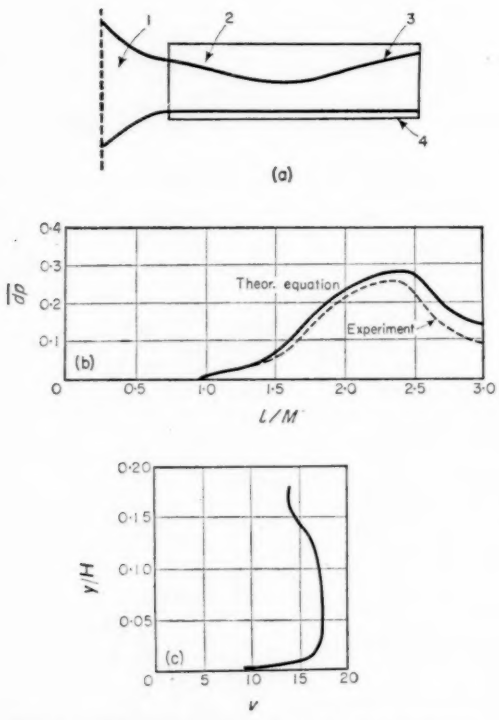

FIG. 1. Working section with longitudinal pressure gradient above a flat surface. (a) Scheme of working section: 1—nozzle, 2—lateral walls of tray, 3—upper curvilinear plate, 4—blowed flat element. (b) Pressure gradient curve. (c) Velocity curve in compressed area of working section.

shaped core of constant velocities. The velocities were measured in some cross-sections so that two-dimensional flow conditions could be maintained. Measurements showed (Fig. 1c) that over the whole working section boundary layers do not close up near the blowed plane and the upper curvilinear surface.

For the direct investigation of flow in the boundary layer above a curvilinear surface we investigated another type of working section, i.e. flow above the wing. The stream was limited by the curvilinear surface on one side and by the flat walls of the tray on two lateral sides.

The experiment showed that with nozzle dimensions of 190 × 380 mm the core of the constant velocities is preserved for a length of

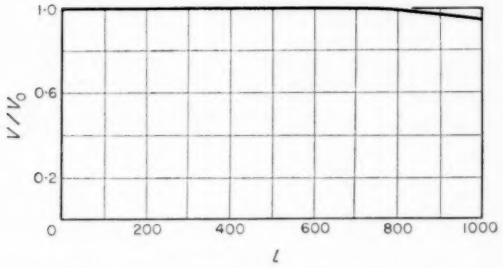

FIG. 2. Velocity curve in a core of constant velocities in a tray above a wing.

about 2 m (Fig. 2), this allows one to investigate the gradient flow under conditions imitating the flow of an infinite flat-parallel flow over a wing. The velocity remains practically invariable over the whole length of the tray.

Curves of the velocity within the boundary layer in the tray, which are plotted according to experimental data, coincide well with analogous curves obtained by other authors in a wind tunnel of an ordinary type (Fig. 3).

For a solution of the problem of whether the form of the working section influences the character of flow turbulence, measurements of pulsations were carried out with the help of an electrothermo-anemometer near the curvilinear surface. The results of measurements (Fig. 4) cause one to believe that a longitudinal pulsation component is invariably preserved in the flow core but while approaching the curvilinear surface the pulsations increase both in relative and in absolute calculus.

The pressure distribution on the wing surface was measured in the range of attack angles from 0° to 12° and in the range of velocities from 30 to 120 m/s.

At different attack angles and at the constant velocity $v = 120$ m/s the pressure curves give a high rate of coincidence with data known in the literature and obtained for general conditions (Fig. 5). In our experiment a wing of 11 per cent thickness with a maximum at a distance of 0·4 l from the nose was blown.

The experimental points of a pressure value ($\overline{\Delta p} = 2\Delta p/\rho v^2$) which are obtained for equal velocities practically coincide (Fig. 6). One may conclude that the distribution of pressure is

Vol. 3 1961

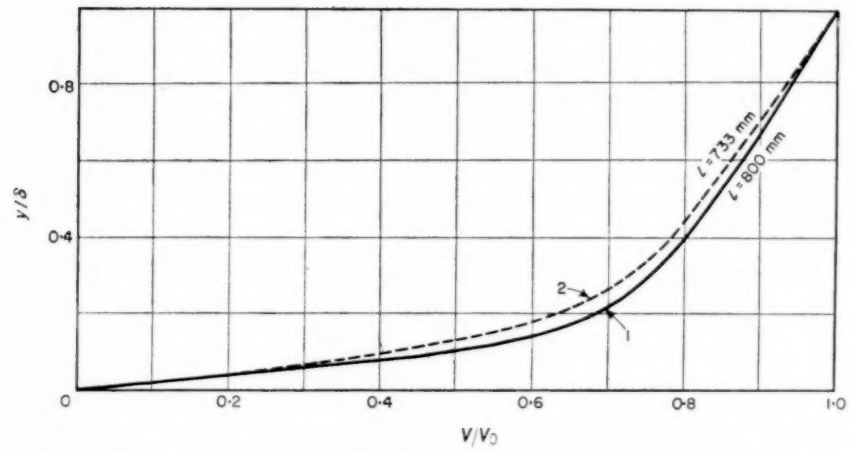

FIG. 3. Velocity curve in a boundary layer above a wing: 1—measurements made in the Kiev Polytechnical Institute: 2—measurements made in Göttingen.

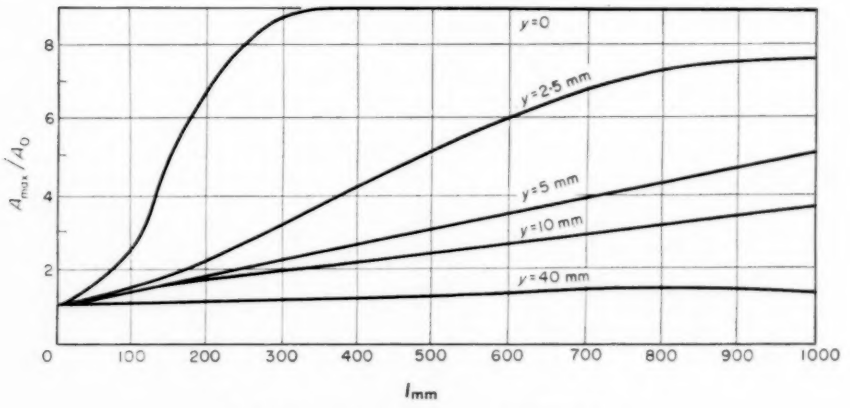

FIG. 4. Distribution of pulsations above a wing.

preserved in rather a wide range for different outflow velocities from the nozzle.

At large attack angles a separation zone was determined with the help of the electrothermo-anemometer by the screen of a cathode oscillograph. When the probe of the electro-thermo-anemometer reaches the separation zone, the amplitudes and frequencies of pulsations increase sharply. In this way the separation zone is determined rather precisely and simply.

Results of the experimental investigation of a boundary layer at gradient flow in the tray show that the application of new types of working section allows one:

(1) To investigate a two-dimensional problem imitating the flow profile by the infinite flow.

(2) To carry out an experiment on a model whose length exceeds by about 10 times the dimensions of the nozzle.

(3) To carry out an experiment at the minimum possible power of delivery pumps. Thus, for example, technical possibilities of the stand made in the Kiev Polytechnical Institute (compression ratio 1:8; mass flow rate 8 kg/s)

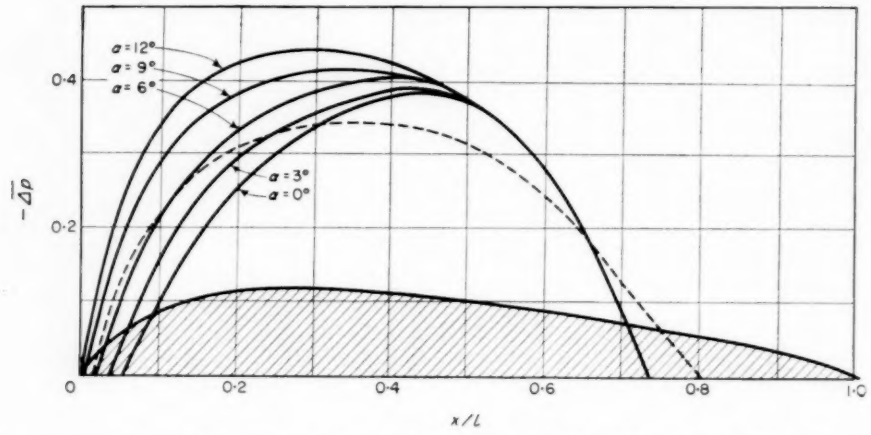

FIG. 5. Pressure curves above a wing both at velocity of running flow (120 m/s) and different attack angles. Pressure curve is shown by a dashed line for blowing of an approximately analogous profile in a wind tunnel of an ordinary type.

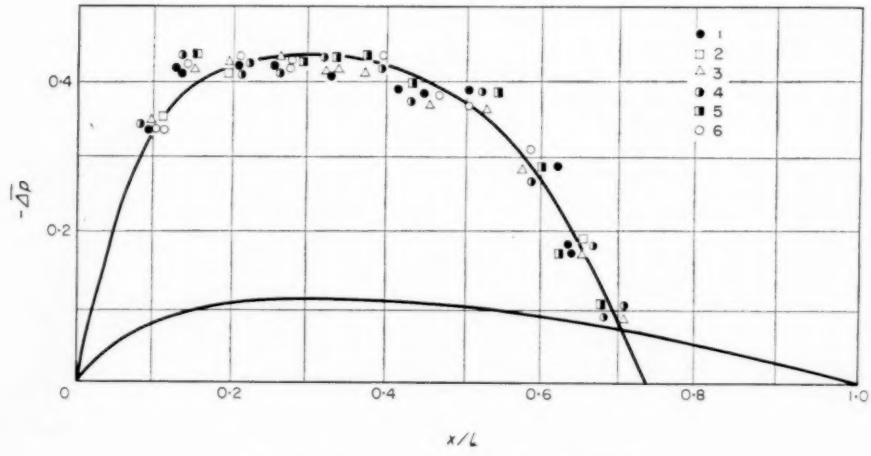

FIG. 6. Pressure curve at attack angle of 12°.
1—v = 43 m/s; 2—v = 68 m/s; 3—v = 88 m/s; 4—v = 92 m/s; 5—v = 105 m/s; 6—v = 114 m/s.

allows one to carry out investigations at velocities up to 120 m/s, at Reynolds numbers up to 4×10^7 and at the chord length of a profile of about 2 m.

Besides the electrothermo-anemometer, a micrometer screw which was remote-controlled and with three-dimensional travel was applied. The travel length of the micrometer screw carriage was 2000 mm along the working section, 400 mm across and 400 mm along the vertical line. The measurement accuracy of horizontal displacements was 0·5 mm and of vertical displacements 0·05 mm. The displacement was carried out along micrometer screws by the rotation of nuts with the help of reversible motors PD-09. The displacement was controlled both visually and remotely by a rheo-chord scheme.

In the vertical screw there was a longitudinal axial hollow into which was inserted the probe of

Vol. 3 1961

the electrothermo-anemometer and pneumo-packings to measure velocity and static pressure.

On the two types of working section described above the heavy electric and magnetic fields, resonators and ultrasound were applied as a physical influence upon a turbulent layer. When applying the first method, the separation point of the turbulent boundary layer is displaced on account of its additional turbulization; the effect due to the application of the second method is explained by the decrease in the second (volumetric) air viscosity when the ultrasound is passing; when applying the third method the ions, formed by natural or artificial ionization, are accelerated along a flow communicating energy to the air in a region near the wall and thus eliminating the separation.

At present, investigations of qualitative and quantitative properties of the mentioned methods of boundary-layer regulation are being carried out.

ol.
3
961

Int. J. Heat Mass Transfer. Vol. 3, pp. 188–197. Pergamon Press 1961. Printed in Great Britain.

ON AERODYNAMICS OF RAREFIED GASES AND PROBLEMS OF HEAT TRANSFER

A. S. PREDVODITELEV

Department of Molecular Physics, Moscow State University, U.S.S.R.

(*Received* 23 *January* 1961)

Abstract—Poor agreement between experimental data and theoretical expressions for acoustic dispersion in a rarefied gas which are obtained on the basis of the Burnett and super-Burnett solutions of the Boltzmann equation is shown in the present paper; the classical theory based on the Navier–Stokes hydrodynamics brings more successful results. The above-mentioned appears to be valid also when considering a temperature jump and slip. Contradictions between the Euler equations and the molecular-kinetic theory are also revealed while considering the conformability of these equations to the rarefied gas. The generalization of the Euler equations is fulfilled in the paper by introducing a parameter of non-ideal continuity.

Résumé—Cet article montre le mauvais accord qui existe entre les données expérimentales et les expressions théoriques obtenues pour la dispersion acoustique dans les gaz raréfiés d'après les solutions Burnett et super-Burnett de l'équation de Boltzmann; la théorie classique basée sur l'hydrodynamique de Navier–Stokes apporte des résultats plus heureux. La conclusion ci-dessus semble également être valable quand on considère un saut de température et un glissement. Des contradictions apparaissent également entre les équations d'Euler et la théorie cinétique moléculaire quand on applique ces équations aux gaz raréfiés. La généralisation des équations d'Euler est faite dans cet article en introduisant un paramètre exprimant que la continuité n'est pas parfaite.

Zusammenfassung—Für die akustische Dispersion in verdünnten Gasen wird die geringe Übereinstimmung zwischen den experimentellen und theoretischen Werten, wie sie sich auf Grund der Burnett- und Super-Burnett-Lösung der Boltzmanngleichung ergeben, aufgezeigt. Die klassischen Navier–Stokessche Theorie vermittelt bessere Ergebnisse. Das scheint auch für Temperatursprünge zu gelten. Widersprüche zwischen den Eulerschen Gleichungen und der molekular-kinetischen Theorie ergaben sich bei dem Versuch, die Gleichungen auf die verdünnten Gase anzuwenden. Die Verallgemeinerung der Eulerschen Gleichungen wurde hier dadurch erreicht, dass man einen Parameter nicht-idealer Kontinuität einführte.

Аннотация—В статье показывается, что теоретические выражения для акустической дисперсии в разреженном газе, полученные на основе барнетовских и супербарнетовских решений уравнения Больцмана, плохо согласуются с данными экспериментов; более удачные результаты даёт классическая теория, основанная на гидродинамике Навье-Стокса. Это оказывается справедливым и для случая рассмотрения явлений температурного скачка и скольжения.

При рассмотрении уравнений Эйлера применительно к разреженному газу также вскрываются их противоречия с молекулярно-кинетической теорией. В работе проведено обобщение уравнений Эйлера путём введения параметра неидеальной сплошности.

NOMENCLATURE

p, pressure;
ω, circular frequency;
η, dynamic viscosity;
T_w, wall temperature;
T_g, gas temperature;
k, temperature jump coefficient;
h, mean free path of molecules;
f, measure of affinity with molecules of a solid body;
W, flow velocity;
U, slip velocity near a wall;
R, gas constant;
ζ, slip coefficient;

Vol. 3 1961

M, molecular weight of a gas; Mach local number;
u, v, w, components of molecular velocity;
F, function of molecular distribution;
C, shortest distance between rectilinear trajectories;
V, relative velocity of colliding molecules;
φ, angle;
$d\omega = du \cdot dv \cdot dw$;
ρ, density;
γ, ratio of specific heat;
r, distance along radius } polar system reference;
l, distance along axis }
θ, angle;
η_3, parameter of non-ideal continuity.

1

AT PRESENT various problems of heat and mass transfer in rarefied gases represent a whole field of knowledge. There are scores of works in this direction. Designers of various reactive machines, engineers and scientists working on industrial processes involving low gas densities come across various problems on aerodynamics and heat and mass transfer theory in rarefied gases. Improving the construction of powerful gas pumps brings out the necessity for a profound understanding of the phenomena in rarefied gases. However, in spite of the intensive development of the molecular-kinetic theory the problems mentioned are still being solved by methods which raise serious doubts because of the contradictions they give. Thus, it follows that it is necessary to look through all the principal concepts which are the basis of the aerodynamic equations and laws of heat and mass transfer in rarefied gases.

Thus, first it is necessary to search for some methods of experimental examination of the problems mentioned.

2

A very direct and simple method for such an examination is based on the theory of propagation of acoustic waves in rarefied gases. Indeed, until the length of an acoustic wave exceeds by many times the average length of the free path of molecules, the acoustic wave will propagate normally provided that there are no substance transformations in the gas. But if the length of an acoustic wave is comparable with the average length of the free path of molecules, then in this case the phenomenon of acoustic dispersion begins. The laws of this dispersion may be predicted starting from various forms of equations of aerodynamics of a rarefied gas. Thus, there is a possibility of direct examination of the principal states of the equations indicated.

As is known the momentum equations as well as that of energy transfer are deduced in the modern molecular-kinetic theory on the basis of the solutions of the so-called Boltzmann integro-differential equation. The solution of the Boltzmann equation in its first approximation, i.e. when the velocity and temperature gradients effects on the average length of the free path of molecules can be neglected, brings to the gas motion equations of the Navier–Stokes form. The second approximation obtained by Burnett using the Enskog–Chapman method introduces into the system of momentum and heat flow equations essentially new terms which alter dispersion laws of acoustic waves. In this case, to some extent, the variation of velocity and temperature gradients on the average length of the free path of molecules has already been taken into account. The solution of the Boltzmann equation in its third approximation exists already. It is known as the super-Burnett solution. The solution gives new corrections for the equations of momentum and heat flow. Consequently, it must give a more precise expression for acoustic disperson in rarefied gases.

The dimensionless value $r = (p/\omega\eta)$ is used as the independent variable for the experimental examination of theoretical formulae of acoustic dispersion which are deduced from different aerodynamic equations of rarefied gases.

It is easy to show that this value is proportional to the ratio of the acoustic wave length to the average length of the free path of molecules. Consequently, it is convenient for the estimation of the emergence of acoustic dispersion.

The classical theory based on the Navier–Stokes equations gives as a result the known formulae of the Stokes–Kirchoff acoustic dispersion. For values of r exceeding 10, i.e. when we deal with relatively low acoustic frequencies and high pressures, the relative value of the

sound absorption coefficient is not great. Therefore, the velocity of its propagation remains practically a constant value. Consequently, there is no acoustic dispersion.

The relative absorption of sound increases at decrease of r; the velocity of its propagation becomes the function of r and the Stokes–Kirchoff acoustic dispersion begins. The absorption is maximum if the value of r is equal to unity. The absorption is somewhat lower with further decrease of this value.

The corresponding calculations based on the Burnett and super-Burnett momentum equations give qualitatively the same results. At great values of r the coefficient of sound absorption as the function of r coincides with the corresponding functions obtained from the Burnett and super-Burnett equations. However, the divergence between the corresponding functions begins to increase with decrease of r. The highest divergence is at the value of $r = 1$. This divergence is so considerable that it can be easily found experimentally. In 1953 Greenspan and Thompson carried out a detailed experimental investigation of the velocity and absorption of ultrasound waves in rarefied gases. The results of these highly precise experiments revealed that the classical theory based on the Navier–Stokes hydrodynamics gives correct results in a considerably wider range of r than the theories based on the Burnett and super-Burnett equations. Moreover, the super-Burnett equations obtained from the more precise solutions of the Boltzmann equation gave the worst results.

3

However, the phenomenon of acoustic dispersion is not the only method of verification of concepts of aerodynamics of rarefied gases.

At Moscow State University, in the Department of Molecular Physics, the phenomena of slip of the gas flow and the temperature jump between a wall and a gas were investigated.

The theory of the temperature jump and flow slip near a wall, as is known, is based on the solution of the Boltzmann equation in its first approximation and was verified by Kundt, Warburg, Smolukhovskii, Lazarev, Millikan, Timiryazev and others.

If we designate the corresponding temperature of a wall and a gas as T_w and T_g, then the heat transfer between a wall and a gas is regulated by the formula:

$$k \frac{\mathrm{d}\theta}{\mathrm{d}n} = T_w - T_g$$

moreover, the temperature jump coefficient k according to molecular-kinetic calculations is equal to:

$$k = \frac{15}{4\pi} L \frac{2-f}{f}.$$

Here L is the average length of the free path of molecules and f is the measure of affinity with those of a solid body.

The analogical formula also exists for the slip of a rarefied gas flow near a wall. Let us designate by W the velocity of the flow; by U the slip velocity near a wall, then we get:

$$\zeta \frac{\mathrm{d}W}{\mathrm{d}n} = -U$$

and moreover, the slip coefficient ζ according to the molecular-kinetic calculations, has the form:

$$\zeta = \frac{2-f}{f} \frac{\eta}{p} \sqrt{\left(\frac{\pi RT}{2M}\right)} = \frac{A_0}{p}.$$

R is the gas constant, M is the molecular weight of the gas. Now from the above-mentioned relations for the slip constant A_0 and for the temperature jump coefficient k, we can get the following important formula:

$$A_0 = \frac{8}{15} kp.$$

As we have noted earlier all these formulae are valid only at extremely low values of both temperature gradient and velocity gradient along the average length of the free path of molecules. If the given gradients are high, then we should search after correct terms for the given formulae. It is quite possible to find these correct terms theoretically, but they can be determined experimentally as well.

Gribkova and Shtemenko developed a very

Vol. 3 1961

interesting method of simultaneous measurements of the temperature jump and slip under conditions of such flows of rarefied gas where it was quite possible to have considerable gradients of temperature and velocities along the average length of the free path of molecules. The method is based on longitudinal flow along a thin heated thread, i.e. the flow of a rarefied gas in a cylindrical tube in which the diameter of an internal continuous cylinder was very small in comparison with the external one. Gribkova developed the theory of such an apparatus which was used in the solution of this problem.

The results of the investigations carried out appeared to be quite unexpected. In spite of the fact that both the gradients of temperature and velocities along the average length of the free path of molecules were considerable, results of the application of the classical theory to the temperature jump and slip appeared to be correct.

After a thorough analysis of the results of their experiments the authors of these investigations came to the following conclusion. Apparently, at motion of a rarefied gas near the surface of a solid in cases when the range of temperature change along the average length of the free path of molecules is 1–10°C, and the velocity of the mass motion variation is 50–60 m/s near the surface of a body, the law of distribution of heat velocities corresponding to the solution of the Boltzmann equation (in the first approximation) occurs.

4

(1) The described disagreement of the molecular-kinetic theory with the observed facts makes us think seriously of the reasons which cause these contradictions.

If we assume that the solution methods of the Boltzmann equation, which were worked out by mathematicians, are quite correct, then we should find an explanation of the described contradictions in imperfections of this equation.

As is known, two operations of the function of molecular distribution F, according to heat velocities, are equated with each other in the Boltzmann equation.

The variation of the function F per unit in time, co-ordinates and velocities is calculated with the help of the first operation. It may be written in the following way:

$$\frac{DF}{Dt} = \frac{\partial F}{\partial t} + u\frac{\partial F}{\partial x} + v\frac{\partial F}{\partial y} + w\frac{\partial F}{\partial z} + X\frac{\partial F}{\partial u} + Y\frac{\partial F}{\partial v} + Z\frac{\partial F}{\partial w} \qquad (1)$$

and moreover, we take into consideration the equalities:

$$\frac{\partial u}{\partial t} = X; \quad \frac{\partial v}{\partial t} = Y; \quad \frac{\partial w}{\partial t} = Z.$$

The variation of the same function per time unit due to collisions of molecules is calculated with the help of the second operation.

If components of the molecular velocity of the first type molecules are designated by u_1, v_1, w_1 and components of the second type molecules are designated by u_2, v_2, w_2 till the moment of their collision among themselves, then the measure of probability of their approach may be taken as equal to F_1F_2. The subscripts denote in this expression from which components of heat velocities we should take the function of distribution.

After collision, the components of velocities of molecules of both types acquire the following values:

$$(u_1', v_1', w_1'); \quad (u_2', v_2', w_2').$$

The product of F_1' F_2' will serve as a measure of probability of their repulsion.

Thus, each collision of one molecular group with that of another will be characterized by a difference:

$$F_1'F_2' - F_1F_2 = \delta F_1F_2.$$

If we summarize all these differences along the whole phase volume, we shall get the variation of the function F per time unit which is due to collision of molecules,

$$\frac{DF}{Dt} = \int \ldots \int \delta F_1F_2 V db d\omega_1 dq \qquad (2)$$

Here the product $Vdbd\omega_1dq$ denotes an element of a phase space; V denotes the relative velocity of colliding molecules, b is the shortest distance

between rectilinear trajectories of molecules; φ is the angle between the plane of the trajectories of the relative motion of the first type molecule and a certain constant plane passing through V; finally, $d\omega$, denotes the product du, dv, dw.

Consider whether these two operations are always equal to each other. The first operation by its nature can give continuous values from the co-ordinates of a phase space. As for the second operation it is not evident. We are inclined to suppose that the second operation must bring discontinuous values because the variation $\delta F_1 F_2$ is not always an infinitely small value. It means that we cannot equate in the main the operations with each other. As is known, both operations are equated without any proof that the variation $\delta F_1 F_2$ is the continuous co-ordinate function of a phase space. In our opinion such equalization will be more valid, the higher the density of a gas. The validity of the given equalization becomes less lawful as a gas is rarefied. Therefore, the solutions of the Boltzmann equation for rarefied gas must give unsatisfactory results. Probably the reason lies in the fact that the phenomena of acoustic dispersion in rarefied gases and phenomena of the temperature jump and slip of the gas flow near a wall cannot be restricted by the solutions of the Boltzmann equation according to the Enskog–Chapman method.

(2) However, recently another possible point of view has been discussed in literature. We mean the works by Truesdell.

In one of his works he says the following:

"Up to now there is no solution of the Boltzmann equation. It is true that there is a great number of so-called solutions. But the Maxwell theory was a paradise for conjectures and dogmatism, and it was a desert for precise mathematics. The methods named in this theory as integration are without any exception purely formal. Their convergence has never been proved but moreover there are no indications that classical methods of solution have significance for this equation. The above mentioned refers in equal degree to investigations of physicists as well as to the outstanding work by the great mathematician Gilbert." And further: "All the classical investigations are extremely overloaded with calculations. A great number of investigations are devoted to the study of the Boltzmann equation and to attempts to solve it with the help of special series. One always speaks of approximation and the order of magnitude, etc. However, complexity of the analysis makes difficult the understanding of the principal course of arguments."

In his work Truesdell goes further as he has doubts about the concept of the gas-kinetic theory and speaks of a modern crisis in the kinetic theory of gases. In his work, under such a title, he analyses the already formed situation in the kinetic theory of gases and shows that the problem of convergence of successive approximations is not trivial at all. In one concrete example he illustrates that there might exist such cases where all the approximations appeared to be worse than the first one, which is the asymptotic solution. It is quite possible that in a strict statement of the problem this asymptotic solution will be closer to the Navier–Stokes equations than all the existing approximate solutions of the Boltzmann equation. Now it is very difficult to say which point of view mentioned above is correct. It is clear that modern techniques are necessary to begin to solve this problem which is of great importance and deserves the most serious attention on the part of physicists and mathematicians.

Vol. 3 1961

5

(1) The well-known imperfection of our concepts in the kinetic theory may be revealed not only from attempts to obtain exact equations of momentum and heat flow for a viscous rarefied medium, it is also possible to show that the Euler equations do not agree well with molecular-kinetic concepts of media properties. We shall try to explain this in a concrete example.

Let us consider a rectilinear vortex cord of an infinite length in an ideal medium. In this case the rotor of a velocity of a partial motion beyond the vortex cord will be equal to zero. Consequently, motion of a medium beyond the vortex cord will be potential. Therefore, according to the Euler equation for the steady iso-entropic motion of an ideal continuous medium, we can write such an equality for a velocity field beyond the vortex cord:

$$\frac{W_0^2 r_0^2}{2r^2} + \frac{p_0}{\rho_0^\gamma} \frac{\gamma}{(\gamma - 1)} \rho^{\gamma - 1} = \text{const.} \qquad (3)$$

Here the subscript "0" denotes the values of quantities taken on the surface of the vortex cord. The equation obtained is valid provided that the medium is continuous. Only in this case are all the mathematical operations which have to be fulfilled while deriving the given equations quite lawful. But if the medium is discrete, there is no reason to consider that these operations are lawful. In this case, following the Klein example, we must use finite difference and derive the equation of motion from purely physical concepts independently of the Euler equations.

(2) In discrete medium we must take as the hydrodynamic element of the volume such a volume as would contain rather a great number of molecules. Only in this case can we expect that the averaged velocities of the regulated motion can change continuously from one point to another.

Let us cut out a ring with a thickness equal to Δl and width Δr in a region beyond the vortex cord. Further, let us cut a curvilinear parallelepiped out of this ring by two planes and let the angle between these planes be equal to $\Delta\theta$. Then, the volume of this parallelepiped can be written in such a form:

$$\Delta\sigma = \bar{r}\Delta\theta\Delta l\Delta r.$$

Here $\bar{r}$ is the average arithmetic value of two radii of the ring. We must choose this hydrodynamic volume thus that it will catch rather a great number of molecules.

Let us designate the average angular velocity of the curvilinear parallelepiped volume as $\bar{\omega}$. Then the centripetal force effecting this hydrodynamic volume will be equal to:

$$\bar{\rho}\,[(r_2^2 - r_1^2)/2]\Delta\theta\Delta l\bar{r}\bar{\omega}^2.$$

where $\bar{\rho}$ is the average density. On the other hand the pressure on the average surface of a curvilinear parallelepiped will be equal to:

$$(p_2 - p_1)\,\bar{r}\Delta\theta\Delta l.$$

Comparing these two forces with each other we shall have:

$$\frac{r_2^2 - r_1^2}{2}\Delta\theta\Delta l\bar{r}\bar{\omega}^2 = -\frac{p_2 - p_1}{\bar{\rho}}\bar{r}\Delta\theta\Delta l. \qquad (4)$$

If the phenomenon occurs in an iso-entropical way, such an equation can be easily obtained from the Poisson equation:

$$p_1 - p_2 = \frac{\gamma}{(\gamma - 1)}\bar{\rho}(\rho_1^{\gamma - 1} - \rho_2^{\gamma - 1})A$$

$$= \frac{p_0}{\rho_0^\gamma}\frac{\gamma}{(\gamma - 1)}\bar{\rho}(\rho_1^{\gamma - 1} - \rho_1^{\gamma - 1}).$$

Now equation (4) can be transformed in the following way:

$$\frac{r_2^2 - r_1^2}{2}\bar{\omega}^2 = \frac{p_0}{\rho_0^\gamma}\frac{\gamma}{(\gamma - 1)}(\rho_1^{\gamma - 1} - \rho_2^{\gamma - 1}). \qquad (4a)$$

In order to obtain from this equation the relation (3) which follows from the Euler equation it is necessary to exclude $\bar{\omega}^2$. This elimination reserves all the details which result from the necessity of a transition from the discrete medium to the continuous one. Indeed, we suppose that a motion velocity of internal and external points of a ring is determined correspondingly by relations:

$$\frac{W_0 r_0}{r_1} = \omega_1 r_1 = W_{1r}; \qquad \frac{W_0 r_0}{r_2} = \omega_2 r_2 = W_{2r}. \qquad (5)$$

Each of these relations is the effect of the potentiality of the flow. If we assume this, then the average angular velocity ω will be equal to:

$$\bar{\omega} = \frac{W_0 r_0}{2}\left(\frac{1}{r_1^2} + \frac{1}{r_2^2}\right) = \frac{W_0 r_0}{r_1^2 r_2^2}\bar{r}^2.$$

Or substituting the arithmetical mean of $\bar{r} = (r_1 + r_2)/2$ for the geometrical one of $\sqrt{(r_1 r_2)}$ we shall get:

$$\bar{\omega} = \frac{W_0 r_0}{r_1 r_2}.$$

Now we may reduce the equality (4a) to:

$$\frac{W_0^2 r_0^2}{2r_2^2} + \frac{p_0}{\rho_0^\gamma}\frac{\gamma}{(\gamma - 1)}\rho_2^{\gamma - 1}$$

$$= \frac{W_0^2 r_0^2}{2r_1^2} + \frac{p_0}{\rho_0^\gamma}\frac{\gamma}{(\gamma - 1)}\rho_1^{\gamma - 1}.$$

As we see, the obtained equality coincides

essentially with the equality (3) which was found from the Euler equation.

However, we made an unfounded assumption that external and internal surfaces of a physically small volume have various angular velocities throughout, but for determination of continuously changing average velocities of a regulated motion we must assign a specific physically small volume attributing to it some angular velocity and a corresponding radius-vector. This choice must be accomplished in such a way that the equality will be always valid:

$$\frac{W_0 r_0}{r_i} = \omega_i r_i'.$$

Here r_i determines the location of the physically small volume. It is seen from this equality that we can change arbitrarily the angle velocity ω_i and the radius-vector r_i'. However, from the physical considerations it is clear that the angle velocity of the physically small volume must be constant (ω). Consequently, only the radius-vector r_i' must be chosen in accordance with the physically small volume. It means that the following equalities must be valid for the motion of external and internal surfaces of the physically small volume:

$$\frac{W_0 r_0}{r_1} = \omega r_1'; \qquad \frac{W_0 r_0}{r_2} = \omega r_2'.$$

Hence, it follows:

$$\frac{r_1}{r_2'} = \frac{r_2'}{r_1'} = \beta; \qquad \omega = \frac{W_0 r_0}{r_2 r_1}\beta.$$

If we introduce the value of the angular velocity ω into the equality (4a) we shall obtain:

$$\frac{W_0^2 r_0^2}{2r^2}\beta^2 + \frac{p_0}{\rho_0^\gamma}\frac{\gamma}{(\gamma-1)}\rho^{\gamma-1} = \text{const}.$$

This equation differs from equation (3). In order to get it with the help of mathematical transformations which require continuity of a medium, we must improve the Euler equations in a suitable manner. It is not difficult to perceive that the improved Euler equation of a motion must have such a form as:

$$\frac{\partial \mathbf{W}}{\partial t} + \beta^2 \operatorname{grad}\frac{W^2}{2} = -\frac{1}{\rho}\operatorname{grad} p. \qquad (6)$$

It is convenient to substitute the value β^2 for the following:

$$\beta^2 = 1 - \eta_3.$$

The quantity η_3 is the measure of media continuity with respect to the given hydrodynamic motion. Therefore, we may call this measure a parameter of non-ideal continuity.

By extrapolation of the obtained equation up to the heat velocities it is possible to show that the value of η_3 is equal to:

$$\eta_3 = \frac{2}{3}\frac{L}{D}M.$$

Here, L is the average length of the free path of molecules; D is geometrical sizes of region of flow investigated; M is the Mach local number.

It is impossible to obtain the correction which we have found by solving the Boltzmann gas-kinetic equation, as the possibilities of this equation are restricted, i.e. it solves only the problem of transition of a visible motion into heat.

Vol. 3 1961

6

(1) The above-mentioned generalization of the Euler equations allows one to obtain new information on heat transfer phenomena in the flow of a rarefied gas.

As is known, in the problem of gas motion in a cylindrical tube we must take into consideration two equations:

$$\frac{\rho}{2}\frac{\partial W_z^2}{\partial r} + \frac{\partial p}{\partial r} = 0; \quad \frac{\partial p}{\partial z} = \eta\frac{1}{r}\frac{\partial}{\partial r}\left(r\frac{\partial W_z}{\partial r}\right).$$

If we consider the same problem for a flow along a tube of non-ideal continuous media, then proceeding from the Euler generalized equations, we must take into account the following two equations:

$$\rho\frac{(1-2\eta_3)}{2}\frac{\partial W_z^2}{\partial r} + \frac{\partial p}{\partial r} = 0;$$

$$\frac{\partial p}{\partial z} = \eta\frac{1}{r}\frac{\partial}{\partial r}\left(r\frac{\partial W_z}{\partial r}\right).$$

Near a wall the first equation can be transformed with the help of the equation of state

and relations for the temperature jump and slip, i.e. we can use the following formulae:

$$\zeta \frac{\partial W_z}{\partial r} = -W_s; \quad k \frac{\partial T}{\partial r} = \Delta T;$$

$$\frac{\partial p}{\partial r} = R \frac{\mathrm{d}T}{\mathrm{d}r} \rho = \frac{R \Delta T \rho}{k}.$$

As a result of such a transformation, we shall get:

$$\frac{(1 - 2\eta_3) W_s^2}{\zeta} = \frac{R \Delta T}{k}. \tag{7}$$

On the other hand, proceeding from the law of conservation of energy, we have:

$$\frac{\rho W_s^2}{2} + p = p_0.$$

Hence:

$$W_s^2 = 2R_0 \Delta T.$$

Now equation (7) can be rewritten in such a form:

$$2(1 - 2\eta_3)k = \zeta. \tag{7a}$$

Due to investigations carried out by Gribkova and Shtemenko the relation obtained is of great interest. Indeed, if the relation ζ/k remains constant for all the viscous molecular flows and is equal to 8/15, then from equation (7a) it is possible to calculate a parameter of non-ideal continuity. Its value will be equal to 0·367. On the other hand we know the parameter of non-ideal continuity in an explicit form. Therefore, it can be written:

$$\eta_3 = \frac{2}{3} \frac{L}{D} M = 0{\cdot}367.$$

Hence:

$$\frac{L}{D} M = 0{\cdot}550.$$

For the Mach number equal to unity the size of the flow region where the jump of temperature and flow slip occur will be equal to 1·82L, i.e. about two lengths of the average path of the molecular wandering. Since in this case the Mach number is calculated according to the local value of the velocity of molecules the calculated value of sizes of the region of a flow where the temperature jump and slip occur will be maximum.

Thus, the physically small volume for a molecular-viscous flow must exceed by approximately eight times the volume of a cube whose edge is equal to the average length of the free path of molecules. This result is of great interest from the viewpoint of physics. It shows that it is not obligatory to have a great number of molecules in one cubic centimetre while dealing with continuum consideration of a medium. Consequently, the classical equations which were derived in a phenomenological way are also valid for sufficiently deep rarefication of a gaseous medium.

(2) It is possible to extend the generalization of the Euler equations obtained from the analysis of turbulence in ideal medium to a viscous gas as well. In this case only the equations of motion and energy need corrections; the continuity equation remains unchanged.

If we write the Navier–Stokes equation of motion in symbols:

$$\frac{\mathrm{d}\mathbf{W}}{\mathrm{d}t} = \mathbf{S}$$

then after taking into account the corrections for non-ideal continuity we shall have:

$$\frac{\mathrm{d}\mathbf{W}}{\mathrm{d}t} = S + \eta_3 \{\tfrac{1}{2} \operatorname{grad} W^2 + \mathbf{W} \operatorname{div} \mathbf{W} + [\operatorname{rot} \mathbf{W}_1 \mathbf{W}]\}.$$

As is known, in aerodynamics of a viscous liquid we write the equation of energy in its general form as follows:

$$\rho c_v \frac{\mathrm{d}T}{\mathrm{d}t} + p \operatorname{div} \mathbf{W} = E_s.$$

Taking into consideration the corrections for non-ideal continuity the equation can be written as follows:

$$\rho c_v \frac{\mathrm{d}T}{\mathrm{d}t} + p \operatorname{div} \mathbf{W} = E_s + \rho \eta_3 W^2 \operatorname{div} \mathbf{W} + \rho \eta_3 \left(\mathbf{W}, \operatorname{grad} \frac{W^2}{2}\right).$$

The degree of fitness of the equations obtained for the description of the motion of rarefied gases

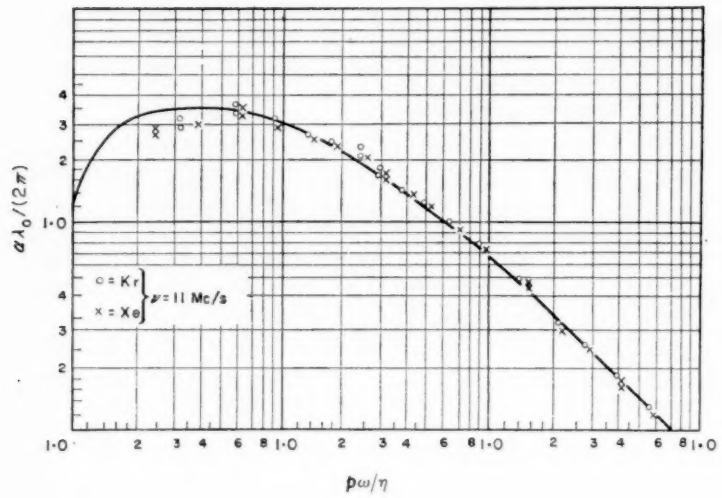

FIG. 1.

Plot of the values $\frac{\alpha}{\beta_0} = \frac{\alpha\lambda_0}{2\pi}$ versus $r = \frac{p}{\omega\eta}$

×, ○ —experimental data, ——— —calculated curve according to author's formulae.

Vol. 3 1961

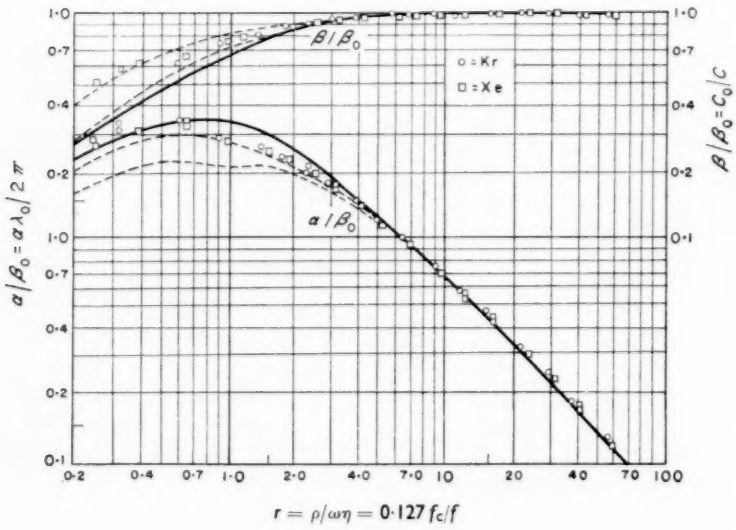

FIG. 2.

Plot of the values $\frac{\alpha}{\beta_0} = \frac{\alpha\lambda_0}{2\pi}$ versus $r = \frac{\rho}{\omega\eta}$

○, □ —experimental data, ——— —calculated curve according to Stokes–Kirchoff,
– – – – – —calculated curve according to second approximation Burnett,
— — — —calculated curve according to third approximation Burnett.

can be obtained while examining the dispersion of acoustic waves in an experimental way. It is not difficult to obtain formulae of acoustic dispersion if we use the conditions of compatibility by Hugonio–Hadamard. As is known, the above-mentioned conditions characterize the process of formation and propagation of a front. They allow one to find without any integration (i.e. only by segregation of discontinuity surfaces), the velocity of motion of the latter throughout a space. The peculiarity of any acoustic front results in the fact that when passing through it from the disturbance region to that of rest the first and second derivatives entering the closed system of momentum equations suffer a break of continuity. Not dwelling upon the detailed calculations the author of this paper succeeded in finding the following formulae for the sound absorption coefficient in a rarefied gas:

$$\alpha = \frac{(0{\cdot}7r + 0{\cdot}23)\sqrt{r}}{(r + 0{\cdot}575)^2\sqrt{(r + 0{\cdot}575)}}.$$

The calculations were fulfilled for monatomic gases which were investigated by Greenspan and Thompson. The above-mentioned dimensionless value is designated by r in the given formula.

The Greenspan data on the dispersion of ultrasound waves in xenon and krypton are given in Fig. 1. The continuous curve is plotted according to the theoretical formula.

As is seen, the coincidence of observed and predicted values of the absorption coefficient of acoustic waves may be considered rather good.

It is interesting to compare this result with that of the Navier–Stokes, Burnett and super-Burnett equations.

The Greenspan data obtained from experiments in krypton and xenon and calculations according to theoretical formulae are given in Fig. 2. The continuous curve corresponds to the Stokes–Kirchoff equations. The short dashed curve corresponds to the Burnett equations and the long dashed curve corresponds to the super-Burnett equations.

Hence, the formulae of acoustic dispersion based on the Navier–Stokes equations describe the experiment better than the formulae based on the Burnett and super-Burnett equations.

As for our formula, it coincides completely with the Stokes–Kirchoff formula over the whole range. This formula gives a better agreement with experimental data only at values approximately equal to unity.

Thus, the analysis of this problem carried out in a different manner to the Truesdell analysis leads to just the same conclusion. Undoubtedly, we deal with a crisis in the molecular-kinetic theory when we relate equations of aerodynamics and heat theory for rarefied gases.

Int. J. Heat Mass Transfer. Vol. 3, pp. 198–221. Pergamon Press 1961. Printed in Great Britain.

A REVIEW OF BINARY LAMINAR BOUNDARY LAYER CHARACTERISTICS†

J. F. GROSS, J. P. HARTNETT,‡ D. J. MASSON and CARL GAZLEY, JR.
The RAND Corporation, Santa Monica, California

(*Received* 4 *April* 1960)

Abstract—Available analyses of the binary laminar boundary layer are examined in some detail. It is demonstrated that the exact predictions of heat transfer and skin friction in the presence of mass-transfer cooling with a foreign gas can be approximated by simple expressions which should be of value for engineering design calculations.

Résumé—Les principales études de couche limite laminaire binaire sont examinées en détail. Dans cet article, on montre que les valeurs exactes du transfert de chaleur et du frottement, en présence d'un refroidissement par transport de masse à l'aide d'un autre gaz, peuvent être approchées par des relations simples qui devraient être très utiles pour les calculs des projets.

Zusammenfassung—Verschiedene Untersuchungen binärer laminarer Grenzschichten werden eingehend geprüft. Es zeigt sich, dass die exakte Berechnung des Wärmeübergangs und der Oberflächenreibung bei der Stoffübergangskühlung mit einem Fremdgas durch einfache Ausdrücke angenähert werden kann. Das ist für die techcnishe Berechnung von Auslegungsdaten von Bedeutung.

Аннотация—В статье приводится анализ бинарного ламинарного пограничного слоя. На основании проведенного анализа даётся простой и достаточно точный для инженерной практики приближенный метод расчёта теплообмена и поверхностного трения для случая охлаждения тел путём подачи в пограничный слой инородного газа.

Vol. 3 1961

NOMENCLATURE

c_p, specific heat at constant pressure;
c_v, specific heat at constant volume;
c_f, local skin friction coefficient, $\tau_w/\frac{1}{2}\rho_e u_e^2$;
c_{f_0}, local skin friction coefficient evaluated for solid wall exposed to same free stream conditions and held at same temperature as the actual wall;
c_H, local heat transfer Stanton number, $q/\rho_e u_e c_{p_e}(T_r - T_w)$;
c_{H_0}, local Stanton number evaluated for solid wall exposed to same free stream conditions and held at same temperature as the actual wall;
c_M, mass transfer Stanton number, $\dot{m}/\rho_e u_e Y_w$;
C, Chapman–Rubesin parameter defined in equation (17);
D_{12}, ordinary diffusion coefficient;
f, dimensionless stream function;
H, enthalpy associated with change of phase;
h, heat-transfer coefficient, equation (19);
k, thermal conductivity;
m, refers to wedge flows, where free stream velocity, u_e, varies as x^m;
m_1, molecular weight of coolant gas;
m_2, molecular weight of pure air;
$\dot{m}_x$, mass flow rate of coolant gas at position x along the surface;
p, pressure;
p_1, partial pressure of coolant gas;
q, local heat transfer rate per unit area, $k_w(\partial T/\partial y)_w$;
q_0, local heat-transfer rate per unit area evaluated for solid wall exposed to same free stream conditions and held at same temperature as actual wall;

† A condensed version of this paper was presented at the Conference on Heat and Mass Transfer, B.S.S.R. Academy of Sciences, Minsk, 5–9 June, 1961.

‡ Consultant, The RAND Corporation and Professor, Department of Mechanical Engineering University of Minnesota.

r, recovery factor;
R, universal gas constant;
T, temperature;
T^*, reference temperature defined in equation (9);
T_r, recovery temperature, defined as the wall temperature where $k_w(\partial T/\partial y)_w = 0$;
u, v, component of velocity parallel and normal to surface, respectively;
x, y, co-ordinates along and normal to the body, respectively;
Y, mass fraction of coolant gas.

Greek symbols

ρ, density;
μ, dynamic viscosity;
η, transformed co-ordinate defined in text;
ψ, stream function;
θ, dimensionless temperature;
Φ, dimension mass fraction;
λ, defined in equation (17);
ν, kinematic viscosity;
γ, ratio of specific heats, c_p/c_v;
τ_w, local shearing stress.

Dimensionless numbers

M, Mach number, ratio of local speed to local speed of sound;
Pr, Prandtl number, $\mu c_p/k$;
Sc, Schmidt number, ν/D_{12};
Re_x, local Reynolds number, $u_e x/\nu_e$.

Subscripts

1, refers to pure coolant;
2, refers to pure air;
e, evaluated at outer edge of the boundary layer;
r, refers to recovery conditions, i.e. where $k_w(\partial T/\partial y)_w = 0$;
w, evaluated at wall conditions;
x, refers to local conditions.

Superscripts

*, evaluated at the reference temperature, equation (9).

1. INTRODUCTION

RECENTLY, the alleviation of the high heating rates encountered by surfaces of hypersonic vehicles has been recognized as an important problem. One of the cooling methods that appears to have great ultimate promise is mass-transfer cooling, wherein a "foreign" material is transferred from the surface into the boundary layer. This has a two-fold advantage in alleviation of the heat-transfer problem. The transferred coolant may absorb heat from the boundary layer through a phase change (sublimation, evaporation, melting, etc.) and/or by acting as a dispersed heat sink. It will be advantageous, therefore, to employ coolants with high heats of sublimation (or evaporation, melting, etc.) as well as high thermal heat capacities. In addition, it has been shown that the introduction of a material (with its normal velocity component) at the surface acts to decelerate the flow and consequently, to reduce the skin friction. This also implies a reduction in heat transfer at the wall.

The usual boundary-layer equations are complicated by the appearance of (a) an equation defining the conservation of the species at any point in the boundary layer, and (b) transport terms which result from thermodynamic coupling coefficients such as thermal diffusion coefficient, etc. There are a number of methods for effecting the injection of a foreign material into the boundary layer, and the following descriptions have been advanced to describe specific mass-transfer cooling schemes:

(1) Transpiration cooling.
(2) Film cooling
  (a) using liquid as a coolant
  (b) using gas as a coolant.
(3) Ablation
  (a) sublimation
  (b) other ablation phenomena, such as melting, erosion, fusion, etc.

These schemes are diagrammatically shown on Fig. 1 [1].† With the exception of film cooling with a gas, these methods all involve the same mechanism in the gaseous phase of the boundary layer. However, there is a difference in the boundary conditions at the wall which distinquish the three methods from a thermodynamic as well as a mechanical viewpoint. Transpiration cooling involves the introduction of a coolant gas through a porous surface. Consequently, the rate of fluid injection through the surface and

† Figures in square brackets refer to references presented at the end of text.

into the boundary layer may be arbitrarily adjusted by purely mechanical means and the temperature at the surface may thereby be regulated depending upon the injection rate and storage temperature of the coolant gas. It should be noted that a transpiration-cooling system requires pumps, storage tanks, pressure regulators and accessory plumbing. In addition, the fabrication and maintenance of porous surfaces represents a difficult engineering problem.

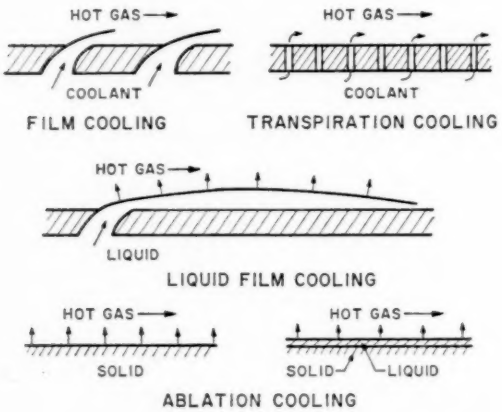

FIG. 1. Various cooling methods.

A film-cooling system involves pumping a liquid or gas on to the surface through an inlet slot configuration such that a thin film of the material covers the surface. This acts as an insulating coating and, in the case of a liquid, absorbs heat by vaporization. These systems are usually limited by such characteristics as the stability of the liquid film and the pumping power available. Film-cooling systems require essentially all the plumbing and control equipment of a transpiration-cooled operation; however, the surface construction is mechanically simpler.

A sublimation-cooling system is self-controlled through the relation between the vapor pressure and surface temperature of a solid, the Clausius–Clapeyron equation:

$$\ln p_1 = \frac{-\Delta H_s}{RT} + B \qquad (1)$$

where

p_1 = vapor pressure of subliming material,
R = universal gas constant,
H_s = heat of sublimation per mole,
B = constant of integration.

Heat is absorbed by the material as it sublimes. Thus, the heat transfer into the interior is reduced in two ways: (a) direct absorption in the form of heat of sublimation, and (b) reduction of heat transfer because of the movement of the sublimed mass away from the surface. The mass release at the surface depends upon the heat of sublimation and the temperature of the surface. Furthermore, the surface temperature can no longer be arbitrarily controlled and, in fact, will always find "its own level" depending upon the heat load, heat sublimation, and the external flow situation. It should be noted that film cooling with a liquid is essentially a sublimation process provided that the surface is completely covered by a liquid layer.

In addition to sublimation, more complex ablation cooling schemes may be visualized. Depending upon the surface material and the flight conditions, it is possible to have such phenomena as fusion of the surface material, mechanical erosion, dissociation of both air and surface material, ionization, and chemical reactions between the components in the boundary layer. The obvious complications involved in an analysis of these complex ablating systems have prevented any really accurate description of the mechanism.

There is another method of classifying these systems which may be helpful conceptually—by specifying the method of controlling the rate of injection. In the case of transpiration cooling, as we have seen, the rate is arbitrarily controlled depending upon certain mechanical requirements such as the porous surface and pumping power available. This may be considered an arbitrarily-controlled system. For a subliming or ablating surface, however, the rate of injection is determined by the heat of sublimation and the surface temperature. For a set of flight conditions and a surface material, the steady-state injection is fixed thermodynamically. We may call this a self-controlled system. Film cooling

Vol. 3 1961

may be considered a mixed system, with the rate of mass transfer into the boundary layer being self-controlled, but the flow rate of liquid or gas over the surface remaining arbitrary.

2. BINARY LAMINAR BOUNDARY-LAYER THEORY

Baron [2, 3], Eckert *et al.* [4–6], Sziklas and Banas [7] and Gross [8] have investigated theoretically the problem of mass-transfer cooling in the laminar boundary layer on a flat plate. The introduction of a species conservation equation as well as the appearance of thermodynamic coupling terms in both the species and energy equations complicates the mathematical analysis of the boundary layer.

The equations have been derived by Hall [9] who first treats the multicomponent fluid system and then from an order-of-magnitude argument obtains the boundary-layer equations for a binary boundary layer. The final binary boundary-layer equations for flow over a flat plate, neglecting the effects of thermal diffusion may be reproduced as follows:

Continuity:

$$\frac{\partial}{\partial x}(\rho u) + \frac{\partial}{\partial y}(\rho v) = 0. \tag{2}$$

Momentum:

$$\rho u \frac{\partial u}{\partial x} + \rho v \frac{\partial u}{\partial y} = \frac{\partial}{\partial y}\left(\mu \frac{\partial u}{\partial y}\right). \tag{3}$$

Energy:

$$\rho c_p u \frac{\partial T}{\partial x} + \rho c_p v \frac{\partial T}{\partial y} = \frac{\partial}{\partial y}\left(k \frac{\partial T}{\partial y}\right) + \mu \left(\frac{\partial u}{\partial y}\right)^2 + \rho D_{12}(c_{p_1} - c_{p_2}) \frac{\partial T}{\partial y} \frac{\partial Y}{\partial y}. \tag{4}$$

Species:

$$\rho u \frac{\partial Y}{\partial y} + \rho v \frac{\partial Y}{\partial y} = \frac{\partial}{\partial y}\left[\rho D_{12} \frac{\partial Y}{\partial y}\right]. \tag{5}$$

The boundary conditions for this system of equations follow from physical considerations:

$$\left.\begin{aligned} u &= 0 \\ T &= T_w \\ Y &= Y_w \end{aligned}\right\} \text{ at } y = 0 \tag{6}$$

$$\left.\begin{aligned} u &= u_e \\ T &= T_e \\ Y &= 0 \end{aligned}\right\} \text{ at } y \to \infty. \tag{7}$$

Since we are concerned with a seventh-order system of equations, another boundary condition must be specified. This condition may be obtained by noting that the mass velocity of the air molecules disappears at the surface of the plate; that is to say, there is no net mass transfer of the boundary layer air into the plate surface. Therefore, the mass flow of air by convection away from the surface must be equal and opposite to the diffusive flow of air toward the surface. This consideration yields the following boundary condition:

$$v = -\frac{\rho D_{12}}{1 - Y} \frac{\partial Y}{\partial y} \text{ at } y = 0. \tag{8}$$

This system of equations (2–8), forms the starting point for the various investigators cited above. In all cases, a transformation of the coordinates is next introduced with the result that the system of partial differential equations is changed into a new set of interdependent ordinary differential equations. This system of equations is still difficult to solve since, in general, all of the physical properties are functions of the local temperature and concentration of the particular gas mixtures being investigated. To obtain a representative number of solutions in a reasonable time requires the use of high speed electronic computers. Although the same basic system of differential equations was used by the various investigators (equations 2–8), somewhat different assumptions were imposed to obtain the final solution. A brief review of the available analyses is given below.

3. REVIEW OF AVAILABLE BINARY LAMINAR BOUNDARY-LAYER ANALYSES

Constant property analysis [10]

Considerable insight into the mass-transfer cooling process is obtained if it is assumed that the injected coolant has physical properties not markedly different from those of the main stream, thereby permitting the assumption of constant physical properties. The advantage of such a constant property solution is that the dimensionless heat transfer and skin-friction

results are dependent on a minimum number of parameters. This is indicated in Figs. 2 and 3 which compare the dimensionless quantities which are of importance for the solid-wall, heat-transfer case and those arising in the presence of mass transfer. For the solid wall, it has been demonstrated [11, 12] that the constant property solutions for the dimensionless skin friction, Nusselt number and recovery factor have additional value in that they may be used even when large

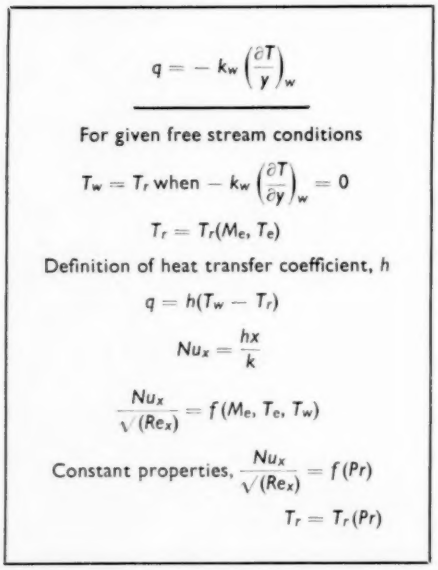
$q = -k_w \left(\frac{\partial T}{y}\right)_w$
For given free stream conditions
$T_w = T_r$ when $-k_w \left(\frac{\partial T}{\partial y}\right)_w = 0$
$T_r = T_r(M_e, T_e)$
Definition of heat transfer coefficient, h
$q = h(T_w - T_r)$
$Nu_x = \frac{hx}{k}$
$\frac{Nu_x}{\sqrt{(Re_x)}} = f(M_e, T_e, T_w)$
Constant properties, $\frac{Nu_x}{\sqrt{(Re_x)}} = f(Pr)$
$T_r = T_r(Pr)$

FIG. 2. Flat plate: solid wall, no mass transfer.

variations in physical properties are encountered (including dissociation), provided the properties are evaluated at a so-called reference temperature, T^*, which may be given explicitly in terms of the surface, the free stream and the recovery temperatures:

$$T^* = T_e + 0{\cdot}5\,(T_w - T_e) + 0{\cdot}22\,(T_r - T_e). \quad (9)$$

It will be demonstrated this temperature, T^*, will also prove of value in correlating the mass transfer results.

It should be noted from Fig. 3 that the heat transfer, q, is defined in terms of the temperature gradient at the wall. This definition is convenient in that this quantity, q, represents the convective

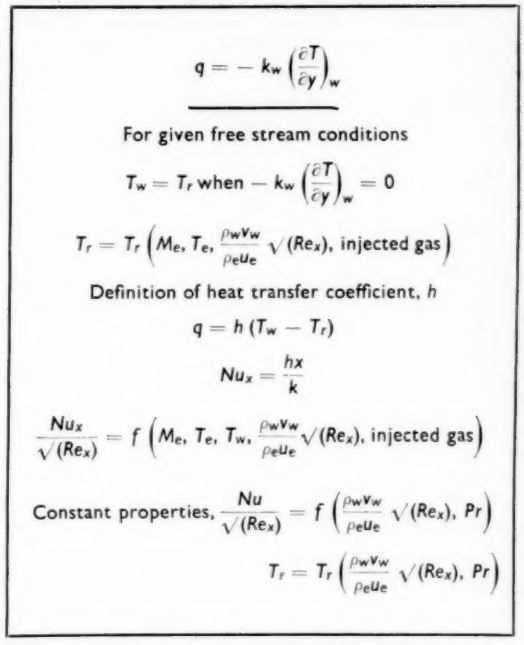
$q = -k_w \left(\frac{\partial T}{\partial y}\right)_w$
For given free stream conditions
$T_w = T_r$ when $-k_w \left(\frac{\partial T}{\partial y}\right)_w = 0$
$T_r = T_r\left(M_e, T_e, \frac{\rho_w v_w}{\rho_e u_e}\sqrt{(Re_x)}, \text{injected gas}\right)$
Definition of heat transfer coefficient, h
$q = h(T_w - T_r)$
$Nu_x = \frac{hx}{k}$
$\frac{Nu_x}{\sqrt{(Re_x)}} = f\left(M_e, T_e, T_w, \frac{\rho_w v_w}{\rho_e u_e}\sqrt{(Re_x)}, \text{injected gas}\right)$
Constant properties, $\frac{Nu}{\sqrt{(Re_x)}} = f\left(\frac{\rho_w v_w}{\rho_e u_e}\sqrt{(Re_x)}, Pr\right)$
$T_r = T_r\left(\frac{\rho_w v_w}{\rho_e u_e}\sqrt{(Re_x)}, Pr\right)$

FIG. 3. Flat plate: mass transfer.

heat transferred to the surface from the boundary layer, and in this sense the boundary-layer heat transfer is considered separately from the enthalpy carried across the surface by the coolant. To be consistent with this point of view, the recovery temperature, T_r, is defined as that temperature where the wall-temperature gradient vanishes; in this case there still exists a transport of enthalpy across the surface, by virtue of the coolant flow, but there is no convective heat transferred to the wall from the boundary layer.

Returning to the solutions of equations (2–8) it is obvious that the energy equation is linear and consequently, the general solution of the complete equation may be obtained from the addition of (a) a general solution of the homogeneous equation (that is, neglecting the dissipation term) and (b) a particular solution of the complete equation. The particular solution results in the specification of the recovery factor, a direct measure of the temperature assumed by the surface if it is allowed to come to equilibrium with the surroundings by convection alone.

Vol. 3 1961

We need, therefore, only to direct our attention to the general solution of the homogeneous equation. To accomplish this solution, a stream function, ψ, is first introduced to satisfy the continuity equation, and a new independent variable, η, and the new dependent variables defined below are substituted into the original equations:

Stream function:

$$u = \frac{\partial \psi}{\partial y}, \quad v = -\frac{\partial \psi}{\partial x} \tag{10}$$

$$\left.\begin{aligned} f &= \psi/\sqrt{(\nu u_e x)} \\ \eta &= (y/x)\sqrt{(u_e x/\nu)} \\ \theta &= (T - T_w)/(T_e - T_w) \\ \phi &= (Y_w - Y)/Y_w \end{aligned}\right\} \tag{11}$$

The following equations result:

Momentum:

$$\frac{d^3 f}{d\eta^3} + \tfrac{1}{2} f \frac{d^2 f}{d\eta^2} = 0. \tag{12}$$

Energy:

$$\frac{d^2 \theta}{d\eta^2} + \tfrac{1}{2} Pr\, f \frac{d\theta}{d\eta} = 0. \tag{13}$$

Diffusion:

$$\frac{d^2 \phi}{d\eta^2} + \tfrac{1}{2} Sc\, f \frac{d\phi}{d\eta} = 0. \tag{14}$$

Boundary conditions:

$$\left.\begin{aligned} \frac{df}{d\eta} &= 0 \\ \theta &= 0 \\ \phi &= 0 \\ f_w &= -2(v_w/u_e)\sqrt{(u_e x/\nu)} \end{aligned}\right\} \text{ at } \eta = 0 \tag{15}$$

$$\left.\begin{aligned} \frac{df}{d\eta} &= 1 \\ \theta &= 1 \\ \phi &= 1 \end{aligned}\right\} \text{ at } \eta \to \infty. \tag{16}$$

An important observation common to all flat-plate binary laminar boundary-layer solutions is that the mass transfer into the boundary layer must vary as $1/\sqrt{x}$ if we are to arrive at a system of ordinary differential equations. Further, we have assumed an isothermal surface and it will be shown that this is completely compatible with the imposed mass-transfer distribution.

The velocity profiles for the constant property mass-transfer system are shown in Fig. 4 for several different injection rates. Inspection of these profiles brings out the following conclusions:

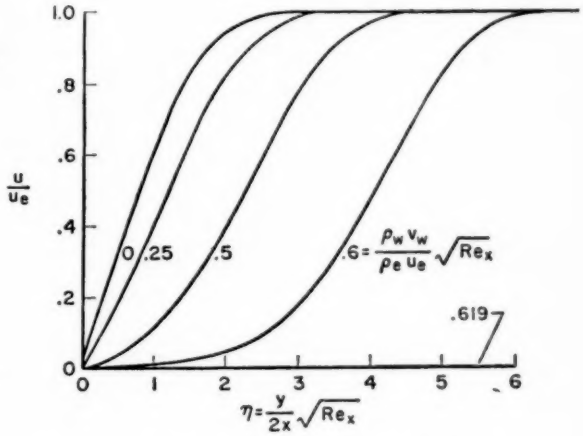

FIG. 4. Effect of air injection on velocity profile: flat plate–constant properties: laminar flow.

(a) The effect of mass addition is to thicken the velocity boundary layer.
(b) The velocity profile becomes S-shaped with mass addition, and since this is known to be an unstable type of profile, it may be concluded that mass transfer is destabilizing.
(c) The boundary layer "lifts off" the wall at a relatively low value of mass transfer; i.e. at $(\rho_w v_w/\rho_e u_e)\sqrt{(u_e x/\nu)} = 0{\cdot}619$. Apparently the boundary-layer equations fail to describe the flow field at this mass transfer condition.

The skin friction coefficient and Nusselt number, presented in Figs. 5 and 6, are seen to decrease with increasing mass transfer, both going to zero at the limiting value where the

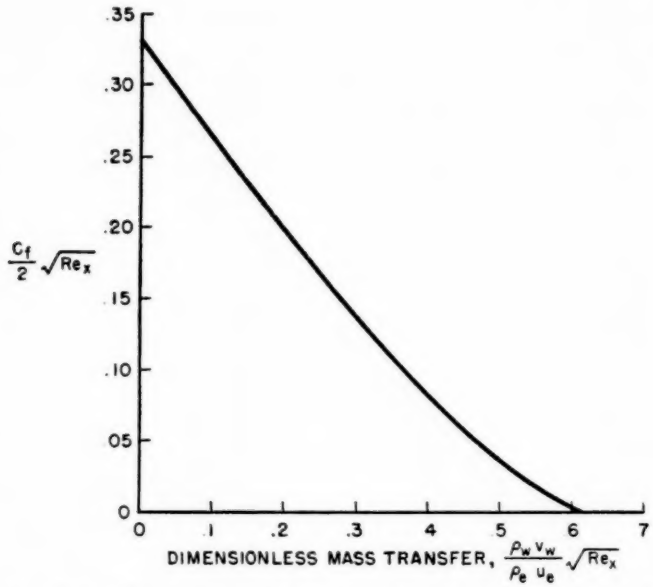

FIG. 5. Effect of air injection on local skin friction: flat plate–constant properties: laminar flow.

Vol. 3 1961

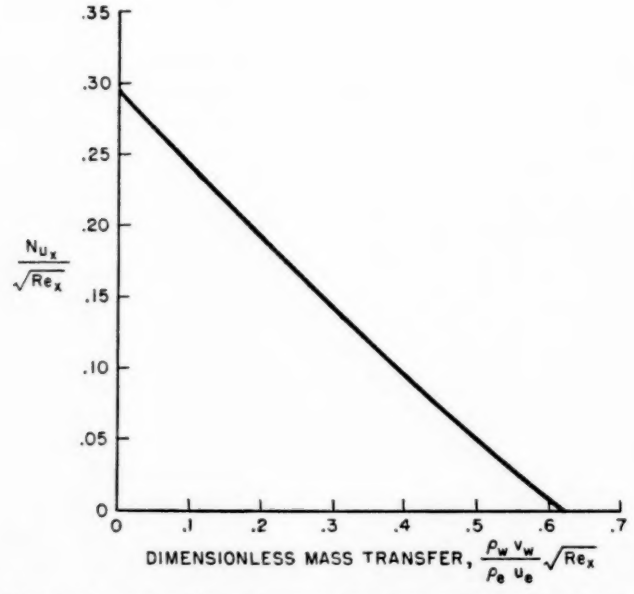

FIG. 6. Effect of air injection on local Nusselt number: flat plate–constant properties–$Pr = 0{\cdot}7$ constant wall temperature: laminar flow.

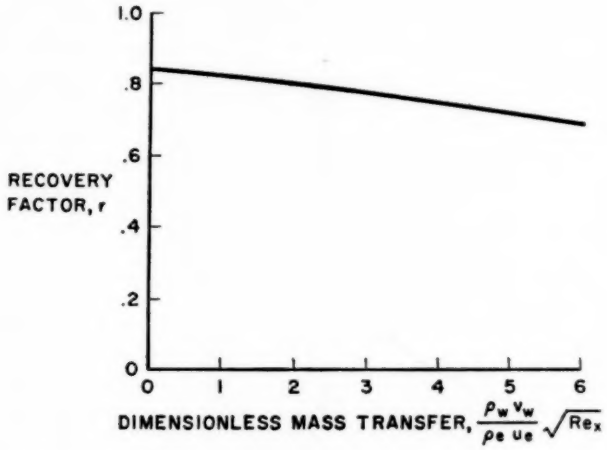

FIG. 7. Effect of air injection on recovery factor: flat plate–constant properties–$Pr = 0{\cdot}7$: laminar flow.

boundary layer "leaves" the wall. The recovery factor, shown in Fig. 7, is somewhat reduced by mass transfer but not as markedly as the Nusselt values. At hypersonic velocities the actual heat transfer to the surface is proportional to the product of the Nusselt number and the recovery temperature, and we conclude that a considerable reduction in heat transfer is obtainable with modest amounts of coolant. This is the feature which has drawn attention to this cooling scheme.

It may be noted that the heat-transfer solutions reveal that the local heat rate, q_x, is proportional to $1/\sqrt{x}$, which is precisely the distribution of the injected coolant. A simple heat balance on a sublimation or transpiration system yields the following expression.

$$\dot{m}_x[\Delta H + c_{p_i}(T_w - T_i)] = q_x$$

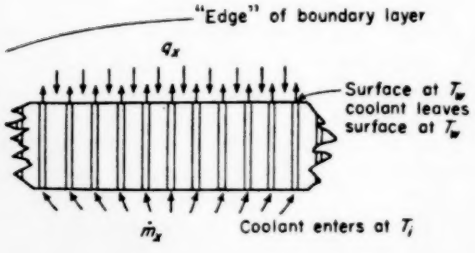

where

$\dot{m}_x$—mass flow rate of coolant,

ΔH—change in enthalpy due to phase change,

c_{p_i}—specific heat of the pure coolant.

Thus for the situation where the coolant enters the wall at a constant temperature, T_i, or if the surface is subliming, the resulting wall temperature must be a constant. We have, therefore, demonstrated the consistency of the assumed boundary conditions.

It may be of interest to investigate the validity of the modified Reynolds analogy (which holds for solid-wall conditions) under the new conditions when mass transfer is employed. If the analogy is valid, the parameter

$$(C_H\, Pr^{2/3}) \div (C_f/2)$$

would equal unity. As seen in Fig. 8, the departure from unity is not significant at low mass transfer rates, with the analogy being accurate to 15 per cent up to a dimensionless mass transfer value of 0·3; at higher mass transfer rates the use of the analogy may lead to considerable error.

Analysis of Baron [2, 3]

Baron was successful in introducing the influence of variable physical properties on mass-transfer cooling, while at the same time keeping

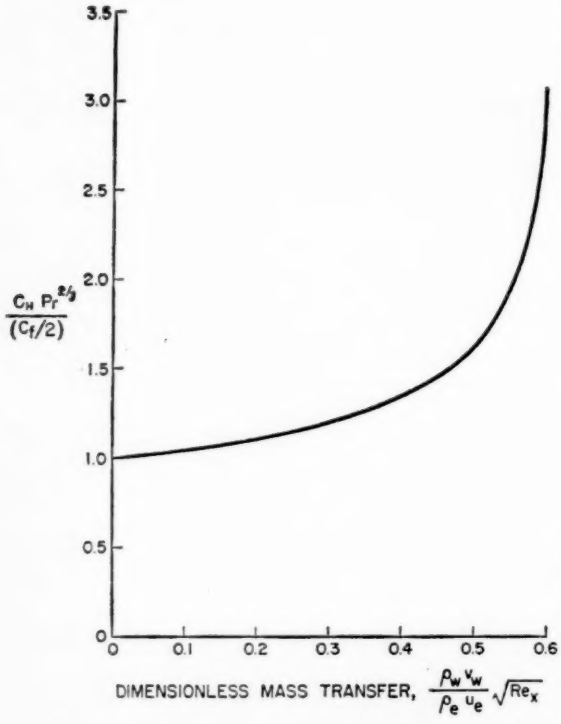

FIG. 8. Effect of mass transfer on modified Reynolds analogy: constant properties–flat plate–$Pr = 0{\cdot}7$.

the number of independent parameters at a minimum. To accomplish this, he adopted an approach similar to that used earlier by Chapman and Rubesin [13] for the solid flat plate. Baron introduces the so-called Chapman–Rubesin constant, C, for the product of the density and viscosity of the *air* only. He notes:

$$\frac{\rho\mu}{\rho_e \mu_e} = \left(\frac{\rho_2 \mu_2}{\rho_e \mu_e}\right)\left(\frac{\rho\mu}{\rho_2 \mu_2}\right) = C\lambda \qquad (17)$$

where

$$C = (\rho_2 \mu_2)/(\rho_e \mu_e) = \text{Chapman–Rubesin constant for } \textit{air} \text{ only}$$

$$\lambda = \frac{\rho\mu}{\rho_2 \mu_2} = \frac{\mu}{\mu_2}\left[1 + \left(\frac{m_2}{m_1} - 1\right) Y\right]^{-1}.$$

The factor, C, is independent of the concentration, while the other factor, λ, is rigorously a function of both temperature (through μ/μ_2) and concentration. However, for helium and carbon dioxide, the gases considered by Baron, the viscosity term μ/μ_2 is relatively insensitive to temperature and is primarily dependent on the concentration.† Consequently, Baron assumes that λ is a function *only* of concentration. Using this assumption, Baron presents two approaches:

Approach 1:

Baron introduces:

$$\left.\begin{aligned} u &= \frac{\rho_e}{\rho}\frac{\partial\psi}{\partial y}, \quad v = -\frac{\rho_e}{\rho}\frac{\partial\psi}{\partial x} \\ \eta &= \frac{1}{2}\sqrt{\left(\frac{u_e}{\nu_e x C}\right)}\int_0^y \frac{\rho}{\rho_e}\,\mathrm{d}y \\ \psi &= \sqrt{(\nu_e x u_e C)}\, f(\eta). \end{aligned}\right\} \qquad (18)$$

Using these transformations along with the additional assumption that the Schmidt number is a function only of concentration (an independent check shows this to be a realistic assumption), Baron obtains a set of three ordinary differential equations, similar in form but more complex than equations (12–16). The net result of these substitutions is that none of the terms appearing in the momentum and diffusion equations are dependent on temperature and consequently these two equations may be solved simultaneously, but independently of the energy equation. Using this approach Baron obtains the velocity profiles, the concentration profiles and the skin-friction parameter, $c_f\sqrt{(u_e x/\nu_e C)}$, as a function only of the mass-transfer parameter $(\rho_w v_w)/\rho_e u_e)\sqrt{(u_e x/\nu_e C)}$. Any temperature effect is completely contained in the constant C.

The energy equation remains to be solved and, Baron reports that all the coefficients appearing in this equation were only mildly affected by temperature, allowing the assumption that all coefficients are functions *only* of concentration. This is a considerable simplification for now the energy equation is linear in temperature, since all coefficients are known functions of the dimensionless parameter, η, by virtue of the previously obtained solutions of the momentum

† This assumption is valid for hydrogen as well.

Vol. 3 1961

and diffusion equations.† As in the constant-property situation, the resulting energy equation, being linear, may be solved by first treating the non-dissipative case and then adding the adiabatic-wall solution. It follows that the low speed non-dissipative heat-transfer coefficients may be used for the high-speed case if the adiabatic-wall temperature replaces the free-stream temperature in the definition of the heat-transfer coefficient

$$q = h(T_r - T_w). \tag{19}$$

The recovery temperature, T_r, determined from the adiabatic-wall solution is reported in terms of a recovery factor, r, which for a given injected gas is a function only of the mass-transfer parameter $(\rho_w v_w/\rho_e u_e)\sqrt{(u_e x/\nu_e C)}$. In addition to the recovery factor, Baron also presents dimensionless heat-transfer coefficients for two binary systems, helium–air and carbon dioxide–air mixtures.

The second approach used by Baron is not as realistic as the above and will be mentioned only briefly. In this case he assumed that λ is a constant to be evaluated at wall condition and the following transformations are then applied to equations (2–8):

Approach 2:

$$\left.\begin{aligned} u &= \frac{\rho_e}{\rho}\frac{\partial\psi}{\partial y}, \quad v = -\frac{\rho_e}{\rho}\frac{\partial\psi}{\partial x} \\ \eta &= \frac{1}{2}\sqrt{\left(\frac{u_e}{\nu_e x C\lambda_w}\right)}\int_0^y \frac{\rho}{\rho_e}\,\mathrm{d}y \\ \psi &= \sqrt{(\nu_e x u_e C\lambda_w)}\, f(\eta). \end{aligned}\right\} \tag{20}$$

Baron obtained some representative solutions for this simplified case and compared them with the more realistic case outlined above. This comparison is shown for helium injection on Fig. 9 and the agreement is only fair.

In a later publication [3] Baron generalizes his analysis to include the influence of pressure gradients. In addition, he presents a summary of his flat-plate results.‡

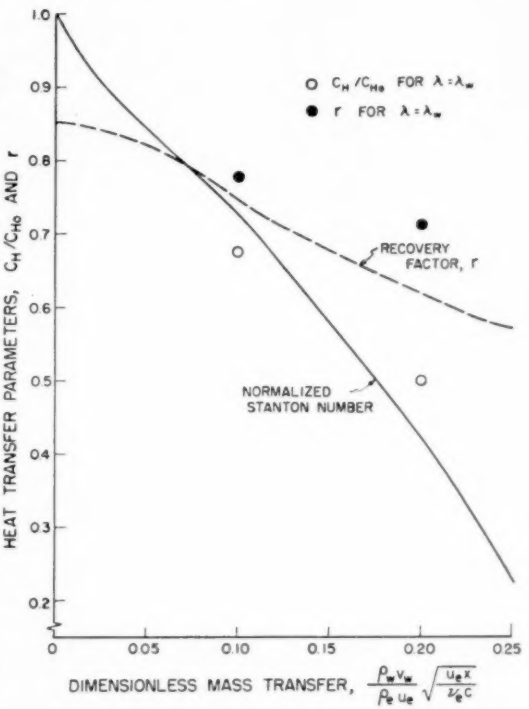

FIG. 9. Helium results of Baron.

Analysis of Eckert and co-workers [4–6]

Before attempting the complete binary problem including heat transfer, Eckert and Schneider first solved the isothermal case with hydrogen as the injected gas. The physical properties were allowed to vary with concentration and the methods outlined in Ref. 4 were used to calculate the variation. The resulting velocity distributions and skin friction are compared to the constant property results on Figs. 10 and 11. This comparison reveals that unstable S-shaped velocity profiles occur at relatively low values of the dimensionless mass transfer when compared

† There appears to be an error in Baron's final energy equation in Ref. 2. This results when he replaces u_e^2 by $(\gamma_e - 1)c_{p_2}M_e^2$ rather than the correct expression $(\gamma_e - 1)c_{p_e}M_e^2$. Consequently, the left hand side of Baron's energy equation 6:15, should be multiplied though by c_{p_2}/c_{p_e} to get the correct form.

‡ Care should be taken in using this reference since there is some confusion in nomenclature. The mathematical development utilizes a somewhat different transformation from that used by Baron in Ref. 2, although the figures are all shown in terms of the original variables of Ref. 2.

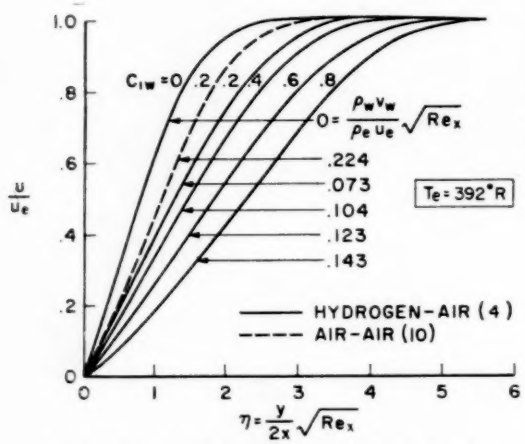

FIG. 10. Effect of light gas injection on laminar velocity profiles: isothermal case–flat plate.

with the constant property situation. The greater influence of a light gas on skin friction is obvious in Fig. 11, where at the same values of dimensionless mass transfer considerably lower skin friction occurs for the hydrogen injection. We, therefore, conclude that the light gas is more effective in reducing skin friction but on the other hand is more de-stabilizing to a laminar boundary layer.

In the analysis of the binary system including heat transfer, again using hydrogen as the mass-transfer medium, Eckert and his colleagues used the following transformation in dealing with equations (2–8).

$$\left.\begin{aligned} u &= \frac{\rho_e}{\rho}\frac{\partial \psi}{\partial y}, \quad v = -\frac{\rho_e}{\rho}\frac{\partial \psi}{\partial x} \\ \eta &= \frac{1}{2}\sqrt{\left(\frac{u_e}{\nu_e x}\right)}\int_0^y \frac{\mu_e}{\mu}\,dy \\ \psi &= \sqrt{(x u_e \nu_e)}\, f(\eta). \end{aligned}\right\} \quad (21)$$

The transformed equations were then solved using the best available property information for hydrogen–air mixtures. These exact solutions, which were obtained using an iterative procedure on an ERA 1103 electronic computer, are rigorously only valid for the specific conditions selected. (See Figs. 2 and 3.) An example of these results is shown in Fig. 12 where the dimensionless heat-transfer coefficients are shown for zero Mach number for two different wall-temperature conditions with the free stream at 392°R.

Vol. 3 1961

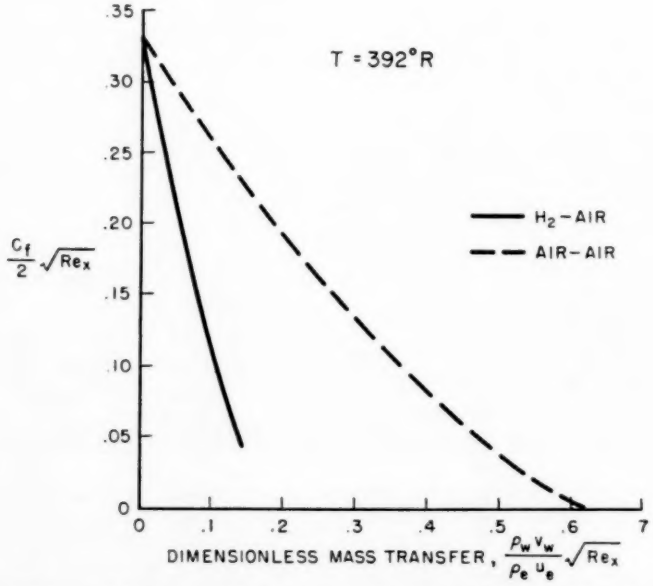

FIG. 11. Effect of light gas injection on skin friction: isothermal conditions–laminar flow: flat plate [4].

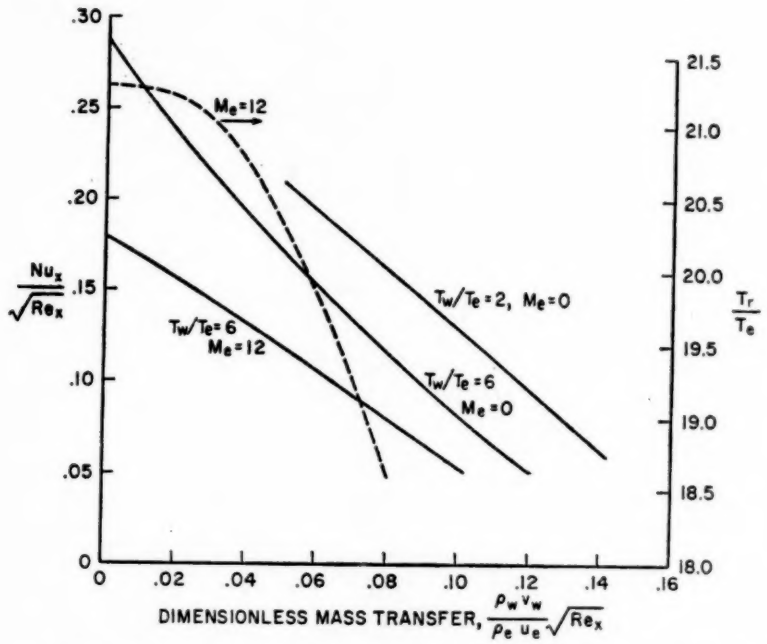

FIG. 12. Effect of hydrogen injection on laminar heat transfer: flat plate–T_e = 392°R. [5, 6].

Additionally, for Mach 12, the Nusselt number and recovery temperature, both of which must be known to determine the heat transfer, are shown for a set of specific conditions. In every case we find a considerable reduction in the heat transfer when only small amounts of hydrogen are transferred away from the wall into the boundary layer. The effectiveness of light-gas injection in decreasing the heat transfer in a high-speed boundary layer is obvious from this figure.

Analysis of Sziklas and Banas [7]

Sziklas and Banas report solutions for a number of different coolants: hydrogen, helium, water vapor, and air. In arriving at the final form of the energy equation they assumed that the specific heat ratio, γ, is the same for the injected coolant as for the main stream gas ($\gamma_1 = \gamma_2$). They then use the standard Blasius $\eta-$ transformation essentially as given in equation (11). In obtaining their solutions the physical properties (including specific heat) were allowed to vary with both temperature and concentration. Methods of kinetic theory were used in the determination of these properties. As was the case with the results of Eckert, the results of Sziklas and Banas are applicable only to the specific conditions imposed in the analysis. Representative results for the helium study are given on Fig. 13, where, again, large reductions in heat transfer accompany small mass-transfer rates.

Analysis of Gross [8]

The isothermal laminar binary boundary layer on a flat plate was investigated by Gross [8] for three different injectant gases; hydrogen, carbon dioxide and iodine vapor. To obtain a solution of the governing equations (equations 2, 3 and 5), Gross used the standard Blasius transformation to arrive at a system of ordinary differential equations. These were then solved using a Runge–Kutta numerical method with the aid of a high-speed electronic computer.

The resulting values of the skin friction

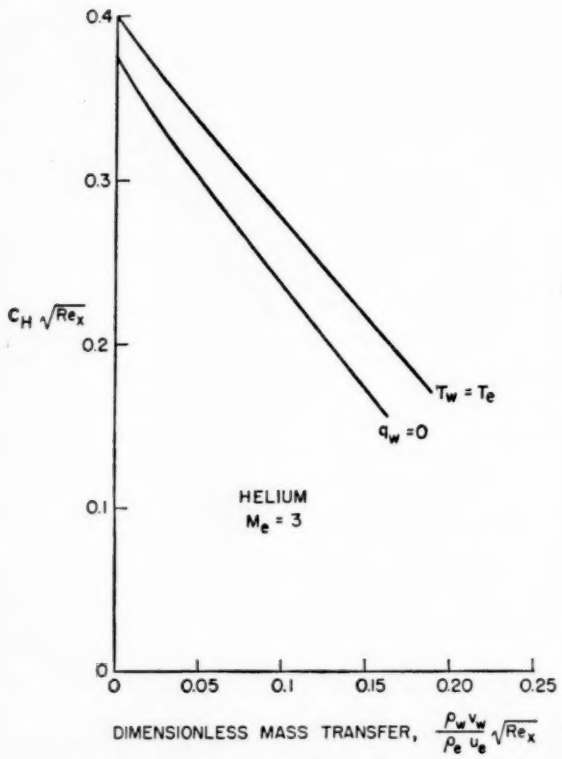

FIG. 13. Variation of laminar heat transfer with helium injection: Theory of Sziklas and Banas [7]. $T_e = 393°R$.

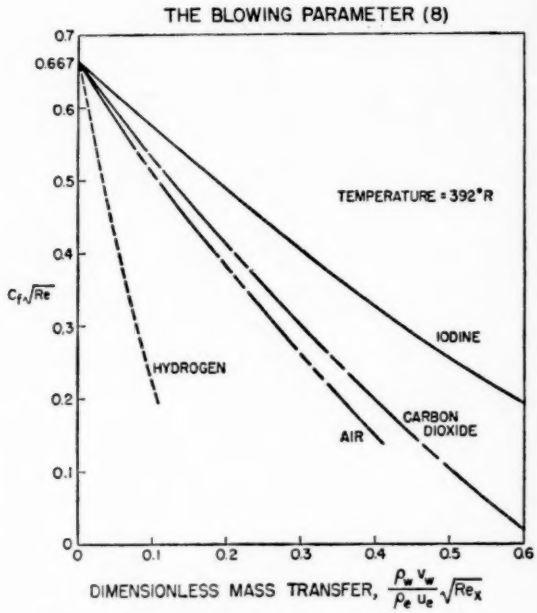

FIG. 14. Friction coefficient as a function of the blowing parameter [8].

coefficient for the three gases investigated are shown on Fig. 14. These results demonstrate that the addition of a heavy gas such as iodine vapor (molecular weight 253·8) is much less effective in reducing the skin friction coefficient than the lighter gases.

4. GENERALIZED PRESENTATION OF LAMINAR FLAT PLATE BINARY BOUNDARY LAYER RESULTS

It is our goal in this section to develop a generalized presentation which may be conveniently utilized by design engineers for predicting skin friction and heat transfer in the presence of mass-transfer cooling for laminar flow over surfaces with zero pressure gradient. The available analytical solutions briefly described above are used as the basis for the generalization. Since heat transfer and skin friction for solid surfaces in the absence of mass-transfer cooling can be calculated at the present time with a measure of confidence, the approach adopted here is to present the correction factors which must be applied to such solid wall calculations to account for the effect of mass addition. Thus the normalized skin-friction coefficient and heat transfer will be given as c_f/c_{f_0}, and q/q_0, respectively, where the subscript zero implies that the quantity is to be evaluated for the same free-stream and wall-temperature conditions neglecting the influence of mass transfer.

It was found that these normalized results for any one gas could be presented as a unique function of the mass-transfer parameter proposed by Baron, $(\rho_w v_w/\rho_e u_e)\sqrt{(u_e x/\nu_e C^*)}$, provided that the Chapman–Rubesin constant, C, was evaluated at the so-called reference temperature, T^*, given by equation (9). The success of this generalized presentation for skin friction is demonstrated in Figs. 15 and 16 which apply to hydrogen–air and helium–air binary systems, respectively. It appears that this representation

Vol. 3 1961

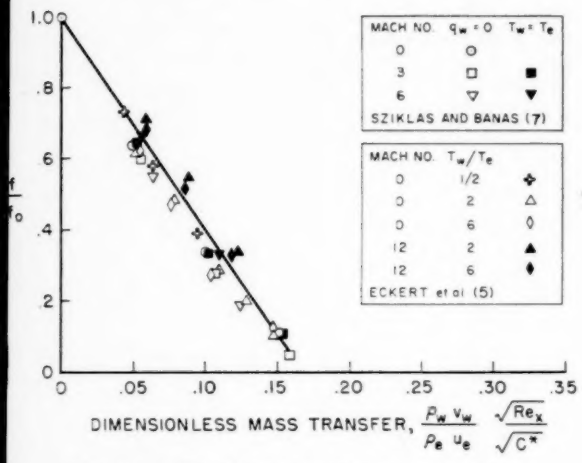

FIG. 15. Effect of mass transfer on skin friction: hydrogen–air: laminar flow–flat plate.

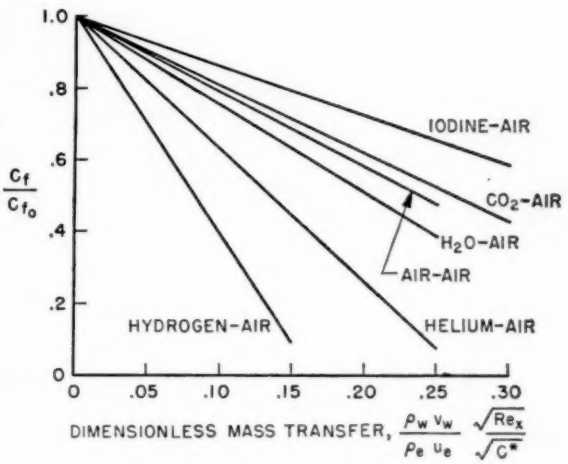

FIG. 17. Effect of mass transfer on skin friction: summary: laminar flow–flat plate.

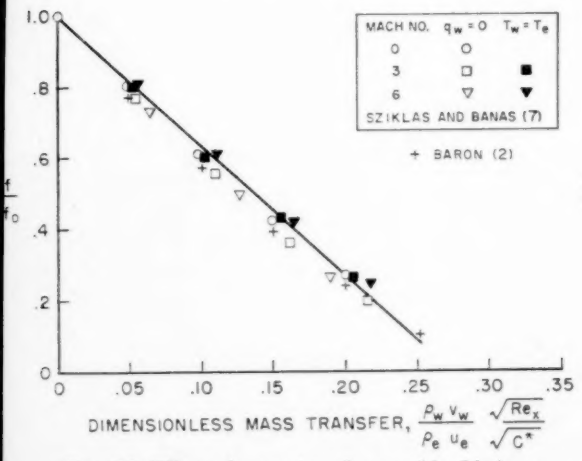

FIG. 16. Effect of mass transfer on skin friction: helium–air: laminar flow–flat plate.

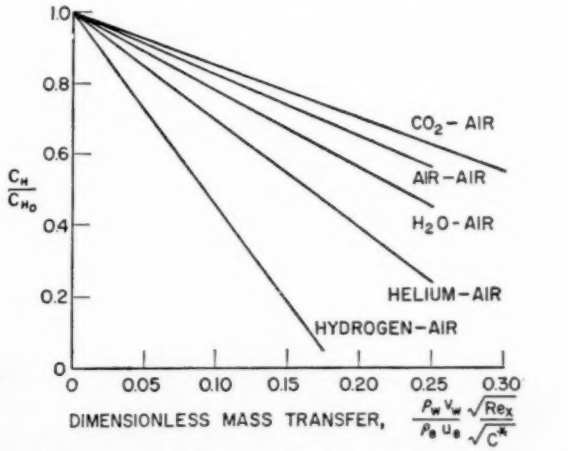

FIG. 18. Effect of mass transfer on Stanton number: laminar flow–flat plate.

is valid over a wide range of wall-temperature conditions and free-stream Mach numbers. This conclusion is true for the other binary systems as well and the reader is referred to the Appendix for verification of this conclusion. A summary of available skin-friction results for six gases is given on Fig. 17.

This same presentation was successful in correlating the normalized Stanton number, with the final results as shown on Fig. 18. Since the determination of the actual heat transfer requires the knowledge of the recovery factor as well as the Stanton number, the normalized recovery factor is shown on Fig. 19. It may be seen that some disagreement exists for the light-weight gases. Apparently the recovery factor is somewhat more sensitive to the different assumptions, particularly physical property variations, adopted by the various investigators. The effect on the final heat transfer prediction of this disagreement in recovery factor is reduced if the normalized heat transfer is directly considered

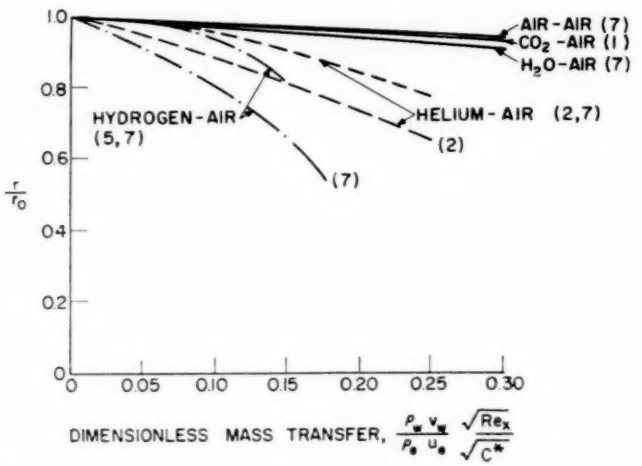

FIG. 19. Effect of mass transfer on recover factor: laminar flow–flat plate.

rather than the Stanton number. The resulting normalized heat transfer is shown on Figs. 20–22. It should be pointed out that some effect of the disagreement in recovery factor is still present in this presentation through the presence of C^*. However, for practical applications the wall temperature in general will be markedly lower than the recovery temperature; for this situation, inspection of the defining equation (9) for T^* reveals that any uncertainty in the recovery temperature has only a minor effect on the reference temperature itself, and consequently, only a minor effect on C^*.

It is apparent from Figs. 17 and 22 that the light gases are much more effective than the heavier gases in reducing heat transfer and skin friction. Inspection of these figures indicates that the normalized skin friction coefficient c_f/c_{f_0} and heat transfer q/q_0 vary linearly with the dimensionless mass-transfer parameter for all the gases shown. In particular, the results for air into air may be expressed by the following two equations.

$$q/q_0 = 1 - 1{\cdot}82\ \{(\rho_w v_w/\rho_e u_e)\ \sqrt{(Re_x/C^*)}\}$$

$$c_f/c_{f_0} = 1 - 2{\cdot}08\ \{(\rho_w v_w/\rho_e u_e)\ \sqrt{(Re_x/C^*)}\}.$$

It is of technical importance to determine whether the other gases can be made to agree with these equations by the simple expedient of multiplying the Baron dimensionless mass transfer parameter by a molecular weight ratio (m_2/m_1), raised to a constant exponent. This question can be answered by plotting the dimensionless mass transfer versus the molecular weight at a constant value of q/q_0 (or c_f/c_{f_0}). This is accomplished in Fig. 23 where it is seen that 1/3 represents a fair compromise for the value of the exponent although the very light gases as well as the heavier gases such as iodine show a significant departure. Recognizing that

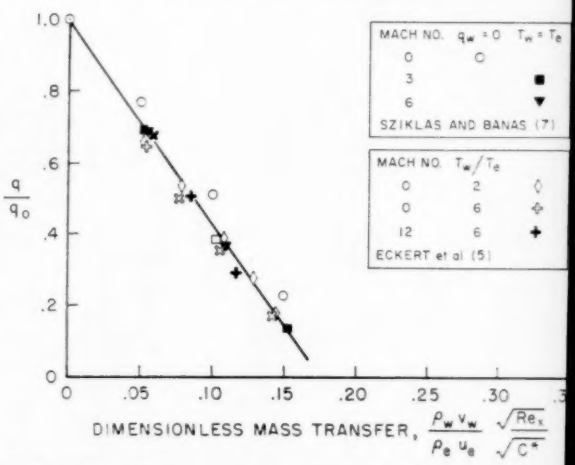

FIG. 20. Effect of mass transfer on heat transfer: hydrogen–air.

Vol. 3 1961

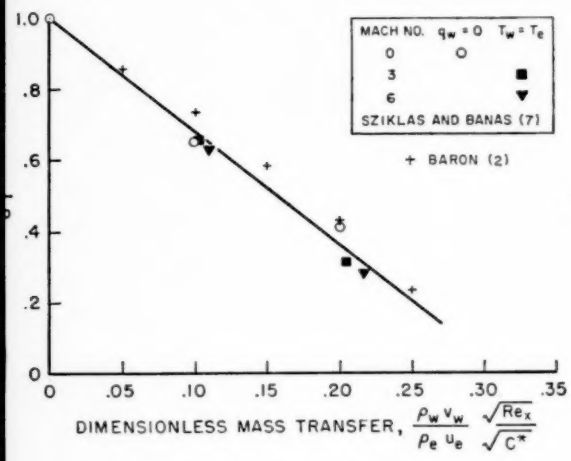

FIG. 21. Effect of mass transfer on heat transfer: helium–air.

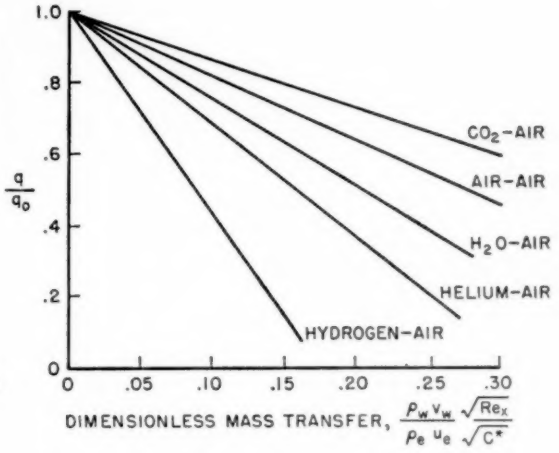

FIG. 22. Effect of mass transfer on heat transfer: summary.

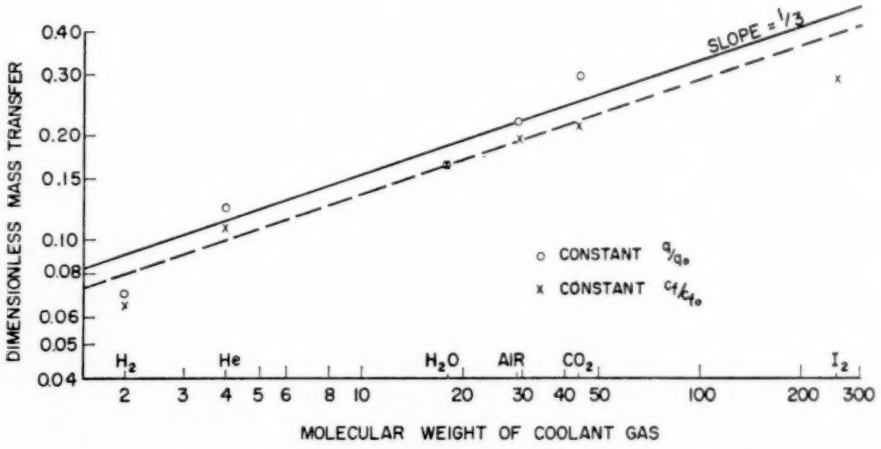

FIG. 23. Dimensionless mass transfer parameter versus molecular weight of coolant gas: laminar flow–flat plate.

such discrepancies do occur for the heavier and light gases, it nevertheless appears that the following equations represent the heat transfer and skin friction reasonably well.

$$\frac{q/q_0}{} = 1 - 1{\cdot}82\,\{(m_2/m_1)^{1/3}(\rho_w v_w/\rho_e u_e)\sqrt{(Re_x/C^*)}\}$$

$$\frac{c_f/c_{f_0}}{} = 1 - 2{\cdot}08\,\{(m_2/m_1)^{1/3}(\rho_w/v_w/\rho_e u_e)\sqrt{(Re_x/C^*)}\}$$

It is recommended that these equations be used to predict the heat transfer and skin friction performance for mass-transfer cooling in a binary laminar boundary layer on a flat plate.

5. EFFECT OF PRESSURE GRADIENT ON LAMINAR MASS-TRANSFER COOLING

Up to the present time, little effort has been directed to the solution of the binary laminar

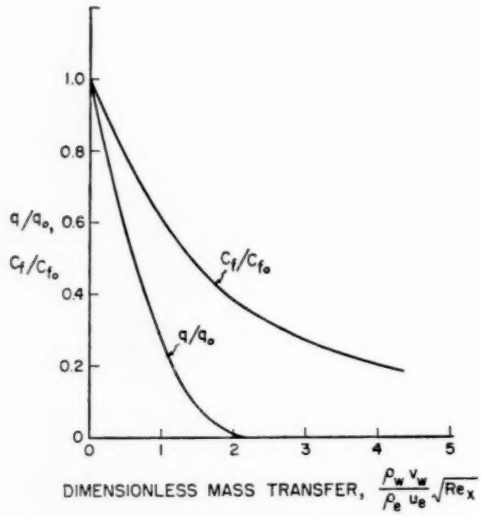

FIG. 24. Effect of air injection on heat transfer and skin friction coefficient: plane stagnation laminar flow [15] $Pr = 0{\cdot}7$.

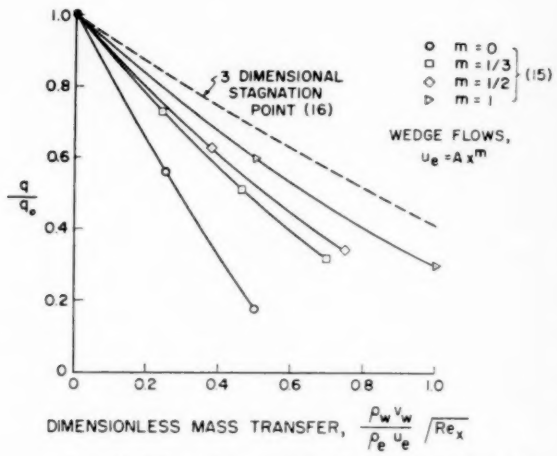

FIG. 25. Effect of pressure gradient on mass-transfer cooling: constant physical properties, $Pr = 0{\cdot}7$.

boundary-layer equations with finite pressure gradients. However, a measure of the influence of a pressure gradient on mass-transfer cooling can be obtained by returning to the constant-property boundary-layer model with normal injection (air-into-air) since solutions have been reported in this case for wedge-type pressure gradients (i.e. the free-stream velocity is described by $u_e = Ax^m$). Examination of these solutions [15] reveals that the presence of a favorable pressure gradient leads to more stable velocity profiles and, consequently, it appears that larger values of the dimensionless mass-transfer parameter, $(\rho_w v_w/\rho_e u_e)\sqrt{(Re_x)}$, may be obtained without causing transition to turbulence. Furthermore, the skin-friction coefficient remains finite in a favorable pressure gradient, with no apparent failure of the boundary-layer equations even for very large mass-transfer rates. However, the heat transfer does decrease to a diminishing value, with the thermal boundary layer displaced from the wall surface toward the free stream. An example of this skin-friction and heat-transfer behavior is given in Fig. 24 for the plane stagnation case ($m = 1$), and it may be seen that the heat transfer goes to zero at a value of the mass-transfer parameter of approximately 2 (as contrasted to 0·619 for the flat plate), while the skin friction is still approximately 40 per cent of its solid-wall value.

A direct comparison of the reduced heat flow, q/q_0, for four different pressure gradients ranging from the zero pressure gradient flat plate to the plane stagnation flow is given in Fig. 25. If a comparison is made at a fixed value of the dimensionless mass-transfer parameter, it is apparent that the greatest reduction in heat transfer occurs for the zero pressure gradient flat plate with the least reduction accompanying the plane stagnation flow. Therefore, to obtain a given reduction in heat flow, q/q_0, it is necessary to go to higher values of the dimensionless mass transfer as the pressure gradient increases. Since there exists considerable interest in the three-dimensional stagnation flow, Fig. 25 also presents the reduced heat transfer q/q_0 for air injection into such a region [16].

It finally remains to determine whether the relative position of the various coolant gases found for the flat plate geometry is markedly influenced by the presence of a pressure gradient. A recent analysis of Hayday [17] for hydrogen injection into a plane stagnation flow leads to the results shown in Fig. 26 and close inspection suggests that the molecular weight parameter found for the flat plate, i.e. $(m_2/m_1)^{1/3}$, is approximately valid for the plane stagnation flow.

Vol. 3 1961

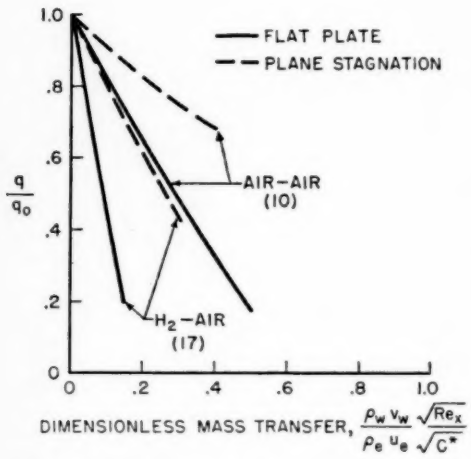

FIG. 26. Effect of pressure gradient on mass-transfer cooling.

As a result, it is suggested that air-into-air results be used to predict the effect of pressure gradient on laminar mass-transfer cooling; if a coolant other than air is transferred into the boundary layer the relative effectiveness of the various coolants is to be estimated from the flat-plate results. This is simply accomplished by using Fig. 25, changing the abscissa to read $[(\rho_w v_w/\rho_e u_e)\sqrt{(Re_x/C^*)}\,(m_2/m_1)^{1/3}]$.

REFERENCES

1. E. R. G. ECKERT, Mass transfer cooling, a means to protect high speed aircraft, presented at *First International Congress of Aeronautical Sciences*, Madrid, Spain, September 1958.
2. J. R. BARON, *The Binary Boundary Layer Associated with Mass Transfer Cooling at High Speed*. Mass. Inst. of Tech. Naval Supersonic Lab. Rpt. 160 (1956).
3. J. R. BARON, The hetrogeneous, laminar boundary layer. *RAND Symposium on Mass Transfer Cooling for Hypersonic Flight*.
4. E. R. G. ECKERT and P. J. SCHNEIDER, *Diffusion Effects in an Isothermal Binary Boundary Layer*. University of Minnesota, Heat Transfer Lab. Tech. Rpt. No. 5, November (1955).
5. E. R. G. ECKERT, P. J. SCHNEIDER, A. A. HAYDAY and R. M. LARSON, Mass transfer cooling of a laminar boundary layer by injection of a light-weight gas. *RAND Symposium on Mass Transfer Cooling for Hypersonic Flight*.
6. E. R. G. ECKERT, P. J. SCHNEIDER, A. A. HAYDAY and R. M. LARSON, Cooling of a laminar boundary layer by injection of a light-weight foreign gas. *Jet Propulsion*, **28**, 34 (1958).
7. E. A. SZIKLAS and C. M. BANAS, Mass transfer cooling in compressible laminar flow. *RAND Symposium on Mass Transfer Cooling for Hypersonic Flight*.
8. J. F. GROSS, *The Laminar Binary Boundary Layer*. RM-1915, The RAND Corporation, September (1956).
9. N. A. HALL, *Flow Equations for Multicomponent Fluid Systems*. University of Minnesota, Heat Transfer Lab. Tech. Rpt. No. 2, August (1955).
10. J. P. HARTNETT and E. R. G. ECKERT, Mass transfer cooling in a laminar boundary layer with constant fluid properties. *Trans. Amer. Soc. Mech. Engrs*, **79**, 247 (1957).
11. E. R. G. ECKERT, Engineering relations for heat transfer and skin friction in high-velocity laminar and turbulent boundary-layer flow over surfaces with constant pressure and temperature. *Trans. Amer. Soc. Mech. Engrs*, **78**, 1273 (1956).
12. M. ROMIG, Stagnation point heat transfer for hypersonic flow. *Jet Propulsion*, **26**, 1098 (1956).
13. D. R. CHAPMAN and M. W. RUBESIN, Temperature and velocity profiles in the compressible laminar boundary layer with arbitrary distribution of surface temperature. *J. Aero. Sci.* **19**, 341 (1947).
14. W. O. CARLSON and P. J. SCHNEIDER, *Transport Properties for Binary Gas Mixtures*. University of Minnesota, Heat Transfer Lab. Tech. Rpt. No. 7, January (1956).
15. W. B. BROWN and P. L. DONOUGHE, *Tables of Exact Laminar Boundary-Layer Solutions when the Wall is Porous and Fluid Properties are Variable*. Nat. Advisory Comm. Aeronaut. Tech. Note 2479, September (1951).
16. E. RESHOTKO and C. B. COHEN, *Heat Transfer at the Forward Stagnation Point of Blunt Bodies*. Nat. Advisory Comm. Aeronaut. Tech. Note 3513, July (1955).
17. A. A. HAYDAY, *Mass Transfer Cooling in a Laminar Boundary Layer in Steady Two-Dimensional Stagnation Flow*. University of Minnesota, Heat Transfer Lab. Tech. Rpt. No. 19, April (1958).

APPENDIX A

Additional verification of the dimensionless presentations

In this section the reduced skin friction c_f/c_{f_0} and heat transfer q/q_0 are plotted as functions of the mass-transfer parameter for all of the injected materials. (Figs. 27 and 28.) It may be seen that the summary curve given in the main body of the report accurately represents the calculated performance.

Furthermore, the Stanton number and recovery factors are given in detail. (Figs. 29–32.) In the latter case, it is apparent that discrepancies exist in the case of hydrogen–air and helium–air,

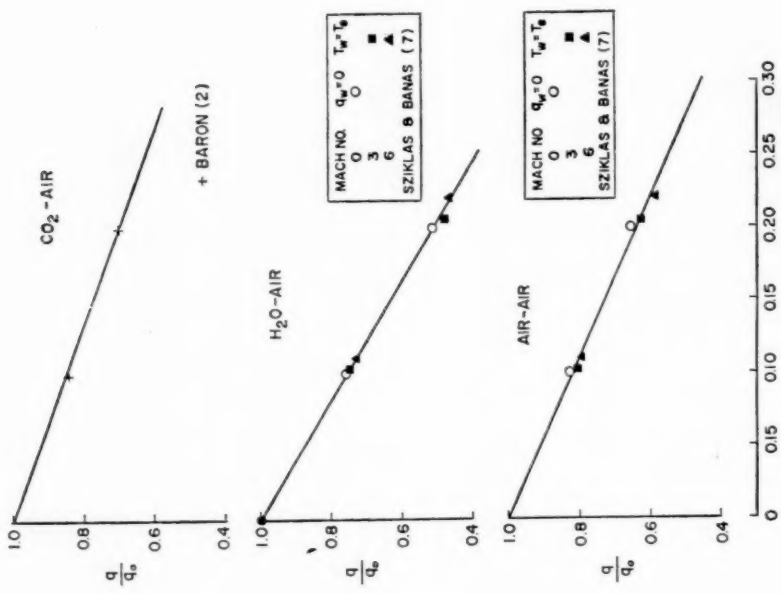

FIG. 28. Effect of mass transfer on heat transfer.

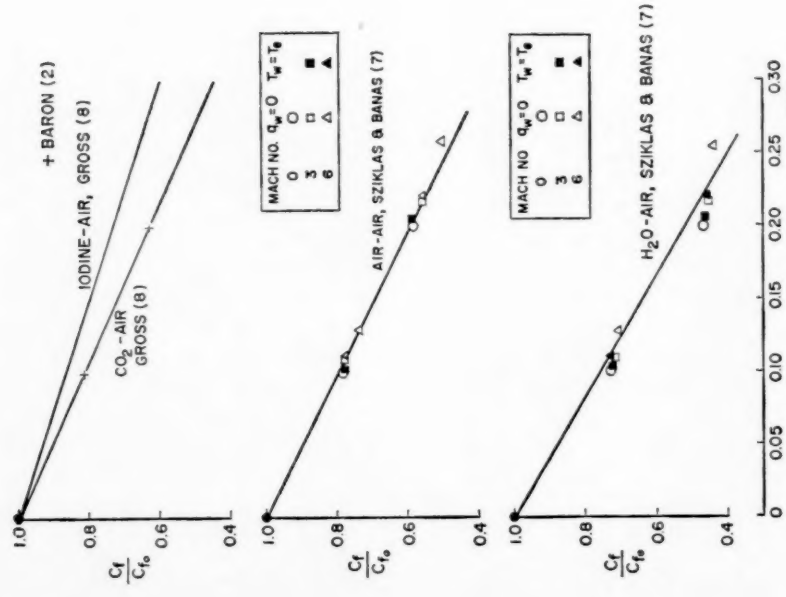

FIG. 27. Effect of mass transfer on skin friction: laminar flow–flat plate.

Vol. 3 1961

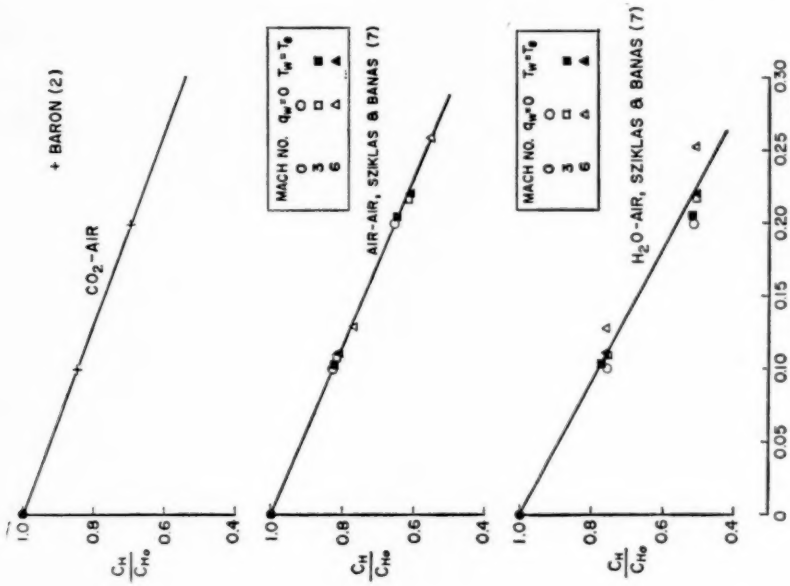

FIG. 30. Effect of mass transfer on Stanton number: laminar flow–flat plate.

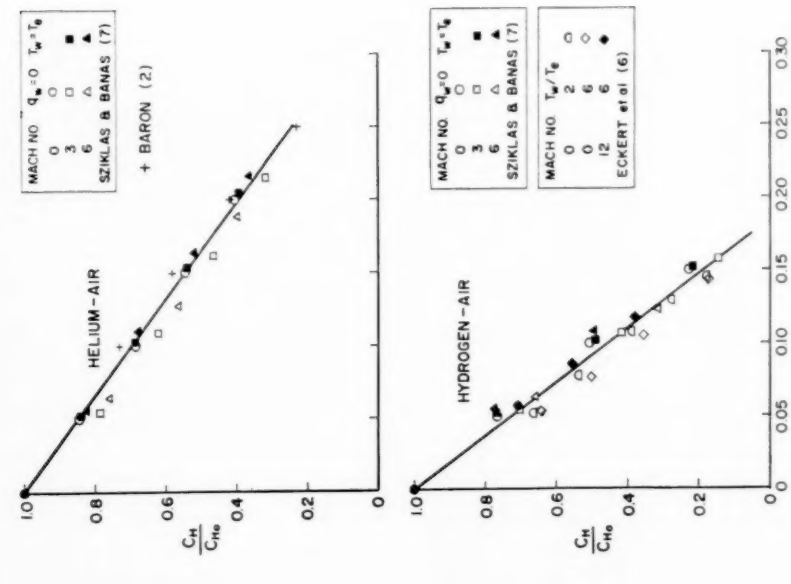

FIG. 29. Effect of mass transfer on Stanton number: laminar flow–flat plate.

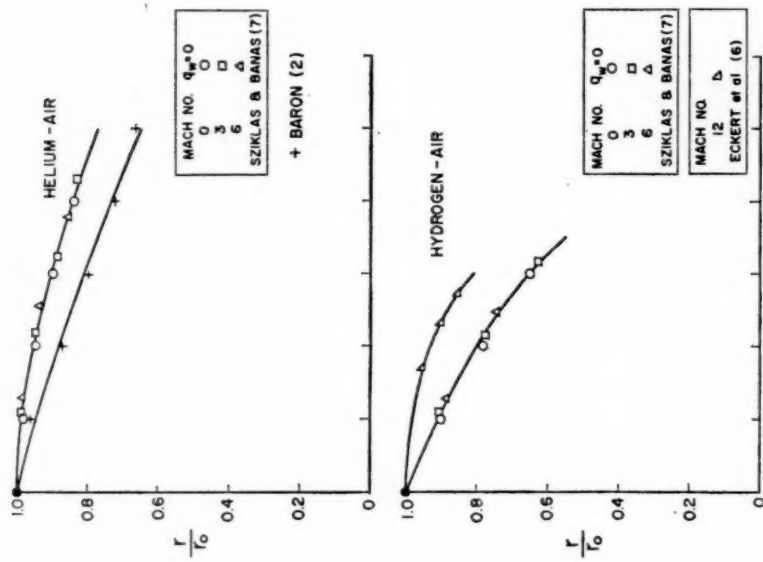

FIG. 32. Effect of mass transfer on recovery factor: laminar flow–flat plate.

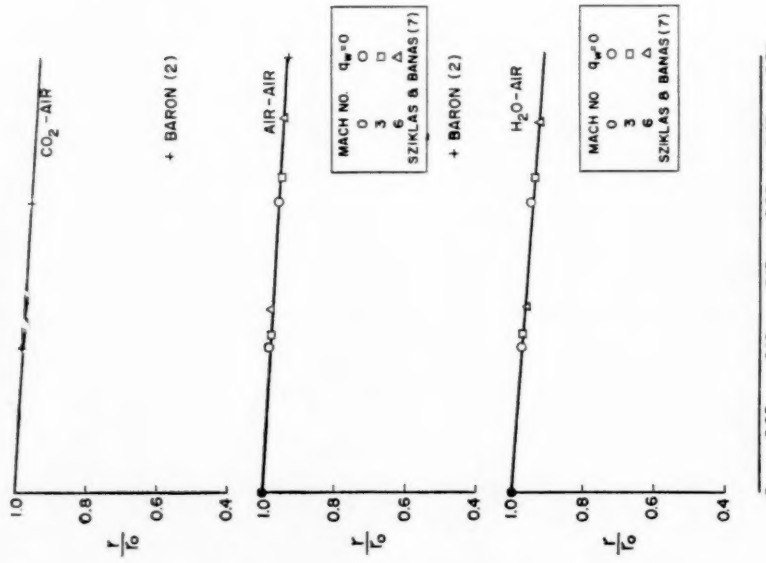

FIG. 31. Effect of mass transfer on recovery factor: laminar flow–flat plate.

Vol. 3 1961

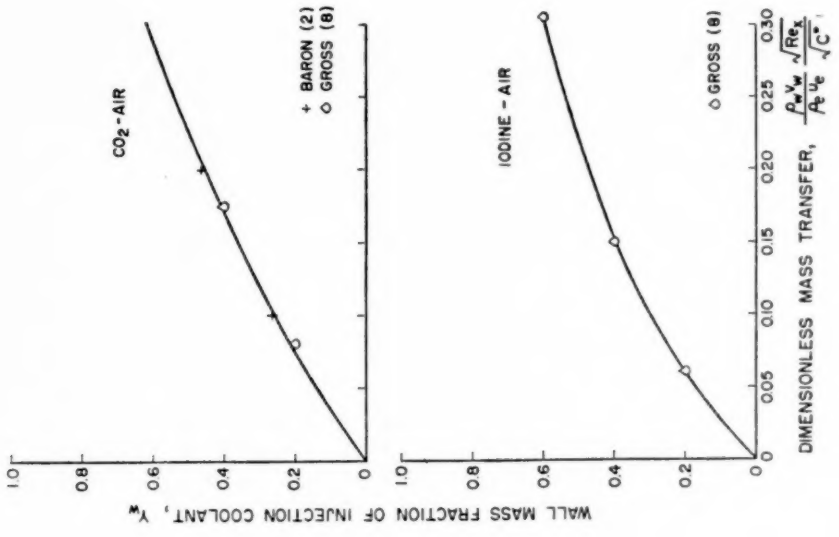
CO_2 - AIR
+ BARON (2)
◇ GROSS (8)
IODINE - AIR
◇ GROSS (8)
WALL MASS FRACTION OF INJECTION COOLANT, Y_w
DIMENSIONLESS MASS TRANSFER, $\frac{\rho_w Y_w \sqrt{Re_x}}{\rho_e u_e \sqrt{C^*}}$

FIG. 34. Wall mass fraction versus dimensionless mass transfer.

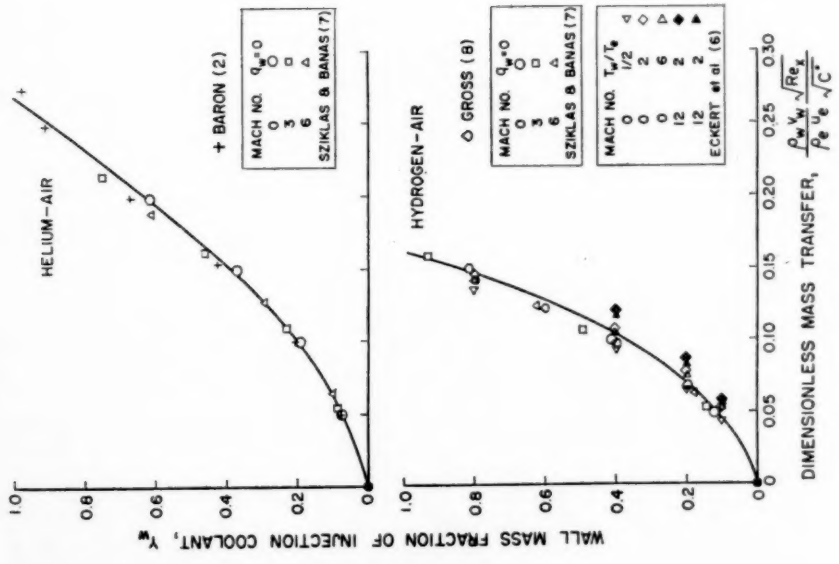

FIG. 33. Wall mass fraction versus dimensionless mass transfer.

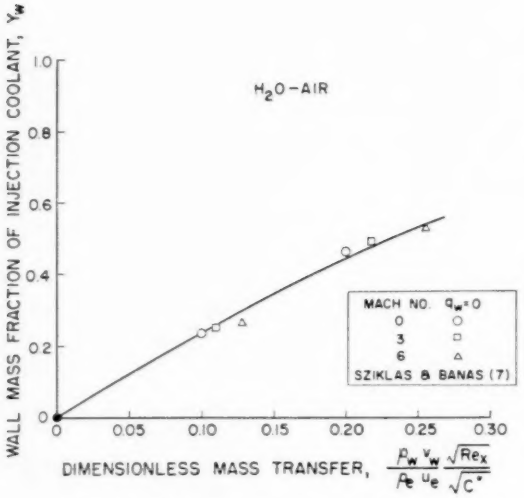

FIG. 35. Wall mass fraction versus dimensionless mass transfer.

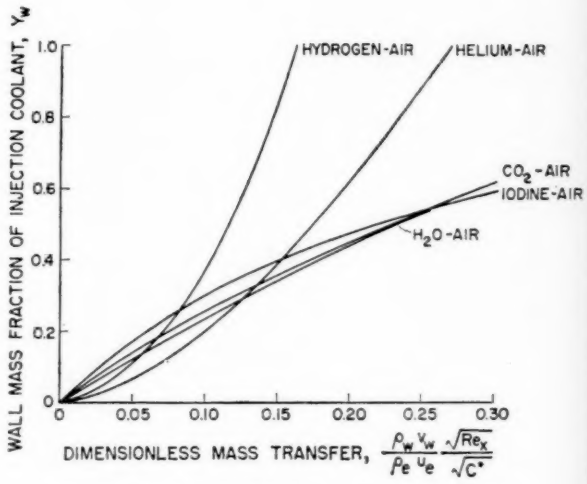

FIG. 36. Wall mass fraction versus dimensionless mass transfer: summary.

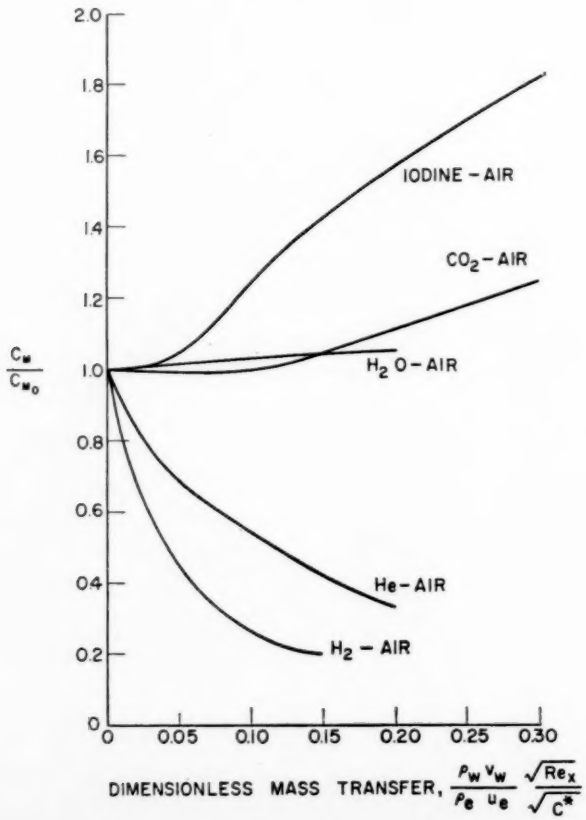

FIG. 37. Effect of mass-transfer rate on the mass transfer Stanton number.

Vol. 3 1961

probably due to the uncertainty in the physical property values under such extreme temperature conditions.

APPENDIX B

Relation between wall concentration and mass transfer parameter

In the treatment of a subliming surface, it is important to know the relationship between the wall mass fraction and the dimensionless mass-transfer rate. A generalized presentation of the wall mass fraction for each gas appears possible with the aid of the Baron variable $(\rho_w v_w/\rho_e u_e)\sqrt{(Re_x/C^*)}$ and these are shown for some five gases in Figs. 33–36. A summarizing curve is also available in Fig. 36.

APPENDIX C

On the use of mass transfer results for prediction of heat transfer

It is rather common practice to experimentally obtain mass transfer Stanton numbers, c_M, using materials which sublime or evaporate, such as naphthalene or water, and to interpret these results directly as solid wall heat transfer Stanton number, c_{H_0} (in some instances a correction factor involving the Lewis number is applied). However, considerable caution must be exercised in this procedure as is obvious from a comparison of Fig. 37 with Fig. 18 of the main text. Fig. 18 shows the heat transfer Stanton numbers in the form of c_H/c_{H_0}, where c_H is the heat transfer Stanton number in the presence of mass transfer, while c_{H_0} is the Stanton number for a solid wall exposed to the same free stream conditions (i.e. c_{H_0} is the limiting value of c_H as the mass-transfer rate goes to zero). Fig. 37 is a similar curve for the mass transfer Stanton number, c_M, again normalized with respect to the value at the zero mass-transfer condition. For water vapor–air and CO_2–air mixtures the limiting Stanton values, c_{H_0} and c_{M_0}, are in good agreement (i.e. $c_{H_0} = c_{M_0}$) and since c_M/c_{M_0} does not depart appreciably from unity over a range of mass-transfer rates, it would appear that the measured mass transfer Stanton number, c_M, for these two systems could indeed be interpreted as solid wall heat transfer Stanton number, c_{H_0}. However, for the other gas mixtures, it must be concluded that considerable error would arise in the use of this procedure.

Int. J. Heat Mass Transfer. Vol. 3, pp. 222–248. Pergamon Press 1961. Printed in Great Britain.

HEAT TRANSFER, A REVIEW OF CURRENT LITERATURE

E. R. G. ECKERT,* T. F. IRVINE, JR.,† E. M. SPARROW‡ and W. E. IBELE‡
Heat Transfer Laboratory, Department of Mechanical Engineering,
University of Minnesota, Minneapolis, Minnesota

(*Received* 25 *April* 1961)

INTRODUCTION

HEAT transfer problems are encountered and have to be solved in almost every engineering activity. They become crucial for various modern developments like high-speed aeronautics and space flight. This is obviously the reason for the fact that research activity in heat transfer is very strong as evidenced by the growing number of publications in this area. Space limitations have prevented us, therefore, from including all references in this literature survey. Many engineering conferences devoted considerable time to a discussion of heat transfer processes. The National Heat Transfer Conference, organized as an annual event by the American Society of Mechanical Engineers and the American Institute of Chemical Engineers, was held in August, 1960, at Buffalo, with an attendance of almost 1000 persons in twelve crowded sessions. A forum for discussion of heat transfer problems on an international basis will be provided by the International Heat Transfer Conference which will be held in September, 1961, at Buffalo. The preceding international conference, held at London in 1951, brought together scientists and engineers from all nations engaged in heat transfer research. The present magazine, the *International Journal of Heat and Mass Transfer*, started publication in 1960. A number of new books present either an introduction to or a cross-section through the present state of the field of heat transfer or related areas (Table 1 in Reference Section).

We have introduced in this review a new section discussing thermodynamic and transport properties because such properties are more and more intimately connected with heat transfer considerations. The available space permitted only the coverage of fluid properties on the basis of a small number of selected papers. They contain correlations and analytical predictions for a range from 3° to 15 000°K; whereas experimental determinations were mainly restricted to temperatures below 1300°K.

A significant increase in the number of papers dealing with radiation becomes immediately apparent by a comparison with last year's review.§ It obviously is caused by the fact that space applications have generally to rely on radiation for energy transport. Surface-to-surface heat transfer is analyzed for a number of geometries, including various types of heat exchangers, and calculation methods for radiative transfer in gas-filled enclosures have been developed.

Papers on heat conduction are almost exclusively of an analytical nature dealing with composite layers, transient condition, and variable properties.

In the field of channel flow, the Graetz problem with its variants is discussed in 15 papers. Experiments cover special fluids like CO_2, hydrogen, and N_2O_4, as well as swirling flow. Boundary-layer analysis was mainly restricted to the development of approximate solutions. Chemical reactions with finite reaction rates (mainly restricted to a Lewis number

* Professor of Mechanical Engineering and Director, Heat Transfer Laboratory, University of Minnesota.
† Professor and Dean of Engineering, State University of New York, Long Island Center.
‡ Professor of Mechanical Engineering, University of Minnesota.

§ *Mech. Engng*, **82** 47–61 (1960).

Vol. 3 1961

equal 1) and the influence of magnetic fields were included. Several reports describing experiments on various models in supersonic or hypersonic flow have found their way into the open literature. Detailed observations and measurements have made it possible to develop analytical models for the description of flow and heat transfer in separated regions. This development has been favored by the fact that engineering interest now includes low Reynolds number flow which is more amenable to an analytic approach. A fairly well developed model describing qualitatively the transition process from laminar to turbulent flow has evolved from flow observations and hot wire measurements.

A significant engineering advance in the effort to obtain high heat transfer coefficients for evaporation and condensation processes has been possible by selection of proper geometries (Fig. 2). A considerable number of papers, mainly experimental, covers the area of heat transfer with change of phase, obviously due to the complexity of this process which prevents analytical predictions in most cases.

CONDUCTION

The problem presented by conduction, steady and unsteady, through a composite wall received increased attention. Extending the generalization of classical problems in heat conduction to include the composite layer case [34A], Vodicka also considers the steady temperature distribution in the specific geometries of an infinite plate [35A] and hollow, infinite, circular and elliptical *n*-layered cylinders [36A]. A semi-infinite, 2-layer body of uniform temperature suddenly encounters a fluid of different temperature [26A] where the heat transfer between fluid and surface is described by a constant film coefficient. Out of a concern for designing a thermal barrier, [31A] uses separation of variables and matrix methods to solve the case of a 2-layer slab, one face of which is adiabatic, the other subjected to sinusoidal temperature variation. It is noted, [5A], that the problem is solvable for a triangular heat impulse through analogy with an appropriate electrical circuit. Steady-state temperature distribution and calculated heat transfer through honeycomb-type sandwich panels for simultaneous radiation and conduction agree to within 15 per cent of experimental values [32A].

Concern with solutions for unsteady state heat conduction problems continues. Thus, for a semi-infinite medium, [6A, 4A] impose boundary conditions involving temperature in a non-linear manner which, in some cases, lead to an integral equation for the surface temperature; [25A] imposes various heat inputs over the surface; and [15A] presents a scheme for computing thick wall temperatures for arbitrary variations of adiabatic wall temperature and heat transfer coefficient. The heating of a plane wall behind a constant velocity plane shock moving parallel to it into a stagnant gas is accurately represented by integral equations solved by successive approximations [33A]. Several approximate solutions for the melting of a semi-infinite slab are noted and compared to exact solution by [8A]. Cooling of solid particles in a fluid by suitable assumptions reduces to system of linear, simultaneous equations with constant coefficients, solvable as eigenvalue problem [24A]. For transient heat conduction in hollow cylinders and slabs, [14A] presents dimensionless temperature for range of heat input for isotropic, constant properties, adiabatic boundary conditions. Disregarding evaporation, [18A] investigates the unsteady temperature and humidity fields in the vicinity of an infinite plate. For variable properties, [13A] considers conduction through a semi-infinite gas medium having a uniform initial and constant boundary temperature, determining integrated air thermal conductivities for oxygen dissociating temperatures.

Additional transient studies, involving melting or freezing, arise from diverse sources. Thus, after onset of melting, [7A] describes simple successive approximation solution of ordinary, non-linear, differential equations which permits the heat input to be arbitrarily varied to a semi-adiabatic slab. The melting rate of a finite slab (initial temperature uniform and below melting point, one face adiabatic or constant temperature) for constant heat input is solved approximately by the heat balance integral [11A]; Ref. [20A] extends previous work to include melting effect; and [19A] removes the prior condition that a molten region exist. Heat flow into an

infinite, homogeneous medium from a moving heat source, represented by a finite cylinder with time dependent radius, is determined [1A] with specific application to secondary oil recovery by underground combustion. A related cooling problem [16A] concerns the steady addition of metal at uniform temperature to an isothermal liquid metal column of different temperature, the bottom temperature of which is constant. Treating conductivity as arbitrarily temperature dependent, [10A] considers transient conduction in a cylinder with one moving boundary using infinite differences and applies results to re-entry problem.

Transient conduction, with heat source, is examined for the case of a cylindrical, isothermal source in a semi-infinite body of constant boundary temperature using integral equation method to yield temperature field and heat flux [17A]. The transient temperature distribution in a uranium rod depends on heat source and removal rates according to [21A]. In the same vein, [28A] examines the two-dimensional heat conduction problem for a uniform volume heat source, cooled by fully developed flow of coolant in circular passages arranged in triangular or square array. The generalization of heating and cooling rates, when the temperature rate of change describes all points in the system and is not influenced by the original temperature distribution, has application to temperature measurements and thermal behavior of complex systems [9A].

Steady state heat conduction in a circular cone with initial, non-uniform, surface temperatures is solved rigorously by [23A]. Ref. [29A] solves numerically the steady, linear, conduction equation when heat generation and conductivity are arbitrary functions of temperature. Using a heat balance error to correct the choice of gradient at the surface, [27A] gives steady-state results for a bar losing heat by radiation. An implicit numerical method for solving the two-dimensional conduction equation includes exact solution in linear case and uses iterative scheme to extend method to non-linear cases [2A].

Variations and extensions of the fin problem occur in [22A] which considers thin, rectangular, triangular, and optimum fins with internal heat generation and in [12A] which discusses the relation between heat transfer and thermal stress in fins. In this connection, [37A] notes the effect of unsteady thermal stress fields upon the formulation of the conduction equation.

Reference [30A] considers the inverse problem of heat conduction: to determine the surface heat flux knowing an internal temperature variation with time. The numerical methods are developed for spheres but apply to other simple geometries.

Finally, [3A] treats the problem of predicting, and correcting for, temperature disturbance caused by thermocouples placed beneath a surface of a heat sink (or calorimeter) exposed to heat flux during re-entry.

CHANNEL FLOW

Laminar heat transfer in the thermal entrance region of ducts continues to be of analytical interest. The classical Graetz problem, in which a hydrodynamically-developed isothermal flow enters a heated section of duct, has been analyzed by new calculation methods and for a broader class of boundary conditions. The eigenvalue problem associated with the solution of the energy equation for the parallel-plate channel or circular tube with uniform wall temperature has been solved to ten figure accuracy [6B]. This same method of analysis is applied to prescribed symmetrical or unsymmetrical heat transfer at the walls of a parallel-plate channel [7B, 8B, 9B]. The effect of heat conduction from the heated fluid into the unheated starting length is examined for a parallel-plate channel and found to be important only at low Peclet numbers [2B]. More accurate solutions of the energy equation very near the entrance section of tubes and channels were obtained by abandoning the eigenvalue approach in favor of a boundary-layer formulation [26B, 25B].

Problems of the Graetz-type have been considered for laminar flow in non-circular ducts. In one case, the eigenvalue problem for a square duct was attacked by a variational method [36B]. In another, the eigenfunctions for a rectangular duct were expanded in terms of slug-flow eigenvalues [14B]. An attempt has been made to bring together laminar heat transfer results for various non-circular ducts, but

Vol. 3 1961

notational difficulties make the final correlations difficult to interpret [39B].

As a variant of the Graetz problem, the simultaneous development of velocity and temperature distributions in the entrance region of tubes and ducts has been analyzed [35B, 29B, 38B]. The first two of these are highly theoretical and are not easily applied. However, [38B] presents Nusselt number results in a relatively simple form and these show favorable comparison with air data [4B].

Fully-developed laminar heat transfer is analyzed in annuli with blowing and suction for the condition of constant longitudinal mass flow [20B]. A circumferentially variable heat flux may lead to large circumferential variations in wall temperature [30B].

Two interesting problems in laminar heat transfer in tubes relate to the effects of non-isothermal chemical reactions [10B] and to non-Newtonian viscosities [28B]. In the latter case, correlations are given with an accuracy of ± 10–15 per cent for flow in tubes having uniform wall temperature.

In contrast to the purely analytical studies for laminar flow, the turbulent case has been treated both analytically and experimentally. For flow in tubes, analytically-derived Nusselt numbers for both the entrance and fully-developed regions are only slightly different for the boundary conditions of uniform wall temperature and uniform wall heat flux when the Prandtl number $\geqslant 0{\cdot}7$ [34B]. An analysis gives heat transfer results when there is an internal heat generation in the flowing fluid [33B]. A critical review of the analogies between heat, momentum, and mass transfer resulted in a correlation for turbulent heat transfer in smooth tubes covering Prandtl (or Schmidt) numbers between 0·46 and 3000 [27B]. Experiments were made on the turbulent flow of gaseous hydrogen in circular tubes at high pressures and high heat fluxes [17B, 24B]. The results could be correlated by Dittus–Boelter type formulas, provided that the fluid properties were properly evaluated. An extensive experimental program covering the Reynolds number range 20 000 to 250 000 produced data for heating and cooling of air and carbon dioxide with large gas-to-wall temperature differences [41B]. It was found possible to correlate data for the low-temperature dissociating system $N_2O_4 \rightleftarrows 2NO_2$ by using suitably-averaged equilibrium properties and a mean kinematic viscosity in the Reynolds number [5B]. Thermal entrance region effects were clearly delineated in an experiment with air in the transition and low turbulent regimes [16B]. In a fundamental experimental study, temperature and velocity profiles were measured in the thermal entrance region of a circular tube (hydrodynamically-developed velocity) [1B]. Eddy diffusivities for momentum ϵ_m and for heat ϵ_h were computed from the data, and the ratio ϵ_h/ϵ_m was found to be almost constant across the section, but rose to high values (~ 3 or 4) near the wall. A complementary analysis of the distribution of the radial heat flux [11B] was found useful in analyzing the data.

Turbulent heat transfer in non-circular ducts has been studied. Calculation of heat transfer at one wall of a parallel plate channel (other side insulated) by using the *heated* periphery in the evaluation of the hydraulic diameter was analytically explored and found to apply only for Prandtl number $= 2$ [19B]. A critical survey of heat transfer data for the annulus led to the conclusion that heat transfer at the outer pipe surface is calculable using the hydraulic diameter with *wetted* perimeter, but that there is no simple rule for the inner pipe [40B]. Analytical heat transfer predictions for turbulent flow in equilateral triangular and square cross-sections were calculated by applying generalized velocity and temperature profiles from circular tubes [13B]. Experiments for air flowing in an electrically-heated duct of isosceles triangular cross-section (11·46° apex angle) reveal thermal entrance lengths in excess of 100 diameters, in contrast to 10–20 diameters for the circular tube [15B].

Unsteady laminar and turbulent heat transfer results corresponding to prescribed time-variations of tube wall temperature were derived by solving the time-dependent energy equation for the fluid [32B, 37B]. Another approach assumes that the turbulent heat transfer coefficient is unchanging with time and position and computes the temperature response of the fluid and tube wall to changes in internal heat generation in the wall [3B]. An experiment ($Re < 2200$)

demonstrates that large increases in heat transfer can be attained by vibrating a duct wall normal to the direction of the main flow [31B].

Several interesting studies relating to swirling and vortex flows were carried out. Experiments with water and air flowing through pipes with several types of inserts and swirl promotors show both large increases in heat transfer and reductions in the pumping power per unit heat transfer [21B]. Additional experimental results on this same problem are also reported in [18B]. Electrically-heated rotating tubes and annuli with throughflow, some running full and others partially filled, provided heat transfer data for water characterized by three distinct flow regimes depending on rotational speed [22B]. The throughflow Reynolds number was under 1000. Two analytical treatments of the vortex tube have appeared, neither fully predictive. In one, an inviscid flow model is assumed which combines a vortex, a sink, and a uniform axial flow [23B]. In the second, a turbulent compressible vortex is postulated in which $\rho\epsilon$ (ρ = density, ϵ = eddy viscosity) is assumed constant, with ϵ undetermined [12B]. It is concluded that energy separation is primarily caused by the turbulent shear work.

BOUNDARY-LAYER FLOW

Boundary-layer solutions

The main emphasis in recent boundary layer heat transfer analysis has been on approximate solutions and calculation methods. However, some work relating to exact solutions and classical-type problems continues. Among these, the requirements for similar solutions of the energy equation were examined for laminar flow [58C]. If the wall temperature is uniform or varies according to a power law, the similarity requirements are identical to those for the velocity problem. Adiabatic wall temperatures for laminar flow of high Prandtl number fluids over a flat plate have been re-examined [37C] and more accurate results calculated. An analysis has provided the heat transfer response of a cylinder or sphere immersed in a fluctuating laminar flow with small mean velocity [27C]. There has been further study of the wall jet (a free jet bounded on one side by a wall) relating to compressibility and heat transfer characteristics [5C]. A study of Reynolds analogy for the laminar flat-plate boundary layer with blowing reveals that the ratio of Stanton number to friction factor increases with the blowing velocity [20C]. Mangler's transformation, which reduces axial-symmetric boundary-layer problems to plane problems, has been successfully applied in the analysis of the high-speed, compressible boundary layer on a cone and results were obtained utilizing prior flat plate solutions [23C]. The unsteady flow and heat transfer on a flat plate moving with time-dependent velocity into a compressible fluid has been attacked using a series-expansion method [19C].

The calculation of heat transfer from non-isothermal surfaces continues to be of interest. A set of variable wall temperature solutions for laminar and turbulent flow over a flat plate is tabulated [4C]. Application is made to laminar flow over a plate whose surface has two separated isothermal zones and is otherwise insulated; mass transfer experiments with naphtalene agree well with the theory [53C]. Lighthill's superposition integral for computing laminar heat transfer with variable wall temperature and variable free-stream velocity has been generalized to include the effects of aerodynamic heating [34C].

The compressible laminar boundary layer with variable free-stream velocity and isothermal wall has been analyzed to various degrees of approximation. In one case, Stewartson's transformation is used to reduce the compressible conservation laws to those for an incompressible fluid and a series solution obtained [42C]. In a second study, the energy equation is eliminated by writing the temperature as a quadratic function of the velocity, which is in turn approximated by a quintic polynomial in the normal coordinate [16C]. Practical calculation procedures for determining the laminar heat transfer on blunt hypersonic vehicles are presented in [41C] and [65C].

An initial study of laminar non-Newtonian boundary-layer flow and heat transfer is based on the assumption that the shear stress is proportional to a power of the velocity gradient [1C]. For the flat plate, it was found that although the velocity solutions obeyed similarity, the temperature did not. Also of particular

Vol. 3 1961

interest are the finite-difference solutions for axially-symmetric blunt bodies which were carried out without similarity assumptions [33C]. Laminar flow and heat transfer on a flat plate with wedge-shaped grooves in the flow direction was analyzed by the Kármán–Pohlhausen method [28C]. Relative to laminar flow over a plane plate, the grooves lead to an increased heat transfer.

Turbulent boundary layers continue to resist exact solution, but there is considerable activity in finding approximate results. Deissler's eddy diffusivity expressions form the basis of an analysis of high-speed flat-plate flow and heat transfer under conditions of variable fluid properties and frictional heating [17C]. Results are given for Mach numbers up to 20. Another approach to this same problem starts by analyzing velocity data and obtains the variation of the shear across the boundary layer [54C]. This information is then utilized to integrate the energy equation for the flat plate [54C, 55C]. This same paper [55C] evolves a relationship between compressible and incompressible turbulent boundary layers with pressure gradient and Prandtl number not equal to unity. The turbulent compressible boundary layer over a slightly yawed cone is made tracable by assuming 1/7-power laws for the velocity distribution and a modified Blasius shear law [7C]. For a highly-cooled, blunt-nose body under hypersonic conditions at an angle of attack, it is demonstrated that the cross-flow velocity is negligible and that heat transfer is calculable by two-dimensional methods [62C]. A relatively simple relation for calculating turbulent heat transfer on a blunt body has been derived by postulating a simple, but unsupported, relation between enthalpy thickness and momentum thickness [64C].

Three interesting Russian papers relating to approximate heat transfer calculations have recently appeared in the literature. For the laminar boundary layer with arbitrary free-stream velocity, a method is proposed in which successive moments of the energy equation are taken [51C]. Various form factors (i.e. thickness parameters) are needed and these are obtained from flat plate and wedge-flow solutions. A second study treats the same problem, but extends consideration to laminar, transition, and turbulent flows [68C]. An integral analysis is utilized, and this is implemented by a semi-empirical law for the convective thickness. The final results require a knowledge of the locations at which transition begins and ends. A third paper considers the heretofore-neglected effects of density fluctuations on compressible turbulent flow and heat transfer about a flat plate [32C].

Dissociation and chemical reactions

Fourier's equation, describing heat conduction in a medium with variable heat conductivity, can be made linear by introduction of a heat flux potential defined as the integral of heat conductivity over temperature. This equation is used to study analytically unsteady heat transfer in a stationary gas with chemical reactions [26C]. A considerable number of papers are concerned with the prediction of laminar heat transfer to high-speed objects, like missiles or satellites, moving or re-entering through the atmosphere. The air surrounding the object is then heated to such a degree that dissociation of the molecules may occur. The problem to determine whether chemical equilibrium or frozen condition with regard to dissociation of oxygen exists is investigated by a comparison of a characteristic residence time of the atoms within the boundary layer to a characteristic chemical reaction time [2C]. The simultaneous effect of a finite re-combination rate of oxygen atoms and of fluid injection has been calculated for Couette flow and for a flat plate of infinite extent suddenly set in motion (Rayleigh's problem) [9C]. A similar calculation using an integral method and the assumption that Prandtl and Lewis numbers are equal to one and that the dissociation is a second order reaction gave the result that for Mach numbers between 10 and 20 and a flight altitude of between 50 000 and 200 000 ft, equilibrium is never approximated within the boundary layer on an adiabatic flat plate [11C]. A similar calculation for flow over blunt bodies is reported in two papers [61C, 12C]. Re-combination may also occur on a catalytic surface even when the dissociation is frozen within the boundary layer itself. A calculation of such a situation assumes a first order surface re-combination, a constant Schmidt number, constant

wall temperature and a gas for which the product of density times viscosity is constant [10C]. The results are well approximated by a simple empirical equation. The postulate of local similarity and use of constant property relations, into which the properties are introduced at a reference enthalpy, leads to heat transfer information which is in good agreement with the results of more involved boundary-layer solutions [18C]. Tables have been prepared from which laminar skin friction and heat transfer parameters can be read for flow of air with equilibrium dissociation over flat plates at angles of attack from 0 to 50°, for wall temperatures from 1000° to 3000°R and free stream velocities of 10 000 to 28 000 ft/s [48C]. Simple relations for the properties of a dissociated gas with frozen chemical composition are reported [22C].

The chemical reaction of a gas released from a surface with a gas flowing in a laminar boundary layer over the surface occurs in a narrow reaction zone, provided the reaction rate is very rapid. The location of this zone is calculated, assuming a gas with Prandtl and Schmidt numbers equal to one and with a constant product of density and viscosity [21C]. A corresponding experimental study has been reported [36C]. The derivation from basic principles of the energy equation of a chemically reacting gas flowing at a low density over a surface indicates that energy transport caused by shear work at the surface has to be considered when slip occurs at the surface [47C].

Magnetohydrodynamics

An excellent introduction into magnetogasdynamics and its possible aeronautical applications discusses the use of magnetic fields to modify the forces and heat transfer on objects exposed to the flow of a conducting fluid [50C]. Air is becoming electrically conducting by ionization at sufficiently high temperatures. The electric conductivity can also be increased by seeding with caesium or potassium. The influence of a magnetic field on heat transfer has been calculated for a number of various geometries and laminar flow situations: flow between two infinite parallel plates with the plate temperature varying stepwise in flow direction and with a magnetic field normal to the plates [39C]; hypersonic flow in the region of a 3-dimensional stagnation point [30C]; wedge-type flow resulting in similar solutions for proper boundary conditions [31C]; flow past an infinite porous flat plate in the presence of a transverse magnetic field and with fluid ejection [25C]; steady and transient free convection on a vertical plate with a transverse magnetic field [24C]; convective motion of a conducting fluid between parallel vertical plates [44C]; free convection in the layer between a lower heated and an upper cooled surface [38C]; free convection of mercury in a closed circular tube with a transverse magnetic field [52C]. The calculations re-confirm the fact that heat transfer can be decreased by the proper application of a magnetic field. However, very large fields are required to get a reasonable reduction. The analogy between the magnetic vector potential and the temperature field, which exists when the electric field in the flow is zero or negligible, has been utilized to obtain information on the magnetic field for various geometries [35C]. The stability of laminar flow in a boundary layer or channel and the influence of a magnetic field has been analyzed by an extension of Tolmien's method [46C]. In general, a magnetic field stabilizes the flow except for conditions where it creates velocity profiles with inflection points. One of the rare experimental studies in magnetofluidmechanics is reported [6C]. A hemispherical model of an eutectic alloy of bismuth with 117°F melting temperature was exposed to a stream of hot water and the melting process was filmed. A coil around the model support and a 6 V battery generated a magnetic field of 5000 G in the water. The velocity in the molten layer decreased and the thickness increased when a magnetic field was applied. A preliminary report [56C] describes experiments on heat transfer to a water-cooled copper tube exposed to a carbon arc discharge with 7000°K temperature or a water plasma jet with 14 000°K. Heat flux densities of 10^6 W/m² and 10^8 W/m², respectively, have been measured.

Experimental investigations

A considerable number of papers reported on experimental investigations measuring heat transfer in supersonic flow to objects with various

Vol. 3 1961

geometries. Use of a shroud with proper design, surrounding the model, gives the possibility to investigate large models in wind tunnels with restricted cross section [15C]. Laminar heat transfer on a cylinder normal to rarefied flow was found to be in good agreement with predictions by Lees' method [60C]. Use of the reference enthalpy method and flat plate relations based on local conditions described satisfactorily turbulent heat transfer on blunt objects [15C]. Simple approximate expressions were developed describing the maximum turbulent boundary layer heating rates on a hemispherical nose [3C]. Experiments on heat transfer in Laval nozzles with flow of superheated steam gave good agreement with a turbulent boundary-layer method by Bartz but showed considerable deviations from tube flow relations [43C]. Measurements on heat transfer to cones arranged in supersonic flow with Mach numbers between 2 and 5 and with various angles of attack [8C, 29C, 59C] indicate that heat transfer at the stagnation line increased up to four-fold with increasing angle of attack. The heat transfer in the separated region was sometimes found to be as large as the heat transfer at the stagnation line. Skin friction in a compressible turbulent boundary layer on a cone is reduced by the injection of air, or Freon-12 and especially of helium [40C]. The reduction was found to decrease with increasing Mach number. The effect of surface cooling on boundary-layer transition was studied on a 15° cone at a Mach number 4 [66C]. Heat transfer to the leading edge of a wing exposed to a high Mach number flow can be considerably reduced if the leading edge is arranged oblique to the flight direction [14C]. Experiments on turbulent heat transfer from a non-isothermal flat plate established the following relations

$$St_T = 0{\cdot}0296\ Re_x^{-0{\cdot}2}\ Pr^{-0{\cdot}4}\ \frac{T_\infty^{0{\cdot}4}}{T_w}$$

(St_T = Stanton number, Re_x = Reynolds number, Pr = Prandtl number, $T\infty$ = upstream fluid temperature, T_w = plate surface temperature) for a constant wall temperature and

$$St/St_T = [1 - (\xi/x)^{9/10}]^{-1/9}$$

describing the Stanton number at location x for a wall temperature which changes at location ξ from T_∞ to T_w [45C, 13C]. Experiments on heat transfer near a convex corner normal to the flow direction [67C] and near a concave corner parallel to the flow direction [57C] were reported. In the latter situation, laminar heat transfer was found to be up to 50 per cent higher near the corner due to shock boundary-layer interaction. Turbulent heat transfer was not influenced by the vicinity of the corner. Free stream turbulence produced by a screen had the following effect on local heat transfer to a cylinder normal to the flow direction: laminar heat transfer increased, transition Reynolds number was reduced, transition in the separated boundary layer occurred earlier, and the low temperature recovery factor at the rear of the cylinder disappeared [49C]. Local heat transfer coefficients on a surface, on which an air jet impinges normally, have been measured [63C]. Some peculiarities of the results are probably caused by the specific test configuration.

FLOW WITH SEPARATED REGIONS

Analytical and experimental studies in the recent past have considerably increased our understanding of the heat transfer process in a separated region. The separated boundary layer behind a step in the surface contour can either be laminar or turbulent. Heat transfer measurements [9D] in the region of a separated flow with laminar boundary layer agreed well with an analysis by Chapman. In flow with a turbulent separated boundary layer, experimental heat transfer coefficients were considerably lower than calculated [9D, 11D]. A maximum heat transfer occurs at the point where the flow re-attaches to the surface. The average heat transfer coefficients are, however, considerably lower for separated flow than for attached boundary layers. This suggests the possibility to utilize separated flow at locations where one wants to have a small heat transfer, for instance, on high velocity aircraft or satellites. The shroud technique described in the boundary-layer section has been successfully applied to study heat transfer on the downstream part of blunt objects [2D]. Accommodation coefficients and Nusselt numbers have been determined for hypersonic gas flow normal

to a cylinder from the free molecule to the continuum regime [13D] and also for a fluid with small Prandtl number [1D].

Pebble bed heaters are widely used to generate a high temperature gas stream, for instance, for supersonic wind tunnels. Experiments on such a heater [8D] established the following relation for the heat transfer to the packed alumina spheres in the heater

$$St\, Pr^{2/3} = 0{\cdot}400\, Re^{-0{\cdot}437}$$

(St = Stanton number, Pr = Prandtl number, Re = Reynolds number). This relation is surprisingly close to the one for a single sphere. Experiments were also concerned with heat transfer to the wall surface in a packed bed [14D] as well as in the bed itself [4D]. An analysis on laminar flow through a pebble bed heater with internal heat generation (nuclear reactors) established the tendency to develop hot spots [5D]. A similar analysis allows calculation of the unsteady temperature distribution in a packed bed for any initial temperature distribution and temperature variation of the entering gas [7D]. Heat transfer coefficients from a moving bed of quartz sand to the walls of a circular tube have been established [6D]. Measurements on heat transfer to the particles in a fluidized bed [10D, 3D] established heat transfer relations and a survey of previous experiments on heat transfer between a fluidized bed and a vertical tube resulted in two correlations, one for fine particles with predominantly viscous flow and another one for coarse particles with predominantly inertial forces [12D]. Considerable deviations between the results of the various experiments demonstrate the relatively poor knowledge of this flow and heat transfer process.

TRANSFER MECHANISM

Knowledge of the laminar or turbulent state of the flow and of the transition location is one of the most important prerequisites to a prediction of heat transfer. Visual observation and hot wire measurements contributed strongly to our understanding of the transition process [6E, 3E, 5E, 8E, 13E, 9E]. The following model of the transition process has evolved from these studies: Transition is usually initiated by instability waves which amplify in downstream direction and roll up into vortices. Such vortices with straight axes in shear flow are unstable and deform in the way that the axis builds loops. At the loops, the fluctuations are especially intense and cause the vortex to break down rapidly into finer and finer vortices (turbulent spots). This transition process occurs also in a separated laminar boundary layer [10E]. The reverse transition from a turbulent into a laminar boundary layer can occur under specific situations [14E]. The effect of an isolated [1E] or distributed [17E] roughness on transition in a supersonic flow can well be characterized by a roughness Reynolds number based on roughness height and velocity at roughness height for subsonic flow or sound velocity corresponding to the state at roughness height for supersonic flow. A shock tube is an excellent tool to study heat transfer and boundary-layer transition at high Mach numbers and temperatures [7E]. The turbulence intensity at the center of a flame holder plane was found to decrease when the ratio of mean free path length to Kolmgoroff scale exceeded a value 0·01 [11E]. Analytical work on the transition process has proceeded [4E] and it is claimed that it now predicts the end of transition as well as its initiation [15E]. The theory of decaying homogeneous turbulence was improved by inclusion of quadruple correlations [2E]. The ratio of eddy diffusivities for momentum and heat is predicted as one by an analytical study [16E]. Van Driest's relation for the friction factor for turbulent flow near a wall is extended to flow at high Mach numbers and large temperature differences [12E].

NATURAL CONVECTION

Analytical and experimental activities covering a broad range of problems in natural convection and combined natural and forced convection have been reported. Among the analytical studies, boundary-layer problems continue to be of interest. The wall temperature variations which permit steady and unsteady similarity-type boundary layers were examined [42F] in a formal manner, but without numerical solutions. Two improvements in the integral method of solution (i.e. Kármán–Pohlhausen) are proposed. In one, velocity and temperature profiles are used which contain both exponentials and

Vol. 3 1961

powers of the distance from the wall [9F]; while in the second, the boundary layer is subdivided into two zones depending on the relative importance of various transport mechanisms [4F]. Generalization of a previous integral solution is made to provide the wall temperature corresponding to an arbitrary variation of wall heat flux [1F]. The natural convection in a heated plume (jet) which rises above a horizontal wire has been analyzed by similarity solutions [5F, 34F]. Blowing or suction through a vertical isothermal plate ($v_w \sim x^{-1/4}$, x vertical) is found to significantly alter the heat transfer [6F]. An integral method is utilized to study the effects of a horizontal magnetic field (B = magnetic intensity $\sim x^{-1/4}$) for the case of an isothermal vertical plate [15F]. Conditions have been derived under which unsteady natural convection in gases can be treated as quasi-steady [37F].

Several papers relating to the analysis of combined natural and forced convection have appeared in the literature. The flow and heat transfer in a vertical tube with a linear temperature gradient in the vertical direction has been solved (once again) by direct mathematical methods [26F]. A new approach appropriate to this thermal boundary condition uses complex variable theory and is illustrated for circular [38F] and rectangular [39F] cross sections. Another method for this type of problem is based on successive use of finite Fourier and Hankel transforms [23F] and solutions are given for the circular sector. Analytical studies have been performed to determine the interaction of a transverse (i.e. horizontal) magnetic field on the flow in a vertical tube [35F] or parallel plate channel [33F]. A correction formula for small buoyancy effects in fully-developed laminar flow and heat transfer in a *horizontal* tube has been found to involve the product of the Reynolds and Rayleigh numbers [27F]. Buoyancy effects have also been studied for low Reynolds number flow about a sphere for both aiding and opposing conditions [21F].

Further analyses have covered a variety of subjects. The thermosyphon, which is a heated tube closed at the bottom and open at the top to a cooled reservoir, has been studied for the condition of a small angle of tilt relative to the vertical [22F]. A small increase in heat transfer is predicted. Closed-loop natural convection inside a horizontal cylinder whose temperature varies sinusoidally over the surface is analyzed by an integral method assuming a boundary layer near the wall and a rotating core [10F]. A mathematical study has been made of the uniqueness of solutions for weak (low Grashof number) convection [8F]. The hot gases produced by a fire experience an upward buoyant force. The characteristics of the ensuing turbulent natural-convection flow are predicted for a fire of arbitrary size in an atmosphere of arbitrary lapse rate [28F]. An order of magnitude estimate leads to the conclusion that natural convection caused by centrifugal forces (e.g. internal cooling of turbine blades) can be important even if the forced-convection mainflow is turbulent [43F]. A new correlation formula

$$Nu = 0{\cdot}11\,(Gr\,Pr)^{1/3} + (Gr\,Pr)^{0{\cdot}1}$$

is proposed [16F] for predicting overall heat transfer from vertical plates and horizontal cylinders over the Grashof–Prandtl range from 10^{-7} to 10^{12}.

Considerable interest, both analytical and experimental, continues in the Benard problem, wherein a thin horizontal layer of fluid is heated from below. For sufficiently large temperature differences, the quiescent state becomes unstable and fluid motion in various cellular patterns sets in. A non-linear theory is advanced to explain the preference for hexagonal cells [31F]. For such a cell pattern, the streamline pattern at the point of instability has been derived [32F]. The heat transfer through such a flow has been determined [29F] and the effects of a superposed magnetic field studied [29F]. When the heated layer is subjected to a time-dependent body force, the Rayleigh number at which instability sets in is found to be much higher than in the steady case [11F]. Another interesting variant of the Benard problem is the superposition of a rotation about the vertical axis of the heated fluid layer. If a metallic liquid such as mercury is thus heated and rotated, the flow pattern at the onset of instability is characterized as overstable oscillations. The characteristics of this flow pattern are explored experimentally [30F] and the heat transfer determined [13F].

A very large increase in free convection heat transfer near the critical point has been reported in past investigations. Additional experiments to explore this phenomenon have recently been undertaken. In one test, an electrically heated horizontal wire was immersed in Freon-114A [14F]. Visual observations at pressures beyond the critical revealed bubble-like aggregates (Fig. 1), but there was no large heat transfer increase as in nucleate boiling. A second experiment carried out with Freon-12 in a natural-circulation loop also failed to find dramatic increases in heat transfer [17F].

Several experiments on unsteady free convection are reported. A vertical plate immersed in water was subjected to a step-function change in wall heat flux [12F]. Interferometric studies of the temperature field revealed that during the transient, the boundary layer overshot its steady state thickness; but, there was no marked overshoot of the wall temperature. The question of whether the transient surface temperature can overshoot the steady state value was further explored with the aid of an electric circuit analogue [2F]. This apparatus was used to analyze overshoot data from an electrically heated wire immersed in a sucrose solution [3F]. Disturbances have been set up in a free convection boundary layer by periodic pulsing with a fine heated wire, and the resulting boundary layer oscillations observed with an interferometer [18F, 19F]. Photographic techniques have also been used to observe the effect of a sound field on free convection about a horizontal cylinder [7F]. Above a certain critical sound pressure level, a flow pattern characterized by the presence of two vortices above the cylinder is formed.

Steady-state natural convection experiments have been carried out for a variety of configurations. The utility of the interferometer as a research tool is discussed and illustrated by photographs of the temperature field about various plates and cylinders [36F]. The measured effect [24F] of tilting a liquid-filled thermosyphon is to decrease heat transfer for small tilt angles (in contradiction to Ref. 22F) and to increase heat transfer at larger angles of tilt. Steady-state heat losses from an inclined tube, heated at the base and filled with air, are reported as a function of inclination angle, tube diameter, and wall conductivity [20F]. No consistent trend with angle is apparent. Temperature distributions and heat transfer have been determined for natural convection within a horizontal cylinder, the two vertical halves of which are maintained at different temperatures [25F]. A detailed investigation of the mean and fluctuating temperatures above a horizontal heated flat plate was performed to gain insight into the structure of the turbulent convection [40F]. The heat transfer characteristics of spheres, both for purely natural convection [41F, 44F] and for combined natural and forced convection [44F], have been furnished by experiment.

CONVECTION FROM ROTATING SURFACES

By extending a previous analysis for a rotating disc, an approximate evaluation of the effect of curvature on the laminar heat transfer from a rotating spherical cap has been investigated [1G]. The theory which is valid for large Prandtl numbers allows an arbitrary meridional distribution of surface temperature. Another study [4G] relates to the heat transfer by laminar flow from a rotating sphere and thus also examines the curvature effect.

A rotating disc with mass injection or suction at the disc surface has been investigated [5G]. Laminar results are given for the velocity, temperature and mass-fraction distributions as well as for the heat transfer, mass transfer, and torque requirements. Asymptotic solutions are given for large suction velocities and it is shown that fluid injection sharply decreases the heat transfer at the disc surface.

An infinitely long rotating circular pipe has been investigated under the conditions of constant rotational speed and a constant axial temperature gradient [2G]. The effects of compressiblity are examined by considering the fluid to be a perfect gas. Another internal flow situation, the motion of a fluid inside a rotating annulus of square cross section, has been studied [3G]. The inside annulus dimensions are taken to be small compared to the distance from the axis of rotation, and the side walls are held at different constant temperatures. Particular attention is paid to the cell-like flow which develops at low thermal Rossby numbers.

The final paper in this series [6G] presents an

Vol. 3 1961

ol.
3
961

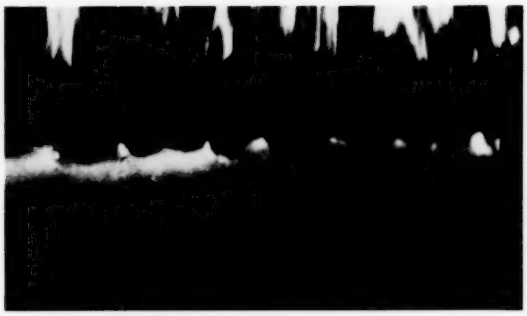

FIG. 1. Bubble-like aggregates in free convection at supercritical pressures (Ref. 14F).

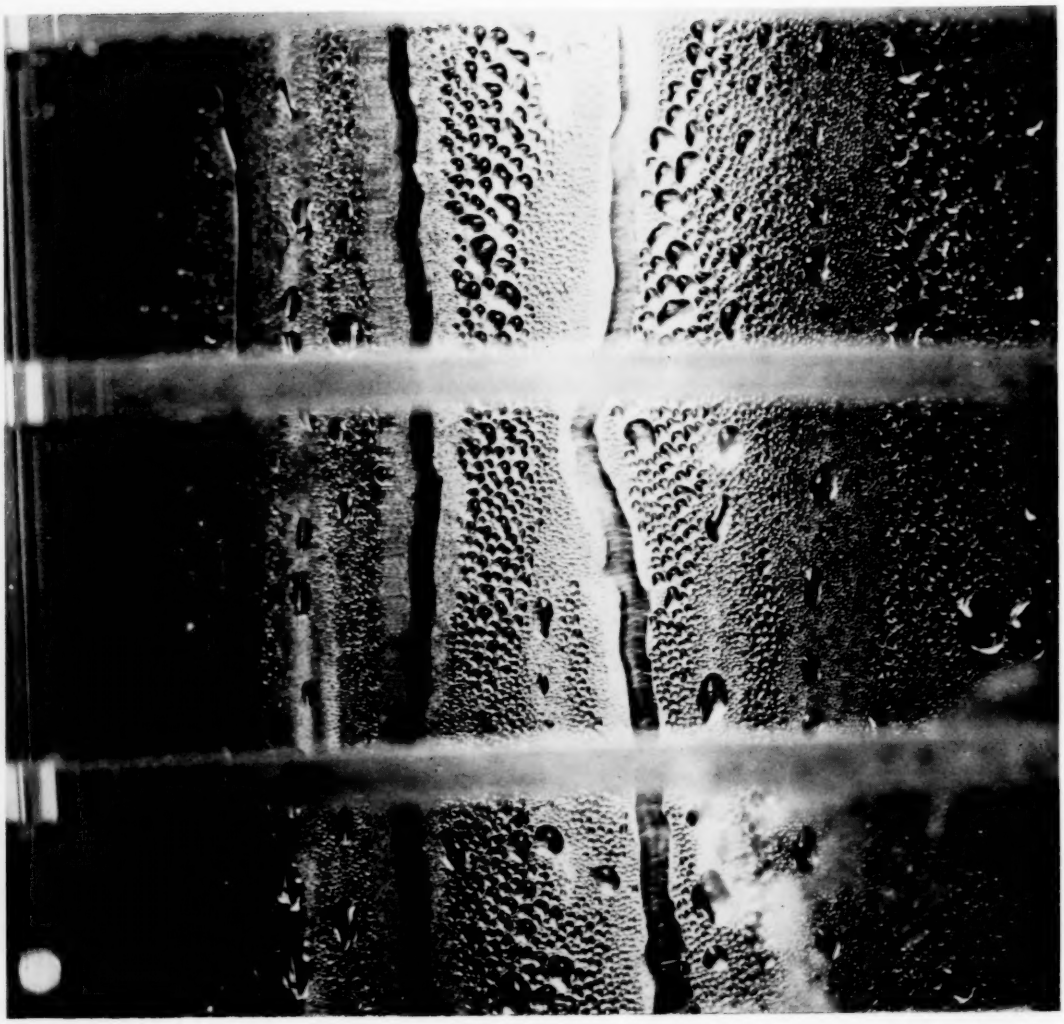

FIG. 2. Mixed dropwise and film condensation on a smooth chrome-plated surface (Ref. 21J).

Vol.
3
1961

analysis of the cellular motions within a horizontal rotating fluid layer which is heated from below. The distortion of the cell boundaries due to rotation are described.

COMBINED HEAT AND MASS TRANSFER

Under the influence of the re-entry problem, a number of papers have been published recently which report mass transfer experiments and design criteria for surfaces under the influence of large heat fluxes. The ablation characteristics of a number of plastics reinforced with inorganic fibers are reported in [20H]. The information which was obtained in a rocket exhaust is reported as "effective heats of ablation" for the various materials. This figure of merit represents the heat absorbed per unit mass of ablated material. A discussion [16H] is given of the agreement between experiment and various analyses when Teflon is exposed to the stagnation enthalpy and pressure levels encountered in hypersonic flight. The study concludes that caution must be exercised in the prediction of mass transfer rates of chemically reacting species.

A simplified analysis is presented of hypersonic ablation in [14H] where it is concluded that the radiation heat flux is negligible compared to the heat absorbed by ablation. A calculation also illustrates the change in shape of a hemispherical nose cone during re-entry. In [10H], the results of ablation tests in a plasma discharge on copper, aluminum, stainless steel, molybdenum, zircon, mullite, alumina, linen bakelite, nylon, and graphite are reported. Heat balances and "effective heats of ablation" are included.

Ablation characteristics of clear and opaque quartz were determined experimentally in an air arc wind tunnel [2H]. Comparison of the data with the analysis of Bethe and Adams showed agreement within 8 per cent. Another analysis of stagnation point melting-ablation [1H] indicated that for glassy materials the thermal diffusivity is an important parameter when designing for minimum weight. In a paper considering sublimation in a hypersonic environment [15H], the pertinent equations are derived for the simultaneous processes of diffusion, convection, and thermal exchange and applied to the vaporization of a refractory material.

A series of studies has been reported which deal with mass injection into turbulent boundary layers. New experimental results [4H] with refined radiation-conduction corrections over previously published results indicate that the Rubesin analysis tends to overestimate the reduction in Stanton number from blowing. Another experimental study [18H] reports on sublimation mass transfer from an adiabatic sharp-edged flat plate under free stream Mach numbers of 0·43, 2·0 and 3·5. An analysis of friction and heat transfer in turbulent compressible flow extended to these low mass transfer rates shows good agreement with the experimental data.

A study of available experimental data has been carried out to evaluate various turbulent theories [8H]. Particular attention was given to the influence of the molecular weight of the injected gas on the reduction in Stanton number. An analysis [21H] is presented for injection into an incompressible turbulent boundary layer under the hypothesis that the effect of injection is restricted to the sub-layer region. Experimental measurements tend to substantiate this hypothesis and the solution for this model is particularly simple for small values of injection and contains no arbitrary parameters. A two-dimensional Laval nozzle with nitrogen injection into a nitrogen free stream has been studied [7H]. Experimental heat transfer measurements are compared to Rubesin's turbulent theory. A series of measurements has also been made [13H] of the skin friction in a compressible turbulent boundary layer on a cone. Injected gases into an air free-stream consisted of helium, air and Freon-12.

An experimental study is reported [12H] of the effect of slot injection angle in film cooling effectiveness. Data were obtained from normal hole configurations and angled slots. The effect of shock generated vorticity on mass transfer effectiveness has been investigated [9H]. It is shown that reduction in heat transfer rates due to mass injection is substantially less than boundary-layer predictions for spheres and cylinders due to this vorticity.

A laminar analysis of helium injection into air has been carried out considering the effect of a free stream pressure gradient [3H]. The influence of the pressure gradient on both the

skin friction and heat transfer was investigated. Another laminar analysis [6H] considers the case where there is constant injected mass flux at the plate surface. This condition is compared to the previous cases investigated of either a blowing velocity distribution that yields a constant surface temperature or one of uniform blowing velocity. Solutions have also been presented [5H] for the compressible laminar boundary layer on yawed cylinders with transpiration cooling. The results indicate that at large Mach numbers and yaw angles an incompressible analysis underestimates the amount of coolant required.

An unusual mass transfer condition has been investigated [17H] where the injected velocity was as large as 19 times the free stream velocity. This was done by examining an evaporating liquid into a low-speed inert gas at pressures near the vapor pressure of the liquid. Another study [11H] has examined the effect of a deceleration force on a melting boundary layer which opposes the downstream flow of the liquid.

The reader's attention is called to a summary article by Professor D. B. Spalding entitled "Heat and Mass Transfer in Aeronautical Engineering" [19H]. Utilizing the mass transfer literature, Professor Spalding develops design procedures for a number of specific technical problems. Typical of the problems considered are the calculation of the rate of burning of a graphite heat shield and the rate of enlargement of the throat area of a solid-propellant rocket motor having a graphite nozzle.

CHANGE OF PHASE

The extensive experimental and analytical work in this area reflects both the broad scope and complexity of the problems.

To gain understanding of the boiling mechanism, experimental studies have examined bubble mechanics. Photographic evidence of nucleate boiling in a rectangular cross section flow channel yields expressions for bubble growth, collapse, and distribution of maximum bubble diameters which are related to bubble energy transport [33J]. Examining the problem of bubble formation in superheated liquids and drops, [22J] reports data and correlations useful in predicting conditions required for homogeneous nucleation, while [4J] gives measured bubble growth in various superheated liquids. Using aqueous solutions of surface-active agents, bubble formation was observed and the increased boiling coefficient attributed either to a decrease in dynamic surface tension or an increase in active nuclei in solution [14J]. High speed photographs show generation and growth of bubbles from a single orifice source in a liquid N_2–O_2 mixture [6J].

A step toward the economic recovery of fresh water appears in the use of thin, evaporating and condensing films (Fig. 2) to yield overall heat transfer coefficients as high as 8000 Btu/h ft² °F [21J]. Heat transfer coefficients for film boiling of Helium I from a single wire agree with those for other liquefied gases [7J]. The forced vaporization of water, carbon tetrachloride, benzene, methanol, and *n*-butyl alcohol in a tapered tube permits the influence of evaporation area to be evaluated [5J] and natural convection boiling results for liquid Freon-12 in a single tube appear in [20J]. Using hydrodynamical model, [36J] examines transition of water from bubble to film boiling for various values of pressure, water velocity, and subcooling. Liquid superheating shows influence on boiling coefficients [34J, 16J] depending on presence or absence of bubbles which originate from active sites determined by surface roughness [16J].

Analytical efforts consider the hydrodynamic boundary condition (i.e. temperature jump and pressure deviation from equilibrium) for evaporation and condensation [15J] and vaporization processes in the hypersonic, laminar boundary layer for a vehicle of arbitrary material [25J]. The correlation of existing data yields generalizations of heat transfer for nucleate boiling [23J, 18J].

Evaporating liquids into low-speed, inert, gas streams at pressures nearly that of the liquid vapor pressure shows the influence of high concentration gradients and evaporative velocities on mass transfer rates for the Graetz number range 0·1 to 1800 [26J]. Observation of rates of evaporation of drops containing dissolved solids in a hot air stream affords a basis for predicting spray-dryer performance [3J]. Evaporation rates predicted for small drops (diameter of order of mean-free-path of steam

Vol. 3 1961

molecules) compare favorably with experimental data and suggests valid use for larger drops [8J]. Further drying implications are inherent in the examination of convective heat exchange between a current of hot air and a flat, wet surface [13J]. Ref. [30J] attributes the diminution of humidity of porous materials in the presence of water saturated atmospheres to capillary effects. The application of energy and mass transfer equations permits an accurate estimate of the reduction of evaporation from a water surface caused by the application of a mono-molecular film [11J].

Continuing earlier work in condensation, [19J] compares theoretical equations with experimental data for laminar and turbulent film condensation and introduces correction factors (accounting for effects of liquid inertia, convective transport, wave motion and variable properties) which give good agreement. Also part of a continuing study is the determination of the influence of vapor drag on heat transfer during condensation for Prandtl numbers 10 and 0·008 [28J]. Considering the inertia forces and energy convection terms neglected by Nusselt, [29J] performs a boundary-layer analysis of laminar film condensation on a horizontal cylinder and reports heat transfer results for the Prandtl number range 0·003 to 100. Factors examined for the influence they exert on condensation are (a) crossflow in the case of steam and steam–gas mixtures condensing on a vertical tube [9J], (b) geometry in the case of Freon-22 condensing on the outer surface of single, horizontal, smooth and ribbed tubes [27J], and (c) viscosity of condensate (water and glycerine) [37J]. Ref. [10J] presents experimentally verified equations for calculating water vapor transfer through composite walls.

Interest in burnout heat flux continues with the reporting of the influence exerted by non-uniform, peripheral heating of steam–water mixtures in vertical tubes [31J]. Further data [1J] for water in a vertical tube (8·2 mm i.d.) at varying pressures (20 to 300 atm), subcooling (0 to 140°C), and tube length (35 to 135 mm) disagree on several counts with previously published data. For the vertical upflow of water in uniformly heated rectangular, burnout heat-flux data at 2000 p.s.i.a. shows correlation with fluid mass velocity and burnout enthalpy [2J]. Further comparisons of tube burnout data for boiling water are made in [32J]. Experiments showing the hydrodynamic instability of a two phase layer are related to burnout heat flux and afford a predictive criterion [17J].

Ablation of solids (naphthalene and camphor spheres) receives photographic study in [35J, 38J], leading to the determination of local ablation rates for Reynolds number range 120 to 16 500. Analytically, [24J] examines the unsteady mass loss and energy accumulation caused by aerodynamic heating of blunt bodies.

Reference [12J] reports measured heat and mass transfer rates for the interesting case where a weak NH_3 in water solution flows down the outside of a water cooled, $\frac{1}{2}$ in o.d. tube while absorbing anhydrous NH_3 at 1 atm.

RADIATION

A unique feature of the past years' radiation literature has been the large number of papers concerned with radiation heat exchangers and the equilibrium temperature of objects in space. Some of the studies deal with a single fin exchanging radiation with specified black environment, and one paper presents an exact formulation of the multi-fin radiation problem which leads to a number of mathematical complexities.

The radiation fin efficiency for a single circular fin has been studied [9K] under the conditions of no incident radiation. Companion papers [23K, 2K] investigate a radiating rectangular thin fin which is irradiated by a uniform source. Optimum fin geometries for minimum weight are investigated. Another paper [36K] reports on the same problem with the inclusion of a discussion of meteorite puncture probabilities. Two papers [38K, 25K] discuss the important problem, as far as space applications are concerned, of the best shaped radiation fin of minimum mass. In the first paper [38K], it is shown that the best shaped fin has 61·2 per cent of the mass of a rectangular fin with the same performance. It should be pointed out, however, that these optimum shapes are always convex and no account has been taken of radiation exchange between different parts of the fin. An exact formulation of the problem of radiating

fins with mutual irradiation as well as radiant interchange with nearby surfaces and the environment is presented in [14K]. The formulation leads to an integro-differential equation.

A unique type of heat exchanger for space applications is described in [37K]. A rotating circular belt picks up waste heat on one point on its circumference and radiates this heat to a sink in its travel around the periphery. The analysis of the temperature distribution in a rotating cylindrical shell which is heated on one side by the sun in space is given in [11K]. The shell is considered to have a finite thermal conductivity. A transient analysis of a similar geometry in space but without rotation and having a specified infinite thermal conductivity is reported in [28K].

Selective non-gray coatings which have a different absorbtivity for solar radiation from their emissivity value have been studied. The use of such coatings for the temperature control of satellites is discussed in [16K]. Another paper [21K] describes the preparation and high temperature stability of selective coatings that will withstand surface temperatures up to 1000°C.

The general problem of radiant interchange within an enclosure continues to receive consideration. A series of three papers [5K] presents an analysis of this situation using the radiation network method. Gas conduction is neglected. The radiation characteristics of long cylindrical cavities have been determined by numerical solutions of the governing integral equation [31K]. Thermal radiation between infinite parallel plates separated by an absorbing and emitting gas is described in [35K]. This analysis also neglects the effects of conduction in the gas. Equations of radiative transfer in gases are formulated for the one dimensional case to include radiation exchange with solid boundaries [15K]. An example of the solution of these equations is given for an infinite flat layer of gas bounded by parallel plane surfaces. In this analysis, the effects of gas conduction are considered.

The four dimensional heat flux integral for diffuse radiation between two surfaces separated by an absorbing gas is considered in [26K]. The complex integral is transformed into a sum of one dimensional integrals for the case of opposite-parallel and adjoining-perpendicular rectangles. The results are suitable for numerical integration techniques. Analytical relations have been obtained [20K] which suggest an experimental procedure for the determination of radiation geometric factors as well as the radiation properties of the surfaces involved.

A new approach to the formulation of the radiation transport equation is described in [12K]. The method involves replacing the standard spectral absorption coefficient with an error function absorption coefficient. The advantages gained are that the error function coefficient is well behaved and has been measured for a number of gases. The paper describes how to rewrite the radiation transport equations in terms of the new coefficients.

A "three measurement" method of measuring the spectral emmisivity and temperature of solid surfaces has been described [33K]. Involved in the procedure is a simultaneous determination of the brightness and color temperatures at three wavelengths. Another interesting experimental paper [32K] describes a high-speed bolometer for measuring large incident radiation fields such as those coming from nuclear fireballs. The response time of this instrument is of the order of 50 micro-seconds.

The normal spectral emissivities of ceramic-coated and uncoated specimens of inconel and stainless steel have been reported [27K]. The measurements were made at temperatures of 900, 1200, 1500 and 1800°F over a wavelength range of from 1·5 to 15 μ. Spectral radiation properties have also been reported [13K] for a number of fabric materials from 1·0 to 23 μ. Materials examined included cotton, linen, silk, orlon and nylon.

A transient technique for measuring the total hemispherical emissivity of highly polished metals has been reported [8K]. The apparatus, which can be operated from 100 to 900°C has an accuracy of 8 per cent. It can also determine the specific heat of the material to within ± 2 per cent. The analytical solution of a constant area fin radiating into a low-temperature environment has been utilized to design an experimental apparatus to measure the total hemispherical emissivity of polished iron in the

Vol. 3 1961

temperature range from 300 to 500°R [7K]. The method has the advantage, important in low-temperature work, that no calorimetric measurements are required.

Two papers have appeared which deal with unsteady heat conduction in a solid with a radiation or non-linear boundary condition. The transient temperature field in an infinite slab with radiation cooling at the surfaces is solved by an integral approach in [29K]. Another study [10K] considers a semi-infinite solid with a non-linear transfer process at the surface. As an example, the temperature distribution in the solid is determined under the conditions of Stefan–Boltzmann radiation at the surface.

Radiation in diathermanous materials such as glass is discussed in [24K]. Analysis and experiment are coupled to investigate the temperature distribution in the glass. Another paper dealing with the same subject [4K] presents a calculation of the spectral radiation emitted normally from the surface of a thin sheet of glass. The results of the calculation are used to design a pyrometer to measure glass temperatures.

The influence of internal radiation exchange in the reduction of temperature differences in solid structures has been examined. A transient analysis [3K] investigates the structural temperature distribution under the conditions of external convective heating. Simple models such as parallel plates are used in [1K] to evaluate the same effect. The use of insulation in the areas of greatest aerodynamic heating is discussed as a method of reducing structural temperature differences.

The subject of radiative transfer through particulate media continues to be of interest. Radiant transfer through fibrous and foamed insulating materials was investigated theoretically and experimentally in [22K]. The optimum diameters of fibers and pores were determined for minimum radiative transfer over the temperature range from 200 to 800°F. A related study [17K] reports on radiative transfer between discrete solid particles in a bed. A theory is presented which accounts for different particle geometries, and experiments are reported which show satisfactory agreement with the analysis.

The analysis of laminar compressible flow in the stagnation region has been modified to examine the effects of foreign gas injection from the surface [18K]. It is found that the overall heat transfer to the surface may be reduced by as much as two-thirds by the injection of a gas having an absorption coefficients several orders of magnitude higher than water vapor. Another analysis [6K] deals with the effect of thermal radiation on the inviscid flow over a blunt body. It is deduced that for practical hypersonic flows, the velocity distribution outside of the boundary layer will not be significantly affected.

An experimental investigation was reported [19K] on the effect of injection of carbon black on the radiation properties of flames. It was found that such injection produced a significant increase in flame emissivity.

The use of the calculus of variations as a tool in radiation analysis has been described [30K]. An example is given of the application of this method to the case of two finite non-black parallel plates and a comparison is made with the exact solution. Among other solution techniques, the variational method described above is utilized to examine the thermal radiation from a finite cylindrical enclosure with a specified wall flux [34K]. The inside temperature distribution is also determined for both gray-diffuse and black surfaces.

LIQUID METALS

A survey covering the current state of knowledge in liquid metal heat transfer has been published [3L]. The large spread among data for tube and duct flows which was highlighted in the 1955 Lubarsky–Kaufman survey remains. Information on free convection, boiling and condensation is given, but in the latter two areas, the data is particularly sparce.

The lack of agreement between theory and experiment is sometimes ascribed to the existence of a surface contact resistance. A static experiment using mercury and chrome-plated copper finds a resistance too small to explain the discrepancy [6L]. In response to reactor applications, information on the maximum temperature in a tube or annulus having a longitudinally-varying sinusoidal wall heat flux has been obtained by correlating mercury data [7L]. Nucleate boiling of mercury (with wetting

additives) in a natural convection loop achieved heat fluxes of 600 000 Btu/h ft² without yet reaching the critical value [9L]. Another boiling study is reported [4L], but a translation could not be found.

Tests and operating experience on heat exchangers utilizing NaK with air or a molten salt are described [5L], and design precepts based on this knowledge set forth [2L]. A feasibility study relating to boiling mercury under zero-gravity was carried out in an airplane flying a zero-gravity arc [8L]. The tests were generally positive, but the effects of non-condensable gases were demonstrated to be particularly important.

An analytical study led to the conclusion that the effects of variable fluid properties on liquid metal heat transfer in tubes is moderate and is not the cause of discrepancies among data [10L]. A modification of Prandtl's mixing length theory is applied to the analysis of turbulent tube flow [1L]. The final equation for the Nusselt number contains a separate dependence on the Prandtl and the Peclet numbers which is neither supported nor refuted by currently available data.

LOW DENSITY HEAT TRANSFER

Experimental and theoretical efforts focused on heat transfer between simple geometries (cylinders and spheres) and high-speed, rarefied gas streams. This concern arises from technological needs of missile, satellite and space vehicle design and because of the interest in the physical processes at work in this region.

Experiments with chromel–alumel wires in crossflow at about Mach 6 covered a Knudsen number range of 0·001 to 15 and yielded Nusselt numbers 0·01 to 10 and accommodation coefficients of 1·0, 0·9 and 0·4 for argon, nitrogen, and helium respectively [9M]. Another study, [8M], gave similar results for a 0·5 in cylinder in continuum and slip flow regimes for the Mach range 1·3 to 5·7. Measuring the heat loss from thin wires ($L/D \gg 1000$) in the transition regime showed the effect of wire diameter [2M]. Collecting new and existing data, [1M] reports a general Nusselt number correlation for transverse and yawed cylinders in continuum, slip, and free molecule air flow at subsonic and supersonic conditions. Excluding dissociation effects, the results cover a Knudsen number range 4×10^{-6} to 37 and a Mach range 0·001 to 6·0.

Application of the complete Navier–Stokes equations to the viscous layer—thin shock and the merged layer—thick shock portions of the transition regime gave heat transfer rates in the stagnation region of adiabatic and highly cooled spheres and cylinders in hypersonic flows [6M]. Considering a hot wire in forced convection with a low Mach number stream, [5M] obtained Nusselt numbers reasonably accurate throughout the transition regime. Introducing slip and temperature jump into an incompressible shock layer analysis, stagnation point heat transfer for blunt bodies in hypersonic streams approaches boundary-layer predictions [4M]. Solutions of the Boltzman equation for parallel plate heat transfer throughout the transition regime are compared with other predictions [3M] and a useful review [7M] cites investigations, kinetic theory developments, and salient features of the free and nearly-free molecule flow regime.

MEASUREMENT TECHNIQUES

Several new techniques for temperature measurement have recently been proposed. An absolute noise thermometer has been developed [7N] in which use is made of the relation between temperature and thermal noise, measured electrically, in a resistor. The method has particular utility at temperatures lower than 140°K.

The accurate measurement of surface temperatures of solids at temperatures in excess of 1500°K has long been a difficult experimental problem. It has been proposed [14N] that measuring the velocity distribution of a beam of atoms which has been reflected from the surface offers a promising method. It appears that the reflected beam is in temperature equilibrium with the surface over a wide range of surface types, smoothnesses, and temperatures. Thus the effect of departure from black body conditions which must be accounted for in pyrometric measurements is absent.

Another paper [12N] discusses the relative merits of thin film probes versus hot wires. The film probe has the advantages of ruggedness and

Vol. 3 1961

low sensitivity to contamination products in the gas stream. Its chief disadvantage is in its considerably greater size.

A number of studies have appeared concerning the measurement of thermal properties. An apparatus has been developed [17N] for the determination of thermal expansion coefficient, specific heat and thermal conductivity of refactories to temperatures up to 3650°C. Another device [9N] measures the thermal conductivity of insulating materials from liquid nitrogen temperature to room temperature. A special feature of the equipment is the short time necessary to reach thermal equilibrium. A measurement can be made at different temperature levels every 15 min.

Ångstrom was the first to show that by subjecting one face of a material to a time dependent and cyclic temperature pulse its thermal conductivity could be determined if the amplitude and phase of the pulse were measured at two interior points. This method has been adapted to measure the thermal conductivity of semiconductors [8N]. Thermal measurements of diathermanous materials in which more than one mode of heat transfer prevails are particularly difficult. A study is reported [2N] dealing with the determination of thermal conductivities of transparent substances.

The last paper in this series [6N] deals with the development of a probe for measuring the thermal conductivity of building materials. The probe is only 0·11 inch in diameter and may be used to determine the thermal conductivity at various locations in the cross sections of structures up to about 1·2 in below the surface.

Another group of papers is concerned with errors which exist in temperature measurements. The study of errors involved in measuring boundary-layer temperatures because of conduction down the leads is reported in [18N]. A similar study [5N] discusses the effect of lead conduction errors when making ground temperature measurements in geological researches. The greatly neglected technique of substituting manganin for copper in a copper–constantan thermocouple is shown to substantially reduce the lead conduction error. A third paper [1N] presents an analysis of the errors when a thermocouple is placed beneath the surface to measure surface temperatures. Two problems considered are the disturbance in the temperature field caused by the presence of the thermocouple and the effect of having the thermocouple removed a certain distance from the surface.

A method of measuring temperatures downstream from a shock wave is discussed in [13N]. The technique is based on the use of the emitting and absorbing characteristics of sodium D lines. Temperatures from 4000 to 5000°K were measured under laboratory conditions with an error of from 100 to 200°K. A probe for the measurement of gas temperatures is described in [23N]. Probe errors of radiation, base conduction and thermocouple wire conduction are minimized by electrically heating the probe base and shield.

Transient temperature measurements are discussed in [16N] and [3N]. In the first paper, a thermocouple installation is described to measure the temperature change on the cylinder wall surface of an internal combustion engine. The temperature measurement is made over an area only 0·25 mm in diameter and the junction is located only 25 μ below the surface. The second paper [3N] discusses a special thermocouple plug developed to measure transient temperatures at relatively large distances from the surface within rocket nozzle walls.

Two thermocouples suitable for the measurement of temperatures up to 2800°C are described in [4N]. They are made from tungsten/26% rhenium–tungsten and tantalum/26% rhenium–tungsten respectively. Important features are the suitability for operation at higher temperatures than is possible for existing thermocouples and their high sensitivity of 15 μV/°C. In connection with thermocouple installations, a quick connector for multipoint thermocouple assemblies is described [11N] which is easily constructed and which affords protection against factors which affect thermocouple calibration.

An improved method for measuring turbulence in wakes [10N] uses a condenser-type microphone and a hot wire annemometer. Results of measurements made with this instrument indicate the contribution of pressure fluctuations to the turbulence characteristics. Another experimental investigation [21N] relates

to the effect of relaxation times on impact-probe measurements. The proper probe size for such measurements under a variety of conditions was determined.

Two new techniques for making flow measurements have been described. The use of nuclear resonance detection in tracers is discussed in [19N]. This technique offers promise in measuring flow rates in blood vessels where conventional methods are difficult to apply. By X-raying with a narrow beam [15N] it is possible to measure both the average vapor content in a channel cross section in two phase flow and the local vapor concentration in a small portion of a boiling-layer.

A pair of general papers complete this section. The first [20N] is a convenient listing of papers in the literature which describe pitot and static probes, their origin, principles, evaluation, performance, modern modifications and applications. The last paper [22N] gives a complete description of a temperature standards laboratory in a research laboratory. A complete list of all the instrumentation is included as well as the accuracies obtainable in the different kinds of calibrations.

HEAT TRANSFER APPLICATIONS

Heat exchangers

Interest remains high on the transient response of heat exchangers. The last paper of a three part series [1P] presents a general solution for the transient temperature distribution resulting from an arbitrary time rate of change of heat generation starting from an arbitrary initial condition. The reader's attention is also directed to the discussion at the end of this paper. The relative merits of "exact" and numerical solutions are presented ably and cogently by adherents of both viewpoints.

Another paper [9P] investigates the transient response and the steady state behavior of a solar heat exchanger wherein the energy transfer processes are by radiation. Other papers related to radiation heat exchangers are discussed in the section on Radiation in the present review.

Experimental data on the effect of flow pulsations on the efficiency of shell and tube heat exchangers are presented in [2P]. Pulsation frequencies of 40, 80, and 160 cycles/min are applied over a tube Reynolds number range from 4000 to 50 000. It is found that the increase in heat transfer caused by the pulsations decreases as the Reynolds number increases.

Two types of special purpose heat exchangers have been investigated [3P, 10P]. The former are nuclear reactor heat exchangers which operate with power densities up to 10 MW/ft^3. Under these severe conditions, critical problems are thermal stresses and methods of metal fastening. The latter paper presents heat transfer and pressure drop data on heat exchangers involving liquid metals and molten salts on the two sides. The two types of flow investigated were through round tubes and flow outside an array of round tubes and parallel to the tubes' axes.

Another pair of papers deals with artificial methods of increasing heat transfer. The study of mechanical wiping on surfaces of evaporation has received attention in [7P]. Analysis which is substantiated by experiment shows large increases in heat transfer over conventional surfaces. The second paper [8P] reports an investigation of the effect of turbulence promoters in three typical heat exchanger designs. Suitable correlations allow the prediction of heat transfer coefficients for these designs under a variety of operating conditions.

Tube sheets of U-tube and bayonet-tube exchangers have been investigated for the strengthening effect of tube-bending reaction [4P]. This effect is evaluated and presented in the form of simple design factors. A regenerative pebble-bed heat exchanger has been constructed to produce large quantities of high temperature air [6P]. Data have been obtained on both the air and bed temperature distributions and compared with predicted values.

Another study has reported the heat transfer and friction characteristics of compact heat exchangers [5P]. The exchangers which were examined have the largest surface to volume ratio of any investigated thus far in the program at Stanford University.

Aircraft, missiles, and satellites

Interest in aeronautics has now mainly shifted to an analysis of the re-entry conditions through the atmosphere of manned and unmanned satellites. It is concluded [4Q] that either a blunt,

Vol. 3 1961

dense vehicle with an ablation cooling system, or a radiation cooled vehicle with drag break or lifting surface is best suited for this purpose. Similar conclusions are reached and simple procedures for a surface temperature prediction have been developed [5Q, 8Q, 2Q, 3Q, 1Q]. These studies consider entry into the atmospheres of other planets as well. The possibility of simulating atmospheric re-entry conditions in experiments with small scale models has been investigated, with the conclusion that such a simulation is possible as far as the thermal stresses and the skin temperatures are concerned [10Q]. The chemical decomposition process on an ablating Teflon wall is investigated [9Q]. Film cooling with water is proposed for the re-entry of satellite vehicles and experimental results for this method are reported [7Q]. The temperature conditions in orbiting satellites are essentially determined by the radiation to and from the surface and by internal conduction and radiation processes. The thermal control of the Explorer satellites is described and analyzed [6Q].

THERMODYNAMIC AND TRANSPORT PROPERTIES

Experimental and theoretical efforts extend from cryogenic to plasma temperatures for a variety of fluids.

Thermodynamic properties

Investigation of the *p-V-T* behavior of water and steam [13R] obtained data in the pressure range 700 to 900 kg/cm² and temperature range 650 to 700°C accurate to 0·06 per cent. Compiled and correlated data for helium resulted in *T-s* and *h-s* charts for the temperature range 3·0 to 20°K and pressure range 0·5 to 100 atm [14R]. Use of statistical mechanics [20R, 6R] predicts equilibrium air properties for temperatures 500 to 15 000°K and pressures from 0·0001 to 1000 atm. Ref. [7R] reports similar data for nonionized N_2–O_2 mixtures to 10 000°K. Hydrogen data from 600 to 5000°K and 0·01 to 100 atm are compiled for calculating rocket performance [12R].

Transport properties

Employing hot wire techniques, [22R] reports thermal conductivities for the nonatomic gases [He, A, Kr, Xe, Hg (vapor)] from 0 to 500°C at 1 atm pressure with a maximum error of 1·8 per cent while [4R, 3R] finds that the $N_2O_4 = 2\ NO_2$ system has conductivities 9 times that computed for equivalent non-reacting systems in the region 20 to 215°C and 0·02 to 1 atm pressure. Coaxial, cylindrical cells yield thermal conductivities of air, A, N_2, CO_2, and steam to 900°C at 1 atm pressure [21R], liquid and gaseous N_2 and A in the region 85 to 200°K and 1 to 135 atm [3R], and D_2O in the region 75 to 260°C and 24 to 294 atm [24R]. Ref. [5R] reports direct Prandtl number measurements for He–air mixtures at 270°K.

Absolute viscosities for air, A, CO_2, D_2O, He, H_2, Kr, Ne, N_2, O_2, and H_2O (vapor) at 20°C by the oscillating-disc method are reported accurate to 0·05 per cent [10R] and the soundness of the method further verified [11R].

Statistical mechanics methods applied to air [6R, 2R] supply estimates of transport properties, from 500 to 15 000°K and from 0·0001 to 100 atm, useful in hypersonic laminar boundary-layer applications [19R]. Based on the Lennard–Jones potential, transport properties from 200 to 1500°K are estimated for He–air mixtures at low pressures [5R] and for the atmospheres of Venus, Mars, and Jupiter [8R]. Ref. [12R] reports equilibrium, hydrogen transport property predictions for the temperature range 600 to 5000°K and warm plasma (an equilibrium mixture of plus ions, neutral particles, and mobile electrons) conductivity is predicted in [17R].

For point source diffusion, [18R] reports the effect of concentration-dependent coefficients on the concentration distribution in one, two, and three dimensions, while [1R] notes that diffusion coefficients may be calculated from the change of asymmetric concentration profiles over known distances.

Addressing the problem of microscopic behavior at elevated temperatures, [16R] reports collision integrals for the exponential repulsive potential and [15R] the effect on these of excitation and charge exchange in mixtures, both important in predicting the transport properties of gases at high temperatures. A useful review of molecular transport properties of fluids is given by [9R].

REFERENCES

Table 1. *Books*

1. *Astronaútics Information Abstracts*, Vol. II, Jet Propulsion Laboratory, California Institute of Technology, Pasadena, Calif. (1960).
2. A. J. CHAPMAN, *Heat Transfer*. Macmillan Company, New York, N.Y. (1960).
3. F. J. CLAUSS (Editor), *Surface Effects on Spacecraft Materials*. John Wiley, New York (1960).
4. S. FLUGGE and C. TRUESDELL (Editors), *Encyclopedia of Physics—I. Fluid Dynamics*. Stromungsmechanik, Vol. 8. Springer-Verlag, Berlin (1959).
5. H. GÖRTLER (Editor), *Symposium on Boundary-Layer Research*. Springer-Verlag, Berlin (1958).
6. R. GREGORIG, *Warmeaustauscher; Berechnung, Konstruction, Betrieb, Wirtschaftlichkeit*. Sauerländer, Frankfurt (1959).
7. W. D. HAYES and R. F. PROBSTEIN, *Hypersonic Flow Theory*. Academic Press, New York (1959).
8. J. O. HINZE, *Turbulence*. McGraw-Hill, New York (1959).
9. C. C. LIN (Editor), *Turbulent Flows and Heat Transfer*. Princeton University Press, Princeton (1959).
10. Anonymous, *Low Temperature Heat Exchangers*. (Symposium issue) Brit. Chem. Eng., Vol. 5, No. 1 (1960).

Conduction

1A. H. R. BAILEY, *Quart. Appl. Math.* **17**, 255 (1959).
2A. G. BAKER, JR. and T. A. OLIPHANT, *Quart. Appl. Math.* **17**, 361 (1960).
3A. J. V. BECK and H. HURWICZ, *Trans. ASME J. Heat Transfer*, C **82**, 27 (1960).
4A. B. A. BOLEY, *Quart. Appl. Math.* **18**, 205 (1960).
5A. W. F. CAMPBELL, *J. Aero. Space Sci.* **27**, 633 (1960).
6A. P. L. CHAMBRE, *J. Appl. Phys.* **30**, 1683 (1959).
7A. S. J. CITRON, *J. Aero. Space Sci.* **27**, 219 (1960).
8A. S. J. CITRON, *J. Aero. Space Sci.* **27**, 317 (1960).
9A. G. N. DULNEV, *Int. J. Heat Mass Transfer*, **1**, Nos. 2/3, 152 (1960).
10A. C. D. FORBES, JR., S. I. SCHLESINGER and L. SASHKIN, *J. Aero. Space Sci.* **27**, 59 (1960).
11A. T. R. GOODMAN and J. J. SHEA, *J. Appl. Mech.* **27**, *Trans. ASME* E **82**, 16 (1960).
12A. H. W. HAHNEMANN, *Z. Ver. Dtsch. Ing.* **102**, 423 (1960).
13A. C. F. HANSEN, R. A. EARLY, F. E. ALZOFON and F. C. WITTEBORN, *N.A.S.A. Tech. Rep.* R-27 (1959).
14A. J. E. HATCH, R. L. SCHACHT, L. U. ALBERS and P. G. SAPER, *N.A.S.A. Tech. Rep.* R-56 (1960).
15A. P. R. HILL, *N.A.C.A. Rep.* 1372 (1958).
16A. G. HORVAY, *Trans. ASME J. Heat Transfer*, C **82**, 37 (1960).
17A. I. A. IOFFE, *Soviet Phys. Tech. Phys.* **4**, 369 (1959).
18A. S. P. KUZNETSOV, *Ref. Zh. Mekh.* no. 10, Rev. 11270 (1958).
19A. W. T. KYNER, *Quart. Appl. Math.* **17**, 305 (1959).
20A. M. LOTKIN, *Quart. Appl. Math.* **18**, 79 (1960).
21A. C. S. LOWTHIAN, *J. Nucl. Energy; Part A, Reactor Science*, **10**, 95 (1959).
22A. W. S. MINKLER and W. T. ROULEAU, *Nucl. Sci. Engng*, **7**, 400 (1960).
23A. R. MUKI and E. STERNBERG, *Z. Angew. Math. Phys.* **11**, 306 (1960).
24A. M. M. NAZARCHUK and N. I. POL'SKII, *Soviet Phys.-Dokl.* **4**, 1227 (1960).
25A. H. PORITSKY and R. A. POWELL, *Quart. Appl. Math.* **18**, 97 (1960).
26A. J. SCHNIEWIND, *Forsch. A.D.G.D. Ing.-Wes.* **25**, 196 (1959).
27A. A. SELLERIO, *Termotecnica*, **12**, 306 (1958).
28A. E. M. SPARROW, *Trans. ASME J. Heat Transfer*, C **82**, 389 (1960).
29A. R. P. STEIN, *J. Appl. Mech.* **26**, *Trans. ASME* E **81**, 685 (1959).
30A. G. STOLZ, *Trans. ASME J. Heat Transfer*, C **82**, 20 (1960).
31A. T. E. STONECYPHER, *J. Aero. Space Sci.* **27**, 152 (1960).
32A. R. T. SWANN, *N.A.S.A. Tech. Note* D-171 (1959).
33A. G. A. TIRSKII, *Soviet Phys.-Dokl.* **4**, 981 (1960).
34A. V. VODIČKA, *Appl. Sci. Res.* A **9**, 190 (1960).
35A. V. VODIČKA, *Z. Angew. Math. Mech.* **40**, 161 (1960).
36A. V. VODIČKA, *Z. Angew. Math. Mech.* **40**, 165 (1960).
37A. K. ZOLLER, *Ing.-Arch.* **28**, 366 (1959).

Channel flow

1B. D. W. ABBRECHT and S. W. CHURCHILL, *J. Amer. Inst. Chem. Engrs*, **6**, 268 (1960).
2B. H. C. AGRAWAL, *Appl. Sci. Res.* A **9**, 177 (1960).
3B. V. S. ARPACI and J. A. CLARK, *Trans. ASME J. Heat Transfer*, C **81**, 253 (1959).
4B. H. D. BAEHR, *Chem.-Ing.-Tech.* **32**, 89 (1960).
5B. R. S. BROKAW, *N.A.C.A. Res. Memo.* E57K19a (1958).
6B. G. M. BROWN, *J. Amer. Inst. Chem. Engrs*, **6**, 179 (1960).
7B. R. D. CESS and E. C. SHAFFER, *Appl. Sci. Res.* A **8**, 339 (1959).
8B. R. D. CESS and E. C. SHAFFER, *Appl. Sci. Res.* A **9**, 64 (1959).
9B. R. D. CESS and E. C. SHAFFER, *J. Aero. Space Sci.* **26**, 538 (1960).
10B. P. L. CHAMBRE, *Appl. Sci. Res.* A **9**, 157 (1960).
11B. S. W. CHURCHILL and R. E. BALZHISER, *Chem. Engng Progr. Symposium Series, Heat Transfer*, **55**, 127 (1959).
12B. R. G. DEISSLER and M. PERLMUTTER, *Int. J. Heat Mass Transfer*, **1**, Nos. 2/3, 173 (1960).
13B. R. G. DEISSLER and M. F. TAYLOR, *N.A.S.A. Tech. Rep.* R-31 (1959).
14B. S. C. R. DENNIS, A. M. MARCER and G. POOTS, *Quart. Appl. Math.* **17**, 285 (1959).
15B. E. R. G. ECKERT and T. F. IRVINE, JR., *Trans. ASME J. Heat Transfer*, C **82**, 125 (1960).
16B. V. K. ERMOLIN, *Int. J. Heat Mass Transfer*, **1**, Nos. 2/3, 147 (1960).
17B. J. M. FOWLER and C. F. WARNER, *J. Amer. Rocket Soc.* **30**, 266 (1960).
18B. H. W. HAHNEMANN, *Z. Ver. Dtsch. Ing.* **101**, 1431 (1959).

Vol. 3 1961

19B. H. Hausen and L. Düwell, *Kältetechnik*, **11**, 242 (1959).
20B. R. M. Inman, *J. Aero. Space Sci.* **26**, 532 (1959).
21B. F. Kreith, *Appl. Sci. Res.* A **8**, 457 (1959).
22B. C. Y. Kuo, H. T. Iida, J. H. Taylor and F. Kreith, *Trans. ASME J. Heat Transfer*, C **82**, 139 (1960).
23B. J. E. Lay, *Trans. ASME J. Heat Transfer*, C **81**, 213 (1959).
24B. J. R. McCarthy and H. Wolf, *J. Amer. Rocket Soc.* **30**, 423 (1960).
25B. A. McD. Mercer, *Appl. Sci. Res.* A **8**, 357 (1959).
26B. A. McD. Mercer, *Appl. Sci. Res.* A **9**, 460 (1960).
27B. A. B. Metzner and W. L. Friend, *Canad. J. Chem. Engng*, **36**, 235 (1958).
28B. A. B. Metzner and D. F. Gluck, *Chem. Engng Sci.* **12**, 185 (1960).
29B. K. Murakawa, *Bull. Jap. Soc. Mech. Engrs*, **3**, 340 (1960).
30B. W. C. Reynolds, *Trans. ASME J. Heat Transfer*, C **82**, 108 (1960).
31B. J. A. Scanlan, *Industr. Engng Chem.* **50**, 1565 (1958).
32B. R. Siegel, *J. Appl. Mech.* **27**, *Trans. ASME* E **81**, 241 (1960).
33B. R. Siegel and E. M. Sparrow, *Trans. ASME J. Heat Transfer*, C **81**, 280 (1959).
34B. R. Siegel and E. M. Sparrow, *Trans. ASME J. Heat Transfer*, C **81**, 152 (1960).
35B. N. A. Slezkin, *J. Appl. Math. Mech.* **23**, 473 (1959).
36B. E. M. Sparrow and R. Siegel, *Int. J. Heat Mass Transfer*, **1**, Nos. 2/3, 161 (1960).
37B. E. M. Sparrow and R. Siegel, *Trans. ASME J. Heat Transfer*, C **82**, 170 (1960).
38B. K. Stephan, *Chem.-Ing.-Tech.* **31**, 773 (1959).
39B. A. G. Temkin, *Soviet Phys.-Tech. Phys.* **4**, 383 (1959).
40B. P. H. Wang, *Scientia Sinica*, **8**, 98 (1959).
41B. H. Wolf, *Trans. ASME J. Heat Transfer*, C **81**, 267 (1959).

Boundary-layer flow

1C. A. Acrivos, M. J. Shah and E. E. Peterson, *J. Amer. Inst. Chem. Engrs*, **6**, 312 (1960).
2C. T. C. Adamson, Jr., *J. Amer. Rocket Soc.* **30**, 358 (1960).
3C. P. D. Arthur and J. C. Williams, *J. Amer. Rocket Soc.* **30**, 207 (1960).
4C. A. C. Baxter and W. C. Reynolds, *J. Aero. Sci.* **25**, 403 (1958).
5C. M. H. Bloom and M. H. Steiger, *Proc. Third U.S. Natl. Congr. Appl. Mech.*, p. 717 (1958).
6C. J. H. Boynton, *J. Aero. Space Sci.* **27**, 306 (1960).
7C. W. H. Braun, *N.A.S.A. Tech. Note* 4208 (1958).
8C. P. B. Burbank and B. L. Hodge, *N.A.S.A. Memo.* 6-4-59L (1959).
9C. P. M. Chung, *N.A.S.A. Tech. Note* D-306 (1960).
10C. P. M. Chung and A. D. Anderson, *J. Amer. Rocket Soc.* **30**, 262 (1960).
11C. P. M. Chung and A. D. Anderson, *N.A.S.A. Tech. Note* D-140 (1960).
12C. P. M. Chung and A. D. Anderson, 1960 *Heat Transfer and Fluid Mechanics Inst.*, p. 150, Stanford Univ. Press, Calif. (1960).
13C. R. J. Conti, *N.A.S.A. Tech. Note* D-159 (1959).
14C. M. Cooper and P. C. Stainback, *N.A.S.A. Memo.* 3-7-59L (1959).
15C. R. J. Cresci, D. A. MacKenzie and P. A. Libby, *J. Aero. Space Sci.* **27**, 401 (1960).
16C. N. Curle, *Proc. Roy. Soc.* **249**, 206 (1959).
17C. R. G. Deissler and A. L. Loeffler, *N.A.S.A. Tech. Rep.* R-17 (1959).
18C. E. R. G. Eckert and O. E. Tewfik, *J. Aero. Space Sci.* **27**, 464 (1960).
19C. N. A. Evans, *Proc.* 1960 *Heat Transfer and Fluid Mechanics Inst.*, Stanford Univ. Press, Calif. (1960).
20C. C. R. Faulders, *J. Aero. Space Sci.* **27**, 628 (1960).
21C. S. K. Friedlander and M. Litt, *Appl. Sci. Res.* **8**, 403 (1959).
22C. R. E. Geiger, *J. Aero. Space Sci.* **26**, 834 (1959).
23C. R. J. Gribben, *Phys. of Fluids*, **2**, 305 (1959).
24C. A. S. Gupta, *Appl. Sci. Res.* A **9**, 319 (1960).
25C. A. S. Gupta, *Z. Angew. Math. Phys.* **11**, 43 (1960).
26C. C. F. Hansen, *J. Amer. Rocket Soc.* **30**, 942 (1960).
27C. C. R. Illingworth, *J. Fluid Mech.* **7**, 442 (1960).
28C. T. F. Irvine, Jr. and E. R. G. Eckert, *Trans. ASME J. Heat Transfer*, C **82**, 325 (1960).
29C. J. D. Julius, *N.A.S.A. Tech. Note* D-179 (1959).
30C. N. H. Kemp, *J. Aero. Space Sci.* **27**, 553 (1960).
31C. J. L. Kerrebrock, *J. Aero. Space Sci.* **27**, 156 (1960).
32C. S. I. Kosterin and Yu. A. Koshmarov, *Soviet Phys.-Tech. Phys.* **4**, 819 (1960).
33C. R. F. Kramer and H. M. Lieberstein, *J. Aero. Space Sci.* **26**, 508 (1959).
34C. B. LeFur, *J. Aero. Space Sci.* **26**, 682 (1959).
35C. D. C. Leigh and G. W. Sutton, *J. Aero. Space Sci.* **27**, 469 (1960).
36C. M. Litt and S. K. Friedlander, *J. Amer. Inst. Chem. Engrs*, **5**, 483 (1959).
37C. D. Meksyn, *Z. Angew. Math. Phys.* **11**, 63 (1960).
38C. Y. Nakagawa, *Phys. of Fluids*, **3**, 87 (1960).
39C. S. D. Nigam and S. N. Singh, *Quart. J. Mech. Appl. Math.* **13**, 85 (1960).
40C. C. C. Pappas and A. F. Okuno, *J. Aero. Space Sci.* **27**, 321 (1960).
41C. H. S. Pergament and M. Epstein, *J. Amer. Rocket Soc.* **30**, 206 (1960).
42C. G. Poots, *Quart. J. Mech. Appl. Math.* **13**, 56 (1960).
43C. W. C. Ragsdale, *Chem. Engng Sci.* **11**, 242 (1960).
44C. S. A. Regirer, *Soviet Phys.-JETP* **37**, 149 (1960).
45C. W. C. Reynolds, W. M. Kays and S. J. Kline, *Trans. ASME J. Heat Transfer*, C **82**, 341 (1960).
46C. V. J. Rossow, *N.A.S.A. Tech. Rep.* R-37 (1959).
47C. S. M. Scala and G. W. Sutton, *J. Amer. Rocket Soc.* **29**, 141 (1959).
48C. J. F. Schmidt, *N.A.S.A. Tech. Rep.* D-8 (1959).
49C. R. A. Seban, *Trans. ASME J. Heat Transfer*, C **82**, 101 (1960).
50C. J. A. Shercliff, *J. Roy. Aero. Soc.* **63**, 518 (1959).

51C. M. B. SKOPETS, *Soviet Phys.-Tech. Phys.* **4**, 411 (1959).
52C. A. G. SMIRNOV, *Zh. Tekh. Fiz.* **28**, 1549 (1958).
53C. H. H. SOGIN, *Trans. ASME J. Heat Transfer*, C **82**, 53 (1960).
54C. D. A. SPENCE, *J. Fluid Mech.* **8**, 368 (1960).
55C. D. A. SPENCE, *Proc.* 1960 *Heat Transfer and Fluid Mechanics Inst.*, p. 62, Stanford Univ. Press, Calif. (1960).
56C. W. SPRINGE, *Z. Ver. Dtsch. Ing.* **102**, 1391 (1960).
57C. P. C. STAINBACK, *N.A.S.A. Tech. Note* D-184 (1960).
58C. D. STOJANOVIC, *J. Aero. Space Sci.* **26**, 571 (1959).
59C. T. TENDELAND, *N.A.S.A. Tech. Note* 4236 (1959).
60C. O. TEWFIK and W. H. GIEDT, *J. Aero. Space Sci.* **27**, 721 (1960).
61C. R. VAGLIO-LAURIN, *Proc.* 1959 *Heat Transfer and Fluid Mechanics Inst.*, p. 95, Univ. of Calif., Los Angeles, Calif. (1959).
62C. R. VAGLIO-LAURIN, *J. Aero. Space Sci.* **27**, 27 (1960).
63C. J. M. F. VICKERS, *Industr. Engng Chem.* **51**, 967 (1959).
64C. G. K. WALKER, *J. Aero. Space Sci.* **27**, 715 (1960).
65C. R. J. WISNIEWSKI, *N.A.S.A. Tech. Note* D-201 (1959).
66C. J. G. WOODLEY, *Aero. Res. Council* (Gt. Brit.) C.P. 479 (1960).
67C. V. ZAKKAY, *J. Aero. Space Sci.* **27**, 157 (1960).
68C. L. M. ZYSINA-MOLOZHEN, *Soviet Phys.-Tech. Phys.* **4**, 564 (1959).

Flow with separated regions

1D. A. A. ANDREEVSKII, *Inzh.-Fiz. Zh.* **2**, 46 (1959).
2D. M. H. BLOOM and A. PALLONE, *J. Aero. Space Sci.* **26**, 626 (1959).
3D. E. BRUN and G. DONNADIEU, *C.R. Acad. Sci., Paris*, **251**, 843 (1960).
4D. P. CALVET and G. DONNADIEU, *C.R. Acad. Sci., Paris*, **250**, 2324 (1960).
5D. L. S. DZUNG, *Int. J. Heat Mass Transfer*, **1**, Nos. 2/3, 236 (1960).
6D. R. ERNST, *Chem.-Ing.-Tech.* **32**, 17 (1960).
7D. A. KLINKENBERG, *Chem. Engng Sci.* **11**, 260 (1960).
8D. R. B. LANCASHIRE, E. A. LEZBERG and J. F. MORRIS, *Industr. Engng Chem.* **52**, 433 (1960).
9D. H. K. LARSON, *J. Aero. Space Sci.* **26**, 731 (1959).
10D. J. F. RICHARDSON and P. AYERS, *Trans. Inst. Chem. Engrs*, **37**, 314 (1959).
11D. R. A. SEBAN, A. EMERY and A. LEVY, *J. Aero. Space Sci.* **26**, 809 (1959).
12D. H. A. VREEDENBERG, *Chem. Engng Sci.* **11**, 274 (1960).
13D. R. N. WELTMANN and P. W. KUHNS, *N.A.S.A. Tech. Note* D-267 (1960).
14D. S. YAGI and D. KUNII, *J. Amer. Inst. Chem. Engrs*, **6**, 97 (1960).

Transfer mechanism

1E. D. CLUTTER and A. M. O. SMITH, *J. Aero. Space Sci.* **27**, 70 (1960).
2E. R. G. DEISSLER, *Phys. of Fluids*, **3**, 176 (1960).
3E. J. W. ELDER, *J. Fluid Mech.* **9**, 235 (1960).
4E. H. GÖRTER, *Z. Flugwiss.* **8**, 1 (1960).
5E. F. R. HAMA, *Phys. of Fluids*, **2**, 664 (1959).
6E. F. R. HAMA, *Proc.* 1960 *Heat Transfer and Fluid Mechanics Inst.*, p. 92, Stanford Univ. Press, Calif. (1960).
7E. R. A. HARTUNIAN, A. L. RUSSO and P. V. MARRONE, *J. Aero. Space Sci.* **27**, 587 (1960).
8E. E. J. HOPKINS, S. J. KEATING, JR. and A. BANDETTINI, *N.A.S.A. Tech. Note* D-328 (1960).
9E. A. L. KISTLER, *Phys. of Fluids*, **2**, 290 (1959).
10E. B. H. LOCHTENBERG, *J. Aero. Space Sci* **27**, 92. (1960).
11E. H. MICKLEY and A. TURANO, JR., *J. Aero. Space Sci.* **27**, 629 (1960).
12E. J. ROTTA, *Z. Flugwiss.* **7**, 264 (1959).
13E. V. A. SANDBORN and R. J. WISNIEWSKI, *Proc.* 1960 *Heat Transfer and Fluid Mechanics Inst.*, p. 120, Stanford Univ. Press, Calif. (1960).
14E. A. A. SERGIENKO and V. K. GRETSOV, *Soviet Phys.-Dokl.* **4**, 275 (1959).
15E. K. G. SEWELL, *Proc.* 1960 *Heat Transfer and Fluid Mechanics Inst.*, p. 106, Stanford Univ. Press, Calif. (1960).
16E. C. L. TIEN, *Appl. Sci. Res.* A **8**, 345 (1959).
17E. E. R. VAN DRIEST and W. D. MCCAULEY, *J. Aero. Space Sci.* **27**, 261 (1960).

Natural convection

1F. R. P. BOBCO, *J. Aero. Space Sci.* **26**, 846 (1959).
2F. R. C. L. BOSWORTH and C. M. GRODEN, *Austral. J. Phys.* **13**, 73 (1960).
3F. R. C. L. BOSWORTH, *Austral. J. Phys.* **13**, 84 (1960).
4F. W. H. BRAUN and J. E. HEIGHWAY, *N.A.S.A. Tech. Note* D-292 (1960).
5F. L. J. CRANE, *Z. Angew. Math. Phys.* **10**, 453 (1959).
6F. R. EICHHORN, *Trans. ASME J. Heat Transfer*, C **82**, 260 (1960).
7F. R. M. FAND and J. KAYE, *J. Acoust. Soc. Amer.* **32**, 579 (1960).
8F. M. M. FARZETDINOV, *Appl. Math. Mech.* **22**, 393 (1958).
9F. T. FUJII, *Bull. Jap. Soc. Mech. Engrs*, **2**, 365 (1959).
10F. G. Z. GERSHUNI and E. M. ZHUKHOVITSKII, *Soviet Phys.-Dokl.* **4**, 102 (1959).
11F. A. W. GOLDSTEIN, *N.A.S.A. Tech. Rep.* R-4 (1959).
12F. R. GOLDSTEIN and E. R. G. ECKERT, *Int. J. Heat Mass Transfer*, **1**, Nos. 2/3, 208 (1960).
13F. I. R. GOROFF, *Proc. Roy. Soc.* A **254**, 537 (1960).
14F. J. D. GRIFFITH and R. H. SABERSKY, *J. Amer. Rocket Soc.* **30**, 289 (1960).
15F. A. S. GUPTA, *Appl. Sci. Res.* A **9**, 319 (1960).
16F. H. HAUSEN, *Allg. Wärmetech.* **9**, 75 (1959).
17F. J. P. HOLMAN and J. H. BOGGS, *Trans. ASME J. Heat Transfer*, C **82**, 221 (1960).
18F. J. P. HOLMAN, H. E. CARTRELL and E. E. SOEHNGEN, *Trans. ASME J. Heat Transfer*, C **82**, 263 (1960).
19F. J. P. HOLMAN, K. E. STOUT and E. E. SOEHNGEN, *J. Aero. Space Sci.* **27**, 463 (1960).

Vol. 3 1961

20F. A. N. KOZLOVA, *Soviet Phys.-Tech. Phys.* **4**, 285 (1959).
21F. L. I. KUDRYASHEV and A. YA. IPATENKO, *Soviet Phys.-Tech. Phys.* **4**, 275 (1959).
22F. F. M. LESLIE, *J. Fluid Mech.* **7**, 115 (1960).
23F. P. C. LU, *Trans. ASME J. Heat Transfer*, C **82**, 227 (1960).
24F. B. W. MARTIN, *Proc. Inst. Mech. Engrs*, **173**, 761 (1959).
25F. W. R. MARTINI and S. W. CHURCHILL, *J. Amer. Inst. Chem. Engrs*, **6**, 251 (1960).
26F. B. R. MORTON, *J. Fluid Mech.* **8**, 227 (1960).
27F. B. R. MORTON, *Quart. J. Mech. Appl. Math.* **12**, 410 (1959).
28F. M. P. MURGAI and H. W. EMMONS, *J. Fluid Mech.* **8**, 611 (1960).
29F. Y. NAKAGAWA, *Phys. of Fluids*, **3**, 82 and 87 (1960).
30F. Y. NAKAGAWA, *Proc. Roy. Soc.* A **253**, 212 (1959).
31F. E. PALM, *J. Fluid Mech.* **8**, 183 (1960).
32F. W. H. REID and D. L. HARRIS, *Phys. of Fluids*, **2**, 716 (1959).
33F. S. A. REGIRER, *Soviet Phys.-JETP* **37**, 149 (1960).
34F. I. G. SEVRUK, *Appl. Math. Mech.* **22**, 807 (1958).
35F. A. G. SMIRNOV, *Soviet Phys.-Tech. Phys.* **4**, 1141 (1960).
36F. E. E. SOEHNGEN, *Ninth Int. Cong. for Appl. Mech.*, p. 475, Brussels (1957).
37F. E. M. SPARROW and J. L. GREGG, *Trans. ASME J. Heat Transfer*, C **82**, 258 (1960).
38F. L. N. TAO, *Appl. Sci. Res.* A **9**, 357 (1960).
39F. L. N. TAO, *Trans. ASME J. Heat Transfer*, C **82**, 233 (1960).
40F. A. A. TOWNSEND, *J. Fluid Mech.* **5**, 209 (1959).
41F. J. VAN DER BURGH, *Appl. Sci. Res.* A **9**, 293 (1960).
42F. K. T. YANG, *J. Appl. Mech.* **27**; *Trans. ASME* E **81**, 230 (1960).
43F. E. I. YANTOVSKII, *Soviet Phys.-Tech. Phys.* **4**, 1280 (1960).
44F. T. YUGE, *Trans. ASME J. Heat Transfer*, C **82**, 214 (1960).

Convection from rotating surfaces

1G. C. B. BAXTER and D. R. DAVIES, *Quart. J. Mech. Appl. Math.* **13**, 247 (1960).
2G. V. N. GOLUBENKOV, *Appl. Math. Mech.* **22**, 1205 (1958).
3G. A. R. ROBINSON, *J. Fluid Mech.* **6**, 599 (1959).
4G. S. N. SINGH, *Appl. Sci. Res.* A **9**, 197 (1960).
5G. E. M. SPARROW and J. L. GREGG, *Trans. ASME J. Heat Transfer*, C **82**, 294 (1960).
6G. G. VERONIS, *J. Fluid Mech.* **5**, 401 (1959).

Combined heat and mass transfer

1H. E. W. ADAMS, *J. Aero. Space Sci.* **27**, 620 (1960).
2H. M. C. ADAMS, W. E. POWERS and S. GEORGIEV, *J. Aero. Space Sci.* **27**, 535 (1960).
3H. J. R. BARON and P. E. SCOTT, *J. Aero. Space Sci.* **27**, 625 (1960).
4H. R. E. BARTLE and B. M. LEADON, *J. Aero. Space Sci.* **27**, 78 (1960).
5H. I. E. BECKWITH, *N.A.S.A. Tech. Rep.* R-42 (1959).
6H. A. Q. ESCHENROEDER, *J. Aero. Space Sci.* **26**, 762 (1959).
7H. L. GREEN and K. L. NALL, *J. Aero. Space Sci.* **26**, 689 (1959).
8H. J. P. HARTNETT, D. J. MASSON, J. F. GROSS and C. GAZLEY, JR., *J. Aero. Space Sci.* **27**, 623 (1960).
9H. H. HOSHIZAKI, *J. Amer. Rocket Soc.* **30**, 628 (1960).
10H. R. M. KRUPKA and D. E. TAYLOR, *Corrosion*, **16**, 91 (1960).
11H. S. OSTRACH, A. W. GOLDSTEIN and J. HAMMAN, *J. Aero. Space Sci.* **27**, 626 (1960).
12H. S. S. PAPELL, *N.A.S.A. Tech. Note* D-299 (1960).
13H. C. C. PAPPAS and A. F. OKUNO, *J. Aero. Space Sci.* **27**, 321 (1960).
14H. L. ROBERTS, *N.A.S.A. Tech. Note* D-254 (1960).
15H. S. M. SCALA, *J. Aero. Space Sci.* **27**, 1 (1960).
16H. S. M. SCALA and N. S. DIACONIS, *J. Aero. Space Sci.* **27**, 140 (1960).
17H. D. E. SEVERSON, A. J. MADDEN and E. L. PIRET, *J. Amer. Inst. Chem. Engrs*, **5**, 413 (1959).
18H. T. K. SHERWOOD and O. TRÄSS, *Trans. ASME J. Heat Transfer*, C **82**, 313 (1960).
19H. D. B. SPALDING, *Aeronaut. Quart.* **11**, 105 (1960).
20H. G. W. SUTTON, *J. Aero. Space Sci.* **27**, 377 (1960).
21H. D. L. TURCOTTE, *J. Aero. Space Sci.* **27**, 675 (1960).

Change of phase

1J. I. T. ALADIEV, L. D. DODONOV and V. S. UDALOV, *J. Nucl. Energy; Part B, Reactor Technology*, **1**, 181 (1960).
2J. D. W. BELL, *Nucl. Sci. Engng*, **7**, 245 (1960).
3J. D. H. CHARLESWORTH and W. R. MARSHALL, *J. Amer. Inst. Chem. Engrs*, **6**, 9 (1960).
4J. P. DERGARABEDIAN, *J. Fluid Mech.* **9**, 39 (1960).
5J. T. ERIKSON and R. J. TYKODI, *J. Chem. Phys.* **33**, 46 (1960).
6J. A. FRANK, *Chem.-Ing.-Tech.* **32**, 330 (1960).
7J. T. H. K. FREDERKING, *J. Amer. Inst. Chem. Engrs*, **5**, 403 (1959).
8J. N. A. FUKS, *Ref. Zh. Mekh.* no. 10, Rev. 11265 (1958).
9J. T. FURMAN and H. HAMPSON, *Proc. Inst. Mech. Engrs*, **173**, 147 (1959).
10J. H. GLASER, *Kältetechnik*, **10**, 386 (1958).
11J. G. E. HARBECK, JR. and G. E. KOBERG, *J. Geophys. Res.* **64**, 89 (1959).
12J. G. G. HASELDEN and S. A. MALATY, *Trans. Inst. Chem. Engrs*, **37**, 137 (1959).
13J. M. I. ISMAILOV, *Ref. Zh. Mekh.* no. 9, Rev. 9987 (1958).
14J. P. D. JONTZ and J. E. MYERS, *J. Amer. Inst. Chem. Engrs*, **6**, 34 (1960).
15J. R. YA. KUCHEROV and L. E. RIKENGLAZ, *Soviet Phys.-JETP* **37**(10), 88 (1960).
16J. H. M. KURIHARA and J. E. MYERS, *J. Amer. Inst. Chem. Engrs*, **6**, 83 (1960).
17J. S. S. KUTATELADZE and V. N. MOSKVICHEVA, *Soviet Phys.-Tech. Phys.* **4**, 1037 (1960).
18J. D. A. LABOONTZOV, *Teploenergetika* no. 5, 76 (1960).

19J. D. A. LABOONTZOV, *Teploenergetika* no. 7, 72 (1957).
20J. V. LAVROVA, *Ref. Zh. Mekh.* no. 6, Rev. 6783 (1958).
21J. E. L. LUSTENADER, R. RICHTER and F. J. NEUGEBAUER, *Trans. ASME J. Heat Transfer*, C **81**, 297 (1959).
22J. G. R. MOORE, *J. Amer. Inst. Chem. Engrs*, **5**, 458 (1959).
23J. K. NISHIKAWA and K. YAMAGATA, *Int. J. Heat Mass Transfer*, **1**, Nos. 2/3, 219 (1960).
24J. L. ROBERTS, *N.A.S.A. Tech. Note* D-41 (1959).
25J. S. M. SCALA and G. L. VIDALE, *Int. J. Heat Mass Transfer*, **1**, No. 1, 4 (1960).
26J. D. E. SEVERSON, A. J. MADDEN and E. L. PIRET, *J. Amer. Inst. Chem. Engrs*, **5**, 413 (1959).
27J. E. SOKOLOVA, *Ref. Zh. Mekh.* no. 6, Rev. 6781 (1958).
28J. E. M. SPARROW and J. L. GREGG, *Trans. ASME J. Heat Transfer*, C **82**, 71 (1960).
29J. E. M. SPARROW and J. L. GREGG, *Trans. ASME J. Heat Transfer*, C **82**, Series C, 290 (1959).
30J. V. YA. STAPRENS, *Ref. Zh. Mekh.* no. 10, Rev. 11264 (1958).
31J. M. A. STYRIKOVICH and I. L. MOSTINSKII, *Soviet Phys.-Dokl.* **4**, 794 (1960).
32J. M. A. STYRIKOVICH, Z. L. MYROPOLSKY, M. E. SHITZMAN, I. L. MOSTINSKY, A. A. STAVROVSKY and L. E. FAKTOROVICH, *Teploenergetika* no. 5, 81 (1960).
33J. G. G. TRESCHOV, *Teploenergetika* no. 5, 44 (1957).
34J. A. S. VOS, *Ingenieur*, **71**, 0.17 (1959).
35J. V. V. VYSHENSKII, *Ref. Zh. Mekh.* no. 1, Rev. 533 (1959).
36J. B. A. ZENKEVICH, *Ref. Zh. Mekh.* no. 1, Rev. 548 (1959).
37J. M. V. ZOZULYA, *Ref. Zh. Mekh.* no. 6, Rev. 6439 (1959).
38J. V. I. ZUBKOV, *Soviet Phys.-Dokl.* **3**, 1121 (1959).

Radiation

1K. R. A. ANDERSON and W. A. BROOKS, JR., *J. Aero. Space Sci.* **27**, 41 (1960).
2K. J. G. BARTAS and W. H. SELLERS, *Trans. ASME J. Heat Transfer*, C **82**, 73 (1960).
3K. R. N. BAYLOR and F. D. SMITH, *Proc. Fourth Midwest. Conf. Solid Mechanics*, p. 298, Univ. of Texas Press (1959).
4K. J. R. BEATTIE, *Brit. J. Appl. Phys.* **2**, 151 (1960).
5K. J. T. BEVANS, *Trans. ASME J. Heat Transfer*, C **82**, 1 (1960).
6K. G. A. BIRD, *J. Aero. Space Sci.* **27**, 713 (1960).
7K. J. A. BRANDT, T. F. IRVINE, JR. and E. R. G. ECKERT, *Proc.* 1960 *Heat Transfer and Fluid Mechanics Inst.*, p. 220, Stanford Univ. Press (1960).
8K. J. H. CAIRNS, *J. Sci. Instrum.* **37**, 84 (1960).
9K. R. L. CHAMBERS and E. V. SOMERS, *Trans. ASME J. Heat Transfer*, C **81**, 327 (1959).
10K. P. L. CHAMBRE, *J. Appl. Phys.* **30**, 1683 (1959).
11K. A. CHARNES and S. RAYNOR, *J. Amer. Rocket Soc.* **30**, 479 (1960).
12K. J. H. CHIN and S. W. CHURCHILL, *Quart. Appl. Math.* **28**, 93 (1960).
13K. R. V. DUNKLE, *Trans. ASME J. Heat Transfer*, C **82**, 64 (1960).
14K. E. R. G. ECKERT, T. F. IRVINE, JR. and E. M. SPARROW, *J. Amer. Rocket Soc.* **30**, 644 (1960).
15K. R. and M. GOULARD, *Int. J. Heat Mass Transfer*, **1**, No. 1, 81 (1960).
16K. G. HASS, L. F. DRUMMETER and M. SCHACH, *J. Opt. Soc. Amer.* **49**, 918 (1959).
17K. F. B. HILL and R. H. WILHELM, *J. Amer. Inst. Chem. Engrs*, **5**, 486 (1959).
18K. J. T. HOWE, *N.A.S.A. Tech. Note* D-329 (1960).
19K. E. H. HUBBARD, *Combustion*, **31**, 34 (1959).
20K. D. T. KOKOREV, *Int. J. Heat Mass Transfer*, **1**, No. 1, 23 (1960).
21K. P. KOKOROPOULOS, E. SALAM and F. DANIELS, *Solar Energy Sci. Engng*, **111**, 19 (1959).
22K. B. K. LARKIN and S. W. CHURCHILL *J. Amer. Inst. Chem. Engrs*, **5** 467 (1959).
23K. S. LIEBLEIN, *N.A.S.A. Tech. Note* D-196 (1959).
24K. G. LUECK, *Chem.-Ing.-Tech.* **32**, 29 (1960).
25K. E. N. NILSON and R. CURRY, *J. Aero. Space Sci.* **27**, 146 (1960).
26K. A. K. OPPENHEIM and J. T. BEVANS, *Trans. ASME J. Heat Transfer*, C **82**, 360 (1960).
27K. J. C. RICHMOND, *J. Amer. Cer. Soc.* **42**, 633 (1959).
38K. W. H. ROBBINS, *N.A.S.A. Tech. Note* D-62 (1959).
29K. P. J. SCHNEIDER, *J. Aero. Space Sci.* **27**, 546 (1960).
30K. E. M. SPARROW, *Trans. ASME J. Heat Transfer*, C **82**, 375 (1960).
31K. E. M. SPARROW and L. U. ALBERS, *Trans. ASME J. Heat Transfer*, C **82**, 253 (1960).
32K. H. E. STUBBS, *Rev. Sci. Instrum.* **31**, 115 (1960).
33K. D. YA. SVET, *Soviet Phys.-Dokl.* **4**, 1375 (1960).
34K. C. M. USISKIN and R. SIEGEL, *Trans. ASME J. Heat Transfer*, C **82**, 369 (1960).
35K. C. M. USISKIN and E. M. SPARROW, *Int. J. Heat Mass Transfer*, **1**, No. 1, 28 (1960).
36K. C. L. WALKER, C. R. SMITH and D. C. GRITTON, *Proc.* 1960 *Heat Transfer and Fluid Mechanics Inst.*, p. 244, Stanford Univ. Press, Calif. (1960).
37K. R. C. WEATHERSTON and W. E. SMITH, *J. Amer. Rocket Soc.* **30**, 268 (1960).
38K. J. E. WILKINS, JR., *Proc.* 1960 *Heat Transfer and Fluid Mechanics Inst.*, p. 228, Stanford Univ. Press, Calif. (1960).

Liquid metals

1L. N. Z. AZER and B. T. CHAO, *Int. J. Heat Mass Transfer*, **1**, Nos. 2/3, 121 (1960).
2L. A. P. FRAAS, *Nucl. Sci. Engng*, **8**, 21 (1960).
3L. S. S. KUTATELADZE, V. M. BORISHANSKII and I. I. NOVIKOV, *J. Nucl. Energy*, **9**, 214 (1959).
4L. C. LIN, Y. YANG, *et al.*, *K'o Hsüeh T'ung Pao* (Chinese People's Republic) No. 24, 832 (1959).
5L. R. E. MACPHERSON, J. C. AMOS and H. W. SAVAGE, *Nucl. Sci. Engng*, **8**, 14 (1960).
6L. T. MIZUSHINA, S. IUCHI, T. SASANO and H.

Vol. 3 1961

TAMURA, *Int. J. Heat Mass Transfer*, **1**, Nos. 2/3, 139 (1960).
7L. V. PETROVICHEV, *Int. J. Heat Mass Transfer*, **1**, Nos. 2/3, 115 (1960).
8L. J. G. REITZ, *Aero. Space Engng*, **19**, 18 (1960).
9L. F. E. ROMIE, S. W. BROVARNEY and W. H. GIEDT, *Trans. ASME J. Heat Transfer*, C **82**, 387 (1960).
10L. R. VISKANTA and Y. S. TOULOUKIAN, *Trans. ASME J. Heat Transfer*, C **82**, 333 (1960).

Low-density heat transfer
1M. L. V. BALDWIN, V. A. SANDBORN and J. C. LAURENCE, *Trans. ASME J. Heat Transfer*, C **82**, 77 (1960).
2M. H. L. BOMELBURG, *Phys. of Fluids*, **2**, 717 (1959).
3M. E. P. GROSS and S. ZIERING, *Phys. of Fluids*, **2**, 701 (1959).
4M. H. HOSHIZAKI, *J. Aero. Space Sci.* **27**, 135 (1960).
5M. H. C. LEVEY, *J. Fluid Mech.* **6**, 385 (1959).
6M. R. F. PROBSTEIN and N. H. KEMP, *J. Aero. Space Sci.* **27**, 174 (1960).
7M. S. A. SCHAAF, *J. Amer. Rocket Soc.* **30**, 443 (1960).
8M. O. K. TEWFIK and W. H. GIEDT, *J. Aero. Space Sci.* **27**, 721 (1960).
9M. R. N. WELTMANN and P. W. KUHNS, *N.A.S.A. Tech. Note* D-267 (1960).

Measurement techniques
1N. J. V. BECK and H. HURWICZ, *Trans. ASME J. Heat Transfer*, C **82**, 27 (1960).
2N. D. BUESSING, *Glastech. Ber.* **33**, 124 (1960).
3N. J. D. CLEM, JR., *Rev. Sci. Instrum.* **31**, 334 (1960).
4N. D. A. DAVIS, *J. Sci. Instrum.* **37**, 15 (1960).
5N. I. G. DONALDSON, *Brit. J. Appl. Phys.* **10**, 252 (1959).
6N. H. J. ERKELENS, *Inst. Heat. Vent. Engrs*, **27**, 281 (1960).
7N. H. J. FINK, *Canad. J. Phys.* **37**, 1397 (1959).
8N. A. GREEN and L. E. S. COWLES, *J. Sci. Instrum.* **37**, 349 (1960).
9N. N. E. HAGER, JR., *Rev. Sci. Instrum.* **31**, 177 (1960).
10N. Y. KOBASHI, N. KONO and T. NISHI, *J. Aero. Space Sci.* **27**, 149 (1960).
11N. R. C. KURTZROCK, *Rev. Sci. Instrum.* **31**, 457 (1960).
12N. S. C. LING, *Trans. ASME J. Basic Engng*, D **82**, 629 (1960).
13N. S. A. LOSEV and N. A. GENERALOV, *Instrum. Exper. Techniques*, **3**, 454 (1959).
14N. J. H. MCFEE, P. M. MARCUS and I. ESTERMANN, *Rev. Sci. Instrum.* **31**, 1013 (1960).
15N. E. I. NEVSTRUEVA, *Soviet Phys.-Dokl.* **5**, 58 (1960).
16N. L. ONGKIEHONG and J. VAN DUNN, *J. Sci. Instrum.* **37**, 221 (1960).
17N. N. S. RASOR and J. D. MCCLELLAND, *Rev. Sci. Instrum.* **31**, 595 (1960).
18N. W. W. SHORT and B. H. SAGE, *J. Amer. Inst. Chem. Engrs*, **6**, 163 (1960).
19N. J. R. SINGER, *Electronics*, **33**, 77 (1960).
20N. J. W. STUART, JR., *J. Aero. Space Sci.* **27**, 136 (1960).
21N. W. F. VAN TASSELL and E. E. COVERT, *J. Aero. Space Sci.* **27**, 147 (1960).
22N. C. E. WHITE, *Instrum. Control Systems*, **33**, 782 (1960).
23N. R. WOOD, *J. Aero. Space Sci.* **27**, 556 (1960).

Heat exchangers
1P. V. S. ARPACI and J. A. CLARK, *Trans. ASME J. Heat Transfer*, C **81**, 253 (1959).
2P. L. K. DORAISWAMY and N. B. PATEL, *J. Sci. Industr. Res.* A **18**, 522 (1959).
3P. A. P. FRAAS, *Nucl. Sci. Engng*, **8**, 21 (1960).
4P. K. A. GARDNER, *J. Appl. Mech.* **27**; *Trans. ASME* E **82**, 25 (1960).
5P. W. M. KAYS, *Trans. ASME J. Engng for Power*, A **82**, 27 (1960).
6P. R. B. LANCASHIRE, E. A. LEZBERG and J. F. MORRIS, *N.A.S.A. Tech. Note* D-265 (1960).
7P. E. L. LUSTENADER, *Trans. ASME J. Heat Transfer*, C **81**, 297 (1959).
8P. A. MCKILLOP and W. L. DUNKLEY, *Industr. Engng Chem.* **52**, 740 (1960).
9P. J. W. TATOM, *J. Amer. Rocket Soc.* **30**, 116 (1960).
10P. M. M. YAROSH, *Nucl. Sci. Engng*, **8**, 32 (1960).

Aircraft, missiles and satellites
1Q. D. R. CHAPMAN, *N.A.S.A. Tech. Rep.* R-11 (1959).
2Q. R. H. EDWARDS and G. S. CAMPBELL, *J. Amer. Rocket Soc.* **30**, 496 (1960).
3Q. A. J. EGGERS, T. J. WONG and R. E. SLYE, *Trans. ASME J. Heat Transfer*, C **81**, 308 (1959).
4Q. C. GAZLEY, JR., *Aero. Space Engng*, **19**, 22 (1960).
5Q. C. GAZLEY, JR., *Trans. ASME J. Heat Transfer*, C **81**, 315 (1959).
6Q. G. HELLER, *J. Amer. Rocket Soc.* **30**, 344 1960).
7Q. R. HERMANN, *Proc. Ninth International Astronautical Congr., Amsterdam*, p. 764, Springer-Verlag, Wien (1959).
8Q. L. LEES, F. W. HARTWIG and C. B. COHEN, *J. Amer. Rocket Soc.* **29**, 633 (1959).
9Q. H. MYERS, *Aero. Space Engng*, **19**, 34 (1960).
10Q. B. L. SWENSON, *N.A.S.A. Tech. Note* D-90 (1960).

Thermodynamic and transport properties
1R. A. W. BLACKMAN, *J. Amer. Rocket Soc.* **30**, 557 (1960).
2R. N. B. COHEN, *N.A.S.A. Tech. Note* D-194 (1960).
3R. K. P. COFFIN, *J. Chem. Phys.* **31**, 1290 (1959).
4R. K. P. COFFIN and C. O'NEAL, JR., *N.A.S.A. Tech. Note* 4209 (1958).
5R. E. R. G. ECKERT, W. E. IBELE and T. F. IRVINE, JR., *N.A.S.A. Tech. Note* D-533 (1960).
6R. C. F. HANSEN, *N.A.S.A. Tech. Rep.* R-50 (1959).
7R. R. A. HORD, *N.A.S.A. Tech. Note* D-2 (1959).
8R. W. E. IBELE and T. F. IRVINE, JR., *Trans. ASME J. Heat Transfer*, C **82**, 381 (1960).
9R. E. F. JOHNSON, *Industr. Engng Chem.* **52**, 447 (1960).
10R. J. KESTIN and W. LEIDENFROST, *Physica* **25**, 1033 (1959).
11R. J. KESTIN, W. LEIDENFROST and C. Y. LIU, *Z. Angew. Math. Phys.* **10**, 558 (1959).

12R. C. R. KING, *N.A.S.A. Tech. Note* D-275 (1960).
13R. V. A. KIRILLIN and A. YE. SHEYNDLIN, *Akad. Nauk SSR. Otdel. Tekh. Nauk. Izv.: Energet. Avtoma.*, No. 2, 44 (1960).
14R. D. B. MANN and R. B. STEWART, *Trans. ASME J. Heat Transfer*, C **81**, 323 (1959).
15R. E. A. MASON, J. T. VANDERSLICE and J. M. YOS, *Phys. of Fluids*, **2**, 688 (1959).
16R. L. MONCHICK, *Phys. of Fluids*, **2**, 695 (1959).
17R. L. MOWER, *Phys. Rev.* **116**, 16 (1959).
18R. R. E. PATTLE, *Quart. J. Mech. Appl. Math.* **12**, 407 (1959).
19R. S. M. SCALA and C. W. BAULKNIGHT, *J. Amer. Rocket Soc.* **30**, 329 (1960).
20R. E. V. STUPOCHENKO, I. P. STAKHANOV, E. V. SAMUILOV, A. S. PLESHANOV and I. B. ROZHDESTVENSKII, *J. Amer. Rocket Soc.* **30**, 98 (1960).
21R. R. G. VINES, *Trans. ASME J. Heat Transfer*, C **82**, 48 (1960).
22R. L. S. ZAITSEVA, *Soviet Phys.-Tech. Phys.* **4**, 444 (1959).
23R. H. ZIEBLAND and J. T. A. BURTON, *Brit. J. Appl. Phys.* **9**, 52 (1958).
24R. H. ZIEBLAND and J. T. A. BURTON, *Int. J. Heat Mass Transfer*, **1**, Nos. 2/3, 242 (1960).

Vol. 3 1961

Int. J. Heat Mass Transfer. Vol. 3, pp. 249–251. Pergamon Press 1961. Printed in Great Britain.

SHORTER COMMUNICATION

EXPERIMENTAL STUDY OF EFFECT OF GAS INJECTION ON RATE OF MASS TRANSFER FROM SOLID TO LIQUID

LIANG-TSENG FAN

Department of Chemical Engineering, Kansas State University, Manhattan, Kansas

(*Received* 16 *May* 1960 *and in revised form* 15 *May* 1961)

LIST OF SYMBOLS

D_p, diameter of pellet, ft;
G_v, volumetric flow rate of gas, ft³/h ft²;
J_d, mass transfer factor based on liquid flow in two phase flow, dimensionless;
J_{d0}, mass transfer factor in single phase flow, dimensionless;
k_1, mass transfer coefficients based on water flow in two phase flow, lb/ft² h;
k_{10}, mass transfer coefficients of single phase flow, lb/ft² h;
L_m, mass velocity of water, lb/h ft²;
L_v, volumetric flow rate of water, ft³/h ft²;
N_{Sh}, Sherwood number, dimensionless;
R, G_v/L_v, dimensionless;
T, temperature, °F;
ϵ, void fraction, dimensionless;
μ, viscosity of liquid.

INTRODUCTION

It is known that the mechanical agitation of the fluid increases the rates of transfer process from a solid to the fluid [1]. When the fluid is a liquid, injection of a gas produces agitation of the liquid. The injection of a gas into the flowing liquid also reduces the space available for the flow of the liquid past the solid surface, thus increasing the linear velocity of the liquid. This intensifies the turbulence and reduces the thickness of the laminar boundary layers around the solid. This should promote the rate of mass transfer. The agitating action of the gas also increases the back-mixing of the fluid in the axial direction of fluid flow. Also the effective transfer area between solid and liquid may be reduced by the presence of the gas. The last two effects should retard the mass transfer.

It can be expected that the first two effects, i.e. the breaking up of the boundary layer and the increased linear velocity of liquid, will predominate when the quantity of injected gas is relatively small; and the last two effects, i.e. increased back-mixing of the liquid and the reduction of the effective transfer area, will be increased as the rate of gas injection is increased. This can be observed in a number of published papers [2, 3] on the effect of gases on the rate of heat transfer between the wall of circular pipes and liquid. Few published data, however, are available concerning the effect of gas injection on mass transfer.

EXPERIMENTAL PROCEDURE

The liquid and gas used in this work were water and nitrogen respectively. The solid used was cylindrical pellets of benzoic acid, with 0·224 in diameter and height.

The test section consisted of a 2 in i.d. by 6 in high cylindrical glass column which was placed above a 14-in section of 2 in i.d. pipe which served as a mixing and calming section. First, 2½ in of inert clay pellets were packed in the column. The clay pellets were of approximately the same size and shape as the acid pellets. The acid pellets were packed into a bed above the inert clay packing. The pellets were then confined by a coarse screen and spring mechanism to reduce the movement of pellets.

Each series of experimental runs consisted of one run without gas injection and several runs with various rates of gas injection. The concentration of benzoic acid in samples obtained from each series of runs was determined by titration.

The degree of randomness of the beds was checked by comparison of single phase (water) flow data with a generalized correlation of solid–fluid mass transfer [4], which was obtained for randomly packed beds.

DISCUSSION AND CONCLUSION

The increase of the mass transfer coefficients due to the injection of inert gas is represented in Fig. 1 as ratios of mass transfer coefficients with gas injection to those under single phase flow.

Figure 1 indicates that the mass transfer rate is accelerated appreciably by injection of relatively small quantities of gas to the flowing liquid. Unlike most of the heat transfer data published, the curves in Fig. 1 do not tend to decline after reaching a maximum point in spite of the fact that the gas injection rate was increased almost five fold in comparison to that used in heat transfer work [2]. This may be explained as follows:

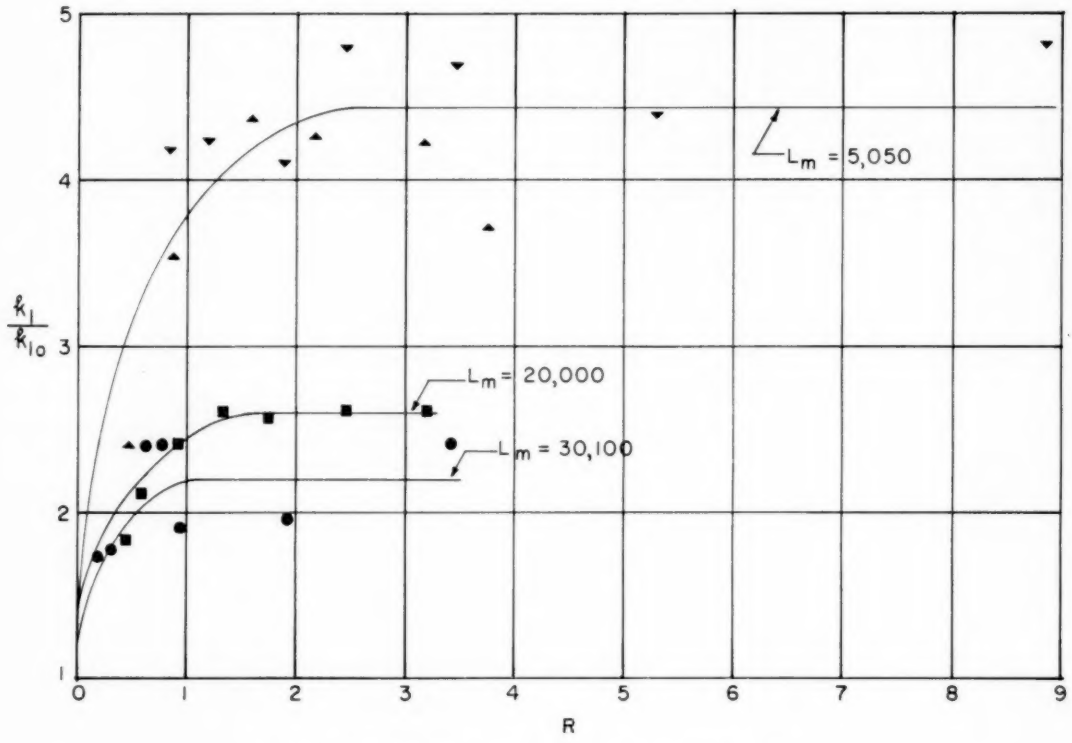

FIG. 1. Effect of inert gas injection on rate of mass transfer.

While the data presented here were obtained in a column packed with particles of benzoic acid, the heat transfer data [2] were obtained in an unpacked plain circular tube. The contact area between the solid and liquid is usually much larger in a packed column than in an unpacked column. A 2 in diameter by 3 in height glass tube packed with 627 benzoic acid particles with a total surface area of 1·06 ft² was used in these experiments. The ratio of the surface area of benzoic acid particles to that of the tube inside was roughly eight. Therefore, it might be expected that more than an eight fold increase in the gas quantity over that used in the heat transfer work [2] would be needed to produce decreased mass transfer rates due to the cover-up of transfer area by the gas.

In a manner similar to the results of heat transfer studies, the effect of gas injection in increasing the mass transfer rate becomes smaller as the liquid flow rate increases. Simple reasoning leads to the conclusion that as the liquid flow rate approaches infinity the injection of finite quantity of inert gas will not produce any effect.

In the range of this work, the following empirical equation approximates the $(k_1/k_{10})_{max}$ or, in term of mass transfer factor, $(J_d/J_{d0})_{max}$.

$$\left(\frac{J_d}{J_{d0}}\right)_{max} = 5{\cdot}0 \exp\left[-1{\cdot}76 \times 10^{-3} \frac{D_p L_m}{\mu(1-\epsilon)}\right]. \quad (1)$$

Since, in general [4]:

$$J_{d0} = 1{\cdot}77 \left[\frac{D_p L_m}{\mu(1-\epsilon)}\right]^{-0{\cdot}44} \quad (2)$$

$$(J_d)_{max} = 8{\cdot}85 \left[\frac{D_p L_m}{\mu(1-\epsilon)}\right]^{-0{\cdot}44} \times \exp\left[-1{\cdot}76 \times 10^{-3} \frac{D_p L_m}{\mu(1-\epsilon)}\right]. \quad (3)$$

From the results of this experimental investigation, the following conclusions could reasonably be drawn:

(1) Injection of gas is a very effective means of accelerating the mass transfer rate from solid to liquid.
(2) When the injection rate of the gas is relatively small, the effect of intensified turbulence due to increased linear velocity of the liquid and mechanical agitation of gas bubbles predominates.

Vol. 3 1961

(3) When the gas velocity is increased further, the effect is partially nullified by the reduction of effective transfer area and by the increased back-mixing of liquid in the direction of flow.
(4) The magnitude of the increase of solid–liquid mass transfer rates due to the injection of gas is comparable to that effected by mechanical pulsation of the liquid [5]. It appears, however, that a much less complicated mechanism is required to inject the gas into the liquid than to induce the pulsation of the flowing liquid [5].

REFERENCES

1. A. I. Johnson and C. J. Huang, Mass transfer in an agitated vessel. *J. Amer. Inst. Chem. Engrs*, **2**, 412 (1956).
2. T. Katzuhara and T. Kazama, Heat transfer in two-phase flow of mixture of air and water. *Trans. Japan Soc. Mech. Engrs*, **24**, 228 (1958).
3. R. F. Knott, R. N. Anderson, A. Acrivos and E. E. Petersen, An experimental study of heat transfer to nitrogen-oil mixtures. *Industr. Engng Chem.* **51**, 1369 (1959).
4. J. C. Chu, J. Kalil and W. A. Wetteroth, Mass transfer in a fluidized bed. *Chem. Engng Progr.* **49**, 141 (1953).
5. T. Shirotsuka and N. Honda, Mass transfer through an inside wall to a pulsation flow. *Chem. Engng, Japan*, **21**, 287 (1957).

Int. J. Heat Mass Transfer. Vol. 3, pp. 252–253. Pergamon Press 1961. Printed in Great Britain.

SHORTER COMMUNICATION

DIMENSIONAL ANALYSIS OF BURNOUT HEAT TRANSFER

S. L. BRAGG and I. E. SMITH

Rolls-Royce Ltd., Derby, England

(*Received* 16 *June* 1961)

IN HIS book on *Heat Transfer in Condensation and Boiling*, Kutateladze [1] states that experimental results on burn-out heat transfer rates can be correlated by the expression

$$\dot{q}_c = (0{\cdot}16 \pm 0{\cdot}03)\, L \,.\, \rho_v^{1/2} \,.\, g^{1/2} \{S \,.\, (\rho_l - \rho_v)\}^{1/4} \quad (1)$$

where

$\dot{q}_c$, is the burn-out heat transfer rate, cal/cm² s;
L, is the latent heat of the liquid, cal/g, which is assumed to be at its saturation temperature;
ρ_l, ρ_v, are the densities of liquid and vapour, g/cm³;
S, is the surface tension of the liquid, dyn/cm.

It is not clear from the text whether the symbol g represents g_φ, the local gravitational acceleration (cm/s²), or whether it stands for g_0, the conversion constant from force to mass units (= 981 g cm/s² g force = 1 g cm/s² dyn) which appears in equations of motion. Although irrelevant to most terrestrial experiments this distinction could be important under space flight or orbital conditions. A dimensional check shows that the correct form of the equation, taking this distinction into account, is

$$\dot{q}_c = (0{\cdot}16 \pm 0{\cdot}03)\, L \,.\, \rho_v^{1/2} \,.\, \{g_\varphi \,.\, g_0 \,.\, S \,.\, (\rho_l - \rho_v)\}^{1/4}. \quad (1a)$$

This formula was brought to our attention by a private communication from Professor D. B. Spalding, who grouped the variables into two dimensionless parameters by introducing the mean bubble size as a reference length. The following note is an attempt to give the simplest possible physical explanation of the form of the equation and the size of the experimental constant. A rather more detailed explanation, in terms of the frequency of bubble shedding and the instability of two-phase flow has been given by Zuber [2].

Consider the stability of a growing bubble on a flat horizontal heating surface. Suppose that at any moment the volume of the bubble is V (cm³) and the radius of the circle of contact r, the angle of contact with the surface being θ. Then the net buoyancy force upwards on the bubble is $V \,.\, (\rho_l - \rho_v) \,.\, g_\varphi/g_0$ and the resolved part of the surface tension force downwards is $2\pi r \,.\, S \,.\, \sin\theta$: since the movement of the centre of gravity of the bubble is negligible as long as it remains attached to the surface, these forces must be in static equilibrium.

As the liquid is heated and the bubble of vapour grows, the buoyancy force, which varies as the volume, must increase faster than the surface tension force, $2\pi r \,.\, S$, so that, to preserve static equilibrium, $\sin\theta$ must increase. The limit is reached when $\sin\theta = 1$. If it is assumed that the bubble is then hemispherical the equation of static equilibrium yields

$$2\pi r \,.\, S = \tfrac{2}{3}\pi r^3 \,.\, (\rho_l - \rho_v) \,.\, g_\varphi/g_0. \quad (2)$$

Any further increase in size makes the system unstable and the bubble is accelerated away from the surface.

Thus the critical size of bubble, r_c (cm), is obtained from equation (2) as

$$r_c^2 = 3S \,.\, g_0/(\rho_l - \rho_v) \,.\, g_\varphi. \quad (3)$$

Burn-out occurs when the whole surface is covered with vapour—that is when the bubbles crowd on each other so fast that there is no room for fresh liquid to reach the surface and keep it cool. Thus to avoid burn-out one bubble must be able to accelerate away from the surface faster than a new one grows into the space it vacates. In the limiting case we may suppose that the bubbles just touch at the moment of release of the second one.

Let us assume that the bubble maintains its hemispherical shape (any other assumption would only introduce a small numerical correction factor) and that the drag is negligible at the small dispatch velocities involved. Then in the time t (s) taken for one bubble to form, the centre of gravity of the preceding bubble must have moved upwards a distance r_c.

Thus

$$r_c = \tfrac{1}{2} a \,.\, t^2 \quad (4)$$

where a (cm/s²) is the acceleration of the centre of gravity of the bubble.

Once the bubble is launched, buoyancy is the sole force acting on it, so its equation of motion is

$$\tfrac{2}{3}\pi r^3 \,.\, (\rho_l - \rho_v) \,.\, g_\varphi = \tfrac{2}{3}\pi r^3 \,.\, \rho_v \,.\, a.$$

That is,

$$a = g_\varphi \,.\, (\rho_l - \rho_v)/\rho_v. \quad (5)$$

If L (cal/g) is the latent heat of the liquid and $\dot{q}_c$ (cal/cm² s) the mean rate of heat transfer at burn-out, the

Vol. 3 1961

time taken to produce a bubble of mass $\frac{2}{3}\pi r_c^3 . \rho_v$ is given by the equation

$$t = \tfrac{2}{3}\pi r_c^3 . \rho_v . L/\dot{q}_c . \pi r_c^2$$

$$= \tfrac{2}{3} r_c . \rho_v . L/\dot{q}_c. \qquad (6)$$

Substituting into equation (4) from equations (5) and (6)

$$r_c = \tfrac{1}{2} g_g . \frac{(\rho_l - \rho_v)}{\rho_v} . \left(\frac{2r_c . \rho_v . L}{3\dot{q}_c}\right)^2$$

therefore

$$\dot{q}_c^2 = \tfrac{2}{9} g_g . (\rho_l - \rho_v) . \rho_v . L^2 . r_c.$$

Substituting for r_c from equation (3)

$$\dot{q}_c^2 = \tfrac{2}{9} g_g . (\rho_l - \rho_v) . \rho_v . L^2 \sqrt{[3S . g_0/(\rho_l - \rho_v) . g_g]}$$

therefore

$$\dot{q}_c = 0{\cdot}62\, L . \rho_v^{1/2} \{g_g . g_0 . S . (\rho_l - \rho_v)\}^{1/4}. \qquad (7)$$

Comparing equations (7) and (1a) it is evident that their form is identical, but the constant in equation (7) is about three or four times as large as that determined experimentally. There are several possible reasons for this.

(1) The minimum clearance between successive bubbles must be greater than the limit assumed, in order to allow for deformation of the bubbles, access of fresh liquid, etc.

(2) The bubbles cover an area less than the total superficial heating area, so their rate of growth for a given mean $\dot{q}_c$ is greater than would be calculated if $\dot{q}_c$ were uniform. Even if the bubbles were regularly spaced on hexagonal centres this would reduce $\dot{q}_c$ by a factor of three-quarters.

(3) In many burn-out tests the heating surface is not horizontal, so the acceleration rate normal to the surface will be less than the vertical buoyant accleration.

A further check on the applicability of equation (3) is obtained by substituting typical values for the physical variables to obtain r_c.

For water at 100°C, on the earth's surface,

$S = 58{\cdot}8$ dyn/cm,
$g_0 = 1$ g cm/s^2 . dyn,
$g_g = 981$ cm/s^2,
$\rho_l = 0{\cdot}958$ g/cm^3,
$\rho_v = 0{\cdot}0006$ g/cm^3,

therefore

$$r_c = \sqrt{(3 \times 58{\cdot}8/0{\cdot}957 \times 981)} = 0{\cdot}43 \text{ cm}.$$

Although this figure would seem to be a little on the high side it is certainly within an order of magnitude of that observed in practice.

Summarizing, then, we would suggest that a possible physical explanation of the observed empirical law is that bubbles break away from the surface as soon as the buoyancy forces are greater than the surface tension forces holding them on; and that burn-out occurs when the buoyant acceleration of the bubbles away from the surface is no longer great enough to keep the bubbles clear of their successors.

REFERENCES

1. S. S. KUTATELADZE, *Heat Transfer in Condensation and Boiling*, 2nd Ed. State Scientific & Technical Publishers of Literature on Machinery, Moscow and Leningrad (1952). Trans. S. J. RIMSHAW as AEC-tr-3770 (United States).
2. N. ZUBER, On the stability of boiling heat transfer, *Trans. Amer. Soc. Mech. Engrs*, **80**, 711 (1958).

Papers accepted for publication in future issues

B. GEBHART: Surface temperature calculations in radiant surroundings of arbitrary complexity—for gray, diffuse radiation

E. Y. NEKHENDZI: Method of a regular regime for the determination of variable thermal coefficients

H. L. EVANS: Mass transfer through laminar boundary layers—6. Methods of evaluating the wall gradient (b'_0/B) for similar solutions; some new values for zero main-stream pressure gradient

H. L. EVANS: Mass transfer through laminar boundary layers—7. Further similar solutions to the b-equation for the case $B = 0$

A. A. ZHUKAUSKAS and A. B. AMBRAZYAVICHYUS: Heat transfer of a plate in a flow of a liquid

BERNARD LE FUR: Convection de la chaleur dans un gaz en régime laminaire dans le cas d'un gradient de pression et d'une temperature de paroi quelconques

E. M. SPARROW and R. D. CESS: The effect of a magnetic field on free convection heat transfer

R. A. SEBAN and L. H. BACK: Velocity and temperature profiles in a wall jet

T. L. PERELMAN: On conjugated problems of heat transfer

B. V. KANTOROVICH and G. N. DELYAGIN: Heat and mass transfer in the process of fuel combustion in an air stream

Minsk Conference Issue

A. V. LUIKOV: The first all-union conference on heat and mass transfer

J. P. HARTNETT and C. GAZLEY: A generalized presentation of mass transfer cooling for laminar flow over a flat plate

V. I. SUBBOTIN, M. K. IBRAGIMOV, M. N. IVANOSKY, M. N. ARNOL'DOV and E. V. NOMOFILOV: Turbulent heat transfer in a flow of liquid metals

S. R. DE GROOT: On the thermodynamics of irreversible heat and mass transfer

S. S. KUTATELADZE: Heat transfer with boiling

D. B. SPALDING: Heat and mass transfer between the gaseous and liquid phases of a binary mixture

P. V. TSOI: Analytical solutions of a set of equations of heat and mass transfer for a semi-restricted medium at different boundary conditions

L. A. VULIS, T. P. LEONT'EVA, Z. B. SAKIPOW and B. P. USTOMENKO: Transfer processes in a free (jet) turbulent boundary layer

A. J. EDE: The heat transfer coefficient for flow in a pipe

I. P. GINZBURG: On possible methods of solving boundary layer problems in the presence of dissociation and diffusion

Vol. 3 1961

Int. J. Heat Mass Transfer. Vol. 3, pp. 255–265. Pergamon Press 1961. Printed in Great Britain.

VELOCITY AND TEMPERATURE PROFILES IN A WALL JET

R. A. SEBAN* and L. H. BACK†

(*Received* 8 *February* 1961, *in revised form* 24 *May* 1961)

Abstract—Conditions approximating those of the wall jet have been obtained by operating a system, involving tangential air injection into a turbulent boundary layer, with very low values of the free stream velocity. Under such conditions the flow is essentially produced by the injected air and measurement of the velocity profiles shows correspondence to the theory for the turbulent wall jet. With some alternation of the eddy diffusivity of that theory the measured temperature profiles can also be predicted and these, together with the velocity profiles, are shown to agree generally with the measured values of the adiabatic wall temperature. The measured heat transfer coefficients are related to the hydrodynamic characteristics by a formulation of the Colburn type.

Résumé—Des conditions se rapprochant de celles du jet à la paroi ont été réalisées avec un dispositif compartant une injection tangentielle d'air dans une couche limite turbulente, les vitesses de l'écoulement libre étant très basses. Dans de telles conditions, l'écoulement est essentiellement produit par l'air injecté et la mesure des profils de vitesses est en accord avec la théorie du jet turbulent à la paroi. Les profils de température mesurés se retrouvent également par cette théorie si l'on fait quelques corrections sur la diffusivité turbulente; ces profils de vitesse et de température sont généralement en bon accord avec la température de paroi adiabatique mesurée. Les mesures des coefficients de transmission de chaleur sont reliées aux caractéristiques hydrodynamiques par une formule du type Colburn.

Zusammenfassung—Durch tangentiales Einblasen von Luft sehr kleiner Freistromgeschwindigkeit in die turbulente Grenzschicht wurden angenähert die bei einem Schlitz auftretenden Verhältnisse erreicht. Die Strömung wird dabei im wesentlichen von der eingeblasenen Luft hervorgerufen und Messungen des Geschwindigkeitsprofils zeigen Übereinstimmung mit der Theorie für turbulente Schlitzströmungen. Nach Änderung der turbulenten Austauschgrösse der Theorie können auch die gemessenen Temperaturprofile vorherbestimmt werden und stimmen, zusammen mit den Geschwindigkeitsprofilen, im Allgemeinen mit den ermittelten Werten der adiabaten Wandtemperatur überein. Die gemessenen Wärmeübergangskoeffizienten sind nach einer Formulierung von Colburn auf die kennzeichnenden hydrodynamischen Grössen bezogen.

Аннотация—С помощью системы, обеспечивающей вдув воздуха по касательной в турбулентный пограничный слой, получены условия, аппроксимирующие условия для струи вблизи стенки (при очень малых значениях скорости невозмущённого потока). При таких условиях поток, по существу, создаётся здуваемым воздухом, а измеренные профили скорости свидетельствуют о соответствии их с теорией турбулентной струи вблизи стенки. Если несколько изменить принятый в этой теории коэффициент диффузии вихря, то измеренные температурные профили могут также быть заданы. Показано, что вместе с профилями скорости они, в общем, согласуются с измеренными величинами температуры адиабатической стенки. Коэффициенты переноса тепла связаны с гидродинамическими характеристиками при помощи аналогии Колбэрна.

NOMENCLATURE

a, b, defined in equations (1) or (2);
c_p, specific heat at constant pressure;
h, local heat transfer coefficient;
s, injection slot height;
t, temperature above free stream, °F; t_s injection air, t_1 free stream, t_a adiabatic wall temperature;
T, absolute temperature, °R;
u, velocity; u_s injection air, u_1 free stream, u_m maximum velocity, U reference velocity;

* Professor of Mechanical Engineering, University of California, Berkeley, California.

† Research Assistant, Institute of Engineering Research, University of California, Berkeley, California.

v, velocity;
x, distance downstream from slot;
x_0, positive distance between the slot and the effective origin of the jet;
y, distance from wall.

Greek symbols

$\xi = x + x_0$, distance downstream from the effective origin of the jet;
δ, distance from wall to the point in the outer region at which $u = u_m/2$;
δ_m, distance from wall to velocity maximum;
$\delta_t = \delta - \delta_m$, distance from velocity maximum to the point where $u = u_m/2$;
$\zeta = y/\delta$, dimensionless distance from wall;
η, similarity variable defined in equation (4);
α, velocity profile parameter;
ν, kinematic viscosity;
ϵ, diffusivity;
τ_0, shearing stress at wall;
σ, Prandtl number;
ρ, density.

Subscripts

s, injection air;
1, free stream;
a, adiabatic wall.

INTRODUCTION

RESULTS have been presented [1] in a previous report for the heat transfer coefficient and for the effectiveness that were obtained from a system involving the tangential injection of air into the turbulent boundary layer produced by an air stream flowing over a plate. This apparatus, which was essentially a model of a film cooling system, was operated with both high and low ratios of the injection velocity to the free stream velocity, and for the high ratios the results for the effectiveness and for the heat transfer coefficient were found to correspond to the earlier results of Jakob [2] that were obtained on a similar system in which the free stream velocity was zero. Without free stream velocity, the flow situation is that of the wall jet and that is the focus of the present consideration even though the free stream velocity could not be eliminated completely in the system from which the present results were obtained. It was the availability of this system for the provision of some detailed hydrodynamic and thermal characteristics that produced the present results, which demonstrate that the major characteristics of the flow agree with the theory of the wall jet as given by Glauert [3] and that the effectiveness and the heat transfer coefficients that have already been correlated empirically do agree with the consequences of that theory.

The system shown in Fig. 1, from which were obtained the present results, consisted of a test surface, 12 in wide and 18 in long, which was one side of the 4 in $\times$ 12 in rectangular test section of a small, once through, wind tunnel. The injection slot, variable in height, spanned the 12 in width of the test surface and was located at its upstream edge, just downstream of the tunnel nozzle. There existed provisions for heating the injection air, heating the plate, and for the determination of the necessary temperatures

Vol. 3 1961

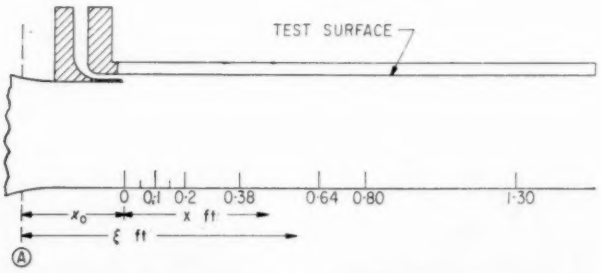

FIG. 1. Slot and test section. Point "A" is the effective origin of the jet.

and pressures. The low free stream velocities that existed for the operation that is considered here were obtained with the tunnel blower inoperative and the main stream flow was also restricted to the point of incipient back flow in the test section.

THE WALL JET

Glauert [3] achieved an analytical specification of the wall jet for both laminar and turbulent flow, for the latter on the basis of a near similarity in which the velocity profiles are relatively invariable for given orders of the Reynolds number. The essential nature of these profiles is characterized by a parameter α, indicative of the proportional extent of the inner flow, between the wall and the velocity maximum, to that of the outer flow between the velocity maximum and the stationary fluid far from the wall. Fig. 2 shows the nature of the velocity profile of the flow, which begins at a source and proceeds downstream, with the maximum velocity diminishing according to a power law, $u_m \sim \xi^a$. The width of the layer, too, follows a power law, $\delta \sim \xi^b$ and the exponents a and b are related to the parameter α in two possible and similar ways,

$$\left.\begin{aligned} a &= \frac{-4\alpha}{5+4\alpha} \\ b &= \frac{4+4\alpha}{5+4\alpha} \end{aligned}\right\} \qquad (1)$$

or

$$\left.\begin{aligned} a &= -\frac{\alpha}{1+\alpha} \\ b &= 1 \end{aligned}\right\}. \qquad (2)$$

The analysis gives the local velocity in terms of a reference velocity U, not easily defined, and an additional parameter λ which depends on α.

$$u = U\left[\frac{4-4b}{\lambda}\left(\frac{U\xi}{\nu}\right)^{4-5b}\frac{df}{d\eta}\right]. \qquad (3)$$

The function f, associated with the stream function, is of course the essential result of the similarity solution. The similarity variable, η, is

$$\eta = \frac{4-4b}{\lambda}\,\frac{yU}{\nu}\left(\frac{U\xi}{\nu}\right)^{-b}. \qquad (4)$$

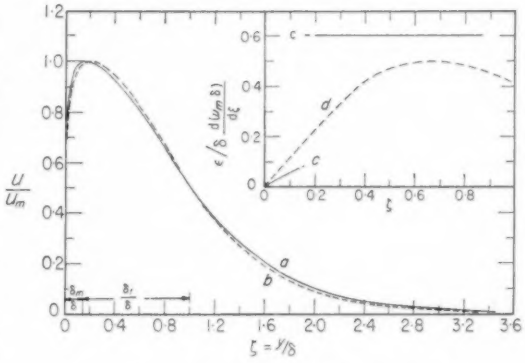

FIG. 2. Velocity profiles from Glauert's theory.

Curve a is the profile for $\alpha = 1{\cdot}2$, curve b for $\alpha = 1{\cdot}3$. The inset shows the distribution of the diffusivity and curve c is that corresponding to the velocity distribution for $\alpha = 1{\cdot}2$. Curve d is a deduction based on the measured temperature profiles.

Fig. 2 shows $df/d\eta$ as a function of η, through co-ordinates which are actually

$$\frac{df}{d\eta}\Big/\left(\frac{df}{d\eta}\right)_m$$

as a function of η/η_δ, with δ being the distance from the wall to that point in the outer region at which the velocity is half of the maximum value; this is the distance most precisely determined by the experimental results. The figure defines also two other distances that are significant, that from the wall to the velocity maximum, δ_m, and δ_l from the velocity maximum to the point where $u = u_m/2$. The flatness of the experimental profile near the velocity maximum makes the latter distances hard to define experimentally, as revealed by the typical theoretical profiles of Fig. 2.

Primarily because of later concern with the temperature profiles it is important to specify the eddy diffusivity from which were predicted the velocity profiles. Since similarity is unattainable if molecular transport is included precisely, the diffusivity ϵ is presumed to include the molecular effects to the extent they are compatible with similarity. A convenient form for illustration gives the diffusivity in the form produced by integration of the momentum equation

$$\frac{\epsilon\xi}{u_m\delta^2(a+b)} = \frac{\epsilon}{\delta[\mathrm{d}(u_m\delta)/\mathrm{d}\xi]}$$

$$= \left[-\left(\frac{2a+b}{a+b}\right)\int_\xi^\infty F'^2\,\mathrm{d}\xi - FF'\right]\frac{1}{F'} \qquad (5)$$

where $F' = u/u_m$ and $\zeta = y/\delta$.

The values of the diffusivity contained on Fig. 2 were evaluated from equation (5) in the outer region but near the wall accuracy required the use of the alternative specification of Ref. 3. The constant value in the outer region can also be specified as 0·85 $(u_m\delta/\epsilon) = 1/\kappa$, so that $\kappa = 0{\cdot}72\,(a+b)\delta/\xi$ and the constant value of κ implied for the outer region is realized if $b = 1$.

VELOCITY PROFILES

Figure 3 shows the experimental velocity profiles obtained downstream of a slot 0·250 inch in height, at seven downstream positions, to reveal that essential similarity was obtained at the station at 0·642 ft ($x/s = 37{\cdot}0$) and beyond. The profile at $x = 0{\cdot}38$ ($x/s = 18{\cdot}3$) is close to these profiles and in fact gives the best correspondence with Glauert's prediction, while the downstream profiles agree with that of Sigalla [4], obtained experimentally on a wall jet. This points to the possibility that the diffusivity in the outer region may be slightly lower than that assumed in the theory.

Figure 4 presents the experimental profiles obtained with a 0·063 in slot for two different injection velocities. The profiles for the injection velocity of 211 ft/s agree better with the theory than do those for the 0·25 in slot, shown on Fig. 3. Only the profile for $x = 0{\cdot}05$ ft ($x/s = 9{\cdot}6$) shows a marked departure and that at the next station, $x/s = 29$, reveals similarity and agreement with the theory. Similar results exist for the lower injection velocity, except for a departure of the profile at the last station, but there the velocities were very low and the accuracy of the determination much diminished. Generally the results for the smaller slot correspond better with the theory, though the results for the larger slot are not inferior and all the profiles support the theory even in the present case in which the finite free stream velocity terminates the profiles in the outer region of the flow. The influence of the free stream flow is indicated to be small even for ratios u_1/u_m as large as 0·40.

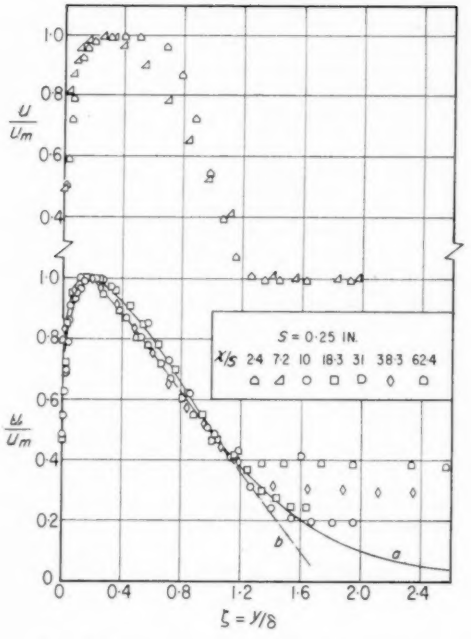

FIG. 3. Velocity profiles for the 0·25 in slot. Curve *a* is the same curve of Fig. 2, curve *b* is the result of Sigalla [4]. The slot Reynolds number was of the order of 6850. Quantities associated with the profiles are as follows.

x/s	u_1 (ft/s)	u_s (ft/s)	u_m (ft/s)	δ (in)	$u_m\delta/\nu$
2·4	9	56	60	0·27	7920
7·2	11	56	56	0·35	9650
10·0	8	58	52	0·37	9400
18·3	9	58	45	0·51	11300
31·0	9	57	40	0·71	13900
38·3	11	55	38	0·86	16000
62·4	11	56	33	1·31	21100

The considerable correspondence between the theoretical and the experimental profiles leads immediately to the question of the degree to which the power law dependence indicated by the theory is borne out by the experimental results. Since that distance is measured from a source at the effective origin of the flow, it must be obtained from a combination of experiment and theory in reference to some feature of the flow and the profiles themselves can be used for this. If the thickness, δ, is specified from equation

Vol. 3 1961

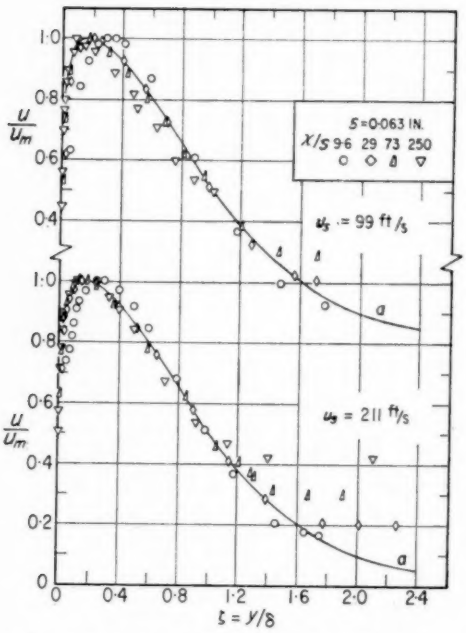

FIG. 4. Velocity profiles for the 0·063 in slot.

The upper set of results is for an injection velocity of 99 ft/s and the lower for 211 ft/s, the slot Reynolds numbers being of the order of 3030 and 6450 respectively. The curves are curve "a" of Fig. 2. Associated quantities are as follows.

x/s	u_1 (ft/s)	u_s (ft/s)	u_m (ft/s)	δ (in.)	$u_m\delta/\nu$
9·6	13	99	107	0·085	4580
29	13	99	69	0·17	6050
73	12	99	47	0·39	9270
250	12	99	28	1·56	22300
9·6	23	211	196	0·10	10100
29	23	211	135	0·20	13600
73	22	211	94	0·43	20500
250	23	211	57	1·44	41700

(4) and the maximum velocity, u_m, from equation (3), then the reference velocity can be eliminated to define the distance ξ; or, equivalently, the (positive) distance from the upstream origin to the slot location.

$$\frac{\xi}{s} = \frac{x}{s} + \frac{x_0}{s} = \left(\frac{\delta}{s}\right)\left(\frac{\delta u_m}{\nu}\right)^{1/4}\left[\frac{4}{0{\cdot}0275}\right.$$

$$\left.\times\left(1 - \frac{4+\alpha}{5+4\alpha}\right)(\alpha + 0{\cdot}07)\eta_t^{-5/4}\left(\frac{f_m}{f'_m}\right)^{5/4}\right]. \quad (6)$$

The function f'_m, f_m, and the distance η_t are given as functions of α in Ref. 3 and the values for x_0/s that are obtained from the profiles of Fig. 3 are contained in Table 1.

Table 1. *Values of* x_0/s, 0·25 *in slot*

From profile at x =	0·208	0·308	1·3
for α = 1·2	13	18	45
1·3	34	50	142

It is clear from the results in the table that the dependence of the upstream distance x_0/s on the parameter α is far too strong in terms of the scant choice in the value of the parameter that can be made from the velocity profiles. A disquieting feature of the tabulated results is the increasing upstream distance that is defined by the profiles at greater downstream distances and consequent implication that a true power law behavior may not exist in the experimental results. Such a situation is possible and may be engendered by the increasing influence of the free stream velocity at large downstream distances, where the maximum velocity becomes low. In any case, equation (6) does not yield consistent results and as an alternative a best fit to a power law behavior was obtained by arbitrary choices of the distance x_0/s. This is not a particularly definitive procedure and a considerable latitude is available in the choice; the value $x_0/s = 12$ was chosen as a magnitude giving the reasonable portrayal contained in Fig. 5. There the experimental values are subject to the empirical generalization of representing $(u_m\delta)/(u_s s)$ and u_m/u_s. This applies fairly for the local value of $u_m\delta$, and the values thereof can be found, within 5 per cent, from the relation

$$\frac{u_m\delta}{u_s s} = 0{\cdot}212\left(\frac{\xi}{s}\right)^{0{\cdot}60}. \quad (7)$$

There is less agreement in the case of the maximum velocity, and in particular the values for the 0·25 in slot reveal a reduced dependence on distance, while those for the 0·063 in slot indicate a small magnitude dependence on the injection velocity. To obtain a single equation,

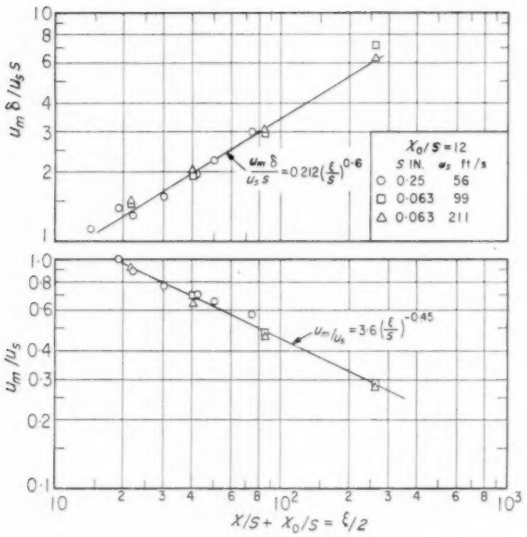

FIG. 5. The maximum velocity and the layer thickness. The curves represent the best fit to the experimental data and are equations (7) and (8).

an approximately 5 per cent tolerance is accepted and the last point for the 0·25 in slot neglected, with the result

$$\frac{u_m}{u_s} = 3{\cdot}6\left(\frac{\xi}{s}\right)^{-0{\cdot}45}. \tag{8}$$

Table 2 contains the individual results for the exponents a and b, for $u_m \sim \xi^a$ and $\delta \sim \xi^b$, and includes the predictions of these exponents for $\alpha = 1{\cdot}2$ and $1{\cdot}3$ from equations (1) and (2). The experimental values of the exponent "a" are a little low, those of "b" a little high, but the degree of dependence is of the same order as is the selection that is available from equations (1) and (2).

SHEAR COEFFICIENTS

Shear coefficients have been determined from the velocity profiles by a semi-logarithmic representation of the values near the wall and the location of this part of the profile in agreement with the law of the wall, taken as

$$\frac{u}{\sqrt{\tau_0/\rho}} = 5{\cdot}5 + 2{\cdot}5\log\frac{y\sqrt{(\tau_0/\rho)}}{\nu} \tag{9}$$

and also with the profile of the transition layer, taken on the Kármán basis as

$$\frac{u}{\sqrt{\tau_0/\rho}} = -3{\cdot}05 + 5\log\frac{y\sqrt{(\tau_0/\rho)}}{\nu}. \tag{10}$$

The use of the transition layer velocity distribution for the appraisal of the friction was dictated by the small extent of the region where the law of the wall could be expected to apply, for in most cases the velocity maximum occurred in the region of $y\sqrt{(\tau_0/\rho)}/\nu = 150$ and the influence of the greater diffusivity that existed there was evident in a departure of the velocity profile from equation (9) in that part of the inner layer near the velocity maximum. The uncertainty in the determination of the friction, particularly due to this effect, made the possible error in the coefficients about 5 per cent for the results for the 0·25 in slot and 10 per cent for those for the 0·063 in slot

Figure 6 shows the values, as coefficients, $\tau_0/\rho u_m^2$, presented as a function of the relative distance ξ/s and demonstrates approximately the power law behavior predicted by the theory, in which it was assumed that near the wall

$$\frac{\tau_0}{\rho u^2} = \frac{0{\cdot}0225}{(uy/\nu)^{1/4}}. \tag{11}$$

If this relation is presumed to hold as far as the velocity maximum then there is indicated a

Table 2. Power law exponents

Slot	u_s	$(a+b)$	a	$(a+b)-a$		a	b
0·250	56	0·60	−0·37	0·97	Equation (1) $\alpha = 1{\cdot}2$	−0·49	0·90
0·063	211	0·60	−0·45	1·05	$\alpha = 1{\cdot}3$	−0·51	0·90
0·063	99	0·63	−0·47	1·10	Equation (2) $\alpha = 1{\cdot}2$	−0·55	1
Equations (7, 8)		0·60	−0·45	1·05	$\alpha = 1{\cdot}3$	−0·56	1

Vol. 3 1961

proportionality of the shear coefficient to $\xi^{-(a+b)/4}$ and Fig. 6 then demonstrates agreement with the values of the exponent that are obtained from equations (1) or (2). In more specific reference to the experimental results, with δ_m/δ

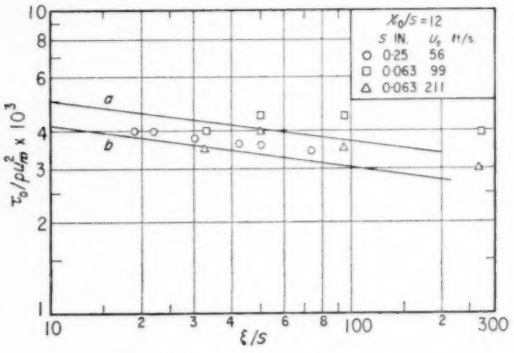

FIG. 6. Skin friction coefficients.

Curves a and b are equation (12) for slot Reynolds numbers of 3500 and 7000 respectively.

taken as 0·18 and equation (7) used for $u_m\delta$, equation (11) becomes

$$\frac{\tau_0}{\rho u_m^2} = \frac{0{\cdot}054}{(u_m s/\nu)^{1/4}} \left(\frac{\xi}{s}\right)^{-0{\cdot}15}. \qquad (12)$$

Fig. 6 contains the indication of equation (12) for two values of the Reynolds number that are typical of the experimental values to demonstrate an acceptable correspondence, particularly at the higher Reynolds number. The results for the lower Reynolds number are above equation (12), but the accuracy of these values is particularly questionable.

TEMPERATURE PROFILES

Temperature profiles were obtained with a 40 gage nichrome–constantan thermocouple, mounted on a fork made of sewing needles. Traverses were made with heated injection and an adiabatic wall, for operating conditions similar to those for which the velocity profiles were determined. These temperature profiles are presented as the ratio t/t_a, where t_a is the observed wall temperature and the few instances in which the ratio exceeds unity at the wall reflect discrepancies between the indication of the thermocouple probe and the thermocouple in the wall. Fig. 7(a) presents the profiles obtained for the 0·25 in slot and reveals essential similarity for those profiles at positions at and downstream of $x/s = 18$ ($\xi/s = 30$). This agrees with the indication of the velocity profiles that it is in this region that similarity is first achieved.

All of these profiles are for an adiabatic wall condition but only those for positions very near the slot show a slope of zero at the wall. At the downstream positions for which similarity is attained the curvature of the profile at the wall is so great that the initial slope of zero is not discernable. This feature exists also in the analytical predictions that are presented later.

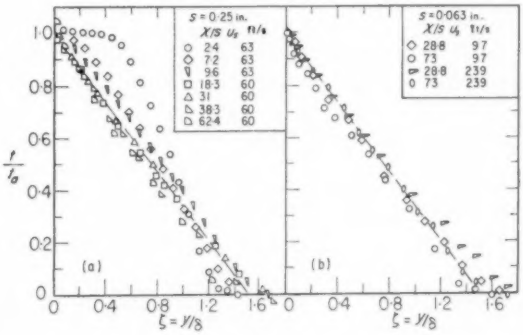

FIG. 7. Temperature profiles.

(a) and (b) show results for the 0·250 and 0·063 in slots respectively. Operating conditions were similar to those for the velocity profiles shown on Figs. 3 and 4. The curve is the mean experimental profile for the 0·250 in slot.

Figure 7(b) presents the few profiles obtained for the 0·063 in slot and also reveals that similarity was attained at least for the first position at $x/s = 28{\cdot}8$. The average experimental curve determined from the profiles for the 0·25 in slot is also shown on Fig. 7(b) and exhibits a good degree of correspondence to the profiles shown on that figure.

Beyond the realization of the expected similarity, the further appraisal of the profiles must deal with the extent to which the theoretical prediction is realized and such a prediction can be made from the hydrodynamic solution if the diffusivities for heat and momentum are taken to be equal. Insofar as the molecular contributions are concerned, this implies of course

a Prandtl number of unity. The energy equation, with dissipation neglected and properties taken as constant, is

$$u\frac{\partial t}{\partial \xi} + v\frac{\partial t}{\partial y} = \frac{\partial}{\partial y}^{(\epsilon \partial t/\partial y)}. \qquad (13)$$

With $u/_m u = F'(\zeta)$, where

$$\zeta = \frac{y}{\delta};\ \frac{\epsilon}{\delta[\mathrm{d}(u_m\delta)/\mathrm{d}\xi]}$$

depending only on ζ; and $t = t_a g(\zeta)$ with $t_a \sim \xi^{-(a+b)}$; this equation transforms to the ordinary differential equation:

$$\frac{\mathrm{d}gF}{\mathrm{d}\zeta} = \frac{\mathrm{d}}{\mathrm{d}\zeta}\left[\frac{\epsilon}{\delta[\mathrm{d}(u_m\delta)/\mathrm{d}\xi]}\right]\frac{\mathrm{d}g}{\mathrm{d}\zeta}. \qquad (14)$$

With an adiabatic wall, $\mathrm{d}g/\mathrm{d}\zeta = 0$ at $\zeta = 0$ and

$$\frac{\mathrm{d}g}{\mathrm{d}\zeta} = \left[\frac{\delta[\mathrm{d}(u_m\delta)/\mathrm{d}\xi]}{\epsilon}\right] gF \qquad (15)$$

and since $g(0) = 1$, there is obtained for the temperature profile

$$g = \exp\left\{-\int F\left[\frac{\delta}{\epsilon}\frac{\mathrm{d}(u_m\delta)}{\mathrm{d}\xi}\right]\mathrm{d}\zeta\right\} \qquad (16)$$

Figure 8 shows the profile predicted from the velocity distribution and diffusivity for $a = 1{\cdot}2$ as they are indicated on Fig. 2, except that the "inner" diffusivity was used as far as $\zeta = 0{\cdot}18$. Comparison with the curve that approximates the experimental profile shows that the predicted resistance near the wall is too large and that in the outer layer, beyond the velocity maximum, it is too small. To show how the prediction is affected by the magnitude of the diffusivity, a prediction is also shown for the case in which the diffusivity of the inner layer has been increased by a factor of 1·65 and that of the outer layer has decreased by a factor of 0·77. This agrees with the experimental values in the inner region and it is to be noted that the increase in the diffusivity that has been used is far greater than might be expected from any consideration that the Prandtl number of the air is 0·70. There is an irregularity in the prediction near the velocity maximum that is due to the sudden increase in the postulated diffusivity but the remainder of the prediction is in accord with experiment out to $y/\delta = 1$. Beyond this, the experimental values themselves are not well represented by the line that is indicated for them, as it is in this region that the existence of the finite free stream velocity apparently diminishes the diffusivity to values below that of the prediction.

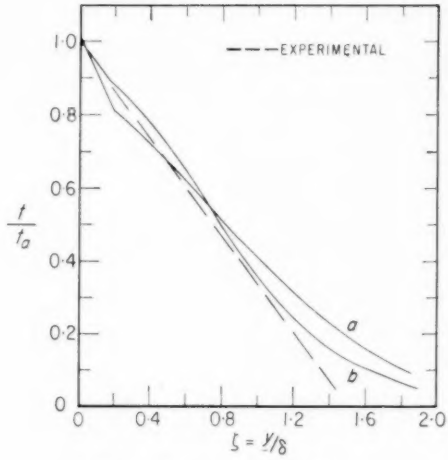

FIG. 8. Temperature profiles.

The experimental curve is that shown in Fig. 7. Curve *a* is that for the diffusivity given by curve *c* on Fig. 2 for $a = 1{\cdot}2$. Curve *b* is that also given by curve *c* on Fig. 2, but with ϵ increased by 65 per cent for $\zeta < 0{\cdot}18$ and decreased 23 per cent for $\zeta > 0{\cdot}18$.

Another view of the value of the diffusivity that is needed for better correspondence is presented in Fig. 2, where there has been indicated the diffusivity that would be required for the realization of the linear temperature profile with the theoretical velocity distribution corresponding to $a = 1{\cdot}2$. This of course is obtainable directly from equation (15) in a particularly simple way when the temperature profile is approximated as linear. The diffusivity obtained in this way varies continuously with ζ and in the outer region there is indicated an average value of the order of $\epsilon/\delta\ [\mathrm{d}(u_m\delta)/\mathrm{d}\xi] = 0{\cdot}40$. In the theory the diffusivity in the outer region is presumed to vary only with distance along the plate according to $u_m\delta_t/\epsilon = 1/\kappa$. From equation (5),

$$\kappa = \left[\frac{\epsilon}{\delta[\mathrm{d}(u_m\delta)/\mathrm{d}\xi]}\right]\frac{(a+b)}{0{\cdot}85}\frac{\delta}{\xi},$$

Vol. 3 1961

and with equations (7) and (8) used to evaluate δ/ξ and to define $(a + b)$, this becomes

$$\kappa = (0{\cdot}069)\left\{\frac{\epsilon}{\delta[\mathrm{d}(u_m\delta)/\mathrm{d}\xi]}\right\}.$$

This gives $\kappa = 0{\cdot}042$ and $0{\cdot}028$ for

$$\left\{\frac{\epsilon}{\delta[\mathrm{d}(u_m\delta)/\mathrm{d}\xi]}\right\}$$

equal to $0{\cdot}61$ and $0{\cdot}40$ respectively and these values are larger than that of $\kappa = 0{\cdot}012$ inferred by Glauert for the radial wall jet.

EFFECTIVENESS

The effectiveness is the ratio of the local adiabatic wall temperature to the temperature of the injection air, and the observations concerning the similarity of the temperature and velocity profiles imply that the effectiveness should be proportional to $\xi^{-(a+b)}$ at downstream distances greater than ξ/s of the order of 30. Fig. 9 shows the values of the effectiveness to indicate this to be true, and that the individual

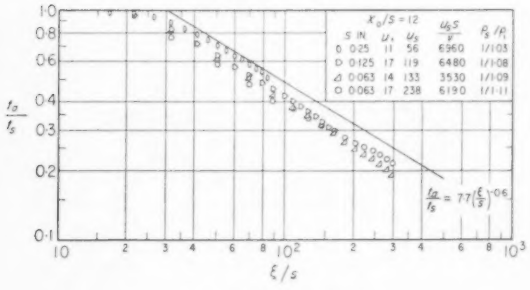

FIG. 9. Effectiveness.
The curve is equation (20) for $\rho_s/\rho_1 = 1{\cdot}0$.

slopes for the three runs illustrated do vary slightly from about $-0{\cdot}60$ for the 0·25 in slot to $-0{\cdot}57$ for the 0·063 in slot with the high speed injection. Table 2 gives $(a + b) = 0{\cdot}60$ for both conditions, as does equation (7).

Further consideration of the effectiveness requires the specification of t_a from an energy balance

$$c_p\rho_s u_s s t_s = \rho_1 c_p u_m t_a \delta \int_0^\infty \frac{\rho}{\rho_1}\frac{u}{u_m}\frac{t}{t_a}\,\mathrm{d}\left(\frac{y}{\delta}\right). \quad (17)$$

For the relatively small temperature differences involved in the results shown in the figure, for which $T_s/T_1 < 1{\cdot}11$, the integral in equation (17) can be approximated as

$$\int_0^\infty \frac{u}{u_m}\frac{t}{t_a}\,\mathrm{d}\left(\frac{y}{\delta}\right) - \frac{t_a}{T_1}\int_0^\infty \left(\frac{t}{t_a}\right)^2 \frac{u}{u_m}\,\mathrm{d}\left(\frac{y}{\delta}\right). \quad (18)$$

The second integral is 0·7 times the first but the coefficient t_a/T_1 is only 0·11 as a maximum, so that the second term of the expression (18) is neglected and equation (17) is approximated in the following form, the denominator then being at most 8 per cent high.

$$\frac{t_a}{t_s} = \frac{\rho_s u_s s}{\rho_1 u_m \delta}\Big/\int_0^\infty \frac{u}{u_m}\frac{t}{t_a}\,\mathrm{d}\left(\frac{y}{\delta}\right). \quad (19)$$

The integral, evaluated from the linear temperature profile of Fig. 7 and the theoretical velocity profile for $a = 1{\cdot}2$, has a value of 0·607, and if equation (7) is used for the ratio $u_s s/u_m\delta$ there is obtained

$$\frac{t_a}{t_s} = 7{\cdot}7\,\frac{\rho_s}{\rho_1}\left(\frac{\xi}{s}\right)^{-0{\cdot}60}. \quad (20)$$

There is risk in this formulation because both the velocity profile used in the integral in equation (19) and $u_s s/u_m\delta$ given by equation (7) were obtained for isothermal conditions, and not for the case of variable density now considered. Also, the value of the integral as used in equation (19) is too high, as noted. Thus equation (20) shown on Fig. 9 with $\rho_s/\rho_1 = 1{\cdot}0$ is at least something less than 11 per cent too high for the 0·063 in slot, the difference decreasing with increasing slot size.

HEAT TRANSFER

Temperature profiles were not obtained for the runs made with heat transfer and the consideration is limited to the comparison of the results previously reported to the evidence about the flow that has been presented here. Fig. 10 shows the pertinent runs portrayed in the correlation previously proposed, as a function of the effective distance ξ. This is essentially the portrayal used originally [1] except that the addition of the distance $x_0/s = 12$ eliminates the need in these runs, at least, for the separate correlation that was used for the region near the

slot. But previous evidence here indicates that the power law dependence

$$\frac{h}{\rho_s u_s c_p}\left(\frac{u_s s}{\nu}\right)^{0.3} = 0.41\left(\frac{\xi}{s}\right)^{-0.60} \qquad (21)$$

shown on Fig. 10 as curve c, should not be expected closer to the slot than $\xi/s = 30$. Beyond this point the correlation is fairly successful, approximating a power law with a scatter of points in a band about 10 per cent in width.

Contrasted to the effectiveness, the heat transfer depends crucially on conditions near the wall, and the solution of equation (13) will need to be matched to some appropriate sublayer assumptions in order to obtain a proper result. In lieu of this there is chosen here the Colburn analogy,

$$\frac{h}{\rho u_m c_p}(\sigma)^{2/3} = \frac{\tau_0}{\rho u_m{}^2}$$

as a possible appropriate relation between the heat transfer and friction coefficients. If this choice is combined with equations (12) and (8), there is obtained the relation

$$\frac{h}{\rho u_s c_p} = \frac{0.25}{(u_s s/\nu)^{1/4}}\left(\frac{\xi}{s}\right)^{-0.60}. \qquad (22)$$

Fig. 10 shows that the prediction of equation (22) is not more than 10 per cent low and that the effect of the difference in the exponents of the slot Reynolds number in equation (22) and the correlation used on Fig. 10 is not a crucial one in the range of Reynolds numbers that is encompassed there. It is noteworthy that the correspondence between the thermal and the hydrodynamic behavior that is achieved for this flow is the equal of that usually found for the more conventional systems of pipe flow and the usual turbulent boundary layer on a plate.

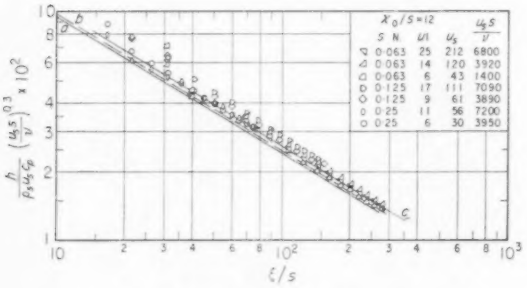

FIG. 10. Heat transfer.

Curves a and b are equation (22) for slot Reynolds numbers of 3000 and 6000 respectively. Curve c is equation (21).

SUMMARY

An approximation to the wall jet, in which the free stream velocity was small but not zero, has been investigated experimentally to appraise the degree to which the behavior of the theoretical flow was realized and to establish the extent to which the measured effectiveness and heat transfer coefficient might be predicted. Generally successful achievement of these comparisons embraced the following items.

The velocity profile in that system considered is practically the same as that predicted and this correspondence holds almost to the point at which exists the free stream velocity; and this agreement existed beyond about 18 slot heights downstream of the slot. Power law behavior exists approximately with respect to downstream distance with exponents being of the order of magnitude that are indicated by the theory, but this is the weakest part of the comparison. The friction factors can be predicted well if the experimental dependence on distance is employed.

Agreement between the predicted temperature profiles and those determined experimentally with an adiabatic wall requires some alteration of the eddy diffusivity and in particular the value in the outer region must be reduced by 30 per cent from that implied by the theory; but other than this, the correspondence is perhaps better than would have been anticipated. When values of the effectiveness are predicted from the hydrodynamic and thermal profiles the prediction agrees with the results for the larger slot but is otherwise high by about 15 per cent.

Heat transfer coefficients, predicted from the flow results, are about 10 per cent below the data; and the prediction, based upon the Colburn analogy, verifies this relation for this system.

Vol. 3 1961

ACKNOWLEDGEMENT

The research which yielded these results was supported by the National Science Foundation under Grant G-10171.

REFERENCES

1. R. A. SEBAN, Heat transfer and effectiveness for a turbulent boundary layer with tangential fluid injection. *Trans. Amer. Soc. Mech. Engrs, J. Heat Transfer*, C **182**, 303 (1960).
2. M. JAKOB, R. ROSE and M. SPILMAN, Heat transfer from an air jet to a plane plate with entrainment of water vapor from the environment. *Trans. Amer. Soc. Mech. Engrs*, **72**, 859 (1950).
3. M. B. GLAUERT, The wall jet. *J. Fluid Mech.* **1**, 525 (1956).
4. A. SIGALLA, Experimental data on a turbulent wall jet. *Aircr. Engr*, **30**, 131–134 (1958).

ol.
3
961

Vol.
3
1961

Int. J. Heat Mass Transfer. Vol. 3, pp. 267–274. Pergamon Press 1961. Printed in Great Britain.

THE EFFECT OF A MAGNETIC FIELD ON FREE CONVECTION HEAT TRANSFER

E. M. SPARROW* and R. D. CESS†

(*Received* 2 *February* 1961 *and in revised form* 22 *May* 1961)

Abstract—Free convection heat transfer due to the simultaneous action of buoyancy and induced magnetic forces is investigated. The analysis is carried out for laminar boundary-layer flow about an isothermal vertical plate. It is found that the free convection heat transfer to liquid metals may be significantly affected by the presence of a magnetic field; but that very small effects are experienced by other fluids.

Résumé—Cet article étudie la transmission de chaleur par convection libre résultant de l'action simultanée des forces de convection naturelle et de forces magnétiques induites. L'étude a été faite pour un écoulement de couche limite laminaire sur une plaque verticale isotherme. On a trouvé que, pour des métaux liquides la transmission de chaleur par convection libre pouvait être notablement affectée par la présence d'un champ magnétique; avec d'autres fluides ces effets sont très petits.

Zusammenfassung—Es wurde der Wärmeübergang durch freie Konvektion bei gleichzeitiger Einwirkung von Auftriebs- und induzierten magnetischen Kräften untersucht, und zwar für die laminare Grenzschicht an der senkrechten isothermen Platte. Es zeigt sich ein starker Einfluss des Magnetfeldes auf den Wärmeübergang bei flüssigen Metallen, bei anderen Flüssigkeiten dagegen nur ein sehr geringer.

Аннотация—В статье рассматривается перенос тепла под действием свободной конвекции и индуцированного магнитного поля. Исследуется ламинарный пограничный слой вокруг изотермической вертикальной пластины. Установлено, что на перенос тепла при свободной конвекции в жидких металлах существенно влияет наличие магнитного поля, в то время как на другие жидкости влияние магнитного поля небольшое.

NOMENCLATURE

B, magnetic induction vector;
B_0, externally imposed y-component of **B**;
F, induced magnetic force;
F_x, x-component of **F**;
f, transformed stream function equation (10);
f_0, f_1, functions of η;
Gr, Grashof number, $g\beta|T_w - T_\infty|x^3/\nu^2$;
g, acceleration due to gravity;
J, current density vector;
k, thermal conductivity;
Pr, Prandtl number, ν/α;
Q, overall rate of heat transfer;
Q_0, Q in absence of magnetic field;
q, local rate of heat transfer per unit area;
q_0, q in absence of magnetic field;
T, static temperature; T_∞, ambient temperature; T_w, wall temperature; $\Delta T = T_w - T_\infty$;
u, velocity component in x direction;
V, velocity vector;
v, velocity component in y direction;
x, co-ordinate measuring distance from leading edge;
y, co-ordinate measuring distance normal to plate.

Greek symbols

α, thermal diffusivity;

* Professor of Mechanical Engineering, Heat Transfer Laboratory, University of Minnesota, Minneapolis, Minnesota, U.S.A.

† Associate Professor of Engineering, State University of New York, Long Island Center, Oyster Bay, New York, U.S.A.

β, thermal expansion coefficient, $-1/\rho\,(\partial\rho/\partial T)_p$;
η, similarity variable, equation (9a);
θ, dimensionless temperature, $(T - T_\infty)/(T_w - T_\infty)$;
θ_1, θ_2, functions of η;
ν, kinematic viscosity;
ξ, magnetic parameter, equation (9b);
ρ, density;
σ, electrical conductivity;
ψ, stream function.

INTRODUCTION

It is common to classify buoyancy forces and induced magnetic forces among the body forces which may occur in fluid mechanics problems. The separate action of each of these forces in establishing and modifying fluid flows has been studied rather extensively. In the present investigation, consideration is given to the situation where buoyancy and magnetic forces act simultaneously.

The specific problem selected for study is the flow and heat transfer in an electrically-conducting fluid adjacent to an isothermal vertical plate. The configuration is pictured schematically in Fig. 1. The plate surface is maintained at a uniform temperature T_w which may either exceed the ambient temperature T_∞, Fig. 1(a), or may be less than T_∞, Fig. 1(b). When $T_w > T_\infty$, an upward flow is established along the plate due to free convection; while when $T_w < T_\infty$, there is a downflow. Additionally, a magnetic field B_0 acts normal to the plate surface. The interaction of the magnetic field and the moving electric charge carried by the flowing fluid induces a force which tends to oppose the fluid motion. Consequently, the resultant flow and the corresponding heat transfer should be decreased relative to the case of pure free convection.

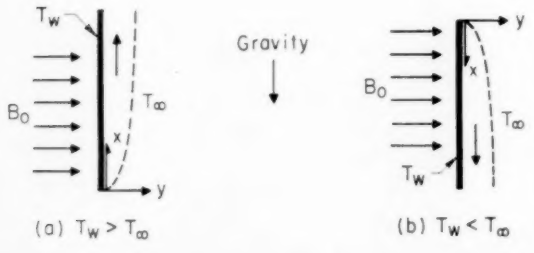

Fig. 1. Physical model and co-ordinates.

There is an interesting distinction between the present problem and others involving magnetohydrodynamic effects in *forced convection* boundary layers. In the latter situation, induced magnetic forces may modify the free stream flow and in turn, this may effect the external pressure gradient or the free stream velocity which is imposed on the boundary layer. Thus, a complete boundary-layer solution would involve a magnetohydrodynamic solution for the inviscid free stream (for example, see Refs. 1 and 2). In some cases, the interaction between the free stream flow and the magnetic field has been treated in an incomplete manner, giving rise to an ambiguity in the boundary-layer results [3]. On the other hand, in the free convection problem, the velocity is zero in the ambient fluid and induced magnetic forces do not exist there. Consequently, the influence of the magnetic field on the boundary layer is exerted only through induced forces within the boundary layer itself, with no additional effects arising from the free stream pressure gradient. As a consequence, the free convection problem may be formulated in a simpler and perhaps more exact manner than the forced convection problem.

The analysis is carried out for the case of uniform surface temperature T_w and uniform imposed magnetic field B_0 (independent of x). These conditions do not lead to a similar solution of the laminar boundary-layer equations. Therefore, solutions of the governing equations have been obtained utilizing a series expansion method. At the time this study was carried out, there were no analyses of the magnetohydrodynamic free convection problem in the readily-available literature. During the process of review by the Journal, some additional references were brought to the attention of the authors. The magnetohydrodynamic free convection problems considered therein are complementary but different from the situation considered here. In Ref. 4 the isothermal vertical plate is analyzed under the assumption that the imposed magnetic field B_0 varies as $x^{-1/4}$. This is the condition required to achieve a similarity boundary layer.

Vol. 3 1961

Approximate solutions were obtained by the Kármán–Pohlhausen integral method. Refs. 5 and 6 also consider similarity-type solutions. In Ref. 5, the isothermal wall case is solved numerically for various Prandtl numbers and magnetic parameters and additionally, asymptotic solutions are given. Ref. 6 explores the relationship between the x-dependence of wall temperature and imposed magnetic field which provides similarity conditions, but numerical results are not given. An imposed field B_0 varying as $x^{1/4}$ along an isothermal plate was considered in Ref. 7. This did not lead to a similarity-type boundary layer and a series expansion method was utilized. The results of Ref. 7 are somewhat in doubt inasmuch as an error was discovered in one of the governing differential equations [5].

ANALYSIS

Mathematical formulation

The starting point of the analysis is the basic conservation laws of mass, momentum, and energy. To obtain the mathematical statement of these laws, we utilize the well-known governing equations for free convection (for example, p. 327 of Ref. 8) to which are added terms appropriate to the magnetic effects. Characterizing the induced magnetic force by **F**, we write

mass:

$$\frac{\partial u}{\partial x} + \frac{\partial v}{\partial y} = 0 \tag{1}$$

momentum:

$$u\frac{\partial u}{\partial x} + v\frac{\partial u}{\partial y} = \pm g\beta\,(T - T_\infty) + \frac{F_x}{\rho} + \nu\frac{\partial^2 u}{\partial y^2} \tag{2}$$

energy:

$$u\frac{\partial T}{\partial x} + v\frac{\partial T}{\partial y} = \alpha\frac{\partial^2 T}{\partial y^2}\,. \tag{3}$$

The plus-minus sign has been attached to the buoyancy force $g\beta(T - T_\infty)$ so that the equations are valid for both the upflow and downflow situations pictured on Fig. 1(a) and 1(b) respectively. Fluid property variations have been considered only to the extent of a density variation which provides a buoyancy force. Viscous dissipation has been neglected in the energy equation (3). Further, since the Joule heating (electrical dissipation) is usually the same order as the viscous dissipation, it too has been neglected.

The magnetic force **F** may, in the absence of excess charges, be written as [9]

$$\mathbf{F} = \mathbf{J} \times \mathbf{B} \tag{4}$$

where **J** and **B** are respectively the current density and magnetic induction vectors. Further, when the external electric field is zero and the induced electric field negligible, the current density is related to the velocity by Ohm's Law as follows

$$\mathbf{J} = \sigma(\mathbf{V} \times \mathbf{B}) \tag{5}$$

where σ denotes the electrical conductivity of the fluid. Next, under the condition that the magnetic Reynolds number is small, the induced magnetic field is negligible compared with the applied field. This condition is usually well satisfied in terrestrial applications, especially so in (low-velocity) free convection flows. So, we write

$$\mathbf{B} = \mathbf{i}_z\, B_0. \tag{6}$$

Bringing together equations (4), (5), and (6), the force component F_x is found to be

$$F_x = -\sigma u B_0^2 \tag{7}$$

and this may then be introduced into the momentum equation (2).

The specification of the boundary conditions is necessary to complete the statement of the problem. At the surface, the velocities are zero to satisfy the conditions of no slip and an impermeable wall. In addition, temperature continuity requires that fluid and solid share the same temperature. Far from the surface, the velocity approaches zero and the temperature approaches that of the surroundings. Formally, these conditions may be stated as

$$\left.\begin{array}{l} u = v = 0 \\ T = T_w = \text{const.} \end{array}\right\} y = 0 \qquad \left.\begin{array}{l} u \to 0 \\ T \to T_\infty \end{array}\right\} y \to \infty\,. \tag{8}$$

Having thus completed the statement of the problem, attention may next be directed toward finding a solution. The first thought would be to

seek a similarity solution; that is, to seek a form of solution in which the velocity and temperature profiles maintain a similar shape at all values of position x. Mathematically speaking, the desirable property of such a solution is that the governing equations (1), (2), (3), and (7) become ordinary differential equations. However, it is found that the conditions that B_0 and T_w are both independent of x cannot be satisfied by a similarity solution. As a consequence, some other approach must be found.

Series solution

Previous experience with non-similar boundary layer problems suggests that a series solution might be useful in the present situation. To this end, the following new co-ordinates are introduced

$$\eta = \frac{y}{x^{1/4}}\left[\frac{g\beta|T_w - T_\infty|}{4\nu^2}\right]^{1/4} = \frac{y}{x}\left(\frac{Gr}{4}\right)^{1/4} \tag{9a}$$

$$\xi = \frac{2\sigma B_0^2}{\rho[g\beta|T_w - T_\infty|]^{1/2}}x^{1/2} = \frac{\sigma B_0^2 x^2/\rho\nu}{(Gr/4)^{1/2}} \tag{9b}$$

where Gr is the Grashof number. The variable η is immediately recognized as the free convection similarity variable. On the other hand, ξ, which is essentially a stretched x co-ordinate, is an index to the relative importance of the magnetic forces. Next, new dependent variables f and θ are defined as

$$f(\xi, \eta) = \frac{\psi}{[64\, g\beta\nu^2|T_w - T_\infty|]^{1/4}x^{3/4}},$$

$$\theta(\xi, \eta) = \frac{T - T_\infty}{T_w - T_\infty} \tag{10}$$

where ψ, the stream function, is related to the velocities u and v in the usual manner

$$u = \frac{\partial\psi}{\partial y},\ v = -\frac{\partial\psi}{\partial x}. \tag{11}$$

This definition of ψ immediately satisfies the conservation of mass equation.

We may then proceed to transform the conservation of momentum and energy equations into the new co-ordinates. To facilitate the transformation, it is useful to have the velocity components explicitly expressed in terms of the new variables. From equation (11) in conjunction with (10) and (9), there is obtained

$$u = 2[g\beta|T_w - T_\infty|]^{1/2}x^{1/2}\frac{\partial f}{\partial\eta} \tag{12a}$$

$$v = -\frac{[64\, g\beta\nu^2|T_w - T_\infty|]^{1/4}}{x^{1/4}}\left[\frac{3}{4}f - \frac{1}{4}\eta\frac{\partial f}{\partial\eta} + \frac{1}{2}\xi\frac{\partial f}{\partial\xi}\right]. \tag{12b}$$

With these, and utilizing the definitions of η, ξ, and θ from equations (9) and (11), the conservation equations (2) and (3) becomes

momentum:

$$2\left(\frac{\partial f}{\partial\eta}\right)^2 - 3f\frac{\partial^2 f}{\partial\eta^2} + 2\xi\left(\frac{\partial^2 f}{\partial\xi\partial\eta}\frac{\partial f}{\partial\eta} - \frac{\partial f}{\partial\xi}\frac{\partial^2 f}{\partial\eta^2} + \frac{1}{2}\frac{\partial f}{\partial\eta}\right) = \theta + \frac{\partial^3 f}{\partial\eta^3} \tag{12}$$

energy:

$$-3f\frac{\partial\theta}{\partial\eta} + 2\xi\left(\frac{\partial f}{\partial\eta}\frac{\partial\theta}{\partial\xi} - \frac{\partial\theta}{\partial\eta}\frac{\partial f}{\partial\xi}\right) = \frac{1}{Pr}\frac{\partial^2\theta}{\partial\eta^2}. \tag{13}$$

It may be noticed that in the absence of a magnetic field, i.e. $\xi = 0$, these equations reduce to the standard free convection equations as first derived by Schmidt and Beckmann (p. 447 of Ref. 10).

Notwithstanding their change in form, equations (12) and (13) are, like their predecessors (2) and (3), partial differential equations. In order to reduce the problem to one involving more tractable ordinary differential equations, we expand the variables f and θ in series as follows

$$f(\xi, \eta) = f_0(\eta) + \xi f_1(\eta) + \xi^2 f_2(\eta) + \ldots \tag{14}$$

$$\theta(\xi, \eta) = \theta_0(\eta) + \xi\theta_1(\eta) + \xi^2\theta_2(\eta) + \ldots \tag{15}$$

These may be substituted into equations (12) and (13) and terms grouped according to powers of ξ. From this, there is obtained the governing equations for the f_0, θ_0, f_1, θ_1, ... as

$$\left.\begin{aligned} f_0''' + 3f_0f_0'' - 2(f_0')^2 &= -\theta_0 \\ \theta_0'' + 3Pr\, f_0\theta_0' &= 0 \end{aligned}\right\} \tag{16}$$

Vol. 3 1961

$$\left.\begin{aligned} &f_1''' + 3f_0f_1'' - 6f_0'f_1' + 5f_0''f_1 = f_0' - \theta_1 \\ &\frac{1}{Pr}\theta_1'' + 3f_0\theta_1' - 2f_0'\theta_1 = -5f_1\theta_0' \end{aligned}\right\} \quad (17)$$

where primes represent differentiation with respect to η and Pr denotes the Prandtl number.

For computational purposes, the series were truncated after the θ_1 and f_1 terms. Formulated in this way, the problem takes the form of a basic free convection flow upon which the effects of the magnetic field constitute a disturbance. From the numerical results to be shown later, it would appear that truncation after the second term is not a too serious restriction.

The boundary conditions (8) may also be rephrased in terms of the new variables. Utilizing the velocity expressions (12) and the definition of θ, equation (10), it is found that

$$\left.\begin{aligned} &f_0(0) = f_0'(0) = 0, \quad \theta_0(0) = 1 \\ &f_0' \to 0, \quad \theta_0 \to 0 \quad \text{as } \eta \to \infty \end{aligned}\right\} \quad (16a)$$

$$\left.\begin{aligned} &f_1(0) = f_1'(0) = \theta_1(0) = 0 \\ &f_1' \to 0, \quad \theta_1 \to 0 \quad \text{as } \eta \to \infty \end{aligned}\right\}. \quad (17a)$$

It may be seen that equation (16) and the corresponding boundary conditions (16a) coincide with the final ordinary differential equations for pure free convection. Numerical solutions of these equations covering the Prandtl number range 0·003 to 1000 have been tabulated in detail in Refs. 11 and 12. The computational task thus remaining for the present study was to solve equations (17) subject to the boundary conditions (17a).

By inspection of these equations, it is seen that since f_1 and θ_1 appear in both equations, simultaneous solution is required. Additionally, it is necessary to utilize the solutions of equations (16) as input data, since f_0, f_0', f_0'', and θ_0', all appear in equations (17). Analytical solutions of equations (17) could not be found, and it was necessary to use numerical means. Solutions were carried out on an IBM 704 electronic digital computer for Prandtl numbers of 0·02, 0·72, and 10. Input data for the lowest of these was taken from Ref. 12, while that for the higher Prandtl numbers came from Ref. 11. From the solutions, the essential information which is needed in the heat transfer computation is $(d\theta_1/d\eta)_{\eta=0}$. These results are listed in Table 1, along with the values of $(d\theta_0/d\eta)_{\eta=0}$ as taken from the references.

Table 1. *Temperature derivatives*

Pr	$\theta_0'(0)$	$\theta_1'(0)$	$\theta_1'(0)/\theta_0'(0)$
10	−1·169	0·125	−0·107
0·72	−0·5046	0·0618	−0·123
0·02	−0·1116	0·0152	−0·137

There are two aspects of these results which deserve mention. First is the fact that $\theta_1'(0)/\theta_0'(0)$ varies only slightly with Prandtl number over the very wide range considered here. This suggests that one may interpolate between or extrapolate beyond the tabulated results without fear of incurring large errors. The second relates to the small magnitude of $\theta_1'(0)/\theta_0'(0) \sim 0{\cdot}1$. Hence, only with fairly large ξ values (e.g. ~ 2) will the second term of the series begin to be important.

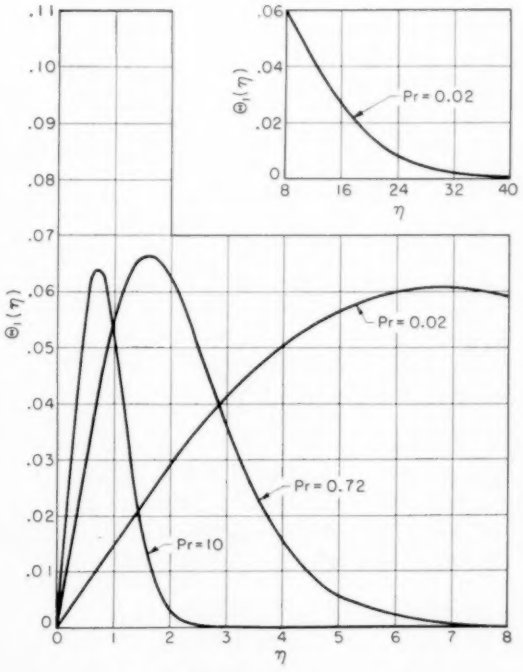

FIG. 2. Variation of the function $\theta_1(\eta)$.

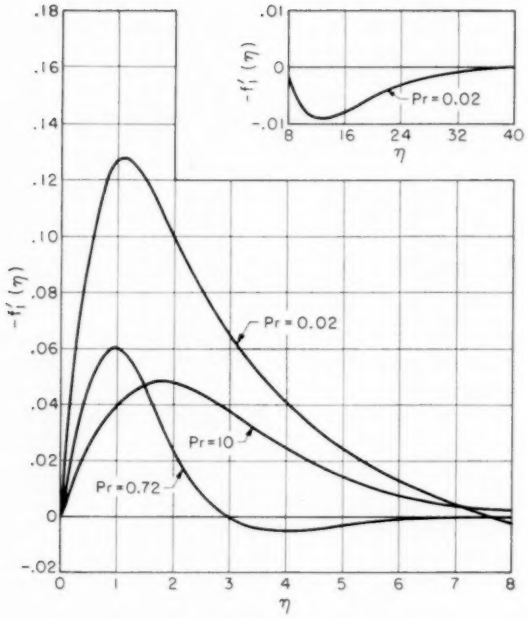

FIG. 3. Variation of the function $f_1'(\eta)$.

Thus, even with truncation after the second term, the theory appears to be able to accommodate fairly large ξ. Of course, small ξ values are accommodated without question.

In addition to the tabulated temperature derivatives which will be used in the heat transfer computation, it appears worthwhile for the sake of completeness to give more detailed information on the new solutions which have been obtained. To this end, the functions $\theta_1(\eta)$ and $f_1'(\eta)$ have been respectively plotted on Figs. 2 and 3 for Prandtl numbers of 0·02, 0·72 and 10. The θ_1 function is associated with the temperature distribution by equation (15); while the f_1' function is associated with the distribution of the velocity component u by equations (12a) and (14). The functions θ_0 and f_0' which are additionally needed in the determination of the temperature and velocity profiles are given in Refs. 11 and 12.

HEAT TRANSFER RESULTS

The local rate of heat transfer flowing from the surface to the fluid may be calculated by Fourier's Law

$$q = -k\left(\frac{\partial T}{\partial y}\right)_{y=0}. \tag{18}$$

Utilizing the definitions of θ and η from equations (10) and (9a), the expression for q can be rephrased as

$$q = -\frac{k}{x}(T_w - T_\infty)\left(\frac{Gr}{4}\right)^{1/4}\left[\frac{d\theta}{d\eta}\right]_{\eta=0}. \tag{19}$$

Then, introducing the series expansion (15) for θ, there is obtained

$$q = \frac{k}{x}(T_w - T_\infty)\left(\frac{Gr}{4}\right)^{1/4} [-\theta_0'(0) - \xi\theta_1'(0) - \ldots] \tag{20}$$

In the absence of a magnetic field, the local heat transfer rate q_0 is given by

$$q_0 = \frac{k}{x}(T_w - T_\infty)\left(\frac{Gr}{4}\right)^{1/4}[-\theta_0'(0)]. \tag{21}$$

The effect of the magnetic field upon the heat flux is then obtained by combining equations (20) and (21), with the result

$$\frac{q}{q_0} = 1 + \left[\frac{\theta_1'(0)}{\theta_0'(0)}\right]\frac{2\sigma B_0^2}{\rho[g\beta|T_w - T_\infty|]}x^{1/2} + \ldots \tag{22}$$

where ξ has been replaced according to equation (9b).

In appraising the influence of the magnetic field, reference is made to the information listed in Table 1. Since $\theta_1'(0)/\theta_0'(0)$ is negative, it follows that the magnetic field reduces the heat transfer, as was expected on physical grounds. Additionally, it is seen that since $\theta_1'(0)/\theta_0'(0)$ is of the order of 0·1, the presence of the magnetic field is significant only if

$$\frac{2\sigma B_0^2 x^{1/2}}{\rho[g\beta|T_w - T_\infty|]^{1/2}}$$

is of the order of one or two.

For 8 N sulphuric acid (1·9 mhos/in) under the reasonable conditions $\Delta T = 50°F$ and $x = 1$ ft, a magnetic field of 25 000 gauss would be required to have a significant effect on heat transfer. Such a magnetic field is exceedingly large and may be considered outside the range of ordinary laboratory practice. For salt water

Vol. 3 1961

(0·64 mhos/in), similar field strengths are required to influence the heat transfer, and even larger fields would be needed for ordinary tap water. In the case of gases, electrical conductivities of technically-interesting magnitudes are not achieved until the gas temperatures are very high. For example, even at a temperature of 5500°F and a density corresponding to 100 000 ft altitude (1/70 of standard sea level density), the electrical conductivity of air is only about 10^{-4} mhos/in (Ref. 13, Fig. D, 34a). For these conditions, a magnetic field of perhaps 20 000 gauss is needed to significantly effect the free convection heat transfer. The combination of such high temperatures and high magnetic fields is difficult to achieve and is not commonly encountered. Somewhat lower temperatures and smaller magnetic fields would be required if the air were seeded with potassium.

At the other end of the scale from these illustrations is the case of liquid metals. For liquid mercury ($2{\cdot}5 \times 10^4$ mhos/in), a 25 per cent reduction in the local heat flux can be achieved with a magnetic field of 1000 gauss for $\Delta T = 50°\text{F}$ and $x = 3$ in. Thus, it would seem that among all the fluids, the liquid metals appear to be most susceptible to the effects of a magnetic field.

Thus far, consideration has been given to the local heat flux q. The overall rate of heat transfer Q from a section of plate from $x = 0$ to $x = x$ may be calculated by integrating as follows

$$Q = \int_0^x q\,\mathrm{d}x. \tag{23}$$

Substituting for q from equation (20) and noting that $Gr^{1/4} \sim x^{3/4}$ and $\xi \sim x^{1/2}$, there is obtained

$$\frac{Q}{Q_0} = 1 + \frac{3}{5}\left[\frac{\theta_1'(0)}{\theta_0'(0)}\right]\frac{2\sigma B_0^2}{\rho[g\beta|T_w - T_\infty|]^{1/2}}\,x^{1/2} + \ldots \tag{24}$$

where Q_0, the overall heat flux for pure free convection, is given by

$$Q_0 = \tfrac{4}{3}\,k(T_w - T_\infty)\left(\frac{Gr}{4}\right)^{1/4}[-\theta_0'(0)]. \tag{25}$$

By comparing equations (22) and (24), it is seen that the presence of the magnetic field has a lesser effect on the overall heat transfer than on the local heat transfer.

Equations (22) and (24) may be regarded as computational formulas for q and Q provided that q_0 and Q_0 are known. These may be evaluated from equations (21) and (25) in conjunction with the $\theta_0'(0)$ values of Table 1. When equations (22) and (24) are used for Prandtl numbers other than those considered here, then results for q_0 and Q_0 are available in Refs. 11 and 12, the former being most useful in the range of high Prandtl numbers and the latter for the liquid metal range.

Comparison with other solutions

It is interesting to see how the results from the present analysis relate to those of other investigations. As previously mentioned, the only reliable results currently available are those for the isothermal plate with a magnetic field which varies as $x^{-1/4}$ (i.e. the similarity case). Although this is different from the uniform field case considered here, it still may be interesting to compare the heat transfer results. One of the possible comparisons is to look at the local heat transfer predictions under the condition that the local values of the magnetic parameter ξ in the two analyses (z in Ref. 5) are identical. The local equality of the ξ parameters at a given x can be achieved by arranging the magnetic field strengths to have identical values at that x.* Making use of the analogue computer solutions of Ref. 5 for the similarity case and of equation (22) and Table 1 for the uniform field case, remarkably close agreement between the heat transfer predictions was found for all Prandtl numbers for ξ up to and including unity. This finding suggests that, at least for situations where the magnetic field has a moderate effect on heat transfer (~10–15 per cent), the local heat transfer reduction is not much influenced by the details of the upstream variation of magnetic field. For ξ values exceeding unity, the analogue computer solutions for the similarity case are available only for a Prandtl number of 0·73. For these higher ξ values, the agreement between the local heat

* The field strength for the similarity case would therefore be larger at smaller values of x.

transfer results from the two analyses is not so good, those from the present study being lower. This deviation may be due either to the differences in the upstream magnetic field variation or perhaps, to the series truncation of equation (22). For the more important low Prandtl range, only approximate results are available for the similarity case for $\xi > 1$.

REFERENCES

1. W. B. Bush, Magnetohydrodynamic-hypersonic flow past a blunt body. *J. Aero. Space Sci.* **25**, 685–690 (1958).
2. W. H. Kemp, Author's reply in Readers' Forum. *J. Aero. Space Sci.* **26**, 672 (1959).
3. Robert V. Hess, Some aspects of magnetohydrodynamic boundary layer flows. *N.A.S.A. Memo* 4-9-59L (1959).
4. A. S. Gupta, Steady and transient free convection of an electrically conducting fluid from a vertical plate in the presence of a magnetic field. *Appl. Sci. Res.* A **9**, 319–333 (1960).
5. Paul S. Lykoudis, Natural convection of an electrically conducting fluid in the presence of a magnetic field. *Tenth Int. Congr. Appl. Mech.*, Stresa, Italy, September, 1960.
6. Barry L. Reeves, Similar solutions of the free convection boundary layer equations for an electrically conducting fluid. *J. Amer. Rocket Soc.* **31**, 557–558 (1961).
7. Y. Mori, On a laminar free-convection flow and heat transfer of electrically conducting fluid on a vertical plate in the presence of a transverse magnetic field. *Trans. Japan Soc. Aero. Space Sci.* **2**, 22–26 (1959).
8. E. R. G. Eckert and Robert M. Drake, Jr., *Heat and Mass Transfer*. McGraw-Hill, New York (1959).
9. Vernon J. Rossow, On flow of electrically conducting fluids over a flat plate in the presence of a transverse magnetic field. *N.A.C.A. Tech. Note* 3971 (1957).
10. Max Jakob, *Heat Transfer*, Vol. 1. John Wiley, New York (1949).
11. Simon Ostrach, An analysis of laminar free-convection heat transfer about a flat plate parallel to the direction of the generating body force. *N.A.C.A. Rep.* 1111 (1953).
12. E. M. Sparrow and J. L. Gregg, Details of exact low Prandtl number boundary-layer solutions for forced and for free convection. *N.A.S.A. Memo* 2-27-59E (1959).
13. Simon Ostrach, Laminar flows with body forces. Section D, Vol. IV, *Princeton Series on High Speed Flow and Jet Propulsion* (1961).

Vol. 3 1961

Int. J. Heat Mass Transfer. Vol. 3, pp. 275–291. Pergamon Press 1961. Printed in Great Britain.

CONVECTION DE LA CHALEUR DANS UN GAZ EN RÉGIME LAMINAIRE DANS LE CAS D'UN GRADIENT DE PRESSION ET D'UNE TEMPÉRATURE DE PAROI QUELCONQUES

BERNARD LE FUR

Laboratoire d'Aérothermique, Sorbonne, Paris, France

(*Received* 20 *April* 1961)

Résumé—Une nouvelle transformation généralisant celle d'Illingworth–Stewartson permet de ramener les équations de la couche limite laminaire compressible aux équations de la couche limite incompressible, lorsque les distributions de vitesse extérieure et de température pariétale sont quelconques. Pour cela, on utilise une enthalpie de référence généralisant celle de Monaghan et l'on néglige les termes de gradient de pression dans les équations transformées.

La comparaison entre les résultats obtenus ainsi et ceux de l'intégration des équations complètes dans les cas étudiés par Cohen et Reshotko montre que les profils de vitesse et de température sont presque identiques, tout au moins quand la température pariétale est comprise entre la moitié et le double de la température totale. Lorsque la température pariétale décroît, l'erreur augmente en restant inférieure à 7,3 pour cent, par exemple, pour le coefficient de convection au point d'arrêt dans un écoulement bidimensionnel, le nombre de Prandtl du gaz étant égal à 1.

Lorsque la température de la paroi d'un obstacle quelconque est faible devant la température totale, la densité de flux de chaleur pariétale est donnée par une formule différant légèrement de celle de Lees.

Abstract—A new transformation, generalizing Illingworth–Stewartson's, transforms the compressible laminar boundary layer equations to the incompressible boundary layer equations, for any external velocity and wall temperature distributions. For this, a reference enthalpy, generalizing Monaghan's formula, is employed; pressure gradient terms are neglected in the transformed equations.

Comparison between results obtained thus and those obtained by Cohen and Reshotko by integrating the full equations shows that the velocity and temperature profiles are almost identical, at least when the wall temperature lies between half and twice the stagnation temperature. When the wall temperature decreases, the error rises while staying below 7·3 per cent, for example, in computing the heat transfer coefficient at a two-dimensional stagnation point with the gas Prandtl number equal to 1.

When the wall temperature of an arbitrary body is small compared with the stagnation temperature, the heat-transfer rate at the wall is given by a formula differing slightly from that of Lees.

Zusammenfassung—Eine neue Transformation, welche die von Illingworth–Stewartson verallgemeinert, gestattet es, die Gleichungen der laminaren, kompressiblen Grenzschicht auf die Gleichungen der inkompressiblen Grenzschicht zurückzuführen bei beliebiger Verteilung der äusseren Geschwindigkeit und der Wandtemperatur. Hierzu wird eine gegenüber Monaghan verallgemeinerte Bezugsenthalpie verwendet; die Terme des Druckgradienten werden in den transformierten Gleichungen vernachlässigt.

Der Vergleich zwischen den so erhaltenen Resultaten und denen der Integration der vollständigen Gleichungen in den von Cohen und Reshotko behandelten Fällen zeigt, dass die Profile der Geschwindigkeit und der Temperatur fast identisch sind, mindestens dann, wenn die Wandtemperatur zwischen der Hälfte und dem Doppelten der Gesamttemperatur liegt. Bei fallender Wandtemperatur wächst der Fehler an, bleibt aber z.B. kleiner als 7,3% für den Übergangskoeffizienten im Staupunkt einer zweidimensionalen Strömung bei einer Prandtlzahl des Gases von 1.

Wenn die Wandtemperatur eines beliebigen Hindernisses klein ist gegen die Gesamttemperatur, lässt sich die Wärmestromdichte an der Wand durch eine Gleichung wiedergeben, die etwas von der Gleichung nach Lees abweicht.

Аннотация—В статье приводится новое обобщенное преобразование Иллингворча–Стюартсона, которое позволяет вывести уравнения ламинарного пограничного слоя для сжимаемого газа из уравнения ламинарного пограничного слоя при любом

распределении внешних пристенных скоростей и температуры. Для этого, в отличие от Монагана, используется обобщенная относительная энтальпия и не учитываются члены градиента давления в преобразованных уравнениях.

Сравнение полученных данных с результатами интегрирования полных уравнений в рассмотренных Кохеном и Решотко случаях показывает, что профили скорости и температуры почти тождественны. С понижением пристеночной температуры погрешность увеличивается, однако остаётся меньше 7,3%, например для коэффициента конвекции в критической точке двумерного потока при числе Прандтля для газа равном $\frac{1}{2}$. Когда температура стенки ниже полной температуры, то плотность потока тепла на стенке может быть выражена уравнением, которое несколько отличается от уравнения Лиса.

NOTATIONS

x, abscisse curviligne prise le long d'un profil ou d'un méridien;
y, ordonnée prise perpendiculairement à la paroi;
R, rayon;
u, composante de la vitesse le long de l'axe des x;
v, composante de la vitesse le long de l'axe des y;
θ, température absolue;
a, célérité du son;
M, nombre de Mach;
ρ, masse volumique;
ψ, fonction de courant;
μ, viscosité;
ν, viscosité cinématique;
τ, tension de frottement;
λ, coefficient de conductibilité;
c_p, chaleur spécifique à pression constante;
γ, rapport des chaleurs spécifiques;
h, enthalpie massique;
Φ_p, densité de flux de chaleur à la paroi;
θ_f, température de frottement;
θ_{eff}, température effective locale;
p, pression statique;
Pr, nombre de Prandtl;
r, facteur thermique pariétal de frottement;
r_h, facteur enthalpique pariétal de frottement;
r_c, facteur enthalpique pariétal de convection local;
α, coefficient de convection local;
R_x, nombre de Reynolds rapporté à x;
C_h, coefficient de transport d'enthalpie (ou nombre de Stanton).

Indices inférieurs

e, écoulement extérieur à la couche limite;
p, conditions à la paroi;
i, conditions à l'arrêt en un point quelconque;
t, conditions à l'arrêt à l'extérieur de la couche limite;
r, grandeurs de référence;
f, conditions à la paroi thermiquement isolée;
1, première approximation;
m, conditions à l'enthalpie moyenne.

Indices supérieurs

$(\ )^*$, grandeurs transformées par la nouvelle transformation;
$(\tilde{\ })$, grandeurs transformées par la transformation de Cohen et Reshotko;
$(\ ')$, grandeurs correspondant à l'équation de l'énergie sans second membre.

INTRODUCTION

Lorsque, dans un gaz, les vitesses et les différences de température ne sont plus très faibles, il faut tenir compte de la variation des propriétés physiques dans les équations de la couche limite laminaire.

Dans le cas particulier où la chaleur spécifique à pression constante c_p est constante, le nombre de Prandtl Pr est égal à 1, la viscosité μ proportionnelle à la température absolue θ et la paroi de l'obstacle thermiquement isolée, les équations de la couche limite peuvent se ramener aux équations de la couche limite incompressible. Cette possibilité avait été démontrée rigoureusement pour la plaque plane par Dorodnitzin [1] et Howarth [2]. Elle a été étendue au cas où la distribution de vitesse extérieure $u_e(x)$ est quelconque par Stewartson [3] et Illingworth [4].

On sait que, si l'on abandonne les hypothèses précédentes, les équations de l'impulsion et de

Vol. 3 1961

l'énergie ne peuvent plus être rendues indépendantes. Nous allons montrer qu'on peut encore se ramener à une couche limite incompressible dans des conditions plus générales et notamment lorsque la température de paroi est quelconque. Pour cela, nous devrons utiliser certaines hypothèses de calcul simplificatrices.

Nous supposerons que le gaz est parfait, mais que c_p est, en général, fonction de θ. D'autre part, la loi de variation de μ en fonction de θ ne sera pas imposée a priori. Le nombre de Prandtl Pr sera supposé constant, mais pas forcément égal à 1.

L'écoulement en dehors de la couche limite sera supposé isentropique.

1. ÉQUATIONS GÉNÉRALES

1.1. *Équations de Prandtl*

On sait que les équations de conservation de la masse, de la composante longitudinale de l'impulsion et de l'énergie dans la couche limite laminaire, dans un écoulement permanent et bidimensionnel, sont:

$$\frac{\partial(\rho u)}{\partial x} + \frac{\partial(\rho v)}{\partial y} = 0, \tag{1}$$

$$\rho u \frac{\partial u}{\partial x} + \rho v \frac{\partial u}{\partial y} = \rho_e u_e \frac{\mathrm{d}u_e}{\mathrm{d}x} + \frac{\partial}{\partial y}\left(\mu \frac{\partial u}{\partial y}\right), \tag{2}$$

$$\rho u \frac{\partial h}{\partial x} + \rho v \frac{\partial h}{\partial y} = \rho_e u \frac{\mathrm{d}h_e}{\mathrm{d}x} + \frac{\partial}{\partial y}\left(\frac{\mu}{Pr} \cdot \frac{\partial h}{\partial y}\right) + \mu\left(\frac{\partial u}{\partial y}\right)^2. \tag{3}$$

1.2. *Équations de von Mises*

Effectuons la transformation de von Mises [5] qui consiste à prendre, comme variables indépendantes, l'abscisse x et la fonction de courant ψ définie par:

$$u = \frac{1}{\rho} \cdot \frac{\partial \psi}{\partial y} \quad \text{et} \quad v = -\frac{1}{\rho} \cdot \frac{\partial \psi}{\partial x}, \tag{4}$$

et telle que $\psi = 0$ lorsque $y = 0$.

Les trois équations de la couche limite (1), (2) et (3) se réduisent à deux:

$$\rho u \frac{\partial u}{\partial x} - \rho_e u_e \frac{\mathrm{d}u_e}{\mathrm{d}x} - \rho u \frac{\partial}{\partial \psi}\left(\mu \rho u \frac{\partial u}{\partial \psi}\right) = 0, \tag{5}$$

$$\rho u \frac{\partial h}{\partial x} - \rho_e u \frac{\mathrm{d}h_e}{\mathrm{d}x} - \rho u \frac{\partial}{\partial \psi}\left(\frac{\mu \rho u}{Pr} \cdot \frac{\partial h}{\partial \psi}\right) = \mu \rho^2 u^2 \left(\frac{\partial u}{\partial \psi}\right)^2. \tag{6}$$

Prenons comme variables dépendantes:

$$\left.\begin{aligned} Z(x, \psi) &= u_e^2(x) - u^2(x, \psi), \\ T(x, \psi) &= \theta(x, \psi) - \theta_e(x), \\ \text{et} \qquad H(x, \psi) &= h(x, \psi) - h_e(x). \end{aligned}\right\} \tag{7}$$

Comme l'enthalpie ne dépend que de θ, $T(x, \psi)$ sera fonction de $H(x, \psi)$ et de $h_e(x)$. En effet:

$$T(x, \psi) = \theta(H + h_e) - \theta(h_e),$$

la fonction $\theta(h)$ étant la fonction inverse de $h(\theta) = \int_0^\theta c_p(\theta)\mathrm{d}\theta$.

Les équations (5) et (6) deviennent, en tenant compte de l'équation d'état des gaz parfaits:

$$\frac{\partial Z}{\partial x} - u \frac{\partial}{\partial \psi}\left(\mu \rho \frac{\partial Z}{\partial \psi}\right) = -\frac{2u_e}{\theta_e} \cdot \frac{\mathrm{d}u_e}{\mathrm{d}x} T, \tag{8}$$

$$\frac{\partial H}{\partial x} - \frac{1}{Pr} \cdot \frac{\partial}{\partial \psi}\left(\mu \rho u \frac{\partial H}{\partial \psi}\right) + \frac{u_e}{\theta_e} \cdot \frac{\mathrm{d}u_e}{\mathrm{d}x} T = -\frac{\mu \rho}{2} \cdot \frac{\partial u}{\partial \psi} \cdot \frac{\partial Z}{\partial \psi}, \tag{9}$$

avec les conditions aux limites:

$$\left.\begin{aligned} &\lim_{x \to 0} Z(x, \psi) = 0, \\ &\lim_{\psi \to 0} Z(x, \psi) = u_e^2(x), \\ &\lim_{\psi \to \infty} Z(x, \psi) = 0, \end{aligned}\right\} \tag{10}$$

et:

$$\left.\begin{aligned} &\lim_{x \to 0} H(x, \psi) = 0, \\ &\lim_{\psi \to 0} H(x, \psi) = h_p(x) - h_e(x), \\ &\lim_{\psi \to \infty} H(x, \psi) = 0. \end{aligned}\right\} \tag{11}$$

1.3. *Enthalpie de référence*

1.3.1. *Plaque plane.* On sait que l'on a pu intégrer numériquement les équations de la couche limite sur une plaque plane à température uniforme en tenant compte de la variation de μ et de Pr en fonction de h. On peut retrouver respectivement les valeurs de τ_p et de Φ_p en utilisant les formules de la couche limite à propriétés physiques constantes dans lesquelles les valeurs de μ, de ρ et de Pr sont celles que posséderait le gaz pour la même pression et pour une enthalpie h_r dite enthalpie de référence.

Eckert [6] a remarqué que l'on pouvait choisir, sans grande erreur, pour le calcul de τ_p et de Φ_p, dans le cas de l'air, la même enthalpie de référence, celle-ci étant une fonction linéaire empirique des enthalpies pariétale h_p, effective h_{eff}† et extérieure à la couche limite h_e:

$$h_r = h_e + 0{,}50(h_p - h_e) + 0{,}22\,(h_{\text{eff}} - h_e), \quad (12)$$

avec:

$$h_{\text{eff}} = h_e + r_c(h_t - h_e), \quad (13)$$

r_c étant le facteur enthalpique pariétal de convection local, égal environ à $[Pr(h_r)]^{1/2}$.

Lorsque le nombre de Prandtl n'est pas constant, l'enthalpie effective n'est égale à l'enthalpie de frottement h_f que si l'on a $\Phi_p = 0$, ($h_{\text{eff}} = h_p$).

Monaghan [7] a montré que l'on avait aussi une bonne approximation en choisissant comme enthalpie de référence la moyenne h_m de l'enthalpie par rapport à u, x étant laissé constant:

$$h_r = h_m = \int_0^1 h\ \mathrm{d}(u/u_e) = \frac{1}{u_e} \cdot \int_0^\infty h(x, \psi)\, \frac{\partial u}{\partial \psi}\, \mathrm{d}\psi. \quad (14)$$

Si l'on remplace dans les équations μ, ρ et Pr par les valeurs μ_m, $\rho_m = \rho_e\theta_e/\theta_m$ et $Pr(h_m)$, on voit qu'elles se ramènent aux équations de la couche limite à propriétés physiques constantes. En remplaçant dans (14) $h(x, \psi)$ et $u(x, \psi)$ par les expressions approchées obtenues ainsi, l'on obtiendra, pour $Pr = 0{,}725$, qui correspond à la valeur moyenne du nombre de Prandtl de l'air, l'expression donnée par Monaghan:

$$h_r = h_e + 0{,}54\,(h_p - h_e) + 0{,}16\,(h_{\text{eff}} - h_e). \quad (15)$$

1.3.2. *Équations simplifiées.* Dans le cas plus général d'une distribution quelconque de pression sur un obstacle à température non-uniforme, nous essaierons de généraliser la notion d'enthalpie de référence. Si nous examinons les équations (5) et (6), nous voyons que les propriétés physiques n'interviennent que par le groupement $\mu\rho u$; il semble donc assez logique d'utiliser l'enthalpie moyenne (14) comme enthalpie de référence, de préférence à l'enthalpie de paroi ou à l'enthalpie de l'écoulement libre.

Nous remplacerons donc, dans les équations (8) et (9), le groupement $\mu\rho$, fonction de x et de ψ, par la valeur $\mu_r\rho_r$, fonction de x seulement, qu'il prendra pour la même pression $p_e(x)$ et l'enthalpie de référence (14). Cette enthalpie sera déterminée a posteriori à l'aide des profils de vitesse $u(x, \psi)$ et d'enthalpie $h(x, \psi)$ obtenus grâce à l'intégration des équations simplifiées.

Les valeurs de la tension de frottement pariétale τ_p et de la densité pariétale de flux de chaleur Φ_p seront obtenues à l'aide des formules suivantes:

$$\tau_p = \lim_{\psi \to 0} \left(\mu\rho u\, \frac{\partial u}{\partial \psi}\right), \quad (16)$$

et

$$\Phi_p = -\frac{1}{Pr} \lim_{\psi \to 0} \left(\mu\rho u\, \frac{\partial h}{\partial \psi}\right), \quad (17)$$

où $\mu\rho$ sera également remplacé par $\mu_r\rho_r$.

1.4. *Équation transformée de l'impulsion*

Nous allons poser:

$$\left.\begin{aligned} x^* &= \int_0^x \frac{\mu_r\rho_r}{\mu_t\rho_t}\, \epsilon(x)\, \mathrm{d}x, \\ y^* &= \epsilon(x) \int_0^y \frac{\rho}{\rho_t}\, \mathrm{d}y, \\ u^* &= u/\epsilon(x), \end{aligned}\right\} \quad (18)$$

$\epsilon(x)$ étant une fonction que l'on déterminera plus loin; μ_t et ρ_t étant la viscosité et la masse

† L'enthalpie effective est celle qui s'introduit dans la définition du coefficient de convection:

$$\Phi_p = \frac{a}{c_p(\theta_p)}\,(h_p - h_{\text{eff}});$$

on trouvera plus loin, 1.5.2, une définition plus précise.

Vol. 3 1961

volumique qu'aurait le gaz à l'extérieur de la couche limite s'il était ramené isentropiquement au repos.

L'équation de l'impulsion s'écrira, en utilisant les grandeurs étoilées, et en posant:

$$\psi^* = \int_0^{y^*} \rho_t u^* \mathrm{d}y^* = \psi, \tag{19}$$

et

$$Z^* = u_e^{*2} - u^{*2}, \tag{20}$$

$$\frac{\partial Z^*}{\partial x^*} - \mu_t \rho_t u^* \frac{\partial^2 Z^*}{\partial \psi^{*2}} = - \frac{2u_e}{\theta_e} \cdot \frac{\mathrm{d}u_e}{\mathrm{d}x^*} \cdot \frac{T}{\epsilon^2} - \frac{2}{\epsilon} \cdot \frac{\mathrm{d}\epsilon}{\mathrm{d}x^*} Z^*. \tag{21}$$

Le second membre de l'équation (21) s'annule lorsque ψ^* croît indéfiniment. Nous allons choisir $\epsilon(x)$ de telle façon que ce second membre s'annule aussi à la paroi.

Il faut donc que:

$$\frac{1}{\epsilon} \cdot \frac{\mathrm{d}\epsilon}{\mathrm{d}x^*} = - \frac{\theta_p - \theta_e}{\theta_e} \cdot \frac{1}{u_e} \cdot \frac{\mathrm{d}u_e}{\mathrm{d}x^*}. \tag{22}$$

$\epsilon(x)$ sera défini par la formule:

$$\epsilon(x) = C^{te} \exp \left[- \int_{x_0}^{x} \frac{\theta_p - \theta_e}{\theta_e} \cdot \frac{\mathrm{d}u_e}{u_e} \right]. \tag{23}$$

La constante et l'abscisse x_0 sont arbitraires et indépendantes; x_0 peut être pris égal à zéro, sauf si la vitesse u_e s'annule à l'origine.

Le second membre de (21) est égal alors à:

$$\left.\begin{aligned} &- \frac{2u_e}{\theta_e} \cdot \frac{\mathrm{d}u_e}{\mathrm{d}x^*} \cdot \frac{1}{\epsilon^2(x)} \\ &\left[\theta - \theta_e - (\theta_p - \theta_e)\left(1 - \frac{u^2}{u_e^2}\right)\right] = \\ &- \frac{2u_e^2}{\theta_t} \cdot \frac{1}{M_e} \cdot \frac{\mathrm{d}M_e}{\mathrm{d}x} \cdot \frac{\mu_t \rho_t}{\mu_r \rho_r} \cdot \frac{1}{\epsilon^3(x)} \\ &\left[\theta - \theta_e - (\theta_p - \theta_e)\left(1 - \frac{u^2}{u_e^2}\right)\right]. \end{aligned}\right\} \tag{24}$$

Ce terme est peu important, lorsque:

(a) soit, u_e est faible;
(b) soit, M_e est élevé;
(c) soit, $\mathrm{d}M_e/\mathrm{d}x$ est faible;
(d) soit, θ_p est voisin de θ_f, Pr étant voisin de 1.

Nous allons à présent négliger le second membre de l'équation (21), qui se ramène alors à l'équation de l'impulsion dans une couche limite fictive à propriétés physiques constantes μ_t et ρ_t:

$$\frac{\partial Z^*}{\partial x^*} - \mu_t \rho_t u^* \frac{\partial^2 Z^*}{\partial \psi^{*2}} = 0. \tag{25}$$

On peut donc utiliser les méthodes générales de la couche limite à propriétés physiques constantes comme, par exemple, celles approchées de Pohlhausen et de Eckert [8] ou celle exacte de Görtler [9]. On pourra également choisir la méthode d'intégration par approximations successives de la Réf. 10.

Une fois calculée la tension de frottement pariétale fictive:

$$\tau_p^* = \mu_t (\partial u^*/\partial y^*)_p,$$

la véritable tension de frottement pariétale τ_p sera obtenue grâce à (16), c'est-à-dire que:

$$\tau_p = \frac{\mu_r \rho_r}{\mu_t \rho_t} \epsilon^2(x) \, \tau_p^*. \tag{26}$$

1.5. *Équation transformée de l'énergie*

Si l'on fait les changements de variables (18), (19) et (20), l'équation de l'énergie deviendra:

$$\frac{\partial H}{\partial x^*} - \frac{\mu_t \rho_t}{Pr} \cdot \frac{\partial}{\partial \psi^*}\left(u^* \frac{\partial H}{\partial \psi^*}\right) + \frac{u_e}{\theta_e} \cdot \frac{\mathrm{d}u_e}{\mathrm{d}x^*} T = - \frac{\mu_t \rho_t}{2} \epsilon^2(x) \frac{\partial u^*}{\partial \psi^*} \cdot \frac{\partial Z^*}{\partial \psi^*}. \tag{27}$$

1.5.1. *Solution particulière.* Soit $(H)_f$ la solution particulière de l'équation (27) correspondant à une densité de flux de chaleur nulle à la paroi et $(T)_f$ la fonction définie par:

$$(T)_f = \theta[(H)_f + h_e] - \theta_e,$$

nous aurons:

$$\frac{\partial (H)_f}{\partial x^*} - \frac{\mu_t \rho_t}{Pr} \cdot \frac{\partial}{\partial \psi^*}\left(u^* \frac{\partial (H)_f}{\partial \psi^*}\right) + \frac{u_e}{\theta_e} \cdot \frac{\mathrm{d}u_e}{\mathrm{d}x^*} (T)_f = - \frac{\mu_t \rho_t}{2} \epsilon^2(x) \frac{\partial u^*}{\partial \psi^*} \cdot \frac{\partial Z^*}{\partial \psi^*}. \tag{28}$$

$(H)_f$ doit obéir aux conditions aux limites suivantes:

$$\left.\begin{aligned} &\lim_{x^*\to 0}(H)_f = 0,\\ &\lim_{\psi^*\to 0}\psi^{*1/2}\cdot\frac{\partial(H)_f}{\partial\psi^*} = 0,\\ &\lim_{\psi^*\to\infty}(H)_f = 0. \end{aligned}\right\} \quad (29)$$

Posons:

$$(H)_f^* = (H)_f/\epsilon^2(x). \quad (30)$$

L'équation (24) devient, en utilisant la relation (22):

$$\left.\begin{aligned} &\frac{\partial(H)_f^*}{\partial x^*} - \frac{\mu_t\rho_t}{Pr}\cdot\frac{\partial}{\partial\psi^*}\left(u^*\frac{\partial(H)_f^*}{\partial\psi^*}\right)\\ &-\frac{2}{u_e}\cdot\frac{\mathrm{d}u_e}{\mathrm{d}x^*}\left[\frac{\theta_p-\theta_e}{\theta_e}(H)_f^* - \frac{u_e^2}{2\theta_e}\cdot\frac{(T)_f}{\epsilon^2(x)}\right] =\\ &\qquad -\frac{\mu_t\rho_t}{2}\cdot\frac{\partial u^*}{\partial\psi^*}\cdot\frac{\partial Z^*}{\partial\psi^*}. \end{aligned}\right\} \quad (31)$$

Le troisième terme du premier membre est, à la paroi, égal à:

$$\left.\begin{aligned} &-\frac{2}{u_e}\cdot\frac{\mathrm{d}u_e}{\mathrm{d}x^*}\cdot\frac{1}{\theta_e\epsilon^2(x)}[(\theta_p-\theta_f)(h_f-h_e)\\ &+(\theta_f-\theta_e)(h_f-h_t)] =\\ &\quad -\frac{2}{\theta_t}\cdot\frac{1}{M_e}\cdot\frac{\mathrm{d}M_e}{\mathrm{d}x}\cdot\frac{\mu_t\rho_t}{\mu_r\rho_r}\cdot\frac{1}{\epsilon^3(x)}\\ &\times[(\theta_p-\theta_f)(h_f-h_e)\\ &\qquad +(\theta_f-\theta_e)(h_f-h_t)], \end{aligned}\right\} \quad (32)$$

où h_f et θ_f sont respectivement l'enthalpie et la température de frottement.

Cette expression est faible dans les cas (a), (b), (c), (d) envisagés au paragraphe 1.4.

Si nous négligeons le troisième terme du premier membre, nous aurons donc:

$$\frac{\partial(H)_f^*}{\partial x^*} - \frac{\mu_t\rho_t}{Pr}\cdot\frac{\partial}{\partial\psi^*}\left(u^*\frac{\partial(H)_f^*}{\partial\psi^*}\right) = -\frac{\mu_t\rho_t}{2}\cdot\frac{\partial u^*}{\partial\psi^*}\cdot\frac{\partial Z^*}{\partial\psi^*}. \quad (33)$$

Cette équation est identique à l'équation de l'énergie dans une couche limite fictive à viscosité et masse volumique constantes, le nombre de Prandtl étant resté le même.

Les conditions aux limites (29) combinées avec (30) montrent que, dans la couche limite fictive, la paroi doit être également thermiquement isolée. Nous pourrons donc calculer le facteur enthalpique pariétal de frottement:

$$r_h = \frac{h_f-h_e}{h_t-h_e} = \lim_{\psi^*\to 0}\left[\frac{2(H)_f^*}{u_e^{*2}}\right]. \quad (34)$$

Si l'on utilise la méthode de la Réf. 11, on voit qu'en première approximation r_h est non seulement indépendant du gradient de pression, mais encore du nombre de Mach de l'écoulement amont:

$$r_h = r_1(Pr) = Pr_2^{1/3}F_1\left(\tfrac{1}{3},\tfrac{2}{3};\tfrac{4}{3};\frac{Pr-1}{Pr}\right), \quad (35)$$

cette formule étant valable lorsque $\frac{1}{2} < Pr < \infty$.

1.5.2. *Équation sans second membre.* Posons:

$$\hat{H} = H - (H)_f \quad (36)$$

et:

$$\hat{T} = T - (T)_f. \quad (37)$$

$\hat{H}$ sera solution de l'équation sans second membre:

$$\frac{\partial\hat{H}}{\partial x^*} - \frac{\mu_t\rho_t}{Pr}\cdot\frac{\partial}{\partial\psi^*}\left(u^*\frac{\partial\hat{H}}{\partial\psi^*}\right) + \frac{u_e}{\theta_e}\cdot\frac{\mathrm{d}u_e}{\mathrm{d}x^*}\hat{T} = 0, \quad (38)$$

et satisfera aux conditions aux limites suivantes:

$$\left.\begin{aligned} &\lim_{x^*\to 0}\hat{H} = 0,\\ &\lim_{\psi^*\to 0}\hat{H} = h_p(x^*) - h_f(x^*),\\ &\lim_{\psi^*\to\infty}\hat{H} = 0. \end{aligned}\right\} \quad (39)$$

Le troisième terme du premier membre de (38) est, à la paroi, égal à:

$$\frac{u_e}{\theta_e}\cdot\frac{\mathrm{d}u_e}{\mathrm{d}x^*}(\theta_p-\theta_f) = \frac{u_e^2}{\theta_t}\cdot\frac{1}{M_e}\cdot\frac{\mathrm{d}M_e}{\mathrm{d}x}\cdot\frac{\mu_t\rho_t}{\mu_r\rho_r}\cdot\frac{\theta_p-\theta_f}{\epsilon(x)}. \quad (40)$$

Cette expression est faible dans les quatre cas envisagés au paragraphe 1.4.

Vol. 3 1961

Si on néglige le troisième terme du premier membre, on obtiendra:

$$\frac{\partial \hat{H}}{\partial x^*} - \frac{\mu_t \rho_t}{Pr} \cdot \frac{\partial}{\partial \psi^*}\left(u^* \frac{\partial \hat{H}}{\partial \psi^*}\right) = 0. \quad (41)$$

Cette équation est identique à l'équation de l'énergie sans second membre, dans une couche limite fictive à viscosité et masse volumique constantes, le nombre de Prandtl étant resté le même.

Nous pourrons donc employer les méthodes de la couche limite à propriétés physiques constantes en y remplaçant $c_p\theta$ par h. Si la température de la paroi est uniforme, on pourra, par exemple, utiliser les solutions d'Eckert [12] correspondant au cas où $u_e^* = cx^{*m}$, comme l'ont fait Brun et Vasseur [13] et Merk [14]. Dans le cas général d'une température de paroi non-uniforme, on pourra appliquer la méthode d'intégration par approximations successives de la Réf. 10, dont la première approximation est décrite dans la Réf. 11.

Une fois calculée la densité pariétale fictive de flux de chaleur:

$$\Phi_p^* = -\frac{\mu_t \rho_t}{Pr} \lim_{\psi^* \to 0}\left(u^* \frac{\partial \hat{H}}{\partial \psi^*}\right), \quad (42)$$

on obtiendra la véritable densité pariétale de flux de chaleur Φ_p grâce à la formule (17), soit:

$$\Phi_p = \frac{\mu_r \rho_r}{\mu_t \rho_t}\, \epsilon(x)\, \Phi_p^*. \quad (43)$$

On peut définir les enthalpies effectives locales dans la couche limite fictive de la façon suivante: supposons que l'enthalpie pariétale $h_p(x^*)$ soit de la forme $h_t + aP(x^*)$, l'enthalpie effective locale $h_{\text{eff}}(x^*)$, en un point d'abscisse x^*, sera la valeur de l'enthalpie pariétale pour laquelle Φ_p^* s'annule lorsque l'on fait varier le paramètre a, les expressions $\mu_r \rho_r$ et $\epsilon(x)$ restant inchangées.

Le coefficient de convection local dans la couche limite réelle sera défini par la formule:

$$\alpha = \frac{\Phi_p\, c_p(\theta_p)}{h_p - h_{\text{eff}}}. \quad (44)$$

Comme h_r et $\epsilon(x)$ dépendent en réalité de h_p, α et h_{eff} en dépendront également et leur considération offre dans ce cas moins d'intérêt que dans celui où les propriétés physiques peuvent être supposées constantes. On présentera en général les résultats des calculs sous la forme de la fonction $\Phi_p(x)$, pour chaque distribution de température pariétale $\theta_p(x)$ envisagée.

2. ÉTUDE DE LA NOUVELLE TRANSFORMATION

La nouvelle transformation prend une forme plus simple dans deux cas particuliers qui se présentent assez souvent en pratique.

2.1. *Paroi thermiquement isolée*

Lorsque c_p est constant, le facteur enthalpique pariétal r_h se ramène au facteur thermique pariétal:

$$r = \frac{\theta_f - \theta_e}{\theta_t - \theta_e}.$$

Si l'on choisit pour r l'expression $r_1(Pr)$ donnée par la formule (35), $\epsilon(x)$ prend une forme très simple.

En effet:

$$\int_{x_0}^{x} \frac{\theta_{f_1} - \theta_e}{\theta_e} \cdot \frac{\mathrm{d}u_e}{u_e} = -\frac{r_1}{2}\,[\operatorname{Log}\theta_e(x) - \operatorname{Log}\theta_e(x_0)]. \quad (45)$$

En choisissant convenablement x_0 et la constante de la formule (23), pour que la couche limite réelle se raccorde, au voisinage du point d'arrêt (où $h_f = h_t$), à la couche limite fictive transformée, on obtient:

$$\epsilon(x) = (\theta_e/\theta_t)^{r1/2}. \quad (46)$$

Lorsque l'enthalpie de référence h_r est prise égale à l'enthalpie de frottement h_f, les formules de transformation (18) où l'on a remplacé $\epsilon(x)$ par (46) sont identiques aux formules obtenies auparavant par Rott [15], Tani [16] et l'auteur [17].

Ces formules avaient été établies en utilisant l'équation globale de la quantité de mouvement et diverses lois hypothétiques de température. On voit qu'ici cette restriction a été levée puisque la loi de température est obtenue à l'aide de la solution de l'équation de l'énergie transformée.

Si l'on suppose, en outre, que $Pr = 1$, on se ramène à la transformation d'Illingworth–Stewartson [3, 4], qui ne serait valable rigoureusement que si la viscosité était proportionnelle à la température absolue.

2.2. *Paroi à température uniforme*

La fonction $\epsilon(x)$ prend également, dans ce cas, une forme simple, lorsque c_p est constant.

En effet:

$$\int_{x_0}^{x} \frac{\theta_p - \theta_e}{\theta_e} \cdot \frac{\mathrm{d}u_e}{u_e} = (k-1)\,\mathrm{Log}\,[u_e(x)/u_e(x_0)] - \frac{k}{2}\,\mathrm{Log}\,[\theta_e(x)/\theta_e(x_0)], \quad (47)$$

où k est le rapport de la température de paroi θ_p à la température totale θ_t.

La forme générale de $\epsilon(x)$ sera donc:

$$\epsilon(x) = \left(\frac{u_e}{u_r}\right)^{1-k}\left(\frac{\theta_e}{\theta_t}\right)^{k/2}, \quad (48)$$

où u_r est une vitesse de référence qui joue le rôle des constantes de la formule (23).

3. PROFILS EN ANAMORPHOSE

3.1. *Équations de Cohen et Reshotko*

Pour savoir si le fait d'avoir négligé certains termes dans les équations de l'impulsion et de l'énergie conduit à des résultats différents de ceux obtenus en intégrant les équations complètes, nous allons examiner un cas où cette intégration a été effectuée.

Nous utiliserons les formules (18) où $\epsilon(x)$ sera pris égal à $(\theta_e/\theta_t)^{1/2}$. Nous désignerons les grandeurs transformées par des lettres surmontées d'un tilde:

$$\left.\begin{aligned} \tilde{x} &= \int_0^x \frac{\mu_r \rho_r}{\mu_t \rho_t}\left(\frac{\theta_e}{\theta_t}\right)^{1/2} \mathrm{d}x, \\ \tilde{y} &= \left(\frac{\theta_e}{\theta_t}\right)^{1/2} \int_0^y \frac{\rho}{\rho_t}\,\mathrm{d}y, \\ \tilde{u} &= u\left(\frac{\theta_t}{\theta_e}\right)^{1/2}. \end{aligned}\right\} \quad (49)$$

On peut montrer que, dans le cas où la température de la paroi θ_p est uniforme, c_p est constant et Pr est égal à 1, les équations de l'impulsion et de l'énergie se ramènent à des équations différentielles lorsque $\tilde{u}_e = c\tilde{x}^m$. Le nombre de Mach M_e à l'extérieur de la couche limite est alors une fonction paramétrique de x de la forme suivante:

$$\left.\begin{aligned} M_e &= c\tilde{x}^m/a_t, \\ x &= \int_0^{\tilde{x}} \frac{\mu_t \theta_r}{\mu_r \theta_t}\left(1 + \frac{\gamma-1}{2}\cdot\frac{c^2}{a_t^2}\tilde{x}^{2m}\right)^{\frac{3\gamma-1}{2(\gamma-1)}} \mathrm{d}\tilde{x}, \end{aligned}\right\} \quad (50)$$

γ étant le rapport des chaleurs spécifiques et $a = \sqrt{\{(\gamma-1)c_p\theta\}}$ étant la célérité du son dans le gaz. La température de référence θ_r est une fonction de $\tilde{x}$ qui sera déterminée après l'intégration des équations.

On doit poser:

$$\frac{u}{u_e} = \frac{\tilde{u}}{\tilde{u}_e} = f'(\beta, k; \tilde{\eta}) \quad (51)$$

ou

$$\psi = \tilde{\psi} = \rho_t \sqrt{\left(\frac{2\nu_t \tilde{u}_e \tilde{x}}{m+1}\right)} f(\beta, k; \tilde{\eta}), \quad (52)$$

et

$$\frac{\theta_i - \theta_t}{\theta_p - \theta_t} = Y_0(\beta, k; \tilde{\eta}) \left(\theta_i = \theta + \frac{u^2}{2}\right), \quad (53)$$

avec

$$\tilde{\eta} = \tilde{y}\sqrt{\left(\frac{m+1}{2}\cdot\frac{\tilde{u}_e}{\nu_t \tilde{x}}\right)}. \quad (54)$$

Les paramètres sont $\beta = 2m/(m+1)$ et k, rapport de la température de paroi θ_p à la température totale θ_t.

Les équations de l'impulsion et de l'énergie deviennent:

$$\left.\begin{aligned} &f''' + ff'' + \beta[1 - f'^2 + Y_0(k-1)] = 0, \\ &Y_0'' + fY_0' = 0. \end{aligned}\right\} \quad (55)$$

Les fonctions $f(\beta, k; \tilde{\eta})$ et $Y_0(\beta, k; \tilde{\eta})$ devront satisfaire aux conditions aux limites suivantes:

$$f(\beta, k; 0) = f'(\beta, k; 0) = 0; \quad Y_0(\beta, k; 0) = 1 \quad (56)$$

et

$$\lim_{\tilde{\eta}\to\infty} f'(\beta, k; \tilde{\eta}) = 1; \lim_{\tilde{\eta}\to\infty} Y_0(\beta, k; \tilde{\eta}) = 0. \quad (57)$$

Le système (55) a été intégré numériquement par Cohen et Reshotko [18] qui ont obtenu ainsi les profils de vitesse $u(x, y)$ et de températures d'arrêt $\theta_i(x, y)$ sous les formes anamorphosées:

$$u = u_e f'(\beta, k; \tilde{\eta})$$

Vol. 3 1961

et

$$\theta_i = \theta_t + (\theta_p - \theta_t) Y_0(\beta, k; \tilde{\eta}).$$

Pour repasser aux profils réels, on utilisera la formule paramétrique:

$$\left.\begin{aligned} y &= \left(\frac{\theta_t}{\theta_e}\right)^{\frac{5\gamma-1}{4(\gamma-1)}} \sqrt{\left(\frac{2\nu_t \tilde{x}}{(m+1)u_e}\right)} \\ &\int_0^{\tilde{\eta}} [1 + (k-1) Y_0(\beta, k; \tilde{\eta}) \\ &\quad - \frac{u_e^2}{2\theta_t} f'^2(\beta, k; \tilde{\eta})]\, \mathrm{d}\tilde{\eta}. \end{aligned}\right\} \quad (58)$$

3.2. *Application de la nouvelle transformation*

Nous allons voir à présent si la nouvelle transformation définie par les formules (18) avec l'expression (48) de $\epsilon(x)$ peut s'appliquer au cas où la distribution du nombre de Mach $M_e(x)$ est exprimée à l'aide des formules paramétriques (50).

A condition que la température de référence soit la même, nous obtiendrons, dans la couche limite fictive:

$$u_e^* = c^* x^{*m^*}, \quad (59)$$

avec

$$c^* = c\left(\frac{c}{u_r}\right)^{\frac{(m+1)(k-1)}{m(1-k)+1}} \quad (60)$$

et

$$m^* = \frac{km}{m(1-k)+1}. \quad (61)$$

On se ramènera donc aux équations de la couche limite à propriétés physiques constantes, dans le cas dit des dièdres, avec:

$$\beta^* = \frac{2m^*}{m^*+1} = \beta k \quad (62)$$

Posons:

$$\frac{u}{u_e} = \frac{u^*}{u_e^*} = f'(\beta k, 1; \eta^*) \quad (63)$$

ou

$$\psi = \psi^* = \rho_t \sqrt{\left(\frac{2\nu_t u_e^* x^*}{m^*+1}\right)} f(\beta k, 1; \eta^*), \quad (64)$$

et

$$\frac{\theta_i - \theta_t}{\theta_p - \theta_t} = Y_0(\beta k, 1; \eta^*), \quad (65)$$

avec

$$\eta^* = y^* \sqrt{\left(\frac{m^*+1}{2} \cdot \frac{u_e^*}{\nu_t x^*}\right)}. \quad (66)$$

Les équations de l'impulsion et de l'énergie dans la couche limite fictive sont:

$$\left.\begin{aligned} f''' + ff'' + \beta k(1 - f'^2) &= 0, \\ Y_0'' + fY_0' &= 0 \end{aligned}\right\} \quad (67)$$

Les fonctions $f(\beta k, 1; \eta^*)$ et $Y_0(\beta k, 1; \eta^*)$ obéissent aux conditions aux limites suivantes:

$$f(\beta k, 1; 0) = f'(\beta k, 1; 0) = 0; \quad Y_0(\beta k, 1; 0) = 1 \quad (68)$$

et

$$\lim_{\eta^* \to \infty} f'(\beta k, 1; \eta^*) = 1; \quad \lim_{\eta^* \to \infty} Y_0(\beta k, 1; \eta^*) = 0. \quad (69)$$

3.2.1. *Profils de vitesse et de température d'arrêt.* Pour pouvoir comparer les profils de vitesse et de température d'arrêt, nous allons déterminer les rapports u/u_e et $(\theta_i - \theta_t)/(\theta_p - \theta_t)$ en fonction de $\tilde{\eta}$, en partant des profils de la couche limite fictive exprimés en fonction de η^*.

En effet, comme $\psi = \tilde{\psi} = \psi^*$, on voit facilement que l'on doit avoir:

$$f(\beta, k; \tilde{\eta}) = f(\beta k, 1; \eta^*). \quad (70)$$

Nous avons porté sur les Figs. 1–5, u/u_e en fonction de $\tilde{\eta}$, pour les cas suivants:

$\beta = 0{,}5$ $\quad k = 0$ $\quad 0{,}2$ $\quad 0{,}6$ et 2,

$\beta = 1$ $\quad k = 2$,

en utilisant les profils de vitesse de la couche limite à propriétés physiques constantes calculés par Smith [19].

Nous avons porté sur les Figs. 6 et 7, $(\theta_i - \theta_t)/(\theta_p - \theta_t)$ en fonction de $\tilde{\eta}$, pour les cas suivants:

$\beta = 0{,}5$ $\quad k = 0$ et 2,

en utilisant les calculs de Görtler [20].

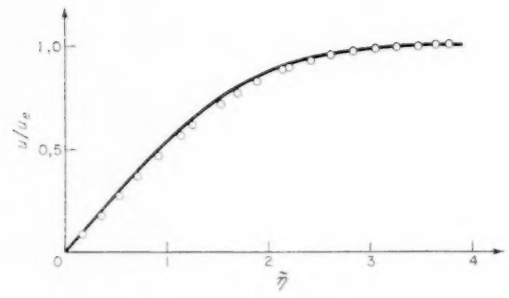

FIG. 1. $\beta = 0{,}5$; $k = 0$; $Pr = 1$
—— Cohen et Reshotko [18]
○ Méthode actuelle.

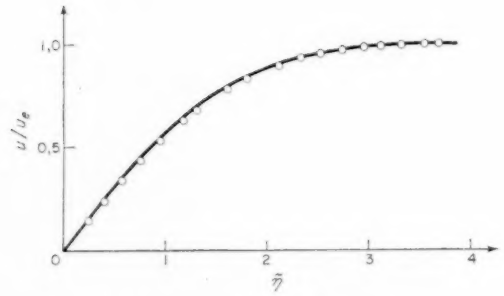

FIG. 2. $\beta = 0{,}5$; $k = 0{,}2$; $Pr = 1$
—— Cohen et Reshotko [18]
○ Méthode actuelle.

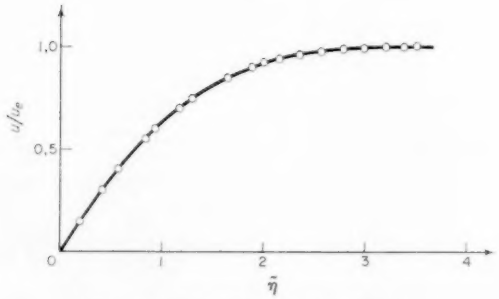

FIG. 3. $\beta = 0{,}5$; $k = 0{,}6$; $Pr = 1$
—— Cohen et Reshotko [18]
○ Méthode actuelle.

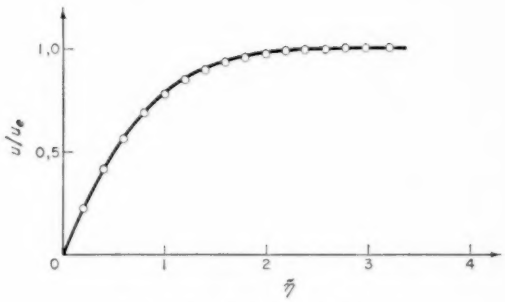

FIG. 4. $\beta = 0{,}5$; $k = 2$; $Pr = 1$
—— Cohen et Reshotko [18]
○ Méthode actuelle.

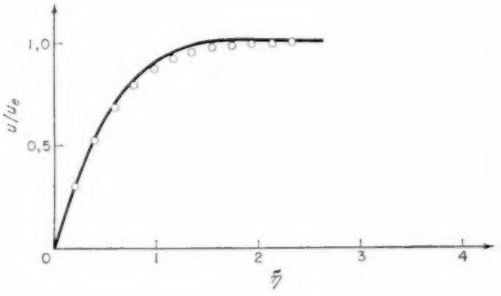

FIG. 5. $\beta = 1$; $k = 2$; $Pr = 1$
—— Cohen et Reshotko [18]
○ Méthode actuelle.

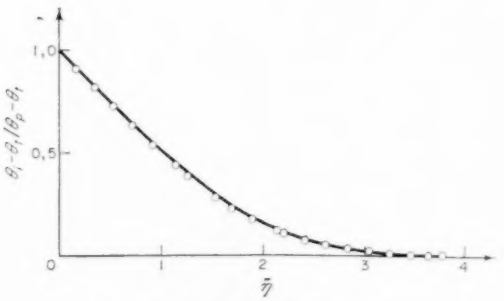

FIG. 6. $\beta = 0{,}5$; $k = 0$; $Pr = 1$
—— Cohen et Reshotko [18]
○ Méthode actuelle.

Vol. 3 1961

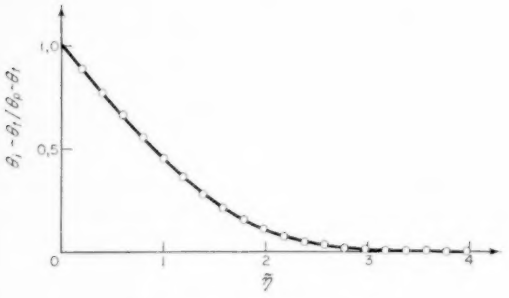

FIG. 7. $\beta = 0{,}5$; $k = 2$; $Pr = 1$
——— Cohen et Reshotko [18]
○ Méthode actuelle.

Les profils de vitesse et de température d'arrêt calculés par les deux méthodes sont presque indiscernables pour $\beta = 0{,}5$, $k = 0{,}6$ et 2. Pour $\beta = 0{,}5$, $k = 0$ et 0,2, les profils obtenus avec la nouvelle transformation sont légèrement inférieurs aux profils de Cohen et Reshotko. Dans le cas $\beta = 1$ et $k = 2$, on n'obtient évidemment pas un profil avec survitesse comme celui de Cohen et Reshotko, mais les profils sont encore assez voisins.

Remarquons que la comparaison a été faite sur les profils anamorphosés à l'aide de la variable $\tilde{\eta}$. Pour repasser aux profils réels, il faut utiliser la formule (58) dans le cas de Cohen et Reshotko, et la formule suivante:

$$y = \left(\frac{\theta_t}{\theta_e}\right)^{\frac{5\gamma-1}{4(\gamma-1)}} \sqrt{\left(\frac{2\nu_t \tilde{x}}{(m+1)u_e}\right)} \int_0^{\tilde{\eta}} [1 + (k-1)\, Y_0(\beta k, 1; \eta^*) - \frac{u_e^2}{2\theta_t} f'^2(\beta k, 1; \eta^*)]\, \mathrm{d}\tilde{\eta}, \quad (71)$$

pour les profils obtenus avec la nouvelle transformation.

3.2.2. *Coefficients de frottement et de transport d'enthalpie.* Soient la tension de frottement pariétale:

$$\tilde{\tau}_p = \mu_t \rho_t \lim_{\tilde{\psi} \to 0} \left(\tilde{u} \frac{\partial \tilde{u}}{\partial \tilde{\psi}}\right), \quad (72)$$

et le nombre de Reynolds:

$$\tilde{R}_x = \frac{\tilde{u}_e \tilde{x}}{\nu_t} = \frac{u_e}{\nu_t} \left(\frac{\theta_t}{\theta_e}\right)^{1/2} \int_0^x \frac{\mu_r \rho_r}{\mu_t \rho_t} \left(\frac{\theta_e}{\theta_t}\right)^{1/2} \mathrm{d}x. \quad (73)$$

Le coefficient de frottement sera donné par:

$$\tilde{C}_f = \frac{2\tilde{\tau}_p}{\rho_t \tilde{u}_e^2} = 2^{1/2} (m+1)^{1/2} f''(\beta, k; 0) \tilde{R}_x^{-1/2}. \quad (74)$$

D'après (26):

$$\tau_p = \frac{\mu_r \theta_t}{\mu_t \theta_r} \left(\frac{\theta_e}{\theta_t}\right)^{\frac{2\gamma-1}{\gamma-1}} \tilde{\tau}_p. \quad (75)$$

Le coefficient de frottement local obtenu à l'aide de l'intégration des équations non simplifiées (55), sera donné, en fonction de $\tilde{R}_x$, par:

$$C_f = \frac{2\tau_p}{\rho_e u_e^2} = \frac{\mu_r \theta_t}{\mu_t \theta_r} \tilde{C}_f = 2^{1/2} \frac{\mu_r \theta_t}{\mu_t \theta_r} (m+1)^{1/2} f''(\beta, k; 0) \tilde{R}_x^{-1/2}. \quad (76)$$

D'autre part, si l'on pose:

$$\tau_p^* = \mu_t \rho_t \lim_{\psi^* \to 0} \left(u^* \frac{\partial u^*}{\partial \psi^*}\right), \quad (77)$$

et:

$$R_x^* = \frac{u_e^* x^*}{\nu_t}, \quad (78)$$

on aura:

$$C_f^* = \frac{2\tau^*}{\rho_t u_e^{*2}} = 2^{1/2} (m^*+1)^{1/2} f''(\beta k, 1; 0) R_x^{*-1/2}. \quad (79)$$

D'après (26):

$$\tau_p = \frac{\mu_r \rho_r}{\mu_t \rho_t} \cdot \left(\frac{u_e}{u_r}\right)^{2(1-k)} \left(\frac{\theta_e}{\theta_t}\right)^k \tau_p^*. \quad (80)$$

Le coefficient de frottement local obtenu à l'aide de la nouvelle transformation et de l'intégration des équations simplifiées (67) sera donné par la formule approchée:

$$C_f = 2^{1/2} \frac{\mu_r \theta_t}{\mu_t \theta_r} (m+1)^{1/2} f''(\beta k, 1; 0) \tilde{R}_x^{-1/2}. \quad (81)$$

La densité de flux de chaleur pariétale dans la couche limite fictive est obtenue à l'aide de l'intégration des équations non simplifiées (55):

$$\tilde{\Phi}_p = -\mu_t c_p (\theta_p - \theta_t) \sqrt{\left(\frac{m+1}{2} \cdot \frac{\tilde{u}_e}{\nu_t \tilde{x}}\right)} Y_0'(\beta, k; 0). \quad (82)$$

Puisque $\theta_{\text{eff}} = \theta_t$ lorsque $Pr = 1$, le coefficient de transport d'enthalpie local sera alors égal à:

$$\tilde{C}_h = \frac{\tilde{\Phi}_p}{\rho_t \tilde{u}_e c_p(\theta_p - \theta_t)} = -\sqrt{\left(\frac{m+1}{2}\right)} Y_0'(\beta, k; 0)\tilde{R}_x^{-1/2}. \quad (83)$$

D'après (43):

$$\Phi_p = \frac{\mu_r \rho_r}{\mu_t \rho_t}\left(\frac{\theta_e}{\theta_t}\right)^{1/2}\tilde{\Phi}_p \quad (84)$$

et

$$C_h = \frac{\Phi_p}{\rho_e u_e c_p(\theta_p - \theta_t)} = \frac{\mu_r \theta_e}{\mu_t \theta_r}\tilde{C}_h = -\frac{\mu_r \theta_e}{\mu_t \theta_r}\sqrt{\left(\frac{m+1}{2}\right)} Y_0'(\beta, k; 0)\tilde{R}_x^{-1/2} \quad (85)$$

D'autre part, on a:

$$\Phi_p^* = -\mu_t c_p(\theta_p - \theta_t)\sqrt{\left(\frac{m^*+1}{2}\cdot\frac{u_e^*}{\nu_t x^*}\right)} Y_0'(\beta k, 1; 0). \quad (86)$$

Le coefficient de transport d'enthalpie local obtenu à l'aide la nouvelle transformation et de l'intégration des équations simplifiées sera donné par la formule approchée:

$$C_h = -\frac{\mu_r \theta_e}{\mu_t \theta_r}\sqrt{\left(\frac{m+1}{2}\right)} Y_0'(\beta k, 1; 0)\,\tilde{R}_x^{-1/2} \quad (87)$$

Nous avons porté sur les Figs. 8 et 9 les courbes représentant les variations des expressions:

$$\tilde{C}_f \tilde{R}_x^{1/2}/(m+1)^{1/2} \text{ et } \tilde{C}_h \tilde{R}_x^{1/2}/(m+1)^{1/2},$$

en fonction de β, pour les deux groupes de formules (76), (81), (85) et (87), k prenant les valeurs 0; 0,2; 0,6; 1 et 2.

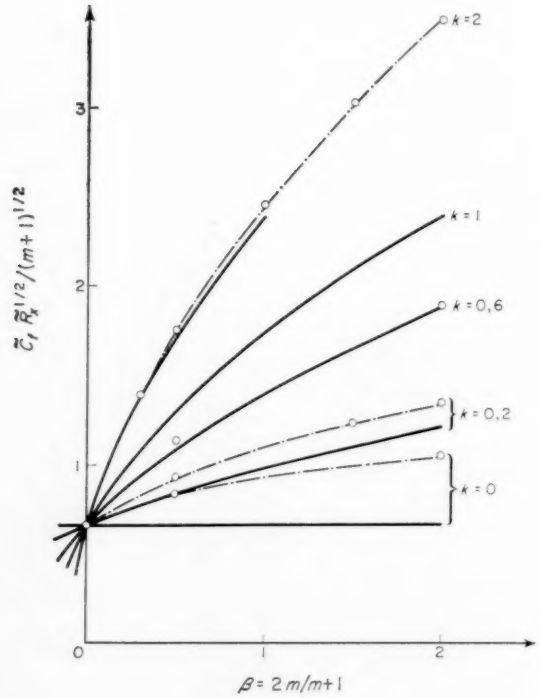

FIG. 8. $Pr = 1$
○ — · — Cohen et Reshotko [18]
——— Méthode actuelle.

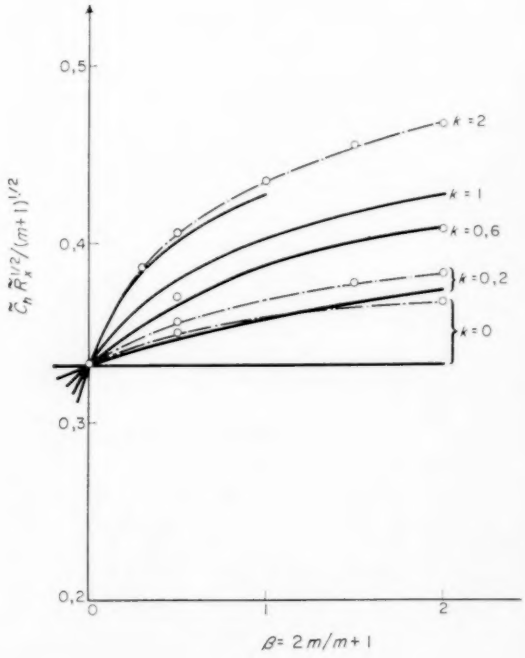

FIG. 9. $Pr = 1$
○ — · — Cohen et Reshotko [18]
——— Méthode actuelle.

Vol. 3 1961

Lorsque $k = 1$, on a évidemment les mêmes courbes. Lorsque $k > 1$, les formules approchées (81) et (87) ne sont valables que lorsque $\beta < 2/k$.

Pour $k = 0{,}6$ et 2, les points calculés par Cohen et Reshotko sont extrêmement voisins des courbes approchées.

Lorsque $k = 0$ et 0,2, les courbes approchées sont en-dessous des courbes de Cohen et Reshotko. Cela concorde avec le fait que les hypothèses introduites aux paragraphes 1.4 et 1.5.1 sont d'autant plus justifiées que $\theta_p - \theta_t$ est faible.

3.3. *Flux de chaleur aux points d'arrêt dans un écoulement bidimensionnel ou de révolution*

Au voisinage d'un point d'arrêt, on a:

$$u_e(x) = x(\mathrm{d}u_e/\mathrm{d}x)_t.$$

On peut alors montrer, comme au paragraphe 3.1, en utilisant la transformation de Mangler [22] pour le cas de révolution, que les profils de vitesse et de température d'arrêt peuvent se mettre, si c_p est constant, sous les formes anamorphosées:

$$\frac{u}{u_e} = f'(\beta, k; Pr; \tilde{\eta}) \tag{88}$$

et

$$\frac{\theta_i - \theta_t}{\theta_p(0) - \theta_t} = Y_0(\beta, k; Pr; \tilde{\eta}), \tag{89}$$

où

$$k = \theta_p(0)/\theta_t$$

et

$$\tilde{\eta} = \tilde{y}\sqrt{\left\{\frac{\tilde{u}_e}{\nu_t(2-\beta)\tilde{x}}\right\}} = \sqrt{\left\{\frac{(1+j)\,(\mathrm{d}u_e/\mathrm{d}x)_t}{\mu_r\rho_r}\right\}}\int_0^y \rho\,\mathrm{d}y. \tag{90}$$

β et j prennent respectivement les valeurs 1 et 0 dans le cas bidimensionnel, et les valeurs $\frac{1}{2}$ et 1 dans le cas de révolution.

Les fonctions $f(\beta, k; Pr; \tilde{\eta})$ et $Y_0(\beta, k; Pr; \tilde{\eta})$ sont solutions des équations:

$$\left.\begin{aligned} &f''' + ff'' + \beta\,[1 - f'^2 + Y_0(k-1)] = 0,\\ &Y_0'' + Pr\,f\,Y_0' = 0,\end{aligned}\right\} \tag{91}$$

avec les conditions aux limites (56) et (57).

La densité de flux de chaleur au point d'arrêt sera donnée par:

$$\Phi_p = \frac{c_p[\theta_p(0) - \theta_t]}{Pr}\sqrt{\{(1+j)\,\mu_r\rho_r(\mathrm{d}u_e/\mathrm{d}x)_t\}}\;Y_0'(\beta, k; Pr; 0). \tag{92}$$

La température effective est égale à la température totale et la température de référence sera donnée par la formule:

$$\theta_r = \theta_t + a(\beta, k; Pr)\,[\theta_p(0) - \theta_t], \tag{93}$$

avec

$$a(\beta, k; Pr) = \int_0^\infty Y_0(\beta, k; Pr; \tilde{\eta})\,f'(\beta, k; Pr; \tilde{\eta})\,\mathrm{d}\tilde{\eta}. \tag{94}$$

Si l'on utilise la nouvelle transformation, on pourra poser:

$$\frac{u}{u_e} = f'(\beta k, 1; Pr; \eta^*), \tag{95}$$

et

$$\frac{\theta_i - \theta_t}{\theta_p(0) - \theta_t} = Y_0(\beta k, 1; Pr; \eta^*), \tag{96}$$

avec

$$\eta^* = y^*\sqrt{\left\{\frac{u_e^*}{\nu_t(2-\beta k)x^*}\right\}} = \sqrt{\left\{\frac{(1+j)\,(\mathrm{d}u_e/\mathrm{d}x)_t}{\mu_r\rho_r}\right\}}\int_0^y \rho\,\mathrm{d}y. \tag{97}$$

Les fonctions $f(\beta k, 1; Pr; \eta^*)$ et $Y_0(\beta k, 1; Pr; \eta^*)$ sont solutions des équations:

$$\left.\begin{aligned} &f''' + ff'' + \beta k(1 - f'^2) = 0,\\ &Y_0'' + Pr\,f\,Y_0' = 0,\end{aligned}\right\} \tag{98}$$

avec les conditions aux limites (68) et (69).

La densité de flux de chaleur au point d'arrêt sera donnée par:

$$\Phi_p = \frac{c_p[\theta_p(0) - \theta_t]}{Pr}\sqrt{\{(1+j)\mu_r\rho_r(\mathrm{d}u_e/\mathrm{d}x)_t\}}\;Y_0'(\beta k, 1; Pr; 0). \tag{99}$$

La température de référence sera:

$$\theta_r = \theta_t + a(\beta k, 1; Pr)\,[\theta_p(0) - \theta_t], \tag{100}$$

avec

$$a(\beta k, 1; Pr) = \int^\infty Y_0(\beta k, 1; Pr; \eta^*)\,f'(\beta k, 1; Pr; \eta^*)\,\mathrm{d}\eta^*. \tag{101}$$

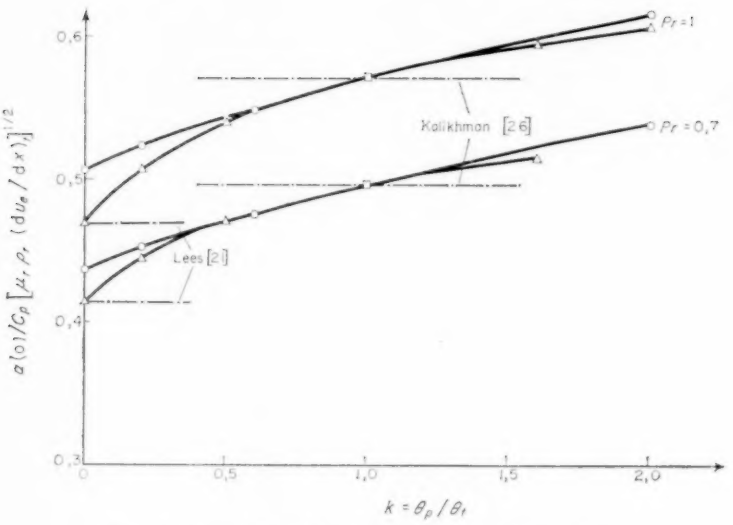

FIG. 10. Point d'arrêt dans un écoulement bidimensionnel

□ Squire [24] ○ Reshotko et Cohen [23] △ Méthode actuelle.

Vol. 3 1961

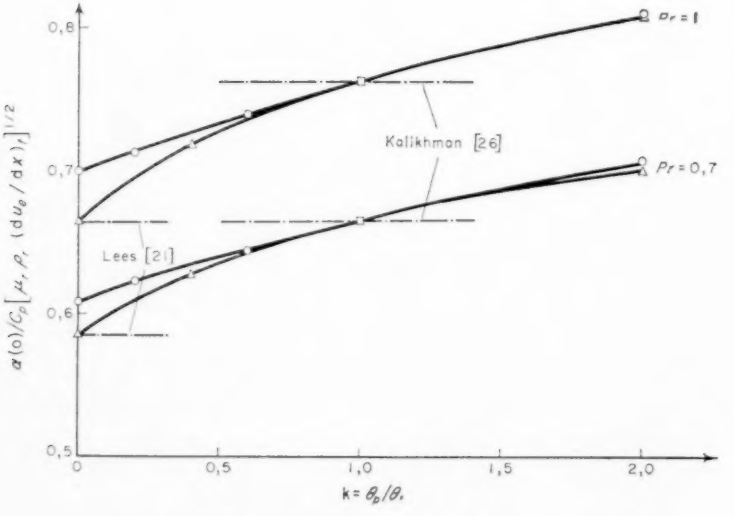

FIG. 11. Point d'arrêt dans un écoulement de révolution

□ Brun et Vasseur [13] ○ Reshotko et Cohen [23] △ Méthode actuelle.

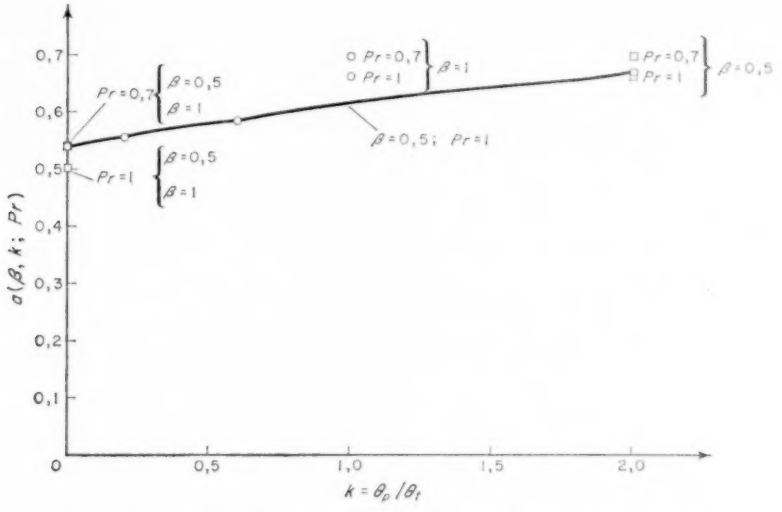

FIG. 12. Point d'arrêt dans un écoulement bidimensionnel ou de révolution
○ Valeurs calculées avec les profils exacts □ Valeurs calculées avec les profils approchés.

On a porté sur les Figs. 10 et 11 les valeurs de $a/c_p\ [\mu_r \rho_r (du_e/dx)_t]^{1/2}$ en fonction de k, pour $Pr = 0,7$ et 1, en utilisant les formules (92) et (99), où les Y_0' ont été calculés, d'une part, par Reshotko et Cohen [23] et, d'autre part, par Eckert [12].

Lorsque $k = 1$, on retombe sur les valeurs de Squire [24] pour le cas bidimensionnel, et sur les valeurs de Brun et Vasseur [25] pour le cas de révolution. On voit que les valeurs obtenues à l'aide de la nouvelle transformation sont voisines de celles obtenues en intégrant les équations complètes, surtout lorsque $0,5 < k < 2$.

On peut passer ainsi d'une façon continue de la théorie de Kalikhman [26] où l'on néglige le terme en $(u_e/\theta_e).\, du_e/dx$ dans (5) et (6), à la théorie de Lees [21] qui correspond au cas où l'on prend $\epsilon(x)$ constamment égal à u_e/u_r, quel que soit k, et où l'on néglige alors le second membre de (21) et le troisième terme du premier membre de (38).

On remarquera qu'on peut traiter, avec la nouvelle transformation, le cas des points d'arrêt en écoulement bidimensionnel ou de révolution, lorsque c_p est variable. On a alors:

$$\alpha = \frac{\Phi_p c_p [\theta_p(0)]}{h_p(0) - h_t}.$$

4. OBSTACLE QUELCONQUE A TEMPÉRATURE UNIFORME FAIBLE DEVANT LA TEMPÉRATURE TOTALE

Lorsque le rapport k tend vers zéro, le gradient de pression dans la couche limite transformée s'annule, car alors $u_e^* = u_r$. On aura alors:

$$\left.\begin{aligned} x^* &= \int_0^x \frac{\mu_r}{\mu_t}\frac{\theta_t}{\theta_r}\cdot\frac{p_e}{p_t}\cdot\frac{u_e}{u_r}\left(\frac{R}{L}\right)^{2j} dx, \\ y^* &= \left(\frac{R}{L}\right)^j \frac{u_e}{u_r}\int_0^y \frac{\rho}{\rho_t}\, dy. \end{aligned}\right\} \quad (102)$$

L'indice j est égal à 0 pour un obstacle bidimensionnel et à 1 pour un obstacle de révolution. Lest une longueur de référence.

La densité de flux de chaleur à la paroi sera égale à:

$$\Phi_p(x) = \frac{\mu_r \rho_r R^j u_e (h_{\text{eff}} - h_p)\, Y_0'(0, 1; Pr; 0)}{Pr[2\int_0^x R^{2j}\, \mu_r\, \rho_r\, u_e\, dx]^{1/2}}, \quad (103)$$

L'enthalpie de référence est donnée par la formule approchée:

$$h_r = h_e + a(0, 1; Pr)\,(h_p - h_e) + b(0, 1; Pr)\,(h_t - h_e), \quad (104)$$

avec

$$a(0, 1; Pr) = \int_0^\infty Y_0(0, 1; Pr; \eta^*) f'(0, 1; Pr; \eta^*)\, d\eta^* \quad (105)$$

et

$$b(0, 1; Pr) = 2\frac{Pr}{r_h} \int_0^\infty f''\, d\eta^* \int_{\eta^*}^\infty f''^{Pr} d\eta^* \int_0^{\eta^*} f''^{2-Pr}\, d\eta^* - a(0, 1; Pr). \quad (106)$$

h_f est l'enthalpie de frottement qui est égale à:

$$h_f = h_t + (r_h - 1)\frac{u_e^2(x)}{2}, \quad (107)$$

avec

$$r_h = 2Pr \int_0^\infty f''^{Pr}\, d\eta^* \int_0^{\eta^*} f''^{2-Pr}\, d\eta^*. \quad (108)$$

Les courbes représentant les variations de $a(0, 1; Pr)$ et de $b(0, 1; Pr)$ en fonction de Pr sont portées sur la Fig. 13.

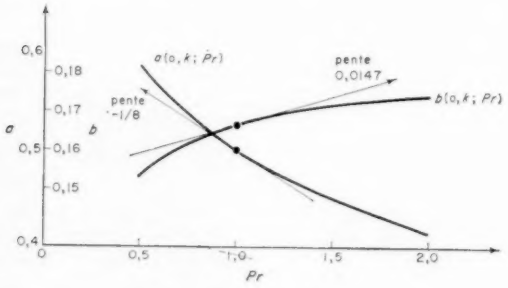

FIG. 13. Plaque plane.

L'enthalpie effective $h_{\text{eff}}(x)$, introduite dans (103), sera calculée en considérant, comme au paragraphe 1.5.2, la convection sur une plaque plane où l'enthalpie pariétale est égale à $h_p - h_f(x)$. Si nous utilisons la méthode de la Réf. 11:

$$h_{\text{eff}_1} = h_t + \frac{r_1(Pr) - 1}{2} x^{*1/4} \int_0^{x^*} (x^{*3/4} - x^{*'3/4})^{-1/3}\, d[u_e^2(x^{*'})]. \quad (109)$$

La formule (103) diffère de la formule de Lees [21] en ce que l'on a choisi l'enthalpie de référence h_r donnée par (104) au lieu de h_e, et l'enthalpie effective h_{eff} donnée par (109) au lieu de h_t.

Eckert et Tewfik [27] ont obtenu un bon accord avec les résultats expérimentaux dans l'air de Kemp *et al.* [28] en utilisant la formule de Lees avec l'enthalpie de référence d'Eckert [6], voisine de celle donnée par (104), et h_f comme enthalpie effective.

CONCLUSION

La transformation présentée ici permet de ramener, moyennant certaines simplifications, les équations de la couche limite dans un gaz parfait aux équations dans une couche limite fictive à viscosité et masse volumique constantes, mais à c_p variable. Dans cette couche limite fictive, la distribution de vitesse extérieure $u_e^*(x^*)$ dépend de la distribution réelle de la température pariétale $\theta_p(x)$ sur l'obstacle.

On peut donc appliquer, dans le cas des propriétés physiques variables, toutes les méthodes mises au point pour la couche limite à propriétés physiques constantes. Les résultats obtenus, dans certains cas particuliers, concordent remarquablement avec ceux obtenus par d'autres auteurs qui ont intégré les équations non simplifiées, tout au moins dans la zone où $0{,}5 < (\theta_p/\theta_t) < 2$. Lorsque $0 < (\theta_p/\theta_t) < 0{,}5$, l'erreur croît au fur et à mesure que θ_p est plus faible et que le gradient de pression est plus élevé, tout en restant inférieure à 7,3 pour cent, pour le point d'arrêt bidimensionnel et $Pr = 1$, par exemple.

Lorsque la température de la paroi est faible devant la température totale, la densité de flux de chaleur à la paroi d'un obstacle quelconque est donnée par une formule différant légèrement de celle de Lees.

Cet article constitue le développement d'une partie de ma thèse préparée sous la direction du Professeur Edmond A. Brun, que je remercie pour les conseils et l'encouragement que j'ai trouvés auprès de lui.

BIBLIOGRAPHIE

1. A. A. DORODNITZIN, Couche limite laminaire dans un gaz compressible (en russe), *Prikl. Matem. I Mekh.* 6 (1942).
2. L. HOWARTH, Concerning the effect of compressibility on laminar boundary layers and their separation, *Proc. Roy. Soc.* **A 194**, 16 (1948).

Vol. 3 1961

3. K. STEWARTSON, Correlated incompressible and compressible boundary layers, *Proc. Roy. Soc.* A **200**, 84 (1949).
4. C. R. ILLINGWORTH, Steady flow in the laminar boundary layer of a gas, *Proc. Roy. Soc.* A **199**, 533 (1949).
5. R. VON MISES, Bemerkungen zur hydrodynamik, *Z. Angew. Math. Mech.* **7**, 425 (1927).
6. E. R. G. ECKERT, Engineering relations for heat transfer and friction in high-velocity laminar and turbulent boundary layer flow over surfaces with constant pressure and temperature, *Trans. Amer. Soc. Mech. Engrs*, **78**, 1273 (1956).
7. R. J. MONAGHAN, On the behaviour of boundary layers at supersonic speeds, I.A.S. Preprint No. 557 (1955).
8. E. A. BRUN, *Introduction à l'étude de la couche limite*, pp. 140 à 148, Gauthier-Villars, Paris (1955).
9. H. GÖRTLER, A new series for the calculation of steady boundary layer flows, *J. Math. Mech.* **1**, 1 (1957).
10. B. LE FUR, Une nouvelle méthode de résolution par itération des équations dynamique et thermique de la couche limite laminaire, Thèse de Doctorat, Paris (1960), à paraître dans les P.S.T. du Min de l'Air.
11. B. LE FUR, Convection de la chaleur en régime laminaire dans le cas d'un gradient de pression et d'une température de paroi quelconques, le fluide étant à propriétés physiques constantes, *Int. J. Heat Mass Transfer*, **1**, Nos. 1/2, 68 (1960).
12. E. ECKERT, Die Berechnung des Wärmeüberganges in der laminaren Grenzschicht umströmter Körper, *Forschungsh. Ver. Dtsch. Ing.* Nr. 416 (1942).
13. E. BRUN et M. VASSEUR, Contribution à l'étude thermique de la couche limite laminaire, *J. Rech. Cen. Nat. Rech. Sci.* No. 6 (1948).
14. H. J. MERK, Rapid calculations for boundary layer transfer using wedge solutions and asymptotic expansions, *J. Fluid Mech.* **5**, 460 (1959).
15. N. ROTT, Compressible laminar boundary layer on a heat-insulated body, *J. Aero. Sci.* **20**, 67 (1953).
16. I. TANI, On the approximate solution of the laminar boundary layer equations, *J. Aero. Sci.* **21**, 487 (1954).
17. B. LE FUR, Calcul de la couche limite laminaire dans un écoulement compressible avec gradient de pression sur une paroi thermiquement isolée. *J. Rech. Cen. Nat. Rech. Sci.* No. 42, 9 (1958).
18. C. B. COHEN et E. RESHOTKO, Similar solutions for the compressible laminar boundary layer with heat transfer and pressure gradient, *N.A.C.A. Rep.* 1293 (1956).
19. A. M. O. SMITH, Improved solutions of the Falkner and Skan boundary layer equation, *Inst. Aero. Sci. S.M. Fairc. Fund. Pap.* FF-10 (1954).
20. H. GÖRTLER, Zahlentafeln universeller Funktioner zur neuen Reihe für die Berechnung laminarer Grenzschichten, *D.V.L. Bericht*, Nr. 34 (1957).
21. L. LEES, Laminar heat transfer over blunt-nosed bodies at hypersonic flight speeds, *Jet Propulsion*, **26**, 259 (1956).
22. W. MANGLER, Zusammenhang zwischen ebenen und rotationssymetrischen Grenzschichten in kompressiblen Flüssigkeiten, *Z. Angew. Math. Mech.* **28**, 97 (1948).
23. E. RESHOTKO et C. B. COHEN, Heat transfer at the forward stagnation point of blunt bodies, *N.A.C.A. Tech. Note* 3513 (1955).
24. voir S. GOLDSTEIN, *Modern Developments in Fluid Dynamics*, Vol. II, p. 631, Clarendon Press, Oxford (1938).
25. E. BRUN et M. VASSEUR, Convection forcée de la chaleur à la surface d'un corps de révolution, *C.R. Acad. Sci., Paris*, **225**, 861 (1947).
26. L. E. KALIKHMAN, Heat exchange in the vicinity of the forward stagnation point in axially symmetrical and two-dimensional gas flow (in Russian), *Izv. Akad. Nauk O.T.N.*8 (1955).
27. E. R. G. ECKERT et O. E. TEWFIK, Use of reference enthalpy in specifying the laminar heat transfer distribution around blunt bodies in dissociated air, *J. Aero. Space Sci.* **27**, 464 (1960).
28. N. H. KEMP, P. H. ROSE et R. W. DETRA, Laminar heat transfer around blunt bodies in dissociated air, *J. Aero. Space Sci.* **26**, 421 (1959).

Vol.
3
1961

Int. J. Heat Mass Transfer. Vol. 3, pp. 293–303. Pergamon Press 1961. Printed in Great Britain.

ON CONJUGATED PROBLEMS OF HEAT TRANSFER

T. L. PERELMAN

Institute of Energetics of the Academy of Sciences of the B.S.S.R., Minsk, B.S.S.R.

(*Received* 25 *March* 1961)

Abstract—The paper deals with the simplest "conjugated" boundary value problems of heat transfer in which heat conduction equations are solved in common for a body with heat sources and for a liquid flowing round the body. The method of the asymptotic solution of integral equations occurring in conjugated problems is presented.

Résumé—L'article traite des problèmes aux limites mixtes les plus simples pour le transport de chaleur, dans lesquels les équations de conduction sont résolues simultanément pour un corps comportant des sources de chaleur, et pour un liquide s'écoulant autour du corps.

On utilise la solution asymptotique des équations intégrales mises en jeu dans ces problèmes conjugués,

Zusammenfassung—Die Arbeit behandelt die einfachsten "konjugierten" Grenzwertprobleme des Wärmeübergangs, bei welchen die Wärmeleitungsgleichungen für den Körper mit Wärmequellen und die ihn unströmende Flüssigkeit gemeinsam gelöst werden können. Für die Integralgleichungen, wie sie bei konjugierten Problemen auftreten, wird die Methode der asymptotischen Lösung angegeben.

Аннотация—В работе рассматриваются простейшие «сопряженные» краевые задачи теплообмена, в которых совместно решаются уравнения теплопроводности для тела с источниками тепла и для жидкости, обтекающей тело. Даётся метод асимптотического решения интегральных уравнений, возникающих в сопряженных задачах.

NOMENCLATURE

- $\theta(x,y)$, liquid temperature;
- $t(x,y)$, solid temperature;
- $\Theta(x)$, surface temperature;
- $p(x)$, normal temperature derivative on the body surface;
- u, v, longitudinal (along the solid) and normal velocity components, respectively;
- K_f, thermal conductivity of liquid;
- K_s, thermal conductivity of solid;
- α, local heat transfer coefficient;
- Nu_x, local Nusselt number;
- Re_x, local Reynolds number;
- Pr, Prandtl number.

1. INTRODUCTION

THE local coefficient of heat transfer between a liquid and a body submerged in it is determined as [1],

$$\alpha = \frac{q}{t_w - t_\infty},$$

where

- t_w = wall temperature at the considered point,
- t_∞ = temperature of the incoming liquid,
- q = density of heat flow through the surface of the immersed body.

Consequently, to determine α, temperature distribution in the liquid and the temperature on the surface of the immersed body must be known.

As a rule, surface temperature of the immersed body—or heat flow through the surface—is considered a given function of co-ordinates [2] and, in particular, of $t_w = \text{const.}$ [3].

In some cases, the setting of the wall temperature instead of its determination from the common solution of heat conduction equations for a liquid and an immersed body is unsatisfactory because of the following:

(1) the wall temperature should not be assigned in the case of intense heat transfer,

(2) in the usual statement of the problem the solution does not contain the dependence on the properties of the immersed body—its thermal constants, size, etc.,

(3) an experimental definition of the wall temperature as a function of co-ordinates is a comparatively complicated problem, whereas it is easier to determine the distribution of sources in the body.*

Therefore the problems, which we shall call "conjugated", are formulated as follows: the common solution of heat conduction equations for the body and the liquid round it is to be found. The velocity distribution in the moving liquid is found by solving the corresponding hydrodynamic problem.

The present paper deals with the simplest conjugated problems. An exact solution of the problem on heat transfer in a slip flow is given in section 2. In section 3 the problem on heat transfer between a thin plate and a laminar boundary layer of incompressible liquid formed on it is solved. The method of the asymptotic solution of one class of singular integral equations to which the problems of the considered type are reduced is given in the Appendix. Therefore, the same method can be applied to the solution of other conjugated problems.

2. CONJUGATED PROBLEM OF HEAT TRANSFER IN SLIP FLOW

Consider a liquid flowing with a constant velocity around a solid occupying a quandrant $x > 0$, $y < 0$ (see Fig. 1). Assume that the component along the axis y is equal to zero. Moreover, heat conduction of the fluid along the axis x is neglected

$$\left(\frac{\partial^2\theta}{\partial x^2} \ll \frac{\partial^2\theta}{\partial y^2}, \text{ "boundary layer"}\right).$$

Thus, the problem is formulated as follows: [$\theta(x,y)$ is the fluid temperature, $t(x,y)$ is the solid temperature].

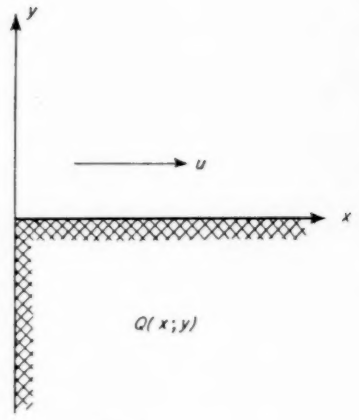

FIG. 1.

For the liquid

$$u\frac{\partial\theta}{\partial x} = \chi\frac{\partial^2\theta}{\partial y^2}, \qquad 0 \leqslant x < \infty, \quad 0 \leqslant y < \infty. \tag{1}$$

For the solid

$$\frac{\partial^2 t}{\partial x^2} + \frac{\partial^2 t}{\partial y^2} = -\frac{1}{K_s}Q(x,y), \qquad 0 \leqslant x < \infty, \quad -\infty < y \leqslant 0. \tag{2}$$

Restrictions on the function $Q(x,y)$ to be made for existence of the solution will be found out below.

On the solid–fluid surface we take:†

$$\theta|_{y=+0} = t|_{y=-0}, \tag{3}$$

$$-K_f\left.\frac{\partial\theta}{\partial y}\right|_{y=+0} = -K_s\left.\frac{\partial t}{\partial y}\right|_{y=-0}. \tag{4}$$

Counting all the temperatures from the temperature of the incoming fluid one may take:

$$\theta|_{x=0} = 0, \tag{5}$$

$$\theta|_{y=\infty} = 0. \tag{6}$$

* The method of determination of the heat transfer coefficient proposed by Academician Luikov is based on it.

† Instead of condition (3) we may take a more general condition (temperature jump) $\theta|_{y=+0} - t|_{y=-0} = f(x)$ where $f(x)$ is the arbitrary given function. The solution of the problem with such a condition is quite analogous. For existence of the solution it is necessary that the transformation (14a) for $f(x)$ should exist and $f_s(\alpha)$ should satisfy the same conditions as the function $g(\xi)$ of (18).

Vol. 3 1961

Let

$$t|_{x=0} = 0. \tag{7}$$

The conjugated problem formulated is of interest when considering some cases of rarefied gas flow with slip near the wall* [4].

The system of equations (1–7) can also be treated as a boundary value problem for the equation of a mixed type with singular coefficients: an elliptic equation at $y < 0$ and a parabolic one at $y > 0$. The general theory of equations of a mixed type and especially the case of a hyperbolic-elliptic equation is considered in [5].

For equation (1) with conditions (5, 6) and with regard to (4) it is easy to get

$$\theta(x,y) = a_1 \int_0^x \frac{\exp\left[-\dfrac{y^2}{4\gamma(x-x')}\right]}{\sqrt{(x-x')}}\, p(x')\,\mathrm{d}x', \tag{8}$$

$$\left.\begin{aligned} &\left.\frac{\partial t}{\partial y}\right|_{y=-0} = \frac{1}{\kappa}\left.\frac{\partial \theta}{\partial y}\right|_{y=+0} \equiv -p(x), \\ &\kappa = K_s/K_f, \quad a_1 = \kappa\sqrt{\frac{\gamma}{\pi}}, \quad \gamma = \frac{\chi}{u}. \end{aligned}\right\} \tag{9}$$

For equation (2) with conditions (7) and (9) we have

$$t(x,y) = K(x,y) - \frac{1}{2\pi}\int_0^\infty \ln\frac{(x+x')^2+y^2}{(x-x')^2+y^2}\, p(x')\,\mathrm{d}x', \tag{10}$$

where

$$K(x,y) = \frac{2}{\pi}\int_0^\infty K_s(\alpha,y)\sin\alpha x\,\mathrm{d}\alpha, \tag{11a}$$

$$K_s(\alpha,y) = \frac{2}{\pi}\int_0^\infty \frac{q_{sc}(\alpha,\beta)}{\alpha^2+\beta^2}\cos\beta y\,\mathrm{d}\beta, \tag{11b}$$

$$q_{sc}(\alpha,\beta) = \int_0^\infty q_s(\alpha,-y)\cos\beta y\,\mathrm{d}y, \tag{11c}$$

$$q_s(\alpha,y) = \frac{1}{K_s}\int_0^\infty Q(x,y)\sin\alpha x\,\mathrm{d}x. \tag{11d}$$

It is seen from (8) and (10) that if the normal derivative on the boundary $p(x)$ is known, then the problem is reduced to quadratures. Taking $y = 0$ in equations (8) and (10), the system of integral equations will be obtained

$$\Theta(x) = a_1\int_0^x \frac{p(y)}{\sqrt{(x-y)}}\,\mathrm{d}y, \tag{12}$$

$$\Theta(x) = K(x,0) - \frac{1}{\pi}\int_0^\infty \ln\left|\frac{x+y}{x-y}\right| p(y)\,\mathrm{d}y, \tag{13}$$

where (see equation (3)) the following designation is introduced

$$\theta|_{y=+0} = t|_{y=-0} \equiv \Theta(x). \tag{14}$$

Subject the system (12, 13) to the generalized Fourier sine-transform [6]:

$$f_s(\alpha) = \lim_{\sigma\to 0}\int_0^\infty f(x)\,\mathrm{e}^{-\sigma x}\sin\alpha x\,\mathrm{d}x. \tag{14a}$$

It is possible to show the validity of changing the order of integrations shown. Finally, eliminating $\Theta(x)$, a singular equation for $p_s(\alpha)$ is obtained:†

$$\left[1+\frac{1}{a\sqrt{\alpha}}\right]p_s(\alpha) = \frac{\sqrt{\alpha}K_s(\alpha)}{a} - \frac{2}{\pi}\int\!\!\!\!\!\!-_0^\infty \frac{p_s(\beta)\beta}{\beta^2-\alpha^2}\,\mathrm{d}\beta, \tag{15}$$

here $K_s(\alpha) \equiv K_s(\alpha, 0)$ (see (11)); $a = a_1\sqrt{\pi}/2$, $\int\!\!\!\!\!\!-$ designates the Cauchy principal value of integral. In equation (15) the change of variables is allowable

$$\alpha = \frac{\sqrt{\xi}}{a^2}, \quad p_s(\alpha) = \varphi(\xi). \tag{16}$$

Equation (15) is reduced to the form

$$\left(1+\frac{1}{\xi^{1/4}}\right)\varphi(\xi) = g(\xi) + \frac{1}{\pi}\int\!\!\!\!\!\!-_0^\infty \frac{\varphi(\eta)}{\xi-\eta}\,\mathrm{d}\eta, \tag{17}$$

where

$$g(\xi) = \frac{\xi^{1/4}K_s(\sqrt{\xi}/a^2)}{a^2}. \tag{18}$$

The general theory of equations of such a type as (17)—singular integral equations with the Cauchy kernel—is considered in [8, 9].

* As suggested by Professor A. A. Gukhman.

† The kernels analogous to those of the integral equation (15) are considered in the Kramers–Kronig transform theory (see, for example, [7]).

Subjecting equation (17) to the Mellin transform and introducing the designation

$$\bar{\varphi}(s) = \int_0^\infty \varphi(\xi)\xi^{s-1}\,d\xi$$

and

$$\bar{g}(s) = \int_0^\infty g(\xi)\xi^{s-1}\,d\xi,$$

we get

$$(1 + ctg\,\pi s)\bar{\varphi}(s) + \bar{\varphi}(s - \tfrac{1}{4}) = \bar{g}(s), \qquad (19)$$

in the range $0 < \mathrm{Re}(s) < 1$.

The latter difference equation for $\bar{\varphi}(s)$ can be reduced to another difference equation with constant coefficients. Omitting simple computations the result is

$$\bar{\varphi}(s) = \bar{\nu}(s) - \tfrac{1}{4}\bar{\varphi}(s-1), \qquad \tfrac{3}{4} < \mathrm{Re}(s) < 1, \qquad (20)$$

where

$$\bar{\nu}(s) = \frac{1}{\sqrt{2}} \cdot \frac{\sin \pi s}{\sin \pi (s + \frac{1}{4})}\,\bar{g}(s) - \frac{1}{2} \cdot \frac{\sin \pi (s - \frac{1}{4})}{\sin \pi (s + \frac{1}{4})}\,\bar{g}(s - \tfrac{1}{4}) - \frac{1}{2\sqrt{2}} \times \frac{\cos \pi s}{\sin \pi (s + \frac{1}{4})}\,\bar{g}(s - \tfrac{1}{2}) + \tfrac{1}{4}\bar{g}(s - \tfrac{3}{4}). \qquad (21)$$

The general solution of equation (20) has the form:

$$\bar{\varphi}(s) = \frac{1}{4^s} \cdot \bar{f}(s) + \int_0^\infty \frac{\nu(\xi)\xi^s}{\xi + \frac{1}{4}}\,d\xi, \qquad (22)$$

where

$$\nu(\xi) = \frac{1}{2\pi i}\int_{\sigma - i\infty}^{\sigma + i\infty} \bar{\nu}(s)\,\frac{ds}{\xi^s}, \quad |\tfrac{3}{4} < \sigma < 1|,$$

and $\bar{f}(s)$ is the arbitrary function satisfying the condition

$$\bar{f}(s) = -\bar{f}(s+1).$$

The function $\bar{f}(s)$ in (22) is chosen to satisfy original equation (19).

$\bar{\varphi}(s)$ being determined, the problem is solved and reduced to the performance of the inverse Mellin transform. The unknown function $p(x)$ will be determined:

$$p(x) = \lim_{\sigma \to 0} \frac{2}{\pi}\int_0^\infty e^{-\sigma a}\,\varphi(a^4 a^2)\sin a\,x\,da.$$

$\Theta(x)$ can be found, for example, from (12).

For illustration, the results will be given when the source has the form:

$$Q(x, y) = Q_0\,\frac{\cos \omega y}{\sqrt{x}}. \qquad (23)$$

The general solution of equation (19) is obtained by the method given above

$$\bar{\varphi}(s) = \frac{\bar{\omega}(s)}{4^s \cdot \sin \pi (s + \frac{1}{4})} + \frac{q_0}{1 + \sqrt{(2)}\,b^{1/4}} \cdot \frac{\pi b^{s - 3/4}}{\sin \pi (s + \frac{1}{4})}, \qquad (24)$$

where

$$q_0 = \frac{Q_0}{K_s} \cdot \sqrt{\left(\frac{\pi}{2}\right)}\,a^3, \quad b = \omega^2 \cdot a^4$$

and $\bar{\omega}(s)$ is the arbitrary function satisfying

$$\bar{\omega}(s) = -\bar{\omega}(s - \tfrac{1}{4}).$$

Apparently we are to take $\bar{\omega}(s) \equiv 0$. Then

$$\varphi(\xi) = \xi^{1/4} \cdot \frac{1}{2\pi i}\int_{\sigma - i\infty}^{\sigma + i\infty} \bar{\varphi}(s - \tfrac{1}{4})\,\frac{ds}{\xi^s} = \frac{q_0}{1 + \sqrt{(2)}\,b^{1/4}} \cdot \frac{\xi^{1/4}}{\xi + b}, \quad |\tfrac{3}{4} < \sigma < 1|$$

and for $p(x)$ and $\Theta(x)$ we get, respectively:

$$p(x) = \sqrt{\left(\frac{2}{\pi}\right)} \cdot \frac{Q_0}{K_s} \times \frac{1}{1 + \sqrt{(2\omega)}\,a}\int_0^\infty \frac{\sqrt{a}\sin a\,x}{a^2 + \omega^2}\,da, \qquad (25)$$

$$\Theta(x) = \sqrt{\left(\frac{2}{\pi}\right)} \cdot \frac{Q_0}{K_s} \times \frac{\sqrt{(2\omega)}\,a}{1 + \sqrt{(2\omega)}\,a}\int_0^\infty \frac{\sin a\,x}{\sqrt{a}\,(a^2 + \omega^2)}\,da. \qquad (26)$$

Note, that the integrals in formulae (25) and (26) converge uniformly relative to x, which makes the study of their properties easier.

Vol. 3 1961

3. HEAT TRANSFER IN A LAMINAR BOUNDARY LAYER OF FLOW ROUND A THIN PLATE WITH INTERNAL HEAT SOURCES

Consider heat transfer between a thin plate with internal heat sources and a laminar boundary layer of incompressible liquid formed on it. Let $t(x,y)$ and $\theta(x,y)$ be temperatures of the plate and liquid, respectively, and $u(x,y)$ and $v(x,y)$ the components of the velocity of a liquid along the axes x and y (Fig. 2). The system of equations for the considered problem is:

$$u\frac{\partial u}{\partial x}+v\frac{\partial u}{\partial y}=\nu\frac{\partial^2 u}{\partial y^2}, \tag{27}$$

$$\frac{\partial u}{\partial x}+\frac{\partial v}{\partial y}=0, \tag{28}$$

with the boundary conditions

$$u|_{y=0}=v|_{y=0},\quad u|_{y=\infty}=U. \tag{29}$$

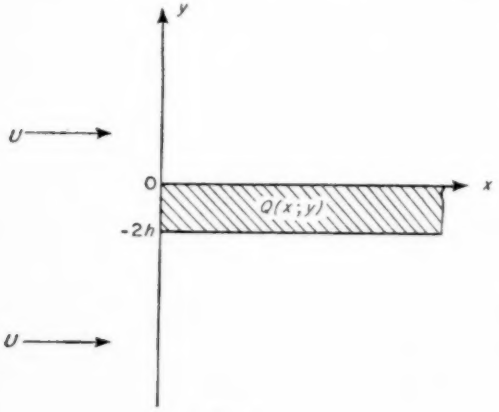

FIG. 2.

For fluid temperature we have

$$u\frac{\partial\theta}{\partial x}+v\frac{\partial\theta}{\partial y}=\chi\frac{\partial^2\theta}{\partial y^2}. \tag{30}$$

If we take the temperature of the incoming liquid as zero, then

$$\text{(a)}\quad \theta|_{x=0}=0,\quad \text{(b)}\quad \theta|_{y=\infty}=0. \tag{31}$$

For the plate

$$\frac{\partial^2 t}{\partial x^2}+\frac{\partial^2 t}{\partial y^2}=-\frac{1}{K_s}\cdot Q(x,y). \tag{32}$$

Restricting ourselves to the sources of the finite power, for which

$$\int Q(x,y)\,\mathrm{d}V<\infty \tag{33}$$

(integration over the whole volume of the plate). All given below is applicable for any source satisfying condition (33). To illustrate, consider the source of the form:

$$Q(x,y)=Q_0\cdot\epsilon(l-x),\quad -2h\leqslant y\leqslant 0, \tag{34}$$

where

$$\epsilon(x)=\begin{cases}1 & x>0\\ 0 & x<0.\end{cases}$$

Due to the symmetry of the problem

$$\left.\frac{\partial t}{\partial y}\right|_{y=-h}=0. \tag{35}$$

On the leading edge of the plate we take

$$t|_{x=0}=0. \tag{36}$$

The latter condition is unessential and can be replaced by another one.

Finally, write out the plate–liquid boundary conditions:

$$\theta|_{y=+0}=t|_{y=-0}, \tag{37}$$

$$-K_f\left.\frac{\partial\theta}{\partial y}\right|_{y=+0}=-K_s\left.\frac{\partial t}{\partial y}\right|_{y=-0}. \tag{38}$$

The exact Blasius solution is known [10] for equations (27, 28) with boundary conditions (29) describing the laminar boundary layer on a flat plate. The problem is similar [11–13]; the variable $\eta=y/2\sqrt{(U/\nu x)}$ being introduced, it is reduced to the ordinary differential equation

$$\frac{\mathrm{d}^3 f}{\mathrm{d}\eta^3}+f\frac{\mathrm{d}^2 f}{\mathrm{d}\eta^2}=0, \tag{39}$$

with boundary conditions

$$f(0)=f'(0)=0,\quad f'(\infty)=2,$$

where $f(\eta)$ is bound with the flow function $\psi(x,y)|u=\partial\psi/\partial y,\ v=-\partial\psi/\partial x|$ by the relation $\psi=\sqrt{(\nu Ux)}\,f$. The solution of equation (39) can be obtained numerically or in the form of power series by η. The latter has the form

$$f(\eta)=\frac{c\eta^2}{2!}-\frac{c^2\eta^5}{5!}+\ldots \tag{40}$$

here $c\equiv f''(0)=1{\cdot}328$.

Let us turn to equation (30). We introduce a new independent variable ψ (flow function) instead of y following [13]. Since ψ is determined to within the arbitrary constant, we take it that when y is equal to zero then $\psi = 0$ as well. Equation (30) and condition (38) will be written:

$$\frac{\partial\theta}{\partial x} = \chi \frac{\partial}{\partial\psi}\left[u \frac{\partial\theta}{\partial\psi}\right], \tag{41}$$

$$u \frac{\partial\theta}{\partial\psi}\bigg|_{\psi=0} = -\kappa\, p(x), \tag{42}$$

where

$$p(x) \equiv -\frac{\partial t}{\partial y}\bigg|_{y=0} \text{ and } \kappa = \frac{K_s}{K_f}.$$

If the Prandtl number is not low, then we may restrict ourselves to the first term in expansion (40). Introducing a new variable [14]

$$z = \tfrac{2}{3}\,\psi^{3/4},$$

we get for (41, 42 and 31), respectively,

$$\frac{4}{\beta} x^{1/4} \frac{\partial\theta}{\partial x} = \frac{\partial^2\theta}{\partial z^2} + \frac{1}{3z} \cdot \frac{\partial\theta}{\partial z}, \tag{43}$$

$$\frac{3^{1/3}\beta}{2^{4/3}\chi} \cdot \frac{z^{1/3}}{x^{1/4}} \cdot \frac{\partial\theta}{\partial z}\bigg|_{z=0} = -\kappa\, p(x), \tag{44}$$

$$\text{(a)}\quad \theta|_{x=0} = 0, \qquad \text{(b)}\quad \theta|_{z=\infty} = 0, \tag{45}$$

where

$$\beta = \frac{\chi\sqrt{(c/2)U^{3/4}}}{\nu^{1/4}}.$$

Equation (43) was studied in [15]; the solution has the form:

$$\left.\begin{aligned}\theta(x,z) = {} & \frac{3z^{1/3}}{2\beta x^{3/4}} \cdot \exp\left(-\frac{3z^2}{4\beta x^{3/4}}\right) \\ & \left\{\int_0^\infty f_1(\lambda) \exp\left(-\frac{3\lambda^2}{4\beta x^{3/4}}\right)\right. \\ & \times I_{1/3}\left(\frac{3\lambda z}{2\beta x^{3/4}}\right) \lambda^{2/3}\, d\lambda \\ & + \int_0^\infty f_2(\lambda) \exp\left(-\frac{3\lambda^2}{2\beta x^{3/4}}\right) \\ & \left. I_{-1/3}\left(\frac{3\lambda z}{2\beta x^{3/4}}\right) \lambda^{2/3}\, d\lambda\right\}.\end{aligned}\right\} \tag{46}$$

The functions $f_1(\lambda)$ and $f_2(\lambda)$ are determined from the boundary conditions. Condition (45a) gives $f_1(\lambda) = -f_2(\lambda) \equiv f(\lambda)$ and it follows from (45b) that $f(\infty) = 0$.

Introducing the designation

$$\theta|_{z=+0} \equiv \Theta(x) \tag{47}$$

and making use of condition (44) it is easy to get

$$\Theta(x) = -\frac{a}{x^{1/2}} \int_0^\infty \psi(u) \exp\left[-\frac{1}{\beta}\left(\frac{u}{x}\right)^{3/4}\right] \frac{du}{u^{1/2}} \tag{48}$$

$$p(x) = -\frac{b}{x^{5/4}} \int_0^\infty \psi(u) \exp\left[-\frac{1}{\beta}\left(\frac{u}{x}\right)^{3/4}\right] \frac{du}{u^{1/4}}, \tag{49}$$

where

$$\psi(u) \equiv f\left(\frac{2}{\sqrt{3}}\, u^{3/8}\right), \quad a = \frac{3}{4\Gamma(\frac{2}{3})\beta^{2/3}},$$

$$b = \frac{3^{5/3}}{8\Gamma(\frac{1}{3})\chi\kappa\beta^{1/3}}.$$

Finally, eliminate $\psi(u)$ from equations (48, 49). Then we have

$$\Theta(x) = \gamma \int_0^x \frac{p(y)\, dy}{(x^{3/4} - y^{3/4})^{2/3}}, \tag{50}$$

here

$$\gamma = \frac{3a}{4\Gamma(1/3) b \beta^{1/3}}.$$

Consider equation (32). The solution of it expressed through $p(x)$ at conditions (34–36) may easily be obtained by the standard methods. We shall directly write the expression for the temperature of the plate surface [see (37, 38 and 47)]:

$$\begin{aligned}\Theta(x) = {} & \frac{Q_0}{K_s}\, x\left(l - \frac{x}{2}\right) \epsilon\,(l - x) \\ & + \frac{Q_0}{K_s}\, \frac{l^2}{2}\, \epsilon(x - l) - \frac{1}{h}\int_0^\infty G(x,y) p(y)\, dy \\ & - \frac{1}{\pi}\int_0^\infty \ln\left[\frac{1 - \exp\left(-\pi\,\dfrac{x+y}{h}\right)}{1 - \exp\left(-\pi\,\dfrac{|x-y|}{h}\right)}\right] p(y)\, dy,\end{aligned} \tag{51}$$

Vol. 3 1961

where

$$G(x,y) = \begin{cases} y & y < x \\ x & y > x. \end{cases} \quad (52)$$

Thus, the problem is brought to the solution of the system of integral equations (50, 51) for unknown functions $\Theta(x)$ and $p(x)$. The knowledge of any of them reduces the determination of $\theta(x,y)$ and $t(x,y)$ to the quadratures.

The system (50, 51) cannot be solved exactly, and moreover, the exact solution need not be given, since the equations of the boundary layer theory (27–29) are applicable only at a distance from the leading edge of the plate; otherwise the complete Navier–Stokes equations should be used. Consequently, the solution is to be sought only in the region $x/h \gg 1$.

The latter remark allows basic simplification of equation (51). Accurate within the terms

$$\sim \text{const.} \exp\left(-\frac{\pi x}{h}\right)$$

we immediately obtain

$$\Theta(x) = \frac{Q_0}{K_s} x\left(l - \frac{x}{2}\right)\epsilon(l-x)$$

$$+ \frac{Q_0}{K_s}\cdot\frac{l^2}{2}\epsilon(x-l) - \frac{1}{h}\int_0^\infty G(x,y)p(y)\,dy$$

$$+ \frac{1}{\pi}\int_0^\infty \ln\left[1 - \exp\left(-\pi\frac{|x-y|}{h}\right)\right]p(y)\,dy. \quad (53)$$

Further, the last term in the right-hand side of equation (53) can be given in the form:

$$\frac{1}{\pi}\int_0^\infty \ln\left[1 - \exp\left(-\pi\frac{|x-y|}{h}\right)\right]p(y)\,dy$$

$$= \frac{x}{\pi}\int_0^\infty \ln\left[1 - \exp\left(-\frac{\pi(y+1)}{h}x\right)\right]$$

$$\times p[x(y+2)]\,dy + \frac{x}{\pi}\int_1^1 \ln\left[1\right.$$

$$\left. - \exp\left(-\frac{\pi x}{h}|y|\right)\right]p[x(y+1)]\,dy.$$

The first of these two integrals can be easily evaluated at high x/h by the Laplace method. It turns out to be equal to

$$-\frac{h}{\pi^2}\exp\left(-\frac{\pi x}{h}\right)p(2x)$$

and should be neglected. For the evaluation of the second integral we show that at

$$\frac{x}{h} \to \infty\ F\left(y;\frac{x}{h}\right) =$$

$$-\frac{3x}{\pi h}\ln\left[1 - \exp\left(-\frac{\pi x}{h}|y|\right)\right]$$

has the limit of $\delta(y)$ in the sense of distribution. It is necessary to show [16] for this, firstly, that $\int_a^b F(y;x/h)\,dy$ is limited from above by a constant independent of a, b and x/h at any a and b. Really, since the function $F(y;\ x/h)$ is non-negative, then

$$\int_b^a F\left(y;\frac{x}{h}\right)dy \leqslant \int_{-\infty}^{\infty} F\left(y;\frac{x}{h}\right)dy = 1.$$

Secondly, at any a and b different from zero

$$\lim_{(x/h)\to\infty}\int_b^a F\left(y;\frac{x}{h}\right)dy$$

$$= \begin{cases} 0 & \text{at } a < b < 0 \text{ and } 0 < a < b \\ 1 & \text{at } a < 0 < b. \end{cases}$$

should be fulfilled, which is easy to check.

Using the latter remark and eliminating $\Theta(x)$ from (50) and (53) we obtain the equation for $p(x)$:

$$\gamma\int_0^x \frac{p(y)\,dy}{(x^{3/4} - y^{3/4})^{2/3}} = \frac{Q_0}{K_s}x\left(l - \frac{x}{2}\right)\epsilon(l-x)$$

$$+ \frac{Q_0}{K_s}\cdot\frac{l^2}{2}\epsilon(x-l) - \frac{1}{h}\int_0^\infty G(x,y)p(y)\,dy$$

$$- \frac{h}{3}p(x). \quad (54)$$

It is easy to see from equation (54) that $p(x)$ depends on the dimensionless variable

$$\sim \frac{Re_x^{1/2}Pr^{1/3}}{\kappa}\cdot\frac{x}{h}$$

where $Re_x = Ux/\nu$ is the local Reynolds number and $Pr = \nu/\chi$ is the Prandtl number. Since Pr and Re_x are not low, then it is sufficient to find the asymptotic solution of equation (54) due to the condition $x/h \gg 1$. For this purpose, having

subjected equation (54) to the Mellin transform we obtain the difference equation

$$(\bar{p}(s) = \int_0^\infty p(x)x^{s-1}\,dx):$$

$$\tfrac{4}{3}\Gamma(\tfrac{1}{3})\gamma \cdot \frac{\Gamma(2-\frac{4}{3}s)}{\Gamma(\frac{7}{3}-\frac{4}{3}s)}\bar{p}(s-\tfrac{1}{2}) =$$

$$-\frac{Q_0}{K_s}\cdot\frac{l^{s+1}}{s(s-1)(s+1)}$$

$$+\frac{1}{h}\cdot\frac{1}{s(s-1)}\bar{p}(s+1)-\frac{h}{3}\bar{p}(s-1), \qquad (55)$$

where

$$0 < \mathrm{Re}(s) < 1.$$

According to the method of the asymptotic solution of some integral equations given in the Appendix a new function $\bar{\varphi}(s)$ will be substituted for $\bar{p}(s)$:

$$\bar{p}(\tfrac{3}{4}s-1) = \overline{\Omega}(s)\bar{\varphi}(s), \quad |\mathrm{Re}(s) > 0|, \qquad (56)$$

where

$$\overline{\Omega}(s) = \frac{\Gamma(2s)\Gamma(2s+\frac{2}{3})\Gamma(s+\frac{5}{3})\Gamma(s+\frac{1}{3})\Gamma(s+2)}{\Gamma(\frac{8}{3}-s)}. \qquad (57)$$

(note, that $\overline{\Omega}(s)$ is analytical in the half-plane $\mathrm{Re}(s) > 0$). The proof of the fact that the function $\varphi(x)$ may be looked for in the form of expansion of x inverse power will be omitted, and the asymptotic expansion for $p(x)$ and $\Theta(x)$ will be given directly. For the sake of brevity we shall deduce the results only for the physically interesting region $x \leqslant l$ where the heat release is going on; l is supposed to be sufficiently large, so that inequalities are taking place

$$h \text{ and } \frac{\kappa}{Re_x^{1/2}Pr^{1/3}}\cdot h \ll x \leqslant l. \qquad (58)$$

$$p(x) = \tfrac{3}{4}\sum_{n=0}^{\infty}\frac{a_n}{x^{n/2}}\overline{\Omega}(\tfrac{2}{3}n+\tfrac{4}{3}), \qquad (59)$$

$$\Theta(x) = \Gamma(\tfrac{1}{3})\gamma\sum_{n=0}^{\infty}\frac{a_n}{x^{n/2-1/2}}\bar{K}(\tfrac{2}{3}n+\tfrac{4}{3}), \qquad (60)$$

where $\overline{\Omega}(s)$ is determined by the relation (57) and

$$\bar{K}(s) = \frac{\Gamma(2s)\Gamma(2s+\frac{2}{3})\Gamma(s+\frac{5}{3})\Gamma(s+\frac{1}{3})\Gamma(s+2)}{\Gamma(3-s)}. \qquad (61)$$

The coefficients a_n satisfy the recurrence relation

$$\left.\begin{aligned} &\bar{K}_1(\tfrac{2}{3}n-\tfrac{4}{3})a_{n-3} - \frac{1}{H}\bar{K}_2(\tfrac{2}{3}n-\tfrac{4}{3})a_n - B\bar{K}_3(\tfrac{2}{3}n-\tfrac{4}{3})a_{n-4} = 0, \quad |n = 1, 2, \ldots|;\\ &a_K \equiv 0 (K < 0);\\ &a_0 = \frac{3^2}{2\cdot 5\cdot 7\,\Gamma^2(\frac{5}{3})\Gamma(\frac{10}{3})}\cdot\frac{Q_0}{K_s}\cdot h. \end{aligned}\right\} \qquad (62)$$

In equation (62) the following designations are used:

$$\left.\begin{aligned} \bar{K}_1(s) &= \frac{\Gamma(2s+\frac{4}{3})\Gamma(2s+2)\,\Gamma(s+\frac{7}{3})\Gamma(s+1)\,\Gamma(s+\frac{8}{3})}{\Gamma(\frac{4}{3}-s)}\cdot s,\\ \bar{K}_2(s) &= \frac{\Gamma(2s+\frac{16}{3})\Gamma(2s+6)\Gamma(s+\frac{13}{3})\Gamma(s+3)\Gamma(s+\frac{14}{3})}{\Gamma(1-s)}\cdot s,\\ \bar{K}_3(s) &= \frac{\Gamma(2s+1)\Gamma(2s+\frac{2}{3})\Gamma(s+\frac{5}{3})\Gamma(s+\frac{1}{3})\Gamma(s+2)}{\Gamma(\frac{8}{3}-s)}(s-\tfrac{4}{3}),\\ H &= \tfrac{3}{4}\Gamma(\tfrac{1}{3})h\gamma, \quad B = h/4\Gamma(\tfrac{1}{3})\gamma. \end{aligned}\right\} \qquad (63)$$

Vol. 3 1961

From (62) and (63) the coefficients a_n are easily evaluated. We shall write out in an explicit form the first terms of the expansions (59) and (60)

$$p(x) = \frac{Q_0}{K_s} h \left\{ 1 - \frac{1}{2^{5/3} \cdot 3^{2/3} c^{1/3}} \left[\frac{\Gamma(\frac{1}{3})}{\Gamma(\frac{2}{3})} \right]^2 \frac{\kappa}{Re_x^{1/2} Pr^{1/3}} \cdot \frac{h}{x} \right.$$
$$\left. - \frac{1}{2^{1/3} \cdot 3^{4/3} c^{2/3}} \left[\frac{\Gamma(\frac{1}{3})}{\Gamma(\frac{2}{3})} \right]^4 \frac{\kappa^2}{Re_x Pr^{2/3}} \left(\frac{h}{x} \right)^2 + 0\,(1/x^{7/2}) \right\} \quad (64)$$

$$\Theta(x) = \frac{Q_0}{K_s} \cdot h \frac{\kappa}{Re_x^{1/2} Pr^{1/3}} \cdot x \cdot \frac{2^{1/3}}{3^{2/3} c^{1/3}} \left[\frac{\Gamma(\frac{1}{3})}{\Gamma(\frac{2}{3})} \right]^2 \cdot \left\{ 1 - \frac{1}{2^{5/3} \cdot 3^{2/3} c^{1/3}} \left[\frac{\Gamma(\frac{1}{3})}{\Gamma(\frac{2}{3})} \right]^2 \frac{\kappa}{Re_x^{1/2} Pr^{1/3}} \cdot \frac{h}{x} \right.$$
$$\left. - \frac{7}{2^{4/3} \cdot 3^{4/3} \cdot 5 \cdot c^{2/3}} \left[\frac{\Gamma(\frac{1}{3})}{\Gamma(\frac{2}{3})} \right]^4 \frac{\kappa^2}{Re_x Pr^{2/3}} \left(\frac{h}{x} \right)^2 + 0\,(1/x^3) \right\}. \quad (65)$$

Hence, for the coefficient of heat transfer and for the local Nusselt number it is easy to get:

$$\alpha = \frac{3^{2/3} c^{1/3}}{2^{1/3}} \left[\frac{\Gamma(\frac{2}{3})}{\Gamma(\frac{1}{3})} \right]^2 K_f \frac{Re_x^{1/2} \cdot Pr^{1/3}}{x} - \frac{3^{1/3}}{2^{5/3} \cdot 5 \cdot c^{1/3}} \left[\frac{\Gamma(\frac{1}{3})}{\Gamma(\frac{2}{3})} \right]^2 K_s \left(\frac{h}{x} \right)^2 \frac{1}{Re_x^{1/2} Pr^{1/3}} \frac{1}{x} + 0(1/x^4), \quad (66)$$

$$\frac{Nu_x}{Re_x^{1/2}} = \frac{3^{2/3} c^{1/3}}{2^{1/3}} \left[\frac{\Gamma(\frac{2}{3})}{\Gamma(\frac{1}{3})} \right]^2 Pr^{1/3} - \frac{3^{1/3}}{2^{5/3} \cdot 5 \cdot c^{1/3}} \left[\frac{\Gamma(\frac{1}{3})}{\Gamma(\frac{2}{3})} \right]^2 \frac{\kappa^2}{Re_x Pr^{1/3}} \left(\frac{h}{x} \right)^2 + 0 \left(\frac{1}{x^{7/2}} \right). \quad (67)$$

In conclusion we shall give once more the range of application of the results obtained:

(a) inequalities (58),
(b) $Pr > 1$,
(c) $Re_x < 3 \cdot 10^5$.

ACKNOWLEDGEMENT

The author wishes to thank Professor A. V. Luikov for his interest in this work.

REFERENCES

1. L. D. Landau and E. M. Lifshitz, *Mekhanika sploshnykh sred.* GITTL (1953).
2. D. R. Chapman and M. W. Rubesin, *J. Aero. Sci.* **16**, 547 (1949).
3. E. Pohlhausen, *Z. Angew. Math. Mech.* **1**, 115 (1921).
4. G. N. Patterson, *Molecular Flow of Gases*, Chap. 5. John Wiley, New York (1956).
5. F. Trikomi, *O lineinykh uravneniyakh v chastnykh proizvodnykh 2-go poryadka smeshannogo tipa.* GITTL (1947).
6. J. R. Macdonald and M. K. Brachman, *Rev. Mod. Phys.* **28**, 393 (1956).
7. N. N. Bogolyubov, B. V. Medvedev and M. N. Polivanov, *Voprosy teorii dispersionnykh soot-noshenii.* Fizmatgiz (1958).
8. N. I. Muskhelishvili, *Singular Integral Equations*, Noordhoff, Groningen (1953).
9. S. G. Mikhlin, *Uspekhi Matematicheskikh Nauk*, III, Vyp. 3 (1948).
10. H. Blasius, *Z. Angew. Math. Phys.* **56**, 1 (1908).
11. L. I. Sedov, *Metody podobiya i razmernosti v mekhanike.* GITTL (1957).
12. A. V. Luikov, *Teoriya teploprovodnosti.* GITTL (1952).
13. V. G. Levich, *Fiziko-khimicheskaya gidrodinamika.* Fizmatgiz (1959).
14. V. G. Levich and N. N. Meiman, *Doklady Akademii Nauk SSSR*, **79**, 97 (1951).
15. W. Sutton, *Proc. Roy. Soc.* **182**, 48 (1943).
16. I. M. Gel'fand and G. E. Shilov, *Obobshchennye funktsii i deistviya nad nimi*, Vyp. 1. Fizmatgiz (1959).

APPENDIX

A number of problems of mathematical physics (including the conjugated problems considered above, some other problems of the transfer theory and dispersion relations of the quantum field theory) are resolved by the integral equations of the form:

$$a(x)\varphi(x) = g(x) + \int_0^\infty k(x/y) x^\alpha y^\beta \varphi(y)\, dy, \quad (A1)$$

where $a(x)$ is the finite sum*

* $a(x)$ can also be a linear differential operator of such a type as $\sum_K a_K x^{\gamma_K} (d^{n_K}/dx^{n_K})$. Thus, equation (A1) can be integro-differential too.

$$a(x) = \sum_K a_K x^{\gamma_K}. \qquad \text{(A1')}$$

Often it is sufficient to get the asymptotic expansion of the solution of this equation.

If as $x \to \infty$ the kernel $k(x)$ does not decrease more quickly than any power of x, then it is impossible to seek $\varphi(x)$ directly in the form of an asymptotic series.

With the help of the method given below the asymptotic solution of equation (A1) may be obtained for many cases at high x.

Subjecting equation (A1) to the Mellin transform we obtain the finite difference equation

$$\sum_K a_K \Phi(s + \gamma_K) = G(s) + K(s + \alpha)\Phi(s + \alpha + \beta + 1), \qquad \text{(A2)}$$

taking place in some band of the complex plane s. Without restriction of the generality we may consider that $0 < \mathrm{Re}(s) < \sigma$ where σ is some positive number.

In equation (A2) we designated

$$\Phi(s) = \int_0^\infty \varphi(x) x^{s-1}\, dx$$

and in an analogous way for the other functions.

Introducing a new unknown function $\Psi(s)$ instead of $\Phi(s)$:

$$\Phi(s + \delta) = \Omega(s)\Psi(s) \quad |\mathrm{Re}(s) > 0|, \qquad \text{(A3)}$$

where δ is the smallest number out of γ_K and $\alpha + \beta + 1$. Equation (A2) will take the form

$$\sum_K a_K \Omega(s + \gamma_K - \delta)\Psi(s + \gamma_K - \delta) = G(s) + K(s + \alpha)\Omega(s + \alpha + \beta - \delta + 1) \times \Psi(s + \alpha + \beta - \delta + 1) \qquad \text{(A4)}$$

The function $\Omega(s)$ is chosen so that, firstly, the inverse Mellin transforms of $\Omega(s)$ as well as of functions $\Omega(s + \gamma_k - \delta)$ and

$$K(s + \alpha)\Omega(s + \alpha + \beta - \delta + 1),$$

being the coefficients in equation (A4) could exist. Secondly, the inverse Mellin transforms of all the functions enumerated must diminish exponentially at $x \to \infty$. To fulfill the latter condition it is necessary that $\Omega(s)$, all the $\Omega(s + \gamma_K - \delta)$ and

$$K(s + \alpha)\Omega(s + \alpha + \beta - \delta + 1)$$

have no singularities in the half-plane $\mathrm{Re}(s) > 0$. Whether it is sufficient depends on the right choice of $\Omega(s)$.

Now we may seek the function $\psi(x)$ in the form of asymptotic expansion, for example,

$$\psi(x) = \sum_{n=0}^{\infty} \frac{c_n}{x^{an+b}}$$

and obtain the recurrence relations for c_n from equation (A4). The unknown function $\varphi(x)$ is easily determined from equation (A3).

For concrete integral equations it is not difficult to select the function $\Omega(s)$ so that it may have the required analytical properties.

As an example consider a simple Volterra equation of the second kind

$$\varphi(x) = 1 - \int_0^x \frac{\varphi(y)}{\sqrt{(x - y)}}\, dy, \qquad \text{(A5)}$$

which belongs to the class of equations (A1). Equation (A5) is taken only for the sake of illustration, since by the standard method it is easy to get its exact solution with the help of the Laplace transformation

$$\varphi(x) = \exp(\pi x)\, \mathrm{erfc}\, [\sqrt{(\pi x)}], \qquad \text{(A6)}$$

where

$$\mathrm{erfc}\,(x) = \frac{2}{\sqrt{\pi}} \int_x^\infty \exp(-t^2)\, dt.$$

Briefly, so as not to introduce the generalized (half-plane) Mellin transforms, we shall present a nonuniform term of equation (A5), for example, in the form of $\lim_{\epsilon \to 0} \exp(-\epsilon\sqrt{x})$ and turn to the limit only at the end.

From equation (A5) we get

$$\lim_{\epsilon \to 0} 2\epsilon^{-2s}\Gamma(2s) - \Phi(s) = \sqrt{\pi}\, \frac{\Gamma(\frac{1}{2} - s)}{\Gamma(1 - s)}\, \Phi(s + \tfrac{1}{2}), \quad |0 < \mathrm{Re}(s) < \tfrac{1}{2}| \qquad \text{(A7)}$$

Introduce instead of $\Phi(s)$ a new function

$$\Phi(s) = \frac{\Gamma(2s)\Gamma(s)}{\Gamma(1 - s)}\Psi(s) \quad |\mathrm{Re}(s) > 0|. \qquad \text{(A8)}$$

Upon elementary transformations equation (A7) will acquire the form

Vol. 3 1961

$$-\lim_{\epsilon \to 0} 2\epsilon^{-2s}\Gamma(-s) - \frac{\Gamma(s)}{s}\Psi(s) =$$

$$2\sqrt{\pi}\Gamma(s + \tfrac{1}{2})\Psi(s + \tfrac{1}{2}), \quad |\mathrm{Re}(s) > 0|. \qquad \text{(A9)}$$

Equations (A8 and A9) are equivalent, respectively

$$\varphi(x) = 2\int_0^\infty J_0(2y^{1/4})K_0(2y^{1/4})\psi\left(\frac{x}{y}\right)\frac{dy}{y} \qquad \text{(A10)}$$

and

$$2 + \int_0^\infty Ei(-y)\psi\left(\frac{x}{y}\right)\frac{dy}{y}$$

$$= 2\sqrt{(\pi x)}\int_0^\infty \exp(-y)\psi\left(\frac{x}{y}\right)\frac{dy}{y}. \qquad \text{(A11)}$$

Here $J_0(x)$ is the Bessel function of the zero order, $K_0(x)$ is the Macdonald function of the zero order and $Ei(x)$ is the integro-exponential function.

Now, it is evident that $\psi(x)$ can be sought in the form of the asymptotic series

$$\psi(x) = \sum_{n=0}^{\infty} \frac{c_n}{x^{an+b}}. \qquad \text{(A12)}$$

From (A8 and A9) or (A10 and A11) we get $a = b = \frac{1}{2}$ and c_n will satisfy the relation

$$c_n = \frac{1}{\sqrt{\pi}} \cdot \frac{1}{n} \cdot \frac{\Gamma(n/2)}{\Gamma[(n+1)/2]} c_{n-1} \quad |n = 1, 2, \ldots| \qquad \text{(A13)}$$

at

$$c_0 = \frac{1}{\pi}.$$

Finally,

$$\varphi(x) = \sum_{n=0}^{\infty} \frac{c_{2n}}{x^{n+1/2}} \cdot \frac{\Gamma(2n+1)\Gamma(n+\frac{1}{2})}{\Gamma(\frac{1}{2} - n)}. \qquad \text{(A14)}$$

It is easy to check that the series (A14) the coefficients of which are determined from equation (A13) coincide with the known asymptotic expansion of the solution of (A6).

Vol.
3
1961

Int. J. Heat Mass Transfer. Vol. 3, pp. 305–309. Pergamon Press 1961. Printed in Great Britain.

HEAT TRANSFER OF A PLATE IN A LIQUID FLOW

A. A. ZHUKAUSKAS and A. B. AMBRAZYAVICHYUS
Institute of Energetics and Electrical Engineering of the Academy of Sciences of the Lithuanian S.S.R.

(*Received* 18 *February* 1961)

Abstract—The paper presents results of the experimental investigation of heat transfer of a plate in a flow of air, water and transformer oil at different directions of heat flow over the range of Re_f numbers from 2×10^4 to 3×10^7 and that of Pr_f—from 0·701 to 380. Formulae were obtained to calculate heat transfer of a plate in a liquid flow.

Résumé—Cet article présente les résultats d'une recherche expérimentale sur la transmission de chaleur d'une plaque dans un écoulement d'air, d'eau et d'huile de transformateur, pour différentes directions du flux de chaleur et des domaines de nombres de Reynolds compris entre 2×10^4 et 3×10^7 et de nombres de Prandtl de 0,701 à 380. Des formules ont été obtenues pour calculer la transmission de chaleur d'une plaque dans un écoulement liquide.

Zusammenfassung—Es werden Versuchsergebnisse mitgeteilt für den Wärmeübergang an einer Platte bei Anströmung mit Luft, Wasser und Transformatorenöl. Die Untersuchungen wurden für verschiedene Wärmestromrichtungen durchgeführt in einem Bereich der Re_f-Zahlen von 2×10^4 bis 3×10^7 und der Pr_f-Zahlen von 0,701 bis 380. Die ermittelten Gleichungen erlauben die Berechnung des Wärmeübergangs an angeströmten Platten.

Аннотация—Представлены результаты экспериментального исследования теплообмена пластины в потоке воздуха, воды и трансформаторного масла при различных направлениях теплового потока в интервале чисел Re_f от 2×10^4 до 3×10^7 и Pr_f от 0,701 до 380. Получены формулы для расчёта теплообмена пластины в потоке жидкости.

NOMENCLATURE

- l_0, length of the heated or cooled portion of the plate;
- l, complete length of the plate with tip;
- t_f, temperature of the liquid outside boundary layer;
- t_w, wall temperature;
- α, heat transfer coefficient;
- w, liquid flow rate;
- λ, thermal conductivity;
- ν, coefficient of kinematic viscosity;
- μ, coefficient of viscosity;
- g, gravity acceleration;
- c_p, heat capacity;
- Nu_{f0}, Nusselt number $(\alpha l_0)/\lambda_f$;
- Re_{f0} Reynolds number $(wl_0)/\nu_f$;
- Re_f, Reynolds number $(wl)/\nu_f$;
- Pr, Prandtl number $(c_p \mu g)/\lambda$.

Subscripts

- f, liquid;
- w, wall.

THE present paper contains results of the experimental investigation of heat transfer of a plate in a flow of a drop liquid at a turbulent boundary layer. In the literature there are data only on heat transfer of a plate in an air flow [1–5].

Experiments were carried out with air, water and transformer oil in hydrodynamic contours, the main scheme of which has been described before [6, 7]. A working liquid was fed by a pump with the efficiency of 200 m³/h from a tank with a capacity of 2 m³, to a tank with a lattice of longitudinal tubes which served to level the flow. The liquid from the tank entered an experimental channel portion of rectangular section through a smoothly contracting entrance, then it interflowed again into the tank through a steel tube 100 mm in diameter, on the straight portion of which there was a normal diaphragm which served to measure the liquid rate. In experiments with air the pump was replaced by a fan.

Electric heaters of plates were fed by direct

current. Plates 50 mm wide were set into the channel of rectangular section 100 × 50 mm and plates 100 mm wide into the channel of 100 × 200 mm section. While determining the velocity in the channel the decrease of the channel section on account of the plate was taken into consideration.

The velocity of air changed from 7 to 70 m/sec, of water from 0·2 to 30·2 m/sec and that of transformer oil from 0·5 to 25·8 m/sec. High flow velocities were obtained by reducing channel height to 40 mm by uniformly graded inserts.

Four plates with water- and electric-calorimeters were applied in experiments. Dimensions of plates with the water calorimeters were 250 × 50 × 10 mm and 250 × 100 × 10 mm, those with electric-calorimeters 58 × 50 × 10 mm and 250 × 50 × 10 mm.

Plates 250 mm long had 23 thermocouples. The short electric plate had 12 thermocouples in its central portion. All the thermocouples were copper–constantan 0·15 mm in diameter. The average wall temperature was determined by graphic integration. The electromotive force of the thermocouples was measured by a potentiometer.

While carrying out experiments with the water plates, the water passing inside them was weighed and temperature change was measured by a pair of differential thermocouples with four junctions.

The electric heaters of the plates were fed by direct current supplied from a generator with an electronic voltage stabilizer. The voltage fall on the electric heaters was measured by the potentiometer through a voltage divider, and the current intensity by an ammeter of 0·5 grade.

Temperature of air ranged from 22° to 28°C, that of water from 12° to 90°C, that of transformer oil from 19° to 60°C. The wall temperature ranged from 10° to 107°C.

Limits of the Reynolds numbers change were from 2×10^4 to 3×10^7. An upper limit was obtained for the complete length of the plate (0·5 m).

In experiments the value of the criterion Pr_f varied from 0·701 to 380.

In order to find the influence of a length of non-heated initial portion upon heat transfer, Turbonit tips were made for each plate 50 mm wide. For plates 250 mm long the tips were made so that the length ratio of the heated portion l_0 (m) to the complete plate length l (m) was equal to 0·5, 0·6, 0·7 and 0·8.

For short plates the tips were made with ratios 0·11, 0·2, 0·3, 0·4 and 0·5. For this plate the tip with the ratio 0·5 (in contrast to all the others made with a semi-circular front edge) was made with a sharp edge, the thickness of which increased smoothly.

Physical parameters of air and water were taken according to the literary data [8]. Physical parameters of transformer oil were determined experimentally.

When primarily treating experimental data, criteria Nu_f, Re_f and Pr_f were determined. Physical parameters referred to the temperature of the liquid outside the boundary layer.

At first the experimental data were presented for plates with the ratio $l_0/l = 1$. The dependence of Nu_{f0} upon Re_{f0} determines the value of exponent at the Re_{f0} criterion equal to $n = 0{\cdot}8$.

Later on the treatment of the experimental data came to the determination of an exponent m at the criterion Pr_f. In a number of works on heat transfer [7–9] it was determined that the value of $m = 0{\cdot}25$ is a good one, where Pr_f is taken by the temperature of a liquid t_f, and Pr_w by that of a wall t_w.

In Fig. 1 the experimental data are given in the form of the dependence:

$$Nu_{f0}\, Re_{f0}^{-0{\cdot}8}\, [Pr_f/Pr_w]^{-0{\cdot}25} = f(Pr_f). \qquad (1)$$

It is seen from the diagram that all the points corresponding to heat transfer of the plate at its heating and cooling lie on a straight line with the exponent $m = 0{\cdot}43$. The inapplicability of the exponent $m = 0{\cdot}33$ is proved by a dashed straight line.

As a result of the further treatment of the experimental data on heat transfer of the plate, the following dependence was obtained:

$$Nu_{f0} = 0{\cdot}037\, Re_{f0}^{0{\cdot}8}\, Pr_f^{0{\cdot}43}\, [Pr_f/Pr_w]^{0{\cdot}25}. \qquad (2)$$

Data obtained on the plates with tips (Fig. 2) are described by the following dependence:

$$Nu_{f0} = 0{\cdot}037\, Re_f^{0{\cdot}8}\, Pr_f^{0{\cdot}43}\, [Pr_f/Pr_w]^{0{\cdot}25}\, [l_0/l]^{0{\cdot}8} \qquad (3)$$

Vol. 3 1961

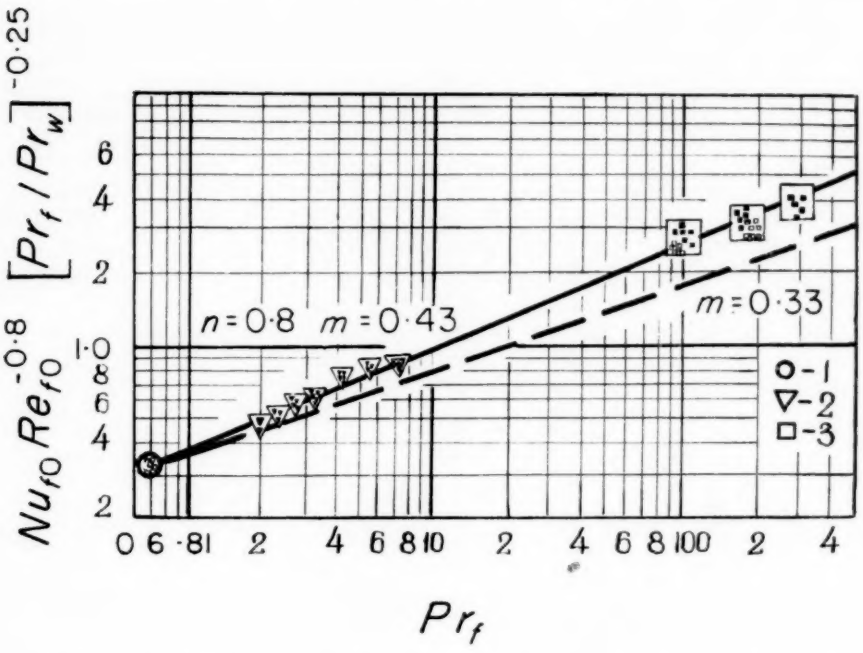

FIG. 1. Determination of exponent at Prandtl criterion. 1—air, 2—water, 3—transformer oil.

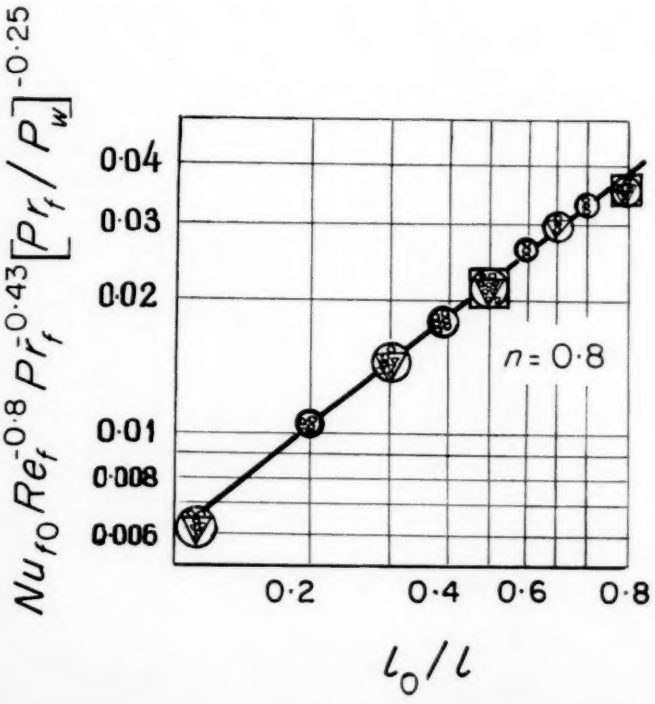

FIG. 2. Dependence of heat transfer from length of non-heated initial portion. See symbols in Fig. 1.

where Nu_{f0} refers to a heated or cooled portion of the plate l_0, and Re_f to the complete length l, or upon reduction:

$$Nu_{f0} = 0{\cdot}037\ Re_{f0}^{0{\cdot}8}\ Pr_f^{0{\cdot}43}\ [Pr_f/Pr_w]^{0{\cdot}25} \quad (4)$$

where Re_{f0} refers to the heated length of the plate l_0. The formulae (4) obtained differs in no way from dependence (2) for plates without non-heated tips. Therefore, it is possible to draw the conclusion that heat transfer of the plate does not depend upon the length of the initial non-heated tip and in calculations both Nu_{f0} and Re_{f0} should refer only to the length taking part in heat transfer.

The experimental data of the final treatment are given in Fig. 3 in the form of the dependence:

$$Nu_{f0}\ Pr_f^{-0{\cdot}43}\ [Pr_f/Pr_w]^{-0{\cdot}25} = f(Re_{f0}). \quad (5)$$

At $Re_f > 1{\cdot}4 \times 10^7$ the upper points are given in the form of the dependence:

$$Nu_{f0}\ Pr_f^{-0{\cdot}43}\ [Pr_f/Pr_w]^{-0{\cdot}25}\ [l_0/l]^{-0{\cdot}8} = f(Re_f) \quad (6)$$

as proof of the identicality of equations (3) and (4).

All the points in the range of the Re_{f0} numbers from 5×10^5 to 3×10^7 lie rather well on a straight line. Points pertaining to the plate with a sharp front edge of the tip lie here as well.

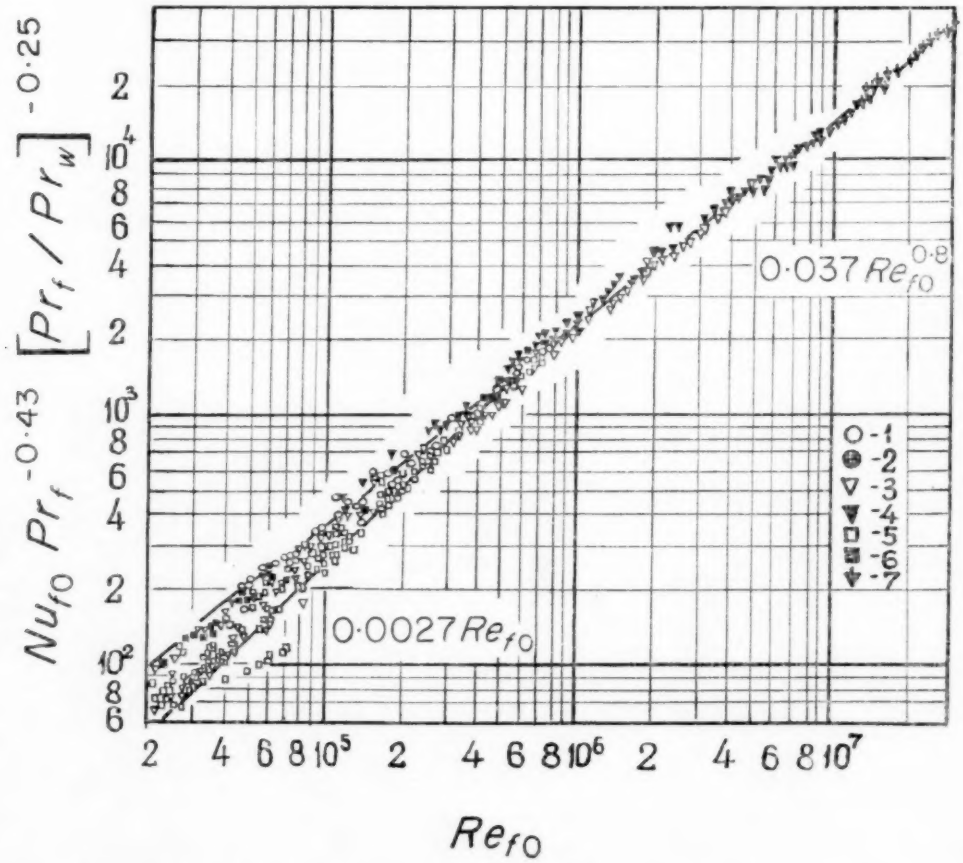

FIG. 3. Experimental data. 1—air heating, 2—air cooling, 3—water heating, 4—water cooling, 5—transformer oil heating, 6—transformer oil cooling, 7—water cooling, equation (7).

Vol. 3 1961

In the transient regime from a turbulent to a laminar boundary layer (Re_{f0} from 2×10^4 to 5×10^5) the experimental points lie between straight lines corresponding to equation (2) and the equation:

$$Nu_{f0} = 0{\cdot}0027\, Re_{f0}\, Pr_f^{0{\cdot}43}\, [Pr_f/Pr_w]^{0{\cdot}25} \quad (7)$$

depending on the intensity of turbulization on the surface of the plate.

Equation (7) shows that for some cases heat transfer in the transient region does not depend on the length of the plate.

For air ($Pr_f = 0{\cdot}702$) equation (4) is simplified and takes the following form:

$$Nu_{f0} = 0{\cdot}032\, Re_{f0}^{0{\cdot}8} \quad (8)$$

that agrees well with experimental data on heat transfer of a plate in a subsonic turbulent air flow [5].

REFERENCES

1. W. Jurges, Der Wärmeübergang an einer ebenen Wand, *Gesundheitsing*. Beiheft 19, Reihe 1 (1924).
2. F. Elias, Die Wärmeübertragung einer geheizten Platte an strömende, *Z. Angew. Math. Mech.* **9**, Heft 6 (1929); **10**, Heft 1 (1930).
3. S. Scesa and F. M. Sauer, An experimental investigation of convective heat transfer to air from a flat plate with a stepwise discontinuous surface temperature, *Trans. Amer. Soc. Mech. Engrs*, **74**, 1251 (1952).
4. W. Tessin and M. Jakob, Influence of unheated starting sections on the heat transfer from a cylinder to gas streams parallel to the axis, *Trans. Amer. Soc. Mech. Engrs*, **75**, 473 (1953).
5. B. S. Petukhov, A. A. Detlaf and V. V. Kirillov, Eksperimentalnoe issledovanie mestnoi teplootdachi plastiny v dozvukovom turbulentnom potoke vozdukha, *Zh. Tekh. Fiz.* **24**, Vyp. 10 (1954).
6. A. B. Ambrazyavichyus and A. A. Zhukauskas, Teplootdacha plastiny v potoke zhidkosti, *Trudy AN Litovskoi SSR* B4 (16), 171 (1958).
7. A. A. Zhukauskas, Teplootdacha pri poperechnom omyvanii tsilindra, *Sbornik, Teploperedacha i teplovoe modelirovanie*, 201, Izdatel'stvo AN SSSR, Moskva (1959).
8. M. A. Mikheev, Osnovy teploperedachi, *Gosenergoizdat*, Moskva (1956).
9. A. B. Ambrazyavichyus and A. A. Zhukauskas, K voprosu o vliyanii napravleniya teplovogo potoka na teplootdachu plastiny v potoke zhidkosti, *Trudy AN Litovskoi SSR* B4 (16), 163 (1958).

Vol.
3
1961

Int. J. Heat Mass Transfer. Vol. 3, pp. 311–320. Pergamon Press 1961. Printed in Great Britain.

METHOD OF A REGULAR REGIME FOR THE DETERMINATION OF VARIABLE THERMAL COEFFICIENTS

E. J. NEKHENDZI
Boiler-Turbine Institute, Leningrad

(*Received* 18 *February* 1961)

Abstract—The present work deals with the application of the theory and methods of a regular thermal regime in the case of cooling (heating) a body at variable thermal coefficients. It is shown that the description of a process by the regular regime formulae is possible and makes sense but in this case thermal coefficients determining the rate m are averaged in some temperature interval $\overline{\Delta t}$. The value $\overline{\Delta t}$ increases with Bi and at mean Bi it approaches the value of the initial excessive temperature ϑ_0.

Therefore, the regular regime method is suitable for the determination of the variable heat capacity $c_p(t)$ and the variable heat transfer coefficient $\alpha(\vartheta)$ at low Bi, but makes no sense for the determination of the variable thermal conductivity $\lambda(t)$ at mean and high Bi.

In the present work the method of variable coefficients is applied to investigating heat capacity of metals in a region of phase conversions of the second kind and heat transfer of a spherical specimen in various media and at various temperatures.

Résumé—Le travail actuel concerne l'application de la théorie et des méthodes du régime thermique régulier dans le cas du refroidissement (ou du chauffage) d'un corps à propriétés thermiques variables. On montre qu'il est possible, grâce aux formules du régime régulier, d'obtenir une représentation valable dans le cas ou les coefficients thermiques déterminant la vitesse m sont pris en moyenne dans un intervalle de température $\overline{\Delta t}$. La valeur de $\overline{\Delta t}$ augmente avec Bi et, comme Bi, approche de la valeur de l'écart de température initial ϑ_0.

Par suite, la méthode du régime régulier peut s'employer pour la détermination d'une chaleur spécifique variable $c_p(t)$ et d'un coefficient de transmission de chaleur variable $\alpha(\vartheta)$ pour de faibles valeurs de Bi, mais n'a pas de signification pour la détermination d'une conductibilité thermique variable $\lambda(t)$.

Dans cette étude, la méthode des coefficients variables est appliquée à la détermination de la chaleur spécifique des métaux au voisinage des conversions de phase de 2ème espèce, à la détermination du transfert de chaleur d'un modèle sphérique de milieux différents à différentes températures.

Zusammenfassung—Die Arbeit behandelt die Anwendung der Theorie und der Methode des regulären thermischen Zustandes auf die Kühlung (Beheizung) eines Körpers bei veränderlichen Wärmekoeffizienten. Es wird gezeigt, dass die Beschreibung eines Vorganges durch die Formeln dieser Theorie möglich und dann sinnvoll ist, wenn die Koeffizienten, die das Verhältnis m bestimmen, über ein Temperaturintervall $\overline{\Delta t}$ gemittelt werden. Der Wert $\overline{\Delta t}$ nimmt mit wachsendem Bi zu und erreicht bei einem mittleren Bi den Wert der anfänglichen Übertemperatur ϑ_0.

Die Methode des regulären thermischen Zustandes ist zur Bestimmung veränderlicher spezifischer Wärmen $c_p(t)$ und veränderlicher Wärmeübergangskoeffizienten $\alpha(\vartheta)$ bei kleinen Bi anwendbar, sie ist jedoch zur Bestimmung veränderlicher Wärmeleitzahlen $\lambda(t)$ unbrauchbar.

Die Methode der veränderlichen Koeffizienten wird angewandt auf die Untersuchung der spezifischen Wärmen von Metallen im Bereich der Phasenumwandlung zweiter Art und auf den Wärmeübergang von einem kugelförmigen Probekörper in unterschiedlichen Medien bei verschiedenen Temperaturen.

Аннотация—Данная работа посвящена применению теории и методов регулярного теплового режима на случай охлаждения (нагрева) тела при переменных тепловых коэффициентах. Показано, что описание процесса формулами регулярного режима воэможно и имеет смысл, но при это и тепловые коэффициенты. определяющие темп m, усредняются в некотором температурном интервале $\overline{\Delta t}$. Величина $\overline{\Delta t}$ возрастает вместе с Bi и уже при средних значениях Bi приближается к величине начальной избыточной температуры ϑ_0.

Поэтому метод регулярного режима пригоден для определения переменной теплоемкости $c_p(t)$ и переменного коэффициента теплоотдачи $\alpha(\vartheta)$ при малых Bi, но не имеет смысла для определения переменной теплопроводности $\lambda(t)$ при средних и больших Bi.

В настоящей работе предложенный метод переменных коэффициентов применяется для исследования теплоёмкости металлов в области фазовых превращений второго рода и теплообмена сферического образца в различных средах и при разных температурах.

NOMENCLATURE

t,	temperature;
τ,	time;
ϑ,	excessive temperature;
t_f,	temperature of medium;
t_w,	temperature of surface;
a,	thermal diffusivity;
c_p,	heat capacity;
λ,	thermal conductivity;
α,	heat transfer coefficient;
m,	rate of cooling (heating);
Bi,	Bio criterion;
R,	radius of specimen;
$f(r)$,	initial temperature distribution;
p_n,	roots of the characteristic equation;
C_n,	coefficients of expansion;
$A_n = C_n \frac{P_n}{R}$,	thermal amplitudes;
Δt,	temperature interval of averaging of thermal coefficients;
$\Delta t_{\text{reg}}(\tau_{\text{reg}})$,	interval of regularization;
$\Delta t_{ik}(\tau_{ik})$,	interval of treating the curve $\vartheta(\tau)$;
$c_{p,\max}$,	height of the heat capacity peak;
$\Delta c_{p,\max}$,	heat capacity jump at the Curie point;
Δt_R,	spatial temperature drop.

1. INTRODUCTION

THE theory and methods of a regular thermal regime of the first kind, developed by Kondratiev [1] and his disciples, are widely applied at present to the investigation of heat transfer processes and to the determination of thermal properties of various materials. The design formulae of the regular regime methods were obtained on the assumption that coefficients of thermal diffusivity a, thermal conductivity λ and of heat transfer α entering both the Fourier equation and a boundary condition of the third kind are constant. It is of interest to extend the regular regime method to the determination of variable thermal coefficients. Lately, much attention has been given to this problem [2–7].

The idea of the method lies in the fact that the curve of cooling (heating) a specimen $\vartheta = f(\tau)$ in the medium with constant temperature is divided into separate intervals $\Delta\tau_{ik}$, Δt_{ik} in which the rate

$$m_{ik} = \frac{\ln \vartheta_i / \vartheta_k}{\Delta\tau_{ik}} \tag{1}$$

is determined. In each interval the thermal coefficients a, λ, c, α and the rate m_{ik} are assumed to be constant values, and calculations are carried out by general formulae of the regular regime. Thus, having determined $m = f(\vartheta)$ for the investigated specimen and $\alpha = f(\vartheta)$ for the given medium, we can obtain the dependences $c_p = f(\vartheta)$, a, $\lambda = f(\vartheta)$ sought for or, vice versa, if we know a, $\lambda = f(\vartheta)$ for the specimen we can determine $\alpha = f(\vartheta)$.

Experimental works [2, 5] consider some particular cases of the determination of variable coefficients and, in the main, of heat transfer coefficient. There are attempts to apply this method to the determination of the variable heat conduction coefficient [5]. However, we cannot find a sufficient analysis or substantiation of the method in the mentioned works.

In theoretical works [6, 7] integral parameters which make it possible to obtain the expression of regularity in a general case of variable thermophysical coefficients were substituted into the heat conduction equation instead of temperature and time. However, this transformation does not yet allow one to propose a concrete method of an experimental determination of variable coefficients (with the exception of a very bulky method of determining α), and the method of dividing the curve $\vartheta(\tau)$ into separate intervals with the application of the regular

Vol. 3 1961

regime equations in a general form preserves its importance.

The present work considers and analyses this method in its general form. The experimental data which can be of original interest are presented here.

2. TEMPERATURE INTERVAL OF AVERAGING OF THERMAL COEFFICIENTS

(1) When substantiating the method it is necessary to ascertain at what actual temperature interval $\overline{\Delta t}$ the thermal coefficients which determine the rate m_{ik} are averaged. This interval of averaging the thermal coefficients $\overline{\Delta t}$ must differ in size from $\overline{\Delta t_{ik}}$. If we do not take into account this fact, dividing into intervals may appear to be a formal procedure without its physical sense. The value Δt should serve as the most important characteristic of the regular regime method for the variable coefficients, since it points out the expediency of the application of this method in various regimes.

The interval of averaging the thermal constants λ, c_p and a of the specimen is determined by a temperature drop Δt_R along the cross-section of the specimen, by regime regularization time τ_{reg} (with the corresponding interval Δt_{reg}) and by the value of the interval of treating the curve $\Delta t_{ik}(\Delta \tau_{ik})$.

In fact, if the time of the regularization of the thermal regime has a finite value, then the rate m_{ik} measured at the interval Δt_{ik} reflects values of the thermal coefficients in the preceding time interval τ_{reg} and in the corresponding temperature interval Δt_{reg}. At the same time, while measuring the rate m_{ik} in the specimen there is a spatial temperature drop Δt_R which is also one of the factors determining the value $\overline{\Delta t}$.

Figure 1 demonstrates graphically a value $\overline{\Delta t}$ of the total interval of averaging at the temperature measurement in the centre of the specimen being cooled:

$$\overline{\Delta t} = \begin{cases} \Delta t_{reg} + \frac{1}{2}\Delta t_{ik} + [\Delta t_R]_k & \text{at } \Delta t_{reg} > \frac{1}{2}\Delta t_{ik} \quad (2a) \\ \Delta t_{ik} + [\Delta t_R]_k & \text{at } \Delta t_{reg} \leqslant \frac{1}{2}\Delta t_{ik}. \quad (2b) \end{cases}$$

Thus, the temperature interval of averaging thermal constants depends only partially on the

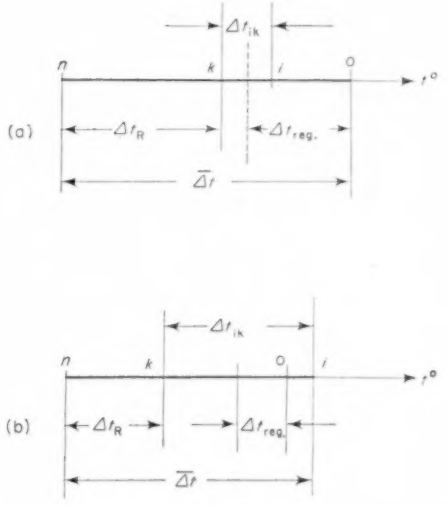

FIG. 1. Temperature interval of averaging of thermal constants $\overline{\Delta t}^\circ$.

way of the treatment of experimental curves $\vartheta(\tau)$ (i.e. on the value Δt_{ik}). The thermal constants are being averaged even at the differentiation of curves ($\Delta t_{ik} \to 0$) in the required minimum interval

$$\overline{\Delta t}_{min} = \Delta t_{reg} + [\Delta t_R]_k. \quad (3)$$

Let us consider in detail each term determining the value $\overline{\Delta t}_{min}$. All the calculations will be made for specimens of a spherical form. The conclusions can be extended to a body of any form.

(2) *Regularization interval*

As is known, the general solution of the Fourier equation has the form

$$\vartheta(r, \tau) = \sum_{n=1}^{\infty} C_n U_n \exp(-m_n \tau) \quad (4)$$

where

$$U_n = \frac{\sin p_n (r/R)}{r}$$

are eigenfunctions for a sphere ($U_n R/p_n = 1$ at the temperature measurement in the centre of the

sphere), p_n are the roots of the characteristic equation

$$Bi = \frac{\alpha R}{\lambda} = 1 - p\,ctg\,p, \tag{5}$$

the numbers

$$m_n = \frac{p_n^2 a}{R^2}, \tag{6}$$

$$C_n = \frac{\int_0^R rf(r) \sin p_n (r/R)\, dr}{\int_0^R \sin^2 p_n (r/R)\, dr} \tag{7}$$

are the constant coefficients of expansion, and the integrand $f(r) = \vartheta(r)|_{\tau=0}$ describes an initial temperature distribution in the specimen.

The regular thermal regime comes after the expiry of the time τ_{reg} of the process regularization when it is possible to neglect all the terms of (4) except the first one:

$$|C_1 U_1 \exp(-m_1\tau)| \gg |\sum_{n=2}^{\infty} C_n U_n \exp(-m_n\tau)|.$$

The theoretical evaluation of the time τ_{reg} or of the continuity of an irregular regime has not been carried out up to now and was thought to be unrealized [1]. However, the value τ_{reg} and the corresponding temperature regularization interval may be calculated if we take some finite quantity of the ratio

$$|\Delta|_{\text{per cent}} = \left| \frac{\sum_{n=2}^{\infty} C_n p_n \exp(-m_n\tau_{reg})}{C_1 p_1 \exp(-m_1\tau_{reg})} \right| . 100. \tag{8}$$

It is reasonable to take $|\Delta| = 4$ per cent (since the usual experimental error is $\Delta m/m = \pm 2$ per cent).

The value τ_{reg} is calculated by equation (8). The numbers p_n, m_n are determined by (5), the coefficients C_n are calculated by formula (7).

Two main and practically important cases should be considered:

(a) $$f(r) = \vartheta_0 = \text{const} \tag{9}$$

a body is heated uniformly at the initial moment; the period of the regime regularization at the beginning of a process is to be found.

(b) $$f(r) = C_1' \frac{\sin p_1'(r/R)}{r} \tag{10}$$

at the initial moment in the specimen there is a regular regime established in the previous interval $\Delta t_{ik}'$ and corresponding to some values of the thermal coefficients a', λ', c', α' and of the criterion Bi'. A period of the regime regularization at the transition into a new interval Δt_{ik} with the thermal coefficients a, λ, c, α and with the criterion Bi is to be obtained.

This case* corresponds to conditions of the method of the variable coefficients.

(3) *The initial condition* $f(r) = \vartheta_0 = const$ (9)

For this case the analysis of the value τ_{reg} depending on various factors is made in Table 1. The time of regularization for typical specific regimes is calculated by means of successive approximations with regard for three terms of a series. The values of thermal amplitudes $A_n = C_n (p_n/R)$ and $p_n = f(Bi)$ are taken from Tables of [8]. The radius of the specimen is taken equal to $R = 2$ cm when calculating the numbers m_n (6). The number m_1 for metallic specimens is in satisfactory agreement with the experimental value of the regular regime rate [4, 9].

The temperature interval of the regularization Δt_{reg} is given by the formula

$$\Delta t_{reg} = \vartheta_0 [1 - 0{\cdot}96\, A_1 \exp(-m_1\tau_{reg})], \tag{11}$$

since

$$\Delta t_{reg} = \vartheta_0 - \vartheta|_{r=0,\ \tau=\tau_{reg}},$$

and

$$\vartheta|_{r=0,\ \tau=\tau_{reg}} = \vartheta[A_1 \exp(-m_1\tau_{reg}) + \sum_{n=2}^{\infty} A_n \exp(-m_n\tau_{reg})]. \tag{12}$$

On the basis of Table 1 and (11) we can arrive at some general conclusions about the time of regularization and the value of the interval Δt_{reg}. The interval Δt_{reg} increases with Bi at Bi = var, a = *idem* (for example, when the heat transfer coefficient varies). At a = var, Bi = *idem* (for example, when heat capacity of the specimen changes in the process of phase conversion) the roots of characteristic equation (5) p_n and the

* G. N. Dulnev draws our attention to the necessity of its detailed consideration.

Vol. 3 1961

Table 1. *The determination of the regularization time* τ_{reg}
(*Spherical specimen* $R = 2$ *cm*)

	Examples	a (cm²/s)	Bi	m_1 (1/s)	m_2 (1/s)	m_3 (1/s)	A_1	A_2	A_3	τ_{reg} (s)	Δ per cent
	1. *Metals*										
1	Carbon steel at the determination of heat capacity near the point A_0	0·11	0·2	0·016	0·57	1·65	1·06	−0·09	0·05	1	−3·8
2	Regime of the determination of a, λ	0·11	4	0·168	0·75	1·85	1·72	−1·23	0·88	5	−3·8
3	The same	0·11	10	0·221	0·89	2·06	1·92	−1·74	1·51	4·7	−3·9
4	Metallic a-calorimeter (practically unrealized case)	0·11	∞	0·271	1·08	2·44	+2·00	−2·00	+2·00	4	−3·8
5	Carbon steel 45, $t_f = 815$°C, lead melt is a medium	0·04	4	0·060	0·27	0·67	1·72	−1·23	0·88	14	−3·8
6	Steel higher the point A_1, $t_f = 670$°C, lead melt is a medium	0·05	7	0·090	0·38	0·90	1·87	−1·57	1·28	10·5	−4·1
7	Steel 45 at the increase of the heat capacity peak near the point A_1, $t_f = 670$°C, lead melt is a medium	0·025	7	0·045	0·19	0·45	1·87	−1·57	1·28	21	−4·1
	2. *Insulators*										
8	Microcalorimeter	0·004	0·1	$0{\cdot}30 \times 10^{-3}$	0·020	0·060	1·03	−0·04	0·03	≲1	−4
9	λ-calorimeter	0·004	4	6×10^{-3}	0·027	0·067	1·72	−1·23	0·88	140	−3·8
10	The same	0·004	10	8×10^{-3}	0·033	0·075	1·92	−1·71	1·51	130	−4
11	a-calorimeter	0·004	∞	$9{\cdot}90 \times 10^{-3}$	0·039	0·089	+2·00	−2·00	+2·00	110	−4·1

coefficients C_n remain invariable and identity (8) leads to the condition $m_n\tau_{reg} = idem$ or $a\tau_{reg} = idem$. Though, in this case, the time of regularization is inversely proportional to the thermal diffusivity a, the value of the interval Δt_{reg} (11) remains constant.

After the establishment of the regular regime in a spherical specimen spatial temperature drop along the radius of it is expressed by the formula

$$\Delta t_R = \vartheta|_{r=0,\ \tau=\tau_{reg}} \left(1 - \frac{\sin p_1}{p_1}\right) \qquad (13)$$

where $\vartheta|_{r=0,\ \tau=\tau_{reg}}$ is determined by (12).

Naturally, at $Bi = \text{var}$, $a = idem$ the spatial drop increases with Bi. At $Bi = idem$ the values A_1, p_1, $m_1\tau_{reg} = idem$, i.e. the drop Δt_R does not change. It means, for example, that if the specimen is under the regular regime conditions, then

the temperature drop along a cross-section of the specimen does not change when the phase conversion of the second kind is going on in it (without heat liberation, $c = \text{var}$, $\lambda = \text{const}$).

On the basis of (11–13) it is possible to write the expression for the minimum temperature interval of averaging thermal constants:

$$\overline{\Delta t}_{\min} = \vartheta_0 \left(1 - 0{\cdot}96\, A_1 \exp\left(-m_1 \tau_{\text{reg}}\right) \cdot \frac{\sin p_1}{p_1}\right). \qquad (14)$$

The consideration of formula (14) confirms the conclusions derived when analysing separately Δt_{reg} and Δt_R: the interval of averaging $\overline{\Delta t}_{\min}$ increases with the increase in *Bi* and does not change with c and a (at $Bi = idem$).

In Table 2 the values of the intervals Δt_{reg}, Δt_R and $\overline{\Delta t}_{\min}$ are calculated depending on the value of *Bi*.

Table 2. The values Δt_{reg}, Δt_R and $\overline{\Delta t}_{\min}$ at various Bi

Bi	$0{\cdot}96\, A_1 \exp\left(-m_1 \tau_{\text{reg}}\right)$	$\frac{\sin p_1}{p_1}$	$\frac{\Delta t_{\text{reg}}}{\vartheta_0}$	$\frac{\Delta t_R}{\vartheta_0}$	$\frac{\overline{\Delta t}_{\min}}{\vartheta_0}$
0·2	0·998	0·91	0·002	0·09	0·09
4	0·72	0·26	0·27	0·54	0·81
7	0·68	0·15	0·32	0·58	0·90
∞	0·65	0	0·35	0·65	1·00

It follows from this table that the thermal constants are being averaged almost in the whole temperature interval of cooling (heating) the specimen irrespective of its initial temperature ϑ_0 already at the mean values of $Bi = 4 + 7$, i.e. in the region of determining heat conduction of metals and insulators.

Thus, the method of the variable coefficients is valid for the investigation of the temperature dependence of the body heat capacity $c_p(t)$ in regimes at low values of *Bi*, but loses its sense when one tries to determine the variable heat conductivity $\lambda(t)$ in regimes at mean and high *Bi*.

It is necessary to bear in mind that just the determination of the variable heat capacity is of the greatest interest since $c_p(t)$ is highly susceptible to structural changes in the specimen whereas heat conduction varies relatively in low degree and monotonously with the temperature.*

The temperature interval of averaging the heat transfer coefficient is less than that of the thermal constants since at $t_f = \text{const}$ the coefficient α is the function of the body surface temperature (ϑ_w) or of its derivatives, for example, of the average boundary-layer temperature, t_m.

However, in the regimes at mean and high *Bi* the value

$$\vartheta_w = \vartheta|_{r=0,\ \tau_{\text{reg}}} \frac{\sin p_1}{p_1}$$

is so small at the end of the regularization interval that any attempt at determining $\alpha = f(\vartheta_w)$ will be senseless. Thus, the determination of the quantitative dependence $\alpha(\vartheta_w)$ is possible only at low *Bi* while at mean and high *Bi* it makes no sense as well as the determination of the variable heat conduction.

The analysis of such an important parameter as an interval of averaging the thermal coefficients $\overline{\Delta t}$, makes it possible to explain such facts as formal observance of the regular regime at intensive cooling of steel specimens in water and oil in the range of ~700–20°C [1], at cooling of refractory materials from ~1000°C to room temperature in the regimes of λ and a-calorimeters (in the regimes of calorimeter work on the determination of thermal conductivity and thermal diffusivity).

(4) *The initial condition* $f(r) = C_1' \dfrac{\sin p_1'(r/R)}{r}$. (10)

To obtain the main conclusions on the application of the method of the variable coefficients it was sufficient to consider the temperature interval of averaging at cooling (heating) a body with uniform temperature distribution (Section 3). However, to specify the values τ_{reg} and Δt_{reg} in the case when thermal coefficients vary in the regular regime already established it is necessary to calculate the expansion coefficients C_n (7) at the initial condition (10). As was shown

* The method of determining the variable heat capacity under the conditions of the regular regime is to a certain extent analogous to methods of thermic analysis which are also bound up with the receipt of curves of cooling (heating) an investigated specimen in a wide temperature interval [10–12].

Vol. 3 1961

above this case has practical value only for regimes at low Bi.

Taking into account that

$$C_1' = \frac{\vartheta_0|_{r=0} \cdot R}{p_1'}$$

(where $\vartheta_0|_{r=0} = f(0)$ is the temperature of the specimen centre at the beginning of the given interval Δt_{ik}) we get for C_n:

$$C_n = \frac{\vartheta_0|_{r=0} \cdot R}{p_1'} \cdot \frac{\int_0^R \sin p_1'(r/R) \sin p_n(r/R)\, dr}{\int_0^R \sin 2 p_n (r/R)\, dr} \tag{15}$$

If the change of $Bi = \alpha R/\lambda$ during a process can be neglected and only heat capacity $c_p(t)$ of the specimen changes essentially, then $p_1' = p_1$ and according to (15) $C_1 = C_1'$; $C_n = 0$ at $n = 2, 3, \ldots$. Thus, at $Bi = idem$, $a =$ var the regularity of the regime is not disturbed, and $\tau_{reg}, \Delta t_{reg} = 0$ despite the fact that the rate $m_{ik}(t)$ varies continuously.

However, in real conditions the value Bi usually changes somewhat, mainly because of the change of the heat transfer coefficient α. Then the values p_1', p_n are the roots of two different equations of the type (5), integrands $\sin p_1'(r/R)$, $\sin p_n(r/R)$ do not form an orthogonal set, and, therefore, all the coefficients $C_n \neq 0$. However, one may expect that

$$C_1 \gg C_n (n = 2, 3 \ldots),$$

since the values Bi' and Bi differ slightly from each other in neighbouring intervals $\Delta t_{ik}'$ and Δt_{ik}.

Having calculated the integrals, the expression (15) may be given in the form most convenient for quantitative calculations:

$$C_n = \frac{\vartheta_0|_{r=0} \cdot R}{p_1'} \cdot \frac{\dfrac{\sin(p_1' - p_n)}{p_1' - p_n} - \dfrac{\sin(p_1' + p_n)}{p_1' + p_n}}{1 - \dfrac{\sin 2 p_n}{2 p_n}}. \tag{16}$$

The calculation of the amplitudes $A_n = C_n \cdot p_n/R$ for typical regimes of the determination of heat capacity and heat transfer coefficient at $Bi = 0{\cdot}2$–$0{\cdot}4$ shows that even at wittingly heightened $|(Bi - Bi')/Bi| = 10$ per cent, the values $A_n \approx 0{\cdot}01\ A_1$, i.e. really all the coefficients of equation (8) are small in comparison with the first one. Taking into account also that the numbers m_n increase with n, one may suppose that in this case $\tau_{reg}, \Delta t_{reg} \to 0$.

Thus, when thermal coefficients vary under the conditions of steady-state regular regime at small values of Bi, then the interval of averaging $\overline{\Delta t}$ is practically determined only by the interval Δt_{ik} and by the volumetric temperature drop Δt_R (2b).

(5) *Single-valued dependence of the rate m on the temperature* ϑ

It is useful to show when substantiating the method of determining the variable coefficients that at the constant temperature of the medium $t_f = idem$ the rate m is simply determined by the value ϑ, irrespective of the initial ϑ_0.

This condition arises logically from the regime regularization concept: the character of the previous thermal regime of a specimen should not influence the value m after the expiry of the time τ_{reg}.

This conclusion is confirmed by experiments. In our work the experiments on cooling the metallic specimens in various media in a wide temperature range $\vartheta_0 \approx 70°$ were duplicated systematically by experiments on cooling the specimens which had been heated to usual excessive temperature $\vartheta_0' \approx 20°$ at the same $t_f = idem$. And in the general interval ϑ_0 the rate m coincides for both groups of experiments in the range of the usual experimental error.

3. APPLICATION OF THE METHOD DETERMINING THE VARIABLE COEFFICIENTS

The method of determining the variable α was applied in the present work to the systematic investigation of external heat transfer at flowing of a spherical specimen in water and oil [9]. The results obtained were used when calculating the variable heat capacity of specimens of steel (of various trade marks) and nickel.

(1) *Determination of nickel heat capacity in the region of the Curie point*

An electrolytic nickel N2 GOST 849-49 (99·2

per cent Ni) was investigated. A nickel specimen was cooled in the medium (high viscous dead mineral oil) in intersecting temperature intervals at $t_f = 310$ and 330°C. The average temperature of a boundary layer $t_m = \frac{1}{2}(t_f + t_w)$ was the determining one for the coefficient of heat transfer. It is seen from Fig. 2 that experimental curves $m = f(t_m)$ obtained when treating photographic records of specimen cooling passes through the

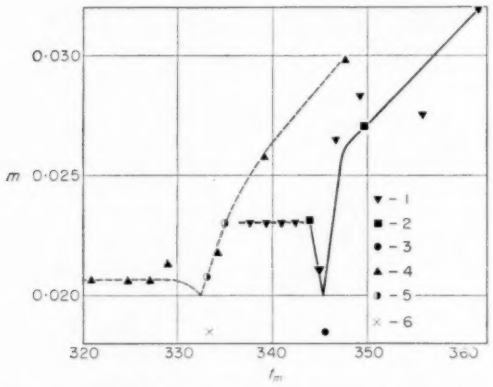

FIG. 2. Results of treating photograms of nickel cooling in the region of the Curie point, m is in s^{-1}.

1—$t_f = 330°$, $\Delta\tau_{ik} = 6$–8 s;
2—$t_f = 330°$, $\Delta\tau_{ik} = 4$ s;
3—$t_f = 330°$, $\Delta\tau_{ik} = 2$ s;
4—$t_f = 310°$, $\Delta\tau_{ik} = 6$–8 s;
5—$t_f = 310°$, $\Delta\tau_{ik} = 4$ s;
6—$t_f = 310°$, $\Delta\tau_{ik} = 2$ s.

minimum corresponding to the heat capacity peak at the Curie point. Both the curves are similar and 10° shifted along the axis t_m which calls forth their coincidence when plotting in co-ordinates $m = f(t)$ (where t is the average temperature of the specimen). Really, the heat capacity values $c_p(t)$ calculated for both groups of experiments lie on the common curve with highly satisfactory accuracy (Fig. 3). This is indicative of the reliability of the experimental results.

The curve $c_p(t)$ forms a clear-cut heat capacity peak at the temperature $t = 362{\cdot}5$°C. The configuration of the peak is typical for heat capacity of a ferromagnetic specimen at the Curie point. The height of the heat capacity peak $c_{p,\,\max}$ has a finite value (the transformation of the second kind) and it depends consider-

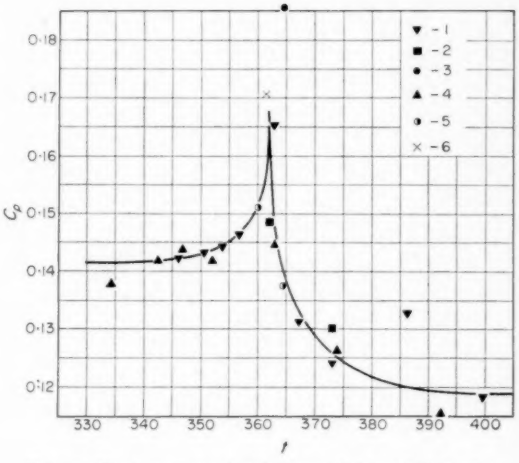

FIG. 3. Heat capacity (cal/g degree) of nickel in the region of the Curie point (by the regular regime method for variable coefficients)

1—$t_f = 330°$, $\Delta\tau_{ik} = 6$ s;
2—$t_f = 330°$, $\Delta\tau_{ik} = 4$ s;
3—$t_f = 330°$, $\Delta\tau_{ik} = 2$ s;
4—$t_f = 310°$, $\Delta\tau_{ik} = 6$ s;
5—$t_f = 310°$, $\Delta\tau_{ik} = 4$ s;
6—$t_f = 310°$, $\Delta\tau_{ik} = 2$ s.

ably on the interval of treating the photograms of $\Delta\tau_{ik}$, i.e. on the interval of averaging the thermal constants $\overline{\Delta t}$. The contraction of the intervals $\Delta\tau_{ik}(\Delta t_{ik})$ makes it possible to approach the true heat capacity $c_{p,\,\max}$ but, on the other hand, error arises as a result of inaccuracy in measuring adjacent ordinates ϑ on the photogram. The optimum value $\Delta\tau_{ik} = 4$ s at $t_f = 310°$ or $\Delta\tau_{ik} = 6$ s at $t_f = 330°$ was established, which corresponds to the interval of averaging the heat capacity $\overline{\Delta t} \approx 10°$ both to the height of the peak $c_{p,\,\max} = 0{\cdot}165$–$0{\cdot}170$ cal/g degree and to the value of the heat capacity jump at the Curie point $\Delta c_{p,\,\max} = 0{\cdot}045$–$0{\cdot}050$ cal/degree. And the error of $\Delta m_{ik}/m_{ik} = \pm 1{\cdot}5$ per cent, the total error of $(\Delta c_p/c_p)_{\max} = \pm 3{\cdot}5$ per cent.

The curve $c_p(t)$ obtained coincides practically with that adduced in the literature, but the values $c_{p,\,\max}$ and $\Delta c_{p,\,\max}$ are higher than in other works ($c_{p,\,\max} = 0{\cdot}155$; $\Delta c_{p,\,\max} = 0{\cdot}035$ cal/g degree). To explain this divergence we carried out the analysis of the experimental installations used by Sykes and Wilkinson [13], Klinkhardt [14] and Moser [15] from the point of view of the

Vol. 3 1961

value of the temperature interval of averaging the heat capacity $\overline{\Delta t}$. In each of these installations the rate of heating the specimen, temperature drop, duration of measuring processes, inertia of measuring instruments and the dissociation of experimental points on the curve $c_p(t)$ determine the value $\overline{\Delta t}$. It turned out that everywhere the value $\overline{\Delta t} > 10°$, and it may lead to the understating of $c_{p,\max}$ in the published works

The control determination of the heat capacity of nickel specimens which were of the same trade mark, N2, was carried out on the installation built in the Leningrad Polytechnical Institute [16]. Particular attention was paid in these experiments to the lowering of Δt (to 2°). And the increase of $c_{p,\max}$ compared to the data adduced in the literature was confirmed. The values $\Delta c_{p,\max} = 0{\cdot}045$ cal/g degree and Curie temperature coincided with the data of the regular regime method.

The considered question on the correct measurement of the true value of $c_{p,\max}$ and $\Delta c_{p,\max}$ has not only a methodological importance, but it is important also for physics of a solid body and, in particular, for the evaluation of the number of magnetons per atom and for more precise definition of the ferromagnetism theory.

(2) *Definition of the carbon steel heat capacity in the region of A_0 point*

The temperature dependence of heat capacity of some carbon steel specimens in the region of the cementite magnetic transformation (A_0 point) obtained by the regular regime method for the variable coefficients is given in Fig. 4. The interval of averaging the heat capacity is estimated in $\overline{\Delta t} = 9{\cdot}5°$, experimental errors of $\Delta m_{ik}/m_{ik} = \pm 1{\cdot}5$ per cent; $(\Delta c_p/c_p)_{\max} = \pm 3{\cdot}5$ per cent.

The clear-cut heat capacity maximum is observed in A_0 point. This corroborates the data obtained by Umino [17], the only author who found the heat capacity peak in the A_0 region.

The efficiency of applying the regular regime method in the present problem is apparently conditioned by a photographical record of the continuous cooling curve at rather low values of $\Delta m_{ik}/m_{ik}$ and $\overline{\Delta t}$.

The validity of the results obtained for the carbon steel is confirmed by the fact that heat capacity of the austenitic and ferrite steel, measured by the same method, increases slightly and monotonously with temperature in the same region forming no maximum.

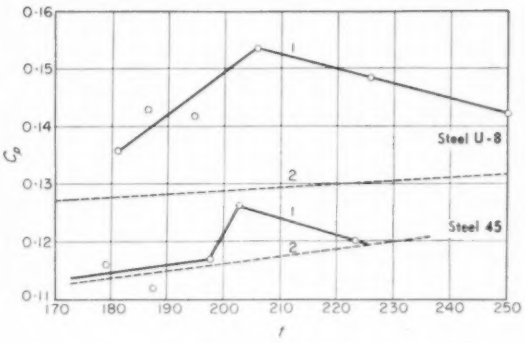

FIG. 4. Heat capacity (cal/g degree) of carbon steel in the region of A_0 point (by the regular regime method for variable coefficients)
1—author's data, $t_f = 165°C$,
2—data from References [18–21]

REFERENCES

1. G. M. KONDRAT'EV, *Regulyarni Teplovoi Rezhim*, GTTI (1954).
2. E. M. SEMYASHKIN, Sravnitel'noi opredelenie srednekh koeffitsiyentov teplotdachi tsilindrov po metodam stadionarnogo i regulyarnogo rezhimov, LITMO Sbornik Statei, Vyp. **8**, 27 (1953).
3. G. N. DULNEV and E. M. SEMYASHKIN, Sravnenie dvukh metodov izmereniya koeffitsienta teplotdachi, LITMO Sbornik Statei, Vyp. **21**, 233 (1957).
4. E. J. NEKHENDZI, Opredelenie teplovykh konstant metallov metdom regulyarnogo rezhima, avtoreferat dissertatsii, Leningrad (1956).
5. Pervaya mezhvuzovskaya nauchno-tekhnicheskaya konferentsiya po teplovomu regulyarnomu rezhimu, *Kratkoe Soderzhanie Dokl.* LITMO, Leningrad (1958); *Inzh. Fiz. Zh.* **1**, 8 (1958).
6. L. I. KUDRYASHOV and A. V. TEMNIKOV, Obobshchenie teorii teplovogo regulyarnogo rezhima na sluchai peremennykh teplofizicheskikh charakteristik, *Inzh. Fiz. Zh.* **1**, 10 (1958).
7. L. I. KUDRYASHOV and V. G. ZHEMKOV, Obobshchenie teorii teplovogo regulyarnogo rezhima na sluchai peremennykh teplofizicheskikh charakteristik. *Inzh. Fiz. Zh.* **2**, 4 (1959).
8. A. V. LUIKOV, *Teoriya Teploprovodnosti*, GTTI (1952).
9. E. J. NEKHENDZI, Opredelenie teploemkosti i teploprovodnosti metallov v usloviyakh regulyarnogo rezhima, *Zh. Tekh. Fiz.* **24**, 8 (1954).

10. C. SYKES, Methods for investigating thermal changes occurring during transformations in a solid solution, *Proc. Roy. Soc.* A **148**, 864, 422 (1935).
11. C. SMITH, Prostoi termicheskii metod kolichestrenuogo opredeleniya udelnoi teploemkosti i skrytoi teploty prevrashchenii (referat), *Metallurg.* **7**, 57 (1940).
12. Y. A. TUROVSKII and G. M. BARTENEV, Opredelenie teploemkosti metallov metodom okhlazhdeniya, *Zh. Tekh. Fiz.* **10**, 6, 514 (1940).
13. C. SYKES and H. WILKINSON, The specific heat of nickel from 100° to 600°C, *Proc. Phys. Soc.*, **50**, 281, 834 (1938).
14. H. KLINKHARDT, Messung von wahren spezifischen Wärmen bei hohen Temperaturen durch Heizung mit Glühelecktronen, *Annalen Physik*, **84**, 17, 167 (1927).
15. H. MOSER, Messung der wahren spezifischen Wärme von Silber, Nickel, β-Messung, Quarzkristall und Quarzglass zwischen +50 und 700°C nach einer verfeinerten Methode, *Z. Phys.* **37**, 21, 737 (1936).
16. G. M. FEENBERG and Y. A. BERMAN, Opredelenie ictinnoi teploemkosti tverdykh tel v shirokom intervale temperatur, *Zavodskaya Laboratoriya*, **9**, 1057 (1953).
17. S. UMINO, *Sci. Rep. Tohoku Univ.* **16**, 798, 1027 (1927); **23**, 665 (1935).
18. C. SYKES and H. EVANS, Specific heat temperature curves of commercially pure iron and certain plain carbon steels, *J. Iron St. Inst.* **138**, 2, 125 (1938).
19. J. H. AWBERY and A. SNOW, Total heat at various temperatures up to 950°C, *Iron St. Inst., Spec. Rep.*, No. 24 (1939).
20. P. L. GRUZIN, G. V. KURDUMOV and R. I. ENTIN, O prirode "tretego prevrashcheniya" pri otpuske zakalennoi stali, *Metallurg.* **15**, 8 (128), 15 (1940).
21. N. T. GUDTSOV, (Redaktor) Konstrukshionye stali (spravochnik), T. I., *Metallurgizdat M.* (1947).

Vol. 3 1961

Int. J. Heat Mass Transfer. Vol. 3, pp. 321–339. Pergamon Press 1961. Printed in Great Britain.

MASS TRANSFER THROUGH LAMINAR BOUNDARY LAYERS—6. METHODS OF EVALUATING THE WALL GRADIENT (b_0'/B) FOR SIMILAR SOLUTIONS; SOME NEW VALUES FOR ZERO MAIN-STREAM PRESSURE GRADIENT

H. L. EVANS

Commonwealth Scientific and Industrial Research Organization,
Division of Food Preservation, P.O. Box 43, Ryde, N.S.W., Australia

(*Received* 2 *February* 1961)

Abstract—The wall gradient (b_0'/B) of the b-boundary layer is evaluated from solutions to the velocity equation by integration. By dividing the range of integration into two parts (a) that over the velocity boundary layer and (b) that for main-stream flow, a formula is derived from which this wall gradient can be evaluated accurately for any value of the Prandtl/Schmidt number. Methods are then given for doing this either with a desk calculator or on a computer. These methods are not convenient however, when the Prandtl/Schmidt number has a high value and there is a high rate of inward mass flow; an asymptotic formula is therefore derived for this case. A table of values of the wall gradient, most of which are new, is then given for the case of zero main-stream pressure gradient. A discussion follows of the asymptotic behaviour of functions of the b-boundary layer when various parameters take extreme values and some of these functions are plotted.

Résumé—Le gradient à la paroi (b_0'/B) de la couche limite est évalué, par intégration, à partir des solutions de l'équation du mouvement. En divisant l'intervalle d'intégration en deux parties: (a) celui qui couvre la couche limite dynamique et (b) celui relatif à l'écoulement principal, on établit une formule à partir de laquelle on peut calculer avec précision le gradient à la paroi, pour une valeur quelconque du nombre de Prandtl/Schmidt. Des méthodes sont ensuite données pour effecteur ce calcul soit à l'aide d'une machine à calculer de bureau soit avec une calculatrice. Toutefois, ces méthodes ne conviennent pas quand le nombre de Prandtl/Schmidt est élevé et lorsqu'il existe un transport de masse important dans la couche limite; pour ce cas, une formule asymptotique a été établie. Une table des valeurs du gradient à la paroi, dont la plupart sont nouvelles, est ensuite donnée quand le gradient de pression est nul dans l'écoulement principal. Suit une discussion sur le comportement asymptotique des fonctions dans la couche limite b lorsque les différents paramètres prennent des valeurs extremes; quelques unes de ces fonctions ont été tracées.

Zusammenfassung—Durch Integration von Lösungen der Geschwindigkeitsgleichung wurde der Wandgradient (b_0'/B) der b-Grenzschicht berechnet. Teilt man den Integrationsbereich (a) in den Bereich der Geschwindigkeitsgrenzschicht und (b) in den Bereich der Hauptströmung, so erhält man eine für beliebige Werte der Prandtl/Schmidtzahl gültige Formel fèr die exakten Werte des Wandgradienten. Diese Berechnung ist für Hand- und Elektronenrechner angegeben. Für grosse Werte der Prandtl/Schmidtzahl und einen grossen, nach innen durch die Granzfläche tretenden Massenstrom ist diese Berechnungsmethode unbequem, deshalb wurde dafür eine asymptotische Formel abgeleitet. Eine Tabelle vorwiegend neuer Werte des Wandgradienten ist für einen Druckgradienten Null der Hauptströmung angegeben. Für Extremwerter einiger Parameter zeigen die Funktionen der b-Grenzschicht ein asymptotisches Verhalten. Einige dieser Funktionen sind als Diagramme mitgeteilt.

Аннотация—Градиент (b_0'/B) пограничного слоя b на стенке вычисляется из решений уравнения скорости путём его интегрирования. Разделив интегралы на две части: (а) по пограничному слою и (б) для основного потока, получим формулу, из которой можно точно вычислить градиент на стенке для любых чисел Прандтля/Шмндта. Также в статье приводится методика вычисления с помощью счётни-вычисли-тельных машин. Однако, эти методы непригодны в случае больших чисел Прандтля/Шмидта

или большой скорости течения; в этом сдучае выводится асимптотическая формула. В конце статьи приведена таблица величин градиента на стенке, большая часть из которых даётся впервые, для случая нулевого градиента давления в основном потоке. Рассматривается асимптотическое поведение функций иограничного слоя b, когда различные параметры принимают крайние значения, а некоторые функции даны графически.

NOTATION

Most of the quantities given below are dimensionless; where they are not the dimensions are given in brackets.

a_m, coefficients occurring in equation (23) and defined in equations (26) to (33);
A_q, coefficients occurring in equation (20) defined in equation (21);
b, conserved fluid property in dimensionless form (see Paper 3 for a discussion of its form and meaning);
b'_0, gradient of b in the fluid at the interface; see equation (10);
B, value of b in the main-stream; it is the driving force for mass transfer (discussed fully in Paper 3);
C, constant occurring in equation (1);
c, abbreviation for (f''_0/f_0^3) which occurs in equations (26) to (34);
d, dimensionless distance occurring in equation (15); it is the value of the "similar" co-ordinate η at which the flow can be regarded as inviscid;
e, abbreviation for (β/f_0^4) which occurs in equations (26) to (34);
f, dimensionless stream function in "similar" co-ordinates defined in equation (4);
f_0, value of f at the interface; see equation (7);
$f''_0, f_0^{(n)}$, values of the derivatives of f at the interface;
F_2, function which measures the rate of growth with distance x of the momentum boundary layer thickness δ_2; see equation (57) and Appendix;
K, diffusion constant; the thermal diffusivity of the fluid for heat transfer, the diffusion coefficient of a mass component in the fluid mixture for mass transfer (ft^2/h);
n, constant occurring in equation (1);
Nu, Nusselt number in terms of the length x;
p, number occurring in equation (22) specifying terms in the expanded form of equation (20);
q, number occurring in equation (21) specifying terms in equation (20);
Re, local Reynolds number $(=u_G x/\nu)$;
u, velocity component parallel to the interface (ft/h);
u_G, value of u in the main-stream (ft/h);
v, velocity component normal to the interface (ft/h);
v_0, value of v at the interface (ft/h);
W, curvature parameter in terms of the convection thickness Δ_2; equation (46);
x, distance parallel to the interface measured from the start of the boundary layer (ft);
X, curvature parameter in terms of the conduction thickness Δ_4; equation (44);
y, distance measured perpendicular to the interface (ft);
Y, function which is a measure of the rate of growth with distance x of the conduction thickness Δ_4; equation (45);
Z, function which is a measure of the rate of growth with distance x of the convection thickness Δ_2; equation (47).

Greek symbols

β, parameter occurring in the velocity equation; it is a measure of the main-stream pressure gradient; equation (2);
γ, fluid property called the "exchange coefficient" given by $K\rho$, (lb/ft h);
δ_1^*, displacement boundary layer thickness in "similar" co-ordinates; defined by equation (13), (ft);
δ_2, momentum boundary layer thickness,

$$= \int_0^\infty \frac{u}{u_G}\left(1 - \frac{u}{u_G}\right) dy, \quad \text{(ft)};$$

δ_4, shear boundary layer thickness,
$= u_G/(\partial u/\partial y)_0$, (ft);

Vol. 3 1961

Δ_2, convection boundary layer thickness, $= \int_0^\infty \frac{u}{u_G}\left(1 - \frac{b}{B}\right) dy$, (ft);

Δ_4, conduction boundary layer thickness, $= B/(\partial b/\partial y)_0$, (ft);

η, "similar" dimensionless length co-ordinate which gives the distance of a point from the interface, equation (3);

μ, dynamic viscosity of fluid (lb/ft h);

ν, kinematic viscosity of fluid $(= \mu/\rho)$, (ft²/h);

ρ, density of fluid (lb/ft³);

σ, Prandtl or Schmidt number $(= \nu/K)$;

φ, integration variable used in section 3.4, defined in equation (18);

ψ, stream function (ft²/h).

Subscripts

G, denotes fluid state in the main-stream;

m, denotes terms in equation (23);

0, denotes fluid state adjacent to the interface;

q, denotes terms in equation (20).

1. INTRODUCTION

1.1. *General remarks*

IN EARLIER papers of the present series it was shown that when the fluid properties are uniform the prediction of mass transfer rates through laminar boundary layers can be reduced to the solution of two simultaneous partial differential equations. The velocity equation governs the distribution in the boundary layer of momentum, shear and other purely mechanical quantities; this was considered in Paper 1, Spalding [1] and Paper 2, Spalding and Evans [2]. The b-equation governs the distribution of other conserved fluid properties; this was discussed in Paper 3, Spalding and Evans [3].

It was also shown that for "similar" flows these equations reduce to ordinary differential equations which can be solved exactly. These "similar" solutions are important not only in their application to strictly "similar" flows but also serve as a basis for more general, if approximate, methods applicable to problems involving non-similar flows.

An important quantity occurring in the b-equation is the "wall gradient" (b_0'/B), where b_0' is the gradient of the conserved fluid property b with respect to the "similar" dimensionless distance η, the suffix denoting the value at $\eta = 0$, and B is the value of b in the main-stream. In principle this wall gradient can be evaluated by integration once the distribution of the stream function is known.

In Paper 3 it was shown that comparatively few exact values of the wall gradient could be found in the literature. Most of them related to the case of zero main-stream pressure gradient and were confined to a fairly narrow range near unity in the Prandtl/Schmidt number σ. Paper 3 also contained tables from which approximate values of (b_0'/B) could be obtained for wide ranges in the main-stream pressure gradient and Prandtl/Schmidt number.

Paper 3a, Evans [4], was concerned with the case of zero mass transfer. Series were given from which the wall gradient could be evaluated accurately for wide ranges in the main-stream pressure gradient and for any value greater than 0·5 of the Prandtl/Schmidt number σ.

1.2. *Outline of the present paper*

The main aims of the present paper are to give methods of evaluating the wall gradient (b_0'/B) accurately and to present a table of values for the case of zero main-stream pressure gradient. This table covers wide ranges in the fluid Prandtl/Schmidt number as well as the mass transfer rate. Formulae and methods of calculation are given in a general form which hold even when the main-stream pressure gradient is not zero, but results for non-zero values of this parameter are to be given in later papers.

After a brief statement of the mathematical problem which has to be solved, an expression is derived for the reciprocal of the wall gradient which greatly simplifies the problem of numerical evaluation. This can be used for any values of the parameters specifying the Prandtl/Schmidt number, main-stream pressure gradient or mass transfer rate.

Values of the wall gradient have been obtained in three ways. When solutions to the velocity equation are known, calculations with a desk calculator can give high accuracy; the method used is described in section 3.2. Most of the

results were, however, obtained on a computer the method for which is outlined in section 3.3. But, when the Prandtl/Schmidt number has a high value and the suction rate is high, neither of these methods is suitable so an asymptotic formula which gives high accuracy under these conditions is derived in section 3.4.

The results obtained for zero main-stream pressure gradient are discussed in section 4 and formulae are given in section 5 from which other functions of the b-boundary layer may be calculated. Since these functions are readily evaluated from the wall gradient and the known values of the various parameters, they are not tabulated in the present paper.

In section 6 an examination is made of the asymptotic behaviour of functions in the b-boundary layer for extreme values of the parameters and in section 7 some of these functions are plotted and discussed.

2. STATEMENT OF THE MATHEMATICAL PROBLEM

The forms which the two-dimensional, laminar boundary layer equations take for "similar" flows have been fully discussed in earlier papers in the present series. For purposes of reference and in order to explain the terminology used, the equations are stated briefly in the present section.

2.1. *The "similar" velocity equation*

In Paper 1, Spalding [1], it was shown that for "similar" solutions to the two-dimensional, laminar boundary layer equations with constant fluid properties, the main-stream velocity u_G obeys the equation:

$$\frac{\mathrm{d}u_G}{\mathrm{d}x} = C\,u_G^n \tag{1}$$

where C and n are constants and x is the distance measured parallel to the wall.

A parameter β is obtained from the constant n by the relationship:

$$\beta = \frac{1}{\left(1 - \frac{n}{2}\right)} \tag{2}$$

and a dimensionless distance co-ordinate η is defined by:

$$\eta = y\left(\frac{1}{\nu\beta}\cdot\frac{\mathrm{d}u_G}{\mathrm{d}x}\right)^{1/2} \tag{3}$$

where y is the distance perpendicular to the wall and ν is the kinematic viscosity. If now a dimensionless stream function f is related to the stream function ψ by:

$$f = \frac{\psi}{u_G}\left(\frac{1}{\nu\beta}\frac{\mathrm{d}u_G}{\mathrm{d}x}\right)^{1/2} \tag{4}$$

velocities in the boundary layer are governed by the ordinary differential equation:

$$f''' + ff'' + \beta(1 - f'^2) = 0 \tag{5}$$

with the boundary conditions:

$$\left.\begin{aligned} &\eta = 0, \quad f = f_0, \quad f' = 0 \\ &\eta \to \infty, \quad f' \to 1. \end{aligned}\right\} \tag{6}$$

In equations (5) and (6) the primes denote differentiation with respect to the independent variable η and the quantity f_0 in equation (6), which is a constant for "similar" flows, is related to the velocity v_0 with which mass flows through the wall by:

$$f_0 = -v_0\left(\frac{\nu}{\beta}\frac{\mathrm{d}u_G}{\mathrm{d}x}\right)^{-1/2}. \tag{7}$$

2.2. *The "similar" b-equation*

This equation is a generalization of the energy equation familiar in the study of heat transfer. It has been fully discussed by Spalding [5] and "similar" solutions to it were considered in Paper 3. In the latter paper it was shown that for a certain restricted class of "similar" solutions a conserved fluid property, represented in suitable dimensionless form by the quantity b, satisfies the ordinary differential equation:

$$b'' + \sigma f b' = 0 \tag{8}$$

with boundary conditions:

$$\left.\begin{aligned} &\eta = 0, \quad b = 0 \\ &\eta \to \infty, \quad b \to B \end{aligned}\right\}. \tag{9}$$

In addition to these boundary conditions the relationship:

$$b_0' = -\sigma f_0, \tag{10}$$

Vol. 3 1961

which relates the b-profile to the f-profile, is also satisfied.

In these equations the primes again denote differentiation with respect to η, f and f_0 are the stream functions occurring in the velocity equation, σ is the Prandtl/Schmidt number and B is the value of b in the main-stream.

From equation (8) it may readily be shown that the distribution of b is given by:

$$\frac{b}{B} = \frac{\int_0^\eta \exp -\{\sigma \int_0^\eta f \, d\eta\} \, d\eta}{\int_0^\infty \exp -\{\sigma \int_0^\infty f \, d\eta\} \, d\eta} \tag{11}$$

and the reciprocal of the wall gradient is given by:

$$\left(\frac{B}{b_0'}\right) = \int_0^\infty \exp -\{\sigma \int_0^\eta f \, d\eta\} \, d\eta. \tag{12}$$

The present paper is concerned with methods of evaluating the right-hand side of equation (12) for any value of σ, given solutions to equation (5) with boundary conditions (6). Since such solutions are given for fixed values of f_0, and in view of the relationship given in equation (10), the problem amounts to evaluating the mass transfer driving force B, given the fluid property σ and the velocity, specified by f_0, at which mass flows through the interface. The main-stream pressure gradient, of course, also affects the distribution of f with η and thereby the value of B obtained using equations (12) and (10).

The table of values of (b_0'/B) to be given later apply to the case when the parameter β occurring in equation (5) is zero.

As well as evaluating the right-hand side of equation (12) the method of calculation could also be adapted to obtaining the distribution of b with η as given in equation (11) but this is not done in the present paper.

3. EVALUATING THE INTEGRAL

3.1. *Formula for numerical integration*

It is known that the relative thicknesses of the velocity boundary layer and the b-boundary layer depend on the value of the Prandtl/Schmidt number σ. For the unique case when the main-stream pressure gradient is zero and σ is unity the two boundary layers are identical. This may be seen by comparing equation (5) for $\beta = 0$ with equation (8) for $\sigma = 1$. The distribution in the boundary layer of the velocity, which is f', is then the same as the distribution of the quantity (b/B) since they obey the same differential equation with the same boundary conditions.

When σ is much greater than unity, however, the b-boundary layer is much thinner than the velocity layer, whereas when σ is much smaller than unity the b-boundary layer is much thicker than the velocity layer.

For low values of σ, therefore, an appreciable contribution to the integral in equation (12) comes from regions in the main-stream where, of course, the flow is inviscid.

The integral in equation (12) can therefore be evaluated in two parts, which will be referred to as Parts I and II respectively.

Part I: extends over the region of the velocity boundary layer and is evaluated by standard procedures for numerical integration; this part is important for large values of σ.

Part II: which extends over regions of main-stream flow, can be expressed in closed form and so is readily evaluated using standard mathematical tables; this part is important for small values of σ.

For intermediate values of σ an appreciable contribution to the integral comes from both parts.

For main-stream flow the stream function f takes on a simple form which is obtained as follows.

In the main-stream $(df/d\eta) = 1$ so that f must be a linear function of η. If the displacement thickness defined in terms of the "similar" distance η is given by:

$$\delta_1^* = \int_0^\infty \left(1 - \frac{df}{d\eta}\right) d\eta, \tag{13}$$

on integrating this formally it is found that for large values of η the stream function takes the form:

$$f = (\eta + f_0 - \delta_1^*). \tag{14}$$

When the fluid density is uniform the difference

in the values of the stream-function at two points in any fluid stream can be regarded as a measure of the amount of fluid which crosses a line joining the two points. Equation (14) conforms with this interpretation since f has the value f_0 at the interface where $\eta = 0$ and the amount of fluid flowing across the line joining the interface and the point η is proportional to $(\eta - \delta_1^*)$, since δ_1^* measures the thickness of the velocity layer (i.e. δ_1^* is the distance through which the mainstream has been *displaced* by the presence of the boundary layer).

In the integral of equation (12), therefore, let Part I be integrated over the range $0 \leqslant \eta \leqslant d$ and Part II over the range $d \leqslant \eta \leqslant \infty$. If the value of d is large enough for equation (14) to be valid at that point the expression for (B/b_0') may be written accurately as:

$$\left(\frac{B}{b_0'}\right) = \int_0^d \exp - \left\{ \sigma \int_0^\eta f \, d\eta \right\} d\eta + \left(\frac{\pi}{2\sigma}\right)^{1/2} \left\{ 1 \pm \operatorname{erf} \left[\left(\frac{\sigma}{2}\right)^{1/2} f(d) \right] \right\} \exp \left\{ \frac{\sigma}{2} \left[f(d) \right]^2 - \sigma \int_0^d f \, d\eta \right\} \tag{15}$$

where $f(d)$, the value of f at $\eta = d$, is:

$$f(d) = (d + f_0 - \delta_1^*). \tag{16}$$

In equation (15) the first term on the right-hand side is Part I, and the second term Part II. In Part II the sign preceding the error function should be opposite to that of $f(d)$. In practice, however, $f(d)$ is almost always positive so that this sign is generally negative; the alternative sign is included so that the formula may retain its general form.

The values of (b_0'/B) to be given later were obtained using equation (15). Use of this formula is reasonably straightforward and accurate; methods of doing so will now be described.

3.2. *Integration using a desk calculator*

To apply this method solutions to the velocity equation are needed in the form of values of the stream function f at regular intervals in η. Many such solutions are given in the literature.

Starting from such a table the first step is to construct a table of the function $\int_0^\eta f \, d\eta$ at regular intervals in η up to a value where equation (14) holds accurately; this point is readily located from the values of f and f_0. This table has to be obtained only once, of course, as it can then be used to evaluate (b_0'/B) for any value of σ.

It should be noted that the displacement thickness δ_1^*, although by definition a quantity which is obtained by integrating throughout the velocity boundary layer, can be obtained from the value of f at large η without the need for such integration. Using this and the known values of β, f_0 and f_0'', the other functions associated with the velocity layer, which were discussed in Papers 1 and 2, can also be evaluated. This procedure has proved to be particularly useful for calculations with a computer; the formulae which are used are given in the Appendix.

The table of $\int_0^\eta f \, d\eta$ is obtained in the following way. The stream function f is first expanded as a Maclaurin series in terms of its gradients at $\eta = 0$, the higher derivations of f needed for this being obtained by successive differentiation of equation (5). For small values of η values of $\int_0^\eta f \, d\eta$ can be obtained directly from this series although the accuracy decreases with increasing η. At some value of η, where it is judged that this expansion is becoming too inaccurate, the method is changed to a step by step application of Simpson's rule using the tabulated values of f. More accurate integration formulae than Simpson's rule can obviously be used if rapid means of computation are available.

Having obtained values of $\int_0^\eta f \, d\eta$ all the functions required for evaluating Part II of equation (15) are known.

Part I is evaluated numerically by again applying Simpson's rule in an obvious manner using the table of values of $\int_0^\eta f \, d\eta$. When mass transfer is zero or inwards and σ is large the b-boundary layer is confined to low values of η. To obtain high accuracy therefore a small interval in η must be used.

On the other hand, where mass transfer is outwards and σ is large the integrand occurring in Part I starts from the value unity at the wall, increases to a maximum within the boundary layer and then decreases to a very low value as

Vol. 3 1961

the main-stream is approached. Since the gradient of $\int_0^\eta f\,d\eta$ with respect to the co-ordinate η is f it may readily be shown that this maximum occurs at the point where f is zero. Most of the contribution to the integral therefore comes from regions within the boundary layer but not near the wall. It would therefore be surprising if an expansion in terms of wall gradients gave high accuracy, although expansion about the point where f is zero should be possible. This will not be considered further in the present paper.

3.3. *Integration by a computer*

The method for evaluating (b_0'/B) by a computer differed in many respects from that just described but since the procedure adopted was fairly conventional only a brief outline will be given here.

The computer programme was designed to be as general as possible so that values of (b_0'/B) could be obtained for any suitable values of the three parameters β, f_0 and σ. The only data required from solutions to the velocity equation were corresponding values of f_0, f_0'', and δ_1^*. In the calculations for the case $\beta = 0$ these quantities were taken from the literature.

For most of the calculations an interval of 0·1 in the independent variable η was used. At high suction rates, namely for large positive values of f_0, the velocity layer is very thin so the interval was reduced to 0·05 for those cases.

At each step in the integration procedure the velocity equation was solved using a fourth order Runge–Kutta process and the functions f, f', f'', $\int_0^\eta f\,d\eta$ and $\int_0^\eta \exp -\{\sigma_i \int_0^\eta f\,d\eta\}\,d\eta$ were evaluated. For any particular solution to the velocity equation the computer dealt with about 40 values of σ simultaneously and σ_i, with $i = 1, 2, 3 \ldots$, signifies this.

At every sixth step Part I and Part II of (B/b_0') occurring in equation (15) were evaluated and summed. This sum is an estimate of (B/b_0') up to that value of η. This was compared with the value obtained six steps previously. If the modulus of the difference between these two values was less than or equal to 5×10^{-5} of the last value obtained the integration was stopped for that value of σ. The programme continued until (B/b_0') had been evaluated for all values of σ.

It is now realized, of course, that such a testing procedure was not necessary since the integration could have continued up to the value $\eta = d$ and stopped there for all values of σ. The method just described was used because the form of Part II of the integral in equation (15) was not known when the programme was first devised.

3.4. *Asymptotic formula for high σ when f_0 is large and positive*

In Paper 3a, Evans [4], which was concerned with the case when no mass flows through the interface, asymptotic series in inverse powers of σ were given from which the wall gradient (b_0'/B) could be evaluated accurately for any value of σ greater than 0·5. An expansion of the same type will now be derived for large positive f_0. It has not been possible to do so for negative f_0 because of the behaviour of the integrand; this was discussed at the end of section 3.2.

The expansion is obtained in terms of the wall gradients of the stream function f. The wall gradient (b_0'/B) relating to the b-boundary layer is regarded as a single entity as expressed in equation (12) and not in two parts as given in equation (15). The accuracy of the expansion improves when each of the parameters σ and f_0 increases.

When f_0 is large and positive and σ is large, the driving force for mass transfer, denoted by B, approaches -1 from above. No physical meaning can be attached to values of B beyond -1. If then the quantity $(1 + B)$ can be evaluated to a certain accuracy for known values of β, f_0 and f_0'', the functions B and (b_0'/B) which are calculated from these, will be known to an even higher percentage accuracy. The expansion obtained below expresses $(1 + B)$ as a series in inverse powers of σ.

Expanding the stream function f in terms of wall gradients the integral $\int_0^\eta f\,d\eta$ takes the form:

$$\int_0^\eta f\,d\eta = f_0\,\eta + \frac{f_0''\eta^3}{3!} + \frac{f_0'''\eta^4}{4!} + \frac{f_0^{IV}\eta^5}{5!} + \ldots \tag{17}$$

This is now substituted into equation (12) and the integration variable changed from η to q where:

$$q = \sigma f_0 \eta. \tag{18}$$

Using the relationship:

$$B = -\frac{\sigma f_0}{(b_0'/B)} \tag{19}$$

equation (12) yields the expression:

$$-B = \int_0^\infty e^{-q} \exp -\left\{ \sum_{q=3}^{\infty} A_q q^q \right\} dq \tag{20}$$

in which the coefficients A_q are given by the general formula:

$$A_q = \frac{\sigma f_0^{(q-1)}}{q!} \frac{1}{(\sigma f_0)^q} \tag{21}$$

where $f_0^{(q-1)}$ denotes the $(q-1)$th derivative of f with respect to η when evaluated at $\eta = 0$.

By expanding the second exponential in the integral of equation (20) in powers of q and using the relationship:

$$\int_0^\infty e^{-q} q^p \, dq = p! \tag{22}$$

which holds for any integral value of p, an expansion is obtained for $(1 + B)$. On collecting terms in the same inverse powers of σ this expansion becomes:

$$(1 + B) = \frac{a_2}{\sigma^2} + \frac{a_3}{\sigma^3} + \frac{a_4}{\sigma^4} + \ldots \tag{23}$$

Using the abbreviations:

$$c = \frac{f_0''}{f_0^3} \tag{24}$$

$$e = \frac{\beta}{f_0} \tag{25}$$

the first eight coefficients in this expansion are:

$$a_2 = c \tag{26}$$

Table 1. *Values of the wall gradient* (b_0'/B) *as*

σ	$f_0 = 1{\cdot}0$ $f_0'' = 1{\cdot}0492$ $\delta_1^* = 0{\cdot}098797$	$3\sqrt{2}$ 4·35164 0·222053	$2{\cdot}5\sqrt{2}$ 3·66267 0·260703	$1{\cdot}5\sqrt{2}$ 2·30831 0·393434	$0{\cdot}75\sqrt{2}$ 1·33703 0·611810	$0{\cdot}5\sqrt{2}$ 1·03077 0·740107	$0{\cdot}25\sqrt{2}$ 0·739383 0·925949
0·0001	0·861969(−2)	0·823657(−2)	0·818854(−2)	0·808927(−2)	0·800763(−2)	0·797698(−2)	0·794290(−2)
0·0002	0·125740(−1)	0·118008(−1)	0·117042(−1)	0·115050(−1)	0·113418(−1)	0·112807(−1)	0·112123(−1)
0·0005	0·211078(−1)	0·191406(−1)	0·188972(−1)	0·183959(−1)	0·179864(−1)	0·178340(−1)	0·176651(−1)
0·001	0·318544(−1)	0·278467(−1)	0·273542(−1)	0·263446(−1)	0·255260(−1)	0·252220(−1)	0·248844(−1)
0·002	0·491721(−1)	0·409560(−1)	0·399591(−1)	0·379212(−1)	0·362786(−1)	0·356717(−1)	0·350027(−1)
0·005	0·912630(−1)	0·698160(−1)	0·672610(−1)	0·620743(−1)	0·579451(−1)	0·564373(−1)	0·547876(−1)
0·01	0·151737	0·107073	0·101803	0·912293(−1)	0·829225(−1)	0·799230(−1)	0·766709(−1)
0·02	0·262281	0·168678	0·157771	0·136087	0·119334	0·113377	0·106992
0·04	0·471320	0·274613	0·251880	0·207115	0·173211	0·161387	0·148901
0·06	0·675149	0·371591	0·336563	0·267946	0·216628	0·198965	0·180508
0·08	0·876936	0·464359	0·416717	0·323693	0·254745	0·231256	0·206911
0·1	0·107768(1)	0·554669	0·494176	0·376309	0·289548	0·260232	0·230055
0·2	0·207609(1)	0·989656	0·862717	0·616249	0·438226	0·379652	0·320693
0·3	0·307231(1)	0·141399(1)	0·121859(1)	0·838959	0·566879	0·478686	0·391302
0·4	0·406815(1)	0·183489(1)	0·156999(1)	0·105450(1)	0·686264	0·568038	0·452110
0·5	0·506425(1)	0·225452(1)	0·191953(1)	0·126639(1)	0·800351	0·651679	0·507066
0·6	0·606060(1)	0·267374(1)	0·226830(1)	0·147627(1)	0·911078	0·731569	0·558066
0·7	0·705730(1)	0·309293(1)	0·261679(1)	0·168500(1)	0·101954(1)	0·808828	0·606209
0·8	0·805430(1)	0·351226(1)	0·296527(1)	0·189307(1)	0·112641(1)	0·884158	0·652184
0·9	0·905153(1)	0·393181(1)	0·331387(1)	0·210078(1)	0·123214(1)	0·958030	0·696464
1·0	0·100490(2)	0·435162(1)	0·366265(1)	0·230831(1)	0·133703(1)	0·103077(1)	0·739382
1·2	0·120443(2)	0·519199(1)	0·436087(1)	0·272330(1)	0·154509(1)	0·117377(1)	0·822041
1·4	0·140403(2)	0·603334(1)	0·506006(1)	0·313857(1)	0·175173(1)	0·131444(1)	0·901516
1·6	0·160366(2)	0·687555(1)	0·575989(1)	0·355433(1)	0·195760(1)	0·145357(1)	0·978645
1·8	0·180331(2)	0·771850(1)	0·646049(1)	0·397066(1)	0·216308(1)	0·159165(1)	0·105399(1)
2·0	0·200308(2)	0·856207(1)	0·716168(1)	0·438757(1)	0·236841(1)	0·172901(1)	0·112795(1)
2·5	0·250280(2)	0·106732(2)	0·891776(1)	0·543219(1)	0·288193(1)	0·207067(1)	0·130845(1)
3·0	0·300249(2)	0·127867(2)	0·106766(2)	0·647966(1)	0·339649(1)	0·241127(1)	0·148475(1)
3·5	0·350222(2)	0·149018(2)	0·124372(2)	0·752938(1)	0·391244(1)	0·275180(1)	0·165841(1)
4·0	0·400201(2)	0·170180(2)	0·141992(2)	0·858088(1)	0·442978(1)	0·309271(1)	0·183038(1)
4·5	0·450182(2)	0·191352(2)	0·159620(2)	0·963379(1)	0·494842(1)	0·343423(1)	0·200123(1)
5·0	0·500167(2)	0·212530(2)	0·177256(2)	0·106879(2)	0·546824(1)	0·377643(1)	0·217136(1)
6·0	0·600143(2)	0·254900(2)	0·212545(2)	0·127985(2)	0·651087(1)	0·446295(1)	0·251044(1)
7·0	0·700125(2)	0·297285(2)	0·247850(2)	0·149115(2)	0·755676(1)	0·515211(1)	0·284894(1)
8·0	0·800112(2)	0·339678(2)	0·283166(2)	0·170262(2)	0·860513(1)	0·584358(1)	0·318751(1)
9·0	0·900100(2)	0·382078(2)	0·318489(2)	0·191422(2)	0·965544(1)	0·653702(1)	0·352651(1)
10	0·100009(3)	0·424483(2)	0·353818(2)	0·212591(2)	0·107074(2)	0·723212(1)	0·386611(1)
15	0·150006(3)	0·636547(2)	0·530513(2)	0·318516(2)	0·159816(2)	0·107249(2)	0·557442(1)
20	0·200005(3)	0·848643(2)	0·707246(2)	0·424507(2)	0·212686(2)	0·142340(2)	0·729759(1)

The values given in the table must be multiplied by the powers of ten given in brackets.
Values within the region marked off by broken lines may be inaccurate (see text).

Vol. 3 1961

$$a_3 = -c - e \tag{27}$$

$$a_4 = c + e - 10c^2 \tag{28}$$

$$a_5 = -c - e + (34 + 2\beta)c^2 + 35ce \tag{29}$$

$$a_6 = c + e - (86 + 8\beta)c^2 - (122 + 6\beta)ce - 35e^2 + 280c^3 \tag{30}$$

$$a_7 = -c - e + (194 + 22\beta)c^2 + (317 + 26\beta)ce + (122 + 6\beta)e^2 - (2016 + 168\beta)c^3 - 2100c^2e \tag{31}$$

$$a_8 = c + e - (414 + 52\beta)c^2 - (732 + 76\beta)ce - (317 + 26\beta)e^2 + (9596 + 1348\beta + 20\beta^2)c^3 + (15\,480 + 1140\beta)c^2e + 5775ce^2 - 15\,400c^4 \tag{32}$$

$$a_9 = -c - e + (858 + 114\beta)c^2 + (1591 + 188\beta)ce + (732 + 76\beta)e^2 - (38\,100 + 6892\beta + 176\beta^2)c^3 - (75\,528 + 9608\beta + 132\beta^2)c^2e - (43\,065 + 2970\beta)ce^2 + (190\,960 + 18\,480\beta)c^4 - 5775c^3 + 200\,200c^3e. \tag{33}$$

For very large values of f_0 it is possible to neglect terms which contain $f^\vee$ and higher powers in the denominator. The remaining terms are then readily summed giving for $(1 + B)$ the much simpler expression:

$$(1 + B) = \frac{c}{\sigma(1 + \sigma)} - \frac{e}{\sigma^2(1 + \sigma)}. \tag{34}$$

a function of the parameters f_0 and σ for $\beta = 0$.

$0{\cdot}1\sqrt{2}$ 0·574341 1·08279	0·0 0·469600 1·21672	$-0{\cdot}1\sqrt{2}$ 0·370008 1·38498	$-0{\cdot}25\sqrt{2}$ 0·232624 1·73941	$-0{\cdot}375\sqrt{2}$ 0·132388 2·21109	$-0{\cdot}5\sqrt{2}$ 0·050229 3·10476	$-0{\cdot}6\sqrt{2}$ 0·004748 5·55229	σ
0·791959(−2)	0·790224(−2)	0·788275(−2)	0·784747(−2)	0·780735(−2)	0·774178(−2)	0·758806(−2)	0·0001
0·111662(−1)	0·111316(−1)	0·110929(−1)	0·110229(−1)	0·109436(−1)	0·108150(−1)	0·105155(−1)	0·0002
0·175503(−1)	0·174650(−1)	0·173697(−1)	0·171975(−1)	0·170036(−1)	0·166922(−1)	0·159824(−1)	0·0005
0·246567(−1)	0·244880(−1)	0·243001(−1)	0·239619(−1)	0·235838(−1)	0·229820(−1)	0·216426(−1)	0·001
0·345524(−1)	0·342204(−1)	0·338521(−1)	0·331919(−1)	0·324612(−1)	0·313151(−1)	0·288372(−1)	0·002
0·536860(−1)	0·528805(−1)	0·519918(−1)	0·504188(−1)	0·487064(−1)	0·460885(−1)	0·407257(−1)	0·005
0·745198(−1)	0·729570(−1)	0·712471(−1)	0·682540(−1)	0·650540(−1)	0·602897(−1)	0·510360(−1)	0·01
0·102818	0·998168(−1)	0·965627(−1)	0·909560(−1)	0·850970(−1)	0·766603(−1)	0·613105(−1)	0·02
0·140867	0·135161	0·129051	0·118728	0·108251	0·937787(−1)	0·694246(−1)	0·04
0·168766	0·160497	0·151720	0·137095	0·122549	0·103022	0·718451(−1)	0·06
0·191557	0·180821	0·169505	0·150852	0·132593	0·108630	0·719143(−1)	0·08
0·211164	0·198031	0·184270	0·161791	0·140084	0·112130	0·707666(−1)	0·1
0·284811	0·260351	0·235249	0·195593	0·159157	0·115446	0·588487(−1)	0·2
0·338878	0·303712	0·268160	0·213326	0·164775	0·109634	0·456862(−1)	0·3
0·383480	0·337956	0·292480	0·223728	0·164761	0·101000	0·344045(−1)	0·4
0·422345	0·366675	0·311650	0·229906	0·161816	0·915567(−1)	0·254141(−1)	0·5
0·457308	0·391675	0·327344	0·233353	0·157202	0·821497(−1)	0·185098(−1)	0·6
0·489421	0·413909	0·340517	0·234908	0·151608	0·731757(−1)	0·133326(−1)	0·7
0·519353	0·434045	0·351770	0·235091	0·145447	0·648219(−1)	0·951733(−2)	0·8
0·547553	0·452504	0·361506	0·234249	0·138983	0·571669(−1)	0·674334(−2)	0·9
0·574340	0·469599	0·370010	0·232623	0·132390	0·502297(−1)	0·474804(−2)	1·0
0·624569	0·500533	0·384118	0·227678	0·119265	0·384281(−1)	0·231853(−2)	1·2
0·671350	0·528095	0·395254	0·221211	0·106661	0·291124(−1)	0·111454(−2)	1·4
0·715505	0·553073	0·404147	0·213798	0·948634(−1)	0·218818(−1)	0·529480(−3)	1·6
0·757590	0·575994	0·411282	0·205813	0·839989(−1)	0·163402(−1)	0·249258(−3)	1·8
0·797998	0·597234	0·417006	0·197509	0·741075(−1)	0·121353(−1)	0·119008(−3)	2·0
0·893408	0·644638	0·426652	0·176388	0·534947(−1)	0·565916(−2)	0·174046(−4)	2·5
0·982946	0·685961	0·431503	0·155889	0·380732(−1)	0·258539(−2)	0·242495(−5)	3·0
0·106831(1)	0·722840	0·433034	0·136746	0·268051(−1)	0·116374(−2)	0·349591(−6)	3·5
0·115055(1)	0·756303	0·432160	0·119268	0·187095(−1)	0·518048(−3)	0·472703(−7)	4·0
0·123039(1)	0·787046	0·429495	0·103544	0·129671(−1)	0·228659(−3)	0·650696(−8)	4·5
0·130831(1)	0·815561	0·425468	0·895475(−1)	0·893467(−2)	0·100252(−3)	0·889758(−9)	5·0
0·145980(1)	0·867277	0·414497	0·663457(−1)	0·418286(−2)	0·189793(−4)	0·163868(−10)	6·0
0·160700(1)	0·913470	0·400947	0·486592(−1)	0·193029(−2)	0·353953(−5)	0·297344(−12)	7·0
0·175116(1)	0·955414	0·385849	0·353998(−1)	0·881242(−3)	0·652947(−6)	0·533743(−14)	8·0
0·189307(1)	0·993968	0·369870	0·255831(−1)	0·398992(−3)	0·119460(−6)	0·950259(−16)	9·0
0·203330(1)	0·102974(1)	0·353460	0·183865(−1)	0·179467(−3)	0·217144(−7)	0·168095(−17)	10
0·272007(1)	0·117962(1)	0·273194	0·332596(−2)	0·310040(−5)	0·404659(−11)	0·273508(−26)	15
0·339674(1)	0·129881(1)	0·204611	0·566654(−3)	0·503795(−7)	0·709825(−15)	0·418995(−35)	20

4. VALUES OF THE WALL GRADIENT (b_0'/B) WHEN THE MAIN-STREAM PRESSURE GRADIENT IS ZERO

4.1. *General discussion of Table* 1

Values of the wall gradient (b_0'/B) as a function of the fluid property group σ and the mass flow parameter f_0 for the case $\beta = 0$ are given in Table 1. The solutions to the velocity equation from which these were calculated, namely corresponding values of f_0, f_0'', and δ_1^*, were taken from Emmons and Leigh [6] except for the case $f_0 = 10$ which was taken from Watson [7]. The values of these parameters are given at the head of the appropriate column in Table 1.

Most of the values of (b_0'/B) were calculated by a computer using the method described in section 3.3. When both σ and f_0 were large, however, the values given by the computer were inaccurate because the interval in η was too great. For the bottom left hand corner of Table 1, therefore, the values were calculated from the series expansion given in section 3.4.

For various other reasons, such as error in supplying the input data, the computer also gave incorrect values at isolated positions in other parts of the table. These values were then recalculated by the method described in section 3.2 using values of $\int_0^\eta f\,\mathrm{d}\eta$ supplied by the computer.

4.2. *Accuracy of Table* 1

The method of computation described in section 3.3 was designed to give values of the wall gradient (b_0'/B) with an error less than 5×10^{-5} of its own value. Generally, therefore, the error in the fifth significant digit should be small but considerable error could occur in the sixth significant digit.

The accuracy of the results may be judged by comparing the value of (b_0'/B) for $\sigma = 1{\cdot}0$ with the corresponding value of f_0'' given at the top of the table. They should be equal but generally differ by a few units in the sixth significant digit. The sixth place has therefore been retained in Table 1 but it should be emphasized that no great reliance can be placed on it. This applies particularly to negative values of f_0 since even the quantities f_0'' and δ_1^* are not known to high accuracy there.

During the present work it was found, when working with a computer and using accurate integration formulae, that very high accuracy in wall gradients is often desirable. This was also found by Eckert *et al.* [8] who, when studying the velocity equation, required the wall gradient f_0'' to ten significant digits in order to obtain solutions for the case $\beta = 1{\cdot}0, f_0 = -3{\cdot}0$. Knowledge of the value of the sixth significant digit in (b_0'/B), although not exact, may therefore prove useful in applying the values to obtain other functions of the b-boundary layer.

Values for high σ in the bottom left-hand corner of the table were calculated by the formula of section 3.4. For lower values of σ, particularly for σ approaching unity, the values obtained by the computer were accurate. There was, however, an intermediate zone where both methods were inaccurate to some extent. By differencing the values and, where necessary, adjusting them so as to give smooth, regular differences, the error in the values given is believed to be confined to the sixth significant digit even here. This does not apply to the values in the first column because, when plotting Δ_2/Δ_4 as a function of $(v_0\Delta_2/K)$ (see Fig. 3), a few of the values obtained from this column did not form a continuous curve with points taken from the other columns. It is therefore suspected that some of the values in this column are in error in the fifth significant digit.

In the part of the table where mass flow is outwards (f_0 negative) and $\sigma \geqslant 2$ there may be some inaccuracy for the following reason. Here the integrand in equation (12) starts from unity at the wall, increases to a maximum and then diminishes to a low value in the main-stream. For large σ this curve reaches a very high value and has steep gradients. In order to obtain good accuracy with such a curve a very small interval in η should be used, whereas the values quoted were obtained with an interval of 0·1. No estimate has been made of the probable error due to this but it would be surprising if the values of (b_0'/B) were inaccurate by more than a few per cent of their own values.

4.3. *Comparison with earlier values*

Of all the two-dimensional, laminar boundary layer flows considered in the literature the case when both the main-stream pressure gradient

Vol. 3 1961

and the rate of mass transfer through the interface are zero has received the greatest attention; this is the case $f_0 = 0$ in Table 1.

In order to compare the present results for this case with exact values given in the literature Table 2 has been drawn up. This table contains some values for low σ not included in Table 1; these were calculated by the method described in section 3.2.

Table 2. Comparison with published values for $\beta = 0, f_0 = 0$

(a) Present values (b) Published values

σ	(b_0/B)		Reference
	(a)	(b)	
0·003	0·0415366	0·041537	[10]
0·006	0·057595	0·057593	[10]
0·01	0·072957	0·072959	[10]
0·03	0·119346	0·11935	[10]
0·1	0·198031	0·1953	[9]
0·5	0·366675	0·3664	[9]
0·6	0·391675	0·3915	[9]
		0·3917	[11]
0·7	0·413909	0·4139	[9]
		0·4137	[10]
0·8	0·434045	0·4340	[9]
		0·4342	[11]
0·9	0·452504	0·4525	[9, 11]
1	0·469599	0·46960	[6]
		0·4695	[9, 11]
2	0·597234	0·5971	[11]
7	0·913470	0·9135	[9]
10	1·02974	1·0298	[9]
15	1·17962	1·1796	[9]

The numbers in the last column give the publication in the reference list.

From this table it may be seen that values in the literature sometimes disagree with each other by a few units in the fourth significant digit. The error in the value given by Merk [9] for $\sigma = 0{\cdot}1$ is more serious, however, as it appears to be 1·4 per cent too low. The agreement between the present values and those given by Sparrow and Gregg [10] for low values of σ is very good, which confirms the formula for Part II given in equation (15) since this Part dominates for very low σ.

This case when $\beta = 0$ and $f_0 = 0$ was also considered in Paper 3a, where an asymptotic formula was given for calculating (b_0'/B) for any high value of σ. It appears from the present results that the formula gives an accuracy of one unit in the fourth significant digit even when σ is as low as 0·5.

The only extensive results giving values of (b_0'/B) in the presence of mass transfer were those by Mickley *et al.* [11], which were also for the case $\beta = 0$. On the whole the present values agree with their results to the same extent as for the case of no mass transfer given in Table 2. This does not hold, however, for large σ and high blowing rates (large negative f_0). The greatest difference occurs for $f_0 = -0{\cdot}5\sqrt{2}$ and $\sigma = 5{\cdot}0$, the highest blowing rate and the largest value of σ considered by the earlier authors. Whereas they obtained for (b_0'/B) the value $0{\cdot}9963 \times 10^{-4}$, the present value is $1{\cdot}0025 \times 10^{-4}$, a difference of 0·6 per cent. A possible source of error in the present results for this part of the table has been given in section 4.2.

5. FORMULAE FOR OBTAINING OTHER FUNCTIONS FROM (b_0'/B)

It was shown in Paper 3 that many other functions relating to the b-boundary layer can be calculated from values of (b_0/B) for known values of the parameters β, σ and f_0. For ease of reference these are quoted below but will not be discussed; the reader is referred to other papers in the present series for more detailed discussion of these functions.

The right-hand sides of the following equations are written in terms of "similar" functions. Some of these expressions differ from the forms used in Paper 3; this is merely so that the quantities on the left may be evaluated directly in terms of functions occurring in Table 1 without intermediate calculation. A few of these functions are identically zero for the particular case $\beta = 0$ but are included to make the list complete.

$$\frac{Nu}{Re^{1/2}} = \frac{1}{(2-\beta)^{1/2}}\left(\frac{b_0'}{B}\right) \tag{35}$$

$$\frac{\Delta_2 Re^{1/2}}{x} = \frac{(2-\beta)^{1/2}}{\sigma}\left\{\left(\frac{b_0'}{B}\right) - \sigma f_0\right\} \tag{36}$$

$$B = -\frac{\sigma f_0}{(b_0'/B)} \tag{37}$$

$$\frac{v_0 \Delta_2}{K} = f_0 \left\{ \sigma f_0 - \left(\frac{b_0'}{B} \right) \right\} \tag{38}$$

$$\frac{\Delta_2}{\Delta_4} = \frac{1}{\sigma} \left(\frac{b_0'}{B} \right) \left\{ \left(\frac{b_0'}{B} \right) - \sigma f_0 \right\} \tag{39}$$

$$\frac{\Delta_4^2}{\nu} \frac{\mathrm{d}u_G}{\mathrm{d}x} = \frac{\beta}{(b_0'/B)^2} \tag{40}$$

$$\frac{u_G}{\nu} \frac{\mathrm{d}\Delta_4^2}{\mathrm{d}x} = \frac{2(1-\beta)}{(b_0'/B)^2} \tag{41}$$

$$\frac{\Delta_2^2}{\nu} \frac{\mathrm{d}u_G}{\mathrm{d}x} = \frac{\beta}{\sigma^2} \left\{ \left(\frac{b_0'}{B} \right) - \sigma f_0 \right\}^2 \tag{42}$$

$$\frac{u_G}{\nu} \frac{\mathrm{d}\Delta_2^2}{\mathrm{d}x} = \frac{2(1-\beta)}{\sigma^2} \left\{ \left(\frac{b_0'}{B} \right) - \sigma f_0 \right\}^2 \tag{43}$$

$$X \equiv \left\{ \frac{\Delta_4 \delta_4}{\nu} \frac{\mathrm{d}u_G}{\mathrm{d}x} - \frac{v_0 \Delta_4}{\nu} \right\} = \left(f_0 + \frac{\beta}{f_0''} \right) \frac{1}{(b_0'/B)} \tag{44}$$

$$Y \equiv \frac{1}{K} \left(\frac{\delta_4}{u_G} \right)^{1/2} \frac{\mathrm{d}}{\mathrm{d}x} \left\{ \Delta_4^3 \left(\frac{u_G}{\delta_4} \right)^{3/2} \right\} = \frac{3}{2} \frac{\sigma f_0''}{(b_0'/B)^3} \tag{45}$$

$$W \equiv \left\{ \frac{\Delta_2^{1/2} \delta_4^{3/2}}{\nu} \frac{\mathrm{d}u_G}{\mathrm{d}x} - \frac{\Delta_2^{1/2} \delta_4^{1/2}}{\nu} v_0 \right\} = \left(f_0 + \frac{\beta}{f_0''} \right) \left\{ \frac{(b_0/B) - \sigma f_0}{\sigma f_0''} \right\}^{1/2} \tag{46}$$

$$Z \equiv \frac{1}{K} \left(\frac{\delta_4}{u_G} \right)^{1/2} \frac{\mathrm{d}}{\mathrm{d}x} (u_G \Delta_2)^{3/2} = \frac{3}{2} \frac{1}{(\sigma f_0'')^{1/2}} \left\{ \left(\frac{b_0'}{B} \right) - \sigma f_0 \right\}^{3/2}. \tag{47}$$

Note that the functions X, Y, W and Z form the basis of an approximate method of estimating boundary layer thicknesses which is most accurate for large values of σ. For low σ the use of different functions would probably result in better accuracy.

6. THE ASYMPTOTIC BEHAVIOUR OF FUNCTIONS IN THE *b*-BOUNDARY LAYER

In this section a brief examination will be made of the asymptotic behaviour of functions relating to the *b*-boundary layer for extreme values of some of the parameters. The conclusions arrived at will then be used in section 7 to draw curves showing the relationships between some of these functions.

6.1. *The limiting case* $\sigma \to 0$

On examining equation (15) it may be seen that as $\sigma \to 0$ Part I tends to the value d; this, in similar co-ordinates, is the distance from the interface at which the flow is virtually inviscid. At the same time, Part II tends to the value $(\pi/2\sigma)^{1/2}$ since both the factor containing the error function and the exponential factor tend to unity. For very small σ Part I is clearly negligible compared with this, so the following approximations apply:

$$\text{As } \sigma \to 0 \begin{cases} \left(\dfrac{b_0'}{B} \right) = \left(\dfrac{2\sigma}{\pi} \right)^{1/2} & (48) \\ \dfrac{\Delta_2}{\Delta_4} = \dfrac{2}{\pi} = 0{\cdot}636620. & (49) \end{cases}$$

It is interesting to note that equation (49) applies exactly for purely inviscid flow when $\sigma = 0$.

For small values of σ the mass transfer rate, as measured by the value of the parameter f_0, has only a small effect on (b_0'/B). Referring to the smallest value of σ included in Table 1, namely $\sigma = 0{\cdot}0001$, for which $(2\sigma/\pi)^{1/2} = 0{\cdot}00797885$, the extreme values of f_0 considered, namely $+10$ and $-0{\cdot}6\sqrt{2}$, give values of (b_0'/B) of 0·00861969 and 0·00758806 respectively. For smaller values of σ these values of (b_0'/B) would be nearer to $(2\sigma/\pi)^{1/2}$ and would therefore cover a narrower range.

6.2. *The limiting case* $\sigma \to \infty$

The behaviour of boundary layer functions for large σ when no mass flows through the interface may be estimated from the asymptotic formulae given in Paper 3a. This case will not, therefore, be discussed here except to state that for accelerated and slightly decelerated flows (b_0'/B) is proportional to $\sigma^{1/3}$ and for flows very near to or at the separation point (b_0'/B) is proportional to $\sigma^{1/4}$.

Contrary to what happens for low values of σ, the mass transfer rate has a large effect on

Vol. 3 1961

(b_0'/B) when σ is large. For positive values of f_0, for example, the driving force B is very close to -1 as soon as f_0 has a non-zero value, so that the following approximation then applies:

$$\sigma \text{ large, } f_0 \text{ positive: } \left(\frac{b_0'}{B}\right) = \sigma f_0. \qquad (50)$$

When f_0 is negative, on the other hand, B tends to infinity as soon as f_0 is non-zero and (b_0'/B) tends to zero.

Accurate numerical values of (b_0'/B) for positive f_0 and large σ can be obtained from the asymptotic formula given in section 3.4. Negative values of f_0 would require some modification of the methods already described.

6.3. *Intensive suction*

When considering the velocity boundary layer the case of intensive suction gives rise to the well-known asymptotic suction profile. In an analogous manner the b-profile can be shown to approach the asymptotic profile:

$$\left(\frac{b}{B}\right) = (1 - e^{-\sigma f_0 \eta}). \qquad (51)$$

Instead of using this, however, the case of intensive suction can be examined more accurately by referring to equation (34). Since f_0'' is almost equal to f_0 for sufficiently large f_0, the following relationships hold:

$$(1 + B) = \frac{1}{\sigma(1+\sigma) f_0^2} \qquad (52)$$

$$\left(\frac{b_0'}{B}\right) = \frac{\sigma f_0}{1 - [1/\sigma(1+\sigma) f_0^2]} \qquad (53)$$

$$\frac{v_0 \Delta_2}{K} = \frac{1}{(1/\sigma f_0) - (1+\sigma)} \qquad (54)$$

$$\frac{\Delta_2}{\Delta_4} = \frac{1}{(1+\sigma) - (2/\sigma f_0^2)}. \qquad (55)$$

When f_0 is very large the last two relationships reduce to:

$$-\frac{v_0 \Delta_2}{K} = \frac{\Delta_2}{\Delta_4} = \frac{1}{(1+\sigma)}, \qquad (56)$$

which may also be obtained by evaluating the convection thickness Δ_2 for the asymptotic suction profiles relating to the velocity and the function (b/B) respectively.

6.4. "*Separation*" *on a flat plate*

When the main-stream pressure gradient is zero and the blowing rate reaches the value $f_0 = -0{\cdot}875745$, the wall shear, represented in "similar" co-ordinates by f_0'', becomes zero. The velocity layer is then said to separate. This case has been discussed by Emmons and Leigh [6] in giving similar solutions to the velocity equation for flow over a flat plate.

For this and all higher blowing rates the following relationship holds:

$$F_2 \equiv \frac{u_G}{\nu}\frac{d\delta_2^2}{dx} = 2\frac{v_0 \delta_2}{\nu}. \qquad (57)$$

A physical interpretation of this is that the momentum boundary layer thickness δ_2 grows with distance x at a rate which is proportional to the blowing rate, since the group $(v_0\delta_2/\nu)$, which can be shown to be numerically equal to f_0^2, is a suitable measure of the blowing rate (see Papers 1 and 2).

An analogous situation must also apply to the b-boundary layer. In terms of equation (12) the integral on the right-hand side becomes infinite so that $(b_0'/B) = 0$. Since $b_0'(= -\sigma f_0)$ is still finite this means that B is infinite. This clearly holds for the case $\sigma = 1{\cdot}0$ by direct analogy with the velocity equation, but it must apply whatever the value of σ.

The following relationships therefore hold for all f_0 beyond the value $f_0 = -0{\cdot}875745$:

$$\left(\frac{b_0'}{B}\right) = 0 \qquad (58)$$

$$B = \infty \qquad (59)$$

$$\Delta_4 = 0 \qquad (60)$$

$$\frac{v_0 \Delta_2}{K} = \sigma f_0^2 \qquad (61)$$

$$\frac{\Delta_2}{\Delta_4} = 0 \qquad (62)$$

$$\frac{u_G}{K}\frac{d\Delta_2^2}{dx} = 2\frac{v_0 \Delta_2}{K} = 2\sigma f_0^2. \qquad (63)$$

In view of these relationships and the success obtained with the velocity equation when the mass transfer parameter $(v_0\delta_2/\nu)$ was used, it may be an advantage, in some respects, to use the parameter $(v_0\Delta_2/K)$ instead of $B\{=(v_0\Delta_4/K)\}$ for the b-boundary layer.

7. CURVES OF FUNCTIONS OF THE b-BOUNDARY LAYER

7.1. *Variation of Nusselt number with mass transfer driving force*

Equation (35) shows that the wall gradient (b_0'/B) is a measure of the local Nusselt number Nu. Figs. 1 and 2 show how this gradient, when multiplied by an appropriate power of σ, varies with the mass transfer driving force B for various values of σ. The ordinate contains the power of σ in order to bring closer together curves for different values of σ. Fig. 1 is concerned with high values of σ and Fig. 2 with low values.

(a) *High values of* σ. Fig. 1 is an extension to wider ranges in the values of the driving force B and the Prandtl/Schmidt number σ of Fig. 2 in Paper 3. The behaviour of the curves has already received some discussion in that paper so only a few additional remarks will be made here.

The sections shown as broken lines for high positive values of B indicate that the curves have either been drawn between widely separated points or have been extrapolated by giving them

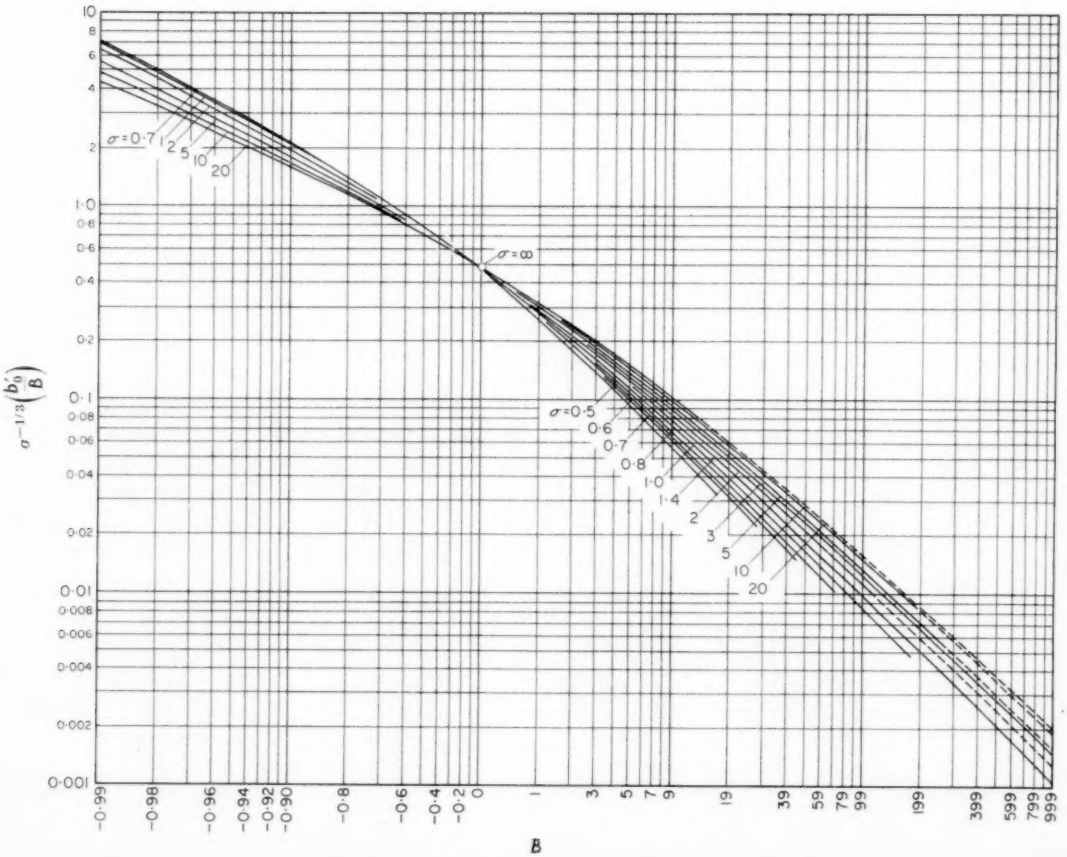

FIG. 1. Variation of the function $\sigma^{-1/3}\,(b_0'/B)$ with mass transfer driving force B for high values of σ.

Vol. 3 1961

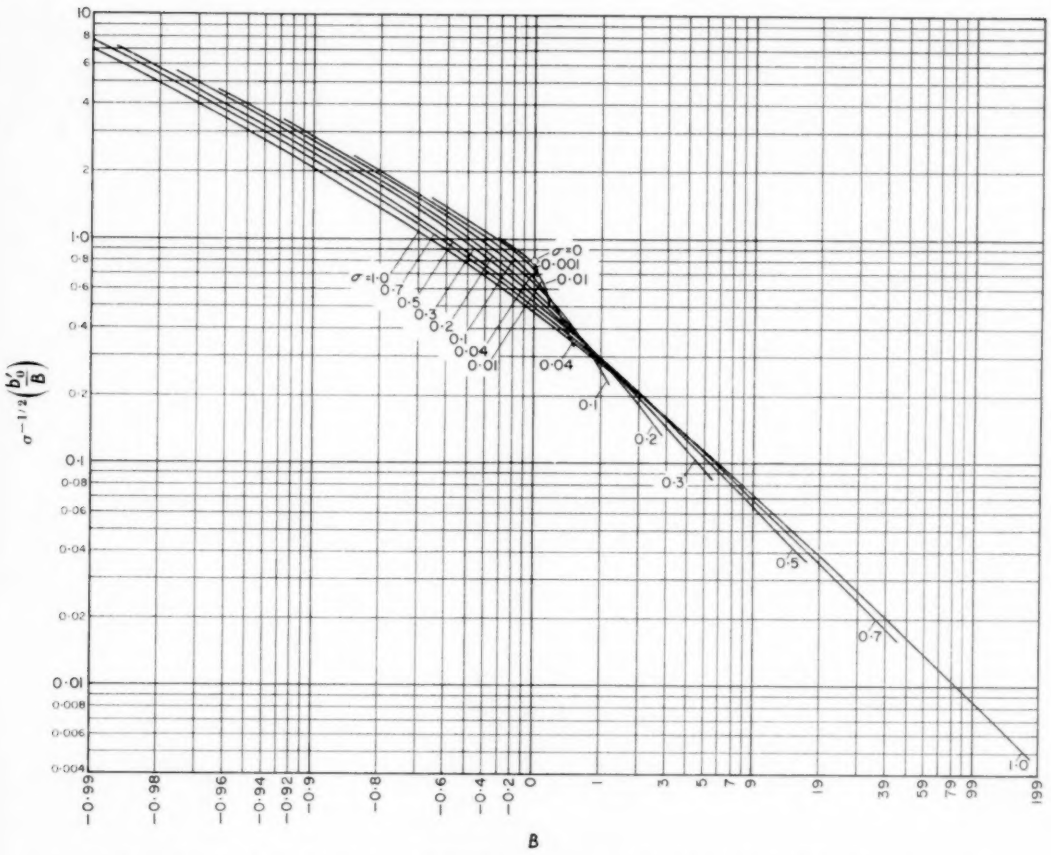

FIG. 2. Variation of the function $\sigma^{-1/2}(b_0'/B)$ with mass transfer driving force B for low values of σ.

the same shape as neighbouring curves whose shape was known. On this scale the error brought about by this would be very small.

For negative values of B, some lines have been omitted for clarity. Of the values of σ near unity, for example, only curves for $\sigma = 0{\cdot}7$ and $1{\cdot}0$ have been included because the curves for other values, at least down to $\sigma = 0{\cdot}5$, are virtually coincident with these.

The point indicated as $\sigma = \infty$ on the line $B = 0$ is given by:

$$\sigma^{-1/3}\left(\frac{b_0'}{B}\right) = \frac{3}{\Gamma(\frac{1}{3})}\left(\frac{f_0'}{3!}\right)^{1/3} = 0{\cdot}479017 \quad (64)$$

where Γ denotes the gamma function. This relationship has been discussed in Paper 3a.

(b) *Low values of* σ. It was shown in section 6.1 that for small values of σ the wall gradient (b_0'/B) is proportional to $\sigma^{1/2}$. In Fig. 2, therefore the ordinate is $\sigma^{-1/2}(b_0'/B)$. The ends of the curves in this figure correspond to the extreme values of f_0 included in Table 1.

The most striking feature about these curves is their behaviour when B is positive, i.e. when mass flows outwards through the interface. For any fixed value of σ the ordinate quantity decreases as B increases. As the value of σ decreases, however, the curves descend more and more rapidly. From the discussion already given in section 6.4 each of these curves must tend to zero on the right when the blowing rate is high enough to cause the velocity layer to separate.

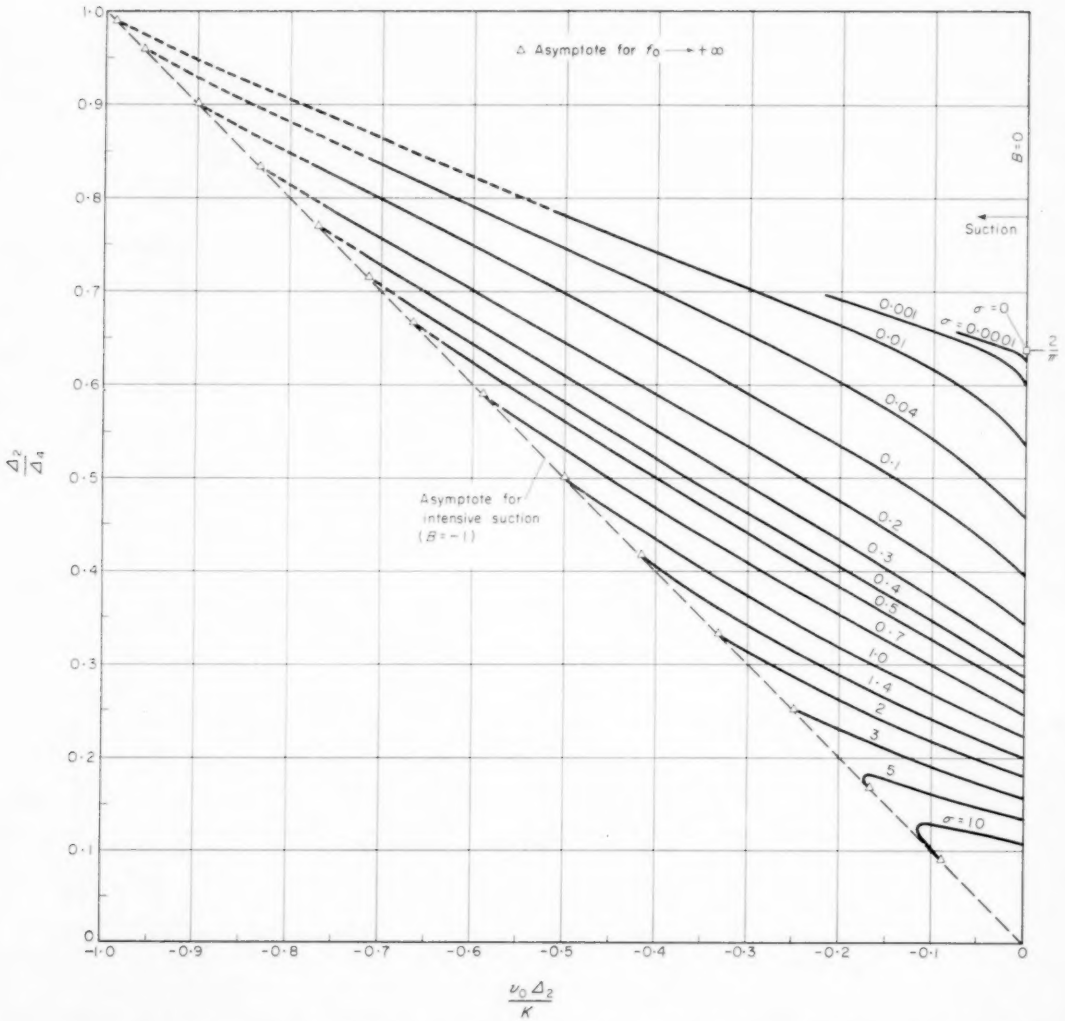

FIG. 3. Variation of the ratio of boundary layer thicknesses (Δ_2/Δ_4) with ($v_0\Delta_2/K$) when mass transfer is inwards.

The point shown as $\sigma = 0$ is given by:

$$\sigma^{-1/2}\left(\frac{b_0'}{B}\right) = \left(\frac{2}{\pi}\right)^{1/2} = 0{\cdot}797885. \qquad (65)$$

7.2. *Variation of the ratio Δ_2/Δ_4 with mass transfer*

(a) *Inward mass transfer*. It has already been seen in section 6.2 that for intensive inward mass transfer the driving force B approaches -1 and the wall gradient (b_0'/B) becomes very large. In order to accommodate such points on Figs. 1 and 2 the co-ordinate axes must be extended both upwards and to the left. It is not, of course, possible to include the asymptote itself since B is then -1 and (b_0'/B) is infinite.

On the other hand the ratio Δ_2/Δ_4 and the mass transfer parameter $-(v_0\Delta_2/K)$ are always between 0 and 1 when the mass transfer is inwards. Fig. 3 shows the relationship between these quantities for constant values of σ. This figure is analogous to part of Fig. 2 in Paper 2 where the ratio $H_{24}(=\delta_2/\delta_4)$ was plotted as a function of the mass transfer parameter $(v_0\delta_2/\nu)$

Vol. 3 1961

(note that v_s in the earlier paper is here denoted by v_0).

Since the ratio of the abscissa to the ordinate for any point on these curves gives the value of $B\{=(v_0\Delta_4/K)\}$, lines of constant B are straight lines of slope $1/B$ passing through the origin.

The full lines in this figure cover the range of mass transfer included in Table 1, namely, up to an inward mass flow rate corresponding to $f_0 = +10$. The broken portions of these lines represent extrapolations to the point on the asymptote, represented by a triangle, which satisfies equation (56). Extrapolations have not been included for the two lowest values of σ as it was difficult to judge the shapes of the curves over such a long distance. They are almost, but not exactly, linear in this region.

For any point on these curves or the extrapolations the wall gradient (b_0'/B) can be calculated from the formula:

$$\left(\frac{b_0'}{B}\right) = \frac{\Delta_2}{\Delta_4}\,\frac{\sigma^{1/2}}{\{(v_0\Delta_2/K) + (\Delta_2/\Delta_4)\}^{1/2}}\,. \qquad (66)$$

Clearly the accuracy of this diminishes as the asymptote is approached since $-(v_0\Delta_2/K)$ and Δ_2/Δ_4 are then almost equal.

Two points should be noted regarding the general shapes of these curves. Firstly, it was noted when discussing Fig. 2 in section 7.1 that, for the case of outward mass transfer, the ordinate descended more and more rapidly with increasing values of B as the value of σ decreased. This effect seems to be evident even on the suction side in Fig. 3. Secondly, the approach to the asymptote for intensive suction is from below when σ is small (i.e. $\sigma \leqslant 2$), whereas when σ is large the approach is from above.

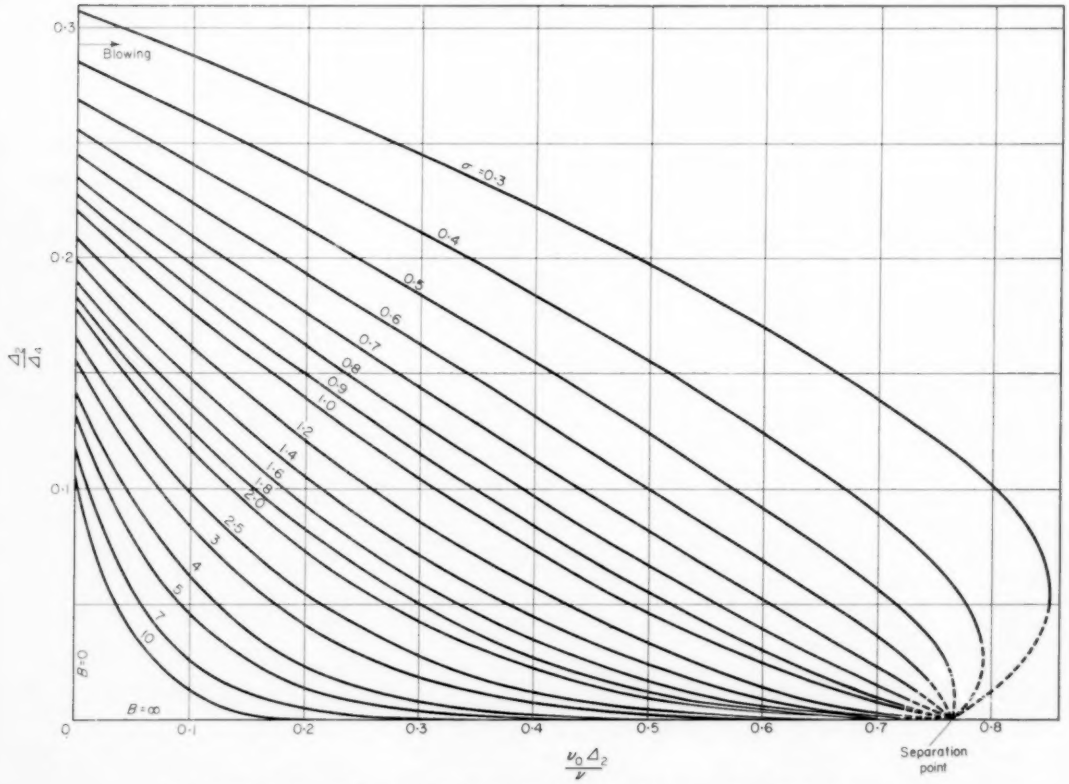

FIG. 4. Variation of the ratio (Δ_2/Δ_4) with $(v_0\Delta_2/\nu)$ when mass transfer is outwards.

(b) *Outward mass transfer*. It was shown in section 6.4 that when the velocity boundary layer separates from the interface, B is infinite and (b_0'/B) is zero for all values of σ. This point also cannot be included in Figs. 1 and 2. Instead of using the mass transfer parameter $(v_0\Delta_2/K)$ along the abscissa as in Fig. 3, however, it follows from equation (61) that the parameter $(v_0\Delta_2/\nu)$ would be better since the point of separation would then be the same for all σ.

The relationship between the ratio (Δ_2/Δ_4) and this mass transfer parameter is shown in Fig. 4. All the curves are seen to converge on the point where $(\Delta_2/\Delta_4) = 0$, $(v_0\Delta_2/\nu) = 0{\cdot}766929$.

Again the full lines represent the results contained in Table 1 and the extensions, shown as broken lines, join the point for $f_0 = -0{\cdot}6\sqrt{2}$ to the separation point. For very low values of σ the curves form a wide arc to the right before returning to cut the abscissa.

These extrapolations to the separation point can clearly be used to extend Figs. 1 and 2 to the right. The accuracy of this would depend largely on the accuracy to which (Δ_2/Δ_4) can be estimated since inaccuracy in the function $\{(v_0\Delta_2/K) + (\Delta_2/\Delta_4)\}^{1/2}$ occurring in equation (66) would introduce only a small error.

ACKNOWLEDGEMENTS

The present work forms part of the research programme of the Division of Food Preservation, C.S.I.R.O., Australia. The author is indebted to Dr. J. M. Bennett and his staff at the Adolph Basser Computing Laboratory, University of Sydney, in particular Mr. R. Whitfield, who computed most of the values of the wall gradient given in Table 1. He is also grateful to Miss J. D. Hayhurst who calculated the other values.

REFERENCES

1. D. B. SPALDING, Mass transfer through laminar boundary layers—1. The velocity boundary layer. *Int. J. Heat Mass Transfer*, **2**, Nos. 1/2, 15 (1961). Referred to as Paper 1.
2. D. B. SPALDING and H. L. EVANS, Mass transfer through laminar boundary layers—2. Auxiliary functions for the velocity boundary layer. *Int. J. Heat Mass Transfer*, **2**, No. 3, 199 (1961). Referred to as Paper 2.
3. D. B. SPALDING and H. L. EVANS, Mass transfer through laminar boundary layers—3. Similar solutions to the *b*-equation. *Int. J. Heat Mass Transfer*, **2**, No. 4, 314 (1961). Referred to as Paper 3.
4. H. L. EVANS, Mass transfer through laminar boundary layers—3a. Similar solutions to the *b*-equation when $B = 0$ and $\sigma \geqslant 0{\cdot}5$. *Int. J. Heat Mass Transfer*, **3**, No. 1, 26 (1961). Referred to as Paper 3a.
5. D. B. SPALDING, A standard formulation of the steady convective mass transfer problem. *Int. J. Heat Mass Transfer*, **1**, Nos. 2/3, 192 (1960).
6. H. W. EMMONS and D. LEIGH, Tabulation of the Blasius function with blowing and suction. *Harvard University, Combustion Aerodynamics Lab. Interim Tech. Report* No. 9 (1953).
7. E. J. WATSON, The asymptotic theory of boundary layer flow with suction. *Brit. Aero. Res. Council R. and M.* 2619 (1952).
8. E. R. G. ECKERT, P. L. DONOUGHE and B. J. MOORE, Velocity and friction characteristics of laminar viscous boundary layer and channel flow with ejection or suction. *N.A.C.A. Tech. Note* 4102 (1957).
9. H. J. MERK, Rapid calculations for boundary-layer transfer using wedge solutions and asymptotic expansions. *J. Fluid Mech.*, **5**, 460 (1959).
10. E. M. SPARROW and J. L. GREGG, Details of exact low Prandtl number boundary-layer solutions for forced and for free convection. *N.A.S.A. Memo.* 2-27-59E (1959).
11. H. S. MICKLEY, R. C. ROSS, A. L. SQUYERS and W. E. STEWART, Heat, mass and momentum transfer for flow over a flat plate with blowing and suction. *N.A.C.A. Tech. Note* 3208 (1954).

Vol. 3 1961

APPENDIX

The displacement and momentum boundary layer thicknesses of the velocity layer are usually evaluated by integrating certain quantities throughout the boundary layer. The stream function is, however, known in the main-stream whether solutions are taken from tables in the literature or evaluated on a computer. The formulae given below can be used for calculating functions associated with the velocity layer without the need for integration. The first two formulae are definitions of δ_1^* and δ_2^*. The importance and applications of the succeeding functions have been discussed in Papers 1 and 2 of the present series.

$$\delta_1^* = \int_0^\infty \left(1 - \frac{\mathrm{d}f}{\mathrm{d}\eta}\right) \mathrm{d}\eta \qquad \text{(A1)}$$

$$\delta_2^* = \int_0^\infty \frac{\mathrm{d}f}{\mathrm{d}\eta}\left(1 - \frac{\mathrm{d}f}{\mathrm{d}\eta}\right) \mathrm{d}\eta \qquad \text{(A2)}$$

$$\delta_1^* = \{\eta + f_0 - f\}_{\eta \text{ large}} \qquad \text{(A3)}$$

$$\delta_2^* = (f_0'' - f_0 - \beta\,\delta_1^*)/(\beta + 1) \qquad \text{(A4)}$$

$$H_{12} = \frac{\delta_1^*}{\delta_2^*} \tag{A5}$$

$$H_{24} = f_0'' \, \delta_2^* \tag{A6}$$

$$\frac{v_0 \delta_2}{\nu} = -f_0 \, \delta_2^* \tag{A7}$$

$$\frac{\delta_2^2}{\nu} \frac{\mathrm{d}u_G}{\mathrm{d}x} = \beta(\delta_2^*)^2 \tag{A8}$$

$$F_2 \equiv \frac{u_G}{\nu} \frac{\mathrm{d}\delta_2^2}{\mathrm{d}x} = 2\{1 - \beta\}(\delta_2^*)^2 \tag{A9}$$

Vol.
3
1961

Int. J. Heat Mass Transfer. Vol. 3, pp. 341–346. Pergamon Press 1961. Printed in Great Britain.

SURFACE TEMPERATURE CALCULATIONS IN RADIANT SURROUNDINGS OF ARBITRARY COMPLEXITY—FOR GRAY, DIFFUSE RADIATION

B. GEBHART

Sibley School of Mechanical Engineering, Cornell University, Ithaca, New York

(*Received* 14 *December* 1960)

Abstract—The question of calculating the temperatures of opaque and non-opaque surfaces subject to assigned net rates of radiant flux is considered. It is shown that, for gray surfaces, any opaque surface in radiant balance in an enclosure of arbitrary complexity achieves a steady state temperature which is independent of the emissivity (or absorptivity) of the surface. Relations are developed for the temperature of opaque and non-opaque surfaces subjected to an assigned net radiant flux.

Résumé—On considère le calcul des températures de surfaces, opaques ou non, soumises à des densités de flux de rayonnement bien déterminées. On montre que, dans le cas de corps gris, une surface opaque quelconque, en équilibre de rayonnement dans une enceinte de complexité arbitraire, acquiert, en régime permanent, une température qui est indépendante de ses coefficients d'absorption ou d'émission. Des relations sont données pour la température de surfaces, opaques ou non, soumises à des flux de rayonnement bien déterminés.

Zusammenfassung—Die Berechnung von Temperaturen strahlungsundurchlässiger und durchlässiger Oberflächen bei gegebener Strahlungsmenge wird untersucht. Jede undurchlässige Oberfläche eines grauen Strahlers in einer willkürlich aufgebauten Umhüllung nimmt im Strahlungsgleichgewicht eine gleichmässige Endtemperatur an, unabhängig vom Emissionsvermögen (oder Absorptionsvermögen) der Oberfläche. Die Abhängigkeit der Temperatur undurchlässiger und durchlässiger Oberflächen von der zugeführten Strahlungsmenge ist angegeben.

Аннотация—Рассматривается проблема вычисления температур непрозрачных и прозрачных поверхностей, через которые проходит определённый результирующий поток излучения. Показано, что для серых поверхностей любая непрозрачная поверхность в условиях равновесия при окружающей системе произвольной сложности достигает стационарной температуры, которая не зависит от излучательной (или поглощательной) способности поверхности. Выведены соотношения для нахождения температуры непрозрачных и прозрачных поверхностей при прохождении определённого результирующего потока излучения.

NOTATION

a, absorptivity (absorptance) of a surface;
A, radiating area of a surface;
B_{ij}, absorption factor;
F_{pi}, angle factor, the fraction of the emission of surface p directly incident upon surface i;
q_j, net rate of radiant energy loss from surface j;
T, absolute temperature;
a_{pi}, $= F_{pi}\rho_i$;
ϵ, total hemispherical emissivity (emittance) of a surface;
ρ, reflectivity (reflectance) of a surface;
σ, universal constant for thermal radiation.

INTRODUCTION

IN ENGINEERING practice there are many circumstances in which thermal radiant energy exchange rates may be calculated with sufficient accuracy under the assumptions of gray, diffuse radiation *in vacuo*. The absorption factor method developed and elaborated upon by the present

writer [1–3] is well adapted to such calculations and applies to enclosures of arbitrary complexity. Although this method requires the solution of a number of simultaneous linear equations (as must any method which accounts for multiple inter-reflections) the method is conceptually simple and is well suited to machine techniques of equation solution or matrix inversion.

The absorption factor method also permits, due to its simplicity, the demonstration of many of the important characteristics of radiant exchange processes. In the original paper, for example, absorption factor reciprocity was shown to be a simple consequence of the assumptions of gray, diffuse radiation and of uniform irradiation without reference to the second law of thermodynamics.

The present paper is concerned with the application of this method to calculations concerning opaque and non-opaque surfaces in radiant surroundings of arbitrary complexity which are subject to assigned rates of net radiant flux. Such a surface condition appears in many cases of modern technology; for example, in electrically heated walls and windows, in reactor elements in the absence of a coolant, in electrical circuit elements in a vacuum, and for surfaces subject to solar or other irradiation.

An interesting particular case, the opaque surface in radiant balance, sometimes called an "adiabatic" surface, is treated in detail. This condition often appears in equipment such as: gas turbine and jet engine combustors, furnaces, electronic components, electronic equipment, and satellite and spacecraft components. It is proven that the temperature of a surface in radiant balance is independent of its surface properties. This characteristic is sometimes alluded to, e.g. Eckert [4] in the language of Oppenheim's method [5] of analysis, but has not been proven.

The assumed condition of gray, diffuse radiation and reflection is met in many circumstances of practical importance. Many studies have indicated that even highly non-gray, specular surfaces are often essentially gray and diffuse under the conditions of actual use as a result of surface coatings, corrosion, erosion, or other types of surface alteration.

GENERAL RELATIONS

Any surface A_j in an "enclosure"* of n gray surfaces loses radiant energy at the net rate of q_j,

$$q_j = W_jA_j - B_{1j}W_1A_1 - B_{2j}W_2A_2 - \ldots$$
$$= W_jA_j - \sum_{i=1}^{n} B_{ij}W_iA_i \qquad (1)$$

where B_{ij}, the absorption factor, is the fraction of the radiant energy arising at surface A_i which is absorbed at surface A_j. WA denotes the rate at which energy is radiated from a surface to the space above it (other than by reflection). For an opaque surface, WA becomes merely the hemispherical emissive power $\epsilon\sigma T^4A$ where ϵ is the total hemispherical emissivity.

For diffuse radiation and reflection, the absorption factors are given by:

$$\left.\begin{aligned}
(a_{11}-1)B_{1j} &+ a_{12}B_{2j} + \ldots + a_{1n}B_{nj} + F_{1j}\epsilon_j = 0\\
a_{21}B_{1j} &+ (a_{22}-1)B_{2j} + \ldots + a_{2n}B_{nj} + F_{2j}\epsilon_j = 0\\
&\vdots\\
a_{n1}B_{1j} &+ a_{n2}B_{2j} + \ldots + (a_{nn}-1)B_{nj} + F_{nj}\epsilon_j = 0
\end{aligned}\right\} \qquad (2)$$

$$a_{pi} = F_{pi}\rho_i$$

where F_{pi} is the fraction of the emission of surface A_p directly incident upon A_i, ϵ_i is the total hemispherical emissivity of surface A_i, and ρ_i is the reflectivity of surface A_i. In general,

* The term "enclosure" is meant to denote the assembly of all radiant conditions relevant to the surface under consideration. Under this definition of an enclosure, all radiation circumstances are "enclosure" problems.

Vol. 3 1961

opaque surfaces in radiant balance, other than A_j, are assigned a reflectivity of 1·0.*

The absorption factor relations may be written more compactly as:

$$\sum_{i=1}^{n} (\alpha_{pi} - \delta_{pi})B_{ij} + F_{pj}\epsilon_j = 0 \qquad (3)$$

where δ_{pi} is Kronecker's delta. The reciprocity relations among the n^2 values of B_{ij} for any combination of opaque and non-opaque surfaces are:

$$\epsilon_i B_{ij} A_i = \epsilon_j B_{ji} A_j. \qquad (4)$$

* Since the temperature of such a surface may not be arbitrarily specified, the total hemispherical emissive power is not known. This assumption, of unit reflectivity, satisfies the condition of radiant balance and removes the unknown from the equation, e.g. equation (1).

TEMPERATURE OF AN OPAQUE SURFACE IN RADIANT BALANCE

Taking A_j as an opaque surface in radiant balance, denoted hereafter as A_a, the value of q_a is zero. By equations (1) and (4), we have

$$q_a = W_a A_a - \sum_{i=1}^{n} B_{ia} W_i A_i$$

$$= A_a \epsilon_a \sigma (T_a^4 - \sum_{i=1}^{n} B_{ai} T_i^4) = 0. \qquad (5)$$

The B_{ai} are given by (2) or (3) as

$$B_{ai} = \frac{D_{ai}}{D} \qquad (6)$$

where D_{ai} and D denote the following two determinants:

$$D_{ai} = \begin{vmatrix} (\alpha_{11} - 1) & \alpha_{12} & \cdots & \alpha_{1,(a-1)} & -F_{1i}\epsilon_i & \alpha_{1,(a+1)} & \cdots & \alpha_{1n} \\ \alpha_{21} & (\alpha_{22} - 1) & \cdots & \alpha_{2,(a-1)} & -F_{2i}\epsilon_i & \alpha_{2,(a+1)} & \cdots & \alpha_{2n} \\ \cdot & & & & & & & \\ \cdot & & & & & & & \\ \cdot & & & & & & & \\ \cdot & & & & & & & \\ \alpha_{n1} & & & & & & & (\alpha_{nn} - 1) \end{vmatrix} \qquad (7)$$

$$D = \begin{vmatrix} (\alpha_{11} - 1) & \alpha_{12} & \cdots & \alpha_{1,(a-1)} & \alpha_{1a} & \alpha_{1,(a+1)} & \cdots & \alpha_{1n} \\ \alpha_{21} & (\alpha_{22} - 1) & \cdots & \alpha_{2,(a-1)} & \alpha_{2a} & \alpha_{2,(a+1)} & \cdots & \alpha_{2n} \\ \cdot & & & & & & & \\ \cdot & & & & & & & \\ \cdot & & & & & & & \\ \cdot & & & & & & & \\ \alpha_{n1} & & & & & & & (\alpha_{nn} - 1) \end{vmatrix}. \qquad (8)$$

Combining (5) and (6), we obtain

$$T_a^4 = \frac{\sum_i D_{ai} T_i^4}{(D - D_{aa})}; \quad i = 1, 2, \ldots, (a-1), (a+1), \ldots, n \qquad (9)$$

It is seen from equation (7) that ϵ_a, which is equal to $(1 - \rho_a)$, does not appear in the D_{ai} for $i \neq a$. Therefore, the numerator of equation (9) does not depend upon ϵ_a. D and D_{aa} are written as follows, moving the ath column into the first column position in both determinants.

$$D = (-1)^{a-1} \begin{vmatrix} F_{1a}\rho_a & (a_{11}-1) & a_{12} & \cdots & a_{1n} \\ F_{2a}\rho_a & a_{21} & (a_{22}-1) & \cdots & a_{2n} \\ \cdot & & & & \\ \cdot & & & & \\ \cdot & & & & \\ (F_{aa}\rho_a - 1) & a_{a1} & a_{a2} & \cdots & a_{an} \\ \cdot & & & & \\ \cdot & & & & \\ \cdot & & & & \\ F_{na}\rho_a & a_{n1} & a_{n2} & \cdots & (a_{nn}-1) \end{vmatrix}$$

$$D_{aa} = (-1)^{a-1} \begin{vmatrix} -F_{1a}\epsilon_a & (a_{11}-1) & a_{12} & \cdots & a_{1n} \\ -F_{2a}\epsilon_a & a_{21} & (a_{22}-1) & \cdots & a_{2n} \\ \cdot & & & & \\ \cdot & & & & \\ \cdot & & & & \\ -F_{na}\epsilon_a & a_{n1} & a_{n2} & \cdots & (a_{nn}-1) \end{vmatrix}.$$

Both determinants are the same except for the first column. Call N_k the value of the minor of the term in the first column in the kth row. Note that none of the N_k contain ϵ_a or ρ_a. The kth term of $(D - D_{aa})$ where $k \neq a$ is written as

$$(-1)^{k+1}(-1)^{a-1}(F_{ka}\rho_a N_k + F_{ka}\epsilon_a N_k) = (-1)^{k+1}(-1)^{a-1}N_k F_{ka}. \tag{10}$$

None of these terms contain ϵ_a. For the term $k = a$,

$$(-1)^{a+1}(-1)^{a-1}[(F_{aa}\rho_a - 1)N_a + F_{aa}\epsilon_a N_a] = (-1)^{a+1}(-1)^{a-1}N_a(F_{aa}-1). \tag{11}$$

Again ϵ_a is absent. Therefore, $(D - D_{aa})$ is independent of ϵ_a. Since neither the numerator nor the denominator depend upon ϵ_a (or ρ_a), T_a is independent of the surface properties of A_a and depends only upon the temperature and emissivities or surface conditions of the other surfaces of the radiant surroundings.

The results in (10) and (11) indicate that the denominator of equation (9) may be written in the following simpler form for calculations;

$$D_a = D - D_{aa} = (-1)^{a-1} \begin{vmatrix} F_{1a} & (a_{11}-1) & a_{12} & \cdots & a_{1n} \\ F_{2a} & a_{21} & (a_{22}-1) & \cdots & a_{2n} \\ \cdot & & & & \\ \cdot & & & & \\ \cdot & & & & \\ (F_{aa}-1) & a_{a1} & a_{a2} & \cdots & a_{an} \\ \cdot & & & & \\ \cdot & & & & \\ \cdot & & & & \\ F_{na} & a_{n1} & a_{n2} & \cdots & (a_{nn}-1) \end{vmatrix}. \tag{12}$$

Vol. 3 1961

The foregoing analysis shows that the temperature of an opaque surface in radiant balance is independent of its surface property emissivity, i.e. the temperature may be calculated from equation (9) using any value of ϵ_a in equations (7) and (8). However, it is not necessary to assume a value of ϵ_a since equations (12) and (9) may be used. This same result may be expressed as follows:

$$T_a^4 = \frac{\sum_i^n D_{ai} T_i^4}{(-1)^{a-1}\left[(-1)^{a+1}(F_{aa}-1)N_a + \sum_k^n (-1)^{k+1} F_{ka} N_k\right]}; \quad i \neq a \text{ and } k \neq a. \tag{13}$$

OPAQUE SURFACES WITH ASSIGNED NET RADIANT LOSS

A surface (in a radiant surrounding of arbitrary complexity) whose temperature level adjusts to result in a given net rate of energy loss by radiation amounts to the assignment of a given value of q_a. The necessary temperature level is found from equation (5) as

$$T_a^4 = \frac{\sum_i^n D_{ai} T_i^4}{D_a} + \frac{q_a D}{A_a \epsilon_a \sigma D_a}; \quad i \neq a. \tag{14}$$

Although the first term on the right is independent of ϵ_a, the second is not and the resulting temperature depends upon ϵ_a. Equation (14) is suitable for calculations.

NON-OPAQUE SURFACES

The general formulations, equations (1), (2) and (3), apply for enclosures which contain windows, openings, or any other surfaces whose radiation characteristics are gray and diffuse. For any surface A_j the equations take into account the effects of the radiant energy transmission across all non-opaque surfaces under the assumption that none of the thermal radiation transmitted outside of the enclosure is again incident upon the outside of the transmitting areas due, for example, to reflections. This is a reasonable assumption in many practical circumstances.

If A_j is opaque, then q_j is the net rate of radiant energy loss from A_j. If A_j is non-opaque, q_j is the net rate of radiant energy loss from the "enclosure" side of A_j. The rate of energy transmission through A_j is

$$(q_T)_j = \frac{\tau_j}{a_j} \sum_{i=1}^{n} B_{ij} W_i A_i = \tau_j \sigma A_j \sum_{i=1}^{n} B_{ji} T_i^4 \tag{15}$$

where τ_j and a_j are, respectively, the transmissivity and absorptivity of A_j.

The calculation of the temperature of a non-opaque surface with an assigned net (or zero) radiant energy loss rate takes into account both sides of the surface and the two different enclosures A and B with which the two sides exchange energy. The n surfaces in enclosure A are numbered 1, 2, . . . , i, . . . , n and the N surfaces in B are numbered 1, 2, . . . , m, . . . , N. The surface under consideration is denoted by a and its net rate of radiant energy loss is

$$q_a = (q_a)_A + (q_a)_B = (W_a A_a - \sum_{i=1}^{n} B_{ia} W_i A_i)_A + (W_a A_a - \sum_{m=1}^{N} B_{ma} W_m A_m)_B. \tag{16}$$

If the two sides of surface a are of equal area and emissive power, this result may be written as

$$q_a = 2W_a A_a - \sum_{i=1}^{n} B_{ia} W_i A_i - \sum_{m=1}^{N} B_{ma} W_m A_m. \tag{17}$$

Employing the reciprocity relation and solving for T_a^4, we have

$$[2 - (B_{aa})_A - (B_{aa})_B]\, T_a^4 = \frac{q_a}{\epsilon_a \sigma A_a} + \sum_{i}^{n} B_{ai} T_a^4 + \sum_{m}^{N} B_{am} T_m^4 \tag{18}$$

where $i \neq a$ and $m \neq a$.

For the case of a non-opaque surface in radiant balance, q_a is zero. However, it is not true that T_a is independent of ϵ_a for a non-opaque surface.

CONCLUSION

The foregoing analysis has shown that the temperature achieved by an opaque surface in radiant balance is independent of its surface properties. Relations are derived for temperature

calculations for opaque and non-opaque surfaces subject to an assigned net thermal radiant exchange rate.

Although the absorption factor method may be used in analysing enclosures containing emitting and absorbing media, the present treatment applies only in the absence of such radiation effects. However, if the principal effect of such an intervening medium is convection at the various enclosure surfaces, its presence may be simply accounted for by an iterative method of calculating the temperature of an assigned net flux surface. A temperature is assumed, the rate of convection loss is calculated and subtracted from the assigned rate of loss to obtain the net rate of radiant loss. From this, a surface temperature is computed which is compared with the assumed value.

This absorption factor method applies, within the limits of the initial assumptions, to enclosures of arbitrary complexity, i.e. for arbitrarily large values of n. It has been pointed out [3] that the inaccuracies inherent in the assumption of uniform irradiation of each surface by each other surface may be reduced continually toward zero by further subdivision of the surfaces of the enclosure.*

If a given area in radiant balance in an enclosure is subject to highly non-uniform irradiation, its temperature will be far from uniform. More accurate estimates of the temperature achieved by such a surface may be obtained by subdividing it into separate zones for which individual temperatures are calculated. By this means a temperature distribution is obtained.

REFERENCES

1. B. GEBHART, Unified treatment for thermal radiation transfer, *ASME Paper* 57-A-34, presented at the ASME Annual Meeting, December (1957).
2. B. GEBHART, A new method for calculating radiant exchanges, *Trans. ASHRAE* **65**, 321 (1959).
3. B. GEBHART, *Heat Transfer*. McGraw-Hill, New York (1961).
4. E. R. G. ECKERT and R. M. DRAKE, JR., *Heat and Mass Transfer*, 2nd Ed., p. 411. McGraw-Hill, New York (1959).
5. A. K. OPPENHEIM, Radiation analysis by the network method, *Trans. ASME*, **78**, 725 (1956).

* This subdivision procedure must be judiciously employed, however. The number of numerical operations which must be carried out to obtain a solution is proportional to n^3.

Vol. 3 1961

Int. J. Heat Mass Transfer. Vol. 3, p. 347. Pergamon Press 1961. Printed in Great Britain.

SHORTER COMMUNICATION

A DISCREPANCY IN THE PUBLISHED RESULTS ON HEAT TRANSFER TO CRYOGENIC FLUIDS*

WILLIAM SQUIRE

Engineering Analysis Section, Department of Mechanical Sciences, Southwest Research Institute, San Antonio 6, Texas

THE purpose of this communication is to call attention to conflicting experimental results on heat transfer to cryogenic fluids. The problem is of some importance in connection with the design of rockets using liquid hydrogen and/or oxygen as propellants.

Kramer, Lowell and Rodebush [1] have reported calculations of the aerodynamic heating of tanks of liquid hydrogen utilizing a curve for the heat transfer from the wall to the liquid hydrogen based on measurements reported by Mulford and Nigon [2]. These measurements of the heat transfer from a 12 mm copper tube to liquid hydrogen at 520 mm pressure indicated a critical temperature difference of 2°K for the transition from nucleate to film boiling. The corresponding maximum heat flux was 6 W/cm². It was stated that measurements with liquid nitrogen paralleled the hydrogen curve at somewhat larger ΔT, the critical temperature difference being 4°K and the peak heat flux 6 W/cm².

On the other hand, Ruzicka [3] made an extensive set of measurements of heat transfer from platinum wires and copper wires and tubes ranging in diameter from 0·051 to 20 mm to liquid nitrogen at 1 atm and found a critical temperature difference of 12°K and a peak heat flux of 11 W/cm².

Weil and Lacaze [4, 5] measured the heat loss from copper, platinum and lead wires to liquid nitrogen over a range of pressures. At 1 atm they found a critical temperature difference of 10°K and a heat flux of 10 W/cm² which agrees reasonably well with Ruzicka. Furthermore, the pressure variation would not explain the discrepancy with the measurements of Mulford and Nigon.

Weil and Lacaze [6] also reported heat loss measurements from lead wires to liquid hydrogen at 1 atm. While their value of the critical temperature difference, 2°K, agrees with Mulford and Nigon, Weil and Lacaze found a peak heat flux of only 3 W/cm² and the shape of the heat flux–temperature difference curve differed markedly.

It should be noted that Mulford and Nigon and Weil and Lacaze state that their results are not affected by large changes in the geometrical configuration, thus making it very difficult to account for these discordant results.

* Work supported by NASA under Contract NASw-146.

REFERENCES

1. J. L. KRAMER, H. H. LOWELL and W. H. RODEBUSH, Numerical computations of aerodynamic heating of liquid propellants, *NASA Tech. Note* D-273 (1960).
2. R. M. MULFORD and J. P. NIGON, Heat exchange between copper surface and liquid hydrogen and nitrogen, *LA*-1416, *Tech. Info. Service, U.S. Atomic Energy Commission* (1952).
3. J. RUZICKA, Heat transfer to boiling nitrogen, *Problems of Low Temperature Physics and Thermodynamics*. Pergamon Press, London (1959).
4. L. WEIL and A. LACAZE, *C.R. Acad. Sci., Paris*, **230**, 196 (1950).
5. L. WEIL and A. LACAZE, *Bull. Inst. Int. du Froide*, 1955-2, 85–88 (1954).
6. L. WEIL and A. LACAZE, *J. Phys. Radium*, **12**, 890 (1951).

Vol.
3
1961

Int. J. Heat Mass Transfer. Vol. 3, pp. 349–350. Pergamon Press 1961. Printed in Great Britain.

ANNOUNCEMENTS

SECOND CONFERENCE ON KINETICS, EQUILIBRIA, AND PERFORMANCE OF HIGH TEMPERATURE SYSTEMS

The Combustion Institute, Western States Section

To be held at University of California at Los Angeles, 16–18 April 1962.

INVITATIONS are extended for papers for the Western States Section's Second Conference on Kinetics, Equilibria, and Performance of High Temperature Systems. The First Conference was held in November 1959, and approximately 40 papers were presented, dealing largely with the calculation of equilibrium chemical compositions of high temperature systems. These papers have recently been published by Butterworths. In the Second Conference it is intended to deal primarily with nonequilibrium aspects of high temperature systems, i.e., those in the temperature range from 3000° Rankine to 10 000° Rankine and above, although any new contributions in the field of chemical equilibrium will receive careful consideration. In this regard, attention might be directed toward analysis of multiphase systems, calculation of equilibrium at low exit temperatures (around 1000°R) in large expansion ratio nozzles, evaluation of the problem of a general freezing point for expansions to temperatures as low as about 500°R, and, importantly, consideration of the effects of iteration tolerance, accuracy of basic property data, and curve fitting approximations upon equilibrium performance results.

Thermodynamic and thermochemical species data

The preparation of the JANAF Thermochemical Tables by Dr. Daniel R. Stull and associates at the Dow Chemical Company has satisfied an urgent need, expounded at the First Conference, for provisional standards. Despite the great number of chemical species represented in the JANAF Tables, there remain some species of interest in high temperature calculations which are not represented, and for which compilations of appropriate data would be valuable. This is especially true of ions and other odd species which put in an appearance above 10 000°R in plasmas and some detonation waves. There is, of course, always interest in, and need for, presentation of new experimental data to effect revisions in previous "best" values. Standard data for reactants might be compiled, and hopefully by the time of the Second Conference a number of special fuels and oxidizers of present interest may be declassified, at least as regards basic thermochemical and thermophysical properties.

Theoretical equilibrium engine performance

As regards declassification, the publication of Dobbins's comprehensive calculational results, for theoretical rocket engine performance, in unclassified report form lends hope that other, even more comprehensive, compilations can be made on an unclassified basis if the numbers are separated from the various application contracts on which many of them were derived. Perhaps a small committee might work together to compile a master collection of performance numbers, and then analyze the results for general results attributable either to chemical composition or to energy level. The effect of low chamber pressure operation upon theoretical performance in a variety of chemical systems would be of particular interest, as would also the theoretical performance of high temperature electrical and magnetic propulsion schemes.

Calculations for engine design

At the First Conference, a few calculational schemes were presented for jet propulsion engine design, with a limited amount of theoretical results. It is likely that since that time a variety of computer programs have been produced which deal with various aspects of engine performance and which incorporate means for evaluating constants and verifying models by correlation of computer output parameters with experimental data. Included in this category would be programs for the design of air-breathing engine inlets, supersonic combustors, and exhaust nozzles.

Evaluation of kinetic processes in engines

As always, there is much need for experimental data of an ordered nature, explained in terms of physical and chemical processes and thus reduced to appropriate terms for general application. In particular, there might be noted the kinetics of vaporization, combustion reactions, and reassociation reactions during exhaust gas expansion, as well as the characteristics of two-phase (gas plus particle) flow.

Other high temperature systems

While all of the above discussion is centered around engine considerations, particularly jet propulsion engines, the concept of the Second Conference will include other high temperature systems than those created by jet propulsion fuels and oxidizers, over the approximate temperature range of 3000°R to 10 000°R above. This means inclusion of such diverse fields as detonation waves of all sorts, ablation heat transfer, chemical processing at elevated temperatures, and thermokinetics of flames generally and of high temperature materials technology.

The Western States Section's standing technical committee on Kinetics, Equilibria, and Performance of High Temperature Systems is chairmaned by Mr. Gilbert S. Bahn, 16902 Bollinger Drive, Pacific Palisades, California. Communications relative to the program

generally, such as brief abstracts of possible papers, should be addressed to Mr. Bahn. Also serving actively on the committee at the present time are Messrs. Harold E. Brandmaier, S. E. Stephanou, H. J. Vale, Alfred Büchler, and D. S. Villars. Organization of the full committee in terms of programming for the Second Conference is now under way, and additional appointments will be made in the near future. Specific papers offered for the Second Conference will be reviewed by Dr. Melvin Gerstein, Papers Review Committee Chairman for the Western States Section, and members of his committee. Completed texts of papers should be sent directly to Dr. Gerstein, whose address is Dynamic Science Corp., 1445 Huntington Drive, South Pasadena, California.

Prospective authors should note that 300 copies of preprints will be required to be furnished to the Section for distribution to Conference registrants, and should arrange well in advance of the Conference to complete any requisite security review of their papers.

THE NINTH INTERNATIONAL SYMPOSIUM ON COMBUSTION

THE Ninth International Symposium on Combustion will be held at Cornell University, Ithaca, New York, during the week of 27 to 31 August 1962, inclusive. It will be the fourth symposium organized under the auspices of The Combustion Institute. The local arrangements are being made by the Department of Thermal Engineering at Cornell. The Institute and the local sponsors welcome the participation of all members of the organization, together with all scientists and engineers interested in combustion.

Local arrangements for the meeting

Headquarters for the meeting will be Upson Hall of the Sibley School of Mechanical Engineering, which is situated on the engineering campus of the university. This is located at the south end of the main campus, within walking distance of the dormitories and the eating facilities on the campus.

Dormitory rooms will be available, mainly in the recently built student dormitory block. Some rooms will be available for single women and couples can be accommodated. The surrounding district contains a number of hotels and motels for which information will be provided in the next announcement. Meals will be available by special arrangement with the University Department of Residential Halls and there are many nearby restaurants.

If you plan to attend the 1962 Symposium, kindly write, at your earliest convenience, to

Combustion Symposium Office, Upson Hall
Sibley School of Mechanical Engineering
Cornell University
Ithaca, New York.

Symposium agenda

The technical program of the Ninth International Combustion Symposium is planned to include two *Discussions*, three *Colloquia* and *Contributed Papers*. The Discussions and Colloquia are intended to lead to interchange of information in specific areas where an intensive review of the known theoretical and experimental facts is desirable. Contributed Papers will be accepted in all areas of the Combustion Field. When parallel sessions are unavoidable, an effort will be made to schedule papers in the same general area of interest at such times as to make attendance at all of them possible.

Discussions

The Discussion topics are (a) *Fundamental Flame Processes* (with emphasis on the Structure of Flames) and (b) *Detonations*. The Discussions will revolve around *invited preprinted* papers, available for distribution several weeks before the Symposium.

Combustion Symposium participants are urged to take an active part in the Discussions. Their value and success depends to a large measure on the quality of the contributions from the audience. A brief summary by the authors of the highlights of their papers will be followed by extended discussions from the floor. It is particularly desirable to present unpublished material that is germane to the topics of the Discussions. Participants are requested to procure preprints and to prepare their comments prior to the meeting. The papers and relevant comments will be published in the Symposium Proceedings. Further information will be given in the Second Announcement.

Colloquia

The Colloquia topics are (a) *Modeling Techniques* (Engines, Furnaces, Fires), (b) *Chemical Reactions and Phase Changes in Supersonic Flow* (with emphasis on Nozzle Flow), (c) *Reciprocating Engine Combustion Research*. The Colloquia papers will be presented in full, followed by comments from the floor. The papers will not be preprinted but will be published in the Symposium Proceedings. Further details can be obtained from the Chairman, Papers Subcommittee.

Contributed papers

The Papers Subcommittee will select Contributed Papers on the *basis of* 800–1000 *word Abstracts*, with a view to technical content and suitability for public presentation. Three copies of the Abstracts are to be submitted to The Combustion Institute, 936-B Union Trust Building, Pittsburgh 19, Pennsylvania, not later than 1 February 1962.

Three copies of the manuscripts of the complete Contributed Papers are due at The Combustion Institute on or before 1 May, 1962, and will be reviewed prior to publication in the Symposium Proceedings. It is requested to restrict the length of the papers to 4000 words or less.

Time alloted to individual Contributed Papers is 15–20 minutes, with 5–10 minutes for comments. Abstracts (revisable up to 1 May 1962) of all accepted papers will be bound together for distribution at the Symposium.

Vol. 3 1961

Int. J. Heat Mass Transfer. Vol. 3, pp. 351–357. Pergamon Press 1961. Printed in Great Britain.

HEAT TRANSFER BIBLIOGRAPHY

E. R. G. ECKERT, E. M. SPARROW and W. E. IBELE

Heat Transfer Laboratory, Department of Mechanical Engineering,
University of Minnesota, Minneapolis 14, Minnesota, U.S.A.

APPLICATIONS

D. M. ADAMS, How Finned Streamlined Heat Exchanger Tubes Perform. *Heat. Pip. Air Condit.* **33**, No. 2, 131 (1961).

E. L. ARMI and C. G. KIRKPATRICK, Temperature Control by Means of the Peltier Effect. *Aircr. Engng*, **33**, No. 383, 12 (1961).

D. C. BRIGGS and A. L. LONDON, The Heat Transfer and Flow Friction Characteristics of Five Offset Rectangular and Six Plain Triangular Plate-Fin Heat Transfer Surfaces. *Dept. of Mechanical Engng, Stanford University, Stanford, Calif., Tech. Rep.* 49 (1960).

S. C. BROWNING and J. J. S. SEBASTIAN, Ceramic Heat Exchangers for High-Temperature Heat Transfer from Helium. *Industr. Engng Chem.* **53**, No. 3, 191 (1961).

D. BUSHNELL and A. D. KRAUS, Thermal Equilibrium of Space Vehicles. *Sperry Rev.* **13**, No. 4, 26 (1960).

R. W. DETRA and H. HIDALGO, Generalized Heat Transfer Formulas and Graphs for Nose Cone Re-entry into the Atmosphere. *J. Amer. Rocket Soc.* **31**, No. 3, 318 (1961).

B. N. DEVYATOV, Transient Effects in Continuously Acting Thick-Walled Heat Exchangers. *Soviet Fiz. Dokl.* **5**, No. 1, 54 (1960).

L. S. DZUNG, A Cooling Problem of Pebble-Bed Nuclear Reactors. *Int. J. Heat Mass Transfer*, **1**, Nos. 2/3, 236 (1960).

F. C. GRANT, Modulated Entry. *NASA TN* D-452 (1960).

R. I. HODGE, A Comparison Between the Measured and Predicted Cooling Performance of an Internally Spanwise Ventilated Turbine Nozzle Blade. *Aero. Res. Coun. Lond., Curr. Pap.* 494 (1960).

R. I. HODGE, A Turbine Nozzle Cascade for Cooling Studies: Part 1, The Measurement of Mean Nusselt Numbers at the Blade Surface. *Aero. Res. Coun. Lond., Curr. Pap.* 492 (1960).

A. H. LEFEBVRE, Heat-Transfer Processes in Gas-Turbine Combustion Chambers. *Proc. Instn Mech. Engrs, Lond.* **174**, No. 12, 463 (1960).

M. H. LEIPOLD and J. L. TAYLOR, Ultra-High-Frequency Oxide Induction-Heating Furance. *Jet Propulstion Laboratory, California Institute of Technology, Pasadena, Calif., Tech. Rep.* 32-32 (1961).

R. J. MARCUS and H. C. WOHLERS, A New Solar Furnace —Design and Operation. *Industr. Engng Chem.* **52**, No. 10, 825 (1960).

R. MARLOW, Peltier Cooling of Electrical Components in Telemetering Packages. *J. Amer. Rocket Soc.* **31**, No. 2, 263 (1961).

F. T. MCCLURE, R. W. HART and J. F. BIRD, Heat Release Rate, Temperature and Pressure in Solid Rocket Instability. *J. Amer. Rocket Soc.* **31**, No. 3, 367 (1961).

L. D. NICHOLS, Effect of Shield Position and Absorptivity on Temperature Distribution of a Body Shielded from Solar Radiation in Space. *NASA TN* D-578 (1961).

D. R. OLANDER, Design of Direct Contact Cooler-Condensers. *Industr. Engng Chem.* **53**, No. 2, 121 (1961).

W. S. PELLINI, Materials Requirements of Hypersonic Flight Vehicles. *J. Metals*, **12**, No. 12, 952 (1960).

H. A. PERRY, Reinforced Plastics Pierce Heat Barrier. *Mater. Res. Stand.* **1**, No. 2, 122 (1961).

E. T. PITKIN, Optimum Radiator Temperature for Space Power Systems. *J. Amer. Rocket Soc.* **29**, No. 8, 596 (1959).

D. READSHAW, Predicting Temperature Rises Due to Aerodynamic Heating. *Aircr. Engng*, **33**, No. 383, 8 (1961).

R. J. ROSA, Physical Principles of Magnetohydrodynamic Power Generation. *AVCO Everett Research Laboratory, Everett, Mass., Research Rep.* 69, AFBMD TR-60-36 (1960).

K. SCHACK, Wärmetausch von Gasen hoher Temperatur in kombiniertem Gleich- und Gegenstromverfahren. *Chem.-Ing.-Tech.* **33**, No. 3, 163 (1961).

J. N. STEINMETZ, JR., Hydrogen Jets Match Re-entry Heat. *Missiles & Rockets*, **8**, No. 8, 24 (1961).

A. M. STOLL, The Role of the Skin in Heat Transfer. *J. Heat Transfer*, C **82**, No. 3, 239 (1960).

S. L. SULLIVAN, JR. and C. D. HOLLAND, Double Pipe Heat Exchangers. *Industr. Engng Chem.* **53**, No. 4, 285 (1961).

J. TAYLOR, Beating the Heat Barrier. *Royal Aircraft Establishment* (*Gt. Brit.*), *RAE Tech. Note Structures*, 286 (1960).

C. L. WALKER, C. R. SMITH and D. G. GRITTON, Weight Optimization of Heat Rejection Systems for Space Applications. *Proc. Heat Transfer and Fluid Mechanics Institute, Stanford, Calif., June* 15–17, 1960; *Stanford University*, p. 244 (1960).

E. L. WATSON, A. A. MCKILLOP, W. L. DUNKLEY and R. L. PERRY, Flow Characteristics—Plate Heat Exchangers. *Industr. Engng Chem.* **52**, No. 9, 733 (1960).

C.-Y. WEN and E. N. MILLER, Heat Transfer in Solids–Gas Transport Lines. *Industr. Engng Chem.* **53**, No. 1, 51 (1961).

L. D. WING and K. E. CAMERON, Solar Collectors for Use in Thermionic Power Supply Systems in Space. *J. Amer. Rocket Soc.* **31**, No. 3, 327 (1961).

R. M. WOOD and T. J. ASHLEY, Missile Has Special Protective "Skin". *Missiles & Rockets*, **8**, No. 5, 42 (1961).

BOOKS

Astronautics Information Open Literature Survey, Vol. III, No. 4, Jet Propulsion Laboratory, California Institute of Technology, Pasadena, Calif. (1961).

C. W. BECKET, W. S. BENEDICT, L. FANO, J. HILSENRATH, H. J. HOGE, J. F. MASI, R. L. NUTTALL and Y. S. TOULOUKIAN, *Tables of Thermodynamic and Transport*

Properties of Air, Argon, Carbon Dioxide, Carbon Monoxide, Hydrogen, Nitrogen, and Steam. Pergamon Press, Lond. (1960).

J. L. DELCROIX, *Introduction to the Theory of Ionized Gases.* Interscience, New York (1960).

N. A. FUCHS, *Evaporation and Droplet Growth in Gaseous Media.* Pergamon Press, New York (1959).

B. GEBHART, *Heat Transfer.* McGraw-Hill, New York (1961).

T. R. HARRISON, *Radiation Pyrometry and Its Underlying Principles of Radiant Heat Transfer.* John Wiley, New York (1960).

B. G. KORENEV, *Certain Problems in Theory of Elasticity and Heat Conduction Solved in Terms of Bessel Functions.* Gosudarstvennoe Izdatel'stvo Fiziko-Matematicheskoi Literatury, Moscow (1960).

Precision Measurement and Calibration, Selected Papers: Vol. 2, *Heat and Mechanics.* U.S. NBS Handbook 77, U.S. Government Printing Office (1961).

A. I. VEINIK, *Approximate Calculation of Heat Conduction Processes.* Gosudarstvennoe Energeticheskoe Izdatel' stvo, Moscow (1959).

BOUNDARY LAYER FLOW

J. R. BARON and P. B. SCOTT, The Laminar Diffusion Boundary Layer with External Flow Field Pressure Gradients. *Massachusetts Institute of Technology, Naval Supersonic Laboratory*, AFOSR TN 59-1268 (1959).

I. E. BECKWITH and N. B. COHEN, Application of Similar Solutions to Calculation of Laminar Heat Transfer on Bodies with Yaw and Large Pressure Gradient in High-Speed Flow. *NASA TN* D-625 (1961).

R. P. BERNICKER, An Experiment with a Transpiration-Cooled Nozzle. *Massachusetts Institute of Technology, Naval Supersonic Laboratory, Tech. Rep.* 447, AFOSR TN 60-1484 (1960).

M. H. BLOOM and M. H. STEIGER, Perturbed Boundary Layer Solutions Applied to the Wall Jet and Blasius Profile. *Polytechnic Institute of Brooklyn, Dept. of Aerospace Engng and Applied Mechanics, PIBAL Rep.* 471, AFOSR TN 60-1340 (1960).

L. J. CHALLIS, K. DRANSFELD and J. WILKS, Heat Transfer Between Solids and Liquid Helium II. *Proc. Roy. Soc.* A **259**, No. 1299, 31 (1961).

P. M. CHUNG and A. D. ANDERSON, Heat Transfer to Surfaces of Finite Catalytic Activity in Frozen Dissociated Hypersonic Flow. *NASA TN* D-350 (1961).

W. H. DORRANCE, Dissociation Effects Upon Compressible Turbulent Boundary Layer Skin Friction and Heat Transfer. *J. Amer. Rocket Soc.* **31**, No. 1, 61 (1961).

A. FERRI and V. ZAKKAY, Measurements of Stagnation Point Heat Transfer at Low Reynolds Numbers. *Polytechnic Institute of Brooklyn, Dept. of Aerospace Engng and Applied Mechanics, ARL Rep.* 38 (1961).

G. E. GADD, W. F. COPE and J. L. ATTRIDGE, Heat-Transfer and Skin-Friction Measurements at a Mach Number of 2·44 for a Turbulent Boundary Layer on a Flat Surface and in Regions of Separated Flow. *Aero. Res. Coun. (Gt. Brit.), ARC R & M* 3148 (1960).

A. F. GOLLNICK, JR., Heat Transfer Rates and Insulated Wall Temperatures for a Transpiration Cooled Hemisphere. *Massachusetts Institute of Technology, Naval Supersonic Laboratory, Tech. Rep.* 433, AFOSR TN 60-1483 (1960).

R. A. GRANVILLE and G. BOXALL, Measurement of Convective Heat Transfer by Means of the Reynolds Analogy. *Brit. J. Appl. Phys.* **11**, No. 10, 471 (1960).

G. R. GUINN, Aerodynamic Heating of Plane Bodies of Low Thermal Diffusivity. *J. Amer. Rocket Soc.* **31**, No. 1, 158 (1961).

C. R. GUNN, Heat-Transfer Measurements on the Apexes of Two 60° Sweptback Delta Wings (Panel Semiapex Angle of 30°) Having 0° and 45° Dihedral at a Mach Number of 4·95. *NASA TN* D-550 (1961).

J. G. HALL and T. C. GOLIAN, Heat Transfer to Sharp and Blunt Yawed Plates in Hypersonic Airflow. *Cornell University, Cornell Aero. Laboratory, Inc., Rep.* AD-1052-A-11, AFOSR TN 60-938 (1960).

F. K. HILL, Turbulent Boundary Layer Measurements at Mach Numbers from 8 to 10. *Phys. Fluids*, **2**, No. 6, 668 (1959).

J. P. IRVING and J. M. SMITH, Heat Transfer in a Chemically Reacting System (Nitrogen Tetroxide-Dioxide). *J. Amer. Inst. Chem. Engrs*, **7**, No. 1, 91 (1961).

H. KENNET and S. L. STRACK, Stagnation Point Radiative Transfer. *J. Amer. Rocket Soc.* **31**, No. 3, 370 (1961).

J. KESTIN, P. F. MAEDER and H. H. SOGIN, The Influence of Turbulence on the Transfer of Heat to Cylinders Near the Stagnation Point. *Z. Angew. Math. Phys.* **12**, No. 2, 115 (1961).

J. KESTIN and P. D. RICHARDSON, Heat Transfer Across Turbulent Incompressible Boundary Layers. *Division of Engineering, Brown University, Providence, R.I., Rep.* AF-774911 (1961).

O. KRISCHER, Wärme- und Stoffaustausch bei überströmten oder durchströmten Körpern verschiedener geometrischer Form. *Chem.-Ing.-Tech.* **33**, No. 3 155 (1961).

T. Y. LI, Effect of Surface Mass-Transfer on the Impulsive Motion of an Infinite Plate at Hypersonic Speeds in a Viscous Compressible Fluid. *Rensselaer Polytechnic Institute, Dept. of Aeronautical Engng, TR AE* 6005, AFOSR TN 60-956 (1960).

T. Y. LI, Recent Advances in Nonequilibrium Dissociating Gasdynamics. *J. Amer. Rocket Soc.* **31**, No. 2, 170 (1961).

J. G. MARVIN, Surface Pressures and Heat Transfer on Unswept Blunt Plates in Helium at High Mach Numbers. *NASA TN* D-688 (1961).

F. W. MATTING, D. R. CHAPMAN, J. R. NYHOLM and A. G. THOMAS, Turbulent Skin Friction at High Mach Numbers and Reynolds Numbers in Air and Helium. *NASA TR* R-82 (1960).

J. P. MORAN and P. B. SCOTT, A Mass Transfer Finite Difference Formulation Employing Crocco Variables. *Massachusetts Institute of Technology, Naval Supersonic Laboratory, Tech. Rep.* 443, AFOSR TN 60-846 (1960).

R. A. NEWLANDER, Effect of Shock Impingement on the Distribution of Heat-Transfer Coefficients on a Right Circular Cylinder at Mach Numbers of 2·65, 3·41 and 4·44. *NASA TN* D-642 (1961).

W. S. NORMAN and V. MCINTYRE, Heat Transfer to a Liquid Film on a Vertical Surface. *Trans. Instn Chem. Engrs, Lond.* **38**, No. 6, 301 (1960).

A. A. POMERANTSEV, Wall Heating by a Supersonic Gas Flow. *Int. J. Heat Mass Transfer*, **2**, Nos. 1/2, 8 (1961).

R. I. ROTHENBERG and J. M. SMITH, Heat Transfer to a Surface Reacting Fluid in Turbulent Flow. *Canad. J. Chem. Engng*, **38**, No. 1, 184 (1960).

S. M. SCALA and C. W. BAULKNIGHT, Transport and Thermodynamic Properties in a Hypersonic Laminar

Vol. 3 1961

Boundary Layer: Part 2, Applications. *J. Amer. Rocket Soc.* **30**, No. 4, 329 (1960).
J. P. SELLERS, JR., Effect of Two-Dimensional Heat Transfer on Wall Temperatures in a Tubular Thrust Chamber. *J. Amer. Rocket Soc.* **31**, No. 3, 445 (1961).
V. A. SMIRNOV, G. E. VEREVOCHKIN and P. M. BRDLICK, Heat Transfer Between a Jet and a Held Plate Normal to Flow. *Int. J. Heat Mass Transfer*, **2**, Nos. 1/2, 1 (1961).
D. B. SPALDING, Mass Transfer Through Laminar Boundary Layers—1. The Velocity Boundary Layer. *Int. J. Heat Mass Transfer*, **2**, Nos. 1/2, 15 (1961).
P. C. STAINBACK, Heat-Transfer Measurements at a Mach Number of 4·95 on Two 60° Swept Delta Wings with Blunt Leading Edges and Dihedral Angles of 0° and 45°. *NASA TN* D-549 (1961).
T. TENDELAND, H. L. NIELSEN and M. J. FOHRMAN, The Flow Field Over Blunted Flat Plates and Its Effect on Turbulent Boundary-Layer Growth and Heat Transfer at a Mach Number of 4·7. *NASA TN* D-689 (1961).
J. WILKINSON, The Steady Incompressible Boundary-Layer Flow Past a Flat Plate with a Parabolic Leading Edge. *Quart. J. Mech. Appl. Math.* **13**, No. 2, 199 (1960).

CHANGE OF PHASE

M. ALTMAN, R. H. NORRIS and F. W. STAUB, Local and Average Heat Transfer and Pressure Drop for Refrigerants Evaporating in Horizontal Tubes. *J. Heat Transfer*, C **82**, No. 3, 189 (1960).
C. W. BOWMAN, D. M. WARD, A. I. JOHNSON and O. TRASS, Mass Transfer from Fluid and Solid Spheres at Low Reynolds Numbers. *Canad. J. Chem. Engng*, **39**, No. 1, 9 (1961).
R. D. CESS, Laminar-Film Condensation on a Flat Plate in the Absence of a Body Force. *Z. Angew. Math. Phys.* **11**, No. 5, 426 (1960).
J. F. DAVIDSON and B. O. G. SCHULER, Bubble Formation at an Orifice in a Viscous Liquid. *Trans. Instn Chem. Engrs, Lond.* **38**, No. 3, 144 (1960).
J. DLOUHY and W. H. GAUVIN, Evaporation Rates in Spray Drying. *Canad. J. Chem. Engng*, **38**, No. 4, 113 (1960).
T. FREDERKING, Wärmeübergang bei der Verdampfung der verflüssigten Gase Helium und Stickstoff. *Forsch. IngWes.* **27**, No. 1, 17 (1961).
A. FRIEDMAN, Free Boundary Problems for Parabolic Equations: Part 3, Dissolution of a Gas Bubble in Liquid. *J. Math. Mech.* **9**, No. 3, 327 (1960).
J. C. Y. KOH, E. M. SPARROW and J. P. HARTNETT, The Two Phase Boundary Layer in Laminar Film Condensation. *Int. J. Heat Mass Transfer*, **2**, Nos. 1/2, 69 (1961).
A. J. MADDEN and F. J. HALFEN, Temperature Depressions for Evaporating Spheres at Low Pressures. *J. Amer. Chem. Engrs*, **7**, No. 1, 160 (1961).
P. F. MASSIER, A Forced-Convection and Nucleate-Boiling Heat-Transfer Test Apparatus. *Jet Propulsion Laboratory, California Institute of Technology, Pasadena, Calif., JPL TR* 32-47 (1961).
B. METAIS, Einfluss der Gesausscheidung auf den Wärmeübergant bei der Erwärmung von Flüssigkeiten. *Chem.-Ing.-Tech.* **33**, No. 3, 182 (1961).
V. V. MIRKOVICH and R. W. MISSEN, Non-Filmwise Condensation of Binary Vapors of Miscible Liquids. *Canad. J. Chem. Engng*, **39**, No. 2, 86 (1961).
K. NIU, Flow of Condensing Vapour with Temporary Supersaturated State Due to Heat-Removal Effect. *J. Phys. Soc. Japan*, **16**, No. 4, 798 (1961).
H. F. STEINLE, An Experimental Study of the Transition from Nucleate to Film Boiling Under Zero Gravity Conditions. *Proc. Heat Transfer and Fluid Mechanics Institute, Stanford, Calif., June* 15–17, 1960; *Stanford University*, p. 208 (1960).
M. S. STYRIKOVICH and E. I. NEVSTRUEVA, Investigation of Vapour-Content Distribution in Boiling Boundary Layers by the Beta-Radioscopy Method. *Soviet Fiz. Dokl.* **5**, No. 1, 58 (1960).
T. WOODWARD, Heat Transfer in a Spray Column. *Chem. Engng Progr.* **57**, No. 1, 52 (1961).
N. ZUBER, The Dynamics of Vapor Bubbles in Nonuniform Temperature Fields. *Int. J. Heat Mass Transfer*, **2**, No. 1/2, 83 (1961).
N. ZUBER, On the Variable-Density Single-Fluid Model for Two-Phase Flow. *J. Heat Transfer*, C **82**, No. 3, 255 (1960).
S. A. ZWICK, Growth of Vapor Bubbles in a Rapidly Heated Liquid. *Phys. Fluids*, **3**, No. 5, 715 (1960).

CHANNEL FLOW

C. F. BONILLA, J. S. BUSCH, H. G. LANDAU and L. L. LYON, Formal Heat Transfer Solutions. *Nucl. Sci. Engng*, **9**, No. 3, 323 (1961).
P. BRO and S. STEINBERG, Entrance Effects in the High Temperature Heat Transfer From Dissociated Gases. *J. Amer. Rocket Soc.* **31**, No. 3, 375 (1961).
G. FRANKE, Wärmeübergang und Geschwindigkeitsverlauf bei pulsierender Rohrströmung. *Allg. Wärmetech.* **10**, No. 2, 36 (1961).
J. I. GONZALEZ, Air-Gap Heat Transfer. *Mach. Design*, **33**, No. 3, 131 (1961).
S. C. GUPTA, A Variational Principle for Fully Developed Laminar Heat Transfer in Uniform Channels. *Appl. Sci. Res.* A **10**, No. 2, 85 (1961).
F. C. HAAS and A. H. NISSAN, Experimental Heat Transfer Characteristics of a Liquid in Couette Motion and with Taylor Vortices. *Proc. Roy. Soc.* A **261**, No. 1305, 214 (1961).
R. LEMLICH and C.-K. HWU, The Effect of Acoustic Vibration on Forced Convective Heat Transfer. *J. Amer. Inst. Chem. Engrs*, **7**, No. 1, 102 (1961).
L. M. MACK, The Compressible Viscous Heat-Conducting Vortex. *J. Fluid Mech.* **8**, No. 2, 284 (1960).
S. D. NIGAM and S. N. SINGH, Heat Transfer by Laminar Flow Between Parallel Plates Under the Action of Transverse Magnetic Field. *Quart. J. Mech. Appl. Math.* **13**, No. 1, 85 (1960).
S. PAHOR and J. STRNAD, Heat Transfer from Laminar Flow Through Cylindrical Tubes. *Z. Angew. Math. Phys.* **12**, No. 1, 80 (1961).
S. PAHOR and J. STRNAD, A Note on Heat Transfer in Laminar Flow Through a Gap. *Appl. Sci. Res.* A **10**, No. 1, 81 (1961).
A. REYNOLDS, On the Dynamics of Turbulent Vortical Flow. *Z. Angew. Math. Phys.* **12**, No. 2, 149 (1961).
E. M. ROSEN and T. J. HANRATTY, Use of Boundary-Layer Theory to Predict the Effect of Heat Transfer on the Laminar-Flow Field in a Vertical Tube with a Constant-Temperature Wall. *J. Amer. Inst. Chem. Engrs*, **7**, No. 1, 112 (1961).
H. SENFTLEBEN and P. SCHNABEL, Heat Transfer Between Concentrical Cylinders in Liquids and Gases. *Z. Angew. Phys.* **11**, No. 11, 428 (1959). (In German).
D. G. THOMAS, Heat and Momentum Transport Characteristics of Non-Newtonian Aqueous Thorium Oxide

Suspensions. *J. Amer. Inst. Chem. Engrs*, **6**, No. 4, 631 (1960).

W. G. VINCENTI, Calculations of the One-Dimensional Nonequilibrium Flow of Air Through a Hypersonic Nozzle—Interim Report. *Arnold Engng Development Center, Air Force Systems Command, USAF, AEDC-TN*-61-65 (1961).

CONDUCTION

E. I. ANDRIANKIN, Propagation of Thermal Waves from the Boundary of Two Media. *Appl. Math. Mech.* **23**, No. 5, 1420 (1959).

A. E. BERGLES and J. KAYE, Solutions to the Heat-Conduction Equation with Time-Dependent Boundary Conditions. *J. Aero. Space Sci.* **28**, No. 3, 251 (1961).

S.-Y. CHEN, One-Dimensional Heat Conduction with Arbitrary Heating Rate. *J. Aero. Space Sci.* **28**, No. 4, 336 (1961).

J. R. DAVIDSON and J. F. DALBY, Optimum Design of Insulated Compression Plates Subjected to Aerodynamic Heating. *NASA TN* D-520 (1961).

E. DEEG and I. HERTWECK-CRONE, Computation of Non-Stationary Temperature Distribution in Layered Media, with the Help of Electric Analog Computers. *Z. Angew. Phys.* **12**, No. 4, 184 (1960). (In German).

H. R. ELROD, JR., Improved Lumped Parameter Method for Transient Heat Conduction Calculations. *J. Heat Transfer*, C **82**, No. 3, 181 (1960).

R. E. GIBSON, A Linear Heat Problem with a Moving Interface. *Z. Angew. Math. Phys.* **11**, No. 3, 198 (1960).

W. J. GRAFF, Thermal Conductance Across Metal Joints. *Mach. Design*, **32**, No. 19, 166 (1960).

R. S. HARRIS, JR. and J. R. DAVIDSON, An Analysis of Exact and Approximate Equations for the Temperature Distribution in an Insulated Thick Skin Subjected to Aerodynamic Heating. *NASA TN* D-519 (1961).

D. W. JORDAN, Method for Calculating Boundary Value Problems in Heat Conduction for the Cylindrical Cavity and the Half Space, by Means of Convolution Integrals. *Brit. J. Appl. Phys.* **12**, No. 1, 14 (1961).

P. K. KONAKOV, On the Regularities of Composite Heat Transfer. *Int. J. Heat Mass Transfer*, **2**, Nos. 1/2, 136 (1961).

D. KUNII and J. M. SMITH, Heat Transfer Characteristics of Porous Rocks: II. Thermal Conductivities of Unconsolidated Particles with Flowing Fluids. *J. Amer Inst. Chem. Engrs*, **7**, No. 1, 29 (1961).

C. E. LUND and R. M. LANDER, Heat Transfer Through Mineral Wool in Combination with Reflective Surfaces. *ASHRAE Journal*, **3**, No. 3, 47 (1961).

R. E. NETTLETON, Density Fluctuations and Heat Conduction in a Pure Liquid. *Phys. Fluids*, **4**, No. 1, 74 (1961).

T. P. NEWCOMB, Flow of Heat in a Composite Solid. *Brit. J. Appl. Phys.* **10**, No. 5, 204 (1959).

G. F. C. ROGERS, Heat Transfer at the Interface of Dissimilar Metals. *Int. J. Heat Mass Transfer*, **2**, Nos. 1/2, 150 (1961).

A. I. ROZLOVSKII, Refinement of the Solution to the Equation of Heat Conduction in a Flame. *Proc. Acad. Sci. USSR*, **136**, No. 5, 1150 (1961).

C. TIEN, Approximate Solutions of Conduction of Heat Through Non-Homogeneous Medium. *Canad. J. Chem. Engng*, **39**, No. 1, 42 (1961).

G. A. TIRSKII, Two Exact Solutions of Stefan's Nonlinear Problem. *Soviet Fiz. Dokl.* **4**, No. 2, 288 (1959).

T. TSANG, Transient State Heat Transfer and Diffusion Problems. *Industr. Engng Chem.* **52**, No. 8, 707 (1960).

R. M. ZAIDEL', O. S. RYZHOV and E. I. ANDRIANKIN, The Propagation of an Approximately Spherical Heat Front. *Soviet Fiz. Dokl.* **4**, No. 1, 65 (1959).

FLOW WITH SEPARATED REGIONS

J. J. BERNARD and R. SIESTRUNCK, Heat Transfer in Separated Flow. Advances in Aeronautical Sciences, Vol. 1 (*Proc. First International Congress in the Aeronautical Sciences, Madrid, Sept.* 8–13, 1958), Pergamon Press (1959). (In French).

M. H. BLOOM and S. RUBIN, High-Speed Viscous Corner Flow. *J. Aero. Space Sci.* **28**, No. 2, 145 (1961).

J. G. HALL and T. C. GOLIAN, Heat Transfer to Sharp and Blunt Yawed Plates in Hypersonic Airflow. *J. Aero. Space Sci.* **28**, No. 4, 345 (1961).

J. C. Y. KOH and J. P. HARTNETT, Measured Pressure Distribution and Local Heat Transfer Rates for Flow Over Concave Hemispheres. *J. Amer. Rocket Soc.* **31**, No. 1, 71 (1961).

N. C. LAMBOURNE and D. W. BRYER, Some Measurements in the Vortex Flow Generated by a Sharp Leading Edge Having 65 Degree Sweep. *Aero. Res. Coun. Lond., Curr. Pap.* 477 (1960).

I. S. PASTERNAK and W. H. GAUVIN, Turbulent Heat and Mass Transfer from Stationary Particles. *Canad. J. Chem. Engng*, **38**, No. 2, 35 (1960).

LOW-DENSITY HEAT TRANSFER

S. ABARBANEL, Radiative Heat Transfer in Free-Molecule Flow. *J. Aero. Space Sci.* **28**, No. 4, 299 (1961).

J. P. HARTNETT, A Survey of Thermal Accommodation Coefficients. *The RAND Corporation, Santa Monica, Calif., U.S. Air Force Project Rand, Res. Memo. RM-2585* (1960).

YU. N. LUNKIN, Boundary-Layer Equations and Their Boundary Conditions in the Case of Motion at Supersonic Velocities in a Moderately Rarefied Gas. *NASA TT* F-28 (1960).

H. T. NAGAMATSU and T. Y. LI, Hypersonic Flow Near the Leading Edge of a Flat Plate. *Phys. Fluids*, **3**, No. 1, 140 (1960).

D. N. VACHON, On the Erosion of Satellite Surfaces Due to Sputtering in the Free Molecular Flow Region. *Missile and Space Vehicle Dept., Space Sciences Laboratory, General Electric Co., Technical Information Series* R61SD041 (1961).

G. WHITNAH, J. UPTON, R. GRIFFITH, G. MORFITT, G. JORGENSON and D. ROTENBERG, Research on the Effects of Collisions of Small Particles with Bodies Moving at Hypersonic Speeds: Part III, Erosion and Heat Transfer Effects. *Mechanical Division of General Mills, Inc., Research Dept., Minneapolis, Minn., WADC TR* 58-498, Part III (1960).

LIQUID METALS

A. A. ANDREEVSKII, Heat Transfer in Transverse Flow of Molten Sodium Around a Single Cylinder. *Soviet J. Atomic Energy*, **7**, No. 3, 745 (1961).

A. J. FRIEDLAND and C. F. BONILLA, Analytical Study of Heat Transfer Rates for Parallel Flow of Liquid Metals Through Tube Bundles, Part II. *J. Amer. Inst. Chem. Engrs*, **7**, No. 1, 107 (1961).

W. MIALKI, Heat Transmission Through Boiling Metal, Particularly Mercury. *Metall*, **15**, No. 1, 1 (1961).

Vol. 3 1961

MAGNETOHYDRODYNAMICS

A. Bauer, M. A. Cook and R. T. Keyes, Detonation-Generated Plasmas. *Proc. Roy. Soc.* A **259**, No. 1299, 508 (1961).

G. Bekefi and S. C. Brown, Microwave Measurements of the Radiation Temperature of Plasmas. *J. Appl. Phys.* **32**, No. 1, 25 (1961).

R. D. Cess, Magnetohydrodynamic Effects Upon Heat Transfer for Laminar Flow Across a Flat Plate. *J. Heat Transfer*, C **82**, No. 2, 87 (1960).

R. G. Deissler, A One-Dimensional Analysis of Magnetohydrodynamic Energy Conversion. *NASA TN* D-680 (1961).

D. G. Drake, Rayleigh's Problem in Magnetohydrodynamics for Non-Perfect Conductor. *Appl. Sci. Res.* **B8**, No. 5–6, 467 (1960).

R. R. John and W. L. Bade, Recent Advances in Electric Arc Plasma Generation Technology. *J. Amer. Rocket Soc.* **31**, No. 1, 4 (1961).

V. D. Kirillov, Radiation Energy Losses in a Plasma. *Soviet Fiz.-Tekh. Fiz.* **5**, No. 3, 295 (1960).

Y. Nakagawa and I. R. Goroff, Experiments on Heat Transport by Convection in Presence of a Magnetic Field. *Phys. Fluids*, **4**, No. 1, 349 (1961).

J. L. Neuringer, L. Kraus and H. Malamud, Electromagnetic Diffusion into a Cylindrical Plasma Column During the Early Stages of Pinch Formation. *Plasma Propulsion Laboratory, Republic Aviation Corp., Farmingdale, N.Y.*, AFOSR TN 320 (1961).

K. B. Pavlov, Nekotorye svoistva Statsionarnykh Techenii v Magnitnoi Gazodinamike. *Zh. Eksperimental'noi i Teoreticheskoi Fiz.* **39**, No. 2, 304 (1960).

G. Poots and L. Sowerby, Axially Symmetric Stagnation Point Flow with Heat Transfer in Magnetohydrodynamics. *Quart. J. Mech. Appl. Math.* **13**, Pt. 4, 385 (1960).

J. A. Shercliff, One-Dimensional Magnetogasdynamics in Oblique Fields. *J. Fluid Mech.* **9**, Pt. 4, 481 (1960).

R. P. Treat, Ionization in an Electrodeless Discharge. *Plasmadyne Corporation, Santa Ana, Calif.*, AFOSR 473 (1961).

P. K. Watson, Influence of an Electric Field Upon the Heat Transfer from a Hot Wire to an Insulating Liquid. *Nature, Lond.* **189**, No. 4764, 563 (1961).

H. Yoshihara, Plasma Flow Over a Thin Charged Conductor. *J. Aero. Space Sci.* **28**, No. 2, 141 (1961).

V. N. Zhigulev, Theory of the Magnetic Boundary Layer. *Soviet Fiz. Dokl.* **4**, No. 1, 57 (1959).

MEASUREMENT TECHNIQUES

B. Abeles, G. D. Cody and D. S. Beers, Apparatus for the Measurement of the Thermal Diffusivity of Solids at High Temperatures. *J. Appl. Phys.* **31**, No. 9, 1585 (1960).

T. T. Arai and J. R. Madigan, Response of a Thermocouple Circuit to Non-Steady Currents. *J. Appl. Phys.* **32**, No. 4, 609 (1961).

C. R. Barber and W. Blanke, A Platinum Resistance Thermometer for Use at High Temperatures. *J. Sci. Instrum.* **38**, No. 1, 17 (1961).

J. E. Bauerle, Analysis of "Immersed" Thermocouple Error. *Rev. Sci. Instrum.* **32**, No. 3, 313 (1961).

I. I. D'yakonov, Certain Problems in Measuring the Temperature of Rotating Objects. *Measurement Techniques* 1960, No. 1, 44 (1961).

L. M. Fingerson and P. L. Blackshear, Characteristics of Heat Flux Meter for Use in High Temperature Atmospheres. *University of Minnesota, Dept. of Mechanical Engng, Combustion Laboratory Tech. Rep.* 61–1 (1961).

L. M. Fingerson and P. L. Blackshear, Heat Flux Probe for Dynamic Measurements in High Temperature Gases. *University of Minnesota, Dept. of Mechanical Engng, Combustion Laboratory Tech. Rep.* 61-2 (1961).

G. E. Gadd, A Note on the Theory of the Stanton Tube. *Aero. Res. Coun. Lond., Rep. Mem.* 3147 (1960).

L. L. Gorelik and E. A. Lobikov, The Measure of Energy Lost in Plasma by Means of Bolometer Method. *Zh. Tekh. Fiz.* **31**, No. 1, 125 (1961).

A. P. Hatton, Thermal Conductivity and Diffusivity Measurements by an Unsteady-State Method with Application to Insulating Materials Containing Moisture and Ice. *J. Mech. Engng Sci., Lond.* **2**, No. 1, 45 (1960).

H. J. Hoge, Temperature Measurement Based on the Viscous Flow of Gas in a Wheatstone-Bridge Network. *Rev. Sci. Instrum.* **32**, No. 1, 1 (1961).

G. M. Levin and V. I. Vol'mir, Methods for Testing Thermal Inertia in Thermocouples and Resistance Thermometers. *Measurement Techniques* 1960, No. 4, 309 (1961).

M. R. Nadler and C. P. Kempter, Thermocouples for Use in Carbon Atmopsheres. *Rev. Sci. Instrum.* **32**, No. 1, 43 (1961).

R. G. Nagler, Application of Spectroscopic Temperature Measuring Methods to Definition of a Plasma Arc Flame. *Jet Propulsion Laboratory, California Institute of Technology, Pasadena, Calif., Tech. Rep.* 32–66 (1961).

J. R. Philip, The Theory of Heat Flux Meters. *J. Geophys. Res.* **66**, No. 2, 571 (1961).

J. Sagoschen, Temperature Measurement with Thermo-Elements of Platinum Metal. *Metall* **15**, No. 1, 34 (1961).

H. Schneider, Strahlungsmessgeräte. *Z. Ver. Dtsch. Ing.* **103**, No. 8, 360 (1961).

F. Schultz-Grunow and G. Wortberg, Interferometrisch messungen an einer ebenen laminaren Flamme. *Int. J. Heat Mass Transfer*, **2**, Nos. 1/2, 56 (1961).

C. M. Stover, Method of Making Small Pointed Thermocouples. *Rev. Sci. Instrum.* **32**, No. 3, 366 (1961).

D. A. van Meel and H. Vermij, A Method for Flow Visualization and Measurement of Velocity Vectors in Three-Dimensional Flow Patterns Water Models by Using Colour Photography. *Appl. Sci. Res.* A **10**, No. 2, 109 (1961).

R. E. Walker and S. E. Grenleski, Jr., Instrument for Measuring Total Incident Radiant Heat Transfer to a Jet Engine Surface. *J. Amer. Rocket Soc.* **31**, No. 1, 77 (1961).

R. W. Ziemer, Heat Transfer Gage for Use in Highly Ionized Gases. *J. Amer. Rocket Soc.* **31**, No. 1, 78 (1961).

NATURAL CONVECTION

W. H. Braun, S. Ostrach and J. E. Heighway, Free-Convection Similarity Flows About Two-Dimensional and Axisymmetric Bodies with Closed Lower Ends. *Int. J. Heat Mass Transfer*, **2**, No. 1/2, 121 (1961).

E. R. G. Eckert and W. O. Carlson, Natural Convection in an Air Layer Enclosed Between Two Vertical Plates with Different Temperatures. *Int. J. Heat Mass Transfer*, **2**, Nos. 1/2, 106 (1961).

T. W. Jackson, J. M. Spurlock and K. R. Purdy, Combined Free and Forced Convection in a Constant

Temperature Horizontal Tube. *J. Amer. Inst. Chem. Engrs*, **7**, No. 1, 38 (1961).
T. R. MUNSON and R. J. SPINDLER, Transient Thermal Behavior of Decomposing Materials: Part 1, General Theory and Application to Convective Heating. *Research and Development Division, AVCO Corporation, Wilmington, Mass., Tech. Rep.* RAD-TR-61-10 (1961).
A. K. RAO, Unsteady Natural Convection from a Vertical Flat Plate with Suction. *Appl. Sci. Res.* A **10**, No. 2, 141 (1961).
W. R. WILCOX, Simultaneous Heat and Mass Transfer in Free Convection. *Chem. Engng Sci.* **13**, No. 3, 113 (1961).

PROPERTIES

F. H. BROCK, Estimation of Specific Heats at Normal Temperatures. *J. Amer. Rocket Soc.* **31**, No. 2, 265 (1961).
P. CARRUTHERS, Theory of Thermal Conductivity of Solids at Low Temperatures. *Rev. Mod. Phys.* **33**, No. 1, 92 (1961).
W. D. ERICKSON, Real-Gas Correction Factors for Hypersonic Flow Parameters in Helium. *NASA TN* D-462 (1960).
P. HAMMERLING, J. D. TEARE and B. KIVEL, Nonequilibrium Electrical and Radiative Properties of High Temperature Air, Nitrogen and Oxygen. *Proc. Fourth International Conference on Ionization Phenomena in Gases* (*Uppsala, August* 17–21, 1959), p. 1092, North-Holland Publishing Company, Amsterdam (1960).
C. F. HANSEN and M. E. HODGE, Constant Entropy Properties for an Approximate Model of Equilibrium Air. *NASA TN* D-352 (1961).
R. A. HARTUNIAN and P. V. MARRONE, Viscosity of Dissociated Gases from Shock-Tube Heat-Transfer Measurements. *Phys. Fluids*, **4**, No. 5, 535 (1961).
YU. A. KIRICHENKO, Measurements of Temperature Conductivity by the Method of Radial Temperature Waves in a Cylinder. *Measurement Techniques* 1960, No. 5, 406 (1961).
J. R. MCCARTHY and H. WOLF, The Heat Transfer Characteristics of Gaseous Hydrogen and Helium. *Rocketdyne, Canoga Park, Calif., Res. Rep.* RR-60-12 (1960).
E. J. OWENS and G. THODOS, Thermal Conductivity: Reduced State Correlation for Ethylene and Its Application to Gaseous Aliphatic Hydrocarbons and Their Derivatives at Moderate Pressures. *J. Amer. Inst. Chem. Engrs*, **6**, No. 4, 676 (1960).
T.-C. PENG and W. F. AHTYE, Experimental and Theoretical Study of Heat Conduction for Air up to 5000°K. *NASA TN* D-687 (1961).
R. A. SAENGER and G. E. HUDSON, Periodic Shock Waves in Resonating Gas Columns. *J. Acoust. Soc. Amer.* **32**, No. 8, 961 (1960).
C. SAGAN, The Planet Venus. *Science*, **133**, No. 3456, 849 (1961).
TH. E. SCHMIDT, Über die Wärmeleitzahl von Isolierstoffen. *Forsch. IngWes.* **27**, No. 1, 10 (1961).
M. E. STEPHENSON, JR. and M. MARK, Thermal Conductivity of Porous Materials. *ASHRAE Journal*, **3**, No. 2, 75 (1961).
T. S. STORVICK and J. M. SMITH, Application of the Principle of Corresponding States for Polar Substances. *J. Chem. Engng Data*, **6**, No. 1, 28 (1961).
H. TAUTZ, Determination of Thermal Conductivity of Vulcanized Rubbers in Relationship to Elongation. *Exp. Technik Phys.* **7**, No. 1, 1 (1959). (In German).
N. B. VARGAFTIK and A. A. TARZIMANOV, Experimental Investigation of the Thermal Conductivity of Water-Vapour with High Parameters. *Teploenergetika*, **6**, No. 9, 15 (1959).

RADIATION

S. S. ABARBANEL, Time Dependent Temperature Distribution in Radiant Solids. *J. Math. Phys.* **34**, No. 4, 246 (1960).
S. M. BERMAN, Impurity Radiant Energy Loss. *Physical Research Laboratory, Space Technology Laboratories, Los Angeles, Calif.*, STL/TR-60-0000-GR435 (1960).
J. C. BOEHRINGER and R. J. SPINDLER, Radiant Heating of Semi-Transparent Materials. *Research and Advanded Development Division, AVCO Corporation, Wilmington, Mass., Tech. Rep.* RAD-TR-61-8 (1961).
R. GOULARD, A Comment on "Radiation From Hot Air and Its Effect on Stagnation-Point Heating". *J. Aero. Space Sci.* **28**, No. 2, 158 (1961).
I. GRANET and W. MCILROY, Optimum Radiant Straight Fin with Exponential Sides. *J. Amer. Rocket Soc.* **31**, No. 1, 80 (1961).
P. HAMMERLING, Ionization Effects of Precursor Radiation From Shocks in Air. *AVCO Everett Research Laboratory, Everett, Mass., Res. Rep.* 98 (1960).
P. L. HARTMAN and R. C. MERRILL, Reflectivity of Silver Chloride in the Ultraviolet. *J. Opt. Soc. Amer.* **51**, No. 2, 168 (1961).
T. S. HOLDEN, Ways to Calculate Incident Low Temperature Radiation. *ASHRAE Journal*, **3**, No. 4, 51 (1961).
L. P. KADANOFF, Radiative Transport Within an Albating Body. *AVCO Everett Research Laboratory, Everett, Mass., Res. Rep.* 61 (1959).
J. C. KECK, J. C. CAMM, B. KIVEL and T. WENTINK, JR., Radiation from Hot Air: Part II. Shock Tube Study of Absolute Intensities. *Ann. Phys.* **7**, No. 1, 1 (1959).
H. KENNET and S. L. STRACK, Stagnation Point Radiative Transfer. *J. Amer. Rocket Soc.* **31**, No. 3, 370 (1961).
B. KIVEL, Radiation From Hot Air and Its Effect on Stagnation-Point Heating. *J. Aero. Space Sci.* **28**, No. 2, 96 (1961).
C.-Y. LIU, On Optimum Rectangular Cooling Fins. *Quart. Appl. Math.* **19**, No. 1, 72 (1961).
H. T. MANTIS, Observation of Infrared Cooling of a Tropical Air Mass. *J. Geophys. Res.* **66**, No. 2, 465 (1961).
A. D. MOORE, An Electrical Essay—The Radiant Heat Pump. *Elect. Engng*, **80**, No. 2, 118 (1961).
D. G. MURCRAY, F. H. MURCRAY, W. J. WILLIAMS and F. E. LESLIE, Study of 1·4μ and 6·3μ Water Vapor Bands at High Altitudes. *J. Opt. Soc. Amer.* **51**, No. 2, 186 (1961).
L. D. NICHOLS, Effect of Shield Position and Absorptivity on Temperature Distribution of a Body Shielded from Solar Radiation in Space. *NASA TN* D-578 (1961).
U. P. OPPENHEIM, Experimental Verification of Theoretical Relations Between Total Gas Absorptivities and Total Gas Emissivities for CO. *J. Appl. Phys.* **30**, No. 6, 803 (1959).
E. W. PARKES, Influence Coefficients for Radiation in a Circular Cylinder. *Int. J. Heat Mass Transfer*, **2**, Nos. 1/2, 155 (1961).
P. M. REYNOLDS, Spectral Emissivity of 99·7% Aluminum Between 200 and 540°C. *Brit. J. Appl. Phys.* **12**, No. 3, 111 (1961).

Vol. 3 1961

W. H. ROBBINS, An Analysis of Thermal Radiation Heat Transfer in a Nuclear-Rocket Nozzle. *NASA TN* D-586 (1961).

C. SAGAN, The Radiation Balance of Venus. *Jet Propulsion Laboratory, California Institute of Technology, Pasadena, Calif., JPL TR* 32–34 (1960).

V. V. SOBOLEV, Diffusion of the Radiation in a Medium Whose Boundary Reflects the Rays as a Mirror. *Proc. Acad. Sci. USSR*, **136**, No. 3, 571 (1961).

R. H. TOURIN, Measurements of Infrared Spectral Emissivities of Hot Carbon Dioxide in the 4·3μ Region. *J. Opt. Soc. Amer.* **51**, No. 2, 175 (1961).

R. C. WEATHERSTON and W. E. SMITH, A New Type of Thermal Radiator for Space Vehicles. *Aero. Space Engng*, **20**, No. 1, 16 (1961).

C. S. WILLIAMS, Discussion of the Theories of Cavity-Type Sources of Radiant Energy. *J. Opt. Soc. Amer.* **51**, No. 5, 564 (1961).

ROTATING SURFACES

E. A. KEARSLEY, Bounds on the Dissipation of Energy in Steady Flow of a Viscous Incompressible Fluid Around a Body Rotating within a Finite Region. *Arch. Rational Mech. Anal.* **5**, No. 4, 347 (1960).

C. L. TIEN, Heat Transfer by Laminar Flow From a Rotating Cone. *J. Heat Transfer*, C **82**, No. 3, 252 (1960).

M. VINOKUR, Kinematic Formulation of Rotational Gas Flow. *J. Fluid Mech.* **9**, No. 4, 533 (1960).

TRANSFER MECHANISMS

J. M. BIDWELL, Use of the Roughness Criterion to Refute Roughness as the Cause of Reported Transition Reversal. *J. Aero. Space Sci.* **27**, No. 8, 622 (1960).

R. G. DEISSLER, Analysis of Multipoint-Multitime Correlations and Diffusion in Decaying Homogeneous Turbulence. *NASA TR* R-96 (1961).

C. A. EDWARDS and D. M. HIMMELBLAU, Mass Transfer between Liquid Phases. *Industr. Engng Chem.* **53**, No. 3, 229 (1961).

F. H. GARNER and J. M. HOFFMAN, The Transition from Free to Forced Convection in Mass Transfer from Solid Spheres. *J. Amer. Inst. Chem. Engrs*, **6**, No. 4, 579 (1960).

L. LEES and C.-Y. LIU, Kinetic Theory Description of Plane, Compressible Couette Flow. *Guggenheim Aeronautical Laboratory, California Institute of Technology, Hypersonic Research Project, Mem.* 58 (1960).

D. E. ROSNER, Diffusion and Chemical Surface Catalysis in Flow Systems. *Aero Chem Research Laboratories, Inc., Princeton, N.J., Tech. Pub.* 14, AFOSR TN-60-887 (1960).

J. R. STERRETT and J. C. EMERY, Extension of Boundary-Layer-Separation Criteria to a Mach Number of 6·5 by Utilizing Flat Plates with Forward-Facing Steps. *NASA TN* D-618 (1960).

E. R. VAN DRIEST and C. B. BLUMER, Effect of Roughness on Transition in Supersonic Flow. *North American Aviation, Inc., Aero-Space Laboratory, MD* 60-329, AFOSR TN 60-1164 (1960).

L. M. VAUGHAN, The Prediction of Atmospheric Diffusion by Using an Eddy Diffusivity Based on the Vertical Transfer of Heat. *J. Meteorol.* **18**, No. 1, 43 (1961).

R. J. WISNIEWSKI and J. R. JACK, Recent Studies on the Effect of Cooling on Boundary-Layer Transition at Mach 4. *J. Aero. Space Sci.* **28**, No. 3, 250 (1961).

TRANSPIRATION AND MASS TRANSFER COOLING

S. BLECHER and G. W. SUTTON, Comparison of Some Approximate Methods for Calculating Re-entry Ablation of a Subliming Material. *J. Amer. Rocket Soc.* **31**, No. 3, 433 (1961).

M. R. DENISON, Estimating Transient Temperature Distributions During Ablation. *J. Amer. Rocket Soc.* **30**, No. 6, 562 (1960).

S. EVNOCHIDES and G. THODOS, Simultaneous Mass and Heat Transfer in the Flow of Gases Past Single Spheres. *J. Amer. Inst. Chem. Engrs*, **7**, No. 1, 78 (1961).

H. GLASER, Experimentelle Untersuchungen auf dem Gebiet der Wärme- und Stoffübertragung. *Chem.-Ing.-Tech.* **33**, No. 3, 146 (1961).

V. KOLAR, Heat and Mass Transfer in a Turbulent Medium. *Coll. Trav. Chim. Tchécosh.* **26**, No. 2, 335 (1961).

T. KUBOTA, Ablation with Ice Model at M = 5·8. *J. Amer. Rocket Soc.* **30**, No. 12, 1164 (1960).

E. LEGRIVES and P. SARRAT, Untersuchung der Mischungs- und Verbrennungsvorgänge zwischen konzentrischen Strömungen. *Z. Flugw.* **9**, No. 2, 46 (1961).

P. A. LIBBY and R. J. CRESCI, Experimental Investigation of the Downstream Influence of Stagnation-Point Mass Transfer. *J. Aero. Space Sci.* **28**, No. 1, 51 (1961).

J. P. MORAN, Application of Covert's Approximations for the Binary Boundary-Layer to a Porous Cone with a Solid Tip. *Massachusetts Institute of Technology, Naval Supersonic Laboratory, Tech. Rep.* 442, AFOSR TN 60-834 (1960).

A. PALLONE, Non-Similar Solutions of the Compressible Laminar Boundary Layer Equations, with Applications to the Upstream Transpiration Cooling Problem. *AVCO Corporation, Research and Advanced Development Division, Wilmington, Mass., RAD-TR-9-60-8* (1960).

L. ROBERTS, Mass Transfer Cooling Near the Stagnation Point. *NASA TR* R-8 (1959).

L. ROBERTS, Stagnation-Point Shielding by Melting and Vaporization. *NASA TR* R-10 (1959).

L. ROBERTS, A Theoretical Study of Stagnation-Point Ablation. *NASA TR* R-9 (1959).

C. J. SCOTT, Experimental Investigations of Laminar Heat Transfer and Transition with Foreign Gas Injection—A 16° Porous Cone at M = 5. *University of Minnesota, Rosemount Aeronautical Laboratories, UMRAL Res. Rep.* 174, AFOSR TN-60-1370 (1960).

D. L. TURCOTT, The Melting of Ice in a Hot Humid Stream of Air. *J. Fluid Mech.* **8** No. 1, 123 (1960).

Int. J. Heat Mass Transfer. Vol. 3, p. 358. Pergamon Press 1961, Printed in Great Britain.

HEAT TRANSFER BIBLIOGRAPHY

TAKASHI SATŌ

Department of Mechanical Engineering, Kyoto University, Kyoto, Japan

CHANGE OF PHASE

TERUKATSU MIYAUCHI and SAKAE YAGI, Nucleate boiling heat-transfer on horizontal flat surface. *Chem. Engng Japan*, **25**, No. 1, 18 (1961).

KEISHIRO NIU, Flow of condensing vapour with temporary supersaturated state due to heat-removal effect. *J. Phys. Soc. Japan*, **16**, No. 4, 798 (1961).

TAKASHI SATŌ, ITARU MICHIYOSHI, KIICHIRO TAKEUCHI and KEIGO KONDŌ, Experimental studies of the burn-out under the boiling (1st Report, Transient phenomena to meltdown). *Trans. Japan Soc. Mech. Engrs*, **27**, No. 177, 722 (1961).

RYOZO TOEI, Drying rate in the surface evaporation period—Consideration on the Ackermann effect. *Chem. Engng Japan*, **25**, No. 1, 65 (1961).

KINICHI TORIKAI, MASAO HORI and YOSHIHIRO ŌUCHI, The surface boiling burnout in a channel. *J. Atomic Energy Soc. Japan*, **3**, No. 5, 333 (1961).

CONDUCTION

WEN-JEI YANG, Temperature distributions in plate-fin type heat exchangers. *Trans. Japan Soc. Mech. Engrs*, **27**, No. 177, 730 (1961).

LOW DENSITY HEAT TRANSFER

T. TSUBOUCHI and S. SATŌ, Heat transfer between single particles and fluids in relative forced convection. *Rep. Inst. Speed Mech., Sendai* (Tohoku Univ.), **12**, 227 (1960/1961).

MEASUREMENT TECHNIQUES

YUKIHIKO TAKENAKA, Study on radiation pyrometer. *J. Japan Soc. Aero. Space Sci.* **9**, No. 86, 71 (1961).

NATURAL CONVECTION

T. TSUBOUCHI and S. SATŌ, Heat transfer from fine wires and particles by natural convection. *Rep. Inst. Speed Mech. Sendai* (Tokoku Univ.), **12**, 127 (1960/1961).

RADIATION

TAKASHI SATŌ, RYŪICHI MATSUMOTO, KAZUSHIGE UEDA and KEIZO ŌHIRA, Radiant heat transfer from luminous flame (1st Report, Theoretical and experimental studies on the uniform-temperature and particle contents). *Trans. Japan Soc. Mech. Engrs*, **27**, No. 177, 713 (1961).

YASUO YAMASAKI, Calculation of gas radiation from a rectangular parallelepiped gas mass surrounded by transparent gas (3rd Report, Method of calculating heat absorption in boiler furnaces by making use of the area ratio of flame to furnace). *Trans. Japan Soc. Mech. Engrs*, **27**, No. 174, 190 (1961).

TRANSFER MECHANISMS

TSUTAO ŌTAKE and SETSUJI TONE, Mechanism of heat transfer in solid particle beds. *Chem. Engng Japan*, **25**, No. 1, 56 (1961).

TRANSPIRATION AND MASS TRANSFER

TOKURO MIZUSHINA and RYUHŌ ITŌ, Analysis of the unsteady state in the thermal diffusion cell. *Chem. Engng Japan*, **25**, No. 1, 34 (1961).

TADASHI SHIROTSUKA, AKIRA HIRATA, TSUYOSHI MASHIMO and AKIRA MORI, Mass transfer in high velocity compressible fluid. *Chem. Engng Japan*, **25**, No. 1, 50 (1961).

SATIO SUGIYAMA, KATSUMI NAGASAKA, HIDEO HUKUHARA and TAKAO MIYAZAKI, Thermal decomposition of solid. *Chem. Engng Japan*, **25**, No. 4, 265 (1961).

Vol. 3 1961

Int. J. Heat Mass Transfer. Vol. 3, pp. 359–369. Pergamon Press 1961. Printed in Great Britain.

PIONEER PAPERS IN CONVECTIVE MASS TRANSFER

2. WILHELM NUSSELT: Die Verbrennung und die Vergasung der Kohle auf dem Rost, *Z. Ver. Dtsch. Ing.* **60**, 102 (1916). Reprinted by permission of VDI-VERLAG GmbH.

Editor's Foreword

Although the connexion between mass transfer (diffusion) and heat transfer was mentioned by Reynolds in his paper "On the extent and action of the heating surface of steam boilers", forty years passed before the connexion was exploited. In the paper here reprinted, Nusselt introduced two important ideas: the first is that the burning of a carbon surface in a gas stream is controlled by the rate of mass transfer of oxygen to the surface; the second is that this transfer rate can be calculated from the formula which correlates heat transfer data in geometrically similar passages.

The first idea proved to be a highly fruitful contribution to the theory of the combustion of solid fuels. It is however the second which justifies the inclusion of the paper in the present series; for the calculations contained in the paper appear to be the first quantitative exploitation of the analogy between heat and mass transfer. The passages in the text in which the two ideas are explicitly stated are distinguished, for the convenience of readers, by italic printing.

D.B.S.

DIE VERBRENNUNG UND DIE VERGASUNG DER KOHLE AUF DEM ROST*

WILHELM NUSSELT

IM GEGENSATZ zu der hohen technischen Vervollkommnung, welche die Verbrennung und die Vergasung der Kohle in den letzten Jahrzehnten erfahren haben, ist die Theorie dieser Vorgänge in dieser Zeit wenig gefördert worden. Bei der Schwierigkeit der experimentellen Forschung ist auch die vorhandene Zahl guter Versuche sehr gering. Als notwendige Vorarbeit für weitere planmäßige Versuche scheint es mir zunächst erwünscht, eine klare Vorstellung von den im Kohlenbett sich abspielenden physikalischen und chemischen Vorgängen zu besitzen. Diesem Zweck soll die folgende Abhandlung dienen.

Ein ebener Rost möge dauernd und gleichmäßig bis zu einer bestimmten Höhe H, Abb 1, etwa durch eine selbsttätige Wurffeuerung beschickt werden. Die Zusammensetzung der Gase in verschiedenen Abständen von den Roststäben, die dort herrschenden Temperaturen und die in der Zeiteinheit verbrennenden Kohlenmengen sollen bestimmt, und es soll weiter angegeben werden, wie sich diese Größen mit der Menge der zugeführten Frischluft ändern. Diese Luftmenge soll gleichmäßig verteilt unter den Rost eintreten. Dann werden obige Größen nur vom Abstand x über dem Rost abhängen. Die Frischluft habe die normale Zusammensetzung 0,21 Raumteile Sauerstoff und 0,79 Raumteile Stickstoff. Über dem Rost setzt sofort die Verbrennung nach der statischen Verbrennungsgleichung

$$C + O_2 = CO_2 + h_1 \text{ WE}$$

ein; d. h. ein Mol† Kohlenstoff und ein Mol Sauerstoff liefern ein Mol Kohlensäure und h_1 WE. Dieser Heizwert h_1 ist nach der Kirchhoffschen Formel von der Temperatur abhangig, bei der die Verbrennung stattfindet. Bei 15° ist $h_1 = 97\,650$ WE.

* Sonderabdrücke dieses Aufsatzes (Fachgebiet: Dampfkessel) werden an Mitglieder des Vereines sowie Studierende und Schüler technischer Lehranstalten gegen Voreinsendung von 35 Pf. postfrei abgegeben. Andre Bezieher zahlen den doppelten Preis. Zuschlag für Auslandporto 5 Pf. Leiferung etwa 2 Wochen nach dem Erscheinen der Nummer.

† Ein Mol ist die Menge eines Stoffes in kg, die seinem Molekulargewicht gleich ist. Ist also μ das Molekulargewicht, so sind μ kg 1 Mol eines Stoffes. Es sind also 2 kg Wasserstoff 1 Mol Wasserstoff, 32 kg Sauerstoff 1 Mol Sauerstoff usw.

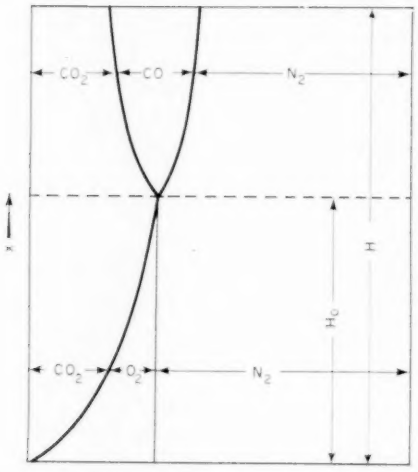

ABB. 1. Änderung der Gaszusammensetzung mit dem Abstand vom Rost.

Aus jener Formel folgt weiter, daß aus einem Raumteil Sauerstoff der gleiche Raumteil Kohlensäure entsteht. Es findet also durch die Verbrennung keine Kontraktion statt. Verfolgt man zunächst die mittlere Gaszusammensetzung über dem Rost, so erkennt man, daß das Gas aus Kohlensäure, Sauerstoff und Stickstoff bestehen wird. Solange noch Sauerstoff vorhanden ist, kann sich kein Kohlenoxyd bilden, aus Gründen, die nachher erörtert werden. Mit zunehmender Höhe nimmt der Sauerstoffgehalt ab, und in einer bestimmten Höhe H_0 über dem Rost ist aller Sauerstoff verbrannt. Daß man am Dampfkessel bei geringem Luftüberschuß neben Sauerstoff Kohlenoxyd in den Abgasen feststellen kann, liegt daran, daß infolge ungleicher Beschickung die Schütthöhe H an manchen Stellen größer und an andern kleiner als die Höhe H_0 ist, in der eben aller Sauerstoff verbraucht ist. An ersteren Stellen besteht das die Kohlenschicht verlassende Gas aus CO, CO_2 und N_2, an letzteren aus CO_2, O_2 und N_2. Durch Mischung in den Zügen, in denen infolge der durch die Wärmeabgabe an die Heizfläche veranlaßten Temperatursenkung keine Verbrennung mehr stattfindet, entsteht das beobachtete Gemisch von CO_2, CO, O_2 und N_2.

Nimmt man der Einfachheit halber an, daß reiner Kohlenstoff verbrannt wird, so besteht in dieser Zone das Gas aus 0,21 vH Raumteilen Kohlensäure und 0,79 vH Raumteilen Stickstoff. In Höhen größer als H_0 verbrennt die Kohle zu Kohlenoxyd unter Zerlegung der vorher gebildeten Kohlensäure nach der Reaktionsgleichung

$$C + CO_2 = 2\,CO - h_2\ \text{WE}.$$

Es ist bemerkenswert, daß jetzt die Verbrennung nicht mehr unter Wärmeentwicklung, sondern mit Wärmeverbrauch stattfindet. Bei 15° ist

$$h_2 = 38\,250\ \text{WE}.$$

Da aus einem Mol Kohlensäure zwei Mole Kohlenoxyd entstehen, wird das Volumen der Verbrennungsgase an das halbe Volumen des gebildeten Kohlenoxydes vergrößert. Sie bestehen jetzt aus Kohlensäure, Kohlenoxyd und Stickstoff. Die Raumteile von Kohlensäure und Stickstoff nehmen mit zunehmendem x ab und der Raumteil vom Kohlenoxyd nimmt zu. Damit ist qualitativ die Art und Veränderlichkeit der Gaszusammensetzung in der Kohle gegeben. Es ist dabei zu beachten, daß es sich hier immer um die Änderung der mittleren Gaszusammensetzung in einer Ebene parallel zum Rost handelte. Die Verbrennung soll nun genauer verfolgt werden, insbesondere soll jetzt die Veränderung der Gaszusammensetzung in den Räumen zwischen den Kohlenstücken untersucht werden.

Zur Vereinfachung der Betrachtung werde angenommen, daß die verbrennende Kohle nicht aus einzelnen Körnern, sondern aus ebenen Platten gebildet sei, die parallel zu einander und senkrecht auf den Rost gestellt seien, Abb. 2. Es soll jetzt die Veränderung der Gaszusammensetzung im Luftspalt längs der Strecke AB im Abstand x vom Rost an gegeben werden. Infolge der hohen Affinität des Sauerstoffes zur Kohle wird bei A und bei B, also an der Oberfläche der Kohle, wenn eine gewisse Mindesttemperatur überschritten ist, aller dort vorhandene Sauerstoff verbrannt sein, so daß dort die Sauerstoffkonzentration null und die Kohlensäurekonzentration demnach 0,21 ist. Die weitere Verbrennung an den Stellen A und B hängt dann von der Menge Sauerstoff ab, die an die Oberfläche der Kohle gelangt. Sobald ein

Vol. 3 1961

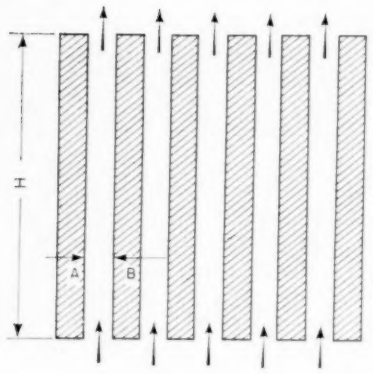

ABB. 2. Ideelles Kohlenbett.

Sauerstoffmolekül auf die Kohlenwand trifft, wird es sofort zu Kohlensäure verbrannt; deshalb ist die Sauerstoffkonzentration bei *A* und B dauernd null. Das Vordringen von Sauerstoff aus dem sauerstoffreichen Kern des Gasstromes nach der Wand erfolgt nun nach den Gesetzen der Diffusion. Es diffundiert Sauerstoff aus dem Innern des Gases nach der Wand und Kohlensäure von der Wand nach dem Innern. Die Gaszusammensetzung wird in ihrer Veränderlichkeit längs AB durch Abb. 3 veranschaulicht. *Die Menge der an der Kohlenfläche also bei A und B in der Zeiteinheit verbrannten Kohle ist demnach lediglich abhängig von der Diffusionsgeschwindigkeit, also von einer rein physikalischen Größe.* Die nach der Wand diffundierte Sauerstoffmenge kann nach den Grundgesetzen der Diffusion berechnet werden. Da mit 32 kg Sauerstoff 12 kg Kohlenstoff verbrennen, ist auch die an der Wand verbrannte Kohlenmenge bekannt. Nach dem Grundgesetz der Diffusion der Gase ist die in der Zeiteinheit durch ein Flächenelement df hindurchströmende Sauerstoffmenge proportional dem Abfall der Dichte des Sauerstoffes auf die Längeneinheit senkrecht zu jenem Flächenelement und proportional der Diffusionszahl k.

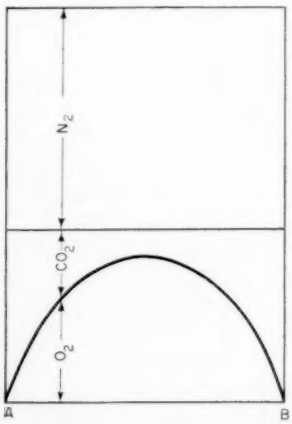

ABB. 3. Änderung der Gaszusammensetzung in einem Horizontalquerschnitt der Verbrennungszone.

Ist

df ein Flächenelement,
dz ein Zeitelement,
dG das in dieser Zeit durch jene Fläche diffundierende Sauerstoffgewicht,
γ die Dichte des Sauerstoffes in kg/cbm und
s die Koordinate auf der Flächennormaler,

besteht die Gleichung

$$\mathrm{d}G = k\,\mathrm{d}f\mathrm{d}z\,\frac{\mathrm{d}\gamma}{\mathrm{d}s}.$$

Die Dimension von k ist $\mathrm{m^2 st^{-1}}$.

Die Diffusionzahl k ist nur dann unabhängig vom Mischungsverhältnis, wenn zwei Gase ineinander diffundieren. Sind mehrere Gase vorhanden, so ist ein Einfluß des Mischungsverhältnisses vorhanden, der merklich ist, wenn die Dichten der diffundierenden Gase stark verschieden sind, wenn man also z. B. Wasserstoff in Luft diffundieren läßt. Bei der Verbrennung hält sich der Dichteunterschied der Gase in Grenzen, die die Diffusionszahl praktisch unveränderlich erscheinen lassen. Die Stickstoffkonzentration ist deshalb unveränderlich, und der Stickstoff beteiligt sich nicht an der Diffusion. Wenn man die Betrachtung ganz eingehend durchführt, ergibt sich, daß der Stickstoff nach der Seite der größeren Sauerstoffkonzentration, also nach dem Gaskern diffundiert.

In der obigen Grundgleichung der Diffusion sollen nun statt der Dichte γ die Volumhundertteile des Sauerstoffes eingeführt werden, und zwar sollen die chemischen Zeichen neben der Art des Gases auch dessen Raumteil in der Volumeneinheit des Gases angeben. Ist p_1 der

Teildruck des Sauerstoffes und p der Gesamtdruck, so ist der Raumteil des Sauerstoffes (numerische Konzentration oder Molenbruch)

$$O_2 = \frac{p_1}{p}.$$

Nach der Gasgleichung ist

$$\gamma = \frac{p_1 \mu}{RT},$$

wenn μ das Molekulargewicht,
R die Gaskonstante 848 und
T die absolute Temperatur bedeuten.

Das Grundgesetz der Diffusion geht dann über in

$$dG = k\, df\, dz\, \frac{\mu p\, dO_2}{848\, T ds}.$$

Ist V das Sauerstoffvolumen beim Zustande p und T, so ist

$$Vp = \frac{G}{\mu} 848\, T$$

und

$$dG = \frac{\mu p}{848\, T} dV.$$

Damit geht die Grundgleichung der Diffusion über in

$$dV = k\, df\, dz\, \frac{dO_2}{ds}.$$

Ist der Zustand mit der Zeit nicht veränderlich, so kann man über die Zeit integrieren und erhält das in der Zeiteinheit durch die Flächeneinheit diffundierende Gasvolumen

$$V = k \frac{dO_2}{ds},$$

d. h. der in der Stunde durch die Flächeneinheit diffundierende Gasraum (beim Gesamtdruck gemessen) ist dem Gefälle der numerischen Sauerstoffkonzentration proportional. Die Kohlensäure diffundiert in der andern Richtung. Da der Gesamtdruck gleichbleibend ist und auch die Stickstoffkonzentration sich praktisch nicht ändert, wird

$$-\frac{dCO_2}{ds} = \frac{dO_2}{ds}$$

und ebenso

$$dV = dV',$$

wenn dV' das in der gleichen Zeit diffundierende Kohlensäurevolumen ist

Daraus folgt, daß die Diffusionszahlen für Kohlensäure und Sauerstoff die gleichen sind.

Die Diffusionszahl k ist proportional dem Quadrate der absoluten Temperatur und umgekehrt proportional dem Gesamtdruck; ist sie beim Zustande p_0 und $T_0 = k_0$, so ist sie bei p und T

$$k = k_0 \frac{p_0}{p} \frac{T^2}{T_0^2};$$

daraus folgt

$$\frac{p}{T} = \frac{k_0\, T\, p_0}{k\, T_0^2}.$$

Durch die Verbrennung von 1 Mol Kohlenstoff (12 kg) werden 1 Mol Sauerstoff (32 kg O_2 oder 24,4 cbm bei 15° und 1 at) verbraucht. Es verbrennen deshalb in der Stunde auf 1 qm der Kohlenoberfläche

$$K = \frac{Vp}{T} \frac{288 \cdot 12}{10\,000 \cdot 24{,}4} = 0{,}01416 \frac{Vp}{T} \text{ kg}$$

Kohle oder nach Einführung obiger Werte für V und $\frac{p}{T}$:

$$K = 0{,}01416 \frac{k_0\, p_0 T}{T_0^2} \frac{dO_2}{ds} \text{ kg}.$$

In dieser Gleichung ist T die Temperatur der Kohlenoberfläche und $\frac{dO_2}{ds}$ das Gefälle der Konzentration des Sauerstoffes an ihr. Die stündlich verbrannte Kohle ist deshalb nur abhängig von der Temperatur und dem Sauerstoffgefälle. Sie ist beiden proportional. Die Temperatur ist ein geläufiger Begriff und auch leicht meßbar. Aber das Sauerstoffgefälle ist zunächst nur eine Rechnungsgröße.

Das Sauerstoffgefälle ist in erster Linie von der mechanischen Strömung, insbesondere von deren Wirbelung abhängig. *Es lassen sich nun glücklicherweise Vergleiche mit einem andern Naturvorgang, der genauer untersucht ist und*

Vol. 3 1961

den gleichen Grundgesetzen gehorcht, anstellen. Die Übertragung der Wärme von einer festen Wand an ein an ihr entlang strömendes Gas befolgt dieselben Gesetze wie die Diffusion in Gasen. Ist λ die Wärmeleitzahl des Gasstromes bei der Temperatur der Wand T und Θ die Temperatur des Gases, so ist die von dem Gas nach dem Flächenelement df der Wand strömende Wärme

$$Q = \lambda \, df \, dz \, \frac{d\Theta}{ds}.$$

Ersetzen wir darin Q durch V, λ durch k und Θ durch O_2, so geht sie in die Diffusionsgleichung über. Greifen wir im Gasstrom ein Raumelement heraus, so wird durch dessen Begrenzung Sauerstoff hinein- und herausdiffundieren. Außerdem wird aber auch durch die mechanische Strömung Sauerstoff in das Element ein- und austreten. Die über die ganze Oberfläche des Volumenelmentes addierte Sauerstoffströmung bedingt dann eine Änderung der Sauerstoffkonzentration des eingeschlossenen Gasvolumens. Diese Betrachtung liefert eine Differentialgleichung, die der Fourierschen Gleichung der Wärmeübertragung in strömenden Medien vollkommen entspricht. Dazu treten die Differentialgleichungen der Strömung, die Stetigkeitsgleichung und die Navier–Stockesschen dynamischen Gleichungen, die für beide Probleme identisch sind. Damit auch die Grenzbedingungen gleich werden, hat man die Temperatur Θ von der Wandtemperatur aus zu zählen. Beim Wärmeübergang ist die Temperatur an der Wand null, und bei der Verbrennung bezw. der Diffusion ist an der Wand die Sauerstoffkonzentration O_2 gleich null.

Man kann deshalb die Lösung dieses Diffusionsproblems aus der Lösung einer Aufgabe der Wärmeübertragung herleiten. Auf dem Gebiete des Wärmeüberganges sind für eine Reihe von Fällen die Lösungen durch Versuche bestimmt worden. Es erwies sich als zweckmäßig, aus den Versuchen die sogenannte Wärmeübergangszahl α zu berechnen. Das ist jene Wärmemenge, die in der Zeiteinheit durch die Flächeneinheit der Oberfläche ausgetauscht wird, wenn der Temperaturunterschied zwischen der Oberfläche und der mittleren Gastemperatur einen Grad beträgt. Demzufolge ist die in der Zeit z durch die Fläche F strömende Wärme

$$Q = \alpha F z u_m,$$

wenn u_m der mittlere Temperaturunterschied ist.

Eine der Wärmeübergangszahl α analoge Größe will ich für die Diffusion und die Verbrennung einführen, die ich die Verbrennungszahl nenne und mit β bezeichne. Sie gibt an, wieviel Raumeinheiten Sauerstoff in der Zeiteinheit für die Flächeneinheit zur Verbrennung gebraucht werden, wenn die mittlere Sauerstoffkonzentration im Querschnitt 1 ist. Dann wird das in z Stunden auf F qm entstehende Kohlensäurevolumen, das ja gleich dem verbrauchten Sauerstoffvolumen ist,

$$V = \beta F z {O_2}^m.$$

Diese Gleichung möge die dynamische Verbrennungsgleichung genannt werden. Sie sagt aus, daß das durch die Verbrennung entstehende Kohlensäurevolumen proportional der Zeit, der Kohlenoberfläche, der mittleren Sauerstoffkonzentration ${O_2}^m$ und der Verbrennungszahl β ist. Die Dimension von β ist mst^{-1}.

Ich will jetzt auf den Fall übergehen, den ich selbst für den Wärmeübergang durch Versuche und theoretisch untersucht habe. Das Gas soll durch ein Rohr strömen, das aus fester Kohle gebildet sei. Der Durchmesser sei d und die Länge des Rohres L. Durch künstliche Mittel möge es auf der stets gleichen Temperatur T gehalten werden. Die Änderung der Konzentration der durch das Rohr strömenden Verbrennungsgase sei gering.

Nun ist nach meinen Versuchen für ein Rohr die Wärmeübergangszahl

$$\alpha = \frac{18{,}86 \, \lambda^{0{,}214}}{d^{0{,}16} \, L^{0{,}054} \, (w\gamma c_p)^{0{,}786}} \, \frac{\text{WE}}{\text{st qm °C}}^{1}.$$

Um daraus die Diffusionszahl für ein Rohr zu erhalter, braucht man nur für λ k zu setzen, und da für die Wärmeübertragung für ein Volumenelement der Energiesatz

$$dQ = dx \, dy \, dz \, \lambda c_p \, d\Theta$$

1. *Z. Ver. Dtsch. Ing.* 1913 S. 199.

lautet und für die Diffusion, die dieser entsprechende Gleichung

$$dV = dx\,dy\,dz\,dO_2$$

gilt, ist $\gamma c_p = 1$ zu setzen.

Es wird also für ein Rohr die Verbrennungszahl

$$\beta = \frac{18{,}86\,k^{0{,}214}\,w^{0{,}786}}{d^{0{,}16}\,L^{0{,}054}}\ \text{m/st.}$$

w, die mittlere Geschwindigkeit, ist hier in msk^{-1}, L und d in m und k in qm/st einzusetzen.

Führt man noch die Diffusionszahl k_0 bei 0° und 1 at ein,

$$k = k_0\,\frac{T^2}{273^2}\,\frac{10\,000}{p},$$

worin p der Gasdruck in kg/qm ist, so geht die Gleichung über in

$$\beta = 12{,}27\,\frac{T^{0{,}428}\,w^{0{,}786}\,k_0^{0{,}214}}{d^{0{,}16}\,L^{0{,}054}\,p^{0{,}214}}.$$

Setzen wir diesen Wert in obige Gleichung ein, so ist in einem Rohr oder einer Gruppe von Kohlenrohren die in z Stunden auf F qm der Kohlenoberfläche verbrannte Kohle in kg

$$K = \frac{p}{T}\,\frac{141{,}6}{10\,000}\,\beta F z O_2$$

$$= 0{,}1736\,\frac{k_0^{0{,}214}\,p^{0{,}786}\,w^{0{,}786}\,F z O_2}{T^{0{,}472}\,d^{0{,}16}\,L^{0{,}054}}$$

Bei sonst gleichen Verhältnissen nimmt also das verbrannte Kohlengewicht mit der Luftgeschwindigkeit zu und ist proportional der Sauerstoffkonzentration. Führt man das durch das Rohr in der Stunde strömende Gasvolumen (bei 15° und 10 000 kg/qm gerechnet) W_0 ein, so wird, da

$$\frac{W_0\,T\,10\,000}{288p} = \frac{d^2\pi}{4}\,w\,3600,$$

$$\frac{wp}{T} = \frac{W_0\,10\,000 \cdot 4}{288\,d^2\pi\,3600}$$

$$= 0{,}01229\,\frac{W}{d^2}:$$

$$K = \frac{4{,}52}{10^5}\,\frac{k_0^{0{,}214}\,T^{0{,}214}\,W_0^{0{,}786}}{d^{1{,}732}\,L^{0{,}054}}\,F z O_2.$$

Um ein Beispiel zu geben, werde angenommen

p = 1 at = 10 000 kg/qm
w = 10 m/sk
F = 1 qm
z = 1 st
O_2 = 0,21
T = 1700°
d = 0,05 m
L = 1,0 m
k_0 = 0,064 qm/st.

Dann verbrennen auf 1 qm Kohlenoberfläche in der Stunde

$$K = 0{,}1736 \cdot \frac{0{,}064^{0{,}214} \cdot 10\,000^{0{,}786} \cdot 10^{0{,}786} \cdot 0{,}21}{1700^{0{,}472} \cdot 0{,}05^{0{,}16} \cdot 1^{0{,}054}}$$

$$= \frac{0{,}1736 \cdot 0{,}882 \cdot 1410 \cdot 6{,}13 \cdot 0{,}21}{31{,}8 \cdot 9{,}26 \cdot 1} = 9{,}45\ \text{kg/st.}$$

Setzt man die Dichte der Kohle gleich 1,25, so wird in der Stunde eine Schicht von 7,55 mm abbrennen.

Ist die Abnahme der Sauerstoffkonzentration merklich längs des Rohres, so ist die hier angewandte Formel durch eine andere zu ersetzen, die man dadurch gewinnt, daß man die dynamische Verbrennungsgleichung für ein Längenelement des Rohres dF ansetzt. Es gilt dafür

$$dV = \beta O_2\,dF,$$

wobei β die mittlere Verbrennungszahl im Rohr und O_2 die Sauerstoffkonzentration an der Stelle dF ist. Außerdem ist aber

$$dV = -W\,dO_2,$$

wenn mit W das in der Stunde durch das Rohr strömende Gasvolumen im Zustande p und T ist. Es wird jetzt

$$W\,dO_2 = \beta O_2\,dF$$

oder

$$\frac{dO_2}{O_2} = \frac{\beta}{W}\,dF$$

und integriert

$$\ln O_2 = -\frac{\beta F}{W} + C.$$

Vol. 3 1961

Setzt man die Konzentration des Sauerstoffes am Eintritt O_2^1 und am Austritt O_2, so wird

$$\ln \frac{O_2}{O_2^1} = -\frac{\beta F}{W}$$

and

$$O_2 = O_2^1 e^{-\beta F/W}.$$

Damit ist die Abnahme der Sauerstoffkonzentration und die an einem Flächenelement verbrannte Kohle längs des Rohres bekannt.

Obige Gleichung für die Verbrennungszahl β gilt bloß für röhrenförmige Körper. Nach der Kenntnis des Wärmeüberganges gelten für anders gestaltete Körper ähnliche Gesetze.[1] Leider sind sie hierfür nicht genau genug durch Versuche sicher gestellt. Insbesondere ist für einen geschichteten Körper, den die Kohle über dem Rost darstellt, nichts ermittelt. Wenn somit auch quantitativ die Ergebnisse obiger Gleichung, angewendet auf die Verbrennung der Kohle über dem Rost, nicht genau stimmen werden, so geben sie doch sicher qualitativ ein annähernd richtiges Bild der Verbrennung, und nur darauf kommt es mir hier zunächst an.

Bisher wurde die Temperatur der Kohle immer als bekannt vorausgesetzt. Sie wechselt natürlich an verschiedenen Stellen über dem Rost. Nachdem nun in der Verbrennungszahl ein Begriff gefunden worden ist, der die Verbrennung regelt, können jetzt ganz allgemein die Gleichungen für die Verbrennung über dem Rost aufgestellt werden. Es seien alle Größen nur von dem Abstand x über dem Rost abhängig. Die zugeführte Luftmenge sei gleichbleibend, und auch die Schütthöhe bleibe unverändert dadurch, daß durch eine Wurffeuerung dauernd beschickt werde. In der ganzen Brennstoffschicht bleibt dann der Zustand unverändert, d. h. an allen einzelnen Stellen herrscht dauernd derselbe Zustand.

Greift man ein Volumenelement von der Dicke dx heraus, so müssen für dieses zwei Bedingungen erfüllt sein: Es müssen die Sätze von der Erhaltung der Energie und der Masse bestehen, d. h. in dem Element darf keine Ansammlung von Energie oder von Masse stattfinden. Ebensowenig darf solche verschwinden. Der Unterschied zwischen der zu- und abströmenden Energie muß gleich der frei werdenden Verbrennungswärme sein.

Es sei n die Anzahl der stündlich auf 1 qm des Rostes zugeführten Luftmole. Da sich bei der Verbrennung die Molzahl nicht ändert, strömt durch jeden Querschnitt x die gleiche Anzahl Mole mit den Verbrennungsgasen. Ist T die Temperatur an dieser Stelle und C die Molekularwärme der Gase daselbst, so strömt mit den Gasen durch die Ebene im Abstand x vom Rost ein Wärmeinhalt

$$J = nCT.$$

C ist natürlich von der Gaszusammensetzung und der Temperatur abhängig, wechselt also mit x. Die Zunahme des Wärmeinhaltes längs dx sei dJ. Die Kohle sinkt abwärts, und zwar mögen m Mole durch die Ebene x treten. m ändert sich mit x. Für $x = 0$ ist auch $m = 0$, d. h. durch den Rost soll keine Kohle fallen. Ist c die Molekularwärme der Kohle, so ist ihr Wärmeinhalt

$$i = cmT$$

Sein Zuwachs längs dx sei di.

Ferner wird die Wärme durch Leitung übertragen. Ist λ die Wärmeleitzahl der Kohlenschicht, so strömt durch die x-Ebene die Wärme

$$q = \lambda \frac{dT}{dx}$$

gegen den Rost. Das Differential dq strömt mehr von oben ein als unten aus.

Durch die Verbrennung wird Wärme in dem Element erzeugt. Ist h der Heizwert von 1 Mol Kohle, so wird in der Schicht dx die Wärme

$$dQ = h\,dm$$

erzeugt. Nach dem Energieprinzip muß dann sein

$$dJ + di + dq - dQ = 0$$

und integriert

$$J + i + q - Q = C_1 \qquad (1)$$

1. Mit den Ergebnissen meines inzwischen erschienenen Aufsatzes, „Das Grundgesetz des Warmeüberganges" *Gesundheitsingenieur* 1915, kann die Verbrennung in ruhender Luft behandelt werden.

Auf Grund der am Anfang aufgestellten dynamischen Verbrennungsgleichung ist die in der Stunde Volumenelement dx verbrannter Kohle

$$\mathrm{d}m = \beta \mathrm{O}_2 \, \mathrm{d}x,$$

wenn O_2 die Sauerstoffkonzentration der Verbrennungsgase an der Stelle x ist, oder als Differentialgleichung geschrieben:

$$\frac{\mathrm{d}m}{\mathrm{d}x} = \beta \mathrm{O}_2 \tag{2}$$

Der Satz von der Erhaltung der Materie verlangt, daß alle in dem Element verbrannte Kohle dieses als Kohlensäure verläßt. Das ergibt die Bedingung:

$$\mathrm{d}m = -\, n \, \mathrm{dO}_2 \tag{3}$$

Da n unveränderlich ist, kann integriert werden. Es wird

$$m = -\, n\mathrm{O}_2 + \mathrm{C}_2 \tag{3}$$

Damit sind drei Gleichungen gewonnen, die genügen, um die drei unbekannten Größen m, T, O_2, als Funktionen von x zu erhalten. Bei der Integration treten 4 Integrationskonstanten auf, die durch die folgenden Bedingungen bestimmt werden:

(1) Für $x = 0$ muß $m = 0$ sein, d. h. es darf keine unverbrannte Kohle durch den Rost fallen.

(2) Für $x = 0$ muß O_2 bei der Verbrennung in Luft = 0,21 sein.

(3) Am Rost, also für $x = 0$ möge die Wärme S_1 durch Leitung an die Roststäbe und durch Strahlung an den Aschenfall abgegeben werden. Die Verbrennungsluft trete mit T_1^0 unter den Rost. Dann muß sein

$$\lambda \frac{\mathrm{d}T}{\mathrm{d}x} = S_1 + nC(T - T_1).$$

(4) Am oberen Ende der Brennschicht mögen S_2 Wärmeeinheiten an die Kesselwand ausgestrahlt werden. Ist T_2 die Temperatur der frischen Kohle, so liefert der Energiesatz dort die Beziehung

$$x = H; \qquad \lambda \frac{\mathrm{d}T}{\mathrm{d}x} = S_1 + mc(T - T_2).$$

Führt man aus Gleichung (3) m in dieG leichung ein und setzt in erster Annäherung β für die (2) ganze Brennschicht unveränderlich, so wird bei Berücksichtigung der Grenzbedingungen

$$\mathrm{O}_2 = 0{,}21 \, e^{-\frac{\beta}{n} x}$$

Der Sauerstoffgehalt nähert sich also nach einer Exponentialfunktion dem Wert null, allerdings erst für unendliche Schütthöhe. In der untersten Zone verbrennt demnach am meisten Kohle; je weiter man nach oben geht, desto weniger lebhaft ist die Verbrennung auf die Längeneinheit. Ebenso wie ein kaltes Gas, das durch ein warmes Rohr strömt, auf Grund der Rechnung erst bei unendlicher Länge die Temperatur der Rohrwand annimmt, braucht man bei der Verbrennung eine unendliche Schütthöhe, um allen Sauerstoff zu verbrennen. Praktisch ist aber schon für eine endliche Schütthöhe aller Sauerstoff verbrannt. Über dieser bildet sich sodann Kohlenoxyd, wobei Wärme gebunden wird.

Ist Kohlensäure in Berührung mit fester Kohle, so stellt sich ein Gleichgewichtzustand ein, derart, daß ein Teil der Kohlensäure in Kohlenoxyd zerfällt, und zwar besteht für jede Temperatur eine bestimmte und bekannte Konzentration. Je höher die Temperatur ist, desto mehr Kohlenoxyd ist vorhanden.

Die Schütthöhe möge jetzt so groß angenommen werden, daß die Höhe, bis zu der aller Sauerstoff verbrannt ist, überschritten wird. Es bildet sich dann Kohlenoxyd, und man spricht nicht mehr von einer Verbrennung, sondern von einer Vergasung des Brennstoffes, weil ein brennbares Gas entsteht. Der Vorgang der Vergasung findet folgendermaßen statt: In jener Grenzhöhe ist die Kohlensäurekonzentration 0,21 und die des Sauerstoffes null. An der Oberfläche verbrennt die Kohle jetzt nach der Gleichung

$$\mathrm{C} + \mathrm{CO}_2 = 2\mathrm{CO} - h_2 \, \mathrm{WE},$$

und zwar ist es sehr wahrscheinlich, daß sich an der Oberfläche die der Temperatur entsprechende Gleichgewichtkonzentration einstellt. Dann sind dort die Kohlensäure- und Kohlenoxydkonzentration nur von der Temperatur abhängig. Die weitere Vergasung geht dann so

Vol. 3 1961

vor sich, daß Kohlenoxyd von der Kohlenoberfläche nach dem Kern des Gasstromes diffundiert, während in dieser Zone die Kohlensäure aus dem Kern gegen die Wand strömt. Eine Abbildung des Vorganges durch ein Problem des Wärmeüberganges ist aber jetzt nicht mehr möglich, da an der Wand aus einem Raumteil Kohlensäure 2 Raumteile Sauerstoff werden. Es ist jetzt eine Strömung vorhanden, bei der an der Begrenzungswand Quellen sitzen, da an der Wand durch den Vergasungsvorgang eine Vergrößerung des Volumens stattfindet. Die Konzentration verteilt sich nach Abb. 4.

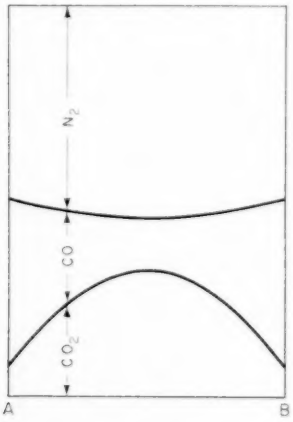

Abb. 4. Änderung der Gaszusammensetzung in einem Horizontalquerschnitt der Vergasungszone.

Ist V das in 1 st und auf 1 qm der Kohle erzeugte Kohlenoxydvolumen, so entsteht dort an der Wand eine Volumenvergrößerung von $\frac{1}{2}V$, und demzufolge strömt das Gas von der Wand mit der Geschwindigkeit $w = \frac{1}{2}V \frac{1}{3600}$ m/sk gegen den Kern. Da CO der Anteil von Kohlenoxyd an 1 cbm ist, werden auf 1 qm $\frac{V}{2}$ CO cbm Kohlenoxyd durch sichtbare Strömung in das Gas geleitet. Dazu kommt die Abgabe von Kohlenoxyd durch Diffusion im Betrage von

$$k \frac{\mathrm{dCO}}{\mathrm{d}s}.$$

Beide zusammen geben das erzeugte Volumen Kohlenoxydgas. Es wird also

$$V = k \frac{\mathrm{dCO}}{\mathrm{d}s} + \frac{V}{2} \mathrm{CO}$$

oder

$$V \left(1 - \frac{\mathrm{CO}}{2}\right) = k \frac{\mathrm{dCO}}{\mathrm{d}s}.$$

Aus dieser Formel kann das erzeugte Volumen Kohlenoxyd und damit die dadurch verbrannte Kohle bestimmt werden, wenn das Konzentrationsgefälle des Kohlenoxydes an der Wand bekannt ist. Ähnlich wie bei der Verbrennung kann man dann bei der Vergasung eine Vergasungszahl γ einführen, die uns sagt, daß an der Kohlenoberfläche

$$k \frac{\mathrm{dCO}}{\mathrm{d}s} = \gamma (\mathrm{CO}_0 - \mathrm{CO}_m)$$

ist, wenn CO_0 die Kohlenoxydkonzentration an der Kohlenoberfläche und CO_m die mittlere Kohlenoxydkonzentration im Gasstrom ist. Durch diesen Ansatz wird die vergaste Kohlenmenge proportional dem Unterschied der Kohlenoxydkonzentration an der Kohlenoberfläche und der mittleren Kohlenoxydkonzentration im Gasstrom gesetzt. Sind Werte von γ hierfür durch Versuche bestimmt, dann kann man wieder die Sätze von der Erhaltung der Energie und der Masse anwenden und durch deren Integration den Temperaturverlauf und die Änderung der Gaszusammensetzung in Generator bestimmen.

Obige Theorie hat aber einen Mangel. Es ist die Stelle, an der aller Sauerstoff aufgebraucht ist, an der also die Verbrennung in die Vergasung übergeht, nicht scharf bestimmt. Man kann ihn vermeiden, wenn man bei der Verbrennung ebenfalls an der Kohlenoberfläche das Vorhandensein des Kohlensäuregleichgewichtes wie in der Vergasungszone annimmt. Das an der Kohlenoberfläche gebildete Kohlenoxyd diffundiert gegen den Kern der Verbrennungsgase und verbrennt mit dem vom Kern gegen die Wand diffundierenden Sauerstoff nach. Maßgabe einer endlichen Verbrennungsgeschwindigkeit. Die an einer Stelle im Gasraum entstehende

Kohlensäure folgt dann nach den Gesetzen der chemischen Dynamik der Gleichung

$$\frac{d[CO_2]}{dz} = f\,[CO]^2[O_2].$$

In dieser Gleichung ist f eine reine Temperaturfunktion; $[CO_2]$, $[CO]$ und $[O_2]$ sind die molaren Konzentrationen von Kohlensäure, Kohlenoxyd und Sauerstoff an einer Stelle. Der Zusammenhang zwischen der molaren Konzentration einer Molekülgattung[1] und deren räumlicher Konzentration ist z. B. für Kohlensäure durch die Gleichung

$$[CO_2] = CO\,\frac{p}{RT}$$

gegeben, wenn R die Gaskonstante 848 und p der gesamte Druck in kq/qm sind.

Abb. 5 gibt die Änderung der Konzentration auf einer Senkrechten zur Kohlenoberfläche an. Die Kohlenoxyd führende Schicht an der Wand

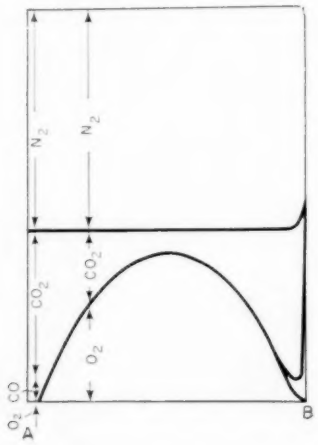

Abb. 5. Änderung der Gaszusammensetzung in einem Horizontalquerschnitt der Verbrennungszone.

wird praktisch außerordentlich klein sein, so daß sich das Bild bis auf diese Grenzschicht mit der Abbildung 3 decken wird. Bei dieser Annahme fällt jetzt Unterschied zwischen Verbrennung und Vergasung ganz fort. Beide Fälle sind in einer Gleichungsreihe enthalten. Aber die Zurückführung auf das Problem des Wärmeüberganges entfällt, und die Einfachheit der Verhältnisse verschwindet. Damit ist das Wesen der Vergasung von Kohlenstoff besprochen, wenn es sich um die Erzeugung von Luftgas handelt.

Es sollen jetzt noch die Vorgänge behandelt werden, die sich bei der Erzeugung von Mischgas abspielen. Es wird hier ein Gemisch von Wasserdampf und Luft unter dem Rost eingeblasen. Wie oben, so stehe ich auch hier wieder auf dem Standpunkt, daß ein chemischer Vorgang nur an der Oberfläche der Kohle stattfindet. In dem Gasraume zwischen den Kohleteilchen findet die Änderung der Gaszusammensetzung nur durch Diffusion statt.

In der unteren Zone verbrennt wieder Kohle zu Kohlensäure. Es kann meines Erachtens kein Kohlenoxyd und auch kein Wasserstoff bestehen, so lange noch Sauerstoff vorhanden ist, denn bei der in der Verbrennungszone herrschenden Temperatur ist die Affinität zum Sauerstoff so groß, daß beide Gase augenblicklich verbrennen. Die Wasserdampfkonzentration ist deshalb gleichbleibend, und Kohlensäure diffundiert von der Wand nach innen, s. Abb. 6.

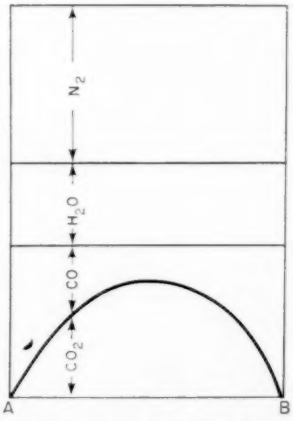

Abb. 6. Änderung der Gaszusammensetzung in einem Horizontalquerschnitt der Verbrennungszone bei der Erzeugung von Mischgas.

In einer gewissen Höhe über dem Rost ist aller Sauerstoff verbrannt, und es ist ein Gemisch von Wasserdampf, Kohlensäure und Stickstoff vorhanden. Von hier an setzt eine andre Reaktion

1. d. i. die Anzahl Mole in der Raumeinheit.

Vol. 3 1961

ein. An der Wand geht die Vergasung der Kohle nach folgenden beiden Gleichungen vor sich:

$$C + CO_2 = 2CO - h_2 \text{ WE}$$

und

$$C + H_2O = CO + H_2 - h_3 \text{ WE}.$$

Es wird also bei beiden Reaktionen Wärme verbraucht, die von der Temperatur abhängig ist. Bei 15° ist

$$h_2 = 38\,250 \text{ WE}$$

und

$$h_3 = 27\,930 \text{ WE}.$$

An der Kohlenoberfläche treten beide Reaktionen auf und verlaufen sehr schnell bis zum chemischen Gleichgewicht, das verlangt, daß die beiden Brüche

$$\frac{[CO]^2}{[CO_2]} = K_1(T)$$

und

$$\frac{[CO]\,[H_2]}{[H_2O]} = K_2(T)$$

eindeutige Funktionen der Temperatur sind. Zieht man beide Reaktionsgleichungen voneinander ab, so erhält man die sogenannte Wassergasreaktion

$$CO_2 + H_2 = CO + H_2O - h_4 \text{ WE},$$

wobei

$$h_4 = 10\,320 \text{ WE}$$

ist.

Diese Gleichung wird vielfach als ausschlaggebend für die Vergasung im Gaserzeuger bezeichnet. Sie stellt aber eine homogene Reaktion dar, und meines Erachtens sind im Gaserzeuger die Temperaturen zu tief und die Zeiten zu klein, als daß im Gaserzeuger eine Reaktion nach der Wassergasgleichung stattfinden könnte. Man hat sich vielmehr den Vorgang so vorzustellen, daß an der glühenden Kohle die Vergasung nach obigen beiden Gleichungen bis zum Gleichgewicht stattfindet. Die gebildeten Gase CO und H_2 diffundieren dann in das an der Kohle entlang strömende Gas, während aus dessen Kern CO_2 und H_2O gegen die glühende Kohle diffundieren und dort die Kohle vergasen. Die Schnelligkeit der Vergasung hängt nur von der Diffusionsgeschwindigkeit ab. Im Gasraum diffundieren jetzt die fünf Gase N_2, CO, CO_2, H_2O und H_2. Bevor eine weitere analytische Behandlung der Vergasungsfrage möglich ist, muß zuerst die Diffusion von Gasen des näheren durch Versuche geklärt werden.

ZUSAMMENFASSUNG

Es wird gezeigt, daß die Verbrennung und Vergasung von Kohle auf dem Rost wesentlich physikalische Fragen sind. Die sichbare und die molekulare Strömung (Diffusion) leiten diese Vorgänge. Die Verbrennung der Kohle wird durch eine Aufgabe der Wärmeübertragung abgebildet und dadurch gelöst.

Papers accepted for publication in future issues

H. L. EVANS: Mass transfer through laminar boundary layers—7. Further similar solutions to the b-equation for the case $B = 0$

V. A. KIRILLIN, A. E. SCHEINDLIN and V. Y. CHEKHOVSKOY: Experimental determination of the enthalpy and heat capacity of molybdenum up to 2337°C

P. N. ROMANENKO, A. I. LEONT'EV and A. N. OBLIVIN: Investigation on resistance and heat transfer at turbulent flow in axisymmetrical channels with longitudinal pressure gradient

P. S. LYKOUDIS: Natural convection of an electrically conducting fluid in the presence of a magnetic field

SH. N. PLYAT: Heat and mass transfer of circular hollow cylinders under boundary conditions of the second kind

V. P. MOTULEVICH: Heat and mass transfer in a frontal point of blunt bodies in a liquid flow at the pressure of heterogeneous chemical reactions

G. POOTS: The application of integral methods to the solution of problems solving the solidification of liquids initially at fusion temperature

G. POOTS: An approximate treatment of a heat combustion problem involving a two dimensional solidification front

I. T. ELPERIN: Terms, letter symbols and definitions on heat and mass transfer used in the Soviet Union

H. L. EVANS: Mass transfer through laminar boundary layers—8. Further solutions to the velocity equation

M. S. SMIRNOV: On a system of differential equations for highly intensive heat and mass transfer

Vol. 3 1961

ol.
3
961